



Viability Assessment of a Repository at Yucca Mountain  
Total System Performance Assessment



U.S. Department of Energy  
Office of Civilian Radioactive Waste Management

Volume 3  
DOE/RW-0508

DOE/RW-0508/V3

# **Viability Assessment of a Repository at Yucca Mountain**

**Volume 3: Total System Performance Assessment**

December 1998



U.S. Department of Energy  
Office of Civilian Radioactive Waste Management  
Yucca Mountain Site Characterization Office

This publication was produced by the U.S. Department of Energy  
Office of Civilian Radioactive Waste Management.

For further information contact:  
U.S. Department of Energy  
Yucca Mountain Site Characterization Office  
P.O. Box 30307  
North Las Vegas, Nevada 89036-0307

or call:  
Yucca Mountain Information Center  
1-800-225-6972

or visit:  
Yucca Mountain Site Characterization Project website  
<http://www.ymp.gov>

 Printed with soy ink on recycled paper.

CONTENTS

|   | Page |
|---|------|
| OVERVIEW .....  | O-1  |
| 1. INTRODUCTION .....   | 1-1  |
| 1.1 DEFINITION OF PERFORMANCE ASSESSMENT AND TOTAL SYSTEM<br>PERFORMANCE ASSESSMENT .....                                 | 1-1  |
| 1.1.1 Explanation of a Total System Performance Assessment.....   | 1-1  |
| 1.1.2 The Performance Assessment Pyramid.....   | 1-2  |
| 1.2 PHILOSOPHY OF TOTAL SYSTEM PERFORMANCE ASSESSMENT .....   | 1-3  |
| 1.2.1 Why Total System Performance Assessments Are Performed .....  | 1-3  |
| 1.2.2 Why Total System Performance Assessments Are the Appropriate Tool for<br>Analyzing Repository Systems .....         | 1-4  |
| 1.3 GENERIC APPROACH FOR CONDUCTING A TOTAL SYSTEM PERFORMANCE<br>ASSESSMENT .....  | 1-5  |
| 1.3.1 Develop and Screen Scenarios .....  | 1-6  |
| 1.3.2 Develop Models .....  | 1-6  |
| 1.3.3 Estimate Parameter Ranges and Uncertainties.....  | 1-6  |
| 1.3.4 Perform Calculations.....   | 1-8  |
| 1.3.5 Interpret Results .....   | 1-8  |
| 2. YUCCA MOUNTAIN SITE CHARACTERIZATION PROJECT TOTAL SYSTEM<br>PERFORMANCE ASSESSMENT FOR THE VIABILITY ASSESSMENT ..... | 2-1  |
| 2.1 OBJECTIVES OF TOTAL SYSTEM PERFORMANCE ASSESSMENT FOR THE<br>VIABILITY ASSESSMENT .....                               | 2-2  |
| 2.2 TOTAL SYSTEM PERFORMANCE ASSESSMENT APPROACH.....   | 2-4  |
| 2.2.1 Development of an Integrated Total System Performance Assessment<br>Approach .....                                  | 2-4  |
| 2.2.2 Components of the Yucca Mountain Repository System Evaluated in the Total<br>System Performance Assessment.....     | 2-10 |
| 2.2.3 Conceptual Description of Processes Relevant to an Evaluation of Postclosure<br>Performance .....                   | 2-15 |
| 2.2.3.1 Water Movement in the Unsaturated Tuffs Above the Repository .....  | 2-16 |
| 2.2.3.2 Water and Water Vapor Movement Around the Repository Drifts .....   | 2-17 |
| 2.2.3.3 Water Movement Within the Engineered Barrier System.....  | 2-19 |
| 2.2.3.4 Water Movement and Radionuclide Migration out of the Engineered<br>Barrier System .....                           | 2-19 |
| 2.2.3.5 Water Movement and Radionuclide Migration Through the<br>Unsaturated Tuffs Below the Repository .....             | 2-22 |
| 2.2.3.6 Water Movement and Radionuclide Migration Through the Saturated<br>Zone Aquifers and Biosphere.....               | 2-22 |
| 2.3 METHODOLOGY .....   | 2-25 |
| 2.3.1 Information Flow Between Component Models.....  | 2-26 |
| 2.3.2 Code Architecture .....   | 2-29 |
| 2.3.3 Treatment of Uncertainty .....  | 2-37 |
| 2.3.3.1 Uncertainty Versus Variability.....   | 2-37 |
| 2.3.3.2 Weighting of Alternative Conceptual Models.....   | 2-38 |
| 2.3.3.3 Uncertainty and the Base Case .....   | 2-39 |
| 2.3.3.4 Presentation and Analysis Techniques for Uncertainty.....   | 2-41 |
| 2.4 DESCRIPTION OF BASE CASE RESULTS .....  | 2-43 |

CONTENTS (Continued)

|  | Page       |
|--|------------|
| 2.4.1 Time of Waste Emplacement to Time of Repository Closure .....  | 2-43       |
| 2.4.2 Time of Repository Closure to Several Hundred Years After Closure.....                                   | 2-43       |
| 2.4.3 Several Hundred Years to Several Thousand Years After Closure .....                                      | 2-43       |
| 2.4.4 Several Thousand Years to Ten Thousand Years After Closure .....   | 2-44       |
| 2.4.5 Ten Thousand Years to Several Tens of Thousands of Years After Closure .....                             | 2-45       |
| 2.4.6 Several Tens of Thousands of Years to One Hundred Thousand Years<br>After Closure.....                   | 2-45       |
| 2.4.7 Several Hundred Thousand Years After Closure.....  | 2-46       |
| <b>3. DEVELOPMENT OF TOTAL SYSTEM PERFORMANCE ASSESSMENT<br/>COMPONENTS FOR THE VIABILITY ASSESSMENT .....</b> | <b>3-1</b> |
| 3.1 UNSATURATED ZONE FLOW .....  | 3-2        |
| 3.1.1 Construction of the Conceptual Model .....   | 3-5        |
| 3.1.1.1 Climate .....  | 3-8        |
| 3.1.1.2 Infiltration .....   | 3-9        |
| 3.1.1.3 Mountain-Scale Unsaturated Zone Flow .....   | 3-10       |
| 3.1.1.4 Seepage into Drifts .....  | 3-11       |
| 3.1.2 Implementation of the Performance Assessment Model .....   | 3-12       |
| 3.1.2.1 Climate .....  | 3-12       |
| 3.1.2.2 Infiltration .....   | 3-13       |
| 3.1.2.3 Mountain-Scale Unsaturated Zone Flow .....   | 3-15       |
| 3.1.2.4 Seepage into Drifts .....  | 3-16       |
| 3.1.3 Results and Interpretation .....   | 3-19       |
| 3.1.3.1 Infiltration .....   | 3-19       |
| 3.1.3.2 Mountain-Scale Unsaturated Zone Flow .....   | 3-20       |
| 3.1.3.3 Seepage into Drifts .....  | 3-23       |
| 3.2 THERMAL HYDROLOGY .....  | 3-23       |
| 3.2.1 Construction of the Conceptual Model .....   | 3-26       |
| 3.2.2 Implementation of the Performance Assessment Model .....   | 3-30       |
| 3.2.2.1 Repository and Waste Package Design .....  | 3-30       |
| 3.2.2.2 The Drift-Scale Model .....  | 3-31       |
| 3.2.2.3 The Mountain-Scale Model .....   | 3-35       |
| 3.2.2.4 Uncertainties .....  | 3-35       |
| 3.2.3 Results and Interpretation .....   | 3-36       |
| 3.3 NEAR-FIELD GEOCHEMICAL ENVIRONMENT.....  | 3-39       |
| 3.3.1 Construction of the Conceptual Models.....   | 3-43       |
| 3.3.1.1 The Near-Field Geochemical Environment Workshop and Highest<br>Priority Issues .....                   | 3-43       |
| 3.3.1.2 Incoming Gas, Water, and Colloids .....  | 3-45       |
| 3.3.1.3 Evolution of the In-Drift Chemistry .....  | 3-49       |
| 3.3.2 Implementation of the Near-Field Geochemical Environment Models.....                                     | 3-57       |
| 3.3.2.1 Incoming Gas, Water, and Colloids .....  | 3-58       |
| 3.3.2.2 Evolution of the In-Drift Chemistry .....  | 3-62       |
| 3.3.2.3 Major Uncertainties Within the Models .....  | 3-65       |
| 3.3.3 Results and Interpretation .....   | 3-66       |
| 3.3.3.1 Gas Compositions .....   | 3-67       |
| 3.3.3.2 Water Compositions .....   | 3-68       |

CONTENTS (Continued)

|         | Page   |       |
|---------|--|-------|
| 3.3.3.3 | Consideration of Spent Fuel Alteration and Secondary Phase Effects<br>on Near-Field Geochemical Environment.....             | 3-72  |
| 3.3.3.4 | Colloid Amounts .....  | 3-73  |
| 3.4     | WASTE PACKAGE DEGRADATION .....  | 3-73  |
| 3.4.1   | Construction of the Conceptual Model .....   | 3-77  |
| 3.4.1.1 | Waste Package Degradation Expert Elicitation.....  | 3-79  |
| 3.4.1.2 | Model Input and Output .....   | 3-80  |
| 3.4.1.3 | Modeled Degradation Modes .....  | 3-80  |
| 3.4.1.4 | Early Waste Package Failure (Juvenile Failure) .....   | 3-81  |
| 3.4.1.5 | General Corrosion .....  | 3-81  |
| 3.4.1.6 | Localized Corrosion .....  | 3-82  |
| 3.4.1.7 | Other Degradation Modes for Waste Packages.....  | 3-83  |
| 3.4.2   | Implementation of Waste Package Degradation Model.....   | 3-85  |
| 3.4.3   | Results and Interpretation: Evaluation of Key Issues and Importance to<br>Performance .....                                  | 3-88  |
| 3.5     | WASTE FORM ALTERATION, RADIONUCLIDE MOBILIZATION, AND<br>TRANSPORT THROUGH THE ENGINEERED BARRIER SYSTEM.....                | 3-90  |
| 3.5.1   | Construction of the Conceptual Model .....   | 3-92  |
| 3.5.1.1 | Input .....  | 3-94  |
| 3.5.1.2 | Output .....   | 3-94  |
| 3.5.1.3 | Components of the Models .....   | 3-94  |
| 3.5.1.4 | Bases for Confidence in the Model .....  | 3-94  |
| 3.5.1.5 | Inventory .....  | 3-95  |
| 3.5.1.6 | Cladding .....   | 3-97  |
| 3.5.1.7 | Dissolution Rates .....  | 3-97  |
| 3.5.1.8 | Solubility Limits .....  | 3-99  |
| 3.5.1.9 | Colloids .....   | 3-99  |
| 3.5.2   | Implementation of the Waste Form Degradation and Mobilization Model.....   | 3-100 |
| 3.5.2.1 | Cladding Model Abstraction .....   | 3-100 |
| 3.5.2.2 | Dissolution Rates .....  | 3-103 |
| 3.5.2.3 | Solubility Limits .....  | 3-103 |
| 3.5.2.4 | Colloids .....   | 3-104 |
| 3.5.2.5 | Secondary Phase Analyses .....   | 3-106 |
| 3.5.2.6 | Engineered Barrier System Transport .....  | 3-106 |
| 3.5.3   | Results and Interpretation: Evaluation of Issues Important to Performance.....   | 3-107 |
| 3.5.3.1 | Cladding Degradation.....  | 3-107 |
| 3.5.3.2 | Waste Form Degradation .....   | 3-108 |
| 3.5.3.3 | Doses from DOE Spent Nuclear Fuel .....  | 3-108 |
| 3.5.3.4 | Releases from Plutonium Waste Forms, High-Level Radioactive<br>Waste, and the Commercial Spent Nuclear Fuel Waste Form ..... | 3-108 |
| 3.5.3.5 | Releases from Naval Spent Nuclear Fuel .....   | 3-108 |
| 3.5.3.6 | Remaining Uncertainties in Engineered Barrier System Analyses .....  | 3-109 |
| 3.6     | UNSATURATED ZONE TRANSPORT .....   | 3-109 |
| 3.6.1   | Construction of the Conceptual Model .....   | 3-113 |
| 3.6.1.1 | Unsatuated Zone Flow Model .....   | 3-114 |
| 3.6.1.2 | Matrix Diffusion Model .....   | 3-116 |
| 3.6.1.3 | Sorption Model .....   | 3-117 |

CONTENTS (Continued)

|         | Page   |
|---------|--|
| 3.6.1.4 | Colloid-Facilitated Transport Model ..... 3-118  |
| 3.6.1.5 | Dispersion Model ..... 3-119   |
| 3.6.1.6 | Chain-Decay Model ..... 3-119  |
| 3.6.2   | Implementation of the Performance Assessment Model ..... 3-120   |
| 3.6.2.1 | Finite Element Heat and Mass Particle Tracking ..... 3-120   |
| 3.6.2.2 | Linkage with Other Models ..... 3-120  |
| 3.6.2.3 | Parameter Inputs ..... 3-121   |
| 3.6.3   | Results and Interpretations ..... 3-123  |
| 3.6.3.1 | Results for the Unsaturated Zone Transport Model ..... 3-124   |
| 3.6.3.2 | Influence of the Unsaturated Zone Flow Model ..... 3-127   |
| 3.6.3.3 | Influence of Matrix Diffusion ..... 3-127  |
| 3.6.3.4 | Influence of Rock Type ..... 3-128   |
| 3.6.3.5 | Summary and Conclusions ..... 3-129  |
| 3.7     | SATURATED ZONE FLOW AND TRANSPORT ..... 3-130  |
| 3.7.1   | Construction of the Conceptual Model ..... 3-132   |
| 3.7.1.1 | Conceptualization of Saturated Zone Flow and Transport<br>Processes ..... 3-132                        |
| 3.7.1.2 | Saturated Zone Flow and Transport Data ..... 3-133   |
| 3.7.1.3 | Saturated Zone Flow and Transport Modeling ..... 3-135   |
| 3.7.1.4 | Saturated Zone Workshop and Expert Elicitation ..... 3-136   |
| 3.7.2   | Implementation of the Performance Assessment Model ..... 3-139   |
| 3.7.2.1 | One-Dimensional Flow and Transport Modeling ..... 3-139  |
| 3.7.2.2 | Model Parameter Uncertainty ..... 3-140  |
| 3.7.2.3 | Integration of Transport Modeling with Total System Performance<br>Assessment Calculations ..... 3-141 |
| 3.7.3   | Results and Interpretation ..... 3-143   |
| 3.8     | BIOSPHERE ..... 3-145  |
| 3.8.1   | Construction of the Conceptual Model ..... 3-146   |
| 3.8.1.1 | Model Basis ..... 3-148  |
| 3.8.1.2 | Pathways ..... 3-150   |
| 3.8.1.3 | Regional Survey ..... 3-151  |
| 3.8.2   | Implementation of the Performance Assessment Model ..... 3-155   |
| 3.8.3   | Results and Interpretation ..... 3-158   |
| 3.8.3.1 | Biosphere Probabilistic Results ..... 3-159  |
| 3.8.3.2 | Biosphere Comparative Analyses ..... 3-160   |
| 3.8.3.3 | Biosphere Scenarios Associated with Volcanic Activity ..... 3-161                                      |
| 4.      | BASE CASE DEFINITION AND RESULTS ..... 4-1   |
| 4.1     | BASE CASE DESCRIPTION ..... 4-2  |
| 4.1.1   | Climate ..... 4-2  |
| 4.1.2   | Unsaturated Zone Flow and Infiltration ..... 4-3   |
| 4.1.3   | Drift Scale Seepage ..... 4-4  |
| 4.1.4   | Drift Scale Thermal Hydrology ..... 4-7  |
| 4.1.5   | Repository Scale Thermal Hydrology ..... 4-7   |
| 4.1.6   | Near-Field Geochemical Environment ..... 4-9   |
| 4.1.7   | Waste Package Degradation ..... 4-9  |
| 4.1.8   | Cladding Degradation ..... 4-12  |

CONTENTS (Continued)

|  | Page  |
|--|-------|
| 4.1.9 Waste Form Degradation and Mobilization.....   | 4-13  |
| 4.1.10 Transport in the Engineered Barrier System.....   | 4-13  |
| 4.1.11 Unsaturated Zone Transport.....   | 4-15  |
| 4.1.12 Saturated Zone Flow and Transport.....  | 4-16  |
| 4.1.13 Biosphere Transport.....  | 4-16  |
| 4.2 DETERMINISTIC RESULTS OF THE TOTAL SYSTEM PERFORMANCE  |       |
| ASSESSMENT BASE CASE.....  | 4-21  |
| 4.2.1 Ten-Thousand-Year Dose Rates.....  | 4-25  |
| 4.2.2 One-Hundred-Thousand Year Dose Rates.....  | 4-35  |
| 4.2.3 One-Million-Year Dose Rates.....   | 4-50  |
| 4.2.4 Cumulative Activity Releases from the Repository and the Engineered Barrier<br>System..... | 4-61  |
| 4.2.5 Summary.....   | 4-62  |
| 4.3 PROBABILISTIC RESULTS OF THE BASE CASE.....  | 4-63  |
| 4.3.1 Uncertainty Analysis.....  | 4-63  |
| 4.3.1.1 Uncertainty Analysis Results.....  | 4-64  |
| 4.3.1.2 Precision of the Base Case Complementary Cumulative Distribution<br>Functions.....       | 4-71  |
| 4.3.2 Sensitivity Analysis.....  | 4-71  |
| 4.3.2.1 Sensitivity Analysis Results.....  | 4-72  |
| 4.3.2.2 Impact of Parameter Uncertainty Ranges on Sensitivity Analyses.....                      | 4-77  |
| 4.3.3 Summary.....   | 4-78  |
| 4.4 EFFECTS OF DISRUPTIVE EVENTS.....  | 4-80  |
| 4.4.1 Initial Selection of Important Issues.....   | 4-81  |
| 4.4.2 Igneous Activity.....  | 4-81  |
| 4.4.2.1 Direct Release Scenario.....   | 4-82  |
| 4.4.2.2 Enhanced Source Term Scenario.....   | 4-84  |
| 4.4.2.3 Indirect Igneous Effects Scenario.....   | 4-85  |
| 4.4.2.4 Results of Igneous Activity Analyses.....  | 4-86  |
| 4.4.3 Seismic Activity.....  | 4-88  |
| 4.4.3.1 Rockfall Scenario.....   | 4-90  |
| 4.4.3.2 Indirect Seismic Effects Scenario.....   | 4-91  |
| 4.4.3.3 Results of Seismic Activity Analyses.....  | 4-92  |
| 4.4.4 Nuclear Criticality.....   | 4-92  |
| 4.4.4.1 In-Package Criticality Scenarios.....  | 4-94  |
| 4.4.4.2 Out-of-Package Criticality Scenarios.....  | 4-96  |
| 4.4.4.3 Results of Nuclear Criticality Analyses.....   | 4-96  |
| 4.4.5 Human Intrusion.....   | 4-99  |
| 4.4.5.1 Technical Bases for Human Intrusion Analyses.....  | 4-100 |
| 4.4.5.2 Results of Human Intrusion Analyses.....   | 4-100 |
| 4.4.6 Summary.....   | 4-102 |
| 4.5 EFFECTS OF DESIGN OPTIONS.....   | 4-102 |
| 4.5.1 Emplacement Drift Backfill.....  | 4-102 |
| 4.5.2 Drip Shields.....  | 4-104 |
| 4.5.3 Ceramic Coating of the Disposal Container with Backfill.....                               | 4-106 |
| 5. SENSITIVITY ANALYSES FOR COMPONENTS.....  | 5-1   |

CONTENTS (Continued)

|   | Page |
|---|------|
| 5.1 UNSATURATED ZONE FLOW .....   | 5-1  |
| 5.1.1 Sensitivity to Climate .....  | 5-1  |
| 5.1.2 Sensitivity to Infiltration .....   | 5-3  |
| 5.1.3 Sensitivity to Mountain-Scale Unsaturated Zone Flow .....   | 5-4  |
| 5.1.4 Sensitivity to Seepage into Drifts.....   | 5-6  |
| 5.2 THERMAL HYDROLOGY .....   | 5-9  |
| 5.3 NEAR-FIELD GEOCHEMICAL ENVIRONMENT .....  | 5-10 |
| 5.3.1 Sensitivity of Water Composition to Spent Fuel Alteration .....   | 5-10 |
| 5.3.2 Sensitivity to Concrete-Modified (Alkaline) Water Compositions .....  | 5-11 |
| 5.3.2.1 Components Affected by Concrete-Modified Water .....  | 5-11 |
| 5.3.2.2 Effect on Dose Rate and Engineered Barrier Release Rate.....  | 5-12 |
| 5.4 WASTE PACKAGE DEGRADATION .....   | 5-14 |
| 5.4.1 Sensitivity to Uncertainty/Variability Assumptions in Alloy 22 General<br>Corrosion Rates.....                    | 5-15 |
| 5.4.2 Sensitivity to Environment (Drip Versus No Drip Conditions).....  | 5-16 |
| 5.4.3 Sensitivity to Percent of Waste Package Surface Wetted Under Dripping<br>Conditions .....                         | 5-16 |
| 5.4.4 Sensitivity to High-pH (Concrete-Modified) Seepage Water .....  | 5-18 |
| 5.4.5 Sensitivity to Microbiologically Influenced Corrosion.....  | 5-19 |
| 5.4.6 Sensitivity to Juvenile Failures .....  | 5-21 |
| 5.4.7 Sensitivity to Corrosion Patch Size.....  | 5-21 |
| 5.5 WASTE FORM ALTERATION, RADIONUCLIDE MOBILIZATION, AND<br>TRANSPORT THROUGH THE ENGINEERED BARRIER SYSTEM.....       | 5-22 |
| 5.5.1 Sensitivity to Seepage into the Waste Package.....  | 5-22 |
| 5.5.2 Sensitivity to Cladding Degradation .....   | 5-23 |
| 5.5.3 Sensitivity to Dissolution Rate and Secondary-Phase Retention of Neptunium....                                    | 5-28 |
| 5.5.4 Sensitivity of Dose to Neptunium Solubility .....   | 5-29 |
| 5.5.5 Sensitivity to Formation and Transport of Radionuclide-Bearing Colloids .....                                     | 5-30 |
| 5.5.6 Sensitivity to Transport in the Engineered Barrier System.....  | 5-31 |
| 5.5.7 Comparison of the Surrogate U.S. Department of Energy Spent Nuclear Fuel<br>to DOE Spent Nuclear Fuel Total ..... | 5-33 |
| 5.5.8 Comparison of Plutonium Waste Form with Commercial Spent Nuclear Fuel<br>Equivalent Waste Form.....               | 5-34 |
| 5.6 UNSATURATED ZONE TRANSPORT .....  | 5-35 |
| 5.6.1 Sensitivity to Matrix Diffusion .....   | 5-35 |
| 5.6.2 Sensitivity to Sorption.....  | 5-36 |
| 5.6.3 Sensitivity to Combined Effects of Source Term and Unsaturated Zone<br>Sorption.....                              | 5-39 |
| 5.7 SATURATED ZONE FLOW AND TRANSPORT .....   | 5-40 |
| 5.7.1 Sensitivity to Dilution .....   | 5-40 |
| 5.7.2 Sensitivity to Alluvium Fraction.....   | 5-41 |
| 5.7.3 Sensitivity to Method of Flow-Tube Combination .....  | 5-42 |
| 5.8 BIOSPHERE .....   | 5-43 |
| 5.8.1 Sensitivity to Biosphere Dose Conversion Factor .....   | 5-44 |
| 5.8.2 Sensitivity to Dilution at the Well and in the Biosphere.....   | 5-44 |
| 5.8.3 Sensitivity to Critical-Group Definition.....   | 5-46 |

CONTENTS (Continued)

|  | Page |
|--|------|
| 6. SUMMARY AND CONCLUSIONS .....   | 6-1  |
| 6.1 SCIENTIFIC DATA AND ANALYSES IN THE TOTAL SYSTEM PERFORMANCE<br>ASSESSMENT FOR THE VIABILITY ASSESSMENT MODELS.....  | 6-2  |
| 6.2 PROBABLE BEHAVIOR OF THE REFERENCE DESIGN .....  | 6-4  |
| 6.3 SENSITIVITY ANALYSES OF THE REFERENCE DESIGN .....   | 6-5  |
| 6.3.1 Sensitivity Analyses over the First 10,000 Years .....   | 6-6  |
| 6.3.2 Sensitivity Analyses from 10,000 to 100,000 Years.....   | 6-8  |
| 6.3.3 Sensitivity Analyses for Times Greater than 100,000 Years .....  | 6-10 |
| 6.4 PRINCIPAL FACTORS AFFECTING POSTCLOSURE PERFORMANCE.....   | 6-11 |
| 6.4.1 Precipitation and Infiltration of Water into the Mountain .....  | 6-14 |
| 6.4.2 Percolation to Depth.....  | 6-14 |
| 6.4.3 Seepage into Drifts .....  | 6-14 |
| 6.4.4 Effects of Heat and Excavation on Flow (Drift Scale) .....   | 6-14 |
| 6.4.5 Dripping onto Waste Packages .....   | 6-14 |
| 6.4.6 Humidity and Temperature Effects on Waste Packages .....   | 6-15 |
| 6.4.7 Chemistry Effects on Waste Packages.....   | 6-15 |
| 6.4.8 Integrity of Inner Waste Package Barrier.....  | 6-15 |
| 6.4.9 Seepage into Waste Packages .....  | 6-15 |
| 6.4.10 Integrity of Spent Fuel Cladding.....   | 6-15 |
| 6.4.11 Dissolution of UO <sub>2</sub> and Glass Waste Form (Waste Form Integrity) .....  | 6-15 |
| 6.4.12 Solubility of Neptunium-237 .....   | 6-16 |
| 6.4.13 Formation of Radionuclide-Bearing Colloids.....   | 6-16 |
| 6.4.14 Transport Within and out of the Engineered Barrier System.....  | 6-16 |
| 6.4.15 Transport Through the Unsaturated Zone .....  | 6-16 |
| 6.4.16 Transport in the Saturated Zone .....   | 6-16 |
| 6.4.17 Dilution from Pumping .....   | 6-17 |
| 6.4.18 Biosphere Uptake.....   | 6-17 |
| 6.5 IMPROVING CONFIDENCE IN THE TOTAL SYSTEM PERFORMANCE<br>ASSESSMENT FOR THE LICENSE APPLICATION .....   | 6-17 |
| 6.5.1 Assessment of Potential Activities to Increase the Confidence in the Total<br>System Performance Assessment Based on the Results of the Total System<br>Performance Assessment for the Viability Assessment..... | 6-18 |
| 6.5.1.1 Precipitation and Infiltration into the Mountain: Unsaturated Zone<br>Flow.....  | 6-18 |
| 6.5.1.2 Percolation to Depth: Mountain-Scale Unsaturated Zone Flow.....  | 6-18 |
| 6.5.1.3 Seepage into Drifts .....  | 6-19 |
| 6.5.1.4 Effects of Heat and Excavation on Flow: Mountain- and Drift-Scale<br>Thermal Hydrology .....   | 6-19 |
| 6.5.1.5 Chemistry of Water on Waste Package: Near-Field Geochemical<br>Environment .....   | 6-21 |
| 6.5.1.6 Waste Package Degradation.....   | 6-22 |
| 6.5.1.7 Waste Form Alteration and Mobilization Models.....   | 6-22 |
| 6.5.1.8 Unsaturated Zone Transport .....   | 6-24 |
| 6.5.1.9 Saturated Zone Flow and Transport .....  | 6-24 |
| 6.5.1.10 Dilution from Pumping.....  | 6-25 |
| 6.5.1.11 Biosphere Transport and Uptake .....  | 6-26 |
| 6.5.2 Insights from the Total System Performance Assessment Peer Review Panel.....   | 6-27 |

CONTENTS (Continued)

|   | Page |
|---|------|
| 6.5.2.1 Physical Events and Processes Considered .....  | 6-28 |
| 6.5.2.2 Use of Appropriate and Relevant Data.....   | 6-29 |
| 6.5.2.3 Assumptions Made .....  | 6-30 |
| 6.5.2.4 Abstraction of Process Models.....  | 6-30 |
| 6.5.2.5 Application of Accepted Analytical Methods .....  | 6-31 |
| 6.5.2.6 Treatment of Uncertainties .....  | 6-33 |
| 6.5.2.7 Other Issues .....  | 6-33 |
| 6.5.3 Comments from the Nuclear Regulatory Commission .....   | 6-34 |
| 6.5.3.1 Radionuclides Tracked in the Performance Assessment.....                                      | 6-34 |
| 6.5.3.2 Consideration of all Significant Features and Processes in the<br>Performance Assessment..... | 6-34 |
| 6.5.3.3 Model Abstraction .....   | 6-35 |
| 6.5.3.4 Documentation of Assumptions .....  | 6-35 |
| 6.5.3.5 Transparency and Traceability of Analysis.....  | 6-35 |
| 6.5.3.6 Container Life.....   | 6-35 |
| 6.5.3.7 Role of Rockfall in Assessing Waste Package Lifetime .....                                    | 6-36 |
| 6.5.3.8 Effectiveness of Engineered Barriers in the Event of Volcanic<br>Activity .....               | 6-36 |
| 6.5.3.9 Neptunium Solubilities .....  | 6-36 |
| 6.5.3.10 Matrix Diffusion .....   | 6-36 |
| 6.5.3.11 Saturated Zone Transport .....   | 6-36 |
| 6.5.3.12 Radionuclide Retardation .....   | 6-37 |
| 6.5.3.13 Treatment of Colloids .....  | 6-37 |
| 6.5.3.14 Basis for Assigning Probabilities to Corrosion Potential Values.....                         | 6-37 |
| 6.5.3.15 Uncertainty in the Results of Expert Elicitation.....  | 6-37 |
| 6.5.3.16 Development of Expert Elicitation Results for Use in Performance<br>Assessment .....         | 6-37 |
| 6.5.4 Concluding Remarks.....   | 6-38 |
| 7. REFERENCES .....   | 7-1  |
| 7.1 DOCUMENTS CITED .....   | 7-1  |
| 7.2 STANDARDS AND REGULATIONS .....   | 7-13 |
| APPENDIX A - GLOSSARY .....   | A-1  |
| A.1 GENERAL GLOSSARY .....  | A-1  |
| A.2 GLOSSARY OF STATISTICS TERMS .....  | A-45 |

**FIGURES**

|      |   | <b>Page</b> |
|------|---|-------------|
| O-1  | Performance Assessment Information Flow Pyramid .....   | O-2         |
| O-2  | Generalized Performance Assessment Approach.....  | O-4         |
| O-3  | Limited Water Contacting Waste Package.....   | O-5         |
| O-4  | Long Waste Package Life Time .....  | O-5         |
| O-5  | Slow Release from Waste Package .....   | O-6         |
| O-6  | Low Concentrations of Radionuclides in Groundwater .....  | O-6         |
| O-7  | Disruptive Events .....   | O-7         |
| O-8  | Potential Radionuclide Release Conditions at About 1,000 Years .....  | O-11        |
| O-9  | Potential Radionuclide Release Conditions at About 10,000 Years .....   | O-12        |
| O-10 | Progressive Loss of Radioactivity Due to the Decay Process .....  | O-13        |
| O-11 | Potential Radionuclide Release Conditions at About 100,000 Years .....  | O-14        |
| O-12 | Potential Radionuclide Release Conditions at About 1 Million Years .....  | O-14        |
| 1-1  | Performance Assessment Information Flow Pyramid.....  | 1-2         |
| 1-2  | Major Steps in a Generic Performance Assessment.....  | 1-7         |
| 2-1  | Major Sources of Information Used in the Development of the Total System Performance Assessment for the Viability Assessment.....                             | 2-6         |
| 2-2  | Major Components of the Total System Performance Assessment for the Viability Assessment .....  | 2-11        |
| 2-3  | Schematic of the Reference Waste Package and Waste Form Designs Used in the Total System Performance Assessment for the Viability Assessment.....             | 2-12        |
| 2-4  | Schematic of the Reference Repository and Engineered Barrier System Designs Used in the Total System Performance Assessment for the Viability Assessment..... | 2-14        |
| 2-5  | Conceptual Illustration of Water Movement Through the Unsaturated Tuffs at Yucca Mountain.....  | 2-16        |
| 2-6  | Conceptual Illustration of Water and Water Vapor Movement Around the Repository Drifts During the Thermal Period.....   | 2-18        |
| 2-7  | Conceptual Illustration of Water Movement into and Within the Engineered Barrier System .....   | 2-20        |

**FIGURES (Continued)**

|  | <b>Page</b> |
|--|-------------|
| 2-8 Conceptual Illustration of Water Movement and Radionuclide Transport out of the Engineered Barrier System .....  | 2-21        |
| 2-9 Conceptual Illustration of Radionuclide Transport Through the Unsaturated Tuffs at Yucca Mountain.....   | 2-23        |
| 2-10 Conceptual Illustration of Radionuclide Transport Through the Saturated Tuffaceous and Alluvial Aquifers and the Biosphere .....  | 2-24        |
| 2-11 Simplified Representation of Information Flow in the Total System Performance Assessment for the Viability Assessment Between Data, Process Models, and Abstracted Models.....              | 2-28        |
| 2-12a Detailed Representation of Information Flow in the Total System Performance Assessment for the Viability Assessment.....   | 2-29        |
| 2-12b Detailed Representation of Information Flow in the Total System Performance Assessment for the Viability Assessment.....   | 2-30        |
| 2-13 Total System Performance Assessment for the Viability Assessment Code Configuration: Information Flow Among Component Computer Codes .....  | 2-32        |
| 3-1 Conceptual Drawing of Unsaturated Zone Flow Processes at Different Scales.....   | 3-3         |
| 3-2 Conceptual Drawing of Projected Climates for Yucca Mountain.....   | 3-4         |
| 3-3 Coupling of the Climate Subcomponent to Other Unsaturated Zone Flow Subcomponents and to Other Total System Performance Assessment for the Viability Assessment Components.....              | 3-5         |
| 3-4 Coupling of the Infiltration Subcomponent to Other Unsaturated Zone-Flow Subcomponents and to Other Total System Performance Assessment for the Viability Assessment Components .....        | 3-6         |
| 3-5 Coupling of the Mountain-Scale Flow Subcomponent to Other Unsaturated Zone Flow Subcomponents and to Other Total System Performance Assessment for the Viability Assessment Components ..... | 3-6         |
| 3-6 Coupling of the Seepage Subcomponent to Other Unsaturated Zone Flow Subcomponents and to Other Total System Performance Assessment for the Viability Assessment Components .....             | 3-7         |
| 3-7 Illustration of the Method Used for Calculating Seepage for Total System Performance Assessment for the Viability Assessment.....  | 3-17        |
| 3-8 Total Percolation Flux at Three Elevations .....   | 3-19        |
| 3-9 Selected Water-Flow Paths from Ground Surface to Water Table .....   | 3-21        |
| 3-10 Breakthrough Curves for Three Climate States.....   | 3-22        |

**FIGURES (Continued)**

|       |   | <b>Page</b> |
|-------|---|-------------|
| 3-11  | Breakthrough Curves for Five Base Case Property Sets .....  | 3-22        |
| 3-12  | Comparison of Base Case and Dual-Permeability/Weeps Model .....   | 3-22        |
| 3-13  | Calculated Seepage Fraction and Seep Flow Rate as Functions of Percolation Flux .....   | 3-23        |
| 3-14  | Conceptual Drawings of Thermal-Hydrologic Processes at Three Stages.....  | 3-25        |
| 3-15  | Conceptual Diagram Illustrating Flow of Liquid Water and Water Vapor in Fractures .....   | 3-26        |
| 3-16  | Coupling of Thermal Hydrology to Other Total System Performance Assessment for the<br>Viability Assessment Components.....  | 3-27        |
| 3-17  | Quantities Passed to Other Total System Performance Assessment for the Viability<br>Assessment Components .....   | 3-28        |
| 3-18  | Plan View of a Typical Emplacement-Drift Segment for Drift-Scale Thermal-Hydrologic<br>Analyses.....  | 3-31        |
| 3-19  | Illustration of the Multiscale Modeling and Abstraction Method .....  | 3-32        |
| 3-20  | Division of the Repository Area into Six Subregions .....   | 3-34        |
| 3-21  | Average Waste Package Temperature History for Six Repository Regions .....  | 3-36        |
| 3-22  | Variability of Temperature History Among Waste Packages .....   | 3-37        |
| 3-23  | Variability of Relative-Humidity History Among Waste Packages.....  | 3-37        |
| 3-24  | Average Waste Package Temperature History for Five Base Case Property Sets .....  | 3-37        |
| 3-25  | Effect of Alternative Hydrologic-Property Sets on Waste Package Temperature .....   | 3-38        |
| 3-26  | Air Mass Fraction for Center and Edge Repository Locations .....  | 3-38        |
| 3-27  | General Near-Field Geochemical Environment Conceptual Processes, Phases, and Design<br>Material.....  | 3-39        |
| 3-28  | Relations Between the Five Near-Field Geochemical Environment Models.....   | 3-41        |
| 3-29  | Interconnections Between Near Field Geochemical Environment Component and Other<br>Total System Performance Assessment for the Viability Assessment Components..... | 3-42        |
| 3-30  | Mountain-Scale Conceptual Picture of Incoming Gas Model Processes .....   | 3-46        |
| 3-31  | Mountain-Scale Conceptual Picture of Incoming Water Model Processes.....  | 3-48        |
| 3-32a | Drift-Scale Near-Field Geochemical Environment Conceptual Processes Time Frame 1—<br>First Few Hundred Years.....   | 3-50        |

FIGURES (Continued)

|   | Page |
|---|------|
| 3-32b Drift-Scale Near-Field Geochemical Environment Conceptual Processes Time Frame 2—<br>Approximately 500 to 10,000 Years.....   | 3-51 |
| 3-32c Drift-Scale Near-Field Geochemical Environment Conceptual Processes Time Frame 3—<br>Approximately 10,000 to 100,000 Years.....   | 3-52 |
| 3-33 Connections Among the In-Drift Water-Solids Chemistry Sub-Models.....  | 3-54 |
| 3-34 Inputs, Outputs, and Bases for the Total System Performance Assessment for the Viability<br>Assessment Near-Field Geochemical Environment Component .....  | 3-57 |
| 3-35 Flow Diagram Depicting the Parameter Exchanges Among all Near-Field Geochemical<br>Environment Models .....  | 3-59 |
| 3-36 Near-Field Geochemical Environment Gas Composition Results for Carbon Dioxide and<br>Oxygen from Time of Waste Emplacement to 100,000 Years.....   | 3-67 |
| 3-37a Near-Field Geochemical Environment Water Composition Results, pH Values, for the Time<br>Frame from Time of Waste Emplacement to 100,000 Years .....  | 3-69 |
| 3-37b Near-Field Geochemical Environment Water Composition Results, Total Dissolved<br>Carbonate Values ( $\Sigma\text{CO}_3^{2-}$ ) for the Time Frame from Time of Waste Emplacement to<br>100,000 Years .....                        | 3-70 |
| 3-37c Near-Field Geochemical Environment Water Composition Results, Ionic Strength Values,<br>for the Time Frame from Time of Waste Emplacement to 100,000 Years .....  | 3-71 |
| 3-38 Example of Input to the Total System Performance Assessment for the Viability<br>Assessment from the Near-Field Geochemical Environment Component Showing<br>Distributions of pH for Incoming Water Reacted with Iron-Oxides ..... | 3-72 |
| 3-39 Results of Simulations for Primary Spent Fuel Reacting with Water to Form Secondary<br>Alteration Phases .....   | 3-73 |
| 3-40 Waste Package Reference Design .....   | 3-74 |
| 3-41 Engineered Barrier System Reference Design .....   | 3-75 |
| 3-42 Waste Package Degradation Schematic .....  | 3-76 |
| 3-43 Waste Package Degradation Information Flow .....   | 3-77 |
| 3-44 Waste Package Degradation Model Logic Diagram .....  | 3-78 |
| 3-45 Corrosion Allowance Material Corrosion Rates and Data .....  | 3-82 |
| 3-46 Abstracted General Corrosion Rate Distributions of Alloy 22.....   | 3-87 |
| 3-47 Waste Package Degradation History of Packages Exposed to Drips .....   | 3-88 |

**FIGURES (Continued)**

|      |   | <b>Page</b> |
|------|---|-------------|
| 3-48 | Dripping Versus No-Dripping Effect on Waste Package Degradation .....   | 3-89        |
| 3-49 | Effect of Alternative Dripping Scenarios on Waste Package Degradation .....   | 3-89        |
| 3-50 | Schematic of Waste Form/Waste Package/Engineered Barrier System.....  | 3-91        |
| 3-51 | Waste Form Degradation/Mobilization/Engineered Barrier System Conceptual Model .....  | 3-92        |
| 3-52 | Inventory Abstraction .....   | 3-98        |
| 3-53 | Colloidal Plutonium Transport .....   | 3-105       |
| 3-54 | Fraction of Commercial Spent Nuclear Fuel Surface Area Exposed as a Function of Time.....   | 3-107       |
| 3-55 | Activity as a Function of Time .....  | 3-108       |
| 3-56 | Coupling of Unsaturated Zone Radionuclide Transport to Other Total System Performance Assessment for the Viability Assessment Components .....                          | 3-110       |
| 3-57 | Conceptual East-West Hydrogeologic Section Through the Unsaturated Zone .....   | 3-111       |
| 3-58 | Color Contour Plot Showing Travel Times from the Repository to the Water Table for Hypothetical Nonsorbing, Nondiffusing Tracer Particles .....                         | 3-124       |
| 3-59 | Color Contour Plot Showing Travel Times from the Repository to the Water Table for Hypothetical Tracer Particles Having the Characteristics of Plutonium.....           | 3-125       |
| 3-60 | Average Locations for Hypothetical Releases from each Repository Grid Cell at the Water Table .....   | 3-126       |
| 3-61 | Comparison of the Effects of Unsaturated Zone Flow Fields on Technetium and Neptunium Transport: Base Case Versus DKM Weeps Flow Models .....                           | 3-127       |
| 3-62 | Comparison of the Effects of Matrix Diffusion on Technetium and Neptunium Transport.....  | 3-128       |
| 3-63 | Comparison of the Influence of Sorption on Devitrified, Vitric, and Zeolitic Rock on Neptunium Transport.....   | 3-128       |
| 3-64 | Summary of Inputs and Outputs for the Saturated Zone Flow and Transport Component of the Total System Performance Assessment for the Viability Assessment Analysis..... | 3-130       |
| 3-65 | Regional Map of the Saturated Zone Flow System.....   | 3-131       |
| 3-66 | Conceptual Model of the Saturated Zone Groundwater Flow System and Processes Relevant to Performance of the Potential Repository at Yucca Mountain.....                 | 3-133       |
| 3-67 | Simulated Particle Paths from the Total System Performance Assessment for the Viability Assessment Three-Dimensional Flow Model for the Saturated Zone .....            | 3-137       |

FIGURES (Continued)

|  | Page  |
|--|-------|
| 3-68 Schematic Diagram of the Conceptual Basis of the Total System Performance Assessment for the Viability Assessment One-Dimensional Transport Model for the Saturated Zone from Below the Repository to 20 km (12 miles) South..... | 3-139 |
| 3-69 Flow Chart for Utilization of the Convolution Integral Method in Saturated Zone Flow and Transport Calculations in Total System Performance Assessment for the Viability Assessment .....   | 3-142 |
| 3-70 Unit Radionuclide Concentration Breakthrough Curves from the Total System Performance Assessment One-Dimensional Transport Modeling for the Saturated Zone at a Distance of 20 km (12 miles) for all Modeled Radionuclides .....  | 3-144 |
| 3-71 Unit Radionuclide Concentration Breakthrough Curves from the Total System Performance Assessment One-Dimensional Transport Modeling for the Saturated Zone at a Distance of 20 km (12 miles) for Technetium-99.....               | 3-144 |
| 3-72 Overview of the Modeling Process Employed in the Biosphere Component of Total System Performance Assessment for the Viability Assessment .....  | 3-146 |
| 3-73 Present-Day Biosphere in the Amargosa Valley .....  | 3-147 |
| 3-74 Satellite Image Showing the Yucca Mountain Area Including the Amargosa Valley Area .....  | 3-149 |
| 3-75 Illustration of the Biosphere Modeling Components and Pathways Contributing to Three Major Dose Categories to Humans.....   | 3-151 |
| 3-76 Map Showing the Number of Permanent Inhabitants Included in the Biosphere Modeling Work Group's Regional Food and Water Consumption Survey .....  | 3-153 |
| 3-77 The Biosphere Regional Food and Water Consumption Survey.....   | 3-154 |
| 3-78 Quantities of Locally Produced Food and Well Water Consumed by Amargosa Valley Residents.....   | 3-154 |
| 3-79 Histogram of the Biosphere Dose Conversion Factor for Neptunium-237 .....   | 3-158 |
| 3-80 Comparison of Biosphere Dose Conversion Factors for Neptunium-237 as a Function of Receptor and Precipitation Regime .....  | 3-160 |
| 4-1 Climate History for the Expected-Value Realization of the Total System Performance Assessment for the Viability Assessment Base Case at Two Different Time Scales.....   | 4-3   |
| 4-2 Infiltration History for the Expected-Value Realization of the Total System Performance Assessment for the Viability Assessment Base Case .....  | 4-4   |
| 4-3 Total System Performance Assessment for the Viability Assessment Base Case Drift-Scale Seepage Model .....   | 4-5   |

**FIGURES (Continued)**

|      |  | <b>Page</b> |
|------|--|-------------|
| 4-4  | Total System Performance Assessment for the Viability Assessment Base Case Percolation Flux at the Repository Level for the "Base Infiltration" Flow Field During the Long-Term Average Climate .....                                | 4-6         |
| 4-5  | Variability of Total System Performance Assessment for the Viability Assessment Base Case, Drift-Scale, Thermal-Hydrologic Parameters (Temperature and Relative Humidity) in the Northeast Region at the Repository Horizon.....     | 4-8         |
| 4-6  | Time Histories of the Near-Field Geochemical Parameters.....   | 4-10        |
| 4-7  | Total System Performance Assessment for the Viability Assessment Base Case Waste Package Degradation Histories.....  | 4-12        |
| 4-8  | Commercial Spent Nuclear Fuel Degradation Rate .....   | 4-13        |
| 4-9  | Configuration of Cells in the RIP Program for Engineered Barrier System Transport in the Total System Performance Assessment for the Viability Assessment Base Case .....  | 4-14        |
| 4-10 | Conceptualization of Unsaturated Zone Transport for the Total System Performance Assessment for the Viability Assessment Base Case .....   | 4-17        |
| 4-11 | Conceptualization of Saturated Zone Transport for the Total System Performance Assessment for the Viability Assessment Base Case .....   | 4-19        |
| 4-12 | Dose Rate to an "Average" Individual Withdrawing Water From a Well Penetrating the Maximum Plume Concentration in the Saturated Zone 20 km (12 miles) Downgradient from the Repository .....   | 4-23        |
| 4-13 | Effects of Climate Change, Seepage Flux, and Waste Package Degradation on Engineered Barrier System Releases and Dose Rates in the First 10,000 Years After Waste Emplacement .....  | 4-27        |
| 4-14 | Performance of the Unsaturated Zone with Respect to Technetium-99 During the First 10,000 Years After Waste Emplacement .....  | 4-29        |
| 4-15 | Performance of the Saturated Zone with Respect to Technetium-99 During the First 10,000 Years After Waste Emplacement .....  | 4-31        |
| 4-16 | Effects of Climate Change, Seepage Flux, and Waste Package Degradation on Engineered Barrier System Releases and Dose Rates in the First 100,000 Years After Waste Emplacement .....   | 4-37        |
| 4-17 | Effects of Matrix Degradation Rate and Inventory Exposure Rate on the Releases of the Three Different Fuel Types: Commercial Spent Nuclear Fuel, U.S. Department of Energy Spent Nuclear Fuel, and High-Level Radioactive Waste..... | 4-39        |
| 4-18 | Performance of the Unsaturated Zone During the First 100,000 Years After Waste Emplacement with Respect to Technetium-99, Neptunium-237, and Plutonium-239.....  | 4-41        |

FIGURES (Continued)

|  | Page |
|--|------|
| 4-19 Performance of the Saturated Zone During the First 100,000 Years After Waste<br>Emplacement with Respect to Technetium-99, Neptunium-237, and Plutonium-239.....  | 4-43 |
| 4-20 Importance of Biosphere Dose Conversion Factors in the First 100,000 Years After<br>Waste Emplacement .....   | 4-45 |
| 4-21 Effects of Climate Change, Seepage Flux, Waste Package Degradation, and Cladding<br>Degradation on Waste Package Releases and Dose Rates in the First 1 Million Years After<br>Waste Emplacement .....  | 4-51 |
| 4-22 Waste Package Releases During 1 Million Years After Waste Emplacement for the<br>Three Inventory Types: Commercial Spent Nuclear Fuel, U.S. Department of Energy<br>Spent Nuclear Fuel, and High-Level Radioactive Waste .....                | 4-53 |
| 4-23 Effects of Saturated Zone Dilution and Biosphere Dose Conversion Factors on<br>1 Million-Year Dose Rates .....  | 4-55 |
| 4-24 Cumulative Fractional Inventory Releases of Technetium-99, Neptunium-237,<br>Plutonium-239, and Plutonium-242 from the Engineered Barrier System and the<br>20-km (12-mile) Saturated Zone Boundary, Normalized to the Initial Inventory..... | 4-57 |
| 4-25 Plots of Cumulative Inventory Released from Different Boundaries of the Repository System<br>Along with the Inventory Decay Curve over a Period of 1 Million Years.....   | 4-59 |
| 4-26 Base Case Distribution of Peak Dose Rates for Three Periods and Their Relation to<br>Dose-Rate Time Histories .....   | 4-65 |
| 4-27 Dose-Rate Time Histories for 10,000- and 1-Million-Year Periods .....   | 4-66 |
| 4-28 Time Variation of Statistical Descriptors of the Calculated Dose-Rate Distribution.....   | 4-66 |
| 4-29 Average Contribution to Peak Dose Rate of Different Radionuclides for Three Periods.....  | 4-67 |
| 4-30 Peak Dose Rate Versus Time of Peak Dose Rate for Three Periods.....   | 4-68 |
| 4-31 Climate History for One Realization .....   | 4-69 |
| 4-32 Number of Failed Waste Packages over Time for the Selected Realizations .....   | 4-70 |
| 4-33 Comparison of Peak Dose Rate Distributions Determined from Simulations with Different<br>Numbers of Realizations .....  | 4-71 |
| 4-34 Most Important Parameters from Stepwise Regression Analysis for Three Periods .....   | 4-73 |
| 4-35 Scatter Plot of Seepage Fraction over 100,000 Years .....   | 4-75 |
| 4-36 Scatter Plot of Mean Alloy 22 Corrosion Rate over 100,000 Years .....   | 4-75 |
| 4-37 Scatter Plot of Seepage Fraction over 1 Million Years .....   | 4-75 |

**FIGURES (Continued)**

|       |   | <b>Page</b> |
|-------|---|-------------|
| 4-38  | Partial Rank Correlation Coefficient as a Function of Time for Six Uncertain Parameters .....               | 4-76        |
| 4-39  | Distribution of Peak Dose Rates for Three Time Periods for the Modified-Parameter Case .....                | 4-78        |
| 4-40  | Most Important Parameters from Stepwise Regression Analysis for the Modified-Parameter Case .....           | 4-79        |
| 4-41a | Alternative Consequences of a Magmatic Dike Intruding the Repository .....                                  | 4-83        |
| 4-41b | Alternative Consequences of a Magmatic Dike Intruding the Repository-Part 2 .....                           | 4-83        |
| 4-41c | Alternative Consequences of a Magmatic Dike Intruding the Repository-Part 3 .....                           | 4-84        |
| 4-42  | Source Term Enhanced by Igneous Activity .....  | 4-85        |
| 4-43  | Indirect Igneous Effects Scenario.....  | 4-86        |
| 4-44  | Volcanic Eruption Scenario Dose Rates.....  | 4-87        |
| 4-45  | Dose-Rate Time Histories from Igneous Enhanced Source Term Scenario Compared with Base Case Dose Rate ..... | 4-87        |
| 4-46  | Peak Dose Rate Complimentary Cumulative Distribution Function for 100,000 and 1 Million Years .....         | 4-88        |
| 4-47  | Contaminant Concentration Profiles Resulting from a Dike Intruding Along the Solitario Canyon Fault.....    | 4-89        |
| 4-48  | Rockfall Scenario .....   | 4-91        |
| 4-49  | Indirect Seismic Effects Scenario.....  | 4-93        |
| 4-50  | Number of Waste Package Failures from Rockfall as a Function of Time .....                                  | 4-94        |
| 4-51  | In-Package Criticality .....  | 4-95        |
| 4-52  | External Criticality Scenarios .....  | 4-97        |
| 4-53  | Radioactivity Levels for In-Package Criticality Model.....  | 4-98        |
| 4-54  | Human Intrusion Scenario .....  | 4-101       |
| 4-55  | Comparison of Human-Intrusion Dose Rates with Base Case Dose Rates .....                                    | 4-101       |
| 4-56  | Engineered Barrier System with Design Enhancements (Backfill, Drip Shield, and Ceramic Coating).....        | 4-103       |
| 4-57  | Effect of Backfill on Temperature and Fraction of Waste Packages Failed over Time .....                     | 4-104       |

**FIGURES (Continued)**

|   | <b>Page</b> |
|---|-------------|
| 4-58 Effect of Dripshield on Waste Package Degradation .....  | 4-105       |
| 4-59 Effect of Dripshield on Dose Rate at 20 km (12 miles) .....  | 4-106       |
| 4-60 Effect of Waste Package Ceramic Coating on Waste Package Degradation .....   | 4-107       |
| 5-1 Comparison of the Expected Value Base Case with a Sensitivity Case in Which all<br>Climate Durations are 50,000 Years.....  | 5-2         |
| 5-2 Comparison of the Total Dose Rate for Expected-Value Base Case with Three Sensitivity<br>Cases in Which There are no Climate Changes .....  | 5-2         |
| 5-3 Comparison of the Base Case Peak-Dose-Rate Distribution with a Sensitivity Case in<br>Which Infiltration and Climate are Uncorrelated .....   | 5-3         |
| 5-4 Comparison of the Base Case Dose Rate Results with a Sensitivity Case Involving<br>Infiltration .....   | 5-4         |
| 5-5 Total Dose Rate History Curves for the Five Base Case Flow Fields, with all Other<br>Parameters Set to Their Expected Values.....   | 5-4         |
| 5-6 Comparison of the Total Dose Rate for Expected-Value Base Case with a Sensitivity Case<br>that Used the Dual-Permeability/Weeps Flow Model Rather than the Base Case Flow<br>Model..... | 5-5         |
| 5-7 Comparison of the Base Case Peak-Dose-Rate Distribution with a Sensitivity Case in<br>Which Dual-Permeability/Weeps Flow Fields are Used Instead of Base Case Flow Fields .....         | 5-6         |
| 5-8 Total Dose Rate History Curves with Seepage Influence .....   | 5-7         |
| 5-9 Dose Rate History Curves for Three Sensitivity Cases.....   | 5-8         |
| 5-10 Comparison of Base Case Peak Dose Rate with Sensitivity Cases Involving Fracture<br>Aperture .....   | 5-8         |
| 5-11 Total Dose Rate History Curves for the Expected-Value Base Case and for Three<br>Sensitivity Cases in Which Different Hydrologic Properties Were Used.....                             | 5-9         |
| 5-12 Comparison of Expected-Value Total Release-Rate Histories from the Engineered Barrier<br>System for Concrete-Modified Water and the Base Case .....                                    | 5-13        |
| 5-13 Expected-Value Time Histories for Individual and Total Radionuclide Release Rates from<br>the Engineered Barrier System for the Concrete-Modified Water Case .....                     | 5-13        |
| 5-14 Comparison of Expected-Value Total Dose-Rate Histories for the Concrete-Modified<br>Water Case and the Base Case .....   | 5-14        |
| 5-15 Effect of Uncertainty in Alloy 22 Corrosion Rate on Package Failure Time.....  | 5-15        |
| 5-16 Effect of Uncertainty in Alloy 22 Corrosion Rate on Total Dose Rate.....   | 5-16        |

**FIGURES (Continued)**

|      |   | <b>Page</b> |
|------|---|-------------|
| 5-17 | Effect of Dripping Conditions on Waste Package Failure for the Base Case .....  | 5-16        |
| 5-18 | Waste Package Degradation Curves for Different Percentages (Alternative Models) of Wetted Surface Area.....   | 5-18        |
| 5-19 | Total Dose Rate Histories for Different Percentages (Alternative Models) of Wetted Waste Package Surface Area.....  | 5-18        |
| 5-20 | Effect of High-pH (Concrete-Modified) Seepage Water on Waste Package Degradation .....  | 5-19        |
| 5-21 | Effect of Microbiologically Influenced Corrosion on Waste Package Degradation .....   | 5-20        |
| 5-22 | Total Dose Rate Histories for Microbiologically Influenced Corrosion Waste Package Degradation Versus the Base Case.....                                  | 5-20        |
| 5-23 | Sensitivity of Dose to Juvenile Failure of Waste Packages.....  | 5-21        |
| 5-24 | Sensitivity of Waste Package Degradation to Corrosion Patch Size.....   | 5-21        |
| 5-25 | Total Dose Rate Histories for Different Sizes of Corrosion Patch Failure .....  | 5-22        |
| 5-26 | Effect of Seepage Collection Factor on Total Dose Rate.....   | 5-23        |
| 5-27 | Effect of Alternative Seepage Model on Total Dose Rate .....  | 5-24        |
| 5-28 | Effect of Cladding Failure Fraction on Total Dose Rate.....   | 5-24        |
| 5-29 | Effect of Alternative Models for Cladding Failure on Total Dose Rate .....  | 5-25        |
| 5-30 | Effect of an Alternative Cladding Model on 10,000-Year, 100,000-Year, and 1 Million Year Peak Dose Rate over Multiple Realizations .....                  | 5-26        |
| 5-31 | Most Important Parameters for the Modified Cladding Model Case .....  | 5-27        |
| 5-32 | Effect of Commercial-Spent-Fuel and High-Level-Glass Dissolution Rates on Total Dose Rate.....  | 5-28        |
| 5-33 | Sensitivity of Total Dose Rate to Reprecipitation of Neptunium in Secondary Mineral Phases .....  | 5-29        |
| 5-34 | TSPA-VA Base Case Neptunium Solubility Distribution Compared to TSPA-1995 Distribution and to Eleven Different Precipitation/Dissolution Experiments..... | 5-30        |
| 5-35 | Effect of Neptunium Solubility on Total Dose Rate .....   | 5-31        |
| 5-36 | Effect of Colloid Distribution Coefficient on Total Dose Rate.....  | 5-32        |
| 5-37 | Effect of Radionuclide Distribution Coefficients in the Concrete Invert on Total Dose Rate at 20 km (12 miles).....                                       | 5-32        |

FIGURES (Continued)

|  | Page |
|--|------|
| 5-38 Sensitivity of Total Dose Rate to an Alternative Engineered Barrier System Transport Model that Assumes the Radionuclide $K_d$ s in the Invert are Equal to Zero.....   | 5-33 |
| 5-39 Expected-Value Total Dose-Rate History at 20 km (12 miles) over 100,000 Years for Sixteen Categories of U.S. Department of Energy Spent Nuclear Fuel.....   | 5-34 |
| 5-40 Comparison of Total Dose Rate for Plutonium Waste Forms (Mixed Oxide Fuel and "Can-in-Canister").....   | 5-35 |
| 5-41 Comparison of Zero-Matrix-Diffusion (in the Unsaturated Zone) Model with Base Case Model.....   | 5-36 |
| 5-42 Effect of Radionuclide Distribution Coefficients in the Unsaturated Zone Matrix on Total Dose Rate at 20 km (12 miles).....   | 5-37 |
| 5-43 Sensitivity of Total Dose Rate to an Alternative Unsaturated Zone Transport Model that Assumes the Actinide $K_d$ s in the Unsaturated Zone Rock Matrix are Equal to Zero.....                                  | 5-38 |
| 5-44 Sensitivity of Neptunium-237 and Plutonium-239 Dose Rate to an Alternative Unsaturated Zone Transport Model that Assumes the Actinide $K_d$ s in the Unsaturated Zone Rock Matrix are Equal to Zero.....        | 5-38 |
| 5-45 Sensitivity of Plutonium-242 Dose Rate to an Alternative Unsaturated Zone Transport Model that Assumes the Actinide $K_d$ s in the Unsaturated Zone Rock Matrix are Equal to Zero.....                          | 5-39 |
| 5-46 Sensitivity of Total Dose Rate to the "Alkaline Plume" Model.....   | 5-40 |
| 5-47 Total Dose-Rate History Curves for the Expected-Value Base Case and Cases that Have Saturated Zone Dilution Factor at the 5th and 95th Percentiles of its Base Case Distribution.....                           | 5-41 |
| 5-48 Total Dose-Rate History Curves for the Expected-Value Base Case and Cases that Have the Fraction of the Saturated Zone Flow Path in Alluvium at the 5th and 95th Percentiles of its Base Case Distribution..... | 5-42 |
| 5-49 Total Dose-Rate History Curves for the Expected-Value Base Case and for Two Sensitivity Cases that Use Different Methods for Combining the Six Flow Tubes Used to Model the Saturated Zone.....                 | 5-43 |
| 5-50 Total Dose-Rate History Curves for the Expected-Value Base Case and Cases that Have Biosphere Dose Conversion Factors at the 5th and 95th Percentiles of Their Base Case Distributions.....                     | 5-44 |
| 5-51 Average Dose Rate as Function of Critical Group Size for the Amargosa Valley, Estimated for the Expected-Value Base Case.....   | 5-46 |
| 5-52 Total Dose-Rate History Curves for the Expected Value Base Case and for Two Sensitivity Cases in Which Different Critical Groups are Assumed.....   | 5-47 |

**TABLES**

|      |  | <b>Page</b> |
|------|--|-------------|
| 2-1  | Principal Factors Affecting Expected Postclosure Performance for the Viability Assessment Reference Design and Their Corresponding Total System Performance Assessment for the Viability Assessment Model Components and Nuclear Regulatory Commission Key Technical Issues..... | 2-5         |
| 2-2  | Principal Sources of Information Used in the Development of the Total System Performance Assessment Model for the Viability Assessment Reference Design.....   | 2-7         |
| 3-1  | Component Models for Process Areas and Corresponding Documentation.....  | 3-1         |
| 3-2  | Expert Elicitations for the Total System Performance Assessment for the Viability Assessment.....  | 3-2         |
| 3-3  | Unsaturated Zone Flow Abstraction/Testing Workshop.....  | 3-7         |
| 3-4  | Data Summary for the Climate Model.....  | 3-13        |
| 3-5  | Average Net Infiltrations and Probabilities for the Infiltration Cases.....  | 3-15        |
| 3-6  | Probabilities for the Mountain-Scale Unsaturated Zone Flow Cases.....  | 3-16        |
| 3-7  | Probabilities for the Process-Model Cases Used to Develop Seepage Distributions.....   | 3-18        |
| 3-8  | Thermal Hydrology Abstraction/Testing Workshop.....  | 3-28        |
| 3-9  | Near-Field Geochemical Environment Abstraction/Testing Workshop.....   | 3-44        |
| 3-10 | Abstracted Periods, Temperatures, Gas Fugacities and Cumulative Gas Fluxes (Per Meter of Drift) Used for the Near-Field Geochemical Environment Component.....   | 3-60        |
| 3-11 | Waste Package Degradation Abstraction/Testing Workshop.....  | 3-79        |
| 3-12 | Waste Form Degradation and Radionuclide Mobilization Abstraction/Testing Workshop.....   | 3-93        |
| 3-13 | U.S. Department of Energy Spent Nuclear Fuel Categories, Typical Spent Fuel in Each Category, and Metric Tons Heavy Metal in Each Category.....  | 3-96        |
| 3-14 | Inventories for Various Waste Forms.....   | 3-96        |
| 3-15 | Solubility Limit Distributions.....  | 3-99        |
| 3-16 | Parameters Used in Reversible Attachment Model.....  | 3-104       |
| 3-17 | Unsaturated Zone Radionuclide Transport Abstraction/Testing Workshop.....  | 3-114       |
| 3-18 | Parameter Values Used for Unsaturated Zone Radionuclide Transport in Total System Performance Assessment for the Viability Assessment.....   | 3-122       |
| 3-19 | Saturated Zone Flow and Transport Abstraction/Testing Workshop.....  | 3-138       |

TABLES (Continued)

|  | <b>Page</b> |
|--|-------------|
| 3-20 Stochastic Parameters for Saturated Zone Flow and Transport .....   | 3-140       |
| 3-21 Climatic Alterations to Saturated Zone Flow .....   | 3-143       |
| 3-22 Biosphere Abstraction/Testing Workshop.....   | 3-148       |
| 3-23 Adults Surveyed for the Food and Water Consumption Model .....  | 3-152       |
| 3-24 Receptor Types Considered in the Total System Performance Assessment Biosphere<br>Modeling Effort .....   | 3-155       |
| 3-25 Selected Uncertain Parameters Used in the Biosphere Modeling .....  | 3-156       |
| 3-26 Sensitivity Analysis for the Three Most Important Radionuclides for the Base Case<br>Scenario .....   | 3-159       |
| 4-1 Importance Ranking of Inputs for Engineered Barrier System Releases at 1 Million Years .....   | 4-77        |
| 4-2 Summary of Calculated Peak Dose Rates at 20 km (12 miles).....   | 4-80        |
| 4-3 Probabilities of Igneous Impacts on Repository.....  | 4-90        |
| 6-1 Significance of Uncertainty in Principal Factors on Post Closure System Performance -<br>Summary of Sensitivity Analysis for Viability Assessment Reference Design ..... | 6-12        |

**ACRONYMS**

|       |  |
|-------|--|
| ASTM  | American Society for Testing and Materials     |
| CCDF  | Complementary Cumulative Distribution Function |
| CFR   | <i>Code of Federal Regulations</i>             |
| CRWMS | Civilian Radioactive Waste Management System   |
| DOE   | U.S. Department of Energy                      |
| EIS   | Environmental Impact Statement                 |
| EPA   | U.S. Environmental Protection Agency           |
| LA    | License Application                            |
| M&O   | Management and Operating Contractor            |
| NRC   | Nuclear Regulatory Commission                  |
| TSPA  | Total System Performance Assessment            |
| USGS  | U.S. Geological Survey                         |
| VA    | Viability Assessment                           |
| YMP   | Yucca Mountain Site Characterization Project   |

**Measurements**

|        |                      |
|--------|----------------------|
| Btu    | British thermal unit |
| cm     | centimeter           |
| Eh     | redox potential      |
| ft     | foot                 |
| g      | gram                 |
| in.    | inch                 |
| kg     | kilogram             |
| km     | kilometer            |
| kPa    | kilopascal           |
| kV     | kilovolt             |
| kVA    | kilovolt-ampere      |
| lin ft | linear feet          |
| m      | meter                |
| mL     | milliliter           |
| mm     | millimeter           |
| MPa    | megapascal           |

|      |                             |
|------|-----------------------------|
| MTHM | metric tons of heavy metal  |
| MTU  | metric tons of uranium      |
| MVA  | megavolt-ampere             |
| nm   | nanometer                   |
| pH   | hydrogen-ion activity       |
| ppm  | parts per million           |
| ppmv | parts per million by volume |
| psi  | pounds per square inch      |
| wt   | weight                      |

## OVERVIEW

The U.S. Congress directed the U.S. Department of Energy (DOE) to include in the Viability Assessment (VA) for a repository at Yucca Mountain, Nevada,

...a total system performance assessment based upon the design concept and the scientific data and analysis available by September 30, 1998, describing the probable behavior of the repository in the Yucca Mountain geological setting relative to the overall system performance standards. (Energy and Water Development Appropriations Act 1997)

This volume presents the results of the Total System Performance Assessment (TSPA) conducted for the VA. This TSPA is one of an iterative series of analyses conducted for Yucca Mountain over the life of the Yucca Mountain Site Characterization Project (YMP). The next TSPA in the series is planned to support the Secretary's decision on site recommendation and the License Application (LA).

The TSPA for the VA (TSPA-VA) analyzes the probable behavior of the reference design for the engineered repository components in the expected natural conditions at the Yucca Mountain site. It also includes sensitivity and uncertainty analyses to illustrate the relative importance of the various TSPA components and parameters. This aspect of the TSPA is particularly useful as a management tool for identifying and prioritizing future work, as reported in Volume 4.

This volume summarizes the TSPA work performed for the VA. Readers wanting all of the supporting information on how the TSPA for the VA was developed and performed are referred to the *Total System Performance Assessment-Viability Assessment (TSPA-VA) Analyses Technical Basis Document (CRWMS M&O 1998i)*.

## HOW THE TOTAL SYSTEM PERFORMANCE ASSESSMENT VOLUME IS ORGANIZED

**Overview**—This overview presents a summary explanation of TSPA, the general role of TSPA in repository development, the contents of the TSPA for the proposed repository system at Yucca Mountain. The section then summarizes results of the TSPA, and provides a perspective on the work remaining to support a decision on site recommendation and the LA.

**Section 1—General Description of the TSPA Process.** Because the subject of TSPA is both important and complex, Section 1 explains in some detail what TSPA is and why it is applicable to repository development and also discusses, from the perspective of the international radioactive waste management community, the general approach for performing a total system performance assessment.

**Section 2—Yucca Mountain TSPA for the Viability Assessment.** This section states the objectives of the TSPA for the VA and then describes the specific way in which the general TSPA approach was adapted for the TSPA-VA. Next is a general description of how, based on current knowledge, the repository system is interpreted and represented in the TSPA. This description traces the eventual release of radionuclides to the biosphere in terms of the four key attributes of the repository safety strategy. The section then explains the method applied to actually build the computer model used for the TSPA, and how the uncertainty and the variability were treated in the analyses. It concludes with a synopsis of TSPA results.

**Section 3—Development of the TSPA-VA Components.** The entire system that comprises the TSPA-VA is represented as a series of models or TSPA "components" representing the processes that are expected to influence the system performance. This section presents a detailed description of how each component was developed and also provides some results of analyses for specific aspects of individual components.

#### Section 4—Base Case Definition and Results.

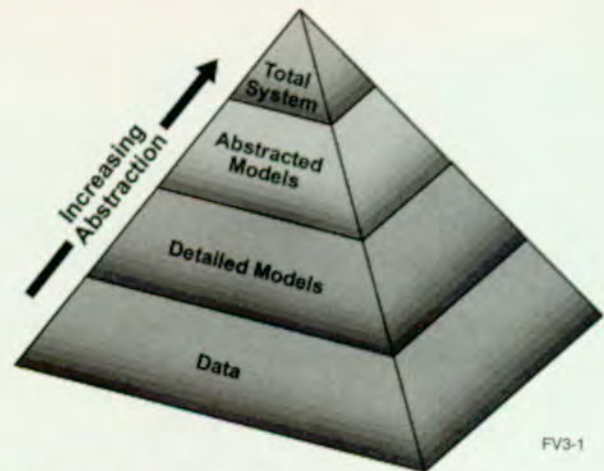
This section explains how and which aspects of the various TSPA components were combined into a total-system model. It then reports TSPA results in terms of an expected “base case” and also as a probabilistic sequence of results. Also shown are the effects of disruptive events, such as volcanism and seismicity. Finally included are analyses of selected design options to the reference design, such as the use of backfill.

**Section 5—Sensitivity Analyses for TSPA-VA Components.** For each of the TSPA components, this section discusses factors about which there are significant uncertainties in our understanding, and it examines their relative importance to repository system performance. It also examines how sensitive those factors are to changes in the values assigned to them.

**Section 6—Summary and Conclusions.** In contrast with the previous section that deals with the uncertainty and sensitivity of various aspects of individual components, this section takes the approach of looking at uncertainty from a total system perspective. It then discusses the additional work recommended by the results of the TSPA-VA, by the Performance Assessment Peer Review Panel, and by Nuclear Regulatory Commission (NRC) to improve confidence in the TSPA to support the decision on site recommendation and the LA. These recommendations are then incorporated, along with other considerations outside of the purview of the TSPA, into the LA Plan in Volume 4.

#### EXPLANATION OF A TOTAL SYSTEM PERFORMANCE ASSESSMENT

The general TSPA process was developed as a cooperative effort involving professionals throughout the international community of radioactive waste management. This process can be visualized as a series of levels going up a pyramid (Figure O-1). The base of the pyramid is built using all of the data and information collected by scientists and engineers involved in site character-



FV3-1

Figure O-1. Performance Assessment Information Flow Pyramid

The process of beginning with many pieces of data from multiple sources and capturing the key attributes of the system through several simplifying stages is represented by the Performance Assessment Information Flow Pyramid.

ization and engineering design. The base is very large because it represents the composite of all the information gathered by a repository program. All of this information feeds, on a very small scale, the conceptualization of how various processes work. An example of this scale is a description of the movement of water molecules as they pass between rock and fractures.

The specific aspects for describing a process on a larger scale are then extracted and incorporated into a computer model. An example is a model for all water flow above the water table, which would incorporate flow interactions between the rock matrix and the rock fractures as well as many other specifics needed to describe how water flows throughout the rock mass. Every piece of information is not generally used, or needed, in the computer model. Only information determined to be the primary driver for the process makes it up the next level of the pyramid.

This abstraction or progressive simplification to a more compact and usable form is depicted by the slightly smaller width of the pyramid. The models that eventually analyze the evolution through time of all the various components of the system are

generally the most compact or abstracted models of all. Abstraction is necessary for many reasons. One of these reasons is that many of the models are much too large to be run efficiently even on very large computers.

The TSPA must be probabilistic (as opposed to deterministic) to capture the uncertainty and variability in the behavior of the repository system, and thus to determine what is the "probable" behavior of the system under defined conditions. The models are run many times using many combinations of parameters. Each of the combinations of parameters has some definite possibility of representing the actual performance of the repository. These probabilistic analyses are intended to reflect the range of behaviors or values for parameters that could be appropriate, knowing that perfect or complete knowledge of the system will never be available and that the system is inherently variable.

A final reason to use abstraction is that, in some cases, an overly complex model would over-represent the actual state of knowledge about a process, so a simpler model is more appropriate.

The visualization of the TSPA process is shown in Figure O-2. Here, collection of site data and incorporation of the data (or estimates, where data are not available) first into conceptual models, then into mathematical equations, next into computer (numerical) models, and, finally, into a total system model is illustrated. The figure is a more graphic representation of the process that is depicted using the TSPA pyramid in Figure O-1.

#### **HOW THE REPOSITORY SYSTEM IS VISUALIZED IN THE TOTAL SYSTEM PERFORMANCE ASSESSMENT FOR THE VIABILITY ASSESSMENT**

In general, the repository system is visualized as a series of processes linked together, one after the other, spatially from top to bottom in the mountain. From a computer modeling point of view, it is important to break the system into "bite-size" portions that relate to the way information is collected. In reality, the operating repository system will be completely interconnected, and

essentially no one process will be independent of other processes. However, the complexity of the system demands some idealization of the system be developed for an analysis to be performed.

The component models are shown on Figures O-3 through O-7 in their relative spatial sequence. Each model in the sequence provides input to the model following it and receives the output of the preceding model or models. The shape of the component model icons shown on these figures is determined by the key attribute of the repository safety strategy they feed. As discussed in Section 2.2.1, the four key attributes are the following:

- Limited water contacting waste packages
- Long waste package lifetime
- Slow release of radionuclides from waste package
- Reduction in the concentration of radionuclides during transport from the waste package

An additional set of icons is used to depict the models associated with off-normal or disruptive events like volcanism, seismicity, nuclear criticality, and human intrusion. These events, if and when they occur, would affect the nominal case processes. The details of the model construction and the input and output parameters are contained in Section 3. The following is an abbreviated description of the expected behavior of the major components.

**Limited Water Contacting Waste Package.** The changes in climate over time provide a range of conditions that determines how much water falls onto the ground surface and infiltrates (Figure O-3). Based on current scientific understanding, the assumption in the TSPA is that the current climate is the driest that the Yucca Mountain site will ever encounter. All future climates are assumed to be either similar to current conditions or wetter. The water that is not lost back to the atmosphere by evaporation or

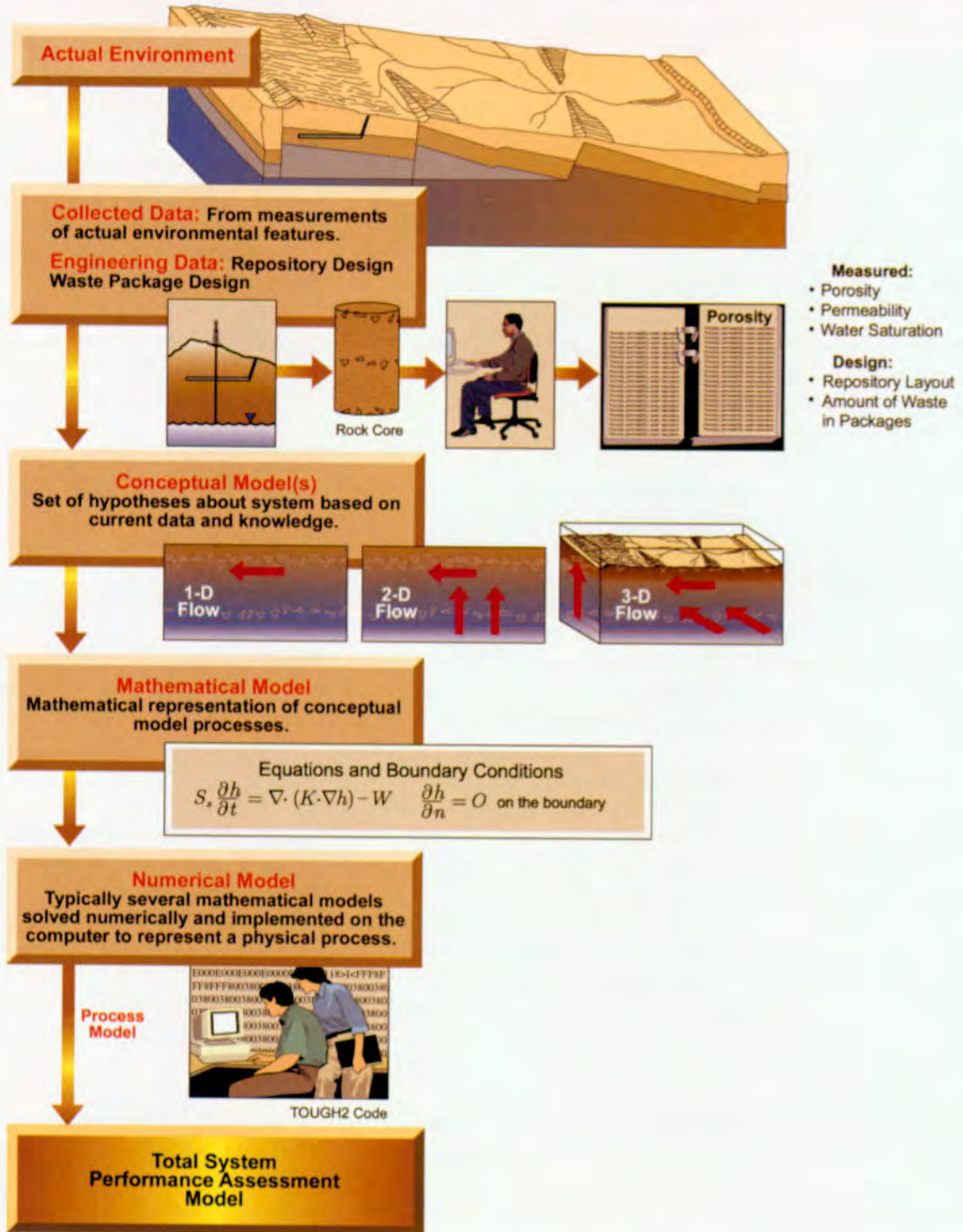


Figure O-2. Generalized Performance Assessment Approach

The generalized performance assessment approach is to develop conceptual models from site and engineering data, to represent the conceptual models using mathematical and numerical systems and to perform a calculation, the outcome of which can be used to describe the performance of the system being studied.

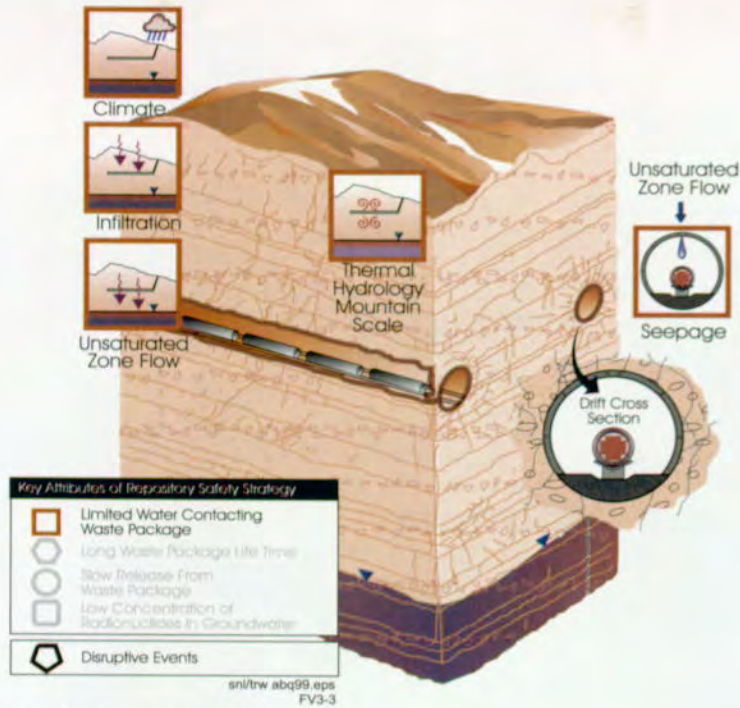


Figure O-3. Limited Water Contacting Waste Package

The five models represented by icons on this figure are used in calculations concerning water movement. Water that falls as precipitation can enter the rock of the mountain by infiltration and may eventually contact waste packages through seeps.



Figure O-4. Long Waste Package Life Time

The three models represented by icons on this figure are used in calculations concerning thermal and chemical environments and the impact of these environments on waste package life time.



Figure O-5. Slow Release from Waste Package

The three models represented by icons on this figure are used in calculations concerning degradation of cladding and the waste form and chemical conditions that affect the rate of release of waste from the waste package.



Figure O-6. Low Concentrations of Radionuclides in Groundwater

The three models represented by icons on this figure are used in calculations concerning the concentration of radionuclides in groundwater and their availability to contribute to exposure of individuals in the accessible environment.

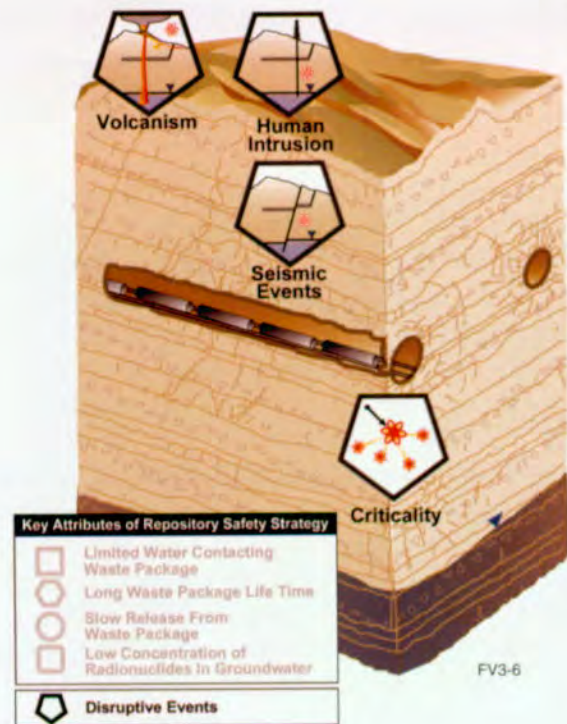


Figure O-7. Disruptive Events  
The four models represented by icons on this figure are used in calculations concerning performance of the engineered and natural systems during disruptive events that could release radionuclides.

transpiration enters the unsaturated zone flow system. Water infiltration is affected by a number of factors related to the climate state, such as increase or decrease in vegetation on the ground surface, total precipitation, air temperature, and run-off.

Water generally moves downward in the rock matrix and fractures. The rock mass at Yucca Mountain is composed of volcanic rock that is fractured to varying degrees as a result of contraction during cooling of the originally nearly molten rock and also due to extensive faulting in the area. Water flowing in the fractures moves much more rapidly than the water moving through the matrix. In some locations, some of the water collects into locally saturated zones in the rock or is diverted laterally by differences in the rock properties. The overall unsaturated flow system is very heterogeneous, and the location of flow paths and velocities and volumes of groundwater flowing along these paths are expected to change many times over the life of the repository system.

The thermal heat generated by the spent nuclear fuel in the repository causes the temperature of the surrounding rock to rise from the time of emplacement until about 3,000–4,000 years after repository closure. The water and gas in the heated rock are driven away from the repository during this thermal pulse. The thermal output of the waste decreases with time; eventually, the rock mass returns to its original temperature, and the water and gas flow back toward the repository. After the water returns to the repository walls, it begins to drip into the repository but only in a relatively few places. The number of seeps that can occur and the amount of water that is available to drip is restricted by the low volume of water flowing through Yucca Mountain, which is located in a semiarid region. Drips also can occur only if the hydrologic properties of the rock mass cause the water to concentrate enough to feed a seep. Over time, the number and location of seeps increase and decrease, corresponding to increased or decreased infiltration based on changing climate conditions.

**Long Waste Package Lifetime.** Because the repository is located above the water table in the unsaturated zone, the most important process controlling waste package lifetime is whether or not water drips on the package (Figure O-4). The location of the seeps providing dripping water depends to some extent on the natural conditions of the rock but also on the alterations caused by repository construction. Alterations such as increased fracturing may be caused by mechanical processes related to drilling the drifts or by thermal heating and expansion of the drift wall. The alterations in the seepage can also be caused by chemical alterations occurring as the engineered materials dissolve in water and re-precipitate in the surrounding rock, closing the pores and/or the fractures. The chemistry in the drift is continually changing because of the complex interactions among the incoming water, circulating gas, and materials in the drift (e.g., concrete from the liner or metals in the waste package). The chemical evolution is strongly influenced by heat during the thermal pulse.

In the reference design, the radioactive waste emplaced in the repository will be enclosed in a two-layer waste package. The layers will be constructed of two different materials that are expected to fail at different rates and from different mechanisms from each other as they are exposed to various repository conditions. The outer layer is made of carbon steel and the inner layer of a high-nickel alloy metal. Where water drips onto the waste packages, the packages corrode and eventually are breached. The breaches are thought to occur as deep, narrow pits or as broader areas called patches. The changing thermal, hydrologic, and chemical conditions in the repository all influence the corrosion rate of the waste packages.

**Slow Release of Radionuclides from Waste Package.** When water eventually enters a waste package through the patches or pits, it can contact the spent nuclear fuel contained within the waste package. The majority of radioactive waste material comes from commercial reactors, but there is also some material in the form of defense high-level radioactive waste and DOE reactor fuels. However, the influence of the commercial

spent nuclear fuel dominates long-term performance of the repository system, so waste from other sources is not included further in this overview discussion.

The water first contacts the very thin layer (about 0.7 mm) of a zirconium alloy that covers the surface of most of the fuel elements. This layer, called cladding, must be breached by mechanical or chemical processes before the radioactive fuel pellets can be exposed. Then the individual fuel elements start to degrade, making the radionuclides available for transport away from the waste form (Figure O-5). The degradation process may involve several stages because the waste forms are sometimes altered to different chemical phases before they reach a phase that will allow the nuclides to be released from the waste. Also, different radionuclides have different chemical properties themselves, so the reaction rates of the individual nuclides with water are greatly variable. In general, however, once the waste form begins to alter, it takes about 1,000 years for the commercial waste forms to completely degrade. The result is that certain nuclides are released much earlier than others are. The results of the TSPA show this effect, as different nuclides become the key contributors to dose rate over time.

To move out of the waste package, the radionuclides are either picked up and carried away from the waste form in flowing water or they move in a thin film of water by diffusion. To escape, the nuclides must exit through a pit or patch in the waste package and move out into the waste emplacement drift.

**Low Concentration of Radionuclides During Transport.** After escaping from the waste package, the radionuclides can then advance through materials on the drift floor, which are mainly concrete and the corrosion products from the waste package. At this point, the nuclides may either adhere to some of the materials on the drift floor, continue to move in the water, or become attached to extremely small particles of clay, silica, or iron called "colloids." Because of their molecular charge and physical size, these colloidal particles move through the rock mass under the

repository somewhat differently than noncolloidal particles.

The radionuclides move downward beneath the repository at different rates based on the chemical characteristics of the nuclides and of the rock they are passing through and on the velocity of the water in which they are contained (Figure O-6). The rock underlying the repository is unsaturated, and the water movement behaves as described earlier. Some water moves rapidly in fractures and some much more slowly in the rock matrix. The transport rate also depends on the tendency of the individual nuclide to interact with the rock through which it moves. Some radionuclides adhere to some minerals in a process called sorption and are bound in the rock for long periods. Sorption can be irreversible in some instances, and the nuclide is bound permanently in the rock. In other cases, the nuclides may desorb at a future time and again move through the system. Other types of nuclides move more quickly through the rock with little or no interaction that delays their transport.

When the radionuclides reach the water table, they are caught in the saturated zone flow system. Beneath Yucca Mountain, the water in the saturated zone flows in a generally southerly direction toward the Amargosa Valley. Nuclide sorption also occurs in the rocks and alluvium along the flow paths in the saturated zone. Because of the differences in chemistry between the unsaturated and saturated zone rock and water, the rates, durations, and nuclides involved in sorption are different for the two regions. As the radionuclides move in the saturated zone along different paths and through different materials, they gradually become more dispersed and the concentration of the nuclides in any volume of water decreases.

If the radionuclides are pumped out of the saturated zone by water wells, the radioactive material can cause doses to humans in several ways. For example, the water from the well could be used to irrigate crops that are eaten by individuals or livestock; to water stock animals that provide milk or meat food products; or to provide drinking water. Also, if the water pumped from irrigation

wells evaporates on the ground surface, the nuclides may be left as fine particulate matter that could be picked up by the wind and then inhaled by humans.

**Disruptive Events.** The key attributes of the system, given in the previous sections, describe the continually ongoing processes that are expected to occur in and around the proposed repository system. The term used to denote the sequence of anticipated conditions is "nominal case." In contrast, "disturbed case" refers to discrete, unanticipated events that disrupt the nominal case system (Figure O-7). The disruptive events include the following:

- Formation of a volcano through or adjacent to the repository
- Earthquake
- Human intrusion into the repository
- Nuclear criticality

Yucca Mountain is in a terrain that has experienced volcanic activity in the geologic past. The rocks in which the repository will be constructed are volcanic in origin. However, scientific studies of the timing, volume, and other aspects of volcanism have concluded that volcanic activity in this area has been waning in the recent geologic past and that the probability of volcanic activity as a repository-disturbing event is highly unlikely. However, for completeness, part of the TSPA analysis is an assessment of the consequences of a small cinder cone formed by a dike that flowed up through, or close to, the repository drifts.

In contrast, earthquakes happen frequently in and around Yucca Mountain. The effects of an earthquake important to postclosure repository performance primarily result from ground motions rather than from direct offset along a fault. The primary effect of ground shaking is to hasten rockfall into the drift.

Human intrusion is treated in a very simplistic manner as an event in which the contents of a

waste package are released to the water table through the borehole of a well drilled directly through the repository. Providing a "reasonable" (i.e., testable) forecast of future human activity is very difficult, if not impossible. The impact of such human intrusion is not included directly in the final presentation of results but is compared against the TSPA results to determine the potential level of influence. In other words, the probability of human intrusion occurring is assumed to be absolute, so it is simply the possible consequences that are evaluated.

In the TSPA calculations, the effects of nuclear criticality are assessed in the waste package and in the rock surrounding the repository. In these analyses, a series of unlikely events is assumed to occur. These unlikely events (such as filling the waste package with water or concentrating specific radionuclides in the rock mass) lead to the concentration of certain nuclides, that, in specific low probability environments, might lead to a nuclear criticality. The result is a change in the nuclear material to more highly radioactive forms. The introduction of these new radionuclides into the source term is then compared against the base case to determine if the relative change in dose rate is significant.

## RESULTS OF ANALYSES

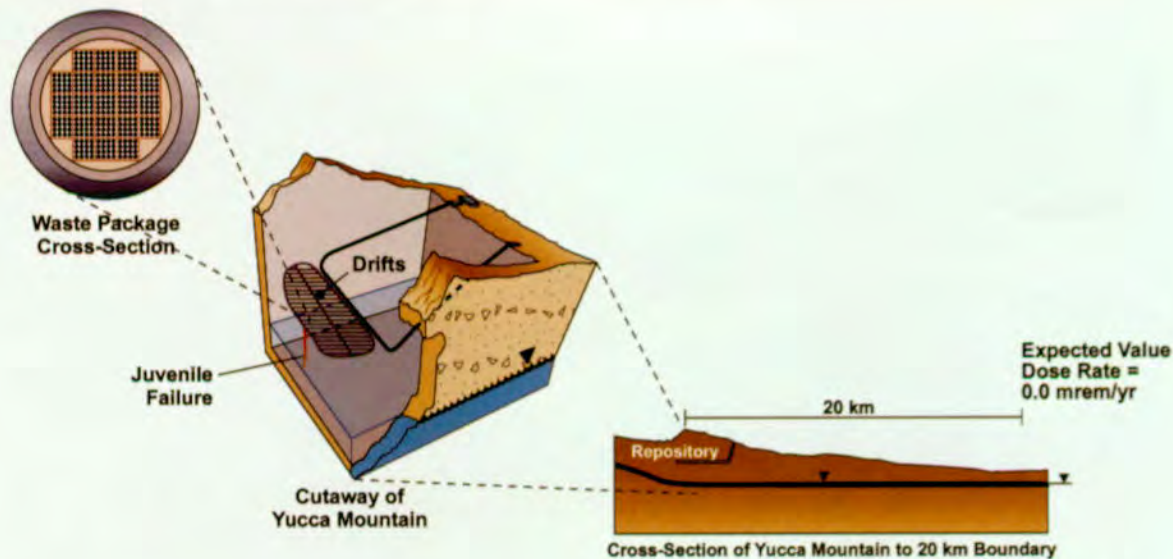
Although the TSPA is usually discussed in terms of a sequence of processes linked one after the other in space (as described in the earlier section), this approach does not readily convey how all of the processes evolve with time. This next section describes the results at various time intervals of interest, attempting to show the evolution in both time and space for the reference design and for the range of nominal-case conditions. However, the assumptions underlying the modeling development drive the results. Different sets of assumptions can give different results. The intent of this TSPA is not only to show how the system is thought to behave but also to provide information on how much uncertainty is associated with each TSPA component, as discussed later. Many of the results shown include a great deal of conservatism and also some large ranges of uncertainty. These areas

of conservatism and uncertainty will help drive the specific issues that the YMP will address in the time before the LA. The results discussed below focus on the forecasted average behavior of the system. This average behavior by itself cannot fully represent the ranges of uncertainty and variability in the system and its possible future states. The full range of behavior is discussed in Section 4.

One aspect of the system that is often unclear is that, while results of the analyses are presented so that they show how the system fails over time, there are even larger parts of the system that remain essentially unaltered. Although this fact is reflected indirectly in the results, it is rarely shown explicitly. The sequence of results in the Figures O-8, O-9, O-11, and O-12 show schematically what a waste package might look like at certain time periods. However, the schematics are only representative of those packages that experience dripping water. The percentage of all packages that experience significant corrosion of the resistant inner high-nickel alloy layer is expected to be small. Even though the location and number of seeps changes with time, the majority of packages will likely never experience any significant seepage at all, even in a million years. Most packages will continue to look essentially like the one depicted in Figure O-8 and not like the ones shown in subsequent figures depicting the TSPA results.

**Waste Emplacement to Several Thousand Years after Repository Closure.** As the waste packages are emplaced in the drifts, their combined heat output causes the drift-wall temperatures to rise and the water and gas in the rock is driven away from the repository. This process progressively dries out the rock mass farther and farther away from the repository. At 100 to 200 years after closure, the surfaces of some of the individual waste packages start to cool below boiling, and the humidity in the drift climbs from preclosure values of about 50 percent to nearly 100 percent. Depending upon the local conditions around each waste package, the degradation of the carbon steel outer layer begins somewhere between a hundred years and several thousand years. The fluids that

**Time = ~1,000 Years**



FV3-8

Figure O-8. Potential Radionuclide Release Conditions at About 1,000 Years  
Elements of the engineered and natural barrier systems showing potential radionuclide release conditions and the resulting dose rate at the 20-km (12-mile) boundary about one thousand years after waste emplacement.

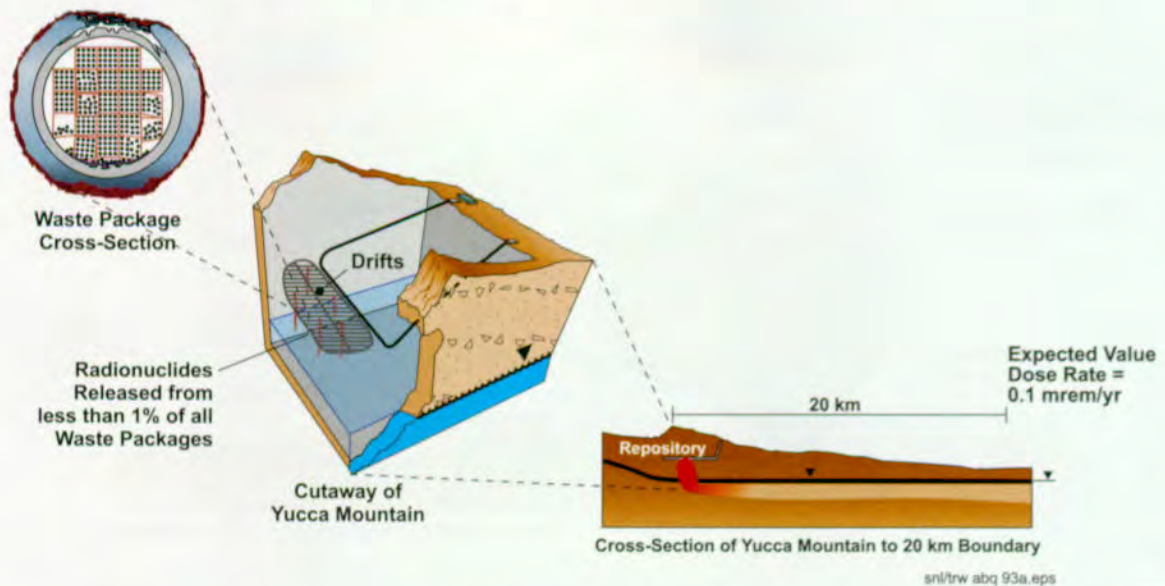
were driven away by the thermal pulse begin to move back toward the repository. Some of the areas that cool more quickly, particularly those toward the edges of the repository, start to experience dripping water. The packages in these areas have accelerated degradation of the outer barrier so that the inner layer of corrosion-resistant metal is exposed.

In Figure O-8, the cut-away of the repository shows schematically the release for one package in the repository. This release represents a single early failure from processes other than corrosion, such as failure caused by a manufacturing defect or a very large rockfall. Of course, the failed package fortuitously must be located under one of the relatively infrequent seeps for the waste form to be altered and the radionuclides to be picked up and carried away from the drift. Even with the early failure added to the analysis, there is not enough time for the nuclides to be carried to an area where it would be available to humans. Therefore, as shown in the final panel of Figure O-8, there is no dose consequence for any of the cases calculated

during this period in the region 20 km (12 miles) downgradient of the repository. The schematic picture of the waste package in Figure O-8 shows the lack of corrosion failures.

**Several Thousand Years to 10,000 Years after Closure.** By this time, the rock surrounding the drift has returned to its original temperature, and the fluid-flow patterns have been reestablished. Some permanent alterations of the rock may remain (such as microfracturing caused by thermal expansion), but this does not appear to be significant in terms of repository performance. The outer layer of the waste package is continuing to corrode. Dripping conditions now occur at discrete locations throughout the repository. Where the entire thickness of the outer layer has been worn away corrosion of the inner-barrier material is initiated (Figure O-9). In the cases where the inner layer has been perforated, the water can enter the waste packages through small openings, alter the fuel, and move out of the engineered barrier system. The repository cutaway in Figure O-9 shows a few paths along which

**Time = ~10,000 Years**



FV3-9

Figure O-9. Potential Radionuclide Release Conditions at About 10,000 Years

Elements of the engineered and natural barrier systems showing potential radionuclide release conditions and the resulting dose rate at the 20-km (12-mile) boundary about ten thousand years after waste emplacement.

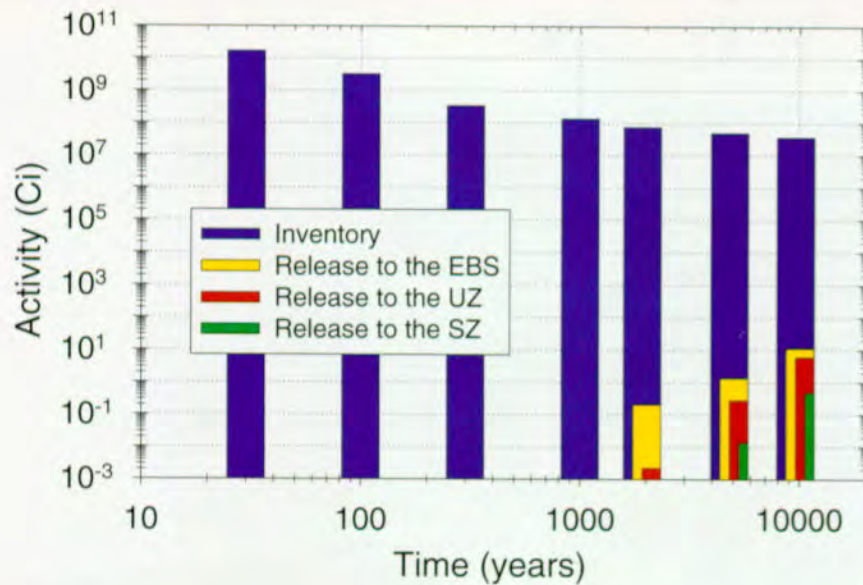
nuclides are being released into the rock under the repository. At this time, the expected value for the number of breached waste packages is less than 1 percent of the total emplaced packages. The expected value for the peak dose rate from a plume in the saturated zone 20 km (12 miles) south-southeast of the repository is calculated to be 0.1 mrem/year. This value is 0.03 percent of the average background radiation from nonmedical sources in the United States, which is about 300 mrem/year. The primary nuclides contributing to the dose rate are technetium-99 and iodine-129.

Another way to assess the benefit of the repository system is to show the radionuclide release information in the context of how much radioactivity remains isolated in the repository versus how much has escaped. Figure O-10 illustrates how the total inventory in the repository at the time of closure (30 years) decays with time, and what amount of the total inventory has escaped from the repository at discrete times over 10,000 years. Using the value for the total amount of radioactivity in the repository at 30 years after waste emplacement, by

about 300 years after closure the decay process has decreased the radioactivity to about 2 percent of the original amount. At 1000 years the amount has decreased further to 0.8 percent, and at 10,000 years the remaining portion of the original total inventory is only about 0.2 percent. Of the 0.2 percent remaining at 10,000 years, 0.00003 percent has gotten to the edge of the repository, 0.00002 percent has reached the water table, and 0.000001 percent has been transported 20 km (12 miles) south of the edge of the repository, where is assumed to be accessible to humans.

#### **Ten Thousand to 100,000 Years after Closure.**

The natural conditions in the rock remain unchanged from the previous period except for the likelihood of a change in climate. The likelihood is that, when the climate changes, a significant increase in infiltration has occurred, causing more water to flow through Yucca Mountain, more seeps into the repository to occur, a larger percentage of packages to fail, and more radionuclides to be transported along the unsaturated and saturated zone pathways. The progression of corrosion of



FV3-10

Figure O-10. Progressive Loss of Radioactivity Due to the Decay Process

The blue portion of the bar shows how much of the total radioactivity (in Curies) remains in the system at several points in time. The yellow portion shows the percentage of the remaining radioactivity that has passed through the floor of the repository into the underlying rock, the green indicates the amount of radioactivity that has reached the water table, and the red shows the amount that has moved to the accessible environment 20 km (12 miles) south of the repository.

the packages experiencing dripping water is shown in Figure O-11.

Those nuclides that at earlier times are limited in their release from the spent nuclear fuel elements because of their chemistry become larger contributors to the dose rate. In particular, neptunium-237 becomes the dominant isotope controlling dose rate. The number of packages failing by the end of this time is about 6 percent of the total number. The expected-value peak dose rate at 20 km (12 miles) is 30 mrem/year, or about 10 percent of the background radiation from natural sources in the United States.

**One Hundred Thousand to 1 Million Years after Closure.** The individual waste packages that are contacted by seeps continue to slowly corrode. By 1 million years, even some packages (around 1–2 percent) that have not been wetted by dripping are breached. The number of packages releasing nuclides by 1 million years after closure is about 30 percent of the total (Figure O-12). Dose rates at the 20-km (12-mile) point continue to climb as

more packages release their inventory, until a maximum is reached at approximately 300,000–400,000 years. The expected value for peak dose rate at this time is 200 mrem/year. Neptunium-237 remains the main contributor to the dose rate, but plutonium attached to colloids is the dominant contributor in about 8 percent of the cases.

#### BASES FOR BUILDING CONFIDENCE IN THE TOTAL SYSTEM PERFORMANCE ASSESSMENT

The confidence that can be placed in the results is a direct function of the confidence placed in the scientific and engineering data and their appropriate incorporation in process and TSPA models used to calculate repository behavior. The task of the YMP site characterization and design organizations is to describe the processes likely to occur at the proposed repository site and then design a system that works in the range of conditions specific to that site. The task of the TSPA is to give feedback to the site and design organizations on the adequacy of the information at

**Time = ~100,000 Years**

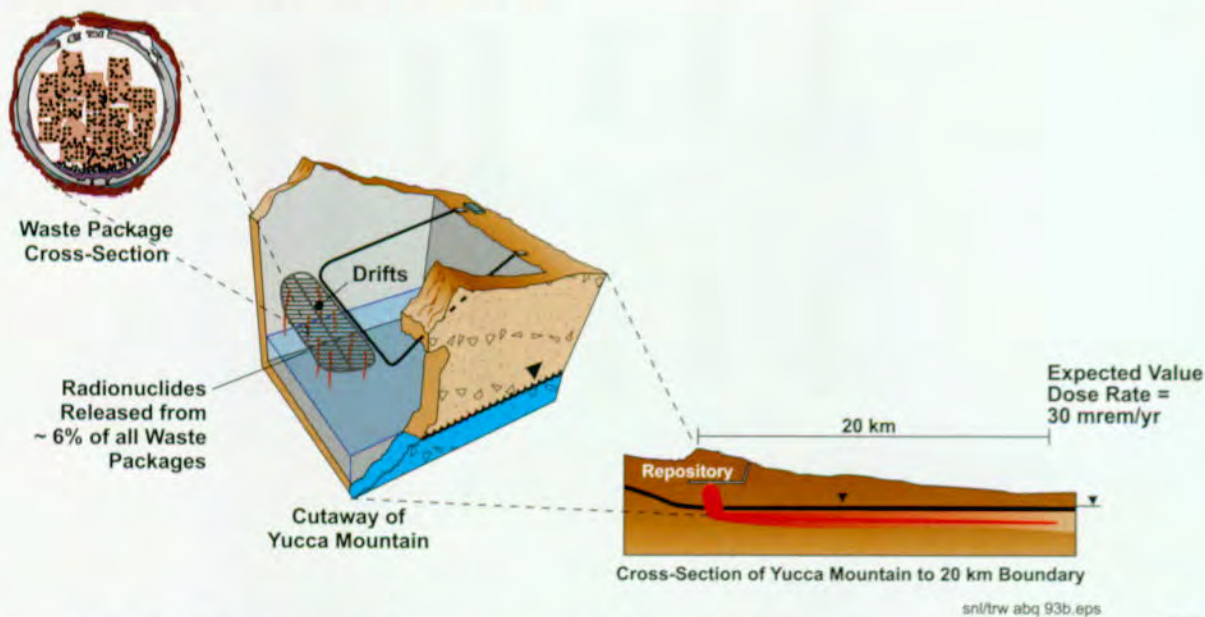


Figure O-11. Potential Radionuclide Release Conditions at About 100,000 Years  
Elements of the engineered and natural barrier systems showing potential radionuclide release conditions and the resulting dose rate at the 20-km (12-mile) boundary about 100,000 years after waste emplacement.

**Time = ~1,000,000 years**

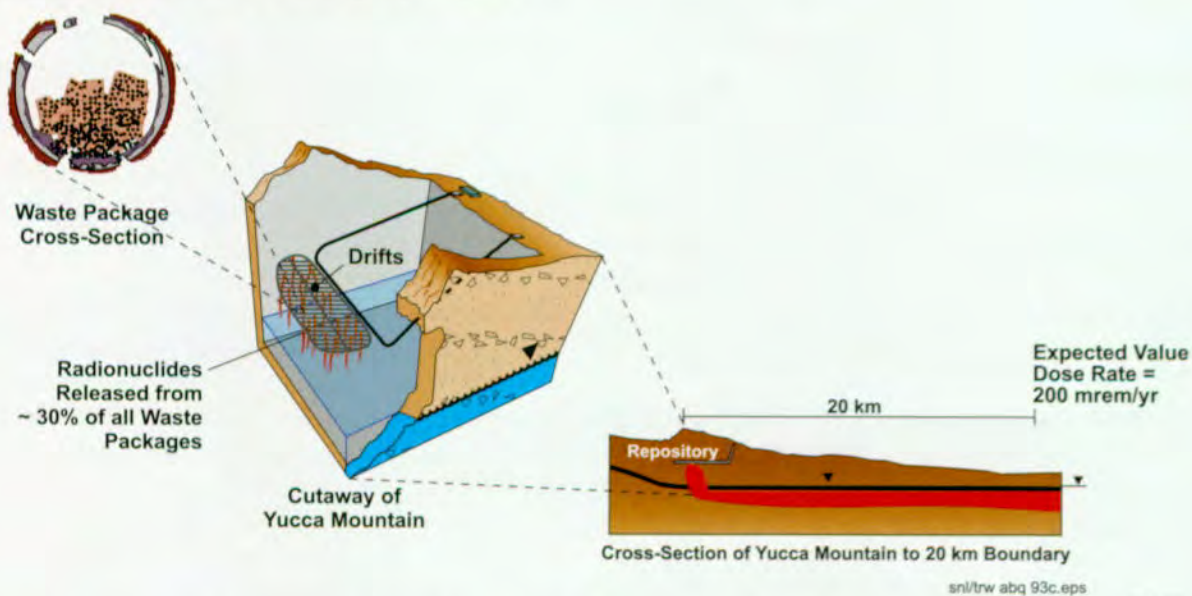


Figure O-12. Potential Radionuclide Release Conditions at About 1 Million Years  
Elements of the engineered and natural barrier systems showing potential radionuclide release conditions and the resulting dose rate at the 20-km (12-mile) boundary about 1 million years after waste emplacement.

any one time and to help determine when new information is unlikely to change the results significantly. In other words, TSPA is a tool that is used to help answer the question "when is enough, enough?" It will never be possible, or necessary, to delete all uncertainty from the TSPA analyses. The forecasts based on the TSPA analyses will always be subject to uncertainty about future events and conditions. They will also depend on the natural variability in the site and design components. The information and understanding about the Yucca Mountain site and the design elements of the proposed repository has progressed a great deal in the past few years. The information has come from many sources, including site and laboratory investigation, computer simulations, and expert judgment.

However, there are still some important areas in which additional work could decrease uncertainty about specific processes that are important to repository performance. This can be accomplished, in part, by performing uncertainty and sensitivity analyses. They are the mechanism for aiding management in determining where more information is needed for the LA, or conversely, where existing information is adequate, or that additional data are unlikely to change the results. There are a number of ways to gain additional confidence. From a site-characterization perspective, adding confidence can include the following:

- Conducting additional, highly focused studies at the site to obtain specific information
- Surveying the national and international scientific literature to glean additional relevant information
- Conducting studies of natural analogs where nature has already performed the experiments in the earth over geologic time scales (the Oklo natural nuclear "reactor" in Gabon is such an example)

The design organization may also develop and implement different or additional engineered struc-

tures or components to deal with aspects of the natural system where uncertainty cannot be decreased for any number of reasons. In these cases, additional studies also may be done to ensure that the behavior of the engineered constituent in the range of natural conditions is as expected.

The sensitivity of repository performance to any specific type of information strongly depends on the way performance is being measured. The question to be answered, in terms of how performance is being measured determines the relative importance of the components. An example of how different performance criteria change the relative importance of the various parts of the system is shown by the variability in the specific TSPA parameters' importance at different times. A different suite or priority of parameters is seen in the uncertainty analyses for 10,000 years versus those for 100,000 or 1 million years.

Mathematical methods of assessing parameter sensitivity, such as regression analyses, are used in the TSPA. In general, the sensitivity analyses do not show, in an absolute sense, the parameters that are most important to performance. Rather, they show, in a relative way, the parameters in which uncertainty most affects the results. In some cases, if future studies could reduce the range in uncertainty, the parameter might no longer appear as a parameter to which performance is highly sensitive. Conversely, if a parameter or component is assigned an inappropriately low uncertainty range, it might not show up as a particularly important parameter. These analyses must be performed with care to gain the necessary understanding about the parameters that are most important to actual repository performance and to identify those parameters that need additional study to achieve the confidence to support the LA. The results of the TSPA uncertainty and sensitivity analyses are provided in the next section in the context of the work that is most important for improving the confidence in the TSPA for the site recommendation and the LA.

## **GUIDANCE FOR THE LICENSE APPLICATION**

This last section focuses on the additional areas where work could increase confidence in certain processes and parameters for the LA. The focus for additional work is directed at the site characterization, design, and performance assessment organizations. For each change in the representation of a natural process or an engineered barrier, the change must be implemented in the TSPA models. Each TSPA model must then be tested to make sure that it is an adequate abstraction of the best understanding of the important features of the process it represents.

Based on the sensitivity and uncertainty analyses of the TSPA results (discussed in Sections 5 and 6 of this volume) and also based on the judgment of the TSPA analysts (discussed in Volume 4), the following aspects of the TSPA components have been determined to be most significant to the dose rates at 20 km (12 miles) from the Yucca Mountain repository. In some cases, the TSPA results point to very specific aspects or parameters used to represent the TSPA components, which, in turn, are captured in the principal factors of the repository safety strategy. Where this information is a subset of a principal factor, the factor with which it is associated is shown in parentheses. The results are shown for three different time periods, since the relative importance of different aspects of the modeled system changes as the system evolves.

### **Postclosure to 10,000 Years after Closure**

- Availability of water to contact the waste package (seepage into drifts)
- Occurrence of premature package failures (loss of integrity of outer waste package barrier or of inner waste package barrier due to manufacturing flaws or mechanical effects)
- Rates of waste package degradation (loss of integrity of outer waste package barrier or of inner waste package barrier due to environmental conditions)

- Rate of cladding failure (integrity of spent nuclear fuel cladding)
- Availability of water to contact exposed waste form surfaces
- Timing and magnitude of climate change (precipitation and infiltration to depth)
- Degree of mixing in the unsaturated zone

### **10,000 to 100,000 Years after Closure**

- Fraction of waste packages under seeps (dripping onto waste packages)
- Rate of waste package degradation
- Amount of water seeping into the drifts (dripping onto waste packages)
- Rate of cladding degradation (integrity of spent nuclear fuel cladding)
- Dilution of nuclides in the unsaturated and saturated zones (transport through the unsaturated zone, transport in the saturated zone)
- Solubility of neptunium-237
- Formation and transport of radionuclide-bearing colloids
- Biosphere dose conversion factor

### **100,000 to 1 Million Years after Closure**

- Fraction of waste packages under seeps (dripping onto waste packages)
- Timing and magnitude of superpluvial climate (precipitation and infiltration to depth)
- Rate of waste package degradation (integrity of inner waste package barrier)
- Amount of water seeping into the drifts (dripping onto waste packages)

- Amount of water seeping into the degraded waste packages (seepage into waste package)
- Cumulative amount of degraded cladding (integrity of spent nuclear fuel cladding)
- Dilution of nuclides in the unsaturated and saturated zones (transport through the unsaturated zone, transport in the saturated zone)
- Neptunium solubility

- Biosphere dose conversion factors (biosphere transport uptake)

The details about which TSPA parameters that feed these factors could be improved is contained in different parts of this document, including Sections 3, 4, 5, and 6. Prioritization of those factors, using input from the TSPA-VA results and other considerations, such as cost, schedule, as well as the plans to address these important parameters and factors is contained in Volume 4.

INTENTIONALLY LEFT BLANK

## 1. INTRODUCTION

This volume reports the development of TSPA for the VA. This first section defines the general process involved in developing any TSPA, it describes the overall TSPA process as implemented by programs in the United States and elsewhere in the world, and discusses the acceptability of TSPA as a process or tool for analyzing a nuclear waste repository system.

Section 2 discusses the more specific use of the TSPA process for the TSPA-VA for Yucca Mountain, including goals, approach, and methods. It also includes a very brief synopsis of TSPA-VA results. Section 3 briefly discusses each of the component models that comprise the TSPA-VA. Each TSPA component model represents a discrete set of processes. The TSPA-VA components are: unsaturated zone flow, thermal hydrology, near-field geochemical environment, waste package degradation, waste form alteration and mobilization, unsaturated zone transport, saturated zone flow and transport, and biosphere. For each of these components, this section introduces the conceptualization of each individual process, describes the data sources, and discusses model parameter development and computer methods used to simulate each component. Section 4 explains the mechanics of how the individual TSPA components were combined into a "base case" and then provides the "expected value" results of a deterministic base case analysis. Section 4 also contains a description of the probabilistic analyses and results that help determine the relative importance of the various TSPA components and the data used to describe the components. Section 5 addresses sensitivity studies run for each of the TSPA components to understand how uncertainty in various parameters within a component change the TSPA results. Section 6 presents the findings of the sensitivity studies run on the various components in Section 5, and prioritizes the findings of the entire set of uncertainty and sensitivity studies of the components relative to each other. Section 6 also discusses the DOE assessment of potential activities to increase the confidence in future TSPAs based on the results of TSPA-VA, gives a synopsis of the insights provided by the TSPA Peer Review

Panel, includes a discussion of comments received by DOE from NRC, and closes with concluding remarks.

### 1.1 DEFINITION OF PERFORMANCE ASSESSMENT AND TOTAL SYSTEM PERFORMANCE ASSESSMENT

Performance assessment and TSPA are terms with very specific meanings in the high-level radioactive waste management community. The process of constructing and implementing a TSPA is often described as a pyramid, where detailed information representing the various processes and components of a total system are distilled and linked into progressively more abstracted models used to analyze system performance.

#### 1.1.1 Explanation of a Total System Performance Assessment

Performance assessment is a method of forecasting how a system or parts of a system designed to contain radioactive waste will behave over time. Its goal is to aid in determining whether the system can meet established performance requirements. A TSPA is the subset of performance assessment analyses in which all of the components of a system are linked into a single analysis.

The word "forecast" rather than "predict" is used to describe the expected outcome of a TSPA. "Predict" implies "inference from facts or accepted laws of nature." Forecast has a similar meaning but also implies anticipating eventualities and differs from predict in being usually concerned with probabilities instead of certainties (Merriam-Webster 1993, p. 457). As discussed in Section 1.3, incorporation of probabilities and uncertainty is a critical aspect of TSPA, which allows determination of reasonable assurance, as defined by regulatory agencies. However, it must be noted that NRC uses the term "predictive models" to express uses what NRC anticipates in 10 CFR 60.102 (a)(2).

The process of performance assessment is somewhat different from a safety assessment and a probabilistic risk assessment. Safety assessments

use a conservative "bounding" assessment of the entire system; performance assessments analyze the best understanding of the system and its components (NEA 1995, pp. 28-36). In a safety assessment, a given process or event is assumed to happen, regardless of the likelihood of its occurrence. A performance assessment incorporates more information than a safety assessment by assuming that some processes or events are more likely to happen than others and treating them accordingly in mathematical modeling (however, for some processes or events where information is limited, bounding analyses may be used in the performance assessment). The benefit of a performance assessment in this case is that a more realistic and, therefore, more defensible case is used. It must be noted that, in the community of nuclear waste management professionals, this distinction between a safety assessment and a performance assessment has become blurred, such that in informal usage they are often used interchangeably. However, it is important to differentiate the two philosophies, that is, use of "conservative" bounding cases versus use of the most realistic models possible. In addition, a safety case, as made before a licensing authority, could include both safety assessments and performance assessments, as defined above.

"Probabilistic risk assessment" is a term generally applied to safety studies of nuclear power plants or other engineered systems, but can be applied to any system that could fail in identifiable ways. Although this type of analysis incorporates variations in probability for different processes, the system and the time periods are very different than for a performance assessment. A probabilistic risk assessment is usually performed for discrete events of limited duration involving an engineered system and its components. Natural events such as earthquakes and volcanic eruptions are considered initiating events that may have an effect on overall system behavior, but are not a part of the system. The components can be tested on a time scale similar to that for the operational life of the system. Therefore, a set of requirements and specifications for these components is available, and the analyses are performed against criteria that have been or can be tested and validated.

A performance assessment treats both the engineered and natural system components. The engineered system is to some extent controllable, but the natural system is not. The responses of the total system extend over periods beyond those for which data have been or can be obtained.

### 1.1.2 The Performance Assessment Pyramid

The process for constructing a TSPA is shown in Figure 1-1 and described in more detail in Section 1.3. The Performance Assessment Pyramid shows how more detailed underlying information builds the technical basis for the total system models. The breadth of the lowest level of the pyramid represents the complete suite of process and design data and information (i.e., field and laboratory studies that are the first step in understanding the system). The next higher level indicates how the data feed into conceptual models that visualize the operation of the individual system components. Most of the information at these lower levels is reported in detail in Volumes 1 and 2.

The next higher level represents the synthesis of information from the lower levels of the pyramid into computer models. At this point, the subsystem



Figure 1-1. Performance Assessment Information Flow Pyramid

The performance assessment information flow pyramid shows how more detailed underlying information builds the technical basis for the total system models. Detail is reduced going up the pyramid; however, key attributes of the system are captured in the TSPA models.

behavior may be described by linking models together into representations, as described in Section 3; at this point performance assessment modeling is usually thought to begin. The term "abstraction" is used at this point to indicate the extraction of essential information. The TSPA models are usually referred to as abstracted models.

The upper level shows the final level of distillation of information into only the most critical aspects to represent the total system. At this point, all of the models are linked together, as discussed in Sections 3.3 and 4.1. These are the models used to forecast system behavior and estimate the likelihood that the behavior will comply with regulations and ensure long-term safety.

As information flows up the pyramid, it generally is distilled into progressively more simplified forms, or becomes more abstracted, as indicated in Figure 1-1. However, abstraction is not synonymous with simplification. If a particular component model can not be simplified without losing essential aspects of the model, it ceases to move up the pyramid and becomes part of the TSPA calculation tool. Thus, an abstracted model in a TSPA may take the form of something as simple as a table of values that were calculated using a complex computer model, or the abstraction may take the form of a fully three dimensional computer simulation. It must be noted that even the most complex models of specific processes are still an abstraction of reality.

There are also some considerations that dictate the level of complexity used to represent a process. One is the sensitivity of the results of the TSPA to that particular process. The more sensitive the process or parameter, the more detailed the model representation tends to be. However, the degree of complexity is also limited by the state of knowledge concerning the model. It is very important not to misrepresent the degree of understanding about a process by embedding it in an overly complicated computer model.

## 1.2 PHILOSOPHY OF TOTAL SYSTEM PERFORMANCE ASSESSMENT

The TSPA has become the internationally recognized method for analyzing system behavior for nuclear waste repositories. It is important to understand why TSPAs are performed, the unique nature of a TSPA compared to other types of analyses, and why the confidence in TSPA as a process has been established at such a global level.

### 1.2.1 Why Total System Performance Assessments Are Performed

Performance assessments are used to forecast how a specific system and all of its components evolve over time. Comparing the results to performance requirements allows analysts to estimate whether the amount of harmful material that may become accessible in the environment is acceptably low. The requirements, usually in the form of regulatory criteria, are generally established by governmental oversight agencies. The ultimate determination of whether a system complies with the requirements lies with the legally responsible regulatory group. The task of those proposing a nuclear waste repository is to provide reasonable assurance that the safety standard will be met, which in turn requires that they

- Understand the proposed system and all of its components
- Can demonstrate the capability to model the system
- Can adequately account for and treat the uncertainties in the analysis
- Can show that the information in the model provides reasonable assurance that safety standards will be met

In addition to providing a tool for determining whether a system meets regulatory requirements, TSPA also provides a rigorous method for aiding management in establishing the priority of information-gathering activities during the site selection, site characterization, and design phases.

As more information is gathered, the TSPA process iterates to incorporate revised and updated information into successive TSPA models and allows a program to progress toward more reasonable and defensible total-system models. Results of each TSPA, particularly the sensitivity and uncertainty studies, provide information about the relative importance of ongoing or proposed information-gathering activities addressing site characterization and design development. Each successive TSPA requires that the total system models become more representative. Several TSPAs by the YMP have been completed to date on the Yucca Mountain repository system (Sinnock et al. 1984; Barnard and Dockery 1991; Barnard et al. 1992; Eslinger et al. 1993; Wilson et al. 1994; Andrews et al. 1994; CRWMS M&O 1995). These efforts, along with studies done by other organizations (NRC 1995; Kessler and McGuire 1996), have contributed to the iterative process of the TSPA for the VA.

A TSPA is unique because it is the analysis that links all the system components together. This linkage is important because it allows each component to be viewed in the context of the behavior of the entire system. Even the simplest system has various aspects that are easier to understand when studied separately. For example, waste package material degradation may be characterized by laboratory tests of corrosion. However, the geologic system in which the waste package is to be emplaced may be analyzed using field studies of the host rock for properties that are only observed on a large scale, such as fracture density, as well as laboratory studies of other aspects, such as water chemistry. In a functioning system, these elements provide feedback to one another. The interaction of the water with the corroded waste package would likely change the water chemistry, which may in turn change the fractures and the way water flows through them. This very simple example shows an obvious potential for feedback. When a very complex system with numerous components is simulated as a single system in a TSPA, interactions among the components that would not otherwise be observed are often found in the analysis.

As discussed in Volume 1, the repository safety strategy for the YMP relies on a multiple barrier system. This isolation strategy means that the components of the natural and engineered systems work together to form a series of barriers. Because the behavior of each component in the series is governed by a different set of physical or chemical processes, this strategy provides a strong argument that the entire system is very unlikely to fail in response to a single mechanism. Also, the use of different types of barriers precludes reliance on complete knowledge about any one process. Therefore, the incorporation of multiple barriers helps to answer the question that frequently arises, how can the analysis account for what is not known? Given the uncertainty inherent in a forecast, one way to deal with an unanticipated response by one component of the system is to have multiple additional components that will still operate as barriers.

The concept of "reasonable assurance," used by NRC in its regulation of nuclear facilities and activities does not require absolute certainty in the results of an analysis. The incorporation of uncertainty into the TSPA, using various mathematical methods, allows the regulator and others to determine if the goal of reasonable assurance has been met. The study of uncertainty is documented in Section 4.3; however, some of the general methods of treating uncertainty include developing distributions to represent various types of data and also assigning probabilities to different conceptual models to encompass a range of potential behaviors or responses of certain components.

### **1.2.2 Why Total System Performance Assessments Are the Appropriate Tool for Analyzing Repository Systems**

A question that often arises is whether or not performance assessment is a useful tool for the purpose of analyzing safety. The consensus of the international waste management community is that, in the realm of providing reasonable assurance, performance assessment is an adequate tool. In support of this consensus, the Nuclear Energy Agency Radioactive Waste Management Committee and the International Atomic Energy

Agency International Radioactive Waste Management Advisory Committee issued a collective opinion that they

...confirm that safety assessments are available today to evaluate adequately the potential long-term radiological impacts of a carefully designed radioactive waste disposal system on humans and the environment, and consider that appropriate use of safety assessment methods, coupled with sufficient information from proposed disposal sites, can provide the technical basis to decide whether specific disposal systems would offer to society a satisfactory level of safety for both current and future generations (NEA 1991a, p.7).

Although TSPAs can never be proven to be absolutely valid, many environmental problems require modeling of long-term interactions of man-made and geologic systems. Using the term "model" acknowledges that whether the descriptions of geologic features, events, and processes are unique and represent absolute reality will never be known. "Validation" of a long-term predictive model means that, on the basis of tests of the assumptions, inputs, outputs, and sensitivities, the model adequately reflects the recognized behavior of the portion of the system it is intended to represent. Adequacy is driven by the needs of the application for which the model is developed (Boak and Dockery 1998, p. 178-180).

Scientists assessing long-term risk use the following mechanisms to establish the adequacy of their models (Boak and Dockery 1998, pp. 181-182):

- Expert judgment to assign appropriate ranges of parameters where data are sparse, controversial, or unobtainable
- Conservatism in assigning parameter values and process descriptions, including ignoring some potentially mitigating processes
- Stochastic simulation to assess the effect of uncertainty in descriptions and the sensi-

tivity of performance predictions to uncertainty and to examine alternative scenarios and process models

The following measures are undertaken to demonstrate that the effort to ensure validity has been comprehensive (Boak and Dockery 1998, p. 182):

- Documentation of the model structures, including justification for assumptions and simplifications as well as the examination of alternative conceptualizations for the system
- Review by the scientific community and those who have a stake in the decisions that these models support

Uncertainty is an inherent part of all total system studies. Information gathering activities are directed at reducing uncertainty as much as is practical. However, because of natural variability in the systems being studied and limited understanding about how processes will operate in the future, uncertainty will always have to be included explicitly in TSPA calculations.

### 1.3 GENERIC APPROACH FOR CONDUCTING A TOTAL SYSTEM PERFORMANCE ASSESSMENT

The TSPA process has been adopted and used throughout the global community for determining how a given waste management system might behave under a range of possible future conditions (NEA 1991b, pp. 24-25). A relatively standardized set of steps has been outlined to guide the performance assessment process, as shown below. The questions to be answered from the requirements form the basis for the details of the performance assessment, including the choice of models, parameters, and boundary conditions. The specifics of the requirements determine aspects of the system that are most sensitive to varying conditions. The steps shown below are not necessarily sequential; they may be performed in parallel. The entire process is iterative, and individual steps can be iterated within themselves.

Figure 1-2 shows the steps in the process of an iterative, total system performance assessment. The five steps shown in that diagram are defined below, and their implementation is discussed in Sections 3, 4, and 5.

### **1.3.1 Develop and Screen Scenarios**

Scenario development in the context of a performance assessment has a very specific meaning. A scenario is a path that, using something resembling an event tree, connects a series of features, events, and processes that could result in a release of waste to the environment. Scenario development is a bookkeeping method that helps a licensing applicant demonstrate that they "thought of everything." Guidance concerning the suite of possible scenarios exists in the form of a Nuclear Energy Agency scenario report (NEA 1991c) that contains a general list of scenario classes.

Scenario development has different uses at different phases of a program. In the first stage of development, all potential pathways are developed. Potential scenarios are organized into a series of feasible futures and demonstrate what has been considered for inclusion in the TSPA. Scenario development helps a program develop logical and effective site characterization and design activities. As more site-specific information is gained, scenarios are screened and the event trees are "pruned" to discard futures that, for one reason or another, are not applicable to that site or design. In the later stages of a program, scenarios assist in ensuring that all connections among the processes are maintained. Scenarios also help describe the details of the conceptual and computer models that must be developed, and they provide a record of what has been considered and discarded in the analysis. The record is needed to make the logic behind the TSPA traceable for other analysts and the regulator. This information is contained in Section 2.2.

### **1.3.2 Develop Models**

In this step, models are developed to represent important scenarios. The models are usually implemented in computer codes. Alternative

computer models are also constructed for different conceptual models of how a system behaves. Complex process models provide the details of physical processes at more fundamental levels and correlate with the second and third levels of the performance assessment pyramid discussed in Section 1.1.2. The models developed at this level are discussed in Section 3.

System-level models contain fewer details but are required for reproducing the essential phenomena of the process. These models are often used at the highest level of the performance assessment pyramid, when the concept of abstraction is introduced.

### **1.3.3 Estimate Parameter Ranges and Uncertainties**

The parameters used in the models described in Section 1.3.2 have natural variability. For example, in a rock mass, the pore space naturally varies from place to place. There is also uncertainty in these parameters that arises from incomplete knowledge, as would happen when the future state of a parameter must be estimated from assumptions rather than from measurements, or when possible incorrect measurements must be adjusted. This uncertainty is accounted for by developing distributions of values for the parameters rather than using any single value. The distributions also are assigned specific shapes that reflect the likelihood of any one value in the distribution occurring. Therefore, these probability distribution functions are used when many computer runs are made, and each run samples from the parameter distributions to allow many possible combinations of values. This method allows less likely values to be used infrequently and highly probable values to be used more often. However, the value selected by the simulation for a specific parameter may restrict the physically possible range of values for another parameter. Correlations among these related parameters also must be maintained mathematically.

Not all parameters have distributions of values. Some parameters may have only a single value, information on the parameter may be extremely

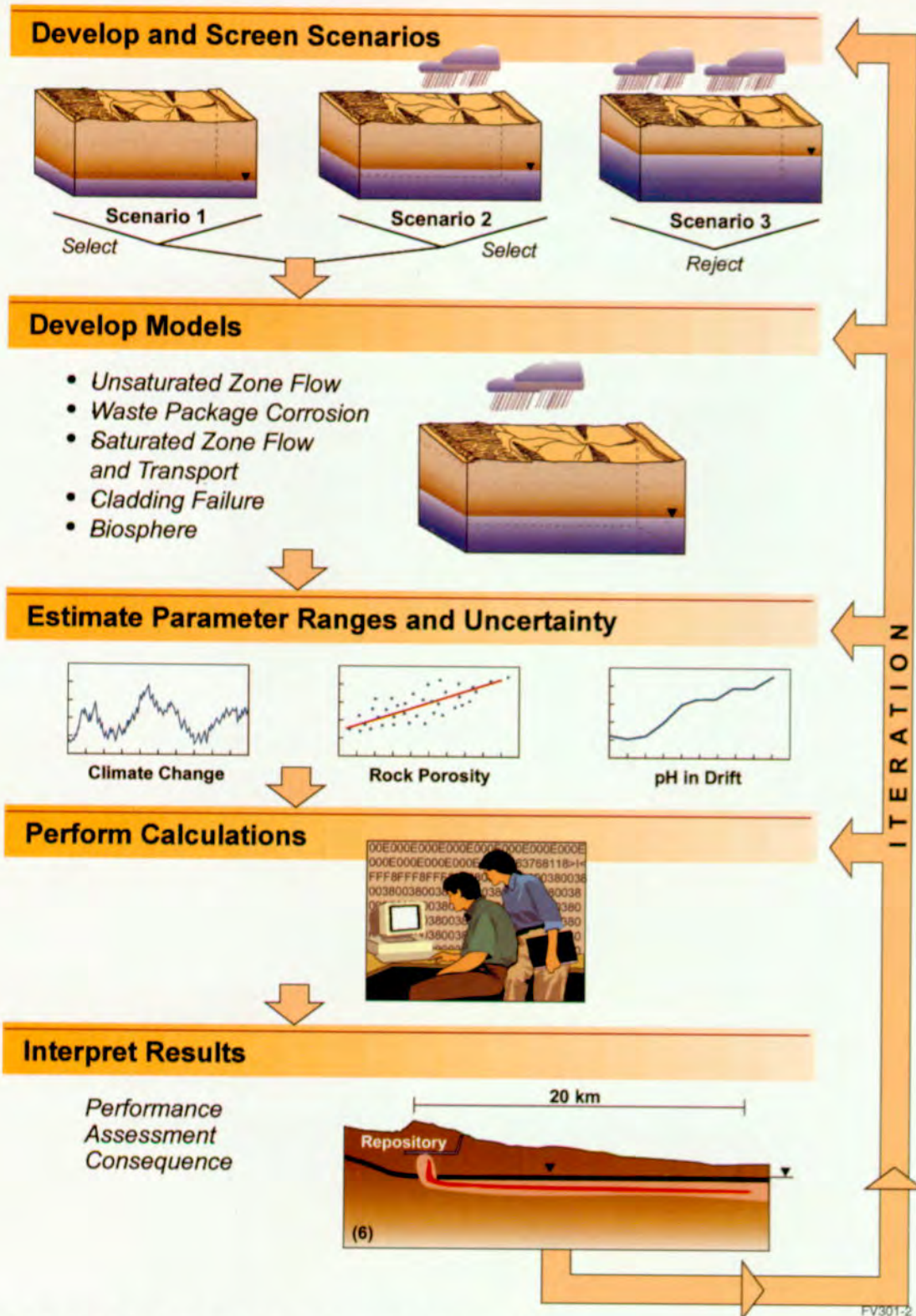


Figure 1-2. Major Steps in a Generic Performance Assessment  
This figure illustrates the standardized sequence of steps in a generic performance assessment. The entire process is iterative between steps and also within individual steps.

limited, or the parameter may be very insensitive, making it unnecessary or inefficient to use a distribution in the calculations. The distributions of values for important variables are discussed in Section 3.

#### **1.3.4 Perform Calculations**

At this point, the work contained in the third or fourth tiers of the performance assessment pyramid has been completed. The next step is to run the subsystem or total system analyses using the distributions of data where distributions are available or necessary. The results of these calculations are reported in Section 4.2 for the total system.

Sections 3 and 5 include the results of subsystem analyses.

#### **1.3.5 Interpret Results**

This final step is very important. The results themselves can be used for the following:

- Further develop or screen scenarios.
- Guide future testing for site characterization, design, and TSPA model development.
- When sufficiently mature, determine whether the system satisfies regulatory requirements.

## 2. YUCCA MOUNTAIN SITE CHARACTERIZATION PROJECT TOTAL SYSTEM PERFORMANCE ASSESSMENT FOR THE VIABILITY ASSESSMENT

The concept of TSPA and the generic TSPA process are described in Section 1 of this volume. The acceptability of TSPA as a tool for analyzing a nuclear-waste repository system was also described in that section. Section 2 of this volume discusses the more specific use of the TSPA process for Yucca Mountain, including the goals, approach, and specific method. The technical basis for this volume is provided in the *Total System Performance Assessment-Viability Assessment (TSPA-VA) Analyses Technical Basis Document (CRWMS M&O 1998i)*.

The objectives of the TSPA for the VA are discussed in Section 2.1. The primary objective, to describe the probable behavior of the Yucca Mountain repository system, was a mandate from the U.S. Congress. To accomplish this objective, available scientific information about the natural geologic setting was used in the TSPA, along with data about the engineered components and their interactions with the geologic setting. Several general assumptions were made in the TSPA because as yet there are no standards to evaluate system performance. These assumptions relate to:

- The appropriate measure of performance
- The time scale of regulatory concern for the analysis

Although a "base case" was used in the TSPA to describe probable behavior of the Yucca Mountain repository system, alternative interpretations were considered to evaluate the significance of the uncertainty in the base case. An important goal throughout the process was to provide the TSPA information in a "transparent" document that describes the assumptions, results, and conclusions of the analyses.

Section 2.2 contains a general discussion of the approach used to analyze the Yucca Mountain repository system in the TSPA-VA. Building the

capability for an integrated system analysis requires significant input from many individual disciplines. In addition, the analyses have benefited from comments received from both internal and external reviewers of previous system analyses conducted for the Yucca Mountain repository. Sources of data and information for constructing the TSPA-VA include previous TSPAs; documented models of the principal components; workshops to abstract, or simplify, the process model components; expert elicitations of key model components; and external review. The eight principal model components are the result of addressing the goal of the Yucca Mountain repository system of minimizing the exposure of humans to radioactive materials. The presence of water is a key factor in initiating release of radionuclides from waste packages and moving them through the environment to a contact point with humans. For this reason, the evaluation of the model components focused on the ability either to keep water from contacting the waste or to minimize releases of radioactivity from the repository if waste packages are breached.

Section 2.3 is a detailed description of the methodology used to analyze the repository system in the TSPA. The previous section discussed the process model components as individual models. This section provides a road map for reassembling, or coupling, the component models into one integral whole. Presented in the section is an overview of the TSPA-VA method for mathematical and numerical modeling of the individual processes, including their uncertainty, and the approach for combining them into an overall model and computer code. This overview includes discussions about information flow between the models and the architecture of the computer program for the TSPA-VA that facilitates the information flow. Also discussed in this section is the method for presenting the key results; in particular, how to show the influence of uncertainty on the performance predictions, and the relationship of uncertainty to the base case.

Section 2.4 summarizes the base case, or the expected performance of the repository system, based on the results of the TSPA-VA. The

expected performance is presented as a series of time slices that demonstrate the system's response to the proposed design concept.

## 2.1 OBJECTIVES OF TOTAL SYSTEM PERFORMANCE ASSESSMENT FOR THE VIABILITY ASSESSMENT

The overall scope and objective of the TSPA for the VA are contained in the Energy and Water Development Appropriations Act (1997):

...a total system performance assessment based upon the design concept and the scientific data and analysis available by September 30, 1998, describing the probable behavior of the repository in the Yucca Mountain geological setting relative to the overall system performance standards.

Assessing the performance of the system requires the following:

- Assimilating all the available scientific data and analyses that describe the geological setting into which the design concept is to be placed
- Defining the design concept that is to be used
- Describing the probable behavior of the repository system
- Identifying the performance standards by which the TSPA will be judged

The total system is comprised of geological and engineering components. Therefore, the TSPA uses the available scientific information about naturally occurring physical and chemical processes at the Yucca Mountain site, which are summarized in Volume 1. In addition, the TSPA includes the design concepts and scientific information about physical and chemical processes caused by the system engineered components, which are summarized in Volume 2.

Currently, there are no overall system-performance standards for the Yucca Mountain repository. The U.S. Environment Protection Agency (EPA) is developing applicable site-specific standards based on the recommendations in a congressionally mandated National Academy of Sciences' report, *Technical Bases for Yucca Mountain Standards* (National Research Council 1995). NRC is revising its licensing regulations. DOE anticipates that both EPA and NRC will develop system-level requirements for evaluating the suitability of the Yucca Mountain repository system for nuclear-waste disposal. This system-level guidance likely will focus on protecting humans from the potential health risks associated with excessive exposure to ionizing radiation at some distance downgradient from the repository.

In the absence of final regulatory guidance, the appropriate measure of system performance is assumed to be the exposure rate to radionuclides for average members of a critical population that may live 20 km (12 miles) downgradient from the repository. This distance was chosen to correspond to Lathrop Wells, the closest existing public or private well to the site, near the intersection of U.S. Highway 95 and Nevada State Route 373. The controlled-area boundary for the DOE Nevada Test Site also is approximately 20 km (12 miles) from the repository. Because the downgradient irrigation wells nearest to the repository are approximately 30 km (18 miles) from the site (near Amargosa Farms), this 20-km (12-mile) distance is believed to be sufficiently conservative for analysis. NRC has used this distance in its performance-assessment calculations (McCartin and Baca 1998).

Not only the geographic domain of interest but also the period of regulatory concern for the analysis must be defined. The previous EPA regulation (40 CFR 191) limited the time to 10,000 years after the facility is permanently closed. The recommendations of the National Academy of Sciences noted that the period of regulatory concern was properly an environmental policy and societal decision that was the responsibility of the implementing agency, in this case EPA. Because there is no formal guidance, the TSPA analyses

examined the 10,000-year period. To evaluate the consequences caused by the repository beyond that period, the analyses are extended to 100,000 and 1 million years in determining when the peak radionuclide doses or peak risk occurs.

DOE also has the goal to assess total system performance quantitatively defining the significance of each of the key components in the repository-safety strategy to assist in a systematic refocusing of the project resources. The statutory goal of the TSPA is to address the probable behavior of the repository system. However, the available scientific information can also suggest alternative interpretations that may also be plausible. When propagated through a quantitative tool such as performance assessment, these alternative interpretations can illustrate the significance of the uncertainty in the base case interpretation chosen to represent the probable behavior of the repository. The information about uncertainty will assist DOE in defining the work required either to minimize uncertainty or to modify the repository design to accommodate for this uncertainty before submitting the LA for constructing the repository system. The quantitative performance analyses assist in identifying those areas where additional scientific and technical work are required to evaluate the site and to prepare a complete, cost-effective, and timely license application. The additional scientific investigations and design analyses believed to be necessary for developing the LA are summarized in Volume 4.

Another indirect use of the TSPA is to provide a vehicle for prelicensing discussions with NRC. The NRC pre-licensing program concentrates on resolving the key technical issues most important to repository performance. An important role of the TSPA is to evaluate the potential significance of these issues to find a common basis for understanding the need for additional scientific and technical work.

Although the goal of the TSPA is to provide a quantitative assessment of the probable behavior of the repository system, it is important to recognize the uncertainties inherent in such analyses. EPA and NRC have recognized the care required in

defining the degree of confidence needed from the analyses. EPA stated that,

Because of the long time period involved and the nature of the events and processes of interest, there will inevitably be substantial uncertainties in projecting disposal system performance. Proof of the future performance of a disposal system is not to be had in the ordinary sense of the word in situations that deal with much shorter time frames. (40 CFR 191.13[a])

NRC also underscored this point in its discussion of reasonable assurance in 10 CFR 60.101(a)(2):

The Commission anticipates that licensing decisions will be complicated by the uncertainties that are associated with predicting the behavior of a geologic repository over the thousands of years during which HLW [high-level radioactive waste] may present hazards to public health and safety. (48 FR 28194 1983; 10 CFR 60)

These inherent uncertainties were recognized in developing the analysis tools that are described in Sections 2.3 and 3 of this volume. The potential effects of many of these uncertainties are presented in Sections 4.3-4.5 and 5.

Given the uncertainty involved in a postclosure performance assessment, an important goal is to produce a transparent document describing the assumptions, the intermediate steps, the results, and the conclusions of the analyses. External review groups have defined what they mean by transparent. The Nuclear Waste Technical Review Board states that "transparency is the ease of understanding the process by which a study was carried out, which assumptions are driving the results, how they were arrived at, and the rigor of the analyses leading to the results" (NWTRB 1998, p. 21). The TSPA Peer Review Panel notes that "transparency is achieved when a reader or reviewer has a clear picture of what was done in the analysis, what the outcome was, and why" (Whipple et al. 1997a, pp. 9-10).

For the reader to have confidence in the analyses, the presentation must illustrate with sufficient clarity the following attributes:

- The conceptual basis for the individual components in the quantitative analyses (i.e., how the system is intended to work, which is presented in Section 2.2)
- How the individual components are combined into an assessment of system behavior (Sections 2.3 and 4.1)
- The scientific understanding used to develop the quantitative analysis tools that describe the system's expected evolution (Sections 3.1-3.8)
- The system's expected evolution as defined by the spatial and temporal response of the system to waste emplacement (Sections 4.1 and 4.2)
- Uncertainty in the system's expected evolution and the significance of that uncertainty to the system performance goals (Sections 4.3-4.5, 5.1-5.8)

Section 2.2 presents a discussion of *what* is being analyzed as part of the TSPA for the Yucca Mountain repository system. This discussion includes *how* the repository system is intended to work and is closely aligned with the repository safety strategy and the principal factors affecting postclosure performance.

Section 2.3 describes how the repository system has been analyzed in the TSPA. Section 3 describes how separate components of the system model have been assembled and the technical and scientific bases for the models used in the analyses.

## 2.2 TOTAL SYSTEM PERFORMANCE ASSESSMENT APPROACH

### 2.2.1 Development of an Integrated Total System Performance Assessment Approach

The Yucca Mountain repository system is a combination of integrated processes that can be summarized in 1 basic tenet, 4 key attributes, and 19 principal factors. The basic objective of the waste disposal system is to contain and isolate the radioactive wastes so that the dose impact to humans is attenuated to a relatively benign level. This tenet manifests itself in the following four key attributes of the DOE repository safety strategy:

- Limited water contacting the waste packages
- Long waste package lifetime
- Low rate of release of radionuclides from breached waste packages
- Radionuclide concentration reduction during transport from the waste packages

The four attributes are associated with 19 principal factors, which are listed in Table 2-1. Also shown in this table are the corresponding TSPA model components analogous to these principal factors.

Building an integrated system analysis capability requires input from the many disciplines that comprise the system. The construction also benefits from comments from internal and external reviewers of previous system analyses conducted for the Yucca Mountain repository. The analyses documented in this volume of the VA have benefited from such interactions. The final approach and methods used in the analyses have been developed over the last two years, following completion of the *Total System Performance Assessment - Viability Assessment (TSPA-VA) Plan* (CRWMS M&O 1996f) and the *Total System Performance Assessment - Viability Assessment (TSPA-VA) Methods and Assumptions* (CRWMS M&O 1997m). The major sources of information that form the bases for the methods, assumptions,

### Oversight

NRC Technical Exchanges, Appendix 7 Meetings  
NWTRB Panel Meetings, Reports to Congress  
TSPA Peer Review Interim Reports 1, 2, and 3  
State of Nevada; Affected Units of Local Government  
Public

### Prior TSPAs

DOE TSPA-91, 93, 95  
NRC IPA-1, -2, -3  
EPRI TSPA Phases 1, 2, and 3

### Expert Elicitation

Probabilistic Volcanic Hazard Assessment  
Probabilistic Seismic Hazard Assessment  
Unsaturated Zone Flow Expert Elicitation  
Saturated Zone Flow and Transport Expert Elicitation  
Near-Field Environment Expert Elicitation  
Waste Package Degradation Expert Elicitation  
Waste Form Alteration and Mobilization Expert Elicitation

### Process Model Abstraction Workshops

Unsaturated Zone Flow  
Thermal Hydrology  
Near-Field Geochemical Environment  
Waste Package Degradation  
Waste Form Degradation and Radionuclide Mobilization  
Unsaturated Zone Transport  
Saturated Zone Flow and Transport

### Site and Design Models

Unsaturated Zone Flow Model  
Seepage Model  
Near-Field Environment Model  
Corrosion Model  
Unsaturated Zone Transport Model  
Saturated Zone Flow and Transport Model

### Site and Design Information

Site Description Document  
Repository Design  
Waste Package Design  
Laboratory Data  
In situ Data  
Analog Data

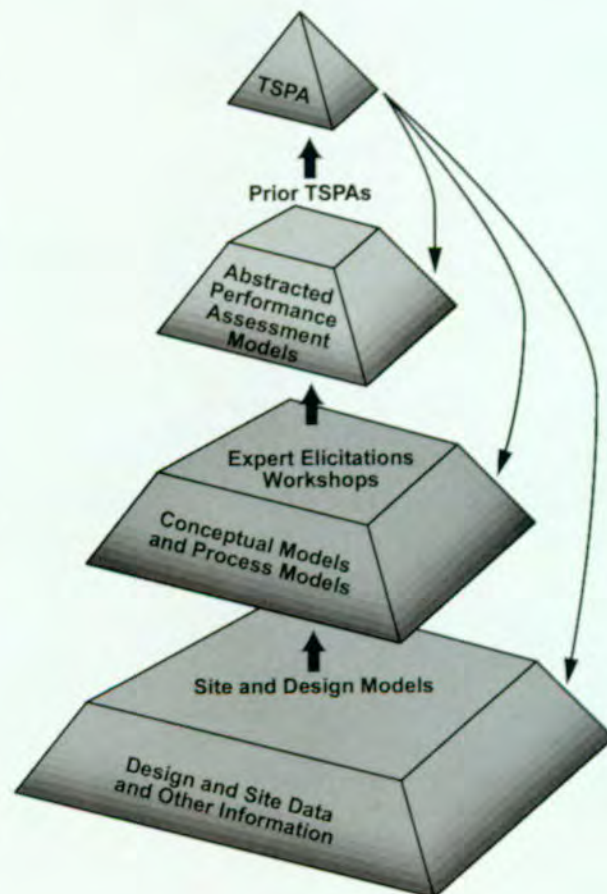


Figure 2-1. Major Sources of Information Used in the Development of the Total System Performance Assessment for the Viability Assessment

This figure illustrates the numerous internal and external sources of information used to develop the models used in the quantitative prediction of postclosure performance.

Table 2-1. Principal Factors Affecting Expected Postclosure Performance for the Viability Assessment Reference Design and Their Corresponding Total System Performance Assessment for the Viability Assessment Model Components and Nuclear Regulatory Commission Key Technical Issues

| Attributes of the Repository Safety Strategy <sup>a</sup>                     | Principal Factors <sup>a</sup>   | TSPA Model Components              | NRC Key Technical Issue <sup>b</sup>  |
|---|--|------------------------------------|---|
| Limited water contacting waste packages                                       | Precipitation and infiltration of water into the mountain                            | Unsaturated Zone Flow              | Unsaturated and Saturated Flow under Isothermal Conditions                            |
|   | Percolation to depth   |                                    |   |
|   | Seepage into drifts  | Seepage                            | Repository Design and Thermomechanical Effects  |
|   | Effects of heat and excavation on flow   |                                    |   |
|   | Dripping onto waste package  |                                    |   |
| Humidity and temperature at waste package                                     | Thermal Hydrology – Mountain Scale<br>Thermal Hydrology-Drift Scale                  | Thermal Effects on Flow            |   |
| Long waste package lifetime   | Chemistry on waste package   | Near-Field Geochemical Environment | Evolution of the Near-Field Environment   |
|   | Integrity of waste package outer barrier<br>Integrity of waste package inner barrier | Waste Package Degradation          | Container Life and Source Term  |
| Low rate of release of radionuclides from breached waste packages             | Seepage into waste package   |                                    |   |
|   | Integrity of spent nuclear fuel cladding   |                                    |   |
|   | Dissolution of UO <sub>2</sub> and glass waste form                                  |                                    |   |
|   | Solubility of neptunium-237  |                                    |   |
|   | Formation of radionuclide-bearing colloids   |                                    |   |
| Transport within and out of waste package                                     |  |                                    |   |
| Radionuclide concentration reduction during transport from the waste packages | Transport through unsaturated zone   | Unsaturated Zone Transport         | Unsaturated and Saturated Flow under Isothermal Conditions and Radionuclide Transport |
|   | Transport in saturated zone  | Saturated Zone Flow and Transport  |   |
|   | Dilution from pumping  |                                    |   |
|   | Biosphere transport  | Biosphere Transport and Uptake     |   |

<sup>a</sup>See Rev. 2 of the DOE repository safety strategy (DOE 1998)

<sup>b</sup>NRC realigned its preclicensing program to focus all its activities on resolving the 10 key technical issues it considered to be most important to repository performance. The Key Technical Issues consist of the following: 1) Total System Performance Assessment (NRC 1998a); 2) Unsaturated and Saturated Flow Under isothermal Conditions (NRC 1997e; 1997f); 3) Evolution of the Near-Field Environment (NRC 1997c); 4) Container Life and Source Term (NRC 1998b); 5) Repository Design and Thermal-Mechanical Effects (NRC 1997a); 6) Thermal Effects on Flow (NRC 1997b); 7) Radionuclide Transport (Sagar 1997); 8) Structural Deformation and Seismicity (NRC 1997d); 9) Igneous Activity (NRC 1998d); 10) Activities Related to Development of NRC High-Level Radioactive Waste Regulations (Sagar 1997). The first nine of these directly or indirectly related to performance assessment. The last one also relates to performance assessment to the extent this tool is used as a basis for setting and showing compliance with regulatory standards. These key technical issues are summarized in NRC staff reports (such as Sagar 1997) and a series of issue resolution status reports, the primary mechanism by which NRC will provide DOE with feedback on the resolution of the key technical issues.

and component models used in the TSPA documented here are illustrated in Figure 2-1 and Table 2-2. The major sources include the following:

- Previous DOE- and non-DOE-sponsored TSPAs of Yucca Mountain
- Documented models describing each of the principal components of the TSPA
- Workshops on abstractions of individual process model components used in TSPA
- Expert elicitations of key process model components used in TSPA
- External reviews of TSPA plans, methods, and assumptions

Table 2-2. Principal Sources of Information Used in the Development of the Total System Performance Assessment Model for the Viability Assessment Reference Design

| Attributes of the Repository Safety Strategy                                  | Principal Factors                                    | Process Model Abstraction/Workshop   | Process Model Expert Elicitation  | Described in Section |
|---|--|--|---|----------------------|
| Limited water contacting waste packages                                       | Precipitation and infiltration into the mountain     | Unsaturated Zone Flow Model Abstraction/Testing (CRWMS M&O 1997t)                          | Unsaturated Zone Flow Expert Elicitation (CRWMS M&O 1997n)                                | 3.1                  |
|   | Percolation to depth                                 |  |   |                      |
|   | Seepage into drifts                                  |  |   |                      |
|   | Effects of heat and excavation on flow               | Thermal Hydrology Model Abstraction/Testing (CRWMS M&O 1997i)                              | N/A*  | 3.2                  |
|   | Dripping onto the waste package                      |  | Near-Field Environment Expert Elicitation (CRWMS M&O 1998d)                               | 3.2                  |
| Long waste package lifetime   | Humidity and temperature at the waste package        | Near-Field Geochemical Environment Abstraction/Testing (CRWMS M&O 1997d)                   | N/A*  | 3.3                  |
|   | Chemistry on the waste package                       |  |   |                      |
|   | Integrity of outer waste package barrier             |  |   |                      |
| Low rate of release of radionuclides from breached waste packages             | Integrity of inner waste package barrier             | Waste Form Degradation and Radionuclide Mobilization Abstraction/Testing (CRWMS M&O 1997o) | Waste Form Degradation and Radionuclide Mobilization Expert Elicitation (CRWMS M&O 1998k) | 3.5                  |
|   | Seepage into waste package                           |  |   |                      |
|   | Integrity of spent nuclear fuel cladding             |  |   |                      |
|   | Dissolution of UO <sub>2</sub> and glass waste forms |  |   |                      |
|   | Solubility of neptunium-237                          |  |   |                      |
|   | Formation of radionuclide-bearing colloids           |  |   |                      |
| Transport within and out of the waste package                                 | N/A*   |  |   |                      |
| Radionuclide concentration reduction during transport from the waste packages | Transport through unsaturated zone                   | Unsaturated Zone Transport Model Abstraction/Testing (CRWMS M&O 1997p)                     | N/A*  | 3.6                  |
|   | Transport in saturated zone                          | Saturated Zone Flow & Transport Model Abstraction/Testing (CRWMS M&O 1997s)                | Saturated Zone Flow & Transport Expert Elicitation (CRWMS M&O 1998g)                      | 3.7                  |
|   |  |  | N/A*  |                      |
|   | Dilution from pumping                                | Biosphere Model Abstraction/Testing (CRWMS M&O 1997a)                                      | N/A*  | 3.8                  |

\* This principal factor was not the subject of an expert elicitation.

- NRC Issue Resolution Status Reports which address the status of key technical issues that are assessed in the TSPA

Each of these sources is described in the following paragraphs. In addition, indirect information derived from other radioactive and non-radioactive waste programs has been used in the development of the approach and methodology used in

TSPA-VA. The more detailed technical basis is presented in the *Total System Performance Assessment-Viability Assessment (TSPA-VA) Analyses Technical Basis Document* (CRWMS M&O 1998i).

DOE contractors completed previous TSPA analyses in 1991, 1993, and 1995. These analyses are documented in *TSPA 1991: An Initial Total-*

*System Performance Assessment for Yucca Mountain* (Barnard et al. 1992), *Total-System Performance Assessment for Yucca Mountain- SNL Second Iteration (TSPA-1993)* (Wilson et al. 1994) and *Total-System Performance Assessment - 1995: An Evaluation of the Potential Yucca Mountain Repository* (CRWMS M&O 1995). The general objective of these scoping analyses was to refine the methods and approach that would be applied in the development of the site recommendation and, ultimately in the LA. An additional objective of these studies was to assist DOE in prioritizing design and scientific investigations on the key components that most significantly impact performance. The knowledge gained in these analyses has assisted DOE in prioritizing the models to include in the TSPA analyses and prioritize the data gathering activities needed to support these models.

Other TSPA analyses, not sponsored by DOE, have been conducted by the Electric Power Research Institute and by NRC. The Electric Power Research Institute's most recent iteration of a TSPA is documented in *Yucca Mountain Total System Performance Assessment, Phase 3* (Kessler and McGuire 1996). NRC has also conducted a recent TSPA (NRC 1995). NRC is conducting an iterative performance assessment (named IPA-3.1.3) in parallel with the DOE TSPA for the VA. Preliminary results of these analyses were reported in a technical exchange held in March 1998 (McCartin and Baca 1998). Each iterative analysis of total system performance, whether performed by DOE and its contractors, NRC and its contractors, or the Electric Power Research Institute and its contractors, leads to improved insights about the expected behavior of the Yucca Mountain repository system. In addition, a review of the conceptual models and parameters used in the analyses provides a basis for defining the significance of the range of uncertainties examined. In general, all of these analyses converge on a few key components that are analogous to the principal factors identified in Table 2-1. These factors are reflected in the NRC key technical issues and recently developed issue resolution status reports that address portions of the key technical issues.

TSPAs are based on a number of building blocks. Principal among these are models that describe how Yucca Mountain behaves in the presence of a repository and how the engineered system behaves within the environmental setting caused by the mountain. These process models indicate that each model is designed to describe the behavior of individual and coupled physical and chemical processes. A significant portion of the DOE site characterization program has been aimed at developing the scientific bases for the most reasonable representation of the Yucca Mountain site and its associated engineered barriers. This scientific basis serves as the foundation for the process models used in the TSPA. The basis for these models is described in more detail in Volumes 1 and 2, and their use in the TSPA is discussed in Section 3 of this volume.

To ensure that this TSPA would be based on the most current scientific knowledge (as defined in the objectives set forth for the VA), a series of workshops were held in 1997 to bring together YMP scientists, engineers, and performance-assessment analysts. These individuals consisted of DOE, national laboratory, U.S. Geological Survey (USGS), and managing and operating (M&O) contractor scientists and engineers. Observers at these workshops included technical staffs of regulatory agencies (such as NRC and EPA) and their contractors, external oversight groups such as the Nuclear Waste Technical Review Board and the Advisory Committee on Nuclear Waste, and the TSPA Peer Review Panel. The aim of these workshops was to develop a strategy for identifying and incorporating the relevant aspects of the individual process models into the TSPA analyses. In addition to defining the appropriate approach for abstracting the important elements of each process model, these workshops assisted DOE in defining and prioritizing the major technical issues that were believed to need addressing in the TSPA. Many of these issues correspond directly with the key technical issues raised by NRC. Each workshop culminated in a plan for incorporating that component in the TSPA and linking that component to other portions of the TSPA. These plans are referenced in Table 2-2 and are summarized in the *Total System*

*Performance Assessment - Viability Assessment (TSPA-VA) Methods and Assumption* (CRWMS M&O 1997m). The approach and methods to implement these plans are discussed in more detail in Section 3.

Acknowledging diverse technical and scientific opinions is an important part of any engineering and scientific endeavor as controversial as analyzing the design and performance of a potential disposal facility for high-level radioactive waste. In addition to the workshops, DOE sponsored five expert elicitations on key process models for the TSPA. The goal of these elicitations was to solicit the judgment of nationally and internationally recognized scientists in quantifying the uncertainty associated with each of these process models and uncertainty in the parameter values used in those models. The process followed the procedures and approaches for eliciting expert judgments that have been formalized in documents such as DOE guidance for the formal use of expert judgment (DOE 1995) and the NRC Branch Technical Position on the use of expert elicitation in the high-level radioactive waste program (Kotra et al. 1996). The assessments and probability distributions that resulted from the elicitations provide a reasonable aggregate representation of the knowledge and uncertainties about issues in evaluating the various processes important to repository performance. The five areas evaluated, in the elicitations were:

- Unsaturated zone flow (CRWMS M&O 1998g)
- Waste package degradation (CRWMS M&O 1998b)
- Saturated zone flow and radionuclide transport (CRWMS M&O 1998g)
- Near-field environment (CRWMS M&O 1998d)
- Waste form degradation (CRWMS M&O 1998k)

The major conclusions of these elicitations are described in Section 3. In addition to these elicitations, DOE conducted external elicitations of the potential hazards associated with either volcanic- or seismic-induced events. The use of these results in the analysis of the potential effects of disruptive scenarios is described in Section 4.4. All of these elicitations helped refine the range of models and parameters that have been considered in the TSPA.

In addition to DOE-sponsored development of the TSPA models, several external oversight groups provided input throughout the process of defining and implementing the approach and methods. These groups include NRC and its contractor, the Center for Nuclear Waste Regulatory Analysis; the NRC Advisory Committee for Nuclear Waste; and the congressionally chartered Nuclear Waste Technical Review Board. An independent peer review panel was convened to comment on development of the TSPA-VA. This panel will review this TSPA to assist DOE in developing more robust performance assessments for the site recommendation report and the LA, which in the current plan occur in the 2001-2002 time frame. These organizations have published a range of technical comments on the TSPA plan and the methods and assumptions documents and have conducted numerous briefings over the last 2 years on the progress of the TSPA. Examples of these comments may be found in the following publications: *Total System Performance Assessment 1995 Audit Review* (Baca and Brient 1996), *NRC High-Level Radioactive Waste Program Annual Progress Report Fiscal Year 1996* (Sagar 1997), *Report to the U.S. Congress and The Secretary of Energy - 1996 Findings and Recommendations* (NWTRB 1997), *Report to the U.S. Congress and The Secretary of Energy - 1997 Findings and Recommendations* (NWTRB 1998), *First Interim Report Total System Performance Assessment Peer Review Panel* (Whipple et al. 1997a), *Second Interim Report Total System Performance Assessment Peer Review Panel* (Whipple et al. 1997b), and *Third Interim Report Total System Performance Assessment Peer Review Panel* (Whipple et al. 1998).

These comments have aided in defining the most appropriate means of describing and analyzing the performance of the Yucca Mountain site and the engineered barriers associated with the reference design and design options. A number of recommendations, however, could not be fully addressed in this TSPA, and will be carried forward to aid the design and planning for the TSPA supporting the site recommendation and LA.

### **2.2.2 Components of the Yucca Mountain Repository System Evaluated in the Total System Performance Assessment**

The Yucca Mountain repository system consists of the geologic setting and engineered barriers that, considered together, are aimed at reducing the exposure of humans to radioactive materials to acceptable levels. This section briefly describes the key aspects of the individual component models identified in Table 2-1 and Figure 2-2.

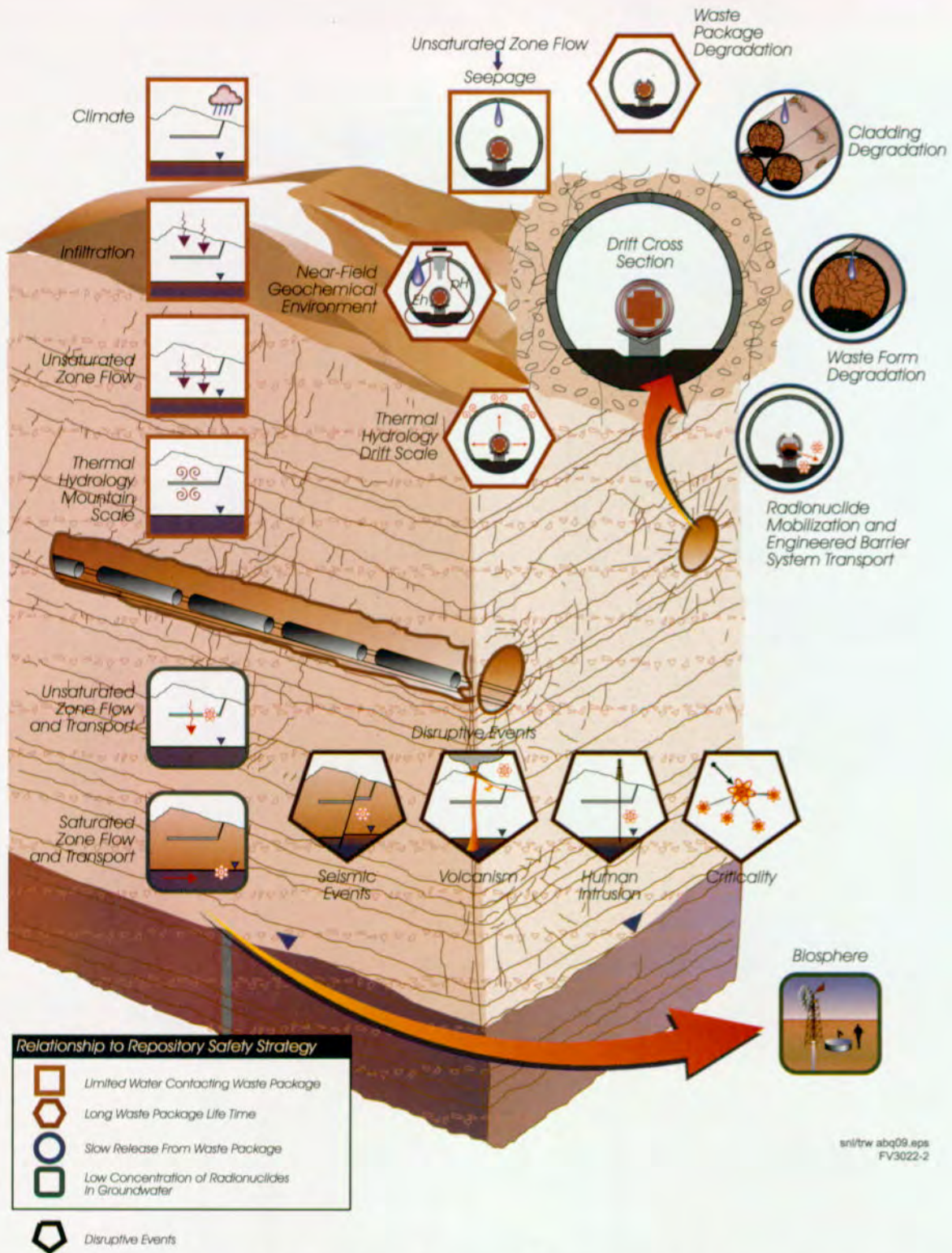
The model components related to the first key attribute in the repository safety strategy—limit the amount of water contacting waste package—include climate, infiltration, unsaturated zone flow, seepage, and mountain-scale thermal hydrology. Together, these components define the temporal and spatial distribution of water flow through the unsaturated tuffs above the water table at Yucca Mountain and the temporal and spatial distribution of water seeps into the repository drifts. There could be long-term (thousands to hundreds of thousands of years) climate variations. In addition, the thermal regime generated by the decay of the radioactive wastes can mobilize water over the first hundreds to thousands of years. For these reasons, the amount of water flowing in the rock and seeping into drifts is expected to vary with time.

The model components related to the second key attribute of the repository safety strategy—extend the time the waste packages contain waste—include all of the above components plus drift-scale thermal hydrology, near-field geochemical environment, and waste package degradation. Together, these components define the spatial and temporal distribution of the times when waste packages are expected to breach. The thermal,

hydrologic, and geochemical processes acting on the waste package surface are the most important environmental factors affecting the waste package containment time. As noted in Volume 2 and Section 4.4, the mechanical degradation processes are insignificant in affecting the containment time. In addition, the degradation characteristics of the waste package materials significantly impact the timing of waste package breaches.

The environmental processes acting on the waste package surface as well as the timing and extent of waste package degradation are directly related to the selected design. Reviewing the key aspects of the VA reference design as they relate to the expected behavior of the repository system is appropriate. Details of the reference design are contained in Volume 2 and are not repeated here. A schematic of the reference waste package design, including the types of waste forms to be emplaced in the Yucca Mountain repository, is depicted in Figure 2-3. Of greatest relevance to performance is that the waste package reference design which consists of two dual-barrier metals—an outer metal consisting of 10 cm (4 in.) of low carbon steel and an inner metal of 2 cm (0.8 in.) of corrosion-resistant high-nickel alloy American Society for Testing and Materials (ASTM) B 575 N06022 (Alloy 22) (ASTM 1994). Volume 2 of this document gives a more detailed description of the properties of these materials and how they are used to construct the waste package. The principal waste forms to be disposed of within these waste packages consist of the following:

- Commercial spent nuclear fuel derived from pressurized water reactors or boiling water reactors
- DOE-owned spent nuclear fuels including N-Reactor fuel from Hanford, research reactor fuel, and naval spent nuclear fuel
- High-level radioactive waste in the form of glass logs placed in stainless-steel canisters from Savannah River, South Carolina; West Valley, New York; Hanford, Washington; and Idaho National Engineering and Environmental Laboratory, Idaho



snl/trw abq09.eps  
FV3022-2

Figure 2-2. Major Components of the Total System Performance Assessment for the Viability Assessment Shown are the individual component models that together must be analyzed in evaluating the behavior of the Yucca Mountain repository system. These components comprise the individual building blocks of the TSPA analysis. The components are correlated to the four attributes of the repository safety strategy.

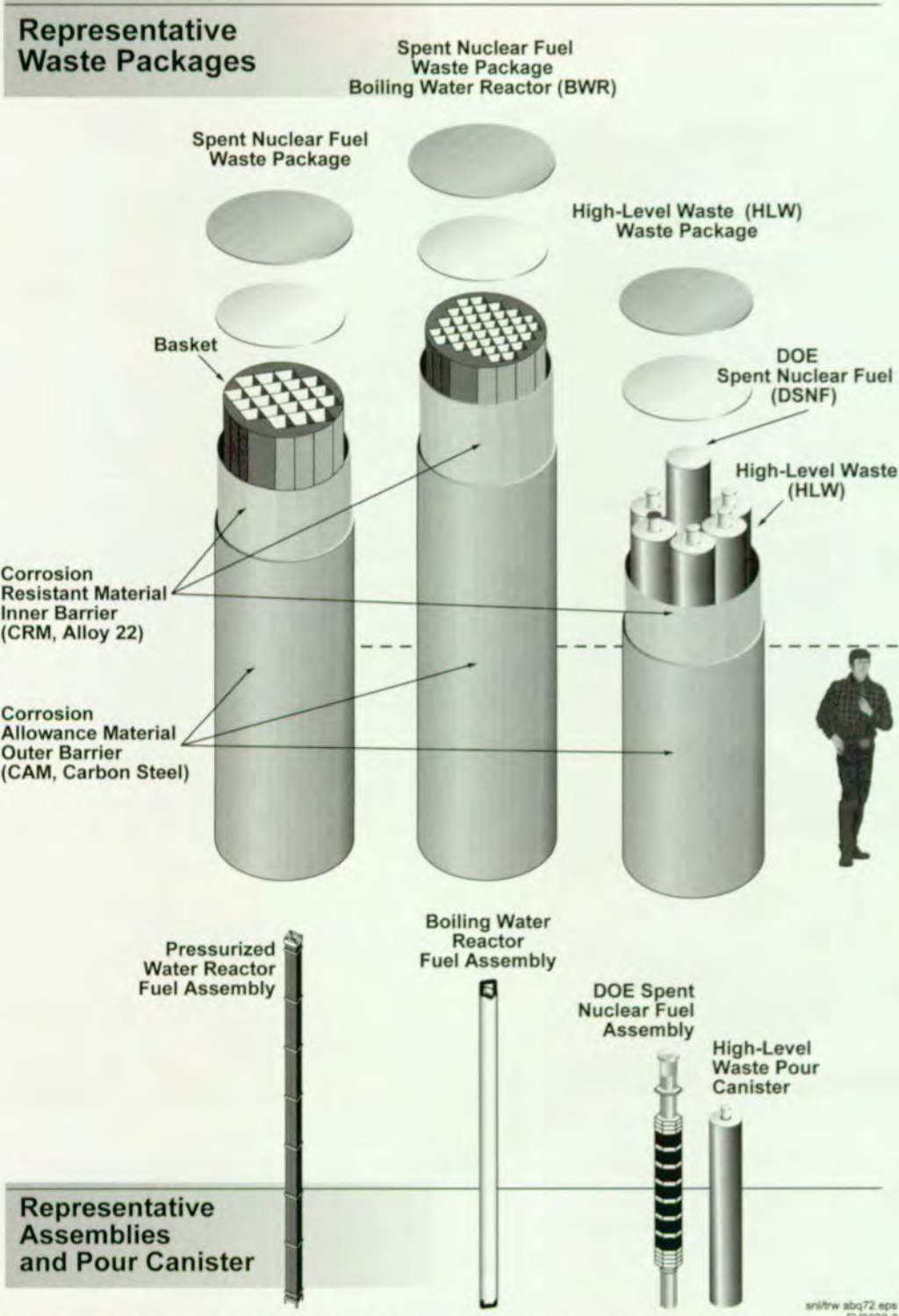


Figure 2-3. Schematic of the Reference Waste Package and Waste Form Designs Used in the Total System Performance Assessment for the Viability Assessment  
This figure illustrates the three major waste form types: commercial spent nuclear fuel (existing as either pressurized water reactor fuel or boiling water reactor fuel), high-level radioactive waste, or DOE-owned spent nuclear fuel. Also illustrated is how these waste form types would be configured in the VA waste package design. More details are presented in Section 5.1 of Volume 2.

- DOE-owned stabilized excess weapons-grade plutonium

The waste packages are designed to contain up to 21 pressurized-water reactor assemblies, 44 boiling-water reactor assemblies, 5 glass logs and co-disposal of DOE-owned spent nuclear fuel assemblies and direct disposal of other canisterized DOE spent nuclear fuels including Naval spent nuclear fuel.

A schematic of the reference repository and engineered barrier system designs is depicted in Figure 2-4. Potential design option features are discussed in Volume 2 and Section 4.5. Key aspects of the repository and engineered barrier system reference design that influence the long-term performance of the disposal system include the following:

- Areal thermal loading, which corresponds to the spacing between waste packages and between emplacement drifts
- Size of the drifts
- Lining of the drifts for mechanical stability
- Characteristics of the engineered materials placed in the drifts to support the waste package (the waste package supports and inverts)

The model components related to the third key attribute—slow release of radionuclides from breached waste packages—include all of the above components plus seepage into the waste package, cladding degradation, colloid formation and stability, waste form degradation, and transport within the waste package. Together, these components lead to a determination of the spatial and temporal distribution of the mass of radioactive wastes released from the waste packages. Each component depends on the thermal, hydrologic, and geochemical conditions inside the waste package, which change with time.

The model components related to the fourth key attribute of the repository safety strategy—low concentration of radionuclides in groundwater—include all of the above components plus radionuclide transport through the engineered barrier system, the unsaturated zone, and the saturated zone; dilution from pumping; and radionuclide transport in the biosphere. Together, these components cause the spatial and temporal variation of radionuclide concentrations in groundwater. The groundwater concentration ultimately yields the mass of radionuclides that may be ingested or inhaled by individuals exposed to that groundwater, which in turn causes a level of radiological dose or risk associated with that potential exposure. Radionuclide transport may either be by advection (radionuclide movement which occur with the bulk movement of the groundwater) or diffusion (radionuclide movement which occurs because of a concentration gradient). The concentration depends on both the mass release rate of the radionuclides as well as the volumetric flow of water along the different pathways in the different components. If the volumetric flow of water from the pumping centers is greater than the volumetric flow in which the radionuclides are contained, then dilution of radionuclide concentrations can occur at the pumping well.

Each of these key attributes and TSPA model components are used to describe the expected or probable (e.g., base case) behavior of the Yucca Mountain repository system. These components describe the features, events, or processes that are expected to occur throughout the period of interest. Other features, events, or processes can occur that could alter the behavior of the system. However, these features, events, or processes have a sufficiently low probability of occurring over the period of interest that they are not considered in the expected behavior. They may be essentially classified as unanticipated processes and events. Examples of such disruptive events include igneous activity, seismic activity, criticality events, and human intrusion. The potential consequences associated with unanticipated processes and events are considered in the TSPA analyses.

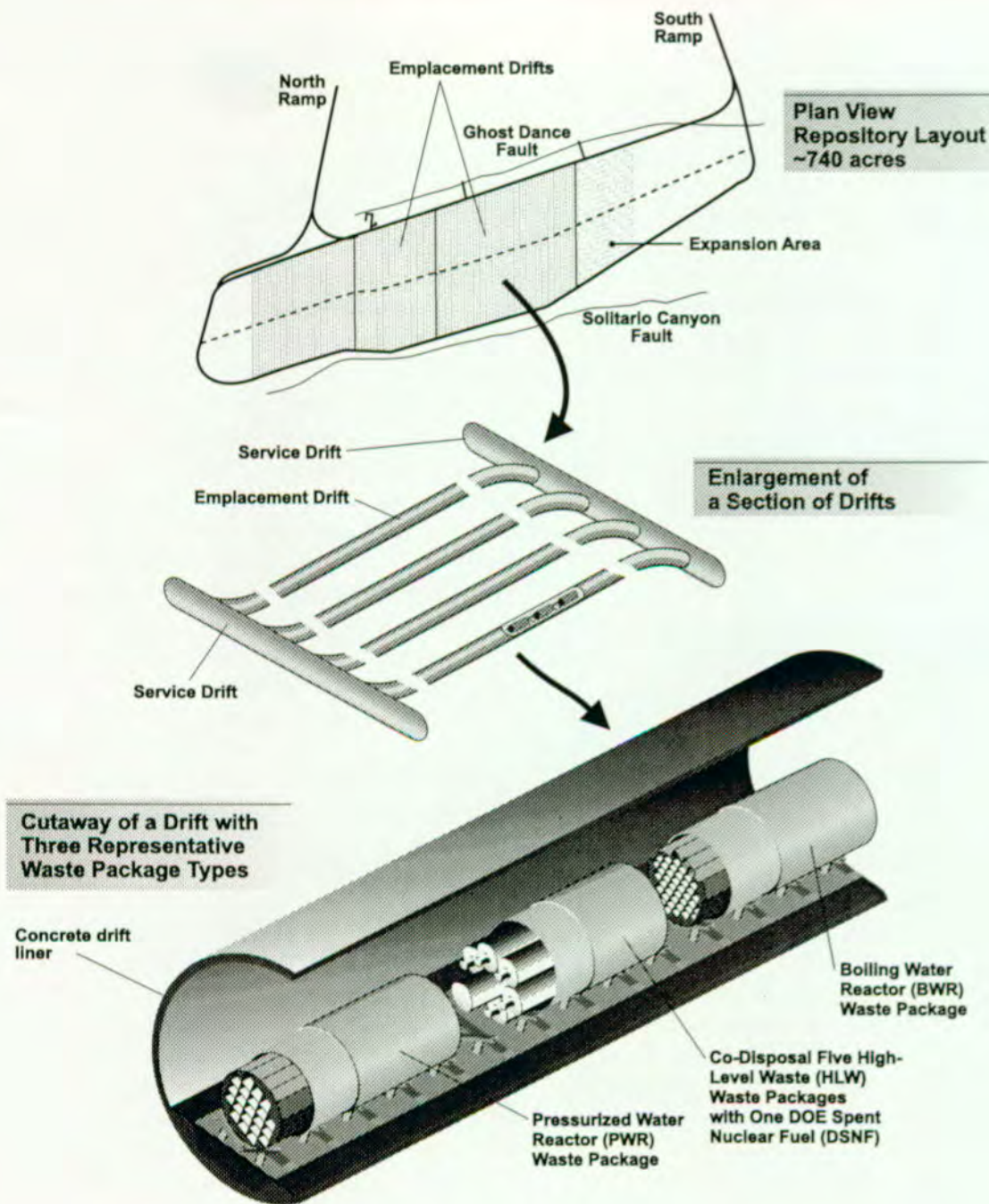


Figure 2-4. Schematic of the Reference Repository and Engineered Barrier System Designs Used in the Total System Performance Assessment for the Viability Assessment  
This figure illustrates the general drift layout within Yucca Mountain to contain the 70,000 metric tons of waste. Also illustrated is the emplacement of the waste packages on supports placed on the drift invert. More details of the reference design are presented in Sections 4.2 and 5.2 of Volume 2.

### 2.2.3 Conceptual Description of Processes Relevant to an Evaluation of Postclosure Performance

TSPA is an analysis of the long-term behavior of the repository system and the uncertainty in the analysis of that behavior. Before discussing how the analysis is performed (see Section 2.3), it is important to describe what is being analyzed. To describe what is being analyzed, it is necessary to describe the overall repository system and the components relevant to the evaluation of the repository system behavior.

The major components to be considered in the assessment of system performance and the relationship of those components to the repository safety strategy were presented in the previous sections. Described in this section are the key concepts of how the repository system is intended to work.

The basic principle of the Yucca Mountain repository safety strategy is to keep water away from the wastes. If water does contact the wastes, then the other principle of the safety strategy is to minimize the release rate of the radioactivity from the engineered barriers and reduce the concentration of any dissolved radionuclides as they migrate from the repository. The discussion that follows will focus on the small group of radionuclides that are mobile in the Yucca Mountain environment. Other radionuclides that either are very insoluble and/or highly retarded in the Yucca Mountain environment pose little risk to the environment.

Because the repository is approximately 300 m (1,000 ft) beneath the land surface and the wastes are all solids, the primary means for the radioactive constituents of the wastes to contact the biosphere, and ultimately humans, is along groundwater pathways. The wastes pose minimal risks to humans unless the following occur:

- Waste forms are exposed to water.
- Radionuclides within these waste forms are dissolved in the water.

- Dissolved radionuclides are transported with the water.
- Radionuclide-containing water is discharged, either naturally or at a pumping well, from the aquifer.
- Humans or any part of the food chain uses this water.

If water is kept away from the wastes, the wastes pose little or no threat to humans.

The presence of water is of primary concern as it contacts the waste and as any dissolved radionuclides migrate within the groundwater to expose humans to the potential effects of radiation. One of the reasons for the primary issue being related to aqueous processes is that in TSPA-VA the performance measure of concern is doses to individuals. Although gaseous transport of some radionuclides (notably iodine-129 and carbon-14) can occur, doses attributed to these release and transport mechanisms are insignificant. In following the water movement through Yucca Mountain, the major components and processes affecting the long-term isolation of radioactive wastes in the Yucca Mountain repository system are described. Also presented is a sketch of how this repository system is intended to work and a series of illustrations that picture the basic concepts that will be quantified in the TSPA.

In addition to tracking the movement of water through the repository system, the following discussion addresses a range of spatial and temporal scales. Being explicit in the definition of the scale being used is important because processes that might be explained at a spatial scale of kilometers must also be discussed at the scale of millimeters. Also, although time scales on the order of days and years are familiar concepts, it is sometimes difficult to extrapolate to the thousands or tens of thousands of years of importance in geologic systems. The discussion has been divided into six topics:

- Water movement in the unsaturated rocks above the repository

- Water and water vapor movement around the repository drifts
- Water movement within the engineered barrier system
- Water movement and radionuclide migration out of the engineered barrier system
- Water movement and radionuclide migration through the unsaturated tuffs below the repository
- Water movement and radionuclide migration through the saturated zone aquifers and biosphere

Each of these areas is discussed below.

### 2.2.3.1 Water Movement in the Unsaturated Tuffs Above the Repository

Figure 2-5 illustrates the key concepts associated with water movement in the unsaturated zone at

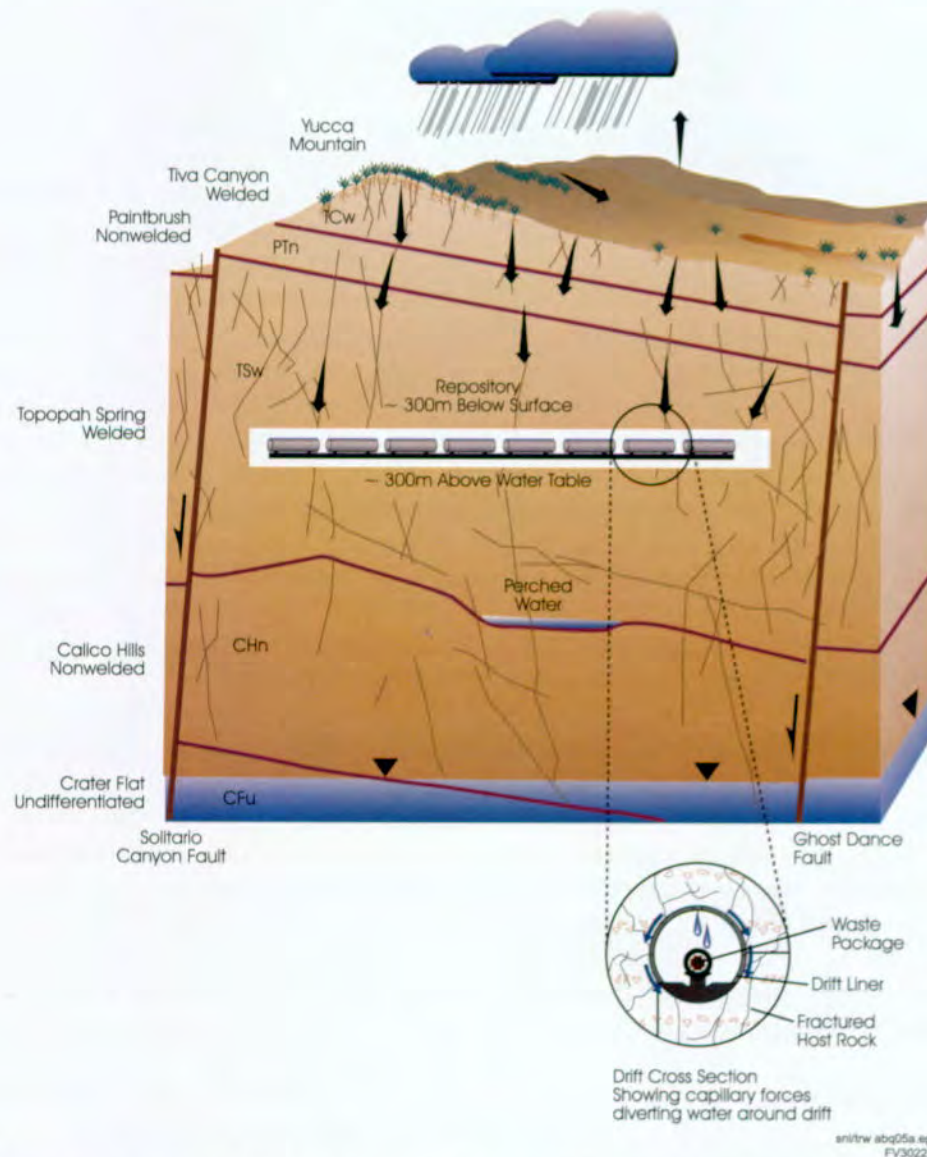


Figure 2-5. Conceptual Illustration of Water Movement Through the Unsaturated Tuffs at Yucca Mountain  
Shown is the gravity-driven flow of water through the geologic units overlying the repository and the effects of capillary forces which prevent a significant fraction of the volumetric flow from entering the drifts.

Yucca Mountain. Water at the repository horizon in the unsaturated zone at Yucca Mountain has as its source precipitation at the surface. This precipitation occurs as rainfall and snow and varies over time and space. The spatial variability is defined by precipitation being generally higher at higher elevations, such as along the crest of Yucca Mountain, and lower at lower elevations. The temporal variability is characterized annually by most of the precipitation occurring in the winter months or during brief summer thunderstorms, with the precipitation being higher during El Niño years. Because of long-term (thousands of years) climatic variations, the average precipitation in southern Nevada is expected to increase from current conditions. These long-term, transient precipitation changes may be affected by human-induced changes.

A significant fraction of the rainfall and snowmelt on the surface of Yucca Mountain either runs off into the washes that bisect the mountain, evaporates from the surface, or transpires from the native plants in the area (Volume 1, Section 2.2.3.2). The remaining water continues downward through the soil horizon and eventually infiltrates into the rock. The net amount of total precipitation that infiltrates is called net infiltration. The net infiltration varies with space and time. The spatial variability is caused by variations in precipitation, soil conditions (permeability, thickness, and antecedent water content), geographic conditions (slope angle and slope direction), and vegetation conditions. The temporal variability is caused by the variability in precipitation.

The net infiltration of water moves downward through the unsaturated zone, driven primarily by gravity (Volume 1, Section 2.2.5.1). In the unsaturated zone, this downward movement of water is called percolation flux to distinguish it from infiltration, or movement of water in the soil horizon. Some lateral diversion of water occurs as it moves downward from the soil horizon through the unsaturated zone. This lateral diversion is caused by the eastward dip of the geologic strata and the heterogeneities in the rock because of the different welded and nonwelded tuffaceous lithologic units between the surface and the repository. Although

the water may be spatially and temporally distributed at depth, this distribution is generally a subdued reflection of the infiltration distribution at the surface because gravity drainage drives the groundwater flow system in the unsaturated zone (CRWMS M&O 1997n).

Water movement or flux in the unsaturated, fractured tuffs occurs in the matrix and the fractures of the rock. Generally, the welded tuff layers have more of the total flux within the fractures because the permeability of the matrix is low, while the non-welded lithologic layers have more of the total flux within the matrix. The capillary forces tend to cause the water to move from the fractures, which are characterized as having a low suction, into the matrix, which has a high suction. This process is called matrix imbibition. The process is more prevalent in rock units with lower matrix saturation (e.g., the Tiva Canyon welded unit) and less significant when the matrix saturation is higher (e.g., the Topopah Spring welded units) or the fracture spacing is large (e.g., the Paintbrush non-welded unit) (Volume 1, Section 2.3.2.2). Although most of the flux occurs in the fractures, most of the water resides in the matrix.

#### 2.2.3.2 Water and Water Vapor Movement Around the Repository Drifts

Figure 2-6 illustrates the key concepts associated with water movement around the repository drifts after waste emplacement at Yucca Mountain. Without heat-producing wastes in the drifts, the water in the unsaturated rocks around the repository drifts will tend to stay in the rocks and flow around the drifts rather than drip into the drifts. Water stays in the rocks because the rock's capillary forces, including the fractures that contain most of the water flux, are greater than the gravitational forces required for causing a seep unless the fractures are almost fully saturated (see Section 3.1).

The characteristics of the rock around the repository openings may change with time. The fracture permeability could increase because of mechanical stress relaxation following the construction of the

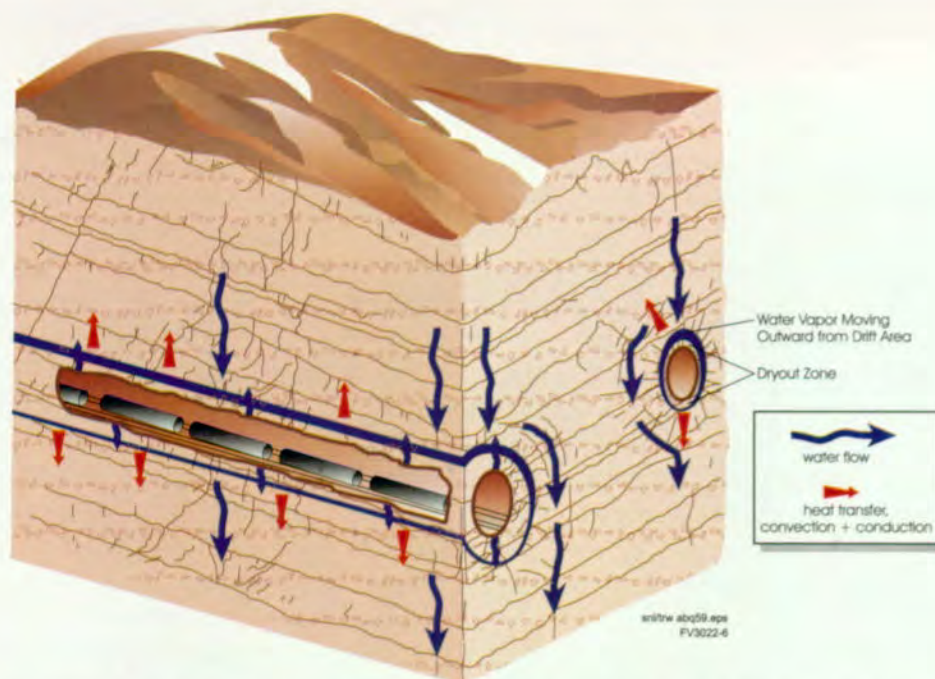


Figure 2-6. Conceptual Illustration of Water and Water Vapor Movement Around the Repository Drifts During the Thermal Period

Shown is the movement of water vapor away from the repository drifts and recondensation in the cooler zones overlying and adjacent to the drifts. This figure represents a time period that extends for several hundred years following waste emplacement.

repository drifts and ultimately the collapse of the drifts. The fracture permeability could decrease because the interaction of emplaced materials causes fractures to plug. The capillary suction of the fractures could either increase or decrease because of these same processes. However, these changes are expected to be within the range of natural variability existing before construction of the facility. The net amount of seepage and the fraction of the repository area in which seepage is expected to occur are important factors in the overall performance assessment, because they determine the likelihood that individual waste packages will be contacted by seepage water (see Section 3.1.1.4).

Water seepage from the rock into the drifts will be affected during the operational phase of the facility by the ventilation of the repository. The ventilation will take moisture from the drifts and the rock in the form of water vapor.

Following waste emplacement, the heat generated by radionuclide decay will drive moisture in the rock away from the heat source, that is, away from the spent nuclear fuel containers in drifts. This water recondenses in areas of lower temperature above, below, and between the hotter drifts. During the first few hundreds to thousands of years, there will be little or no seepage of liquid water into the drifts, because the water is generally being driven away. During this time, water in the drifts is in the form of water vapor or humid air. During the early periods, the relative humidity in the drifts is reduced, but the relative humidity eventually increases to close to 100 percent.

The distribution of liquid water and humid air within and around the repository drifts is variable in space and time. The spatial variability is caused by heterogeneity in the rock properties and variations in the ambient percolation flux. In addition, differences in the thermal output of different waste packages cause a range of thermal-hydrologic conditions in the repository. For example, cooler

regions are expected along the edges of the repository. The temporal variability in water movement around the drifts is caused in the short term (hundreds of years) by the thermal output of the wastes that eventually declines to minimal values; in the long term, the water movement is controlled by the climatic variability discussed above.

### 2.2.3.3 Water Movement Within the Engineered Barrier System

Figure 2-7 illustrates the key concepts associated with water movement within the drifts and the contact of water with the waste package. Water in aqueous or vapor form can cause degradation of the metallic waste package barrier. The dominant degradation mode of the outer mild steel is by aqueous or humid air corrosion. At low relative humidities and in the absence of liquid water, the corrosion rate of mild steel is generally low; however, at high relative humidities or in the presence of liquid water, this metal can corrode, exposing the inner corrosion-resistant metallic barrier composed of a high-nickel alloy, Alloy 22.

The Alloy 22 layer generally degrades only in the presence of liquid water (i.e., when water drips directly on the waste package). Alloy 22 is generally immune to localized pitting and crevice corrosion and most failures will be by slow general corrosion.

The degradation rates of the carbon steel and high-nickel alloys are also affected by the temperature of the waste package surface, the chemistry of the water in contact with the waste package surface, and the degradation characteristics of the metals themselves. Because these environmental parameters are spatially variable and because the metal fabrication is variable, the waste package degradation is also expected to be variable in space and time. Not all of the waste packages are expected to be breached at the same time. In addition, the temporal variability in degradation rate implies that, once a single opening exists through the metallic waste package, it takes additional time before more openings exist through the waste package.

Until the same waste package has been sufficiently degraded to allow an opening to form through the two metallic barriers, there is no possibility for water to come into contact with the wastes. During this period, the wastes are completely contained within the waste package. Once an opening exists, some of the seepage water falling on the waste package could enter the package.

### 2.2.3.4 Water Movement and Radionuclide Migration out of the Engineered Barrier System

Figure 2-8 illustrates the key concepts associated with water moving into the waste package and contacting the waste form. Also illustrated is migration through the engineered barrier system of radionuclides that may exist as either dissolved species or adsorbed onto colloidal particles.

After waste package has been breached, water may enter the waste package and contact the waste forms. For commercial spent nuclear fuel and many types of DOE-owned spent nuclear fuel, this water will first come into contact with the Zircaloy cladding around the spent nuclear fuel pellets. Zircaloy is a highly corrosion-resistant metal alloy; it is even more resistant to the effects of generalized or localized corrosion than is Alloy 22. (Although Zircaloy has been considered as a candidate waste package material, the high cost of this alloy precludes its use in the VA reference design.) Zircaloy eventually will degrade with time under several different mechanisms, but for a certain period it will prevent water from directly contacting the wastes. For high-level radioactive waste, a stainless-steel pour canister surrounds the waste glass. For much of the DOE-owned spent nuclear fuel, the wastes are contained within aluminum or Zircaloy cladding of questionable integrity, which in turn are planned to be placed in stainless steel or other metal alloy canisters. Aluminum and stainless steel are not as corrosion resistant as Zircaloy and do not provide significant protection for the wastes contained within them.

When the material surrounding the actual waste form has degraded, the wastes are exposed to the environment inside the waste package and liquid

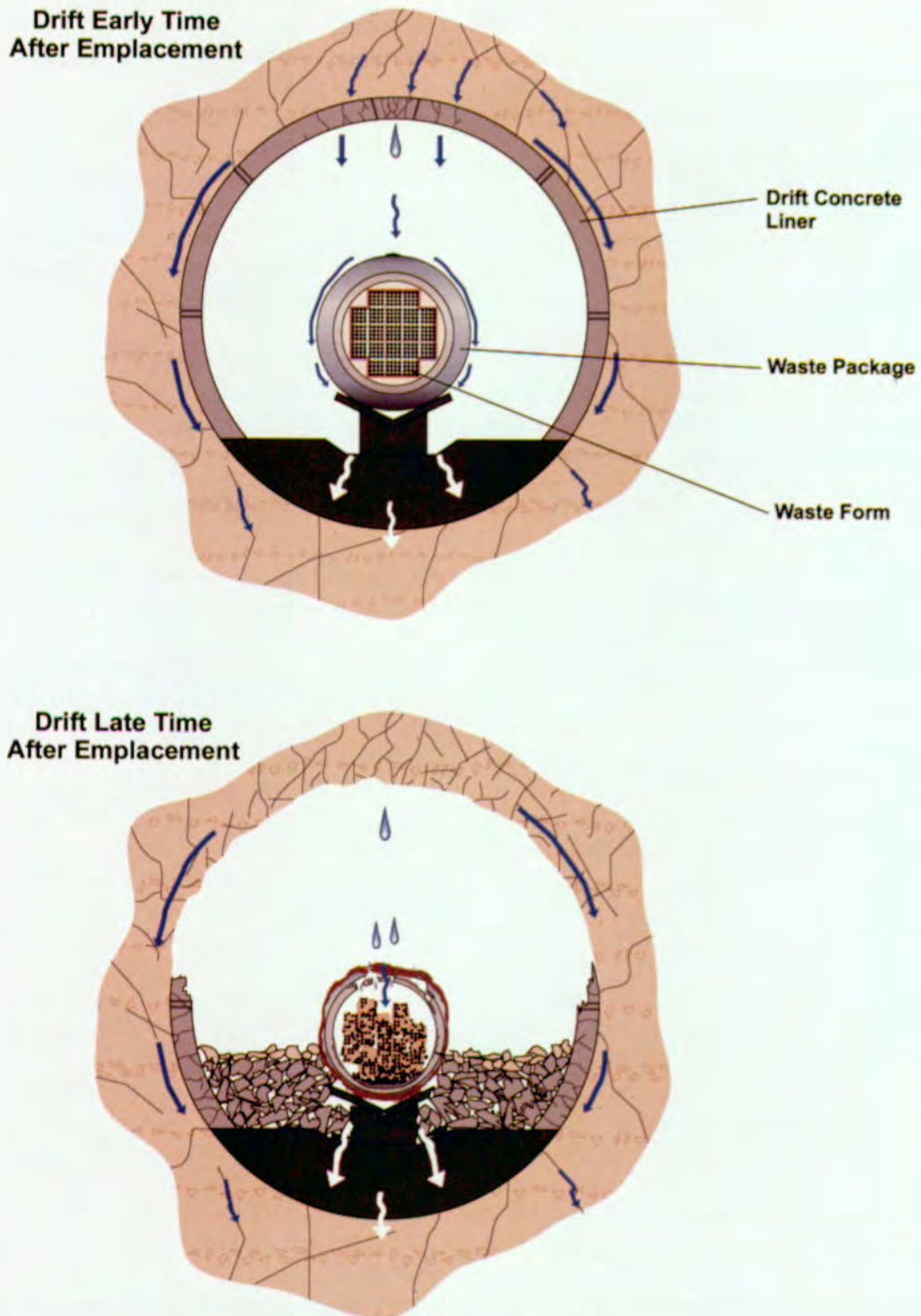
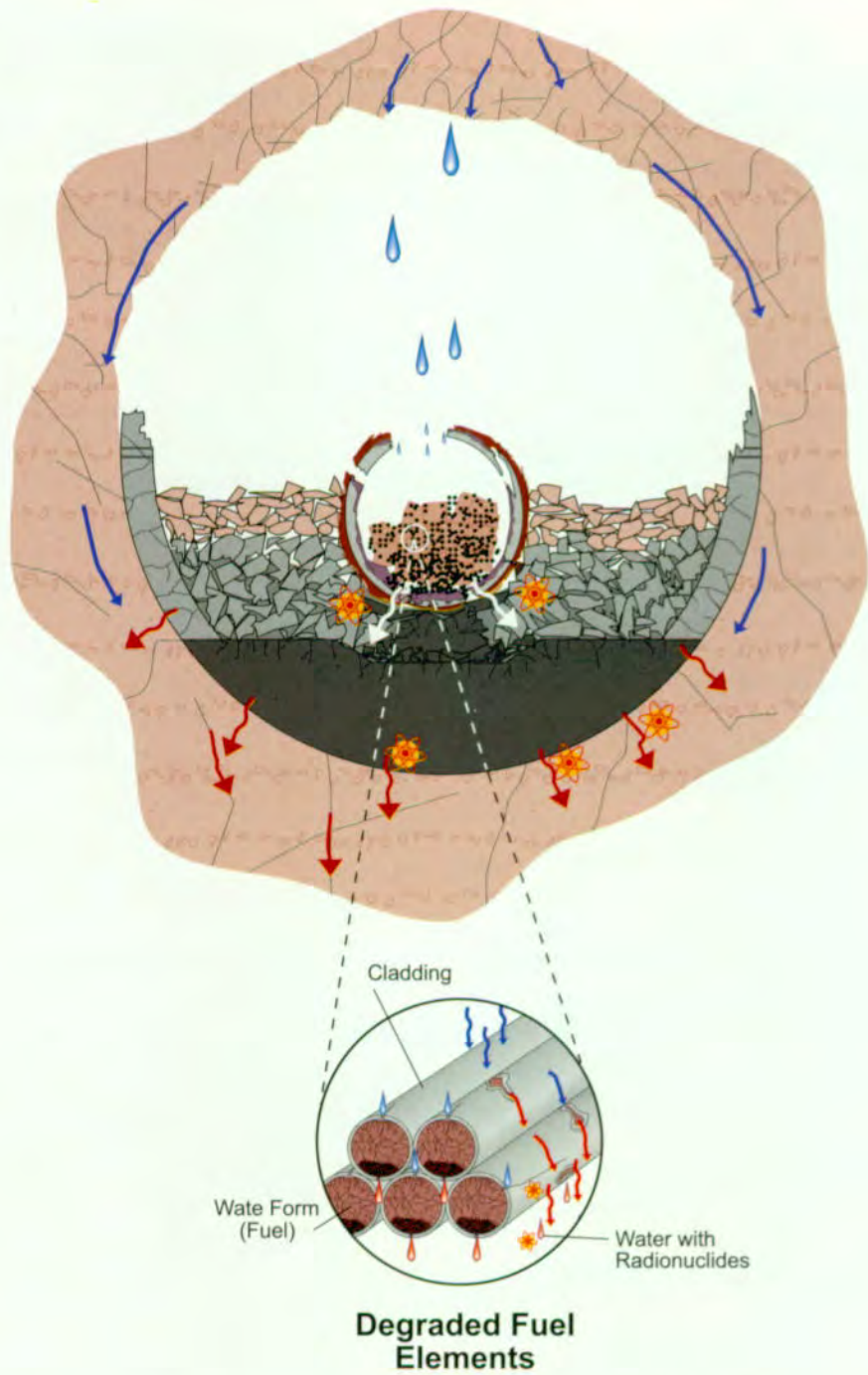


Figure 2-7. Conceptual Illustration of Water Movement into and Within the Engineered Barrier System  
Shown is the movement of water between the drift walls and the waste package prior to the degradation of the waste packages. Also shown is the movement of water through degraded waste packages following the breach of the outer and inner containers by aqueous corrosion. The time for an initial breach of a waste package can vary from several thousand to several million years.



snl/trw abq89.eps  
FV3022-8

Figure 2-8. Conceptual Illustration of Water Movement and Radionuclide Transport out of the Engineered Barrier System  
Shown are potential water pathways within the waste package that may lead to water coming into direct contact with the waste. These pathways would not be initiated until the waste package has been breached, which may take several thousands to millions of years. Once radionuclides have been dissolved in the water, they may be transported along discontinuous pathways within the waste package, through the waste package, and through the drift invert into the unsaturated tuffs.

water can contact a portion of the exposed waste. If water contacts the waste form, the radionuclides can dissolve in the water. Some radionuclides are highly soluble in water, while others are very insoluble in the water that is likely to contact the waste. Some radionuclides may be attached to very small colloids that may also be mobile in the water.

When radionuclides are released from the solid waste form into the mobile liquid phase, they are available for transport. The transport mechanism depends on the distribution of water on the waste form surface and between the waste form surface and the outer edge of the degraded waste package. If water has dripped into the waste package, it is possible that advective transport of radionuclides to the edge of the waste package could occur. If the water has not dripped into the waste package, then a continuous, interconnected water film along which radionuclides may diffuse is required.

After radionuclides are transported through the degraded internal material of the waste package to the edge of the waste package, they may be transported through the degraded invert materials beneath the waste package. Radionuclides may be transported through the degraded invert by either moving water if there is seepage water, or diffusion through the pores of the invert materials. The radionuclides transported through the degraded invert are ultimately released to the tuff rock units to be transported in the unsaturated zone below the repository and ultimately to the saturated zone.

The rate at which radionuclides are released and transported from the repository depends on the following:

- Degradation rate of the engineered barriers
- Dissolution rate of the waste forms
- Form of the released radionuclides
- Solubility of the aqueous radionuclides
- Rate of water movement and volume of water that flows through the engineered barriers

In the absence of any water seepage coming into direct contact with the wastes, radionuclide releases from the engineered barriers will be minimal, with the possible exception of gaseous releases of radionuclides which are of no significant consequence to the public.

#### **2.2.3.5 Water Movement and Radionuclide Migration Through the Unsaturated Tuffs Below the Repository**

Figure 2-9 illustrates the key concepts associated with water movement in the unsaturated rocks beneath the repository and the migration of radionuclides in these rocks. After the dissolved or colloidal radionuclides are released into the unsaturated tuffs beneath the repository, they may be transported with the water to the water table. The rate at which these radionuclides are transported to the water table is a function of the following:

- Percolation flux in the unsaturated tuffs
- Distribution of the percolation flux between fractures and matrix
- Effective velocity of the groundwater within the fractured rocks
- Adsorption of radionuclides within the rock

Because each of these characteristics of the natural environment is variable in space and time, radionuclide transport is also variable. Part of the temporal variability relates to long-term climatic changes that not only change the percolation flux through the system but also cause the water table beneath Yucca Mountain to rise (in the case of wetter climates) or fall (in the case of drier climates).

#### **2.2.3.6 Water Movement and Radionuclide Migration Through the Saturated Zone Aquifers and Biosphere**

Radionuclides that are transported through the unsaturated zone are released to the saturated aquifers beneath the repository. Figure 2-10 illustrates the key concepts associated with water

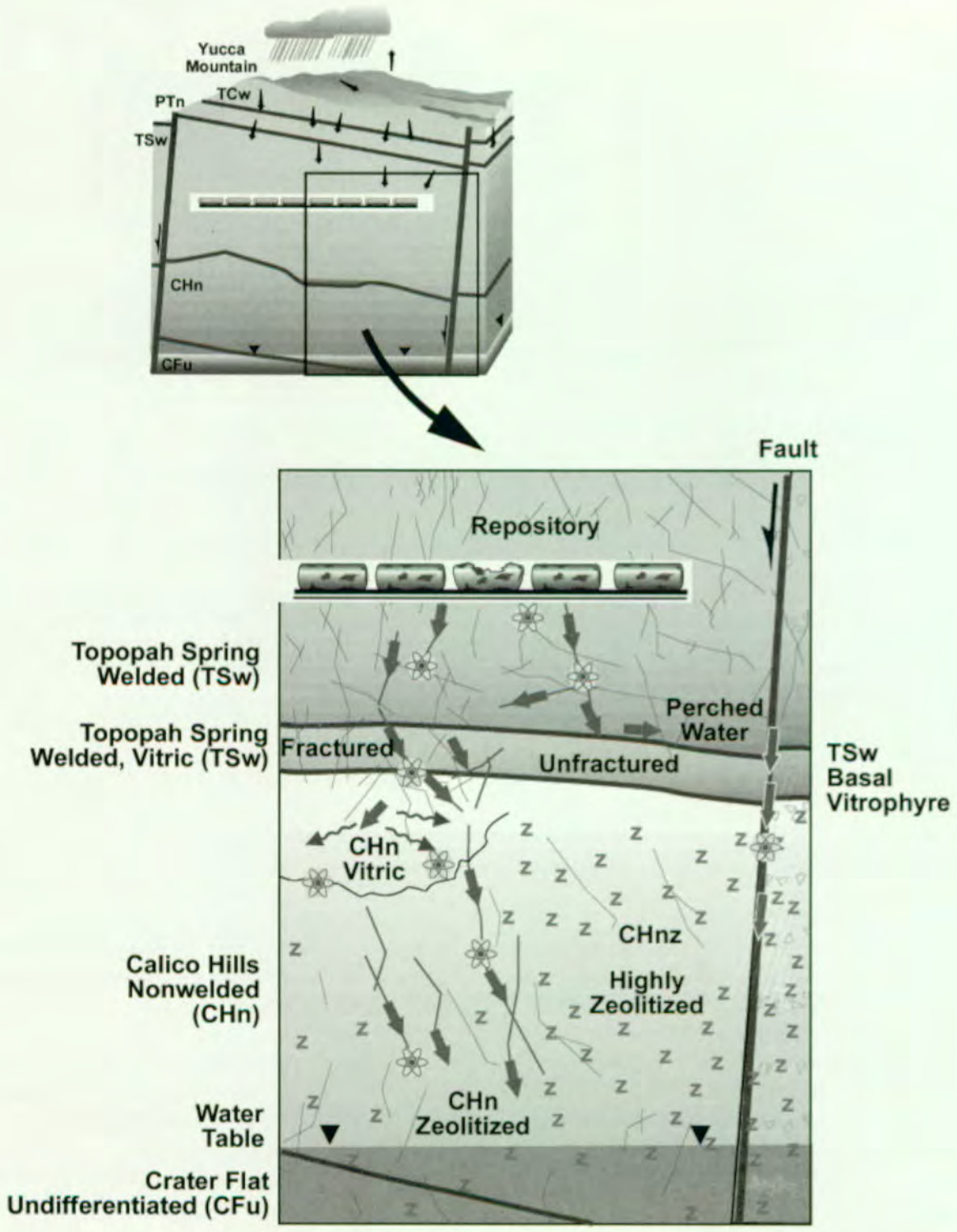


Figure 2-9. Conceptual Illustration of Radionuclide Transport Through the Unsaturated Tuffs at Yucca Mountain  
Shown is the gravity-driven transport of radionuclides through the unsaturated zone. Also illustrated are retardation mechanisms that delay the arrival of radionuclides to the saturated aquifers located several hundred meters beneath the repository. The mean advective travel time through the unsaturated zone is on the order of several thousand years for unretarded radionuclide species in the current climate.

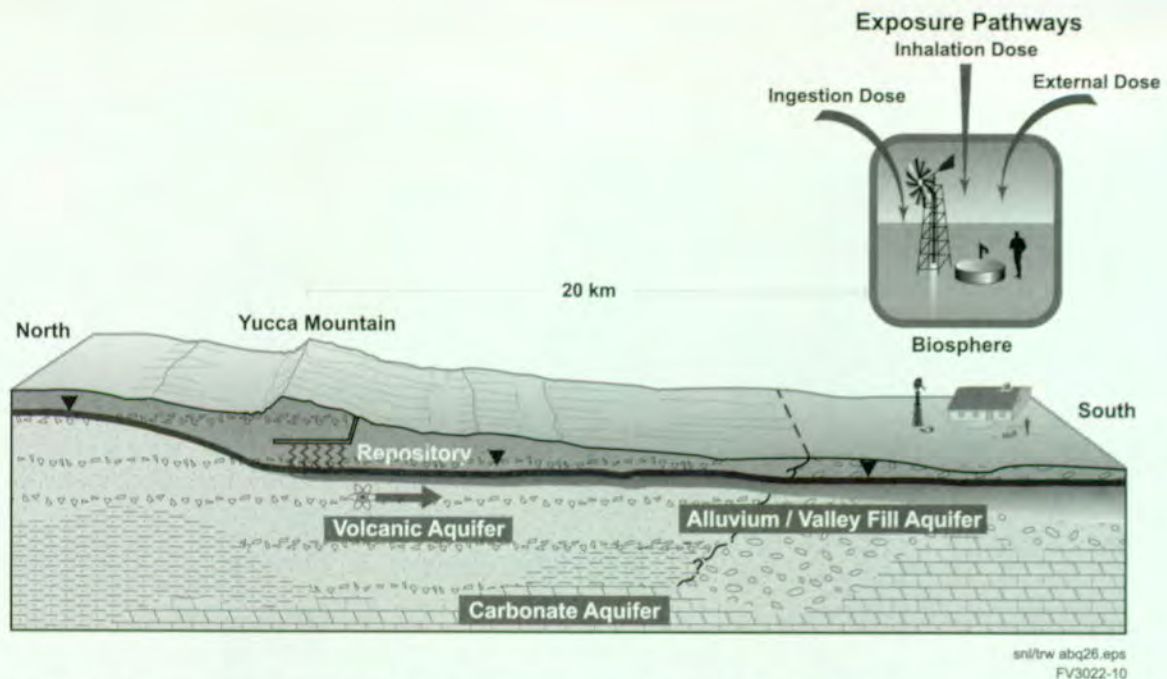


Figure 2-10. Conceptual Illustration of Radionuclide Transport Through the Saturated Tuffaceous and Alluvial Aquifers and the Biosphere

Shown is the lateral migration of any dissolved radionuclides that reach the water table downgradient from the repository. The mean advective travel time through the saturated zone to a point 20 km (12 miles) downgradient is on the order of several thousand years for unretarded species in the current climate. Also shown are potential biosphere pathways by which radionuclides that are dissolved in water may be extracted from the alluvial or tuff aquifers and come into contact with humans.

movement in the saturated aquifers beneath and downgradient from the Yucca Mountain site and the migration of radionuclides in these aquifers. Also illustrated are the pathways by which any dissolved radionuclides may come into contact with humans.

When the radionuclides reach the saturated zone, they will be transported laterally within the saturated zone. The general direction of groundwater flow in the saturated zone is to the southeast, and then possibly to the south and southwest. The concentration of the radionuclides in the saturated zone aquifers at any point downgradient from the repository is a function of the following:

- Radionuclide concentrations in the water that enters the saturated zone
- Dispersion of these radionuclides as they are transported

- Adsorption of these radionuclides on the mineral surfaces along the flow path

The time for radionuclides to reach any specified point downgradient from the repository, such as the 20-km (12-mile) point chosen for evaluating the system performance, depends primarily on the groundwater velocity and the retardation of radionuclides which may sorb on the mineral surfaces within the tuff or alluvial aquifers.

There is minimal risk associated with radionuclide releases as long as the concentration of radionuclides in water that is pumped from the aquifers downgradient from the repository is sufficiently low. Should radionuclides reach a location downgradient from the repository where water is pumped from the aquifer, the potential exists for radionuclides to come into contact with humans through biosphere pathways. The principal biosphere pathways to humans consist of the following:

- Direct consumption of water containing dissolved radionuclides
- Watering of livestock and the subsequent consumption of meat or milk
- Consumption of crops and animal products produced using water containing dissolved radionuclides
- Direct exposure to contaminated soil
- Inhalation of dust that may contain attached radionuclides

The previous discussion outlined how the various components of the Yucca Mountain repository system fit together to describe how the system is intended to work. The general conceptual aspects of each key component and processes that affect the expected behavior of the repository system have been described. The next section (Section 2.3) describes the approach used to assemble the representations of the individual components into a description of the entire system. The details of each of the component models used in the TSPA and the scientific bases for these models are presented in Section 3 and the *Total System Performance Assessment-Viability Assessment (TSPA-VA) Analyses Technical Basis Document* (CRWMS M&O 1998i).

## 2.3 METHODOLOGY

This section presents an overview of the method for mathematical and numerical modeling of each process and component introduced in Section 2.2, including their uncertainty, and the approach for combining them into an overall model and computer code. This overview includes discussions about information flow between the models (Section 2.3.1) and the computer code architecture that facilitates the information flow (Section 2.3.2). This section provides a road map of how to recouple the component models into one integral whole, to reassemble the analyzed pieces and pass information between them to develop reasonable assessments of overall system performance. The method for correctly coupling the component

models to make robust predictions of repository behavior is comprised of the basic activities outlined in Section 1.3. More detail on these activities as they apply to the Yucca Mountain TSPA is given in *Total System Performance Assessment - Viability Assessment (TSPA-VA) Methods and Assumptions* (CRWMS M&O 1997m).

In addition to modeling and analyzing the system, the TSPA methodology presents the key results, focusing on the influence of uncertainty on the performance predictions. As mentioned in Section 2.2, the 1997 Energy and Water Appropriations Act requests an analysis of the "probable behavior of the repository." The base case models described in Section 3 are intended to represent this probable behavior. The exact definition of "base case" depends on the choice of parameter ranges for each component model. In this context, the use of the term "range" is important. In particular, the TSPA-VA base case parameter sets and conceptual models encompass a range of uncertainty for the various parameters rather than just one realization of the parameters. Given the base case definitions of these various parameter ranges for the model components, a base case TSPA model is constructed to predict overall repository performance (see Section 2.3.3). This model represents an assessment of the likely or probable range of future behavior for the overall repository system, which is essentially a combination of the likely ranges of behavior for the various component models, processes, and corresponding parameters.

In addition to base case repository performance, behavior that is considered less likely is captured in the sensitivity cases for alternative models and parameter ranges of the various processes (see Section 5). Besides alternative models and parameter ranges, other sensitivity cases (features, events, and processes not included in the base case) examine the effect of repository design options (see Section 4.5) and disruptive events such as volcanism (see Section 4.4).

Because of the inherent uncertainty in the performance predictions, the TSPA-VA results are provided in two main forms:

- Probability distributions, such as complementary cumulative distribution functions (CCDFs), for peak dose rate to a receptor 20 km (12 miles) downgradient of the repository, during a certain time (see Section 4.3).<sup>1</sup>
- Time histories over 10,000 years, 100,000 years, and 1 million years of the dose rate at 20 km (12 miles) downgradient of the repository, for specific samplings of the input parameters. A dose-rate realization generated by using the expected values from all input parameter distributions is used to describe and explain future repository behavior, in particular, how the various components and subsystems interact with one another (see Section 4.2).

Various sensitivity analysis methods for determining the most influential system parameters are also used (Section 4.3). These analyses include methods for displaying the results in a way that most transparently demonstrates the key natural and engineered barrier parameters and features (e.g., plots of correlation coefficients versus time). This helps prioritize future site-characterization efforts and delineate best possible design options.

### 2.3.1 Information Flow Between Component Models

A stylized conceptualization of the TSPA-VA model hierarchy and information flow is shown in Figures 1-1 and 2-1. These figures indicate a continuum of information and models, from the most basic, detailed level to the level of the total system model. The data and associated conceptual and process-level models rest at the base of the pyramid. These process-level models may be simplified or abstracted,<sup>2</sup> if necessary, because of computational constraints or lack of information. The abstracted performance assessment models may have a one-to-one correspondence with the detailed process-level models or may represent a combined subsystem model<sup>3</sup> covering several aspects of the overall system. The performance assessment models form the components of the overall TSPA model at the top of the pyramid. Total-system model simulations can then be performed in the computationally intensive probabilistic framework necessitated by a Monte Carlo approach to performance assessments.<sup>4</sup>

For this model simplification process, there are two key factors in accurately representing the performance of the overall system. First, information

---

<sup>1</sup> For example, based on uncertainty in the input parameters, the analysis consists of randomly sampling all input parameters 100 times to generate 100 realizations of repository performance. Each realization, being a unique combination of the input parameters, will produce a different prediction of dose rate versus time. From each of these 100 dose rate histories, the peak dose that occurred at any time during a specific time period is selected, for example, during the first 10,000 years after closure of the repository. These peak doses are then plotted as a probability distribution to answer the following question: What is the probability of exceeding dose rate  $x$  during the first 10,000 years?

<sup>2</sup> The word *abstraction* is used to connote the development of a simplified mathematical and/or numerical model that reproduces and bounds the results of an underlying detailed process model.

<sup>3</sup> Examples of various subsystems include the engineered barrier system, the unsaturated zone, and the saturated zone.

<sup>4</sup> Much of the modeling of the repository and its components is complex, uncertain, and variable, involving a variety of coupled processes (thermal-hydrologic-chemical and thermal-hydrologic-mechanical) operating in three spatial dimensions on a variety of different materials (e.g., fuel rods, waste packages, inventory, and host rock) and changing over time. For these reasons, it is often necessary to make some simplifications to the detailed process-level models. The need for simplification is particularly evident in TSPA, which has a significant component of probabilistic risk analysis. The general approach of using probabilistic risk analysis is appropriate because of the inherent uncertainties in predicting physical behavior many thousands of years into the future in a geologic system with properties that can never be fully characterized deterministically. Because of the large number of uncertain parameters in the component TSPA models, probabilistic risk analysis involves a Monte Carlo method of multiple realizations of system behavior, which requires significant computational resources. For this reason, and because the lack of certain data makes some detailed models difficult to quantify, model abstractions are often employed.

passed up the model pyramid must be consistent. For example, an infiltration flux used to generate liquid flow fields from the detailed process model for the unsaturated zone must be used in all subsequent analyses based on those particular flow fields. The same flux must be used when calculating seepage flux in the abstracted seepage subsystem model (see Section 3.1) and when calculating thermal-hydrologic response (temperature and relative humidity) in the near-field environment (see Section 3.2). Second, the parameters that most affect performance in the detailed process models must be appropriately represented in the subsequent subsystem and total system models, including the appropriate uncertainty range of the parameters.

A key feature of the methodology is how to pass uncertainty at one level to uncertainty at another level. As Figure 1-1 illustrates, transfer of uncertainty must go in both directions, from bottom up and from top down. When analyzing uncertainty at the bottom levels (data, conceptual models, and process models), the analyses look at the effect of uncertain parameters on surrogate or subsystem performance measures such as the amount of fracture flow in the unsaturated zone. The sensitivity of the surrogate measure to component model uncertainty is then used to decide whether to carry this uncertainty through to the total system analyses. However, sometimes important parameters at the subsystem level prove to be unimportant at the overall system level and then this information is passed down the pyramid to indicate the relative unimportance of collecting more physical data about this parameter.

Traceability of data transfer amongst models and quality assurance of the data are very important aspects of the information flow process. The *Total System Performance Assessment-Viability Assessment (TSPA-VA) Analyses Technical Basis Document* (CRWMS M&O 1998i), which supports the TSPA results presented here, explicitly identifies the source and status of data, computer codes, and computer input and output files used in the VA. The *Total System Performance Assessment-Viability Assessment (TSPA-VA) Analyses Technical Basis Document* (CRWMS

M&O 1998i) will form the basis for development of the DOE TSPA data qualification plans. Following prescribed procedures, DOE is reviewing the data, assumptions, computer codes, and information used in the TSPA analyses to ensure the models are valid, defensible, and appropriate. DOE has developed a transition plan to take the TSPA reported here to qualified status for the LA. To be fully qualified, there must be clear documentation that the TSPA models are supported by qualified data and the numerical models and computer codes are documented and appropriately controlled.

Figure 2-11 is a more detailed, but still simplified, look at information flow among the eight key component models: unsaturated zone flow (and seepage), thermal hydrology, near-field geochemistry, waste package degradation, waste form alteration and mobilization, unsaturated zone transport, saturated zone flow and transport, and biosphere. It does not show all of the couplings among TSPA-VA component models but does illustrate major model connections, abstractions, and information feeds. "Response surface" means a multi-dimensional table of output from one model to be used as input in another model. When interpolating among points in the table, linearity is generally assumed. Usually a response surface has more than one dependent variable (e.g., both time and percolation flux). However, in the usage in Figure 2-11, sometimes time is the only independent variable, and interpolation is not even necessary between the time points (e.g., the data are provided directly "as is" to the next model).

Figure 2-12 is a more detailed description of information flow in the TSPA-VA, showing the principal pieces of information passed between the various component models. These details of information flow are explained in greater depth in the discussion of the TSPA-VA code architecture in the Section 2.3.2 and in the description of the TSPA-VA base case in Section 4.1. The conceptual and experimental basis for this depiction of information flow is given in detail in Section 3. For example, the division of the repository horizon into six regions based on thermal-hydrologic response and infiltration flux is

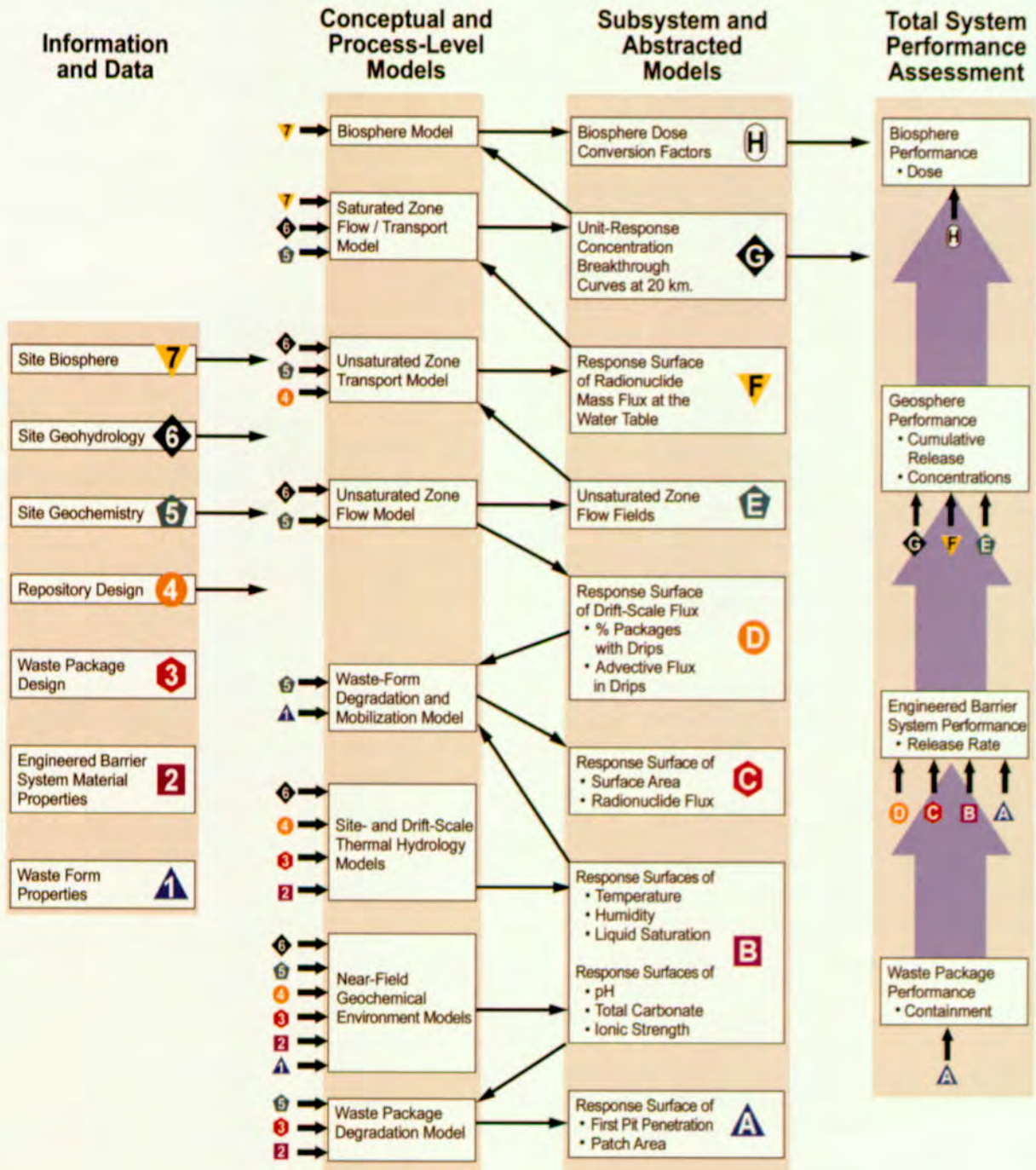


Figure 2-11. Simplified Representation of Information Flow in the Total System Performance Assessment for the Viability Assessment Between Data, Process Models, and Abstracted Models

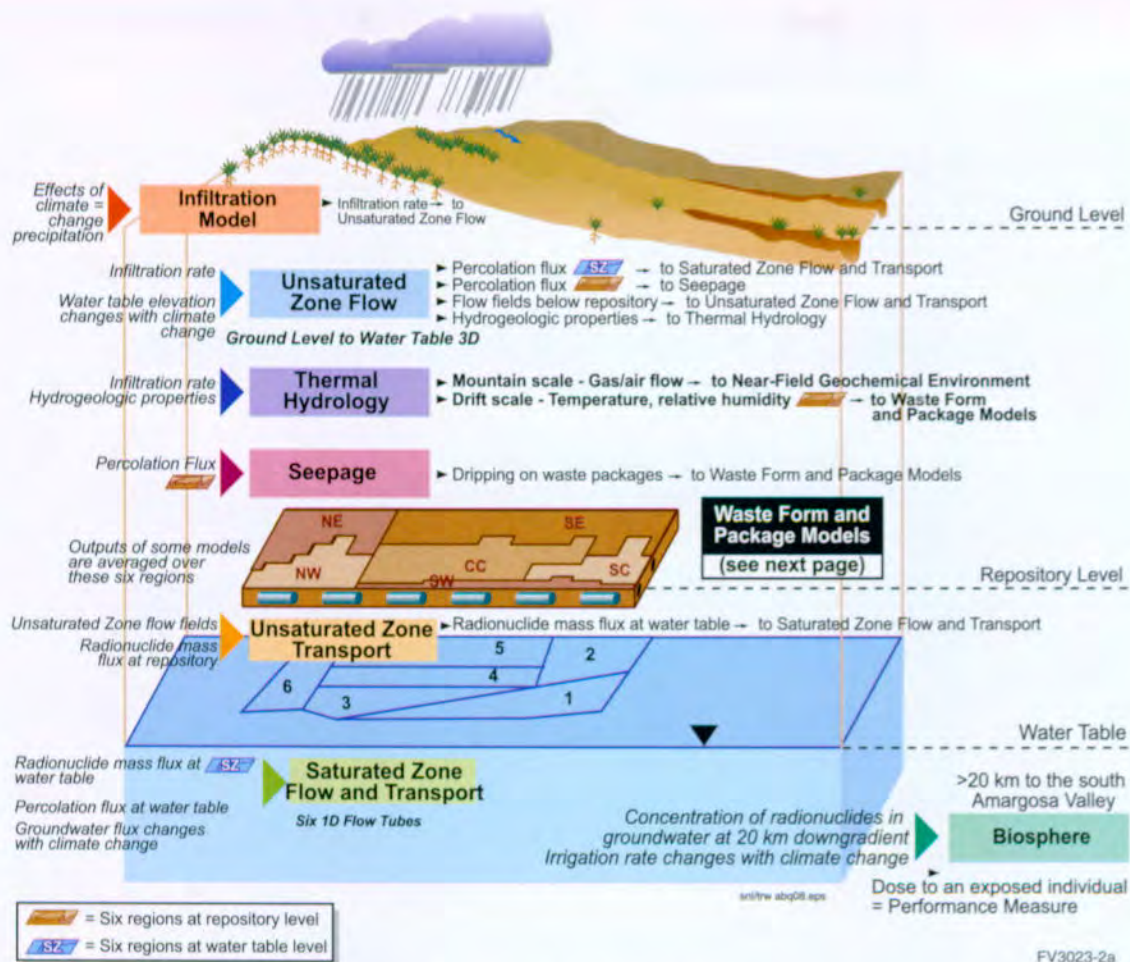


Figure 2-12a. Detailed Representation of Information Flow in the Total System Performance Assessment for the Viability Assessment

This figure is in two parts with the detail of the waste package and waste form models shown in Figure 2-12b.

discussed in Section 3.2; and the division of the saturated zone water table into six regions, unrelated to the six repository regions, based on stratigraphy and other factors is discussed in Section 3.7.

The decoupling of the physical-chemical processes into component models, shown in Figures 2-11, 2-12, and 2-2, is facilitated by a natural division of the repository system into a series of sequentially linked spatial domains (e.g., the waste package, emplacement drift, host rock near the drift, unsaturated zone between the drift and the water table, saturated zone, and biosphere). This division works best from the standpoint of radionuclide transport, which is the primary consideration of the TSPA models. The TSPA-VA model architecture and

information flow becomes, therefore, a sequential calculation in which each spatially based transport model may be run in succession, with output as "mass versus time" from an upstream spatial domain serving as the input of mass versus time for the spatial domain immediately downstream.

### 2.3.2 Code Architecture

The overall model architecture and information flow, discussed in the previous section, forms the basis for the architecture of the overall TSPA-VA computer code. The executive driver program or integrating shell that links all the various component codes is RIP V5.19.01 (Golder Associates, Inc. 1998). It is a probabilistic sampling program that ties all the component

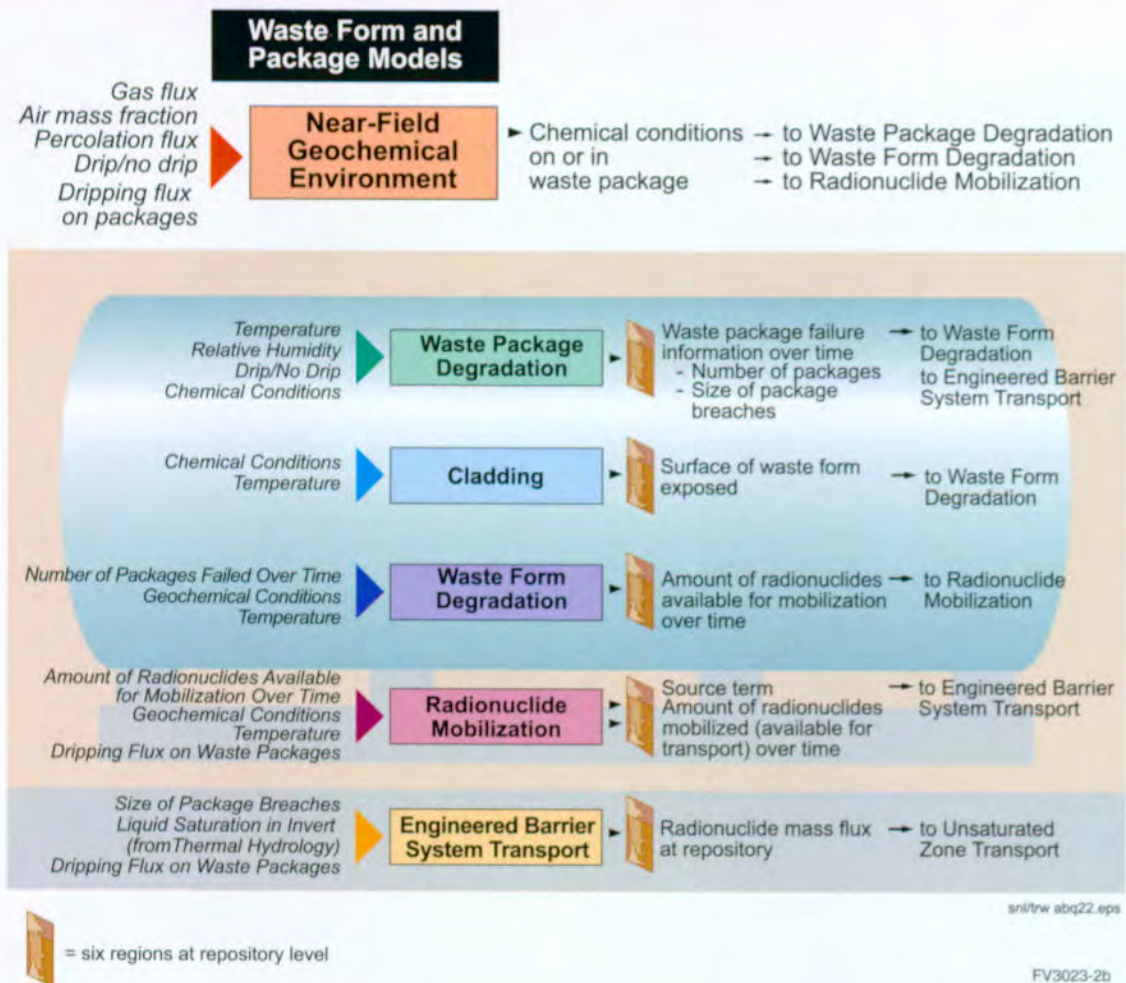


Figure 2-12b. Detailed Representation of Information Flow in the Total System Performance Assessment for the Viability Assessment

models, codes, and response surfaces together in a coherent structure that allows for consistent parameter sampling among the component models. The RIP program is used to conduct either single-realization runs of the entire system (see Section 4.2) or multirealization runs of the system (see Section 4.3). The latter realizations yield a probability distribution of dose rate in the biosphere that shows uncertainty in dose rate based on uncertainty in all the component models.

Because of the need to conduct multiple realizations of the total system behavior, RIP is generally designed to model various components in a simplified fashion. However, the current version of RIP has some very useful features such as cells and environments, that allow certain processes to be

modeled in reasonable detail. The RIP program is also very flexible in representing various component processes in the total system model. The four ways that component models may be coupled into RIP, from most complex to least complex, include the following:

- External function calls to detailed process codes
- RIP cells, which are basically equilibrium batch reactors that, linked in series, can provide a reasonably accurate description of engineered barrier system transport
- Response surfaces, which take the form of multidimensional tables representing the

results of modeling with detailed process models before running the RIP TSPA code

- Functional or stochastic representations of a component model directly built into the RIP architecture

The method used for each TSPA-VA component model is described briefly below and in greater detail in the corresponding sections of Section 3.

As described above for the third coupling method, much of the computational work that goes into the TSPA-VA models is done outside of RIP, before running the actual total system computations. For example, the unsaturated zone flow fields were computed using Transport of Unsaturated Groundwater and Heat TOUGH2 (Pruess 1991), a three-dimensional, finite-volume numerical simulator, with about 80,000 grid blocks representing the entire unsaturated zone model domain (for the dual-permeability model). Similarly, the waste package degradation histories for various values of the uncertain input parameters were run before the RIP runs with a FORTRAN-based simulator called WAPDEG, on UNIX and PC workstations. Other component models that were also run outside of RIP are listed below. The results of these detailed process-level runs were provided as multi-dimensional tables that are read into RIP at run time.<sup>5</sup>

Figure 2-13, in conjunction with Figure 2-12, provides a better understanding of the TSPA-VA code architecture, that is, the actual computer codes used and the connections (information transfer) between codes. It includes both the codes run before the RIP program and those run in real time that are coupled to (external function calls) or within (cells and tables) the RIP program. Based on the schematic information transfer shown in Figure 2-13, some response surfaces generated by codes external to RIP only provide data to other codes external to RIP (e.g., chemical-composition response surfaces (pH) from the near-field

geochemical model will directly feed the external model for waste package degradation, WAPDEG). Other response surfaces, such as liquid saturation, temperature, and seepage flux, will provide data directly into RIP as response surfaces that influence such things as waste form degradation rates. Not all couplings or all models are shown in Figure 2-13, but most are shown (e.g., near-field geochemical modeling is too complex to show all of its aspects in this figure—see Section 3.3).

Coupling of the various models is affected by the climate model, which impacts almost all the other models in one way or another, because it alters water flow throughout the system. The climate is assumed to shift in a series of step changes between three different climate states: present-day dry climate, long-term-average climate (about twice the precipitation of dry climate), and super-pluvial climate (about three times the precipitation of dry climate). These climate shifts are implemented as a series of steady-state flow fields in the unsaturated and saturated zones (including changes in the water-table elevation). Within the RIP program, these shifts require coordination among the coupled submodels because they must all simultaneously change to the appropriate climate state.

In general terms, the coding methods and couplings to be used for the major components are as follows:

- Mountain-scale, unsaturated zone flow (see Section 3.1) is modeled directly with the three-dimensional, site-scale, unsaturated zone flow model developed by YMP, using a volume-centered, integral-finite-difference, numerical flow simulator, called TOUGH2 (Pruess 1991). Steady state flow is assumed, and three-dimensional flow fields are generated for three different infiltration boundary conditions, three different climate states, and several values of rock properties.

<sup>5</sup> Examples of these multidimensional tables include (1) liquid flux and velocity fields for the unsaturated zone as a function  $x, y, z, t$  and uncertain parameters such as infiltration flux and (2) package failures versus time as a function of uncertain parameters such as corrosion rate of the corrosion-resistant metal that forms the inner barrier of the waste package.

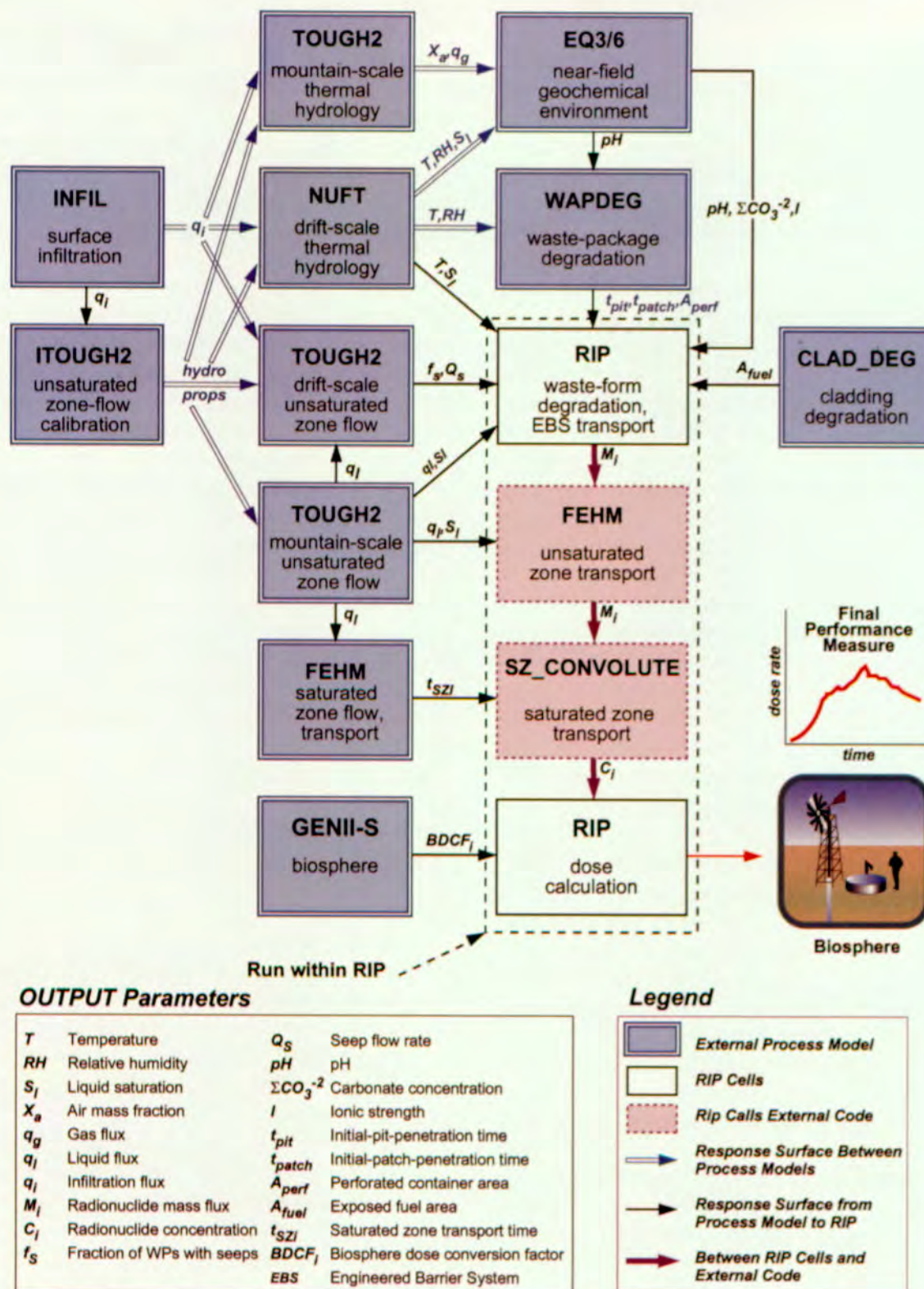


Figure 2-13. Total System Performance Assessment for the Viability Assessment Code Configuration: Information Flow Among Component Computer Codes

These "pre-generated" flow fields (i.e., developed externally and before the RIP simulations) are then placed in a library of files to be read by the Finite Element Heat and Mass (FEHM) code for unsaturated zone transport during the real time RIP simulations. Fracture and matrix liquid fluxes, along with liquid saturation, are passed to FEHM in these tables. To generate the library of flow fields, an inverse model, ITOUGH2 (Finsterle et al. 1996), is used to calibrate the model-predicted liquid saturations to measured liquid saturations in the matrix. This calibration is done when generating the flow fields for the three different infiltration conditions and the different fracture properties at current dry-climate conditions. For future-climate conditions, flow fields are generated based on the dry-climate calibrations. Climate change is modeled within TSPA-VA unsaturated zone calculations by assuming a series of step changes in boundary conditions, meaning that different flow fields are provided at the appropriate time with the assumption of instantaneous pressure equilibrium.<sup>6</sup> The unsaturated zone flow fields are also provided to the TOUGH2 drift-scale seepage models, to the saturated zone streamtube models, and to the engineered barrier system transport models. Unsaturated zone hydrologic properties are passed to the drift-scale, thermal-hydrology model.

- Seepage of water into emplacement drifts (i.e., drift-scale, unsaturated zone flow-see Section 3.1) is also modeled externally and before the RIP simulations using TOUGH2 on a finely discretized grid around the drift.

Simulations are conducted over a heterogeneous fracture permeability field (based on permeability measurements in the Exploratory Studies Facility), at a variety of percolation rates (from the mountain-scale, unsaturated zone flow model) and a variety of mean values and standard deviations for the fracture permeability distribution and the fracture "alpha" distribution (see Section 3.1). These simulations become an uncertain response surface of seepage flux into the drift as a function of percolation flux and a response surface of the number of packages that are dripped on (by seeps) as a function of percolation flux. Both of these response surfaces are input directly into RIP.

- Mountain-scale, unsaturated zone thermal hydrology (see Section 3.2) is modeled with the TOUGH2 code using two-dimensional cross sections taken from the three-dimensional, site-scale, unsaturated zone flow model. Output is several histories of air mass fraction and gas flux as a function of time near the drift, which is provided directly to the near-field geochemical process models.
- Drift-scale, unsaturated zone thermal hydrology is modeled with the finite-difference computer program NUFT (Nitao 1998) in one, two, and three dimensions before the RIP simulations. The drift-scale thermal-hydrology model uses a complicated set of embedded abstractions at different levels of spatial and process detail (e.g., conduction-only versus conduction and convection), as described in Section 3.2. Outputs include:

---

<sup>6</sup> According to the particular history of climate changes sampled by the RIP TSPA model at the beginning of a given realization, the unsaturated zone flow field library is interrogated for a different flow field every time during the simulation that a step change is indicated. This change in a flow field is assumed to apply instantaneously to the transport model. The validity of this approach is discussed briefly in Section 3.6 and in more detail in the *Total System Performance Assessment-Viability Assessment (TSPA-VA) Analyses Technical Basis Document (CRWMS M&O 1998i)*. The durations of each of the three climate states are uncertain parameters sampled at the beginning of each realization of the total system model. However, the sequence of these alternating climate states is the same for all realizations. More details are given in Sections 3.7 and 4.1.1.

- Waste package surface temperature ( $T_{wp}$ ) and waste package surface relative humidity ( $RH_{wp}$ ) for seven different package types within six discrete spatial regions of the repository (see Figure 2-12 for an illustration of the six regions).<sup>7</sup> These values are provided to WAPDEG.
- Average waste form temperature ( $T_{wf}$ ) and liquid saturation in the invert ( $S_l$ ) in each of the six regions. These values are provided to the waste form degradation and engineered barrier system transport models in the RIP program.
- Average drift-wall temperature ( $T_{dw}$ ), relative humidity, and liquid saturation in the invert in the "CC" region of the repository (Figure 2-12). These values are provided to the near-field geochemical models. The outputs are in the form of response surfaces or multi-dimensional tables.
- Near-field geochemical environment (i.e., drift-scale thermal chemistry) is modeled in the base case calculations outside of the RIP simulations by assuming a certain scenario for water flow through the drift and the types of materials the water contacts. Equilibrium batch-reaction calculations with EQ3/6 (Wolery 1992a; Wolery and Daveler 1992) are performed at several places within the drift and then the output from one batch calculation is passed to the input of the next batch calculation at a different spatial location (see Section 3.3 for details). Output is a response surface of various chemical composition parameters. These values are provided both to the waste package degradation model WAPDEG, which is run outside of the RIP program, and to RIP directly as input tables for the waste form degradation and colloid models within RIP.
- Waste package degradation is modeled outside of, and before, RIP runs using a computer code named WAPDEG (CRWMS M&O 1998j), which includes corrosion-rate variability both on a given package and from package-to-package (see Section 3.4). Output is in the form of several tables, read into the RIP program at run time, of the cumulative number of package failures per time, average patch area per package versus time, and average pit area per package versus time. Early or "juvenile" failures, because of the combined effects of large rockfalls, high seismic activity, or possibly undetected material defects, are input directly into RIP as probability distributions.
- Cladding degradation by physical-chemical processes such as creep rupture is modeled outside of RIP runs and then input directly into RIP as a percentage value of failed cladding versus time (exposed waste form area versus time; see Section 3.5). Other cladding degradation modes such as mechanical failure are also input directly into the RIP program, based on other simulations (CRWMS M&O 1998i, Section 6.3.1.1.7).
- Waste form degradation is modeled as an equation within the RIP program using empirical degradation-rate formulas developed from available data and experiments for the three different waste form types: commercial spent nuclear fuel, DOE spent nuclear fuel, and high-level radioactive waste (see Section 3.5). Output from the waste form degradation model is the mass of waste form exposed per time and the volume of water in contact with this waste form versus time, which is used directly in the RIP waste form cells. There are a variety of these waste form cells in the RIP program, corresponding to three different waste form types and several different seepage scenarios. The amount of inventory that can

---

<sup>7</sup> Waste form surface temperature is actually assumed to be equal to the waste package surface temperature.

ultimately enter each waste form cell is a linear function of the number of packages emplaced in each inventory/seepage/thermal-hydrologic environment. There are 72 such environments, representing the product of 6 thermal-hydrologic regions (discussed above), 3 inventory types, and 4 seepage environments (see Section 4.1.7). The entire waste inventory is composed of hundreds of different types of radionuclides. Of these hundreds, 39 were found to be present in sufficient quantity to warrant modeling in the near-field model components of the TSPA. Of these 39, only the nine most important radionuclides—most important from the standpoint of delivering, or potentially delivering, the greatest dose rate at the biosphere location 20 km (12 miles) downgradient of the repository—were tracked through all the system models. These nine radionuclides are: technetium-99, iodine-129, neptunium-237, plutonium-239, plutonium-24, uranium-234, carbon-14, selenium-79, and protactinium-231.<sup>8</sup>

- Engineered barrier system transport is modeled directly within RIP at run time using the RIP cells algorithm. The modeling is based on an idealized representation (basically a linked series of equilibrium batch reactors) of waste form, waste package, and invert, and how radionuclides move through them via diffusion and advection (see Section 3.5). Output from engineered barrier system transport is radionuclide mass flux (for each of the nine radionuclides) at each time step, passed during the RIP simulations to the directly coupled, three-dimensional, dual-permeability, FEHM particle tracker (Robinson et

al. 1997) used for unsaturated zone transport. As shown in Figure 2-12, the repository area is divided into six distinct regions based on infiltration and thermal hydrology, which was modeled with six distinct source-term groups within RIP. The mass releases from these six source-term groups are spread uniformly across the grid blocks in FEHM that reside within the corresponding areas of the six regions. A key part of engineered barrier system transport is waste form or radionuclide mobilization, which is a direct function of both seepage flux and radionuclide solubility in the groundwater. Solubility is input directly into the RIP program as probability density functions (see Section 3.5).

- Unsaturated zone transport is modeled at run-time using the directly coupled, three-dimensional, dual-permeability, finite-element code FEHM (Zyvoloski et al. 1995), which is accessed as an external function by the RIP program. Flow fields and property sets are accessed directly by FEHM from table files residing in the run-time file directory. The unsaturated zone transport model is based on the unsaturated zone flow model and uses the same flow fields (generated by the TOUGH2 unsaturated zone flow code) and the same climate states. As with unsaturated zone flow, a dual-permeability model is assumed, and transport is modeled with the FEHM particle tracker in three dimensions. The FEHM particle tracker transports particles on the same dual-permeability TOUGH2 spatial grid as used in the flow model (using the same material properties, infiltration, and liquid saturation). When the climate shifts, a new TOUGH2 flow field is provided from

<sup>8</sup> The nine radionuclides were chosen based on six criteria (not necessarily in order of significance): high solubility, low sorption affinity, size of inventory (plus ingrowth generated by parent radionuclides), high biosphere dose conversion factor, half-life long enough to survive transport, and existence as colloidal particles. Also, based on previous Yucca Mountain TSPAs (Wilson et al. 1994; CRWMS M&O 1995; NRC 1995; Kessler and McGuire 1996), a number of radionuclides in the list of 39 were inconsequential in their dose effects. Tests of the validity of using only nine radionuclides are presented in Chapter 6 of the *Total System Performance Assessment-Viability Assessment (TSPA-VA) Analyses Technical Basis Document* (CRWMS M&O 1998i).

the run-time file directory, and the particles are assumed to be instantly traveling with the new velocities. In addition, for multirealization runs, a matrix of uncertain property values is created before simulation time by the RIP program and then accessed by FEHM during the simulations. The FEHM code steps through the uncertainty matrix row by row, where each row represents one realization of the uncertain unsaturated zone transport parameters, including  $K_d$ s for each radionuclide, matrix diffusion coefficients, dispersivity, and  $K_c$  values for the plutonium colloids.<sup>9</sup> Output from the FEHM code at each time step is mass flux from the fractures and matrix within each of the six water-table regions (see Figure 2-12 for a depiction of the six water table regions, which have no particular correspondence to the six repository regions). The location of these output grid points is a vertical function of the climate state, increasing in elevation for wetter climates. The fracture and matrix mass fluxes from FEHM are mixed together in a RIP mixing cell and then fed to the saturated zone convolution integral SZ\_CONVOLUTE at each RIP time step (see Chapter 8 of CRWMS M&O 1998i).

- Saturated zone transport is modeled by one-dimensional, effective-continuum, flow-and-transport simulations through six streamtubes using the FEHM computer program. The streamtubes extend from the bottom of the repository at the water table to the 20-km (12-mile) distance downgradient. The locations and directions of the six streamtubes, and the lithology along their flow paths, are determined with a three-dimensional computer model for saturated zone flow, based on the FEHM code and the three-

dimensional, site-scale geologic framework model (see Section 3.7.1.3). These flow and transport simulations are done outside the RIP program for each of the nine radionuclides over 100 realizations of uncertain saturated zone model parameters. These uncertain parameters include effective porosity in the tuff and alluvium;  $K_d$ s in the tuff and alluvium, colloid  $K_c$ , longitudinal dispersivity, fraction of flowpath in the alluvium, and dilution factor (which mimics transverse dispersivity). The choice of six streamtubes is based in part on lithology at the water table and in part on the dilution factors recommended by the saturated zone expert elicitation panel (CRWMS M&O 1998g).<sup>10</sup> The saturated zone expert elicitation panel also recommended the value for the Darcy liquid flux in the dry climate (0.6 m/year), which was used for all realizations in all streamtubes. Output from the FEHM streamtube simulations is concentration versus time at 20 km (12 miles) for a constant mass-release-rate source term. These breakthrough curves reside in files in the RIP run time directory and are accessed when needed by the SZ\_CONVOLUTE external function (which convolves, or integrates, the real source term with the pre-generated unit breakthrough curves) called by the RIP program. For the case of 100 realizations, 6 streamtubes, and 9 radionuclides, there are 5,400 files of breakthrough curves.

- Biosphere transport is modeled within TSPA calculations using biosphere dose-conversion factors that convert saturated zone radionuclide concentration to individual radiation dose rate. The biosphere dose-conversion factors are developed

---

<sup>9</sup>  $K_d$  is the ratio of the mass of a given radionuclide sorbed or residing on the immobile rock phase to the mass dissolved in the aqueous phase.  $K_c$  is the ratio of the mass of a given radionuclide sorbed or residing on colloidal particles to the mass dissolved in the aqueous phase.

<sup>10</sup> The expert panel recommended dilution factors for transport within streamtubes that have the approximate area and liquid flux as the streamtubes chosen for the TSPA-VA model.

outside the RIP program using a computer program named GENII-S (Leigh et al. 1993). The factors are then entered as table values in the RIP front-end menus. These factors are multiplied by the concentrations in the saturated zone streamtubes to compute individual doses, which are the end product of the calculations.

- Disruptive events to be considered are seismic activity, igneous activity (indirect and direct volcanic effects), nuclear criticality, and human intrusion. Models for these events are not shown in Figure 2-13; however, at least one of these events, indirect volcanism, is modeled with the RIP program using a modified source term, specifically different solubilities (because of different mineral phases) for some of the actinides. An example of an indirect volcanic effect is the contact of a magmatic dike with waste packages in which the waste form is recrystallized into other mineral phases that then dissolve at an increased or decreased rate in comparison to the nondisturbed case. Direct volcanic effects (i.e., radionuclides carried by ash plumes from volcanic eruptions) are modeled completely outside the RIP program using the code ASHPLUME (LaPlante and Poor 1997) (see Section 4.4). The codes and methods used in modeling other disruptive events—seismic effects, criticality, and human intrusion—are discussed in Section 4.4.

### 2.3.3 Treatment of Uncertainty

This section describes the various types of uncertainty represented in the TSPA-VA models and how these uncertainties affect the predictions of performance. Section 2.3.3.1 lists the four major types of uncertainty, describes the differences between uncertainty and variability, and introduces the modeling tools (e.g., Monte Carlo sampling) for analyzing uncertainty. Section 2.3.3.2 describes how one type of uncertainty, conceptual model uncertainty, is handled in TSPA-VA and how this leads to a definition of the TSPA-VA base case. Section 2.3.3.3 gives more details on how

uncertainty is handled in the base case and how the base case might be used to explore the “probable” behavior of the repository. A description then follows about the “expected-value” realization, which is used in Section 4 to show how the various component models interact with one another. Finally, Section 2.3.3.4 describes the various sensitivity analysis methods employed in TSPA-VA to determine the most important model parameters affecting the total system performance.

#### 2.3.3.1 Uncertainty Versus Variability

A variable feature, event, or process is one that varies over space or time. Examples include the porosity of a hydrogeologic layer and the temperature and near-field geochemical environment in the repository drifts. If perfect information (complete knowledge) were available, such parameters would best be represented by distributions over space and time.

Uncertainty relates to lack of knowledge regarding a feature, event, or process—one whose properties or future outcome cannot be predicted beforehand. Four types of uncertainty are typically considered: value uncertainty, conceptual model uncertainty, numerical model uncertainty, and uncertainty regarding future events. The treatment of a feature, event, or process as purely variable or purely uncertain can lead to significantly different modeling results. In general, variability can serve to either dilute or concentrate contamination from a repository in either time or space. Uncertainty in the treatment of a feature, event, or process results in uncertain forecasts of future repository behavior. Uncertainty and variability are related in that spatial and temporal variability are generally very uncertain. If the variability can be appropriately quantified or measured, then a model usually can be developed to include this variability. If the variability cannot be physically quantified or measured, then it should be treated as uncertainty (lack of knowledge). However, the ability to model some types of spatial variability can be limited not only by measurement deficiencies but also by computational resources. An example of this is fracture permeability in the volcanic tuffs. Fracture lengths and apertures in the tuff units

occur randomly over a wide variety of spatial scales, from the very large such as distinct fault zones (e.g., the Ghost Dance), to the very small (e.g., cracks on the order of millimeters in length and submicron in width). It is relatively easy to measure air permeabilities (but not necessarily liquid permeabilities) in these large faults and to include these discrete features in numerical models. It is much harder to include spatial heterogeneity on the millimeter scale in the overall flow-and-transport numerical models because of the difficulties of in situ measurement, the inability to comprehensively characterize small-scale permeability over the entire mountain, and a lack of computers large enough to model flow and transport on such a fine scale over the entire mountain. In addition to these considerations, the appropriate quantification of the spatial variability in the models is very much a function of what performance measure is desired at the output side of the model. If a well pumps water over a 100-m (330-ft) screened interval, the appropriate discretization of the spatial variability may be on the order of 10 m (33 ft) per numerical grid block. If it is desired to measure dripping into the drifts, the appropriate discretization of the grid cells may be on the centimeter scale.

Two basic tools used in the TSPA to deal with uncertainty and variability are probability theory and alternative conceptual models. The former is used for uncertainty in specific model parameters and the latter for uncertainty in the understanding of a key physical-chemical process controlling system behavior. In particular, uncertain processes often require different conceptual models. For example, different concepts of matrix-fracture coupling in the unsaturated zone lead to different flow and transport models. Sometimes conceptual models are not mutually exclusive (e.g., both matrix and fracture flow might occur), and sometimes they do not exhaustively cover all possibilities (matrix and fracture flow apparently

do, although the definition of "matrix" depends on the length scale used in the model). These problems indicate that the use of alternative conceptual models, while often necessary to characterize some types of uncertainty, is not always as rigorous as one might like—an unfortunate result of insufficient knowledge in some areas.

For the treatment of uncertainty in specific model parameters and for alternative conceptual models that have been weighted beforehand with specific probabilities, the Monte Carlo sampling method has been used in all TSPAs to date and is the primary method of uncertainty analysis used for this TSPA. The method involves random sampling of the probability distributions for all uncertain input parameters (including any index parameters that might be used to weight alternative conceptual models). Then, numerous realizations of the repository system are calculated based on the sampled realizations of all the inputs. Each total system realization has an associated probability so that there is some perspective on the likelihood of that set of circumstances occurring.<sup>11</sup> The Monte Carlo method yields a range for any chosen performance measure (e.g., peak dose rate to an individual within a given time period at a given location) along with a probability for each value in the range. In other words, it gives an estimate of repository performance plus "error bars" on the estimate. The performance measures and associated probabilities have traditionally been presented as CCDFs that show the probability of exceeding a given performance measure value.

### 2.3.3.2 Weighting of Alternative Conceptual Models

In many subsystems of the overall TSPA system, there are plausible alternative models or assumptions. In some cases, these alternatives form a continuum, and sampling from the continuum of

---

<sup>11</sup> In the standard Monte Carlo method, each realization is equally likely, so the probability is 1 divided by the number of realizations. In more elaborate variants, for example using "importance sampling," some realizations can be less probable than others. The TSPA-VA uses a variant of the Monte Carlo method, called Latin Hypercube Sampling, which better models the tails of the input probability distributions when the number of realizations is small.

assumptions fits naturally within the Monte Carlo framework of sampling from probability distributions. In other cases, the assumptions or models are discrete choices. In particular, some processes are so highly uncertain that there is not enough data to justify developing continuous probability distributions over the postulated ranges of behavior. In other words, a high degree of sampling is unwarranted, and it is better just to look at two or three cases that are assumed to encompass (bound) the likely behavior.

There are two possible approaches to incorporating discrete alternative models within the TSPA: weighting all models into one comprehensive Monte Carlo simulation (lumping), or keeping the discrete models separate and performing multiple Monte Carlo simulations for each discrete model (splitting). There are advantages and disadvantages to both approaches. Lumping has the conceptual advantage that a single CCDF can be said to include all the system uncertainty. Splitting can lead to a profusion of cases that makes it difficult to quantify the relative importance of the various discrete assumptions. The main disadvantage of lumping is the concern that individual cases with poor performance might be diluted within a multitude of more favorable cases. In other words, there could be a combination of the discrete assumptions with poor performance that might not be obvious under the lumped approach but that would stand out if that combination were presented separately. Another potential disadvantage of lumping occurs if there is no good justification for the probabilities used—if the weighting of the alternatives is artificial, then the results will be artificial as well.

For this TSPA, a combination of the two approaches is used. In particular, the TSPA-VA “base case” model, defined in detail in Sections 4 and 4.1, can be considered an implementation of the splitting approach, because it is based on a limited range of uncertainty. Based on expert judgment (and to some extent on finite time and resources that can be applied to the VA effort), the TSPA-VA base case is a best estimate as to the more likely ranges of model behavior and parameter ranges. Some alternative models are not

included in the base case and some parameter ranges of the included models have been narrowed. The level of uncertainty included in the TSPA-VA base case model is based on the current level of knowledge regarding the various processes controlling system behavior. In several instances, the range of uncertainty is set quite large, in a “conservative” manner. Because of this narrowed range of models and parameters, the base case CCDF is conditional (shown in Section 4.3), meaning that it is conditional on certain models and parameters being held constant or having their variance restricted. As described at the beginning of Section 2.3, the primary type of CCDF used to portray repository performance is a CCDF of the peak dose rate occurring within a given time span at a given location, such as the peak dose rate at 20 km (12 miles) that occurs at any time during the first 10,000 years.

Some of the most important processes and parameters (i.e., having the greatest effect on performance or dose rate) not included in the base case also warrant a separate presentation of their uncertainty in the form of several conditional CCDFs based on alternative process models. Alternative models of water seepage into the drift and of fracture-matrix flow in the unsaturated zone are treated in this manner (see Section 5.1). Also, for design options, such as drip shields and ceramic coatings on the waste packages, there is no reasonable conceptual justification for lumping them together into a single probability distribution. Therefore, they must be presented as conditional CCDFs—conditional on the given repository and/or waste package design.

### 2.3.3.3 Uncertainty and the Base Case

Because of the significant amount of uncertainty in most of the component models, the variance associated with most models and parameters can only reasonably be restricted, but not wholly eliminated. Thus, the base case necessarily encompasses much of the underlying uncertainty. It includes some of all four types of uncertainty: value or parameter uncertainty, conceptual model uncertainty, numerical model uncertainty, and future-event uncertainty. Therefore, the base case

by itself also represents the "lumping" approach. Uncertainty not lumped into the TSPA-VA base case is captured discretely in alternative models, alternative features, and alternative events. These alternatives that have been "split" off of the base case, and their effects on performance are described separately as either alternative conditional CCDFs or, as alternative single-realization time histories of performance. Examples of this for the TSPA-VA, with respect to each of the four types of uncertainty, include the following:

- Parameter uncertainty: widened parameter ranges for the cladding degradation models (Section 5.5)
- Conceptual model uncertainty: alternative process models for unsaturated zone flow and seepage (Section 5.1)
- Numerical model uncertainty: one-dimensional flow and transport used in the saturated zone because of uncertainty regarding numerical dispersion in three-dimensional models (Section 3.7)
- Future-event uncertainty: disruptive events, such as volcanism (Section 4.4)

A total "lumped" CCDF, including all of the uncertainty in TSPA-VA, is not presented because of difficulties (i.e., uncertainty) in assigning probabilities to some of the alternatives.

A final type of uncertainty, already mentioned, but not included in the above four and not a candidate for lumping, is "design" uncertainty. This uncertainty is driven by the uncertainty in the natural-system parameters and processes. It represents the desire to design the safest repository possible within certain cost restrictions. However, the "best" design at any given time (for example, the VA design) may not represent the best design in the future (for example, the LA design) because new knowledge may be acquired based on additional

site characterization and additional TSPA analyses. Either of these factors can lead to a new repository and/or waste package design. This type of uncertainty for the VA is examined in the form of various "design options" (Section 4.5).

The 1997 Energy and Water Appropriations Act asks for the "probable behavior of the repository in the Yucca Mountain geological setting." However, it does not define the word "probable" in this context. Any of the random outcomes in the base case CCDF, or for that matter, any of the random outcomes in the alternative CCDFs could be considered "probable", since they all have a finite probability. A more explicit interpretation of the word "probable" might be either "representative" or "most probable". Regarding the latter, the most probable behavior is clearly the "mode" of a CCDF.<sup>12</sup> Since we do not present the total "lumped" CCDF that includes all alternatives, the most probable behavior could be taken as the mode of the base case CCDF. However, other points on the output CCDF are more often chosen as being "representative" of the likely or probable behavior of a stochastic system, including the expected-value (i.e., the mean or average of all peak dose rates) and the median (i.e., the 50th percentile value, above which lie half of the peak dose rates and below which lie the other half). Both the mean and the median of the base case peak-dose-rate CCDF, along with the entire CCDF, are presented in this document to demonstrate probable future repository behavior (see Section 4.3). In addition, other types of analyses are presented, as discussed below.

The CCDFs of peak dose rate are the most important measure of repository performance since they represent the peak, or highest, dose rate within a given time frame. However, to illustrate how the various component and subsystem models interact with one another, it is also useful to display one or more realizations of dose rate versus time over specific time periods. Perhaps the most useful realization of the input parameters for this purpose

---

<sup>12</sup> In the theory of probability, the "mode" of a distribution is the point with the highest probability or highest likelihood of occurrence.

is the expected values (means) of all the input parameters. This single realization is useful because it is time independent; that is, the same values of the input parameters can be used regardless of the time span of interest, whether it be 10,000 years, 100,000 years, or 1 million years. This single realization is called the "expected-value realization" in the rest of this document. (It is not the realization of the input parameters that produces the expected value or mean peak dose rate on any of the peak dose-rate CCDFs because those realizations differ according to the period being examined.)

The expected-value realization for the TSPA-VA base case is examined in Section 4.2 with respect to how it shows the influence of the various base-case component models on each other and on total system performance. The expected-value realizations for alternative models and designs are shown in Section 5 and compared to the expected-value base-case realization. This is one useful way to look at the sensitivity of total-system and subsystem performance to various models and parameters (see Section 2.3.3.4).

In addition to examining the behavior of the expected-value realization, it is also useful to examine the behavior of realizations that lie close to both tails (i.e., both the upper and lower extreme) of the various input parameters. This is usually done one input parameter at a time; that is, all parameters except one are sampled at their expected values. The parameter of interest is then sampled at either its 5th percentile probability or its 95th percentile probability.<sup>13</sup> This is useful because the behavior of the various component models and their influence on one another can be quite different at these values than for the expected-value realization. It is also useful to display these more extreme time histories on the same graph as the expected-value time history because together they give a good indication of the complete range of influence of each of the input parameters on total repository performance during the specified time period, whether it be over the

first 10,000 years, 100,000 years, or 1 million years after closure. This type of analysis is presented in Section 5 for the most influential parameters of the various base-case component models.

#### 2.3.3.4 Presentation and Analysis Techniques for Uncertainty

One goal of the TSPA-VA is to evaluate the performance and associated uncertainty for the reference repository design (see Volume 2) and various design options (see Section 4.5). Another important goal is to determine the characteristics of the engineered and natural systems that have the most influence on repository performance. This information provides input to the design and site-characterization organizations about additional data that could provide the greatest improvement in confidence about the repository. Beyond these formal goals, there is the simple need to understand the results and make them clear to all interested parties. A number of methods are used to explain the results and quantify the sensitivities.

Total system performance is a function of sensitivity (i.e., if a parameter is varied, how much do the performance measures change?) and uncertainty (i.e., how much variation of a parameter is reasonable?). For example, the TSPA results could be very sensitive to a certain parameter, but the value for the parameter is exactly known. In the uncertainty analysis techniques described below, that parameter would not be regarded as important. Many parameters in the TSPA-VA analyses do, however, have uncertainty associated with them and do end up with a high ranking for their importance to performance. On the other hand, the level of their ranking can depend on the width of the assigned uncertainty range. Therefore, uncertainty analyses must be carefully interpreted (i.e., the width of the uncertainty ranges must be considered). Most of the important parameters with possibly limited uncertainty ranges in the base case are examined in alternative models that either expand the range of their parameters beyond the expected range of uncertainty or change the

<sup>13</sup> Other samplings are possible, such as the 1st and 99th percentiles. We have chosen 5th and 95th as being representative of "extreme" behavior.

weighting of the parameter distribution. For example, this type of analysis is performed for alternative models of seepage (Section 5.1) and cladding degradation (Section 5.5).<sup>14</sup>

System performance also may be sensitive to repository design options, but models and parameters for these various options are not assigned any uncertainty. Therefore, even though they can be important (see Section 4.5), they do not show up in the tables of key parameters based on uncertainty analysis.

The determination of the parameters or components that are most important depends on the particular performance measure being used. This point was demonstrated in the 1993 TSPA (Andrews et al. 1994; Wilson et al. 1994) and the 1995 TSPA (CRWMS M&O 1995). For example, these two TSPAs showed that the important parameters are different for 10,000-year peak doses than for 1-million-year peak doses.

Some methods for investigating sensitivity are discussed below:

- **Scatter plots**—Scatter plots are a good qualitative method of looking for sensitivities based on multi-realization simulations of the system. The final results (e.g., dose rate) are plotted against the input parameters and visually inspected for trends. If there is a visible trend, it is an indication of sensitivity. The performance measures can also be plotted against various subsystem outputs or surrogate performance measures (e.g., waste package lifetime) to determine whether that subsystem or performance surrogate is important to performance.
- **Regression analysis**—In regression analysis, a mathematical relationship between the outputs (performance measures) and inputs (model parameters) of a Monte Carlo simulation is developed. Typically, a method called stepwise linear regression is used in which only a subset of the input parameters is used for the regression, with parameters added one at a time based on calculated correlation coefficients. Parameters that have little influence on the performance measure are those that, when added, only marginally change the variance of the output. This method produces a ranking of input parameters according to their impact on the performance and a quantitative measure of the impact (basically, the correlation coefficient for the performance measure versus the input parameter). A more detailed description of regression analysis is presented in Section 4.3 and in the *Total System Performance Assessment-Viability Assessment (TSPA-VA) Analyses Technical Basis Document* (CRWMS M&O 1998i).
- **Differential analysis**—Another quantitative method for ranking important parameters is differential analysis, in which the partial derivatives of the performance measure with respect to the input parameters are calculated to find the amount that performance is affected when one parameter is varied while the others are held constant. A significant drawback of this method is that it is local, that is, the derivatives are calculated about a point in the parameter space and only represent the sensitivity at that point. In contrast, regression analysis of Monte Carlo results is more global; that is, the sensitivities are determined and ranked taking into account the whole parameter space.

---

<sup>14</sup> The parameter uncertainty ranges established for the base case are usually based on site characterization data and expert judgment. Often times these ranges are expanded beyond the existing data in order to "bound" possible behavior. In such a case, if the performance is not sensitive to the given parameter, then there is generally no point in future sensitivity analyses for this parameter. On the other hand, if the performance is found to be sensitive to the parameter within the base case range, it is often useful to expand the range to quantify the effect of uncertainty beyond the "expected" base case range.

- **Alternative models or parameter sets**—A useful but less systematic method of sensitivity analysis is to look at discrete cases, for example, some discrete sets of input parameters (as opposed to a systematic sampling) or some discrete choices of alternative models for a given process or subsystem. This method provides qualitative information about the sensitivity to the changes in assumptions (i.e., do the results change a little or a lot?) but not the same type of quantitative ranking produced by the previous two methods. This method is used frequently in Section 5.

## 2.4 DESCRIPTION OF BASE CASE RESULTS

The following paragraphs provide a brief summary of the expected TSPA-VA base case results for the current understanding of the natural system described in Volume 1 and the reference design described in Volume 2. These results are discussed in a series of time slices that synthesize the system response to the proposed design concept. Although there is uncertainty in the probable sequence of events occurring after repository closure, this is a general description that captures the essence of system behavior as modeled in the TSPA. The responses described for each of the periods indicated below are generally applicable. However, various areas of the repository will experience somewhat different conditions over different periods. More detailed descriptions of the expected behavior and the assumptions underlying the results are presented in Sections 3, 4, and 5.

### 2.4.1 Time of Waste Emplacement to Time of Repository Closure

In the TSPA-VA base case calculations, conditions around each waste package will be controlled by the large heat output from decay of the short-lived radionuclides. The temperature on the waste package surfaces will be high, around 200°C (392°F) for the hottest waste package. The relative humidity in the drifts is expected to be low, less than 50 percent. The water in the rock will start to be driven away from the drifts because the temper-

ature next to the drift wall is above boiling. Under these conditions, minimal dry oxidation of the carbon steel outer layer of the waste package is expected. However, the waste packages will remain intact, allowing no release of radionuclides.

### 2.4.2 Time of Repository Closure to Several Hundred Years After Closure

Following repository closure, after an initial period of increasing temperatures, the temperatures around each waste package will begin to decline, although the waste package surface temperature still will be generally above boiling. As the temperature decreases, the relative humidity will increase. The carbon steel outer container material will start to corrode under these humid air conditions. Because the waste package and drift temperatures will be above boiling, the air will be humid and drips will not be present.

The lining around the drifts will start to collapse and its absence will be reflected in the change in chemistry of incoming water and gas, since they will no longer pass through any concrete before dripping into the drift. Water will be being driven away from the drifts, and the liquid saturation in the rock matrix will be reduced from about 90 percent (under ambient preconstruction conditions) to less than 20 percent. The rock out to 10 m (3.3 ft) from the repository will be heated above the boiling temperature of water. Only minimal degradation of the carbon steel material of the outer waste package will occur. For this reason, the waste packages are expected to be intact, and there will be no release of radionuclides.

### 2.4.3 Several Hundred Years to Several Thousand Years After Closure

As discussed in Volume 1, Section 2.2.6.1, after a few thousand years the ground support of the repository drifts would be expected to have failed and most of the repository drifts would be expected to have sufficient rockfalls that a portion of the waste package would be covered by debris. The crushed rock around the waste package would insulate the waste package. Given that the thermal output from the individual waste packages is

significantly reduced by this time period, the effects of this on the thermal and hydraulic environment near the waste package is expected to be small. The possible effects of these rockfalls on the waste package degradation are also expected to be minimal because at this time the bulk of the carbon steel on the outer barrier of the waste package is still intact.

During the period of several hundreds to several thousands of years after closure, the temperature on the waste package surfaces will drop below boiling, causing the relative humidity in the drift to rise to almost 100 percent. Also, the rock temperature around the repository generally will drop below boiling at about 1000 years. Under these conditions, aqueous (in the presence of drips) corrosion of the layer of carbon steel that forms the outer barrier of the waste package can begin. So dripping water is likely to begin falling on some of the waste packages; but whether and exactly where these dripping conditions occur is uncertain.

The degree of degradation of the outer carbon steel layer of the waste package is expected to be variable from place to place in the repository and on the surface of each waste package. As a result, some carbon steel on some waste packages may corrode sufficiently to expose the underlying, corrosion-resistant, nickel-base alloy (Alloy 22) layer to aqueous or humid air conditions. However, the corrosion resistance of the Alloy 22 metal precludes significant degradation of this metal under the likely hydrologic and geochemical conditions at the interface of the two metal barriers.

With the possible exception of some unexpected early failures of a few waste packages, possibly caused by very large rockfalls or undetected poor welds of Alloy 22 metal combined with unexpected rapid degradation of the carbon steel, there will be no release of radionuclides during this period. For prematurely failed waste packages, if water contacts the waste, the waste can be altered and radionuclides released from the waste package to the invert and the unsaturated tuffs around the drift wall. Because only a few waste packages are

even considered to fail prematurely, these releases will be small.

#### **2.4.4 Several Thousand Years to Ten Thousand Years After Closure**

Temperatures in the drift and the surrounding rock will continue to decline, liquid saturation in the rock matrix will continue to increase, and the dripping conditions will continue to be reestablished over a broader area. The environment around the repository will return to its original temperature by 3000–4000 years. However, other properties of the rock mass around the drifts may be altered from the pre-waste emplacement conditions. The variability in the ambient rock property conditions and the uncertainty in the changes induced in response to coupled thermal, hydrologic, mechanical, and chemical processes induced by the presence of the repository are difficult to define quantitatively. Therefore, as a first approximation, the TSPA simply represents the variability that could be induced by these coupled processes by using the values for rock properties based on the natural variability in properties currently present at Yucca Mountain.

There will be sufficient corrosion of the carbon steel outer barrier on virtually all of the waste packages to expose the underlying layer of corrosion-resistant Alloy 22 metal. The degradation of Alloy 22 depends on the presence of water and is a function of the geochemical conditions on the metal's surface. These conditions and the degradation rates are variable, so there may be sufficient degradation to allow small openings through some of the waste packages.

If some waste packages have openings through them, water may contact the exposed waste form surface. The majority of the commercial spent nuclear fuel waste forms is protected by a highly corrosion-resistant Zircaloy cladding. Although some types of cladding may be degraded prematurely (e.g., stainless-steel cladding), the Zircaloy cladding is expected to remain intact for tens of thousands of years. Therefore, only a small fraction of the waste form surface will be exposed and in contact with water. Any water that enters

the waste package will be expected to take a circuitous route as it flows through individual fuel rods within the waste package; however, this flow path is difficult to define. The conservative assumption used in the TSPA-VA allows the water to contact the entire exposed waste form surface.

Once water contacts the waste form surface, the spent nuclear fuel or glass will degrade, releasing some radionuclides to the aqueous phase. The degradation of the waste forms will go through many different geochemical alteration phases, some of which will tend to retain partially soluble radionuclides while others may form colloidal particles. In addition, the actual mobile concentration of radionuclides will depend on the solubility of the radionuclides in water.

More than 99 percent of the radionuclides released into solution by degradation of the waste form will be immobile within the geologic setting. Most are insoluble in the Yucca Mountain waters and will remain near the waste form. Others have an affinity for the metal components of the waste package or other engineered barrier materials or sorb strongly to the minerals in the rock. Only a small fraction of these radionuclides is mobile enough to move in the system.

This small fraction of radionuclides may be transported by water moving out of the repository, down through the unsaturated rock, and then in the groundwater flow below the water table. Some of these radionuclides will move more slowly than others because they sorb to the minerals in the unsaturated and saturated zone rocks to some degree. The radionuclides of concern during this period are highly mobile radionuclides, technetium-99 and iodine-129. These radionuclides may then be transported 20 km (12 miles) to a hypothetical well used as a representative location for the assessment of consequences or dose rates. The water flow velocities through the unsaturated and saturated zones at Yucca Mountain control the time it takes for these radionuclides to reach the hypothetical well 20 km (12 miles) downgradient. These transport times depend on rainfall in the region and the recharge to the flow system and, therefore, depend on the climate.

When the change between the present-day dry climate and the assumed, long-term average climate occurs, the transport times are significantly reduced.

The likely dose rate at the hypothetical well during this period, considering all of the above processes, is 0.1 mrem/year (Figure 4-26). This value is about 0.03 percent of the average value for background radiation from nonmedical sources in the United States (about 300 mrem/year [NCRP 1987, p. 149]).

#### **2.4.5 Ten Thousand Years to Several Tens of Thousands of Years After Closure**

During this period, the natural environment near the drifts generally will have returned to ambient conditions, except that some permanent changes in rock properties around the drifts may have occurred and the climate and corresponding surface infiltration are anticipated to be different than current conditions. Degradation of the corrosion-resistant Alloy 22 barrier will continue to occur, predominantly in the areas of the repository that experience dripping conditions. Degradation of the Zircaloy cladding will also continue.

Radionuclide releases from the engineered barrier system will continue. The release rate of highly soluble species is controlled by the waste package failure rate. The release rate of less soluble species (such as neptunium-237) will be controlled by the cumulative fraction of waste packages that will have failed and the fraction of the waste package surface that will have been degraded. Over this period, the soluble radionuclides will still control the dose rate of several millirems per year at 20 km (12 miles) from the repository.

#### **2.4.6 Several Tens of Thousands of Years to One Hundred Thousand Years After Closure**

The degradation of the corrosion-resistant Alloy 22 barrier will continue, as will degradation of the Zircaloy cladding. As more inventory becomes available for transport with increased waste package failure and more water enters each waste

package that has failed, the solubility-limited radionuclides, in particular neptunium-237, will begin to control the dose rate. The anticipated dose rate is about 30 millirems/year (Figure 4-26).

#### **2.4.7 Several Hundred Thousand Years After Closure**

As time continues, more waste packages will fail, more cladding will be degraded, and more water will enter the failed waste packages and, it is assumed, will contact the exposed waste. As a result, the expected value for the dose rate at a well located 20 km (12 miles) downgradient will continue to increase to more than 100 mrem/year. A major glacial cycle is likely to occur, causing superpluvial conditions in the semiarid region

around Yucca Mountain. A wetter climate would increase still further the fraction of waste packages being dripped on and the amount of water that drips into the drifts and into the waste packages. At the time this climate change occurs, the dose rate would be expected to increase still further to several hundred millirems per year.

This synopsis of results should not be read in isolation but must consider the technical bases presented in Sections 3 and 4—and in more detail in the *Total System Performance Assessment-Viability Assessment (TSPA-VA) Analyses Technical Basis Document* (CRWMS M&O 1998i)—and the uncertainty in these results described in Sections 4.3 and 5.

### 3. DEVELOPMENT OF TOTAL SYSTEM PERFORMANCE ASSESSMENT COMPONENTS FOR THE VIABILITY ASSESSMENT

Because of the difficulty in handling the complexity of the repository system in an analysis, the Yucca Mountain total system was divided into individual parts to make each set of TSPA-VA analyses manageable. Each individual part represents a major process area. The component models that define the process areas are discussed in this section. However, because of the need for brevity, the component models are not described in great detail. The details of each component model are thoroughly documented in the *Total System Performance Assessment-Viability Assessment (TSPA-VA) Analyses Technical Basis Document (CRWMS M&O 1998i)*. The process models are listed in Table 3-1, along with their corresponding section numbers in this volume and chapter numbers in the *Total System Performance Assessment-Viability Assessment (TSPA-VA) Analyses Technical Basis Document (CRWMS M&O 1998i)*. By necessity, the detailed documentation for the component models is many pages longer than the sections in this volume; each chapter of the *Total System Performance Assessment-Viability Assessment (TSPA-VA) Analyses Technical Basis Document (CRWMS M&O 1998i)* is published as a separate volume. In addition to the process areas discussed in this section, the effects of disruptive events (volcanism, seismicity, human intrusion, and nuclear criticality) on repository performance are discussed in Section 4.

It must be noted that the various TSPA component models are represented using different computer codes. The variations in the codes, in terms of their architecture, requires that the form of the input and output parameters is different from code to code. For this reason, in some cases, the models require somewhat different forms for what would appear to be the same input and output parameters. The specific parameters used in the TSPA-VA are given in the *Total System Performance Assessment-Viability Assessment (TSPA-VA) Analyses Technical Basis Document (CRWMS M&O 1998i)*.

Although all of the processes will be strongly inter-related in the actual repository system, the assumption was made that the components could be treated separately if a consistent set of boundary conditions and scenarios was rigorously maintained among all the related components. This section addresses the conceptualization of eight component models and the implementation of these components into the performance assessment analyses. It also provides the results and interpretations of the analyses associated with the component. Section 4 describes how these components were recombined into the total-system model, and Section 5 discusses the sensitivity of the total-system results to various aspects of these components.

The four attributes of the Yucca Mountain repository safety strategy and the NRC key technical issues were discussed in Section 2.2.1. The relationships among the four attributes, the NRC key technical issues, and the TSPA model components are shown in Tables 2-1 and 2-2.

Table 3-1. Component Models for Process Areas and Corresponding Documentation

| Process Area   | TSPA-VA Section | Technical Basis Document Chapter |
|--|-----------------|----------------------------------|
| Unsaturated zone flow                                | 3.1             | 2 (B00000000-01717-4301-00002)   |
| Thermal hydrology                                    | 3.2             | 3 (B00000000-01717-4301-00003)   |
| Near-field geochemical environment                   | 3.3             | 4 (B00000000-01717-4301-00004)   |
| Waste package degradation                            | 3.4             | 5 (B00000000-01717-4301-00005)   |
| Waste form degradation and radionuclide mobilization | 3.5             | 6 (B00000000-01717-4301-00006)   |
| Unsaturated zone transport                           | 3.6             | 7 (B00000000-01717-4301-00007)   |
| Saturated zone flow and transport                    | 3.7             | 8 (B00000000-01717-4301-00008)   |
| Biosphere  | 3.8             | 9 (B00000000-01717-4301-00009)   |

To assure that the TSPA is based on the most current scientific knowledge, eight workshops were held in 1997 to bring together YMP scientists, engineers, and performance assessment analysts. The aim of these workshops was to help define and prioritize the important technical issues to be addressed in the TSPA-VA. The general format of the workshops is described in Section 2.2.1. The workshops are summarized in the discussion of the construction of the conceptual models in Sections 3.1–3.8.

In addition to the workshops, DOE sponsored five expert elicitations on key process models for the TSPA. The goal of these elicitations was to solicit the panel members' judgment in quantifying the uncertainty associated with the process models. These elicitations are listed in Table 3-2. Information on the results of the expert elicitations and their subsequent use in the TSPA model components is summarized, where relevant, in the discussion of the construction of the conceptual model in Sections 3.1–3.8.

Table 3-2. Expert Elicitations for the Total System Performance Assessment for the Viability Assessment

| Process Model  | Elicitation  | Documentation   |
|--|--|-----------------|
| Unsaturated zone flow (Section 3.1)                                | Unsaturated Zone Flow                                | CRWMS M&O 1997n |
| Thermal hydrology (Section 3.2)                                    | Near-Field Environment                               | CRWMS M&O 1998d |
| Waste package degradation (Section 3.4)                            | Waste Package Degradation                            | CRWMS M&O 1998b |
| Waste-Form Degradation and Radionuclide Mobilization (Section 3.5) | Waste-Form Degradation and Radionuclide Mobilization | CRWMS M&O 1998k |
| Saturated Zone Flow and Transport (Section 3.7)                    | Saturated Zone Flow and Transport                    | CRWMS M&O 1998g |

### 3.1 UNSATURATED ZONE FLOW

Unsaturated zone flow at Yucca Mountain will play an important role in repository performance. Water seeping into drifts and dripping onto waste packages can accelerate waste package degradation and radionuclide mobilization. In addition, water moving through fast pathways from the repository to the water table via fractures can decrease the

transport time of radionuclides to the accessible environment.

Four distinct components of unsaturated flow are considered in the TSPA for the VA: climate, infiltration, mountain-scale flow of water, and seepage into repository emplacement drifts. These components include processes at several scales. At the global scale is climate, including changes in solar heating caused by changes in the earth's orbit and inclination, and formation of huge ice sheets during glacial periods. There are also important regional-scale (hundreds of kilometers) climate effects, such as the "rain shadow" caused by the Sierra Nevada mountain range and the proximity of the polar jet stream, that make climate variations at Yucca Mountain different from the global average. Infiltration and flow through the mountain, or mountain-scale flow, are modeled at the scale of the site. The YMP infiltration model covers an area approximately 10 km × 20 km (6.2 miles × 12.4 miles), while the site-scale flow model for the unsaturated zone encompasses a volume approximately 5 km × 9 km × 800 m (3.1 miles × 5.6 miles × 2,600 ft). The site-scale models include effects of surface topography and subsurface hydrogeologic layering. The drift scale is the scale of an emplacement drift, approximately 5 m (17 ft) in diameter. At the drift scale, a seepage model evaluates the interaction of percolating water with an emplacement drift and the amount of water that seeps into the drift. Variations in permeability on scales of a few meters up to about 10 m (several feet up to about 30 ft) are important in modeling seepage. Processes at the scale of individual fractures, in particular those affecting fracture-matrix coupling, or water flow between fractures and the porous rock matrix, are important both to seepage and mountain-scale flow. Fracture-scale processes are not modeled explicitly, but are represented by parameters in the continuum flow models. Some of the important processes for unsaturated zone flow are pictured in Figure 3-1. Yucca Mountain climate is illustrated in Figure 3-2.

The unsaturated zone hydrologic modeling studies and analyses presented in this section were prepared with the view of addressing selected aspects of the NRC Key Technical Issue on

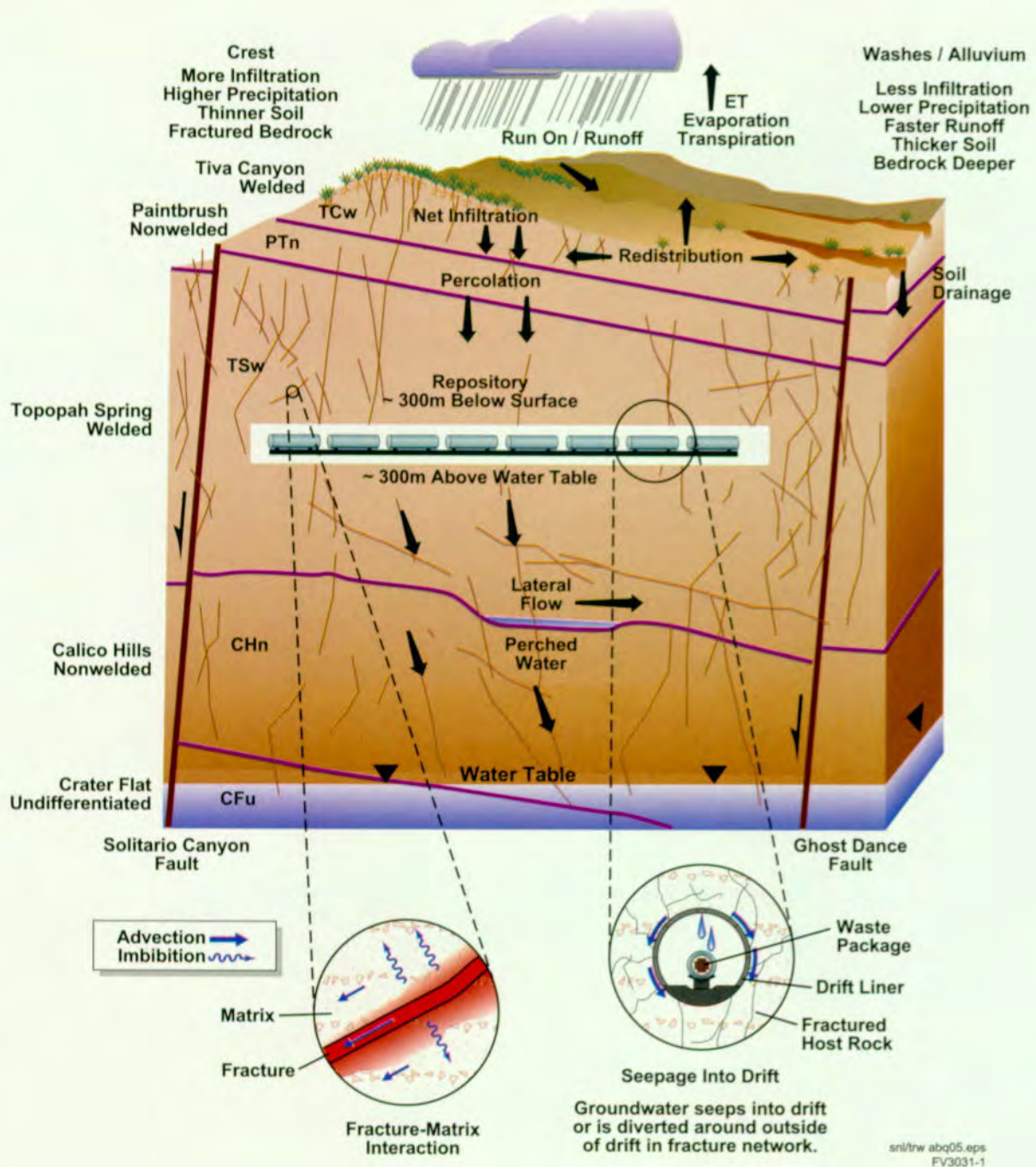


Figure 3-1. Conceptual Drawing of Unsaturated Zone Flow Processes at Different Scales  
Mountain-scale and drift-scale models capture these processes except for fracture-scale processes, which are captured as parameters in continuum flow models.



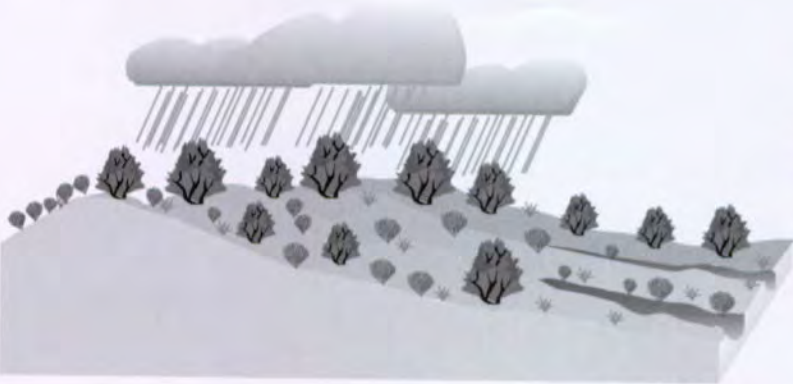
### Dry

**Yucca Mountain**  
precipitation: 170 mm/yr average  
vegetation: desert scrub



### Long-Term Average

analogue: Rainier Mesa, NV  
(like Santa Fe, NM)  
precipitation: 300 mm/yr average  
vegetation: open juniper/sage forest



### Superpluvial

analogue: South Lake, CA  
(like Los Alamos, NM)  
precipitation: 450 mm/yr average  
vegetation: dense juniper forest

snl/trw abq27 eps  
FV3031-2

Figure 3-2. Conceptual Drawing of Projected Climates for Yucca Mountain  
Climate change was modeled as three discrete climate states.

Unsaturated and Saturated Flow under Isothermal Conditions (NRC 1997e; 1997f). Specifically, the information presented is pertinent to four of the eight subissues of this key technical issue, consisting of: range of future climates, hydrologic effects of climate change, amount and distribution of present-day infiltration, and amount and distribution of groundwater percolating through the repository horizon.

Unsaturated zone flow is closely related to other model components, including thermal hydrology, the engineered barrier system, unsaturated zone transport, and flow and transport in the saturated zone. The relationships among the four subcomponents of unsaturated zone flow, and relationships with the other TSPA components, are shown in Figures 3-3–3-6.

Sections 3.1.1 and 3.1.2 summarize development of the climate, infiltration, mountain-scale flow, and seepage models, including the important processes, assumptions, and model implementation. Section 3.1.3 presents results based on the

flow models for the unsaturated zone and interpretations relevant to repository performance. Additional information on unsaturated zone flow can be found in Chapter 2 of the *Total System Performance Assessment-Viability Assessment (TSPA-VA) Analyses Technical Basis Document* (CRWMS M&O 1998i).

### 3.1.1 Construction of the Conceptual Model

Previous TSPAs have determined that unsaturated zone flow is an important contributor to repository performance (Wilson et al. 1994, Sections 14.6.3, 15.5.4; CRWMS M&O 1995, Sections 9.2.5, 9.3.7). Calculated peak doses are sensitive to the current percolation rate at the repository horizon, the amount of increase in the percolation rate under future wetter climate conditions, the partitioning of flow between matrix and fractures, and the amount of seepage into emplacement drifts.

An unsaturated zone flow workshop was held in December 1996 to supplement the previous TSPA determinations about unsaturated zone flow. A

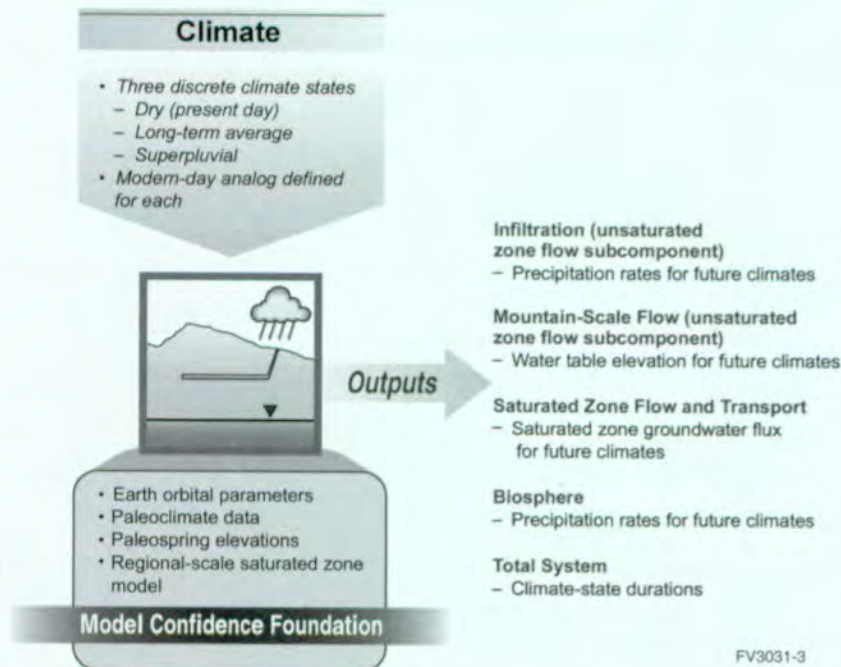
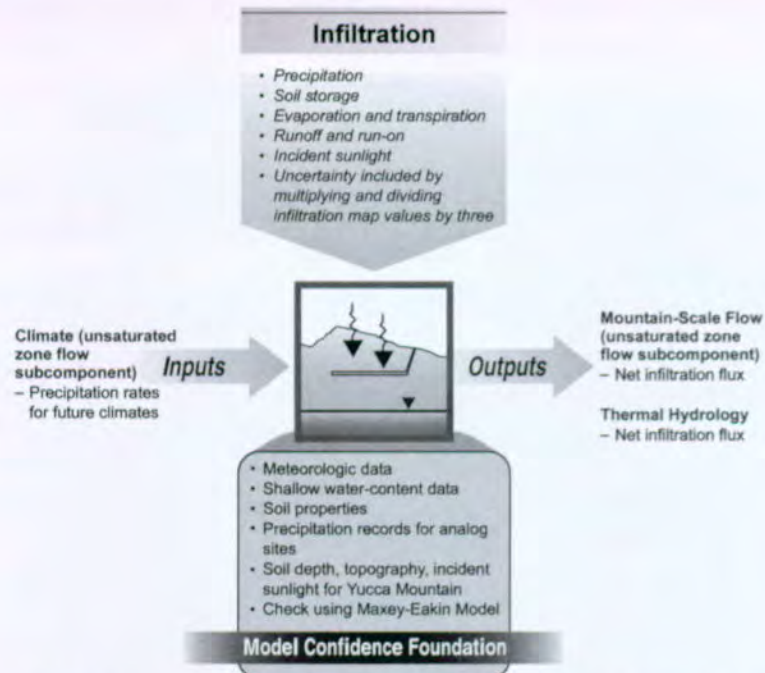
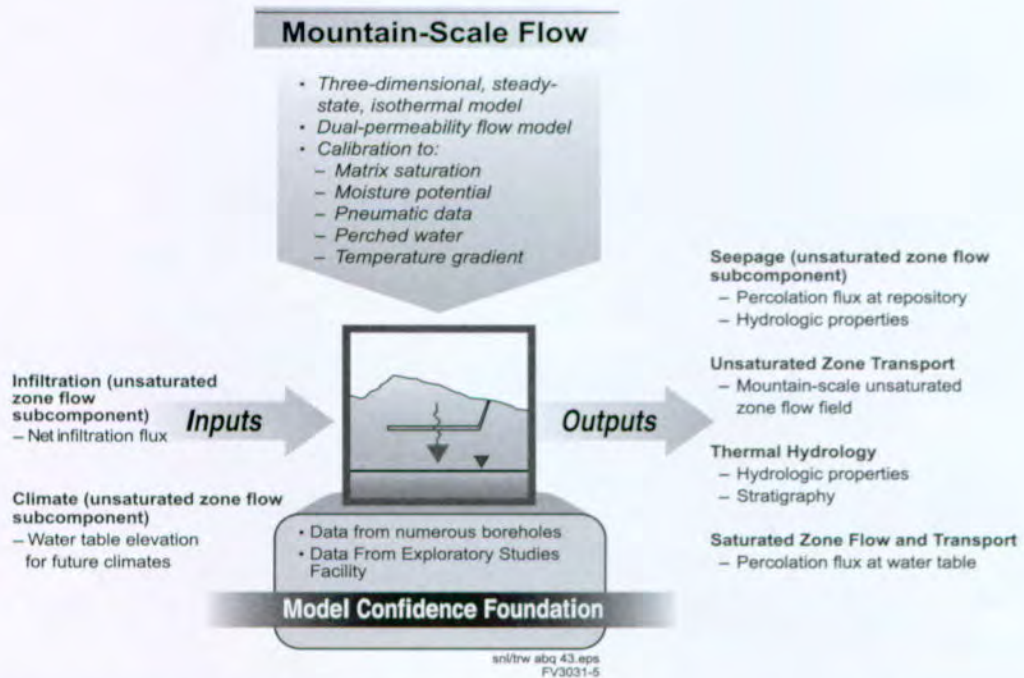


Figure 3-3. Coupling of the Climate Subcomponent to Other Unsaturated Zone Flow Subcomponents and to Other Total System Performance Assessment for the Viability Assessment Components  
The three discrete climates are illustrated in Figure 3-2.



FV3031-4

Figure 3-4. Coupling of the Infiltration Subcomponent to Other Unsaturated Zone-Flow Subcomponents and to Other Total System Performance Assessment for the Viability Assessment Components  
Infiltration variability over the site is captured in the model, which covers 228 square kilometers (88 square miles) around Yucca Mountain.



snl/trw abq 43 eps  
FV3031-5

Figure 3-5. Coupling of the Mountain-Scale Flow Subcomponent to Other Unsaturated Zone Flow Subcomponents and to Other Total System Performance Assessment for the Viability Assessment Components  
The three-dimensional mountain-scale flow model was used directly and not abstracted.

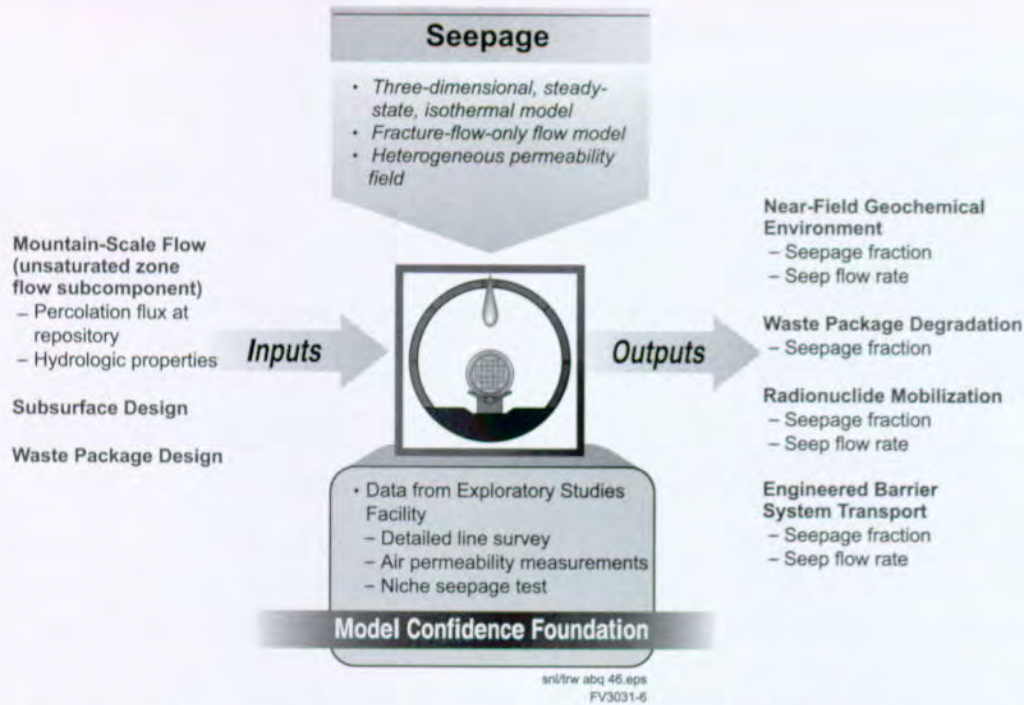


Figure 3-6. Coupling of the Seepage Subcomponent to Other Unsaturated Zone Flow Subcomponents and to Other Total System Performance Assessment for the Viability Assessment Components  
The output "seepage fraction" means the fraction of waste packages receiving drips from seeps.

large portion of the workshop was a discussion of the current knowledge of unsaturated zone flow in Yucca Mountain and the important issues for evaluating unsaturated zone flow. The participants compiled a list of these issues and discussed priorities and approaches for dealing with them in the TSPA-VA (Table 3-3). The issues and priorities developed at the workshop largely determined the methods used for modeling unsaturated zone flow in TSPA-VA. Sections 3.1.2.1 and 3.1.2.2 discuss future climate and infiltration. Section 3.1.2.3 discusses issues related specifically to the unsaturated zone flow at the mountain scale. Section 3.1.2.4 discusses issues related to seepage.

In addition, YMP conducted an unsaturated zone flow model expert elicitation (CRWMS M&O 1997n). Project data and models were presented to a group of experts (mostly from outside the YMP) for their evaluation. The experts were asked to evaluate data and provide estimates of uncertainty in surface infiltration and deep percolation. Probability distributions for infiltration and percolation were elicited from each expert. The mean values

Table 3-3. Unsaturated Zone Flow Abstraction/Testing Workshop

| UNSATURATED ZONE FLOW ABSTRACTION/TESTING WORKSHOP   |  |
|--|--|
| December 11–13, 1996, Albuquerque, NM (CRWMS M&O 1997i)  |  |
| <b>PRIORITIZATION CRITERIA</b>   |  |
| <ul style="list-style-type: none"> <li>• Does the issue have a strong effect on:                             <ul style="list-style-type: none"> <li>- Percolation flux at the repository?</li> <li>- Seepage into the drift?</li> <li>- The partitioning of flow between the fractures and matrix?</li> </ul> </li> <li>• Will the issue be important to flow and transport below the repository?</li> </ul> |  |
| <b>Highest Priority Issues</b>   |  |
| <ul style="list-style-type: none"> <li>• Infiltration and future climate</li> <li>• Model calibration</li> <li>• Lateral flow and perched water below the repository</li> <li>• Flow channeling and seepage into the drift</li> </ul>  |  |
| <b>Analysis Plans</b>  |  |
| <ul style="list-style-type: none"> <li>• Sensitivity studies conducted on the site-scale model to determine abstraction methods for unsaturated zone flow</li> <li>• Seepage into drifts under pre-waste-emplacment conditions</li> <li>• Testing of perched-water concepts and their implications for TSPA-VA calculations</li> <li>• Sub-grid-scale fractures and model calibration</li> </ul>             |  |

of estimated net infiltration ranged from 3.9 mm/year (0.15 in./year) to 12.7 mm/year (0.50 in./year); the mean values of estimated percolation flux at the repository horizon ranged from 3.9 mm/year (0.15 in./year) to 21.1 mm/year (0.83 in./year). These values are commensurate with the current modeled average infiltration of approximately 8 mm/year (0.3 in./year) for the simulated repository region and the modeled spatial variation in percolation flux ranging from near zero to approximately 20 mm/year (0 to 0.8 in./year) (see Section 3.1.2.2)

The experts generally agreed that the infiltration map used shows the general variability of infiltration by location, but several suggested that the map should have more infiltration beneath washes with thin alluvial cover. The experts also agreed that net infiltration is characterized by episodic major storms but that most of the infiltration from each storm is attenuated within the system. Most of the experts agreed that contrasts in the hydrologic properties between units would likely cause lateral diversion of flow above the repository, particularly at the Tiva Canyon welded to Paintbrush nonwelded contact (Figure 3-1); however, the amount of diversion would be limited to scales of several meters to tens of meters. This finding is consistent with the results of the mountain-scale flow simulations, which show nearly vertical flow above the repository. The experts did not address the issue of lateral diversion caused by perched water below the repository. Based on the low matrix permeabilities in the Topopah Spring welded unit, the experts also agreed that the flow in the Topopah Spring welded unit is predominantly in the fractures. This finding is consistent with YMP simulated results. Finally, the experts recommended a number of additional modeling and data-collection activities to improve estimates of infiltration, percolation, and seepage. Many of these recommendations have already been incorporated into this TSPA or are planned in future work.

### 3.1.1.1 Climate

"Climate" refers to the meteorological conditions that characteristically prevail in a particular region. For this TSPA, climate conditions at Yucca

Mountain must be known to determine the hydrology within and around Yucca Mountain. In particular, the amount of precipitation largely determines the amount of infiltration.

The climate in the Yucca Mountain region is presently warm and semiarid, with mean annual temperature of 16°C (61°F) and mean annual precipitation of about 170 mm/year (6.7 in./year). Climate proxies, or the physical remains of substances that carry the imprint of past climates, indicate that the climate in the Yucca Mountain region is not static. For example, climate proxies indicate that during the last glacial period, between 35,000 and 10,000 years ago, most of the world was drier, but the southwest United States was wetter. At that time, the Yucca Mountain region contained wetlands and streams; there were springs at the mouth of Crater Flat and in the Amargosa Desert; there was a lake in Death Valley (Lake Manley) that was over 90 m (295 ft) deep; and sufficient vegetation existed to support a variety of herbivores ranging from mammoths to sheep (CRWMS M&O 1998m, Chapter 4).

Future climate is estimated based on what is known about past climate, with consideration given to climate impacts caused by human activities. Calcite in Devils Hole, a fissure in the ground approximately 40 km (25 miles) southeast of Yucca Mountain, provides the best-dated record of climate change over the past 500,000 years. The record shows continual variation, often with very rapid jumps, between cold glacial climates (for the Great Basin, these are called pluvial periods) and warm interglacial climates similar to the present. The fluctuations average about 100,000 years in length. Because this basic time scale has been corroborated by other climate proxies (e.g., oxygen-isotope variations in marine sediments), it has been selected as the average climate cycle (CRWMS M&O 1998m, Section 4.2.3).

Climate conditions specific to the Yucca Mountain region were estimated from other, more local, climate proxies. Packrat middens are deposits consisting of plant macrofossils cemented by packrat urine that can be dated by radiocarbon methods. Plant life during the last pluvial period

has been reconstructed by analyzing packrat middens. This reconstruction shows an open juniper forest in the lower elevations and a montane conifer forest in the higher elevations of the Yucca Mountain region. From modern locations with open juniper forests, it can be inferred that temperature was then approximately 6 C° (11 F°) colder, and precipitation was approximately two times greater than modern averages. From global climate proxies, in combination with the record from Devils Hole, the last glacial or pluvial period appears to be a rather typical climate, approaching a long-term average climate in the Yucca Mountain region (CRWMS M&O 1998m, Section 4.2.4).

Climate proxies indicate that the last glacial period was not the most extreme climate in the record. The next-to-last glacial period, occurring approximately 150,000 years ago, and a glacial period occurring approximately 600,000 years ago appear to have been markedly colder and wetter. These extreme glacial climates are referred to as superpluvials. During the next-to-last glacial period (150,000 years ago), Lake Manley in Death Valley reached a depth of over 125 m (410 ft). Lake sediments deposited by Owens Lake, north of Death Valley, hold ostracod and diatom remains of species that now live in Canada. Other evidence suggests that the vegetation in the region was mainly a dense juniper forest. This evidence supports the inference (with somewhat less confidence than inferences for the most recent glacial period) that temperature was approximately 10°C (18°F) colder, and precipitation was approximately three times greater than modern averages (CRWMS M&O 1998m, Section 4.2.3).

The wetter environments of the past suggest that more groundwater flowed beneath Yucca Mountain. Several lines of evidence indicate that the water table was 80 to 120 m (250 to 400 ft) higher during the last pluvial period. The first indication is the presence of spring deposits at the mouth of Crater Flat that have been dated to approximately 13,000 years ago. In addition, a strontium-isotope ratio characteristic of the saturated zone has been found in pore waters of rocks over 80 m (250 ft) above the present water

table at Yucca Mountain, and carbon-isotope differences have been found as well. Lastly, water-table rises in this range have been obtained in saturated zone groundwater modeling of future climates. Note that the repository is planned to be over 300 m (1,000 ft) above the present water table, so the repository would still be well above the water table even with a rise of 120 m (400 ft) (CRWMS M&O 1998m, Sections 5.2.6 and 5.2.7).

### 3.1.1.2 Infiltration

Net infiltration is the penetration of water through the ground surface and to a depth where it can no longer be withdrawn by evaporation or transpiration by plants. Once water has entered bedrock or has penetrated below the root zone in soil (a depth of approximately 6 m, or 20 ft, at Yucca Mountain) it has infiltrated. The conceptual model used for infiltration calculations is based on evidence from field studies at Yucca Mountain, combined with established concepts in soil physics and hydrology (Flint et al. 1996). The overall framework of the conceptual model is provided by the hydrologic cycle, including processes on the surface and just below the surface that affect net infiltration.

Important infiltration processes include precipitation (rain and snow); runoff and run-on (flow of surface water off one place and onto another); evaporation; transpiration (removal of moisture from soil by plants); and redistribution of moisture by flow in the shallow subsurface. Localized precipitation depends on meteorological factors, and geographic location and elevation. The generation of runoff depends on precipitation intensity, shallow moisture conditions, soil depth, soil porosity, soil permeability, bedrock permeability, and ground-surface slope. Run-on depends mostly on material surface properties, topography, and channel geometry. Evaporation depends on the amount of sunlight, temperature, and the evaporative capacity of the atmosphere. Transpiration depends on the type of vegetation present. Redistribution of moisture by flow in the shallow subsurface in response to gravity and capillary pressure is strongly dependent on soil and bedrock properties. The removal of water

through evaporation and transpiration (together called evapotranspiration) is closely coupled with redistribution of moisture in the shallow subsurface.

The conceptual model of infiltration was developed based on analysis of an 11-year record of moisture measurements from 99 boreholes on Yucca Mountain (Flint and Flint 1995). Relative changes in water-content profiles were compared to precipitation records, estimates of evapotranspiration, physiographic setting, bedrock geology, and soil cover. Results from field studies indicate that high soil saturation leading to net infiltration primarily occurs during a series of winter storms producing moderate precipitation. These storms tend to occur more frequently during winters with an active El Niño pattern. The timing, intensity, and duration of precipitation; storage capacity of the soil; and evapotranspiration determine the availability of water for net infiltration. In the upland areas of Yucca Mountain with shallow soil cover, the amount of net infiltration depends on the effective conductivity of the underlying bedrock. Lower conductivity leads to moisture being held longer in the soil, where it can potentially be lost to evapotranspiration. During winter, when potential evapotranspiration is at a minimum, smaller amounts of precipitation are needed to develop and maintain saturated conditions at the soil-bedrock contact.

### **3.1.1.3 Mountain-Scale Unsaturated Zone Flow**

Unsaturated zone flow is the percolation of groundwater through rocks above the water table. Unsaturated zone flow varies with the rock strata through which the water flows (CRWMS M&O 1998m, Sections 5.3.4.2, 5.3.4.3). As depicted in Figure 3-1, the unsaturated zone in Yucca Mountain is composed of alternating layers of welded and nonwelded tuffs. The terms welded and nonwelded refer to the degree of consolidation of the rock when it was formed from volcanic ash millions of years ago. Welded tuff is hard, dense rock but is typically very fractured. The welded tuff rock matrix is relatively impermeable, but the total permeability is high because of the fractures.

Nonwelded tuff is softer and typically less fractured. Its matrix permeability is much higher than that of welded tuff matrix, but its total permeability is typically lower. A special case is zeolitic nonwelded tuff, which was altered during the original cooling in such a way that its matrix permeability is very low (similar to the matrix permeability of welded tuff). Zeolitic tuff may also have little fracturing so that its total permeability is very low. Perched-water zones, or localized saturated regions above the water table, have been observed on the zeolitic tuff in several boreholes.

Fractures play an important role in unsaturated zone flow (CRWMS M&O 1998m, Section 5.3.4.3.2). This role is especially important when considering radionuclide transport from a nuclear-waste repository. Flow in fractures is typically much faster than flow in the porous matrix, potentially leading to much faster travel to the water table. A few years ago, most flow in Yucca Mountain was thought to be through the porous rock matrix. This is not consistent with recent higher estimates of infiltration. The current estimate for present-day net infiltration over the repository area is about 8 mm/year (0.3 in./year) and the estimate is much higher for the wetter future climates. The rock matrix flow capacity is much less than 8 mm/year (0.3 in./year) in the welded tuff, implying that most of the flow is moving through fractures. Because the matrix pores are not saturated with water, it is inferred that the flows in fractures and matrix are only weakly coupled; otherwise, the matrix pores would be saturated.

The equivalent-continuum model, in which the fracture and matrix flows are strongly coupled, was widely used for modeling unsaturated zone flow when net infiltration at Yucca Mountain was thought to be 1 mm/year (0.04 in./year) or less. This model was used in the 1993 TSPA (Wilson et al. 1994, Chapter 14) and the 1995 TSPA (CRWMS M&O 1995, Section 4.2). Two other models of fracture-matrix unsaturated flow that have been used in past TSPAs are the generalized equivalent-continuum model in the 1995 TSPA (CRWMS M&O 1995, Section 7.2) and the Weeps model in the 1993 TSPA (Wilson et al. 1994,

Chapter 15). The generalized equivalent-continuum model is a modification of the equivalent-continuum model in which the fracture and matrix flows are strongly coupled, but fractures are assumed to flow more easily above a matrix-saturation threshold. The Weeps model does not consider the rock matrix and assumes that all significant flow is through the fractures.

The generalized equivalent-continuum model and the Weeps model overcome one of the problems with the equivalent-continuum model because they reasonably can be applied with the higher infiltration rates being used now. Most recent modeling (Bodvarsson et al. 1997, Chapter 6) has used the dual-permeability model, which is a more general model in which the fracture-matrix coupling can be strong or weak, depending on the parameter values used. The dual-permeability model has the flexibility to represent almost the entire range of possible flow behavior through variation of fracture-matrix coupling strength. This allows flow behavior to change continuously from the equivalent-continuum model, which is dominated by matrix flow, to a Weeps-type flow almost entirely within the fracture network.

In this TSPA, unsaturated zone flow, unsaturated zone transport, and thermal hydrology are modeled using the dual-permeability model. Thermal hydrology uses the generalized equivalent-continuum model as well (see Section 3.2). In the dual-permeability model, fracture-matrix coupling strength is used as an adjustable calibration parameter that is set so that net infiltration can be relatively high, as implied by the infiltration model, with matrix saturation in the model near observed values and with measured and inferred values of all matrix and fracture hydrologic properties.

The data used to develop the mountain-scale calibrated flow fields for the unsaturated zone come from several surface-based drillholes and from the Exploratory Studies Facility, which is an 8-km (5-mile) long tunnel through Yucca Mountain. These data include rock-matrix saturations, water potentials (the ability for rock to hold

water), and temperatures; perched-water locations and amounts; chemical composition and isotopic abundances of groundwater and mineral deposits; air permeability and air-pressure measurements; rock types and mineralogy; fault locations and offsets; fracture density and orientations; and matrix permeability and saturation/desaturation parameters. More detailed information on data and the calibration procedure are found in Bodvarsson et al. (1997, Chapter 6) and CRWMS M&O (1998m, Section 5.3.4.4).

The effects of discrete fractures and other small-scale features are not included in the dual-permeability model and may be important. The dual-permeability model (as well as the equivalent-continuum model and the generalized equivalent-continuum model) represents flow through the myriad individual fractures and matrix blocks by approximating them as continuous flow fields. The Weeps model is a simplified version of a discrete-fracture flow model and some of its implications are different from those of continuum models. The effects of discrete fractures are not considered directly in this TSPA, and it is uncertain whether some of their effects might be important. This TSPA uses an alternative flow model called the dual-permeability/Weeps model, which is similar to the Weeps model in many respects but which still treats fractures as a continuum rather than as discrete flow paths.

#### 3.1.1.4 Seepage into Drifts

Seepage is the movement of liquid water into emplacement drifts. The basic conceptual model for seepage is that openings in unsaturated media act as capillary barriers and divert water around them. This capillary barrier effect has been tested in the Exploratory Studies Facility by niche tests in which water is injected above a niche (a side tunnel off the main tunnel). Results from the tests indicate that most of the water does not seep into an opening just 2 ft below (CRWMS M&O 1998i, Section 2.4.4.9). In addition, no natural seeps into the Exploratory Studies Facility tunnel have been observed, although the lack of seeps may be partially caused by drying from tunnel ventilation.

For seepage to occur in the conceptual model, the rock pores at the drift wall must be locally saturated. Drift walls can become locally saturated by either disturbance to the flow field caused by the drift opening or variability in the permeability field that creates channelized flow and local ponding. Of the two reasons, the variability effect is more important. Drift-scale flow calculations made with uniform hydrologic properties suggest that seepage will not occur at expected percolation fluxes. However, calculations that include permeability variations do predict seepage, with the amount depending on the hydrologic properties and the incoming percolation flux (CRWMS M&O 1998i, Section 2.4.4).

For the drift-scale flow model used for calculating seepage, the fracture hydrologic properties were defined in the same way as for the mountain-scale flow model (Bodvarsson et al. 1997, Chapter 7). Additional information needed to define the variability of the fracture-permeability field by location was taken from a series of air-permeability tests conducted at the location of the drift-scale thermal test in the Exploratory Studies Facility (CRWMS M&O 1998i, Section 2.4.4.2.1).

As with the modeling of mountain-scale flow, the dual-permeability model is preferred for modeling seepage at the drift scale. However, to simplify the drift-scale calculations, effects of the rock matrix were not considered, and flow was calculated using a model for only the fracture continuum (CRWMS M&O 1998i, Section 2.4.4). This simplification is conservative compared to the dual-permeability model because the effect of including the matrix would be to decrease the fracture flow and reduce the amount of seepage (the large capillary suction in matrix pores prevents matrix flow from seeping into drift openings). Another simplification is to assume steady-state conditions. It is uncertain whether there is episodic flow at the repository and what its effect on seepage would be. Also, as with the modeling of mountain-scale flow, discrete-fracture effects are potentially important.

In the seepage modeling, drift collapse and thermal alteration of hydrologic properties are not considered. It is expected that the drifts will only

be stable for a few hundred to a thousand years. Therefore, long-term repository performance will depend on the amount of seepage into a drift filled with rockfall rubble, rather than into an open drift. In addition, thermal-mechanical and thermal-chemical effects could alter the hydrologic properties around the drifts, possibly even permanently. The impact of these effects is uncertain.

### **3.1.2 Implementation of the Performance Assessment Model**

#### **3.1.2.1 Climate**

Climate calculations are based on a long-term average climate, with relatively short periods of drier or wetter climates. The typical climate, defined to be the long-term average climate, is like the most recent glacial or pluvial period; the drier climate is similar to present day climate; the wetter climate is the superpluvial climate (Figure 3-2). Several factors led to this strategy. First, there is a great deal of uncertainty in estimating future climate, and a complex climate model would give the impression of a greater knowledge of, and certainty about, future conditions. Second, although this TSPA could have been based on a worst-case climate, a superpluvial climate is atypical and seen only rarely in the climate record. Basing the TSPA on a superpluvial climate would be misleading. Third, modeling groundwater flow with a three-dimensional model is complex and time consuming. Because of this complexity, only three discrete climate states were considered.

Models of human impact on future climates, caused by global warming from increased atmospheric carbon dioxide, are speculative, although they are supported by some global-climate modeling and the general increase in global temperature noted this century. At Yucca Mountain the effect of global warming is estimated to increase average precipitation to a level similar to the long-term average. This estimate is based on atmospheric model input and resembles near-continuous El Niño conditions at Yucca Mountain and the near doubling of precipitation that accompanies these conditions. Therefore, any global-warming impact on future climates is

considered to be within the bounds of paleoclimate ranges (CRWMS M&O 1998i, Section 2.4.1.1). However, infiltration might be different because the temperature would be higher (expected to be about 2 C°, or 4 F°, warmer than currently and more than 5 C°, or 9 F°, warmer than the long-term average), but effects of these temperature differences were neglected for TSPA-VA. These effects will be addressed in future TSPAs, as appropriate.

The modeled climate, then, alternates between three states: dry or present-day climate; long-term average climate; which is about twice the dry-climate precipitation; and superpluvial climate, which is about three times the dry-climate precipitation. The length of the first dry climate, or current climate, is sampled uniformly between 0 and 10,000 years, with an expected value of 5,000 years. The length of subsequent dry climates is sampled uniformly between 0 and 20,000 years, with an average of 10,000 years. The duration of long-term average climates is sampled uniformly between 80,000 and 100,000 years, with an average of 90,000 years. The duration of the superpluvial climates is sampled similarly to dry climates, from 0 to 20,000 years. Dry and long-term average climates alternate from the time of repository closure until the long-term average climate that spans the 250,000-year mark. The last part of that long-term average period is replaced by a superpluvial climate of the sampled duration. Then the climate model returns to alternating dry and long-term average climates until the long-term average climate that spans the time of 400,000 years after the first superpluvial. The end of that long-term average climate is again replaced by a superpluvial, and then back to dry, followed by alternating long-term average and dry climates. About 90 percent of the time is spent in the long-term average climate.

The data used in the climate model are summarized in Table 3-4. Additional information on the various components is found in the sections about the models using climate information (see Section 3.7 for additional information about the multiplier for saturated zone flux).

Table 3-4. Data Summary for the Climate Model

| Climate Parameter   | Dry (Present Day)   | Long-Term Average    | Superpluvial   |
|---------------------|---|----------------------|----------------|
| Precipitation       | Current distribution  | 2 x current          | 3 x current    |
| Water-table rise    | 0   | 80 m (260 ft)        | 120 m (390 ft) |
| Saturated zone flux | Current distribution  | 3.9 x current        | 6.2 x current  |
| Duration            | 0-10,000 years for current;<br>0-20,000 years for future dry climates | 80,000-100,000 years | 0-20,000 years |

The connections between climate and the other subcomponents of unsaturated zone flow, and the other TSPA components, are shown in Figure 3-3.

### 3.1.2.2 Infiltration

Distributed net infiltration rates by location were determined for each of the three climate states using the YMP infiltration model (Flint et al. 1996; CRWMS M&O 1998m, Section 5.3.4.1). The infiltration model simulates the water content of the soil profile at each location by determining water balance using precipitation input, a model for evapotranspiration, and available water in the soil profile.

The model covers an area of 228 km<sup>2</sup> (88 miles<sup>2</sup>) around Yucca Mountain, using a regular grid with 30-m (98-ft) spacing. The inputs to the model include daily precipitation; ground-surface elevation; bedrock geology and hydrologic properties; soil type and hydrologic properties; soil depth; and identification of each location as ridge top, side slope, terrace, or channel (Flint et al. 1996, pp. 69-83).

The infiltration model was calibrated using the records of measured water-content profiles from shallow boreholes and records of daily precipitation. Model calibration consisted of qualitative and quantitative comparisons of measured versus simulated water-content changes for the soil profile. The model calibration process adjusted the parameters for evapotranspiration so that a satisfactory fit between measured and simulated time-dependent changes in soil moisture was obtained

for all borehole locations (Flint et al. 1996, pp. 84–85).

Daily precipitation data were obtained using available records or generated using a stochastic model of daily precipitation. Most of the long-term precipitation records in the Yucca Mountain region (southern Nevada and southeastern California) are less than 50 years old. Precipitation models were used to generate longer precipitation sequences and allow the simulation of paleoclimates that do not have present-day analogs. To represent the dry, present-day climate, daily precipitation records from a weather station located approximately 15 km (9 miles) east of the repository site were used. Although this station is lower in elevation than the repository site (1,000 m, or 3,300 ft, versus 1,500 m, or 4,900 ft), it provides the longest, almost-continuous record of daily precipitation near the repository. The precipitation values were scaled upward to compensate for the difference in elevation (Flint et al. 1996, p. 71). The stochastic precipitation model estimated the 100-year-average precipitation to be 150 mm/year (6 in./year), slightly lower than the recently observed average of 170 mm/year (6.7 in./year) (CRWMS M&O 1998m, Section 5.3.4.1.5.1).

Present-day analogs were chosen to represent the wetter future climates. For the long-term average climate, daily precipitation records from Rainier Mesa were used. This weather station is approximately 40 km (25 miles) north of Yucca Mountain and at higher elevation (2,200 m, or 7,200 ft). For the superpluvial climate, records from South Lake, California, were used. South Lake is located on the eastern slope of the Sierra Nevada at an even higher elevation (2,700 m, or 8,900 ft). These analog sites have not been rigorously evaluated for predictions of the expected characteristics of future climates (for example, the expected seasonal distribution of precipitation). The modeled 100-year-average precipitation based on the precipitation record was found to be 289 mm/year (11.4 in./year) for the Rainier Mesa site and 427 mm/year (16.8 in./year) for the South Lake site (CRWMS M&O 1998m, Section 5.3.4.1.5.3).

Because net infiltration is an important contributor to unsaturated zone flow and seepage into drifts, uncertainty about infiltration and how that uncertainty affects repository performance must be considered. By extension, infiltration contributes to other components that use the results of the unsaturated zone flow modeling. For TSPA-VA, uncertainty about infiltration was included by creating three different infiltration maps: the base infiltration map calculated using the infiltration model, and two other maps made by uniformly multiplying or dividing the base map by three. The same procedure was followed for the three climate states, for a total of nine infiltration maps. The factor-of-three increase or decrease was constrained by comparing the calculated mountain-scale flow fields with observations. The flow model was expected to reproduce the observed temperature gradient, which is a function of net infiltration. Infiltrating water introduces an advective component to the ambient heat balance, changing the temperature profile from what it would be if heat transfer were by thermal conduction only (see Bodvarsson et al. 1997, Chapter 11). If increases are greater than about a factor of three, the flow model cannot reproduce the observed temperature gradient for the unsaturated zone. The factor of three reduction has no definite basis, but was done simply to have symmetry in the amount of increase and decrease.

To incorporate the three infiltration maps into a Monte Carlo framework, they were assigned probabilities. Because the base infiltration map represents the current best estimate of infiltration, the probabilities were assigned so that the base infiltration was equal to the statistical mean. The probability for the high infiltration case (base map times three) was determined by balancing the recommendations made by the participants in the unsaturated zone flow model expert elicitation (CRWMS M&O 1997n, Table 3-1) with information such as the temperature gradient implications. A 10 percent probability was assigned to the “base infiltration multiplied by three” case. The requirement that the “base infiltration” case be the mean of the infiltration distribution then uniquely determines the other two probabilities to be 60 percent for the “base infiltration” case and

30 percent for the “base infiltration divided by three” case. The same probabilities are used for the other climate states, and the infiltration rates were assumed to be perfectly correlated among climates (Table 3-5). For example, when climate changes from dry to long-term average with dry-climate infiltration equal to base infiltration divided by three, then long-term average and superpluvial infiltration are also base infiltration divided by three. A more quantitative basis for infiltration probability distributions could be achieved by running the infiltration model in a stochastic mode to derive infiltration uncertainty from input-parameter uncertainties. Estimates of net infiltration for future climates could be improved by inclusion of the effects of temperature and vegetation changes. Note that in addition to the probabilities, Table 3-5 gives the net infiltration averaged over the repository area for each case.

The connections between infiltration and the other subcomponents of unsaturated zone flow, and the other TSPA components, are shown in Figure 3-4.

### 3.1.2.3 Mountain-Scale Unsaturated Zone Flow

The YMP three-dimensional, site-scale flow model for the unsaturated zone (Bodvarsson et al. 1997) was used in calculating mountain-scale, unsaturated zone flow for this TSPA. Three-dimensional modeling was needed primarily because of flow characteristics below the repository, where significant lateral flow is believed to occur because of low-permeability zeolitic layers and perched water. The model uses the dual-permeability conceptual model, as discussed in Section 3.1.1.3. The direct use of the three-dimensional, mountain-

scale flow model eliminated the need to test simplified abstractions against more complex process models. The models were tested directly against site data as part of the calibration procedure. The following paragraphs summarize the most important features of the mountain-scale flow model for the unsaturated zone.

The mountain-scale flow model for the unsaturated zone is based on site data that include core measurements of porosity, permeability, saturation, and moisture potential; perched-water observations; fracture-frequency data from the Exploratory Studies Facility; air pressure monitoring and air permeability tests; and geochemical data. These data were used to estimate hydrologic parameters through direct calculations and calibration methods. In addition, a geologic-framework model was used to define the proper stratigraphy for the unsaturated zone flow model. Numerous sensitivity analyses have been performed to understand the importance of infiltration, hydrologic parameters, fracture-matrix interactions, and features such as faults and perched water.

The YMP site-scale flow model for the unsaturated zone, including its calibration procedures and sensitivity analyses, was used to develop a base case, mountain-scale model for unsaturated zone flow. Although there are considerable data for calibrating the mountain-scale flow model, there can not be enough data to eliminate all uncertainty. Thus, more than one calibrated model can fit the available data. The base case includes uncertainty in both infiltration (Section 3.1.2.2) and hydrologic parameters that were determined to be important through sensitivity analyses (CRWMS M&O 1998i, Section 2.4.3.2). In the base case, the only

Table 3-5. Average Net Infiltrations and Probabilities for the Infiltration Cases

|  | Dry (Present Day) | Long-Term Average | Superpluvial | Probability<br>(All Climate States) |
|--|-------------------|-------------------|--------------|-------------------------------------|
| Low infiltration<br>(base infiltration ÷ 3)  | 2.6 mm/year       | 14 mm/year        | 37 mm/year   | 30%                                 |
| Base infiltration                            | 7.7 mm/year       | 42 mm/year        | 110 mm/year  | 60%                                 |
| High infiltration<br>(base infiltration × 3) | 23 mm/year        | 125 mm/year       | 340 mm/year  | 10%                                 |

Note: 25.4 mm = 1 in.

hydrologic parameters varied are the air-entry parameter for fractures ( $\alpha_f$ ) and the fracture-matrix coupling strength. The fracture air-entry parameter governs capillary pressure in the fractures, and the fracture-matrix coupling strength governs how easily water flows between fractures and the rock matrix. The fracture air-entry parameter is directly proportional to the effective fracture aperture.

For each hydrogeologic unit a range of uncertainty was developed for the fracture air-entry parameter based on measurements of fracture density and air permeability. The fracture-matrix coupling strength was not varied independently but was used as a calibration variable. The fracture-matrix coupling strength was constrained to have only three different values (for welded tuff, nonwelded nonzeolitic tuff, and nonwelded zeolitic tuff) in a given calibration. These three values were chosen to optimize the match with observed borehole matrix saturations and water potential. Additional information on parameters and calibration can be found in CRWMS M&O (1998i, Section 2.4.3).

The base case includes the following independently calibrated models:

- Base infiltration divided by 3 and the fracture air-entry parameter at a minimum for each layer
- Base infiltration divided by 3 and the fracture air-entry parameter at a maximum for each layer
- Base infiltration and the fracture air-entry parameter at the nominal "best estimate" for each layer
- Base infiltration multiplied by 3 and the fracture air-entry parameter at a minimum for each layer
- Base infiltration multiplied by 3 and the fracture air-entry parameter at a maximum for each layer

Five models were used, rather than the full matrix of nine combinations, to reduce computational

requirements. Flow was calculated for each of the five models for the three climate states: dry (present-day), long-term average, and superpluvial. The probabilities for each case are given in Table 3-6. The probabilities for the infiltration cases are discussed in Section 3.1.2.2. The probabilities for minimum and maximum fracture air-entry parameter values are equal because, based on the way the ranges were defined, there is no reason to favor one over the other.

Table 3-6. Probabilities for the Mountain-Scale Unsaturated Zone Flow Cases

|  | Minimum<br>$\alpha_f$ | Nominal<br>$\alpha_f$ | Maximum<br>$\alpha_f$ |
|--|-----------------------|-----------------------|-----------------------|
| Low infiltration (base infiltration $\div$ 3)    | 15%                   | not considered        | 15%                   |
| Base infiltration                                | not considered        | 60%                   | not considered        |
| High infiltration (base infiltration $\times$ 3) | 5%                    | not considered        | 5%                    |

Note:  $\alpha_f$  = fracture air-entry parameter

In addition to the base case, an alternative model called the dual-permeability/Weeps model was considered. This model has a significantly reduced fracture-matrix coupling strength to induce more fracture flow. The biggest difference between the base case model and the dual-permeability/Weeps model is that the dual-permeability/Weeps model shows flow predominantly in fractures even in nonwelded hydrogeologic units while the base case shows flow in nonwelded nonzeolitic units predominantly in the rock matrix.

The connections between mountain-scale flow and the other subcomponents of unsaturated zone flow, and the other TSPA components, are shown in Figure 3-5.

### 3.1.2.4 Seepage into Drifts

The method for modeling seepage into the emplacement drifts is shown in Figure 3-7. The method is summarized as follows:

- The calculation of seepage into drifts is based on a three-dimensional, fracture-continuum flow model that includes a spatially variable permeability field.

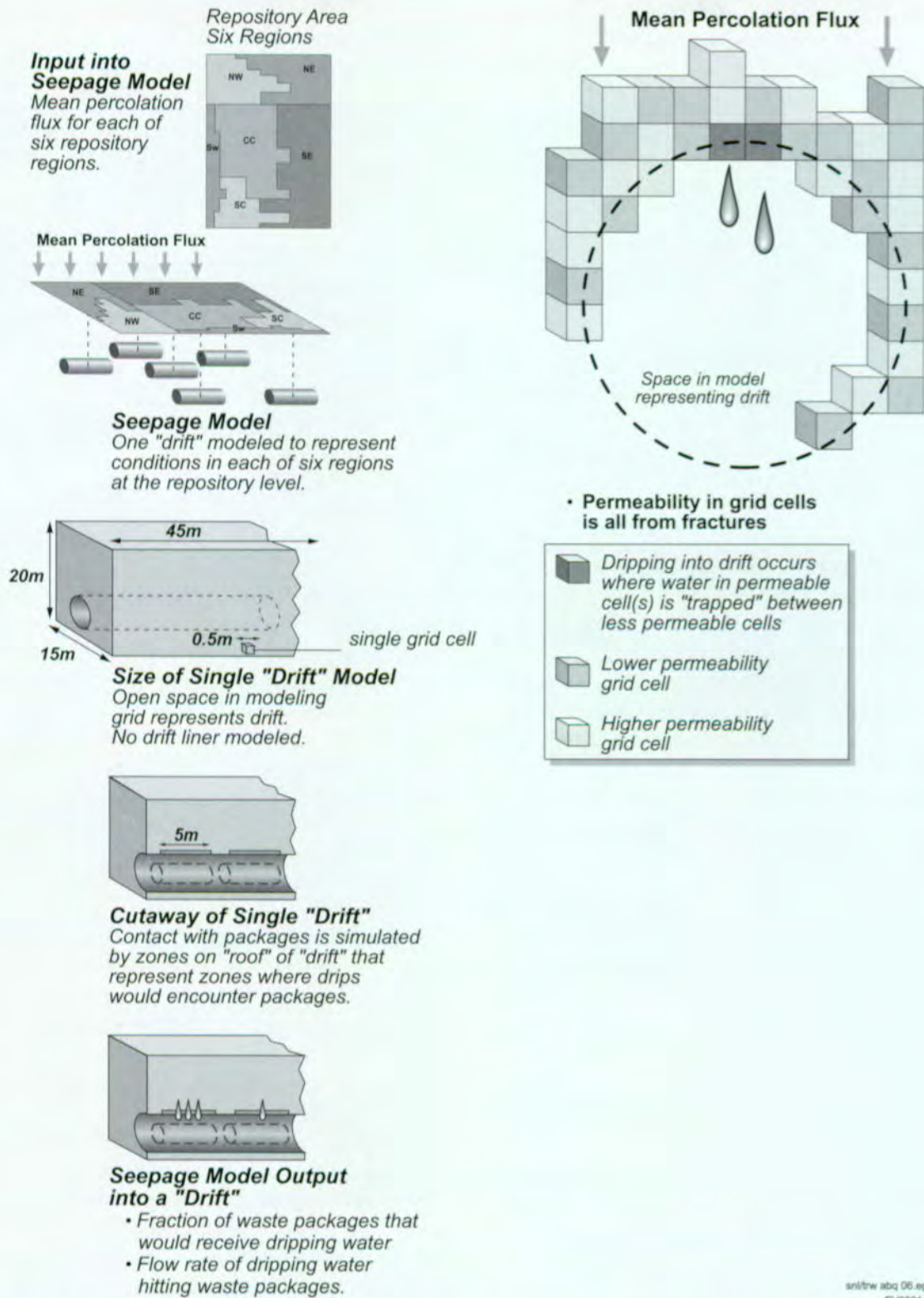


Figure 3-7. Illustration of the Method Used for Calculating Seepage for Total System Performance Assessment for the Viability Assessment

This model calculates two quantities: seepage fraction and seep flow rate.

- Using the three-dimensional process model, the amount of seepage into drifts is calculated as a function of percolation flux. The following quantities are calculated:
  - Seepage fraction, or the fraction of waste packages contacted by seeps
  - Seep flow rate, which is the rate of water flow onto a waste package that is contacted by one or more seeps
- In calculating seepage fraction and seep flow rate, a waste package is conservatively represented by an area of 5 m × 5 m (16 ft × 16 ft), which is approximately the length of a waste package and the width of the drift.
- The TSPA models of near-field processes (e.g., near-field geochemical environment and waste package degradation) include spatial variability by considering six repository regions, as shown in Figure 3-7.
- Percolation flux through fractures is averaged over each of those six regions. The average flux is used to calculate the seepage fraction and seep flow rate, using the functional dependence obtained from the process-model calculations.

Seepage fraction and seep flow rate are not defined as simple functions but rather as probability distributions with mean and standard deviation that are functions of percolation flux. The probability distributions for seepage are developed by assigning distributions to two of the key input parameters that are uncertain in the process model: the mean fracture permeability ( $k_f$ ) and the air-entry parameter for fractures ( $\alpha_f$ ). Similar to the mountain-scale flow model, the distributions are discrete; the values and probabilities are summarized in Table 3-7. The parameter ranges and probabilities were developed from data on air

Table 3-7. Probabilities for the Process-Model Cases Used to Develop Seepage Distributions

|                                      | $\alpha_f = 3 \times 10^{-4}$<br>Pa <sup>-1</sup> | $\alpha_f = 10^{-3}$<br>Pa <sup>-1</sup> | $\alpha_f = 3 \times 10^{-3}$<br>Pa <sup>-1</sup> |
|--------------------------------------|---|--|---|
| Mean $k_f = 10^{-14}$ m <sup>2</sup> | 6.25%   | 12.5%                                    | 6.25%   |
| Mean $k_f = 10^{-13}$ m <sup>2</sup> | 12.5%   | 25%                                      | 12.5%   |
| Mean $k_f = 10^{-12}$ m <sup>2</sup> | 6.25%   | 12.5%                                    | 6.25%   |

Note:  $k_f$  is fracture permeability and  $\alpha_f$  is fracture air-entry parameter; Pa = pascal is a unit of measure for pressure, equal to  $1.5 \times 10^{-4}$  pounds per square inch.

permeability and fracture density (CRWMS M&O 1998i, Section 2.5.2.2).

Nine parameter combinations were used for seepage calculations. Results from the three-dimensional process model were combined with the probabilities shown in the table to develop the probability distributions of seepage fraction and seep flow rate from which values were sampled. The seepage quantities were determined separately for each of the six repository regions; however, the values for the various regions were assumed to be perfectly correlated, and the values for different climate states were also assumed to be perfectly correlated. The values for the six regions were correlated because the probability distributions of hydrologic properties shown in Table 3-7 are assumed to represent uncertainty in the appropriate values, not spatial variability. The values for different climates were correlated to avoid unphysical behavior such as a decrease in seepage when going from a dry climate to a wetter climate. The correlations simplify the analyses because they reduce the number of independent seepage parameters in the TSPA calculations to just two (seepage fraction and seep flow rate), rather than the 36 there could potentially have been (those two times six repository regions times three climates).

The connections between seepage and the other subcomponents of unsaturated zone flow, and the other TSPA components, are shown in Figure 3-6.

### 3.1.3 Results and Interpretation

#### 3.1.3.1 Infiltration

Net infiltration near the repository at the surface as calculated by the infiltration model is shown as the left map in Figure 3-8. Shown are results for the long-term average climate and for the mean (base) infiltration case. In this and most of the remaining figures in this section, the long-term average climate is used for illustration because it is in effect most of the time (approximately 90 percent of the time, on average) for the TSPA simulations.

Some features of the infiltration model can be seen in the figure:

- The modeled infiltration is highly heterogeneous and clearly correlated with topographic features.
- The highest net infiltration occurs along Yucca Crest (the vertical blue band near the center of the map).
- Net infiltration is lower in washes (the roughly horizontal red bands).

The higher net infiltration along the crest and lower net infiltration in the washes are caused by the amount of alluvial cover present. Along the crest, less alluvial cover allows more water to penetrate into the bedrock without being evaporated, but the opposite tends to be true in the washes, where thick

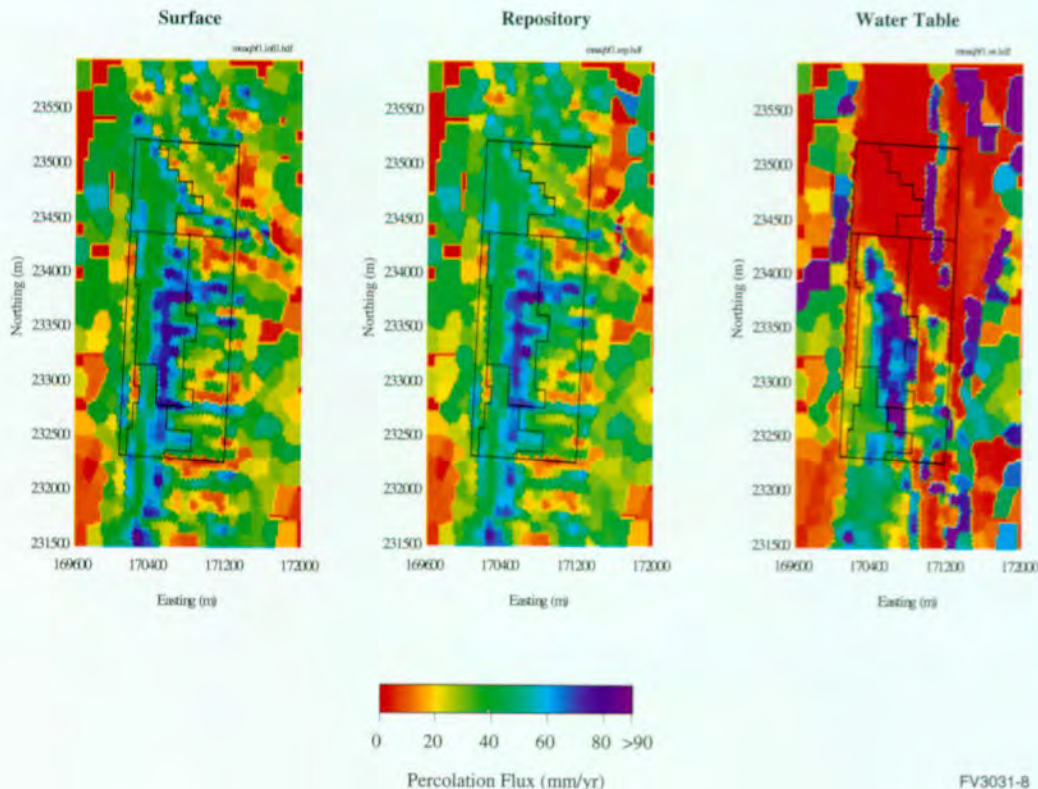


Figure 3-8. Total Percolation Flux at Three Elevations

Total percolation flux (fracture + matrix) at three elevations using long-term average climate, mean infiltration, and base case hydrologic properties. Note that percolation flux at the repository is nearly the same as at the surface, but at the water table the percolation flux is distributed much differently because of lateral flow in the northern part of the repository. An outline of the six regions at the repository level over which data are averaged is placed on each map for reference.

alluvium can store water from storm events long enough for it to be removed by evaporation or transpiration.

### 3.1.3.2 Mountain-Scale Unsaturated Zone Flow

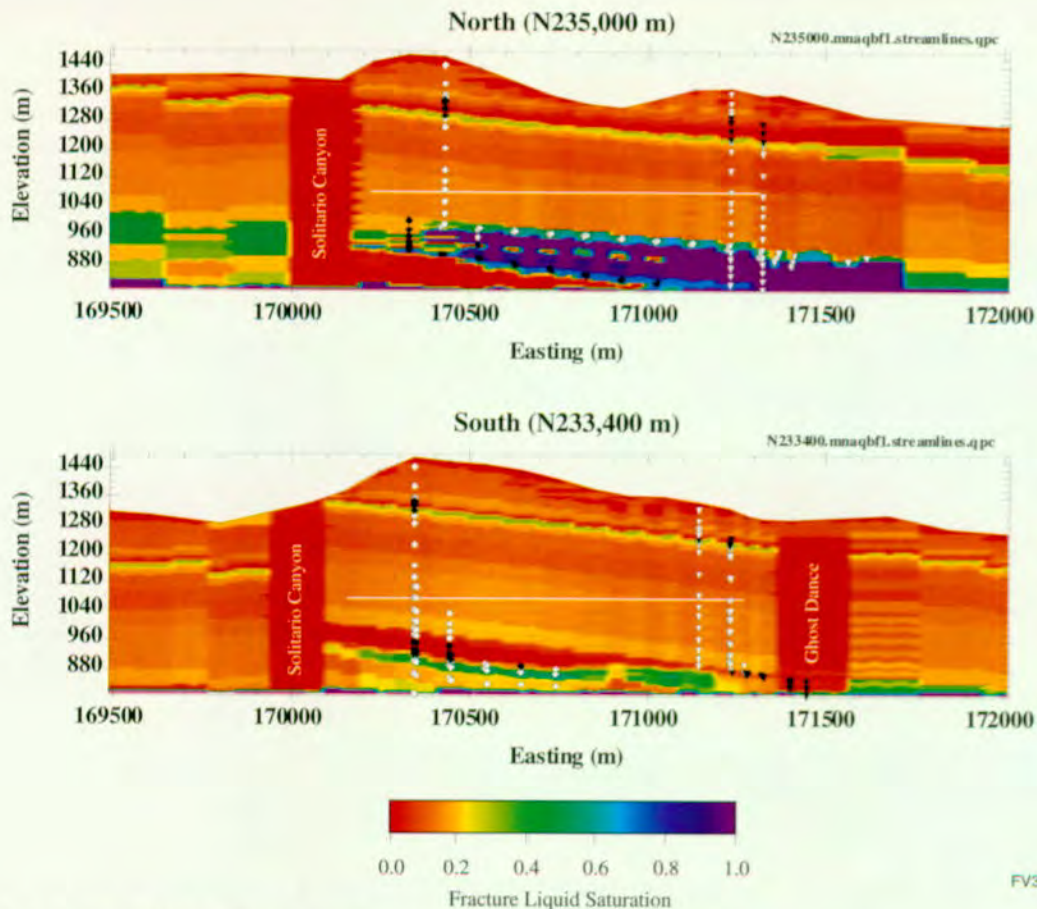
Important results from the mountain-scale flow model for the unsaturated zone are percolation fluxes at the repository horizon and at the water table. These values are shown as the center and right maps in Figure 3-8 for the mean-infiltration, base case model using the long-term-average climate. The location of the repository is shown in each map, as well as the six regions that were defined to account for variations in percolation by location at the repository. The division into regions was defined to limit the variation in percolation within each region. The number of regions was arbitrarily chosen. The center map of percolation flux at the repository level is nearly the same as the left map of surface infiltration, indicating nearly vertical flow from the surface to the repository. However, the right map of percolation flux at the water table is quite different from the other two, indicating significant nonvertical flow between the repository and the water table. In particular, in the large red area to the north, the percolation flux at the water table is low because it is underneath the perched water body; most of the flow is across the top of the perched water and down to the water table at the vertical blue band.

Figure 3-9 shows calculated flow paths of hypothetical tracers (substances with no retardation effect, no hydrodynamic dispersion, and no matrix diffusion) in two west-east, vertical cross sections (labeled north and south). For each cross section, tracers were released at two surface locations above the east and west ends of the repository. White symbols on the cross sections indicate a higher concentration of the tracer in fractures, while black symbols indicate a higher concentration in the matrix; diamonds indicate particles released at the western location and triangles indicate particles released at the eastern location. In both cross sections, flow is nearly vertical above the repository, except for some lateral movement above and in the Paintbrush nonwelded unit (see

Figure 3-1 for location of units). In addition, the flow is contained primarily in the fractures of the welded units and in the matrix of the nonwelded units. In the north cross section, a significant amount of lateral diversion occurs below the repository at the location of the perched water (see Bodvarsson et al. 1997, Chapter 13). Tracers released along the west end of the repository traverse above the perched water for hundreds of meters to the east before reaching the water table. Some of these tracer particles also partition into the matrix upon reaching the perched water and traverse laterally below the perched water. In the south cross-section, although perched water is not prevalent, some lateral diversion beneath the repository still occurs, caused by the contact between the Calico Hills vitric and zeolitic units, where there is a large difference in matrix permeability. The south cross-section shows lateral flow diverting downward at the Ghost Dance fault.

A useful way to compare multiple flow fields is a graph showing the distribution of time for water to travel from the repository to the water table. For example, Figure 3-10 shows the cumulative distribution of travel times (called a "breakthrough curve") for the mean infiltration, base case simulations using the present-day, long-term average, and superpluvial climates. Results show that net infiltration has a strong influence on travel time because higher infiltration results in faster water flow, particularly in the nonzeolitic nonwelded rock. The median arrival times are approximately 2,000, 200, and 90 years for the present-day, long-term average, and superpluvial infiltration rates, respectively. The first arrival times at the water table are very early as a result of fast flow through fractures. In fact, the cumulative breakthrough curves show a bimodal distribution, with over 20 percent of the water for the long-term average and superpluvial simulations taking less than 1 year to reach the water table.

Figure 3-11 shows breakthrough curves for the five base case flow fields for the long-term average climate, illustrating the effects of uncertainty in infiltration and fracture hydrologic properties. The upper parts of the curves represent water particles



FV3031-9

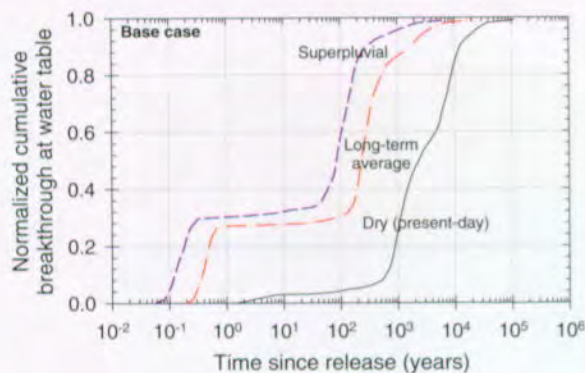
Figure 3-9. Selected Water-Flow Paths From Ground Surface to Water Table

West-east cross sections through the mountain-scale unsaturated zone flow model showing selected water-flow paths from ground surface to water table, using long-term-average climate, mean infiltration, and base case hydrologic properties. See Figure 3-8 for location of cross sections with regard to north-south coordinates. The white symbols denote flow primarily in the fractures, and the black symbols denote flow primarily in the matrix. The background color indicates fracture liquid saturation; dark blue shows perched-water location. The Solitario and Ghost Dance faults are indicated. The white line represents the repository location.

that spent at least part of their time flowing in the matrix between the repository and the water table. The lower parts of the curves represent water particles that were able to travel very quickly in fractures from the repository to the water table. There is a strong dependence of travel time on net infiltration but little dependence on fracture properties (as represented by the fracture air-entry parameter,  $\alpha_f$ ). It is worth noting that the very fast fracture flow does not represent a significant impact on repository performance because travel times from the repository to the water table of 1 year or 100 years are basically indistinguishable in a repository simulation of 10,000 years or more.

Figure 3-12 shows a comparison between the base case model and the dual-permeability/Weeps model for the base infiltration map and long-term average climate. The dual-permeability/Weeps model shows considerably more fast flow through the fractures. Over 50 percent of the particles arrive at the water table before 1 year, and the majority of the remaining particles do not arrive until after several hundred years.

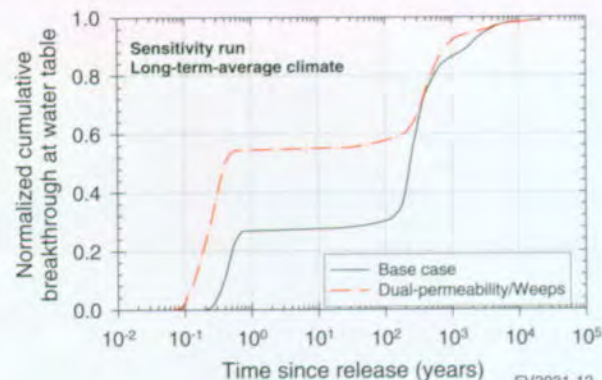
These mountain-scale flow results indicate that net infiltration and fracture-matrix partitioning of flow have a significant influence on the percolation flux and groundwater travel times in the unsaturated



FV3031-10

Figure 3-10. Breakthrough Curves for Three Climate States

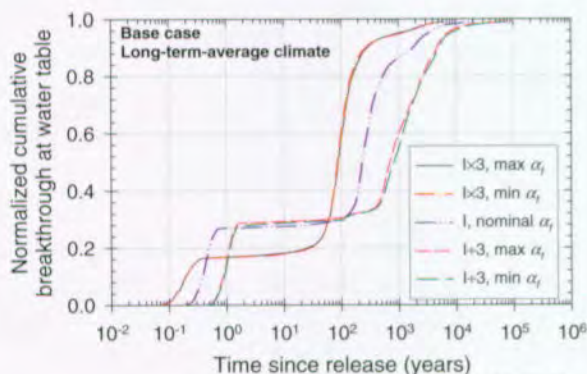
Comparison of travel times of a hypothetical unretarded tracer, released uniformly over the area representing the repository and traveling from the repository to the water table. Breakthrough curves representing arrival times of the tracer at the water table are given for the three climate states using mean infiltration, base case hydrologic properties, and no dispersion or matrix diffusion.



FV3031-12

Figure 3-12. Comparison of Base Case and Dual-Permeability/Weeps Model

Comparison of travel times of a hypothetical unretarded tracer, released uniformly over the area representing the repository and traveling from the repository to the water table. Breakthrough curves representing arrival times of the tracer at the water table are given for two alternative hydrologic-property sets using long-term average climate, mean infiltration, and no dispersion or matrix diffusion.



FV3031-11

Figure 3-11. Breakthrough Curves for Five Base Case Property Sets

Comparison of travel times of a hypothetical unretarded tracer, released uniformly over the area representing the repository and traveling from the repository to the water table. Breakthrough curves representing arrival times of the tracer at the water table are given for the five base case hydrologic-property sets using long-term average climate and no dispersion or matrix diffusion. The effects of varying infiltration rates and hydrologic properties can be seen by comparison of the curves.

zone. The amount of percolation flux at the repository affects performance through seepage and its influence on the engineered systems. Lateral diversion near the perched water has a large effect on the distribution of percolation flux at the water table, which subsequently affects the distribution of radionuclides at the water table. Note that changes in the distribution of radionuclides at the water table will only affect repository performance to the extent that saturated zone travel times or concentrations are different for the different locations (see Section 3.7).

A range of infiltration rates in present-day and future climate scenarios have been considered that give a broad distribution of travel times, and alternative conceptual models (e.g., the dual-permeability/Weeps model) have been considered that provide a range of fracture-matrix partitioning of flow. By this means, uncertainty in mountain-scale flow simulations for the unsaturated zone has been captured, while retaining the realism inherent in the three-dimensional, site-scale flow model for the unsaturated zone.

### 3.1.3.3 Seepage into Drifts

Figure 3-13 shows the final result of the seepage modeling. On the top is a graph illustrating the distribution of seepage fraction, or fraction of waste packages contacted by seeps. On the bottom is a graph illustrating the distribution of seep flow rate, which is the rate of water flow onto a waste package that is contacted by seeps (the sum of the flows if contacted by more than one). Each graph shows a curve representing the mean value as a function of fracture percolation flux (only the fracture component of percolation flux is used in calculating seepage because matrix flow is not expected to seep into openings). In addition,

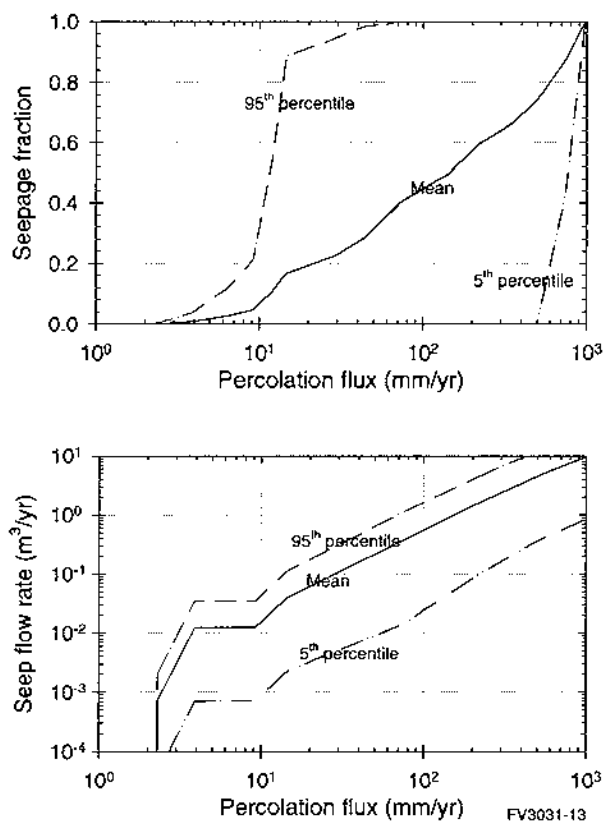


Figure 3-13. Calculated Seepage Fraction and Seep Flow Rate as Functions of Percolation Flux  
Shown are the 5 percent, mean, and 95 percent values of the distributions from which the seepage parameters are sampled.

curves at the 5th and 95th percentiles of the distributions are shown, to indicate the width of the uncertainty band around the mean. With the assumptions that have been made for this TSPA, there is a great deal of uncertainty about seepage, particularly in the fraction of waste packages contacted by seepage. The wide range of seepage fraction results because some combinations of the parameters shown in Table 3-7 cause a relatively large amount of seepage in the three-dimensional process model (especially low values of mean fracture permeability combined with large values of fracture air-entry parameter), while other combinations cause relatively little seepage in the model (especially large values of mean fracture permeability combined with low values of fracture air-entry parameter). If some of the combinations could be ruled out, perhaps with additional data collection or analysis, the uncertainty range could be narrowed. With additional work, it may be possible to rule out some combinations based on correlations between fracture permeability and fracture air-entry parameter (theoretically, they are both related to fracture aperture).

## 3.2 THERMAL HYDROLOGY

Thermal hydrology refers to the study of the effects of heat on hydrology. The Yucca Mountain repository will hold radioactive wastes that emit a large amount of heat from radioactive decay. This heat will influence conditions in the emplacement drifts (near-field conditions) and away from the drifts (far-field conditions). The thermal disturbance to the mountain will depend on how much waste is placed, or loaded, within a given repository area and the heat output of the waste. The areal mass loading for the reference design is specified as 85 metric tons of uranium (MTU)<sup>1</sup> per acre, which has an initial heat output of approximately 100 kW/acre. This loading will cause a significant disturbance in the repository environment for thousands of years after waste emplacement.

<sup>1</sup> The acronyms MTU and MTHM are equivalent for the once-through nuclear fuel cycle (no reprocessed fuel) and can be used interchangeably. MTHM, metric tons heavy metal, is the total amount of heavy metal initially contained in nuclear fuel. For reprocessed nuclear fuels; the initial heavy metal loading contains both uranium and plutonium. For once through nuclear fuels, the initial heavy metal loading consists of only uranium. Thus, for the United States nuclear industry, which uses a once-through fuel cycle, metric tons heavy metal equals metric tons uranium (MTHM = MTU).

The unsaturated zone at the Yucca Mountain site contains in situ water and gas within the pores that will react to the heat generated by radioactive waste. In general, the influence of radioactive decay heat includes vaporization of in situ liquid water, transport of water vapor away from the heat source, condensation of water vapor in cooler regions, and condensate flow driven by gravity and capillary forces. Thermal gradients affect gas and liquid flow in the rock matrix and in fractures, and flow between fractures and matrix. The decay-heat characteristics of the individual waste packages strongly affect the emplacement-drift thermodynamic environment (temperature and relative humidity, partitioning of water between liquid and steam, and flow of water into or out of the drift). The resulting thermodynamic conditions will affect the performance of the repository, particularly of the engineered barrier system, by influencing all of the near-field components of the TSPA-VA.

After waste emplacement, heat will flow from the repository by conduction through the rock and by advection, which means by movement with the gas and water. Through these processes, there will be movement of water vapor, liquid water (both ambient percolating water and heat-mobilized condensate), and heat. Heating will result in elevated temperatures and drying in both the surrounding host rock and regions well away from the repository. The progression of thermal-hydrologic processes through time is pictured in Figure 3-14. Thermally driven mechanical and chemical processes can potentially cause permanent changes to the fluid-flow characteristics of the entire mountain (for example, by changing permeability and porosity).

Thermal-hydrologic processes occur at two important scales: that of the emplacement drifts (a few meters to tens of meters) and that of the mountain (hundreds of meters to thousands of meters). Thermal-hydrologic processes at the drift scale include waste package interactions with other waste packages and the surrounding drift walls and floor. Thermal-hydrologic processes at the mountain scale include the influence of heat on liquid and gas movement above and below the repository. Some of the important processes are

illustrated in Figure 3-15. The "drift-scale" thermal-hydrologic model includes processes at both drift and mountain scales; it provided information to the models of the near-field geochemical environment, waste package degradation, waste form degradation and radionuclide mobilization, and transport of radionuclides within the engineered barrier system. A separate mountain-scale model provided information to models of the near-field geochemical environment (Figures 3-16 and 3-17). Thermal-hydrologic processes at both the drift and mountain scales affect fluid flow and transport in the unsaturated zone; however, for the TSPA-VA it was assumed that there will not be permanent alteration of the hydrologic properties because of thermal-hydrologic-mechanical or thermal-hydrologic-chemical processes and thus the influence of thermal-hydrologic processes would be short-lived. With this assumption, thermal disturbances to seepage into drifts and radionuclide transport from the repository to the water table would only be important during the early period when no waste packages have failed, except for possibly a few juvenile failures. Therefore, thermal effects on seepage and radionuclide transport were neglected.

The thermal-hydrologic modeling studies and sensitivity analyses presented in this section were prepared with the view of addressing selected aspects of the NRC Key Technical Issue on Thermal Effects on Flow (NRC 1997b). Specifically, the information presented is pertinent to two of the three subissues of this key technical issue, namely, sufficiency of thermal-hydrologic modeling to predict the nature and bounds of thermal effects on flow in the near-field and adequacy of total system performance assessment with respect to thermal effects on flow.

Sections 3.2.1 and 3.2.2 summarize the processes, assumptions, and implementation of the thermal-hydrologic models used in the TSPA-VA. Section 3.2.3 presents results from the models and related interpretations. Additional information on the thermal-hydrologic component can be found in Chapter 3 of the *Total System Performance Assessment-Viability Assessment (TSPA-VA) Analyses Technical Basis Document* (CRWMS

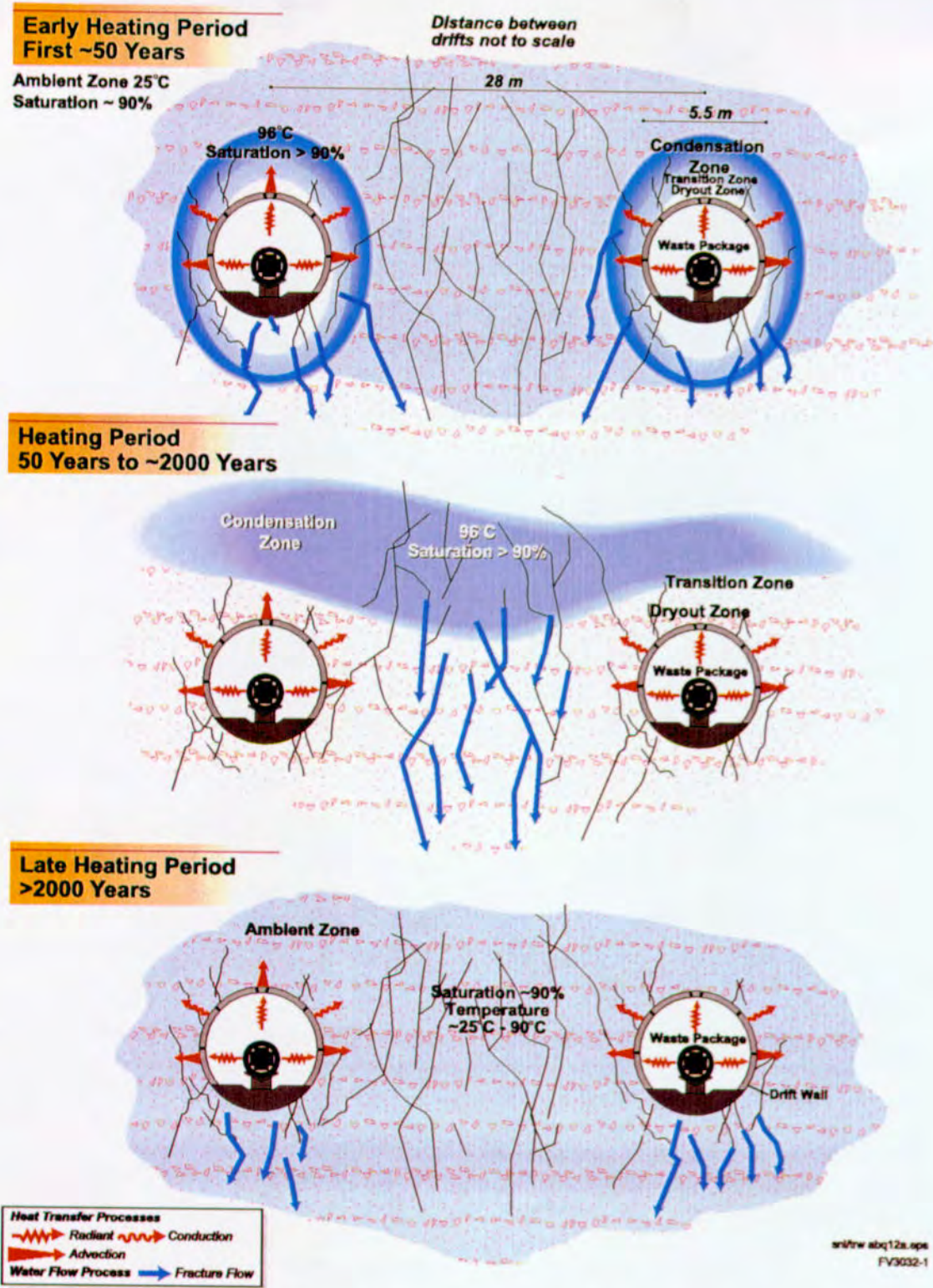


Figure 3-14. Conceptual Drawings of Thermal-Hydrologic Processes at Three Stages  
Heat drives water away from the drifts; water vapor condenses in cooler rock. The condensation zone moves away from the drifts initially, and eventually returns toward the drifts. At all stages water movement in fractures is important.

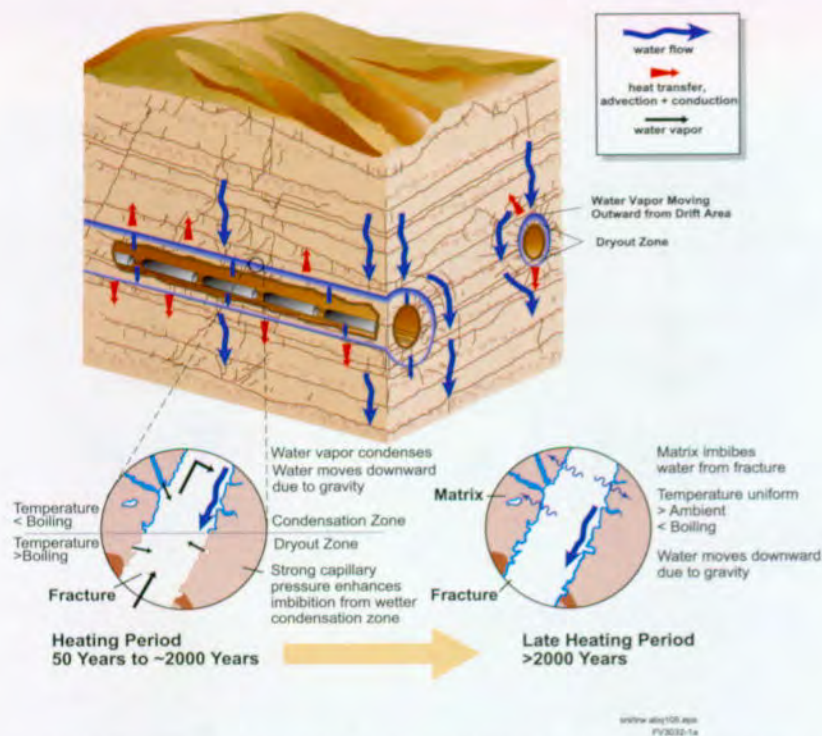


Figure 3-15. Conceptual Diagram Illustrating Flow of Liquid Water and Water Vapor in Fractures  
Condensation of vapor and imbibition of water from fractures into the rock matrix are important processes.

M&O 1998i). Additional information on YMP thermal hydrology can also be found in the *Yucca Mountain Site Description* (CRWMS M&O 1998m, Chapter 7).

### 3.2.1 Construction of the Conceptual Model

Previous TSPAs have included the influence of thermal effects on predictions of radionuclide releases from the repository and subsequent doses to the public. Many of the model assumptions and simplifications in previous TSPA thermal analyses have been improved for the TSPA-VA. These improvements include assumptions about dimensionality and the conceptual flow model for heat and mass transfer. In addition, many recently acquired thermal and hydrologic data have been used in the TSPA-VA.

In the 1993 TSPA, thermal-hydrologic calculations used a model based solely on conduction (Wilson et al. 1994, pp. 10-1 to 10-36). Drift-scale and mountain-scale calculations used three-dimensional models for two different initial thermal loads. The two thermal-load values (heat

generated per repository area), were 57 and 114 kW/acre. Effects on the repository-system hydrology (for example, the extent of rock drying) were inferred from the distance and location of the region where pore water is expected to boil. This approach has limited applicability because it does not explicitly couple heat transfer to fluid flow. Without this coupling, the nature of dry-out and condensation zones may not be properly represented (see Figure 3-15).

In the 1995 TSPA, drift-scale thermal-hydrologic calculations used a two-dimensional model for areal mass loadings of 25 and 83 MTU/acre (CRWMS M&O 1995, pp. 4-1 to 4-39). The calculations were based on the equivalent-continuum model assumption for heat and fluid flow (that is, hydraulic properties of both fractures and rock matrix were combined into a single equivalent continuum). Net infiltration rates of 0.05 and 0.3 mm/year (0.002 and 0.01 in./year) were modeled for a homogeneous, layered system. This modeling was limited because it did not allow for variations in waste package contents or the development of large-scale features such as preferential

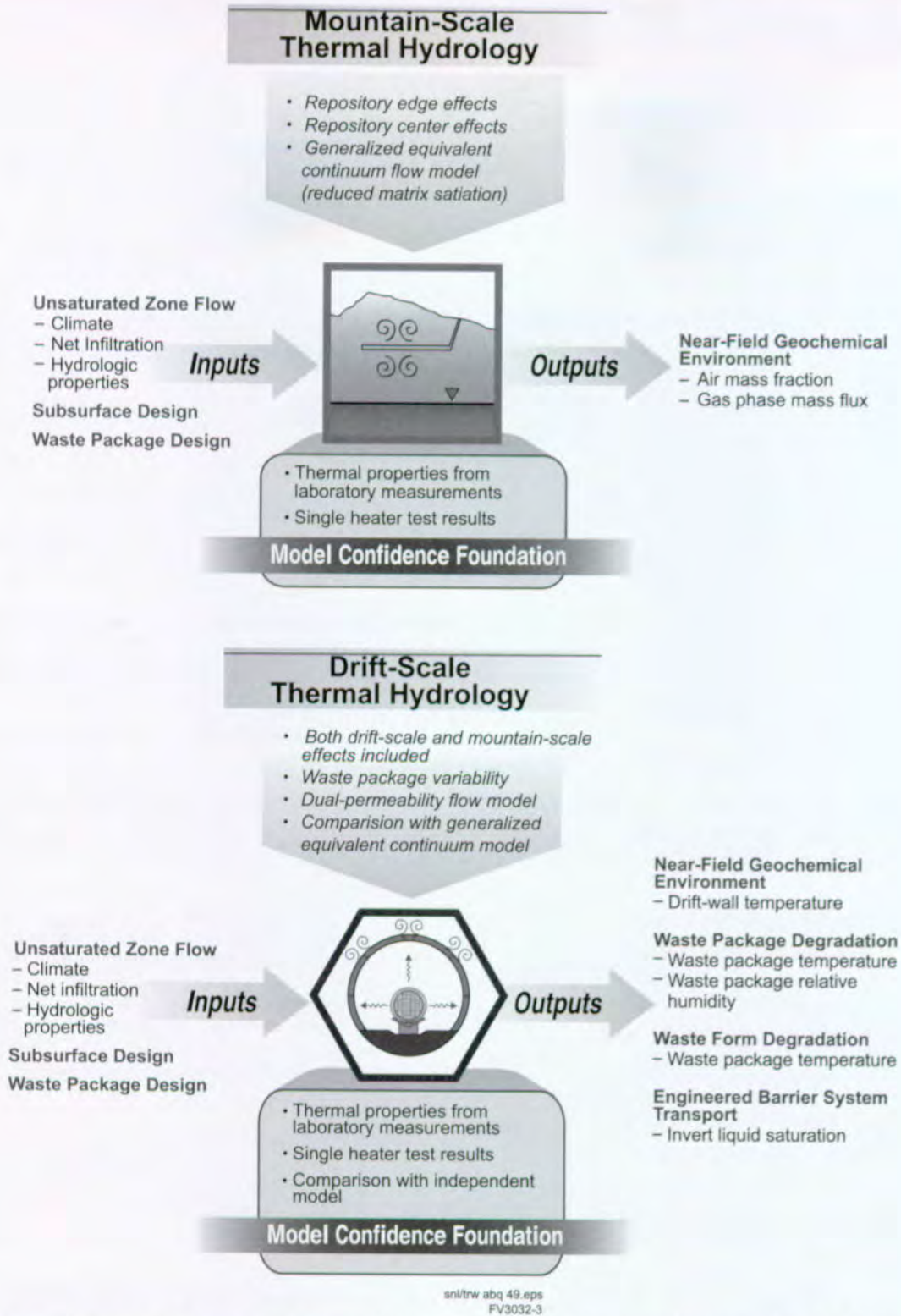


Figure 3-16. Coupling of Thermal Hydrology to Other Total System Performance Assessment for the Viability Assessment Components

The "drift-scale" model is actually a multiscale abstraction that takes into account both drift-scale and mountain-scale processes.

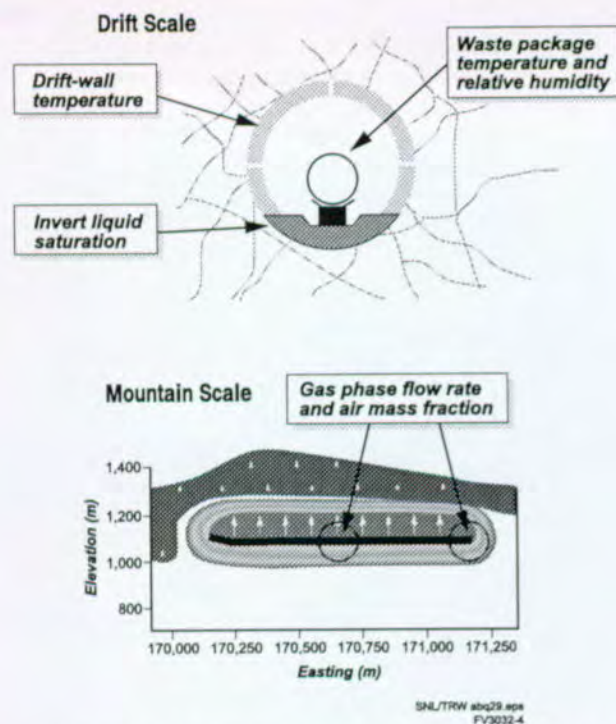


Figure 3-17. Quantities Passed to Other Total System Performance Assessment for the Viability Assessment Components

This figure shows the locations of the important parameters calculated by the mountain-scale and drift-scale models.

cooling around the repository edges or gas-phase convection. The calculations were also based on a conceptual flow model that restricted the amount of flow through fractures during the thermal period.

Thermal-hydrologic models for the TSPA-VA were improved over earlier efforts because of benefits derived from recommendations of the Thermohydrologic Modeling and Testing Program Peer Review (CRWMS M&O 1996e), the YMP thermal testing program, and faster computers. Specific improvements have been made to conceptual flow models, hydrologic and thermal property values, model dimensionality, and infiltration rates.

A key effort in formulating models for this TSPA was a workshop convened by the performance-assessment group in January 1997. Workshop participants developed a list of issues and prioritized them based on criteria for long-term repository performance (Table 3-8). Workshop participants determined that conceptual models allowing for more flow through fractures, in particular

Table 3-8. Thermal Hydrology Abstraction/Testing Workshop

| <b>THERMAL HYDROLOGY ABSTRACTION/TESTING WORKSHOP</b><br>January 21–23, 1997, Albuquerque, NM<br>(CRWMS M&O 1997I) |  |
|--|--|
| <b>PRIORITIZATION CRITERIA</b>   |  |
| •  | Does the process/issue affect the magnitude, spatial distribution, or temporal variation of  |
| –  | Waste package temperature?   |
| –  | Relative humidity around a waste package?  |
| –  | Liquid water flow rate into the drift environment and onto a waste package?  |
| –  | Aqueous flow from the repository to the saturated zone?  |
| <b>HIGHEST PRIORITY ISSUES</b>   |  |
| •  | Thermal-hydrologic processes and parameters  |
| •  | Mountain-scale models  |
| •  | Drift-scale models   |
| •  | Coupled processes  |
| <b>ANALYSIS PLANS</b>  |  |
| •  | Mountain-scale thermal-hydrologic abstraction and testing plan   |
| •  | Abstracting drift-scale temperature, relative humidity, liquid saturation, and liquid-phase flux as a function of location in the repository |
| •  | Thermal-hydrologic modeling of seepage into drifts   |
| •  | Coupled processes abstraction and testing plan   |

during the thermal periods (Figure 3-14), would be the most appropriate. The available conceptual models for increased fracture flow are the generalized equivalent-continuum model and the dual-permeability model (see Section 3.1.1.3). The dual-permeability model gives a more realistic description of a thermally driven system and ensures consistency with flow models for the unsaturated zone (see Section 3.1.1.3). More movement of water through fractures allows condensate or reflux waters mobilized by heat (and ambient percolation) to drain through fractures either back toward the drifts or through the pillars separating drifts.

The workshop participants also considered "coupled processes," or the coupled effects of temperature, hydrology, mechanics, and chemistry. When heated, the rock around the emplacement drifts will expand. This thermal expansion will cause fractures to open and close, which in turn will change the permeability and porosity of the rock and affect movement of gas and liquid. These changes will last only while the rock is heated. In addition, the thermal stresses can potentially cause rock blocks to move and new fractures to form, which again can affect permeability, porosity, and fluid flow. Unlike the simple thermal-expansion effects, these changes to the rock hydrologic properties can be permanent. All of these effects are called thermal-hydrologic-mechanical coupled processes. Heating also can cause chemical changes in the host rock, such as mineral dissolution in some regions and mineral precipitation elsewhere. Mineral dissolution and precipitation can potentially alter the hydrologic properties of the rock permanently, which would in turn alter fluid flow. These effects are referred to as thermal-hydrologic-chemical coupled processes. Based on thermal-hydrologic workshop discussions, some limited follow-up studies of coupled processes were completed.

Preliminary thermal-hydrologic-mechanical modeling (Ho and Francis 1998) was done with a one-dimensional, dual-permeability model at the mountain scale. This modeling indicated that the liquid-phase flow fields are essentially unaffected by non-permanent increases or decreases of a factor of ten

in permeability. Based on this modeling, thermal-hydrologic-mechanical alteration of the flow field is considered negligible.

Preliminary thermal-hydrologic-chemical modeling (summarized in CRWMS M&O 1998i, Section 3.6.8.2; CRWMS M&O 1998c) studied silica within the fracture system in the unsaturated zone. This fully coupled thermal-hydrologic-chemical study was at the drift scale and included reactions for silica-cristobolite-quartz in the system. Changes in fracture and matrix porosity (which also affect permeability) caused by mineral dissolution and precipitation were calculated. Waste package temperature and relative-humidity time histories were not greatly affected by the reactive-transport processes included in the simulation, even though a mineral cap formed above the drifts. However, the effects of a mineral cap above the drift on seepage flow into the drift have not been fully investigated. Because of its complexity, the work that has been done so far only represents a start on addressing the uncertainties associated with thermal-hydrologic-chemical effects.

The near-field environment expert elicitation (CRWMS M&O 1998d) was established to help quantify the large uncertainties associated with thermal-hydrologic-mechanical and thermal-hydrologic-chemical processes. The panel was tasked to consider how these processes occur, both temporally and spatially, and over what range of values the hydrologic properties (for example, fracture permeability) may be influenced.

The elicitation panel examined recent YMP process models and experimental data on coupled processes from the single heater test. They considered thermal-hydrologic-mechanical and thermal-hydrologic-chemical processes, potential changes to hydraulic interactions between fractures and the rock matrix, and effects of rockfall. The panel found that fracture-permeability changes might occur in both the vertical and horizontal directions and in condensate and boiling zones. According to the experts, fracture permeability in the vertical direction can either decrease by 10 to 100 times or increase by 10 to 1,000 times, depending on location and other factors. Fracture

permeability in the horizontal direction may increase by no more than 10 times. Based on the results of the elicitation, the potential for thermally driven alteration of fracture properties (for example, permeability) falls within the range of the natural spatial variability of the system. However, an overall decrease of rock-mass permeability could result. The panel concluded that the mechanical effects would tend to be reversible upon cooling, with the possible exception of horizontal changes in permeability caused by shear stress, but that chemical effects will be more permanent. The panel indicated that the fracture-matrix interaction parameter (see Section 3.1.2.3) used in the dual-permeability models may also be affected because of chemical precipitation or dissolution. Although this effect may be permanent, the magnitude of such changes is uncertain.

Thermal-hydrologic-mechanical and thermal-hydrologic-chemical processes are not included in the base case for this TSPA. Based on the expert-elicitation results and the preliminary modeling studies, it is likely that thermal-hydrologic-mechanical effects are not significant; however, the significance of thermal-hydrologic-chemical effects is more uncertain. In addition, changes to the thermal hydrology caused by drift collapse (and the resultant filling of the drift with rockfall rubble) are not considered in this TSPA.

### **3.2.2 Implementation of the Performance Assessment Model**

As discussed earlier, thermal-hydrologic processes occur on two important scales, drift scale and mountain scale, each passing different information to the other TSPA-VA components (Figure 3-17). The key issues discussed in Section 3.2.1 determined the form of the models developed for thermal-hydrologic analyses. Section 3.2.2.1 describes the reference design, Section 3.2.2.2 describes implementation of the drift-scale model, and Section 3.2.2.3 describes implementation of the mountain-scale model.

#### **3.2.2.1 Repository and Waste Package Design**

Thermal-hydrologic models require specific repository subsurface design and waste package design information. This information includes waste package geometry and decay heat outputs, emplacement drift geometry and layout configuration, and waste stream information including total thermal loading.

The total mass of commercial spent nuclear fuel to be emplaced at Yucca Mountain is 63,000 MTU (CRWMS M&O 1997c, p. 3-14). This mass includes several waste package types of different initial heat outputs (CRWMS M&O 1997e, pp. 45 and 55). Emplacement of about 7,650 commercial spent nuclear fuel waste packages is expected. It is not expected that additional area will be needed for emplacing wastes such as high-level-radioactive waste glass and DOE spent nuclear fuel. The waste packages containing these additional wastes will be placed between the commercial spent nuclear fuel waste packages, with a requirement of at least 1 m (3.28 ft) of separation between waste packages. The total emplaced mass of the expected 2,550 additional waste packages will be 7,000 MTU (2,333 MTU of DOE spent nuclear fuel and 4,667 MTU of high-level radioactive waste glass). These waste packages will include co-disposal waste packages (that is, two types of waste in the same waste package) and waste packages for separate disposal of DOE spent nuclear fuel. The co-disposal waste packages will contain both high-level-radioactive waste glass and DOE spent nuclear fuel; the separate-disposal waste packages will contain only DOE spent nuclear fuel.

The reference-design mass loading of 85 MTU/acre (CRWMS M&O 1997g, p. 23) includes only the amount of commercial waste; DOE spent nuclear fuel and high-level radioactive waste glass are not counted when calculating the mass loading. The reference design specifies point-loading emplacement, meaning that the waste packages are far enough apart that there is little direct thermal communication between packages. A point-loaded drift segment loaded with all three waste package

types (commercial spent nuclear fuel, co-disposal, and separate-disposal) is illustrated in Figure 3-18.

The reference repository design specifies that the emplacement drifts are to contain no backfill. The waste packages are to be placed on carbon steel supports compatible with the waste package outer-barrier composition, on top of and supported by a concrete pier on top of a concrete invert floor (concrete segments put in the bottom of the round emplacement drift to provide a level floor). The thermal-hydrologic calculations for the base case use these design conditions.

Design options are under evaluation that include use of backfill. Design options and alternative design concepts under evaluation that may enhance repository performance are discussed in Section 4.5 and Volume 2, Sections 5.3 and 8.

### 3.2.2.2 The Drift-Scale Model

Output from the drift-scale analyses includes waste package surface temperature and relative humidity, and drift-wall and invert-floor temperature and liquid saturation. Time histories of these quantities

are used in analyses of the engineered barrier system.

Drift-scale modeling must include coupling of drift-scale processes with mountain-scale processes to properly account for effects such as faster cooling of waste packages near the edge of the repository as compared to waste packages near the repository center. A multiscale modeling and abstraction method was developed to couple drift-scale processes with mountain-scale processes. This method uses a series of four mountain-scale and drift-scale submodels to abstract the thermodynamic environment within emplacement drifts throughout the repository area (Figure 3-19). The four submodels are described in the following paragraphs.

**Line-Averaged-Heat-Source, Drift-Scale, Thermal-Hydrologic Submodel.** The line-averaged-heat-source, drift-scale, thermal-hydrologic submodel is a two-dimensional drift-scale model that computes average temperature and relative humidity at the drift wall and liquid saturation of the drift invert. This submodel effectively represents average thermal-hydrologic behavior at any

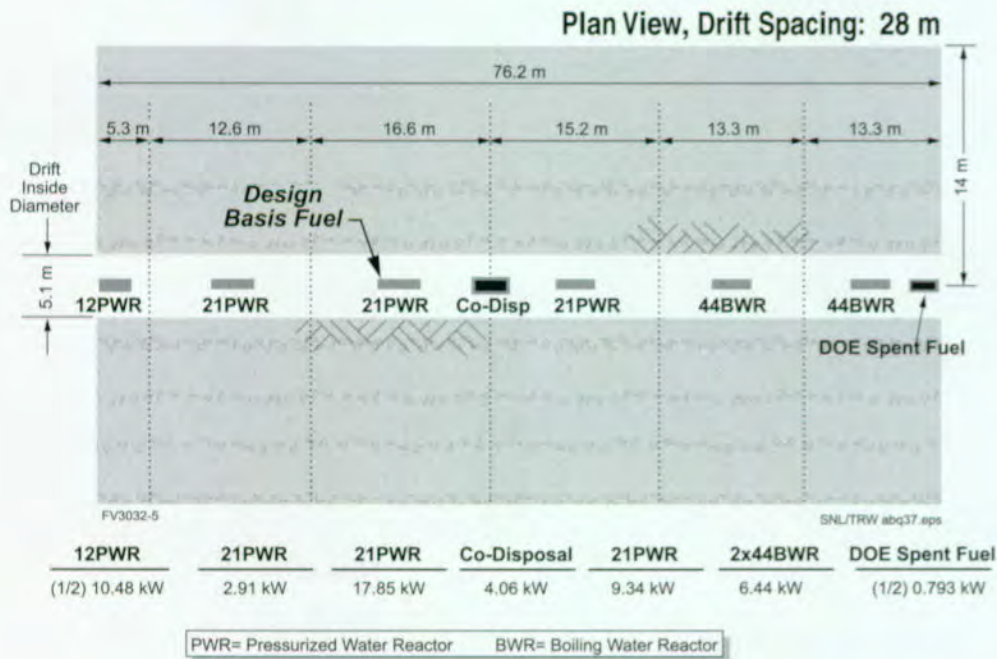


Figure 3-18. Plan View of a Typical Emplacement-Drift Segment for Drift-Scale Thermal-Hydrologic Analyses Heat output is shown for each waste package. The drifts are 28 m (92 ft) apart, center-to-center.

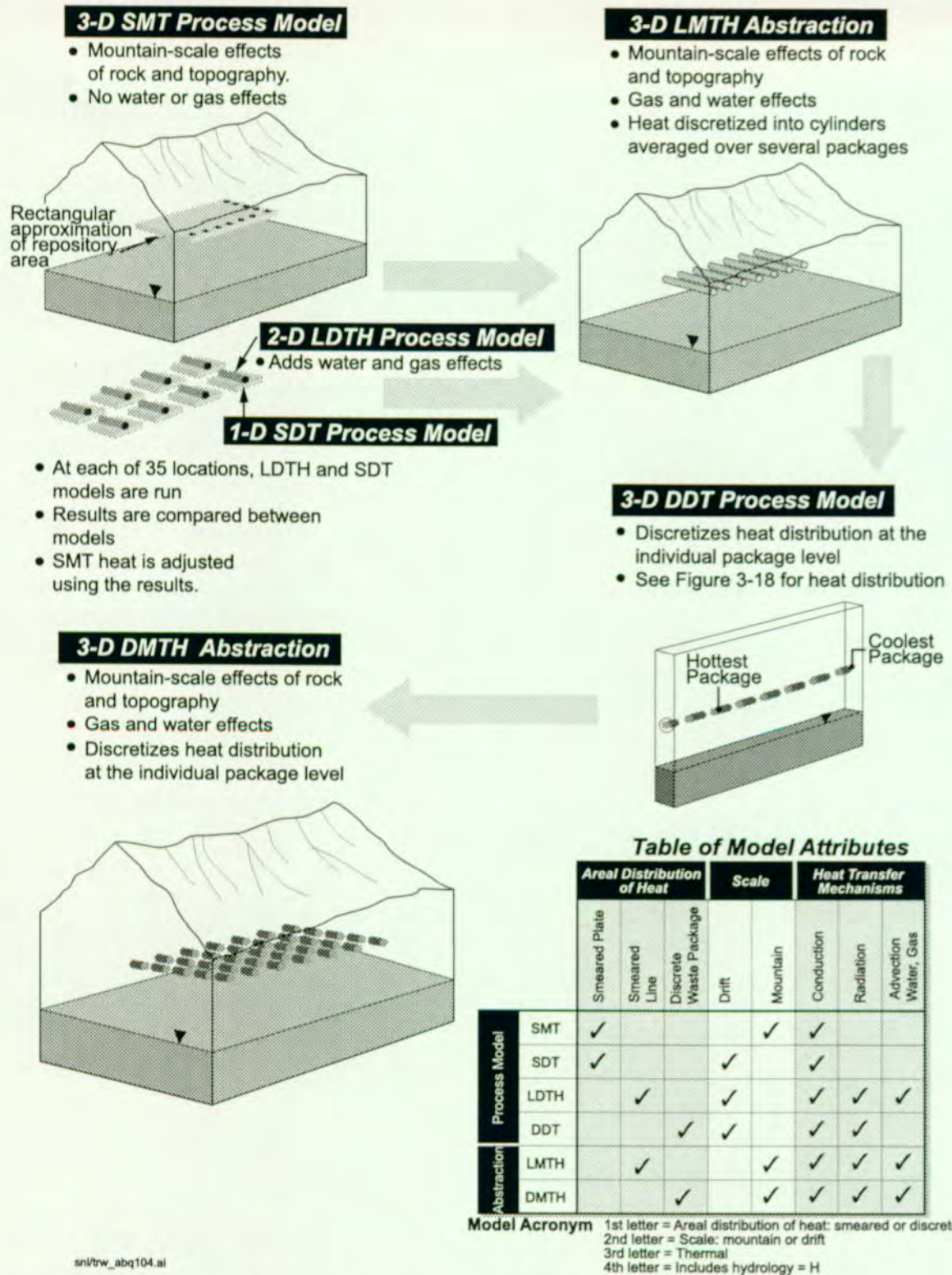


Figure 3-19. Illustration of the Multiscale Modeling and Abstraction Method  
Four models at different levels of abstraction are combined to produce the final abstracted model, which then effectively includes both drift-scale and mountain-scale effects.

specific location within the repository, taking into account the location-specific thermal and hydrologic properties, boundary conditions, and percolation flux. Heat and fluid flow are modeled as dual-permeability, consistent with the mountain-scale unsaturated zone flow model (Section 3.1.1.3). Radiant heat transfer within open drifts is also modeled. This submodel addresses key issues related to modeling of fracture and matrix interactions for fluid and heat flow. It also addresses the issue of the appropriate scale of fracture properties and thermal-hydrologic processes by using hydrologic properties developed for mountain-scale flow by inversion models. Consistency with the mountain-scale unsaturated zone flow model ensures that hydrologic conditions are properly accounted for, including variability of infiltration with location and changes of infiltration with climate.

**Smearred-Heat-Source, Mountain-Scale, and Smearred-Heat-Source, Drift-Scale, Thermal-Conduction Submodels.** Both the smearred-heat-source, mountain-scale, thermal-conduction submodel and the smearred-heat-source, drift-scale, thermal-conduction submodel consider conduction heat transfer only. They are used to establish temperature relationships and to account for the influence of repository edges, topography, and mountain-scale variability in hydrogeologic layering. The smearred-heat-source, mountain-scale submodel is a three-dimensional model that includes the appropriate stratigraphy, topography, and repository location and extent. The smearred-heat-source, drift-scale submodel is a one-dimensional model. These two submodels address key issues related to the differences between repository center and edge locations by coupling the drift-scale submodels with the mountain-scale submodel. The coupling uses the average temperatures of repository host rock obtained from the smearred-heat-source, mountain-scale submodel, corrected for hydrology using a relationship derived from the line-averaged-heat-source, drift-scale submodel and the smearred-heat-source, drift-scale submodel. The resulting "modified" temperatures inherently include repository edge effects because they originated from a full mountain-scale model. The temperature prediction also includes

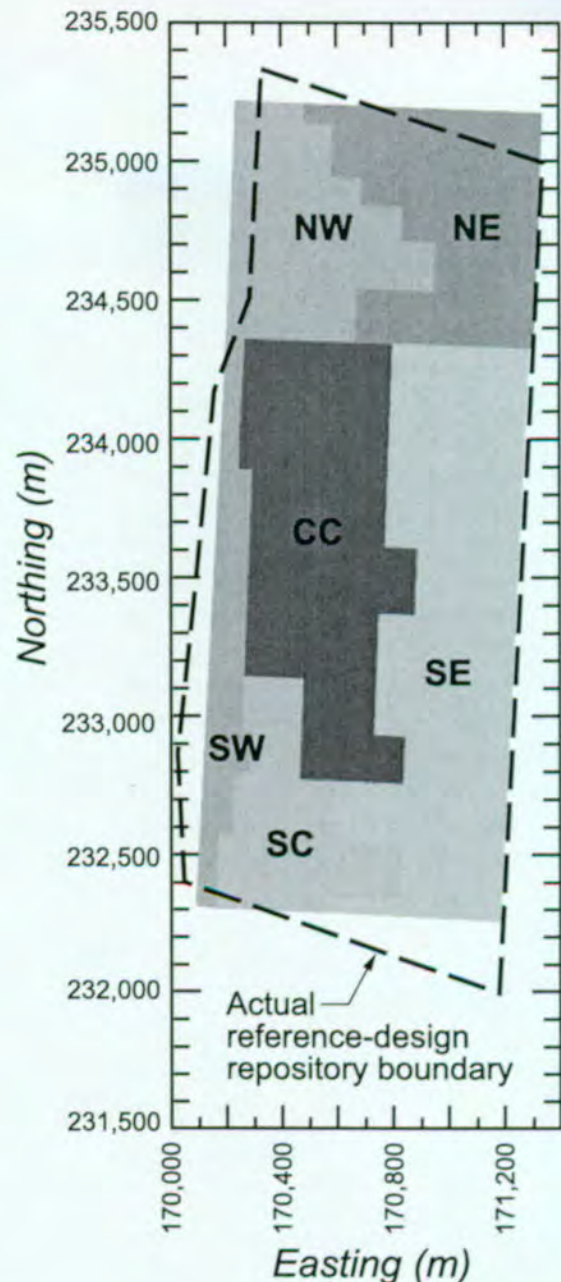
the effects of the system fluid components through the temperature relationship between the two drift-scale submodels. This results in an "abstracted" drift-wall temperature that approximates the effects of the most important thermal-hydrologic processes. A similar procedure provides an abstracted relative humidity at the drift wall.

**Discrete-Heat-Source, Drift-Scale, Thermal Submodel.** The abstracted drift-wall quantities are further modified at the drift wall and at the waste package surface using waste-package-specific deviations computed by the discrete-heat-source, drift-scale, thermal submodel. This submodel provides temperatures and relative humidities for different waste packages along the drift. The discrete-heat-source, drift-scale submodel is a three-dimensional model of a drift segment containing eight representative waste packages of varying heat outputs (Figure 3-18). This submodel includes only conductive heat transfer, plus radiant heat transfer within open drifts. It accounts for variability in temperature and relative humidity among packages along the drifts, which is another of the key issues from the thermal-hydrologic workshop (Section 3.2.1). One limitation of the analyses is that only one type of separate-disposal waste package was modeled. The heat output listed in Figure 3-18 for the separate-disposal package is appropriate for a waste package containing N-Reactor fuel. Some types of DOE spent nuclear fuel are cooler and some are hotter. N-Reactor fuel was modeled because it represents nearly 90 percent of the total MTU of DOE spent nuclear fuel (see Section 3.5.1.5). The inconsistency of using near-field thermal conditions for N-Reactor fuel to represent all types of DOE spent nuclear fuel could affect the release calculations for the other fuel types, but the effect is moderated by the long waste package life (differences in waste package conditions are greatest at early times). In addition, the heat from the naval-spent-fuel component is represented by the 44-assembly boiling-water-reactor waste packages in the modeled drift segment. The 44-assembly boiling-water-reactor allotment in the drift segment is over-represented by about 0.8 percent to account for the naval spent nuclear fuel.

The multiscale modeling and abstraction method involves calculations at a number of repository locations. A repository-wide set of calculations for a given case involves only one computer run using the mountain-scale submodel and only one computer run using the discrete-heat-source, drift-scale, thermal submodel. However, the line-averaged-heat-source, drift-scale, thermal-hydrologic submodel and the smeared-heat-source, drift-scale, thermal submodel are run for 35 locations within the repository and for three different local heating rates. The results of these 105 submodel runs are interpolated over the repository area and as a function of local heating conditions to provide a continuous distribution of the drift-scale thermal-hydrologic variables throughout the repository area. The abstracted temperature and relative humidity are calculated for an array of 425 repository locations, giving reasonable resolution for mountain-scale topographic and stratigraphic effects.

This procedure provides too much information for the near-field TSPA components. Because resource demands increase considerably as the number of waste package groups modeled within RIP (the top-level TSPA program, see Section 2.3) increases, six repository regions were defined for modeling the near-field, as shown in Figure 3-20. The regions were selected to limit variability of net infiltration within the regions, although there is still considerable variability (see Figure 3-8). The regions also represent a range of geometric relations, with Region CC being the region most like the repository center and Region SW being most like the edge. Lastly, the regions represent the variation of hydrogeologic properties around the repository. The reference repository cuts across three hydrogeologic units, the Topopah Spring middle nonlithophysal, lower lithophysal, and lower nonlithophysal units. Region SW is mostly in the lower nonlithophysal; Regions NW, NE, CC, and SC are mostly in the lower lithophysal; and Region SE is mostly in the middle nonlithophysal.

This complex modeling process includes multiple scales (mountain and drift), multiple dimensions



SNL/TRW abq38.eps  
FV3032-7

Figure 3-20. Division of the Repository Area into Six Subregions

The dashed line shows the actual reference-design repository boundary; the solid lines show the idealization of the repository by a rectangle and the six regions used for averaging thermal-hydrologic data. Averaging data values in six zones is an enhancement over averaging data over the entire repository area.

(one-, two-, and three-dimensional models), and varying assumptions regarding the coupling of heat transfer to fluid flow (conduction only and full thermal-hydrologic). To provide greater confidence that this abstraction method adequately represents the thermal-hydrologic behavior of Yucca Mountain, an independent model was also developed. This model incorporates three-dimensional, fully coupled heat transfer and fluid flow but uses a less mechanistic conceptual flow model (generalized equivalent-continuum rather than dual-permeability) and a less sophisticated coupling between drift scale and mountain scale. It uses data from mountain-scale thermal-hydrologic models to approximate edge effects. The computational requirements of the verification model do not allow the many abstraction simulations that are required for a total-system calculation. However, this type of model provides an important check on the abstraction processes. Good agreement was found when the independent modeling approaches were compared at repository center and edge locations. This analysis addresses the key issue of tradeoffs between model dimensionalities. This comparison shows that the combination of one- or two-dimensional models with reduced complexity in heat-transfer models suffices for determining near-field responses associated with waste package heating. This simplicity provides flexibility in producing the many simulations required.

### 3.2.2.3 The Mountain-Scale Model

Mountain-scale thermal-hydrologic models are used to calculate quantities associated with larger scales, such as air mass fraction and gas-phase fluxes. The thermal-hydrologic multiscale modeling and abstraction method is unable to account for gas-phase advection from large-scale temperature and pressure gradients because only conduction is included in its mountain-scale submodel. At the mountain scale, gas-flow patterns from repository heating can only be realized with a fully coupled thermal-hydrologic model. The key issue addressed by this model is the movement of gas and liquid through fractures at the mountain scale. A generalized equivalent-continuum flow model was used to determine gas-phase data for the mountain. Use of this model

reduces the computational requirements of the larger-scale thermal-hydrologic simulations (as compared to use of the dual-permeability model) while still allowing for sufficient mobility of liquid water in fractures.

A mountain-scale model based on east-west cross sections was used for each of the property sets and associated infiltration rates considered. The mountain-scale model includes large-scale features such as mountain topography and variability by location of the net infiltration rate at the ground surface. It also includes repository edge effects and the ability to develop large-scale fluid-flow processes such as buoyant convection, in which fluid moves in response to a density gradient. The cross sections used to calculate gas flow were taken directly from the mountain-scale unsaturated zone flow model (Section 3.1). The model includes the stratigraphy and hydrologic properties established for the unsaturated zone flow model. The mountain-scale model includes the heat output of the entire repository waste stream (scaled for a two-dimensional application) emplaced at the time of repository closure.

The smeared heat source in the mountain-scale model does not allow for important effects such as shedding of condensate between drifts and it does not capture the difference in thermal-hydrologic behavior in the drifts as compared to in the rock between drifts. Because of these limitations, the mountain-scale model probably underestimates reduction in air mass fraction in the drifts during the thermal period.

### 3.2.2.4 Uncertainties

Except for uncertainties associated with repository design (for example, thermal loading, the use of backfill, and waste package configurations), the thermal-hydrologic analyses introduce no new important parameter uncertainties to the analyses. The major uncertainties for thermal hydrology have to do with water and gas flow, and the thermal-hydrologic calculations use the same uncertain parameters as the ambient unsaturated zone flow component (Section 3.1). Some of the most important of these uncertainties are in hydro-

logic properties, infiltration rates, and future climate states. Examples of how these uncertainties influence thermal hydrology are shown in Section 3.2.3.

In addition to the neglect of thermal-hydrologic-chemical coupled processes, the most important limitations of the thermal-hydrologic modeling are those discussed in Section 3.1 for unsaturated zone flow, because the hydrology part of thermal hydrology shares most important issues with the ambient hydrology discussed in Section 3.1.

### 3.2.3 Results and Interpretation

The following selected results illustrate features of the thermal-hydrologic analyses, including effects of variability of waste package heat output and the use of different hydrologic property sets and infiltration rates.

Figure 3-21 shows the variability in average waste package temperature among the six repository regions. The early behavior, when temperature is increasing, is largely influenced by infiltration rates, initial liquid saturation of the host rock, and host-rock thermal properties. During cooldown, faster cooling of regions near the repository edge becomes increasingly noticeable with time.

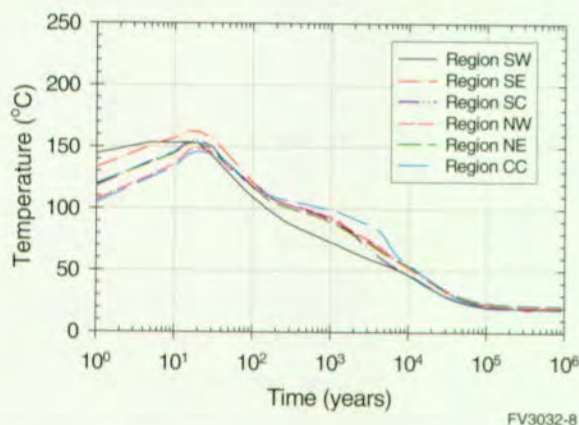


Figure 3-21. Average Waste Package Temperature History for Six Repository Regions  
Average waste package temperature history for six repository regions using commercial spent nuclear fuel, long-term average climate, mean infiltration, and base case hydrologic properties.

Region SW cools off the fastest because it is along the repository edge. Region CC cools off the slowest because it is farthest from the repository edges. After 10,000 years, there is little variability among regions.

Figure 3-21 illustrates temperatures calculated for the entire period using the long-term average climate (see Section 3.1), with an average infiltration of about 40 mm/year (1.6 in./year). In reality, the climate model includes cycling between drier (present-day average infiltration of about 8 mm/year, or 0.3 in./year) and wetter (long-term average) climate states. Climate effects on thermal hydrology are included by making two sets of calculations, one with dry climate for the entire period and one with long-term average climate for the entire period. Switching from one set of calculated results to the other at the time of climate change approximates the influence of climate change on thermal-hydrologic behavior. When this approximation was tested against simulations in which infiltration was varied through time, the response to changes in infiltration was found to be fast enough to use the approximation. Results based on long-term average climate are used for illustration because this climate is in effect most of the time. Temperatures for dry climate are slightly higher because lower infiltration results in less influx of cooler infiltrating water. Only the first climate change, between 0 and 10,000 years, is relevant to thermal hydrology. By the time of the second climate change, between 80,000 years and 110,000 years, temperatures and relative humidities will have essentially returned to ambient conditions (climate-change times are summarized in Table 3-4). Although these illustrations are for commercial spent nuclear fuel waste packages, the results for high-level radioactive waste and DOE spent nuclear fuel are similar.

Figures 3-22 and 3-23 show the variability of waste package temperature and relative humidity within one of the repository regions (Region NE). This variability results primarily from the differences in heat output among waste packages and to a lesser extent from differences in infiltration and stratig-

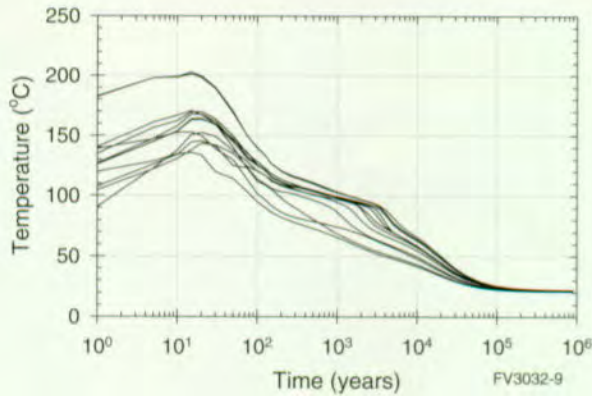
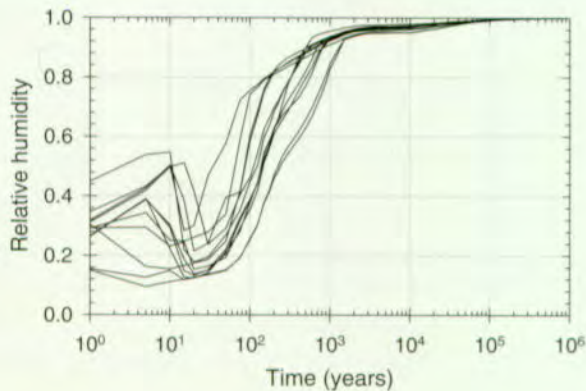


Figure 3-22. Variability of Temperature History Among Waste Packages

Variability of temperature history among waste packages in Region NE (see Figure 3-20) using commercial spent nuclear fuel, long-term average climate, mean infiltration, and base case hydrologic properties.



FV3032-10

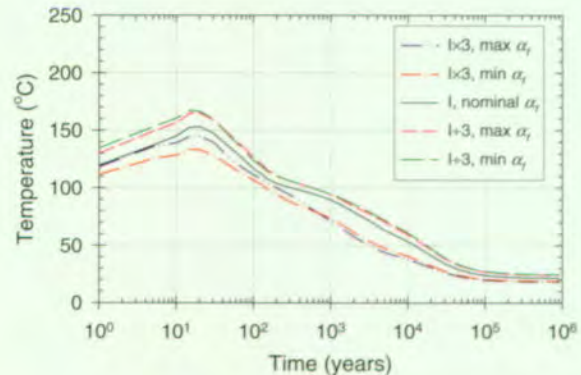
Figure 3-23. Variability of Relative-Humidity History Among Waste Packages

Variability of relative-humidity history among waste packages in Region NE (see Figure 3-20) using commercial spent nuclear fuel, long-term average climate, mean infiltration, and base case hydrologic properties.

raphy within the region. The influence of decay heat is negligible after 100,000 years.

Figure 3-24 shows how average waste package temperature is affected by the uncertainty in unsaturated zone flow incorporated into the base case. The high-infiltration cases (approximately 90 mm/year or 3.5 in./year) have cooler temperatures than the mean-infiltration (approximately 30 mm/year or 1.2 in./year) or low-infiltration (approximately 10 mm/year or 0.4 in./year) cases. This figure shows that the thermal-hydrologic variability associated with infiltration uncertainty dominates the variability associated with hydrologic-parameter uncertainty (represented here by variations in the fracture air-entry parameter  $\alpha_f$ , which is proportional to fracture aperture).

Figure 3-25 shows how waste package temperature is affected by additional hydrologic uncertainty beyond that included in the base case. The dual-permeability/Weeps alternative flow model is described in Sections 3.1.1.3 and 3.1.3.3. The



FV3032-11

Figure 3-24. Average Waste Package Temperature History for Five Base Case Property Sets

Average waste package temperature history in Region NE (see Figure 3-20) for the five base case hydrologic-property sets using commercial spent nuclear fuel and long-term average climate. Shown are effects of variations in infiltration ( $l$ ) and fracture air-entry parameter ( $\alpha_f$ ), which is an important hydrologic property.

“thermal-hydrologic” property set is different from the base case hydrologic properties primarily because of a much lower imbibition diffusivity for the rock matrix of the Topopah Spring lower nonlithophysal hydrogeologic unit, a change suggested by results of the single heater test (CRWMS M&O 1998i, Section 3.4.5). Results in Figure 3-25 are shown for Region SW because the repository is in the Topopah Spring lower nonlithophysal unit in that region, so the difference introduced by the thermal-hydrologic property set is greatest in Region SW. The figure shows that the dual-permeability/Weeps model has a greater effect on waste package temperature than the thermal-hydrologic property set does, but neither one has much effect after the first 100 years.

Figure 3-26 displays the time history of air mass fraction as obtained from the mountain-scale thermal-hydrologic model. This model provides air fractions at repository center and edge locations (Figure 3-17). The center and edge are quite different. Air mass fractions are higher at edge locations because above-boiling conditions subside more quickly as heat is lost to the surrounding unheated rock mass. When temperatures are above boiling, steam generation causes the reduction in air mass fraction as the generated steam drives

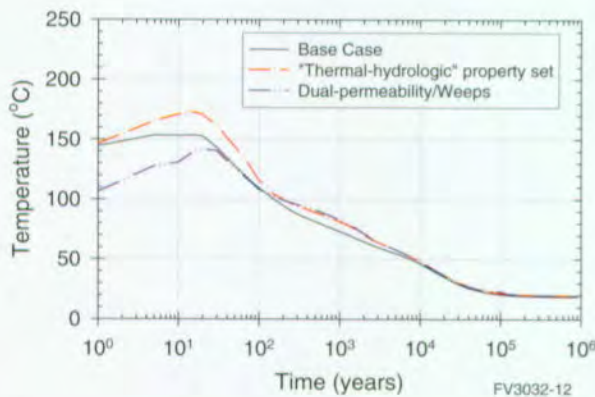


Figure 3-25. Effect of Alternative Hydrologic-Property Sets on Waste Package Temperature  
Effect of alternative hydrologic-property sets on waste package temperature in region SW (see Figure 3-20) using commercial spent nuclear fuel, long-term average climate, and mean infiltration.

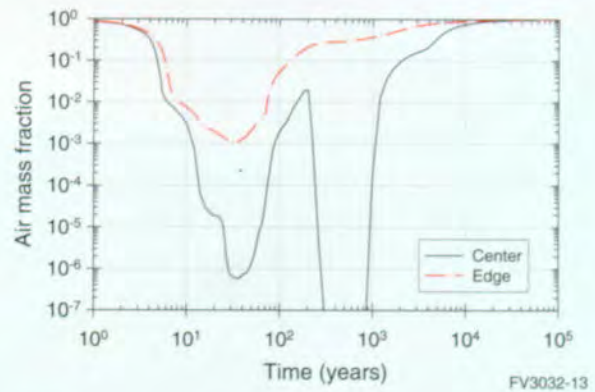


Figure 3-26. Air Mass Fraction for Center and Edge Repository Locations

Air mass fraction for center and edge repository location, from the mountain-scale thermal-hydrologic model using dry (present day) climate, mean infiltration, and base case hydrologic properties. When the air mass fraction is low, it indicates that air has been driven away from the waste packages by steam generation.

away the air. The figure shows that steam generation is only strong enough to drive out the air for a few thousand years at most, and for only a few hundred years near the repository edge. The double-minimum shape of the “center” curve is a result of details of water movement near the repository. There is a pulse of condensate drainage as heat mobilizes water, then a drying period, and then a gradual rewetting as the repository cools.

In summary, thermal-hydrologic models require quantification of processes at two different scales. The use of models at different scales requires different details and refinement to reproduce the important processes caused by emplacement of heat-generating waste in a geologic repository. Because of the complex interaction between heat and fluid flow (for example, phase-change processes), several of the models used to determine the thermal-hydrologic processes important to long-term repository performance are computationally intensive. These thermal-hydrologic models have undergone a significant evolutionary process to address key issues from the thermal-hydrology workshop (CRWMS M&O 1997i) and from recommendations made by the Thermohydrologic Modeling and Testing Program Peer Review (CRWMS M&O 1996e). This process built upon

the knowledge gained through previous TSPAs. Important concerns related to conceptual flow models, use of site-characterization data for hydrologic and thermal properties, and incorporation of results from the thermal-testing program into decisions regarding property sets were implemented in the thermal-hydrology component.

Some important issues remain unresolved, in particular the impact of thermal-hydrologic-mechanical and thermal-hydrologic-chemical coupled processes. As new site data are obtained (for example, from the drift-scale thermal test) they will be incorporated into the thermal-hydrologic models.

### 3.3 NEAR-FIELD GEOCHEMICAL ENVIRONMENT

The near-field geochemical environment component is a description of the changing composition of gas, water, colloids, and solids within the emplacement drifts under the perturbed conditions of the repository environment. The major changes are caused by the planned thermal loading of the

system and the emplacement of large masses of materials that can react with water and gas in the system. Because the system will heat and then cool off, the system will continue to change. Not only will the thermal perturbation affect the movement of gas and water through the unsaturated system (thermal hydrology as described in Section 3.2), but it will also affect the composition of the gas and water. These fluids of altered composition may enter the drifts and react with the materials emplaced during repository construction. Most of these emplaced materials will be very different in chemical composition from the host rock. In the drifts, reactions with materials such as concrete may alter water and gas compositions before they react with the waste package and the waste forms, and along the flow paths for radionuclide transport in the unsaturated zone. The emplaced materials may also provide additional sources of colloids. These colloids from emplaced materials may be more effective in transporting radionuclides than natural colloids. Figure 3-27 is a general view of processes, phases, and design materials that are considered for the near-field geochemical environment.

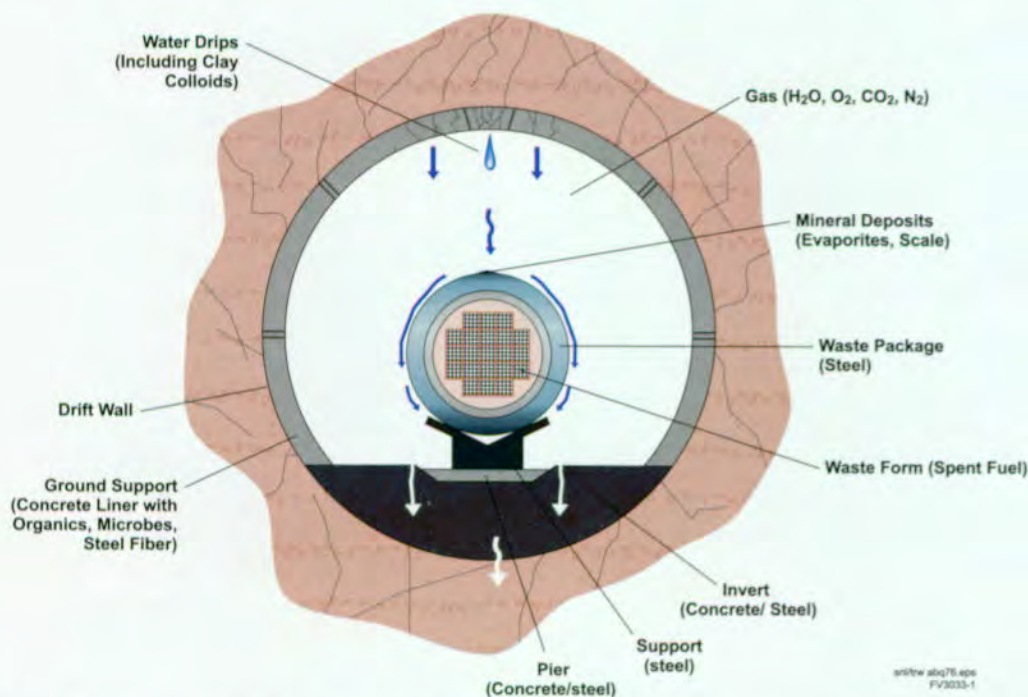


Figure 3-27. General Near-Field Geochemical Environment Conceptual Processes, Phases, and Design Material. This TSPA-VA component describes changing compositions of gas, water, colloids, and solids within the potential emplacement drifts.

The geochemical modeling studies and analyses presented in this section were prepared with the view of addressing selected aspects of the NRC Key Technical Issue on Evolution of the Near-Field Environment (NRC 1997c). Specifically, the information presented is pertinent to three of the four subissues of this key technical issue, namely, effects of coupled processes on seepage, rate of release of radionuclides from breached waste packages, and radionuclide transport through engineered and natural barriers.

The most direct way the near-field geochemical environment may impact long-term performance is by changing the engineered barrier system that inhibits the supply and limits the release rate of radionuclides to the geosphere (to the unsaturated zone component for radionuclide transport, see Section 3.6). Chemical changes to the in-drift environment may affect the amounts and types of mobile radionuclides and the properties of the solids through which they are transported. The near-field geochemical environment is the set of compositional conditions under which the waste package corrodes, the waste forms dissolve and precipitate as secondary phases, the radionuclides mobilize from the waste form, and the radionuclides migrate through the engineered barriers. In addition to these primary effects within the engineered barrier system, perturbed fluids generated in the near-field geochemical environment could react with the host rock. Such alteration may change the flow pathways in the geosphere and change conditions for unsaturated zone transport.

A set of five models has been developed to represent the near-field geochemical environment. These models are:

1. The incoming gas, water, and colloids (compositions of those phases as they enter the drift)
2. The in-drift gas phase (composition of the gas phase relative to major gas sinks in the drift)

3. The in-drift water/solid chemistry (evolution of water composition reacting with major materials and the drift gas phase)
4. The in-drift colloids (stability and quantity of clay and iron-oxide colloids in the drift)
5. The in-drift microbial communities

The relationships between the models for the near-field geochemical environment, including the general flow of information from one model to another and the major components of each submodel, are shown in Figure 3-28. In some cases, these five models contain process-level calculations to represent the evolution of water, solid, and gas reactions in the system. In other cases, the models consist of "bounding" arguments for applying observed values. There are a number of submodels for the water/solids interaction model covering steel corrosion products (iron oxyhydroxides), concrete, waste form (spent nuclear fuel), and mineral precipitates from boiling

The near-field geochemical environment model has several connections with other component models. The near-field geochemical environment models take input from the unsaturated zone flow and thermal-hydrology models and provide output to the waste package corrosion model, the waste form model (degradation, radionuclide mobilization, and engineered barrier system transport), the unsaturated zone radionuclide transport model, and the criticality model. The connections and specific inputs and outputs to and from the near-field geochemical environment component are shown as a flow diagram in Figure 3-29. The interfaces are discussed in more detail below.

*Unsaturated Zone Flow.* The flux of water and dissolved constituents through the near-field geochemical environment is given either as the seepage flux through the drifts or as the average percolation flux at the repository horizon. Seepage flux is used for the in-drift water-solids model and the colloid model. Average percolation flux is used for the in-drift gas model because gas mobility is relatively high near the drifts and, therefore, the

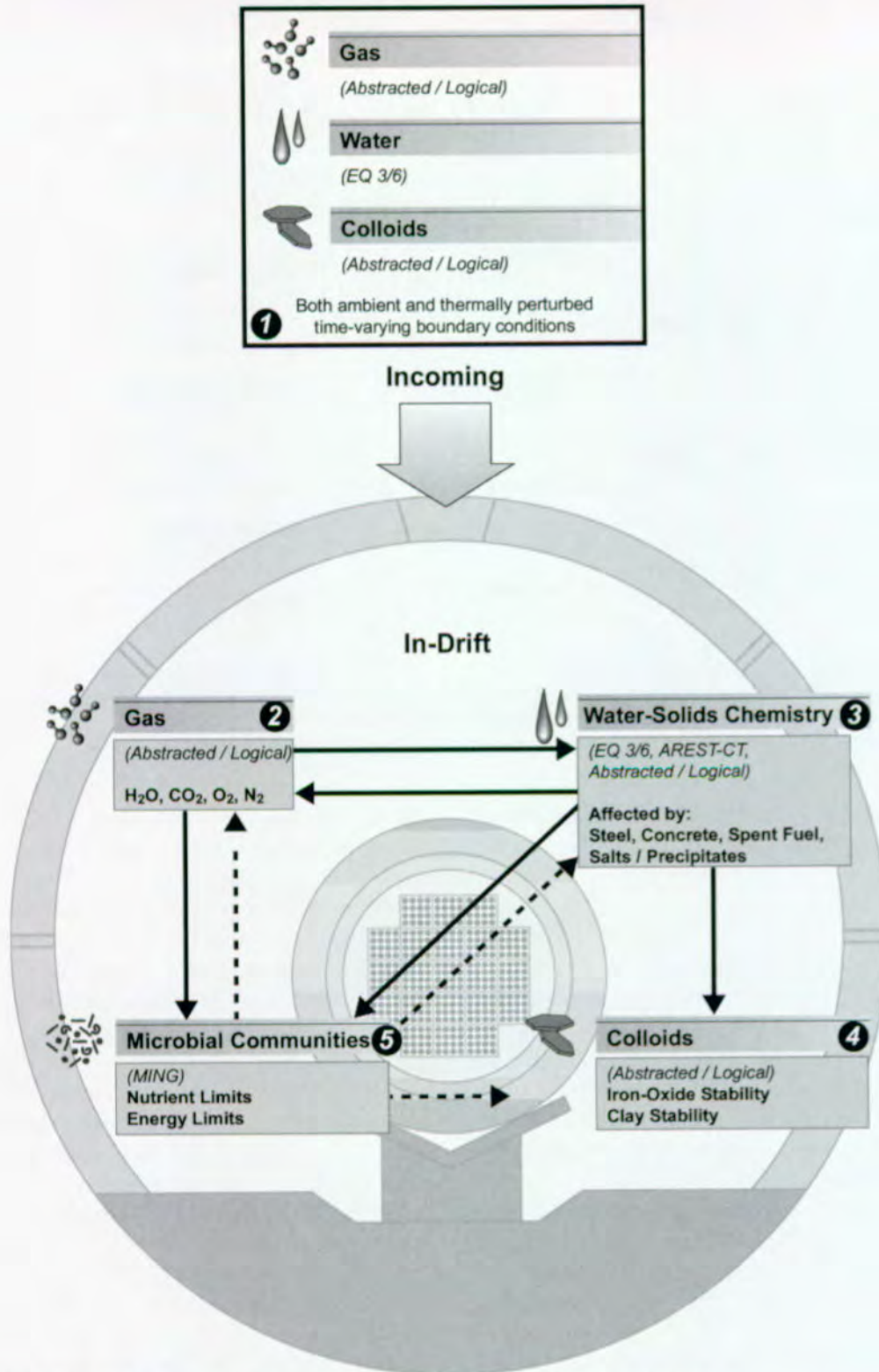


Figure 3-28. Relations Between the Five Near-Field Geochemical Environment Models  
Information flow between models is shown by the arrows. Model implementations are either as abstracted/logical parameter descriptions or via computer codes (MING, EQ 3/6, and AREST-CT).

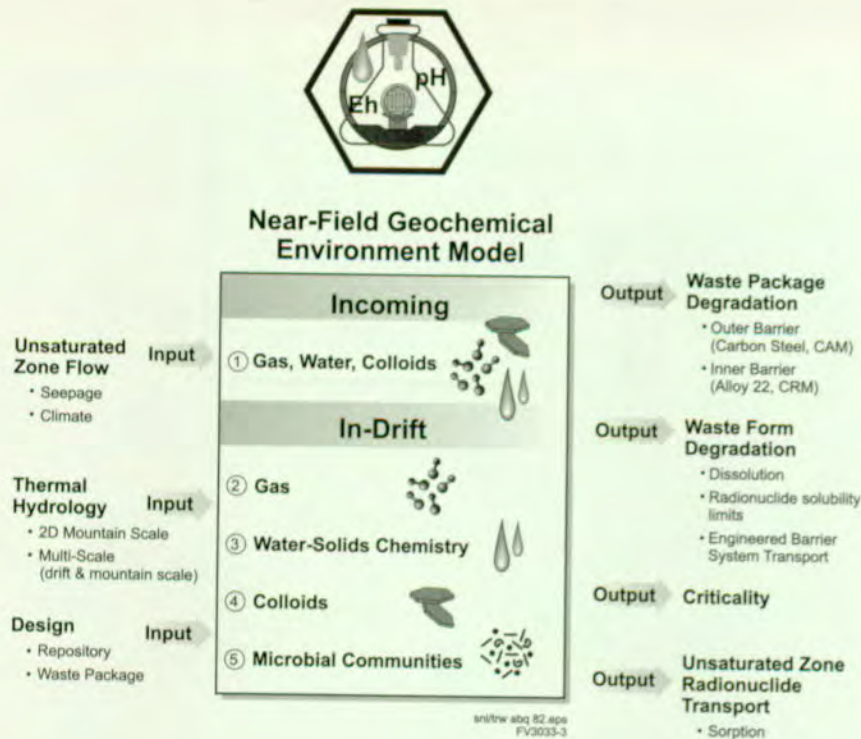


Figure 3-29. Interconnections Between Near Field Geochemical Environment Component and Other Total System Performance Assessment for the Viability Assessment Components (CAM—corrosion allowance material; CRM—corrosion resistant material)

gas composition is in equilibrium with a much greater volume of water than just the seeping water.

*Thermal Hydrology.* The thermal disturbance caused by repository heating provides a number of time-dependent boundary conditions for the near-field geochemical environment model, including the flux of groundwater and gas into the drift, the drift temperature, and the relative abundance of air in the gas. Thermal effects can drive changes in the fluid and gas compositions through changes to temperature-dependent phase equilibria or reaction kinetics. Such changes may also occur within the heated geosphere surrounding the engineered barrier system and change the compositions of those incoming phases. The effects of thermal perturbations may also have long-term consequences for minerals and solids within the drift because of changes in phase stabilities, reaction rates, permeabilities, and porosities.

*Waste Package Degradation.* The in-drift geochemistry may have impacts on corrosion of waste package barrier materials. The composition of water contacting the waste package and the bulk oxidation state within the drifts are supplied by the near-field geochemical environment model. Also, just as the waste package degradation will be affected by the composition of fluids reacting with it, the waste package materials themselves are an extensive mass of introduced materials. These materials and their solid corrosion products can change the aqueous and gas compositions in the drift, as well as provide a source of iron-oxyhydroxy colloids that may enhance migration of certain radionuclides.

*Waste-Form Degradation, Mobilization, and Engineered Barrier System Transport.* The degradation rates of the waste forms (including cladding) depend on the composition of the gas phase and the aqueous phase reacting with the waste form. The near-field geochemical environment component provides the compositions

of water and gas that may react with the waste forms and provides the state of materials through which radionuclide transport will occur in the engineered barrier system. The major chemical constituents of the waste form have also been evaluated for their potential to change the water chemistry from its initial composition.

*Unsaturated Zone Radionuclide Transport.* The overall composition of the water moving from the engineered barrier system into the unsaturated zone transport pathways of the geosphere is determined from the near-field geochemical environment component. Radionuclide transport depends on the water composition, particularly for radionuclide retardation processes, but also for potential alteration of the pathways themselves. The potential altered fluid compositions that may migrate through the unsaturated zone are used as constraints on the cases for altered unsaturated zone radionuclide transport sensitivity analyses (see Section 5.6).

*Criticality.* A portion of this work (Section 4.4) considers the possibility of a critical configuration of fissile material forming within the drift (near-field) environment after release from waste packages ("external" criticality), and its potential performance consequences. This external criticality is linked directly to radionuclide transport processes in the emplacement drifts and depends on the location and time-dependent chemical changes that occur there. In addition, the changes (mainly thermal) caused by a critical event could affect the chemical environment within a drift.

### 3.3.1 Construction of the Conceptual Models

There are several issues and coupled processes relevant to the development of near-field geochemical environment models (CRWMS M&O 1998c). Performance assessment personnel and principal investigators within the scientific program worked together to develop abstracted models of the near-field geochemical environment models. Some of the near-field geochemical environment models are based, in part, on conceptual process models developed within the *Near-Field/Altered-Zone Models Report* (CRWMS

M&O 1998c). Such conceptual models are combined with time-dependent, abstracted results of the potential repository system thermal-hydrologic evolution (see Section 3.2), that were used as constraints for the near-field geochemical environment models of gas composition. This abstraction entailed using average constant values for defined periods with step changes in between them. One primary result of this is that short-term transient effects (for example, lasting less than about 100 years) are included in an average manner. This was assessed as a reasonable way to proceed for this initial model development effort because the TSPA system integration model uses time-steps of at least 100 years (CRWMS M&O 1998i, Section 4.4 and 11.1).

#### 3.3.1.1 The Near-Field Geochemical Environment Workshop and Highest Priority Issues

A workshop about the treatment of the near-field (in-drift) geochemical environment in this TSPA was held in March 1997. The details of the workshop activities and results are documented in *Near-Field Geochemical Environment Abstraction/Testing Workshop Results* (CRWMS M&O 1997d). A brief overview of the workshop is provided because it was the primary initiator for development of the near-field geochemical environment component for this TSPA. The criteria used at the workshop to prioritize issues, the highest priority issues, and the resulting abstraction plans are listed in Table 3-9.

At the near-field geochemical environment workshop, YMP personnel from the design, scientific programs, and performance assessment organizations delineated, discussed, and prioritized issues relevant to chemistry within emplacement drifts that might impact system performance. The two issues given the highest priority focused on evolution of design materials within the drift (that is, the in-drift water/solid chemistry). These two issues are, "the amount of water coming into the drift" and "the introduced material masses and compositions."<sup>2</sup> Three additional issues that were also given high priority for this topic are "aqueous

Table 3-9. Near-Field Geochemical Environment  
Abstraction/Testing Workshop

| <b>NEAR-FIELD GEOCHEMICAL ENVIRONMENT<br/>ABSTRACTION/TESTING WORKSHOP<br/>March 5-7, 1997, Berkeley, CA<br/>(CRWMS M&amp;O 1997d)</b>   |  |
|--|--|
| <b>PRIORITIZATION CRITERIA</b>   |  |
| <ul style="list-style-type: none"><li>• Does the process/issue affect the<ul style="list-style-type: none"><li>- Dissolved radionuclide concentration?</li><li>- Colloidal radionuclide abundances?</li><li>- In-drift sorption capacities?</li><li>- In-drift porosity and permeability?</li></ul></li></ul>  |  |
| <b>HIGHEST PRIORITY ISSUES</b>   |  |
| <ul style="list-style-type: none"><li>• Solid phases throughout the drift:<ul style="list-style-type: none"><li>- Volume and flux of water in drift</li><li>- Compositions, abundances, and distribution (cement, alloys, organics, microbes, ceramics)</li><li>- Aqueous and gas reactions on materials</li><li>- Aqueous and gas reactions (corrosion) on waste package</li><li>- In-drift system open or closed</li></ul></li><li>• Gas phase throughout the drift:<ul style="list-style-type: none"><li>- Gas flux</li><li>- Reactions with solids and microbes (excluding waste package)</li><li>- Reactions with waste package</li><li>- Thermal effects (water reactions)</li><li>- Temporal heterogeneity</li><li>- Climate effects</li></ul></li><li>• Aqueous phase throughout the drift:<ul style="list-style-type: none"><li>- Aqueous phase reactions with major introduced materials (excluding waste package)</li><li>- Open versus closed system</li><li>- Aqueous phase reactions with waste package</li><li>- Temporal evolution of aqueous phase composition</li><li>- Perturbed water composition entering drift</li><li>- Aqueous reactions with waste form</li><li>- Thermal effects on aqueous phase compositions</li><li>- Aqueous phase reactions with evaporite minerals</li><li>- Microbial process effects on aqueous composition</li><li>- Reversibility of radionuclide sorption onto colloids</li><li>- Water-composition effects</li><li>- Waste form</li></ul></li><li>• Other (introduced materials in rock)<ul style="list-style-type: none"><li>- Temporal heterogeneity</li><li>- Microbial processes</li><li>- Temperature effects</li></ul></li></ul> |  |
| <b>ANALYSIS PLANS</b>  |  |
| <ul style="list-style-type: none"><li>• Incoming Gas, Water, and Colloids</li><li>• Gas composition evolution in the drift</li><li>• Water solid chemistry model</li><li>• Colloid-facilitated radionuclide transport</li><li>• Effects of microbial communities</li></ul>   |  |

and gas reactions with materials," "aqueous and gas reactions with the waste package," and "open versus closed system behavior." The gas composition issue given top priority was "gas flux into the drift." The third-highest overall prioritized issue relates to the in-drift water composition, "effects from reactions with introduced materials." Workshop participants gave high priority to two other issues related to in-drift water chemistry: "open versus closed system," and "aqueous reactions with the waste package." The highest priority issue related to in-drift colloids was assessed to be "reversibility of sorption." The issues "water composition effects" and "waste form" were also given high priority for colloids in the drift. These priorities, together with the group discussion of issues in each topic area, provided the bases for development of the component models.

The workshop itself, together with post-workshop synthesis and planning, led to the five model areas for the near-field geochemical environment:

- Incoming gas, water, and colloids (compositions of those phases as they enter the drift)
- The in-drift gas phase (composition of the gas phase relative to major gas constituent sinks in the drift)
- The in-drift water/solids chemistry (evolution of water composition reacting with major materials and the gas phase in the drift)
- The in-drift colloids (stability and quantity of clay and iron-oxide colloids)
- The in-drift microbial communities

The conceptual models for each of these areas are summarized in Sections 3.3.1.2 and 3.3.1.3. Their specific implementations for the analyses are given in Section 3.3.2.

<sup>2</sup> Although the waste package is a design material, it was considered separately from other potential repository-design materials for clarity because it is also a major component of the engineered barrier system.

### 3.3.1.2 Incoming Gas, Water, and Colloids

The near-field geochemical environment model provides values for the time-varying compositions and fluxes of gas, water, and colloids entering the drift. Changes to these variables are primarily driven by the thermal changes to the system. Reactions between the gas, water, and minerals in the rock occur as the system is heated and pore water boils. These processes change the system by changing phase stabilities or increasing rates of reaction for existing phases. The time evolution of the system was divided into two thermal regimes; a boiling regime and a cooling regime. These two regimes are further subdivided based on large changes to the gas composition (mainly within the boiling regime) or the changing temperature of the cooling system (within the cooling regime). The periods are defined to have constant chemical conditions so that the description of the near-field geochemical environment evolution consists of a set of step changes in system conditions.

**Conceptual Model for Incoming Gas.** In the conceptual model for incoming gas, gas composition is represented by the major gas constituents: steam ( $H_2O$ ), oxygen ( $O_2$ ), carbon dioxide ( $CO_2$ ), and nitrogen ( $N_2$ ). The primary sources of these gases and the mountain scale processes affecting their quantities are shown in Figure 3-30. Steam (or water vapor) is generated during the boiling period and affects the rate at which waste packages corrode. The other three gas constituents are components of air considered in this model.<sup>3</sup> Oxygen is included because of its role in metal oxidation. Carbon dioxide directly affects the pH of solutions (which affects waste form dissolution) and can strongly affect actinide complexes (increasing their dissolved concentrations). Finally, nitrogen generally comprises most of the air component of the gas and may serve as a nutrient source for microbial activity.

Because gas is less soluble at higher temperature, heating drives dissolved gases out of the water and into the gas phase. Rapid gas movement in the

fractures may transport those dissolved gas constituents away from the heated water they came from and towards cooler water (that is, down the temperature gradient) where they can redissolve. This process tends to deplete the heated water and enrich the cooler water in these gas species. As the temperature of the mountain increases farther away from the repository, these gas species are remobilized and transported farther away from the drifts in a continual process of revaporization and redissolution. In the rock near the heat sources temperatures will rise above the boiling point of water, generating abundant steam, causing an overall dilution of the air component.

The major source of both oxygen and nitrogen is the atmosphere, so dilution of these two constituents by steam (from boiling) is accounted for by a direct reduction in their atmospheric partial pressures. For carbon dioxide, the system is somewhat more complex. Measurements of gas compositions from various unsaturated zone boreholes demonstrate that unsaturated zone  $CO_2$  gas concentrations are elevated above atmospheric  $CO_2$  partial pressures (about 350 ppmv [parts-per-million by volume]) by about a factor of three (CRWMS M&O 1998i, Section 6.2.7.2, pp. 6.2-40). The values of unsaturated zone pore-gas composition analyzed for the site indicate that the  $CO_2$  content of pore gases tends to average about 1,000 ppmv (ibid., Section 5.3.4.2.4.6, pp. 5.3-173). These elevated values could be the result of mixing of  $CO_2$ -rich gases generated in the soil zone with the rest of the gas volume of the mountain (ibid., Section 5.3.4.2.4.6, pp. 5.3-173). Because the rock contains the mineral calcite ( $CaCO_3$ ) and there is a non-negligible amount of dissolved carbonate in the water, these phases may act as sources of carbon dioxide that must be accounted for in the assessment of the air composition diluted by steam. However, because gas flow is much more rapid than water flow, the near-field geochemical environment model assumes that the water composition will be primarily controlled by the gas composition diluted by steam for most of the thermal period. Nevertheless, there are indica-

<sup>3</sup> Air does not necessarily imply atmospheric composition of these gases but is the term for the gas ingredient "other than steam" in the thermal-hydrologic models (see Section 3.2).

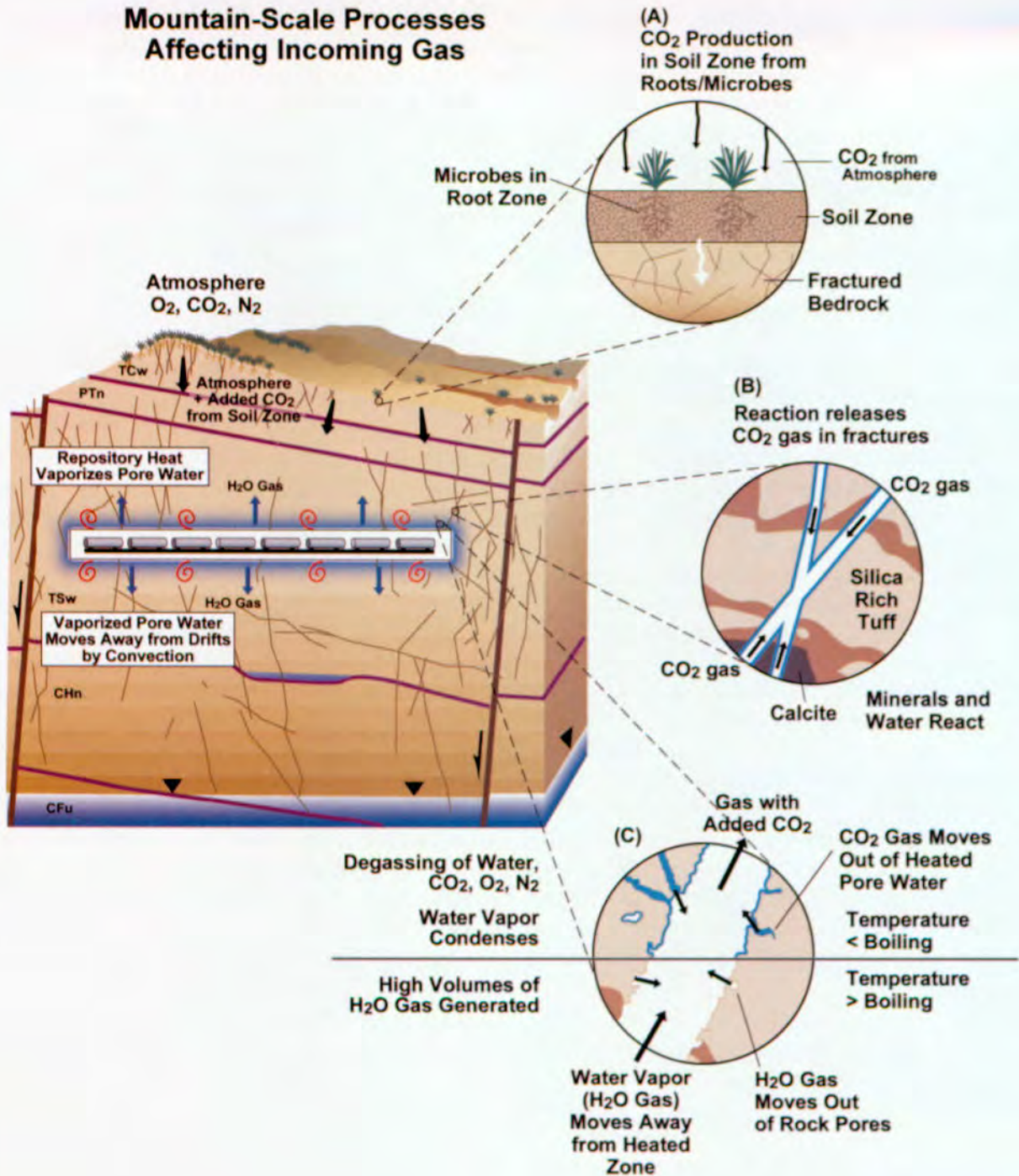


Figure 3-30. Mountain-Scale Conceptual Picture of Incoming Gas Model Processes  
Incoming gas picks up added carbon dioxide content as it passes through the soil zone. Carbon dioxide gas migrating in rock fractures reacts with minerals and water in the tuff rock. Heating caused by waste packages in the repository causes water to boil, to steam, and move away from the heated area in vapor form until it reaches a cooler area where it condenses.

tions from water compositions in the single-heater test that calcite may be reacting to release carbon dioxide during the heating stage (CRWMS M&O 1998c, Section 6.2.1). In addition, the potential exists for short-term increases in the carbon dioxide content (of the air) as it is released from heated water (CRWMS M&O 1998i, Section 4.4). Therefore, a brief period with an elevated level of carbon dioxide in the air, which is then diluted by steam, was included at the start of the model to represent these potential sources of carbon dioxide.

The incoming gas model also assesses constraints on the fluxes of the gas constituents into the drift. These values are used in analyses that evaluate the potential for depletion of these constituents by reaction with the solids in the drift, and the potential effects on water/solids chemistry of those reactions (discussed below). For each of the gas constituents in the model, the cumulative gaseous flux of that chemical component into the drift is given by the product of the cumulative gas phase flux and the fraction of that constituent in the gas for a given period. In the conceptual models for the gas and water/solids chemistry in the drift, the fluxes of these gas constituents that could be derived from their dissolved counterparts in the water flux were also included. For this model, the fluxes of the dissolved gas constituents were based on the percolation flux for the drift cross-section. This water flux is larger than that given by the seepage model, which only has a fraction of the percolation flux entering the drift. Because gaseous diffusion for carbon dioxide or oxygen gas species is relatively rapid at this scale, the gas composition may be buffered by water just outside the drift. Therefore, this larger water flux should represent a more realistic bound on the masses of these gas constituents available for reaction in the drift (CRWMS M&O 1998i, Section 4.4).

**Conceptual Model for Incoming Water.** In the conceptual model for incoming water, water composition is represented by the major dissolved constituents and by some of the less abundant dissolved constituents that participate in some of the dominant mineral reactions within the system. The compositional components considered for the water in the model are pH, sodium ( $\text{Na}^+$ ),

potassium ( $\text{K}^+$ ), calcium ( $\text{Ca}^{2+}$ ), magnesium ( $\text{Mg}^{2+}$ ), iron ( $\text{Fe}^{2+}$ ,  $\text{Fe}^{3+}$ ), aluminum ( $\text{Al}^{3+}$ ), silica ( $\text{SiO}_2$ ), chloride ( $\text{Cl}^-$ ), fluoride ( $\text{F}^-$ ), carbonate ( $\text{CO}_3^{2-}$ ), and sulfate ( $\text{SO}_4^{2-}$ ). These constituents represent the total masses of these components within the fluid, and each may be comprised of a number of different species in solution. In addition, the dissolved oxygen content is included as constrained by the oxygen fugacity (approximately the partial pressure), and this value is used to calculate the equilibrium oxidation potential (Eh) of the system. Figure 3-31 shows the major processes at the mountain scale affecting the concentrations of these constituents in the incoming water.

The composition of ambient water moving through fractures and entering the drift has been constrained by examination of the various fluid compositions observed both at the site, and near Yucca Mountain. Pore water in unsaturated tuffs appears to have higher concentrations of some constituents like sulfate and chloride (CRWMS M&O 1997d, Appendix 3 Table I; Bodvarsson et al. 1997, Chapter 14; CRWMS M&O 1998m, Section 6.2.5 and 6.2.8) compared to the water in the saturated zone tuffs (Figure 3-31, Inset A). However, the composition migrating through the unsaturated zone fractures into the drift is assumed to be that observed within the saturated zone tuff aquifer (from well J-13, Figure 3-31, Insets B and C). This assumption is based on compositional similarities between the perched water bodies, fracture fluids collected at Ranier Mesa (a nearby mountain of unsaturated volcanic tuffs analogous to Yucca Mountain), and groundwater samples from the J-13 well (CRWMS M&O 1998c, Section 6.2 Table 6.2-1; CRWMS M&O 1998i, Section 4.4).

The processes that change ambient water composition are driven by heating of the system and are closely linked with the processes shown in Figure 3-30 for evolution of the gas composition entering the drift. In the conceptual model for the incoming water composition, the time-varying gas composition is imposed as an equilibrium constraint on the water composition at the temperature of the system because the gas transport is fast relative to

### Mountain-Scale Processes Affecting Incoming Water

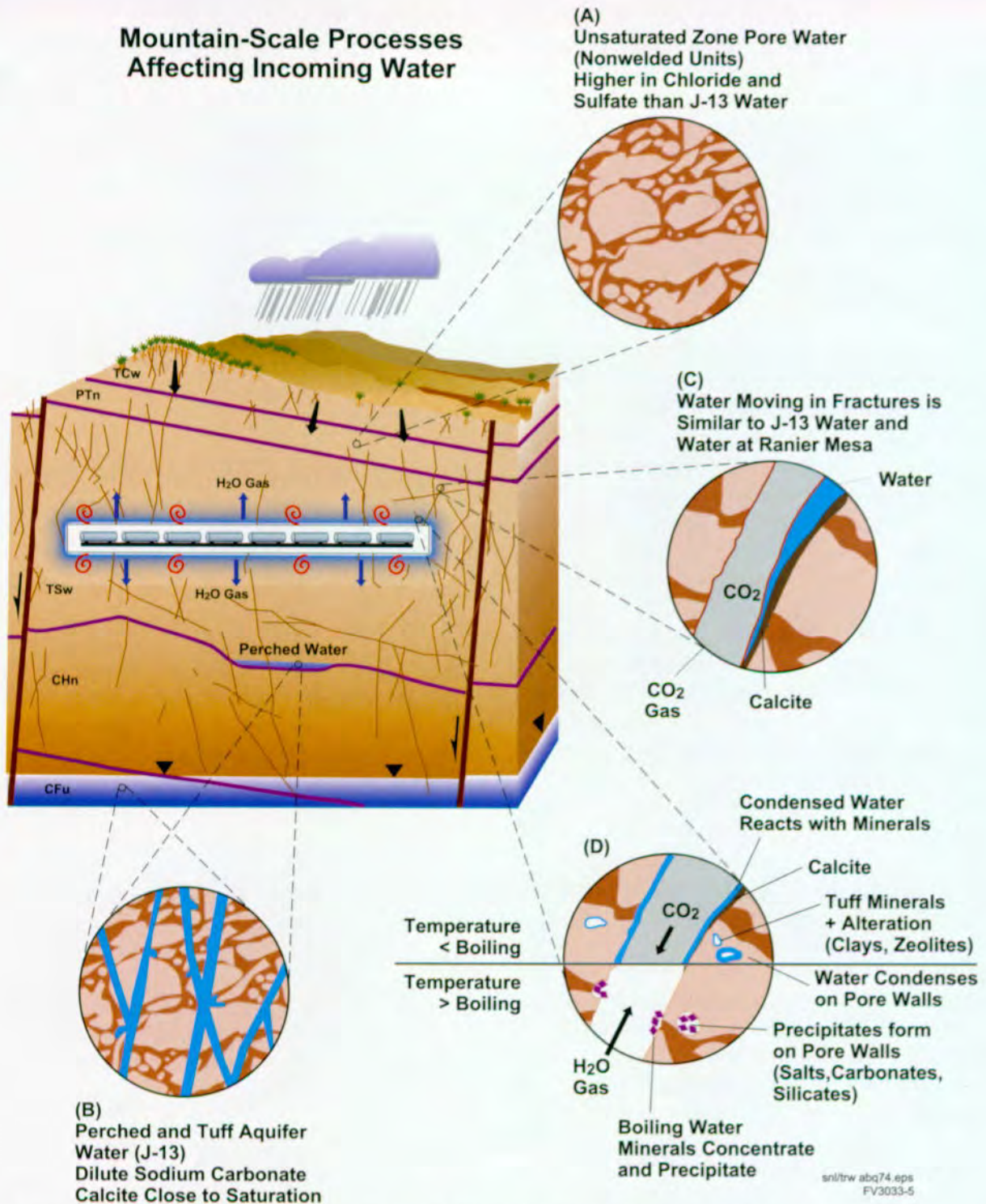


Figure 3-31. Mountain-Scale Conceptual Picture of Incoming Water Model Processes

A variety of ambient water compositions has been observed in unsaturated pores, saturated pores, and perched water. Water composition moving in fractures is similar to that in well J-13, which is used as ambient, undisturbed, water for modeling. Heating caused by waste packages in the repository causes boiling of water and increased gas movement away from the heated area. Evaporation of water in the heated zone leaves behind mineral precipitates and condensed water in the cooler zone reacts with minerals.

the water flow (that is, the changes to gas composition from the dilution by steam generation are expected to be very large compared to the other compositional changes to the gas in the geosphere and therefore these perturbed gas compositions are imposed directly (CRWMS M&O 1998i, Section 4.4). Water composition is also changed by reaction with minerals in the tuff and in the fracture linings at various temperatures (CRWMS M&O 1998c, Section 5). In addition to the heated reaction of water, gas, and minerals, the thermal change is projected to be large enough to create a boiling zone around the drifts (see Section 3.2).

The boiling process will affect water chemistry in a number of ways (Figure 3-31, Inset D). First, the gas composition changes as discussed above (Figure 3-30, Inset C). Second, many of the dissolved mineral constituents become more concentrated as the water boils (CRWMS M&O 1998c, Section 6.2). Some of these constituents concentrate to the point where solids (such as calcite and silica) precipitate and further constrain the water composition (CRWMS M&O 1998c, Section 6.2). When the water boils away completely, some of the precipitated phases are relatively soluble salts that will react later with water and steam to create concentrated salt solutions. In addition, salt will cause water to condense from steam at a lower relative humidity than salt-free systems, forming concentrated salt solutions earlier and at higher temperatures if salt is in the fractures. During the period of boiling, the reaction of water, gas, and minerals was calculated at 95°C (203°F), just below boiling (at the elevation of the proposed repository). As the system cools, the boiling front will migrate back into the drift, ending up at the surface of the waste package. The potential amount of salt buildup within a drift (as discussed below) was assumed to depend on the composition of the starting fluid and the cumulative flux of that fluid through the fractures.

**Conceptual Model for Incoming Colloids.** The near-field geochemical environment component also contains a conceptual model for incoming colloids. Natural colloids are minute particles (from about  $1 \times 10^{-8}$  m, or 100 angstroms, up to

about  $1 \times 10^{-5}$  m,  $1 \times 10^5$  angstroms), which may be transported by the groundwater. Radionuclides can attach to these colloids and be transported through the system at a different rate than their dissolved counterparts. The colloids entering the drift are assumed to be those found in the natural system for the ambient saturated zone water. These natural colloids are a small mass of entrained particles composed of clays, silica, and iron oxyhydroxides (about 20 to 30 ng/mL—Triay et al. 1996 page 9, Table I; CRWMS M&O 1998m Section 6.3.6.1). Because the iron-oxyhydroxide colloids generated within the drift represent a much larger potential source than the incoming natural iron-oxyhydroxide colloids, the incoming colloids are represented by the clay component of the natural colloids. The amounts of the clay and iron-oxyhydroxide colloids are constrained by the ionic strength of the fluid in the drift. This relation is based on colloid concentrations in groundwaters of various ionic strengths from around the world (CRWMS M&O 1998m Section 6.3.6.1; CRWMS M&O 1998c, Section 4.4).

The models of the incoming gas, water, and colloids provide time-dependent boundary conditions for the models of chemical reactions in the drift. The processes for incoming gas, water, and colloids in the near-field geochemical environment component are shown at the drift scale as Inset A in Figures 3-32a, 3-32b, and 3-32c. Figure 3-32 delineates three generalized time frames for the physical-mechanical evolution of the materials in the drift, based in part on a more detailed description of this evolution (CRWMS M&O 1998c, Section 2.2).

### 3.3.1.3 Evolution of the In-Drift Chemistry

Once the model compositions of gas, water, and colloids entering the drift have been established, the chemical processes within the drift can be considered. Within the drifts, the coupling of the physical-mechanical deterioration of the introduced design materials (CRWMS M&O 1998c, Section 2.2) plays a large role in the reaction of water and materials because of changes to the flow pathways. Representations of these processes (pathways for fluid migration through the drifts

## Time Frame 1 First Few 100s of Years

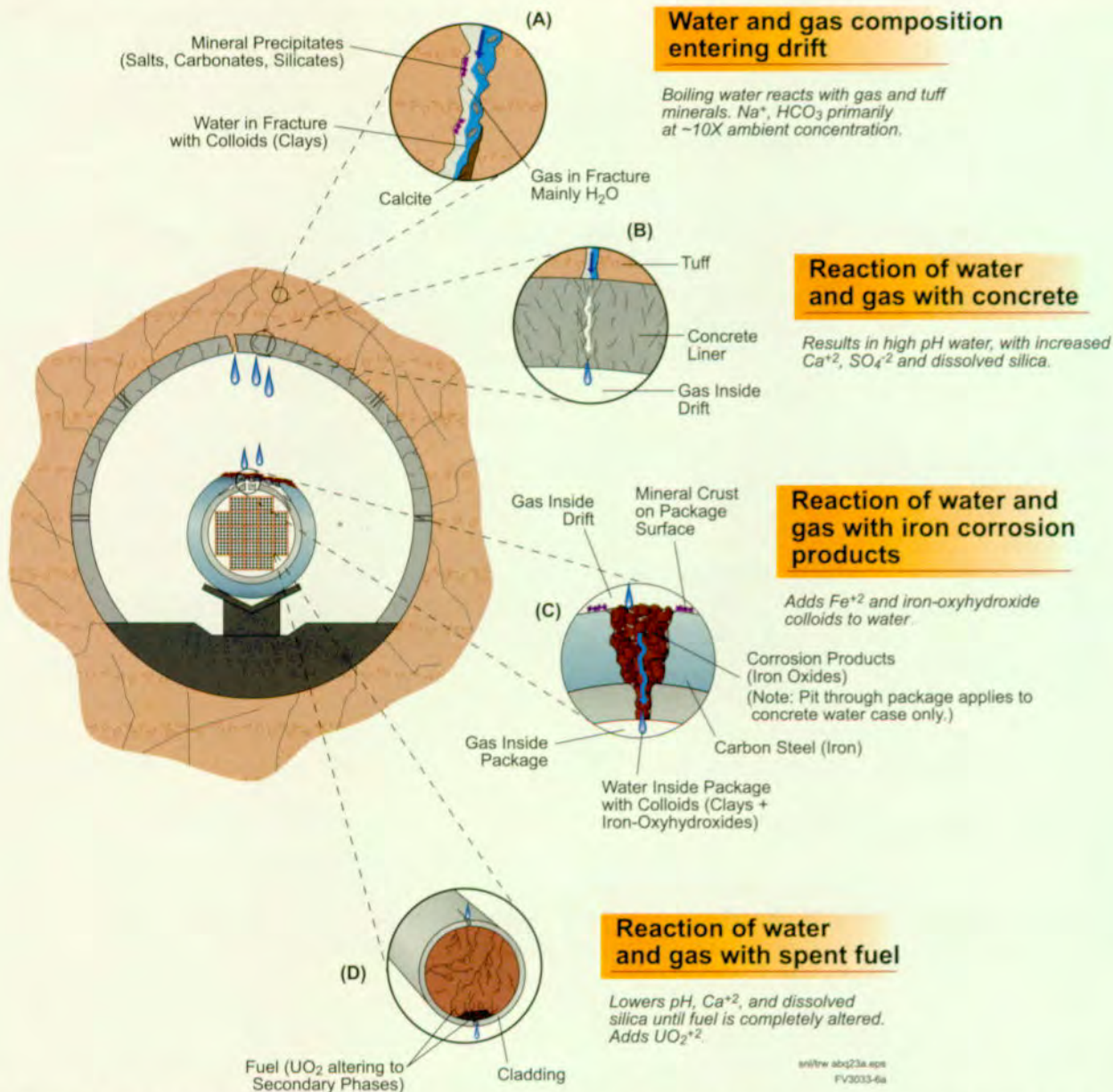


Figure 3-32a. Drift-Scale Near-Field Geochemical Environment Conceptual Processes Time Frame 1—First Few Hundred Years

Within fractures intersecting the drift (Inset A), boiling water reacts with gas and minerals, causing higher concentration sodium-bicarbonate fluid, and carries, natural colloids (primarily clays) into the drift. Water reacting with concrete (Inset B) at these conditions becomes highly alkaline (high pH). Water dripping through areas without concrete would precipitate mineral crusts directly onto the waste package (Inset C) but would not be affected by the concrete's alkaline constituents. Any water moving into the package would react with corrosion products (iron oxyhydroxides) along pitted pathways through the package (Inset C). Reaction of water with spent fuel (Inset D) decreases the pH and scavenges some other cations from the solutions while primary  $\text{UO}_2$  is actively altered to secondary phases. At this time the waste package has not been breached in a manner that would allow a release, only areas seeing alkaline fluids and/or scale crusts are substantially corroded. Clay colloids enter the drift and iron oxyhydroxide colloids are generated from materials within the drift.

Time Frame 2 ~500 Years to 10,000 Years

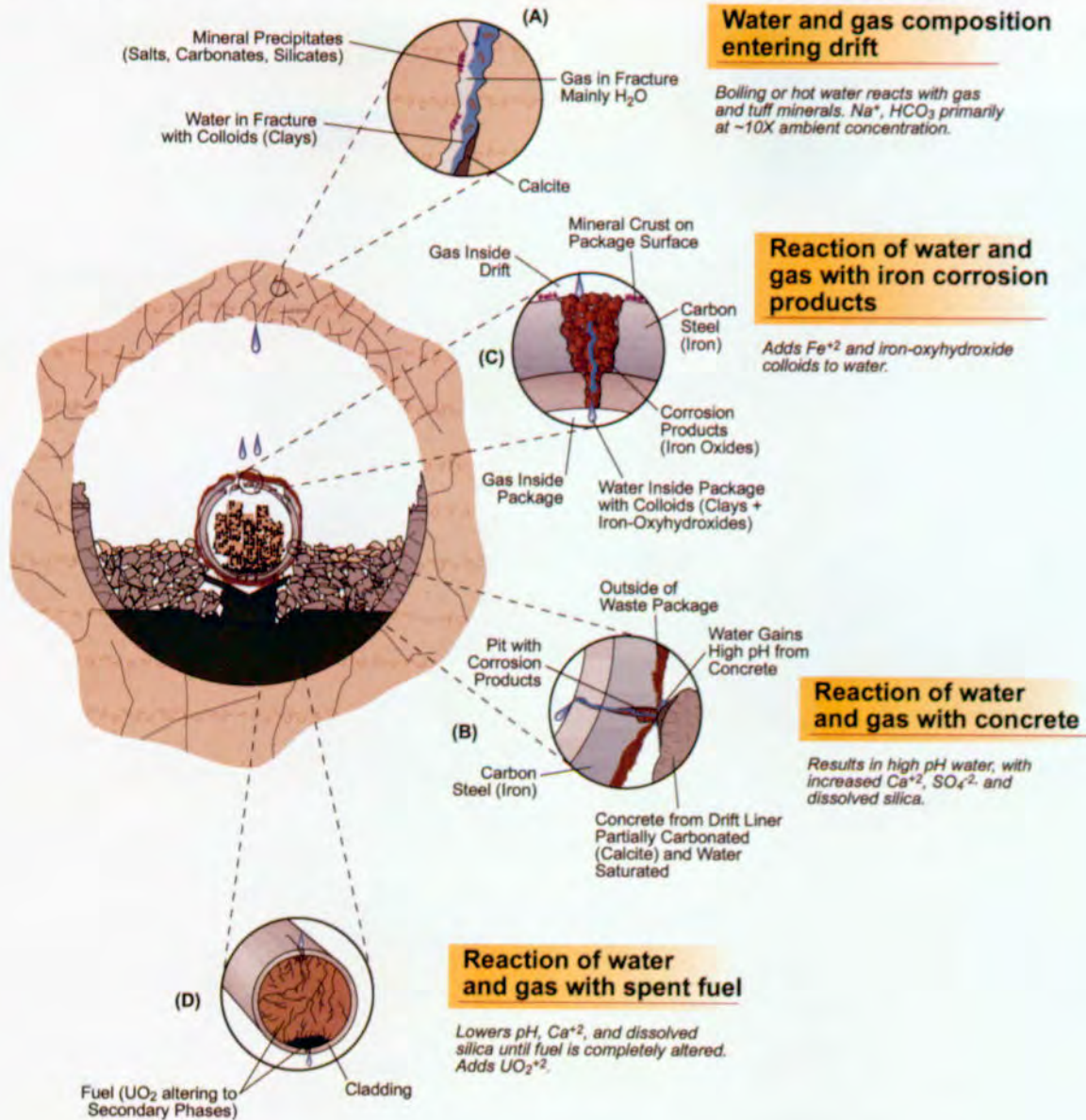
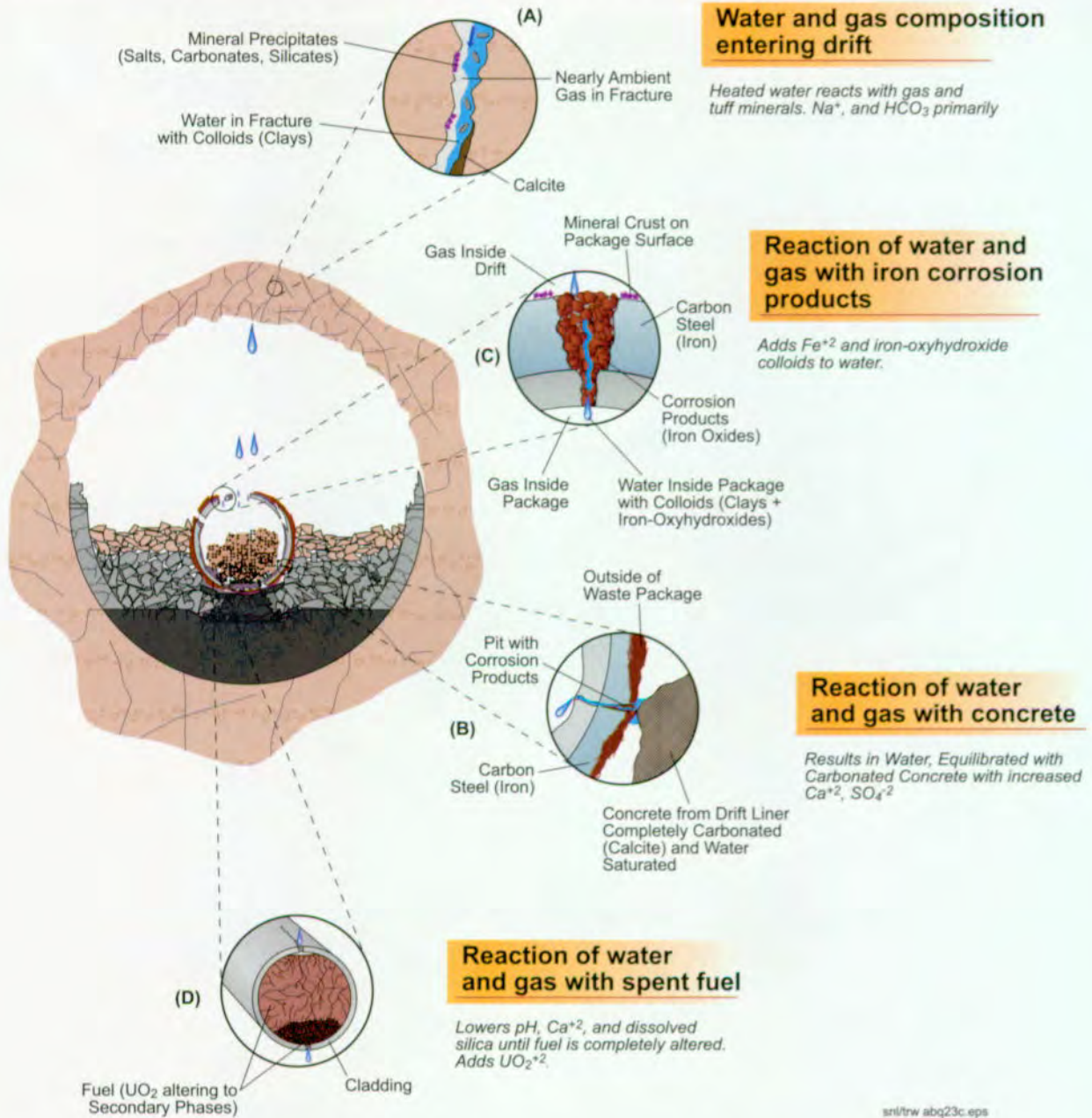


Figure 3-32b. Drift-Scale Near-Field Geochemical Environment Conceptual Processes Time Frame 2—Approximately 500 to 10,000 Years

Water at the interface of concrete blocks and the waste package surface (Inset B) is highly alkaline from reactions with the cement in the concrete. Carbonation of the cement constituents (making calcite— $\text{CaCO}_3$ ) is ongoing but not complete during this time frame. The process is not complete enough to neutralize the concrete's alkalinity. In the post-boiling portion of this time frame, microbial activity is able to start. At this stage the concrete drift liner is assumed to have collapsed and may be lying against the waste package wall. The waste package has corroded substantially in areas receiving drips.

**Time Frame 3 ~10,000 Years to 100,000 Years**



sni/trw abq23c.eps  
FV3033-6c

Figure 3-32c. Drift-Scale Near-Field Geochemical Environment Conceptual Processes Time Frame 3—  
Approximately 10,000 to 100,000 Years

Rock-fall is extensive and the liner and waste package support have fully collapsed. Water entering the drift (Inset A) is only slightly heated at the beginning of this time frame and is cooled to ambient by the end of it. Concrete becomes virtually fully neutralized by reaction with carbon dioxide at the early part of this time frame (Inset B). Corrosion pathways are lined with iron oxides that react with water entering the package (Inset C). The effects on fluid composition of reaction of the secondary uranium phases are relatively minor (Inset D). Microbial growth increases and maximizes during this stage. At this stage the concrete drift liner, support holding the package, and the invert are significantly deteriorated. The waste package is substantially breached by corrosion and radionuclides are released from the package.

and reaction with materials along those pathways) at the drift scale are shown in Figure 3-32a, 3-32b, and 3-32c. The major physical aspects of the system that change are the location and integrity of the concrete that comprises the lining and other ground support, and the integrity of the waste package and its support. While the concrete lining is still intact during the first few hundred years, any water dripping out of the rock will react with it before dripping on the waste package (Figure 3-32a). However, once the lining has collapsed, concrete-modified water is most likely to contact the waste package where concrete blocks lie against the container (Figure 3-32b and 3-32c, Inset B), or below that point. All of the boiling occurs within Time Frames 1 and 2 (Figures 3-32a and 3-32b), even for the center portions of the repository block. The system is at ambient temperatures by the end of Time Frame 3 (Figure 3-32c).

**In-Drift Gas.** The composition of the in-drift gas phase is assumed to be constant throughout the drift because of rapid migration of gas constituents at this scale, particularly for higher temperatures (Figures 3-32a, 3-32b, and 3-32c). However, the mass of each gas constituent available to react with the water and materials in the drifts is limited by the flux of that gas into the drift. If for a given period the amount of gas needed for a reaction exceeds the amount available because of the gas flux, the water flowing close to the drift wall can degas dissolved volatile constituents to supply the reactions taking place. However, once that reservoir of gas is exhausted, the concentration in the gas phase of the reacting gas constituent will decrease until a new equilibrium concentration is reached. This new level depends in a complex manner on reaction rates that change with compositional changes, but the capacity to use up a particular gas constituent in a given period can be assessed using mass balance relations. Steel (or iron) is the major material that will act as a sink for the oxygen in the system as it oxidizes to either hematite ( $\text{Fe}_2\text{O}_3$ ) or goethite ( $\text{FeO}(\text{OH})$ ). The cement phases (portlandite and calcium-silicate hydrates) in concrete are the major sink for carbon dioxide because reaction with calcium in the cement will lead to calcite precipitation. The

degree to which these reactions may affect the gas composition is discussed in Section 3.3.2.

**In-Drift Water-Solids Chemistry.** The model for the in-drift water-solids chemistry is comprised of a number of submodels. Some of these submodels are used quantitatively within the performance assessment analyses and others are used for conceptual scenario development for other components and analyses. A flow chart depicting the detailed relations among the submodels of the in-drift water-solids chemistry portion of the near-field geochemical environment is shown in Figure 3-33. Both the incoming water submodel and in-drift gas model feed water composition and gas constraints directly into the water-solids chemistry submodels. As shown in Figure 3-33, the calculated fluid composition is provided by one submodel and used by another submodel that represents materials "downstream" in the conceptual flow pathway through the system (Figure 3-32). The four features (submodels) of the water-solids chemistry model (corrosion products, concrete, spent nuclear fuel, and precipitates/salts) are described below, following some general conceptual discussion of reaction between water and solids in the drift.

For water that has entered the drift, model calculations were done to evaluate the reaction with the major solids in the drift, in particular with concrete and the corrosion products of the steel (represented by iron oxides). Constraints for the composition of water reacting with the waste form were derived from these models. These reactions between water and solids in the drift are assumed to occur at the conditions for gas fugacities and gas fluxes derived from the in-drift gas model. The reactions will proceed to equilibrium depending on the relative magnitude of gas sinks versus gas fluxes into the drift.

For reaction with repository design and waste package design materials in the repository, the in-drift water-solids chemistry model represents local equilibrium (water movement is slow compared to the reaction rates of the dripping water and reacting solids). This local equilibrium would correspond to reaction along permeable matrix pathways,

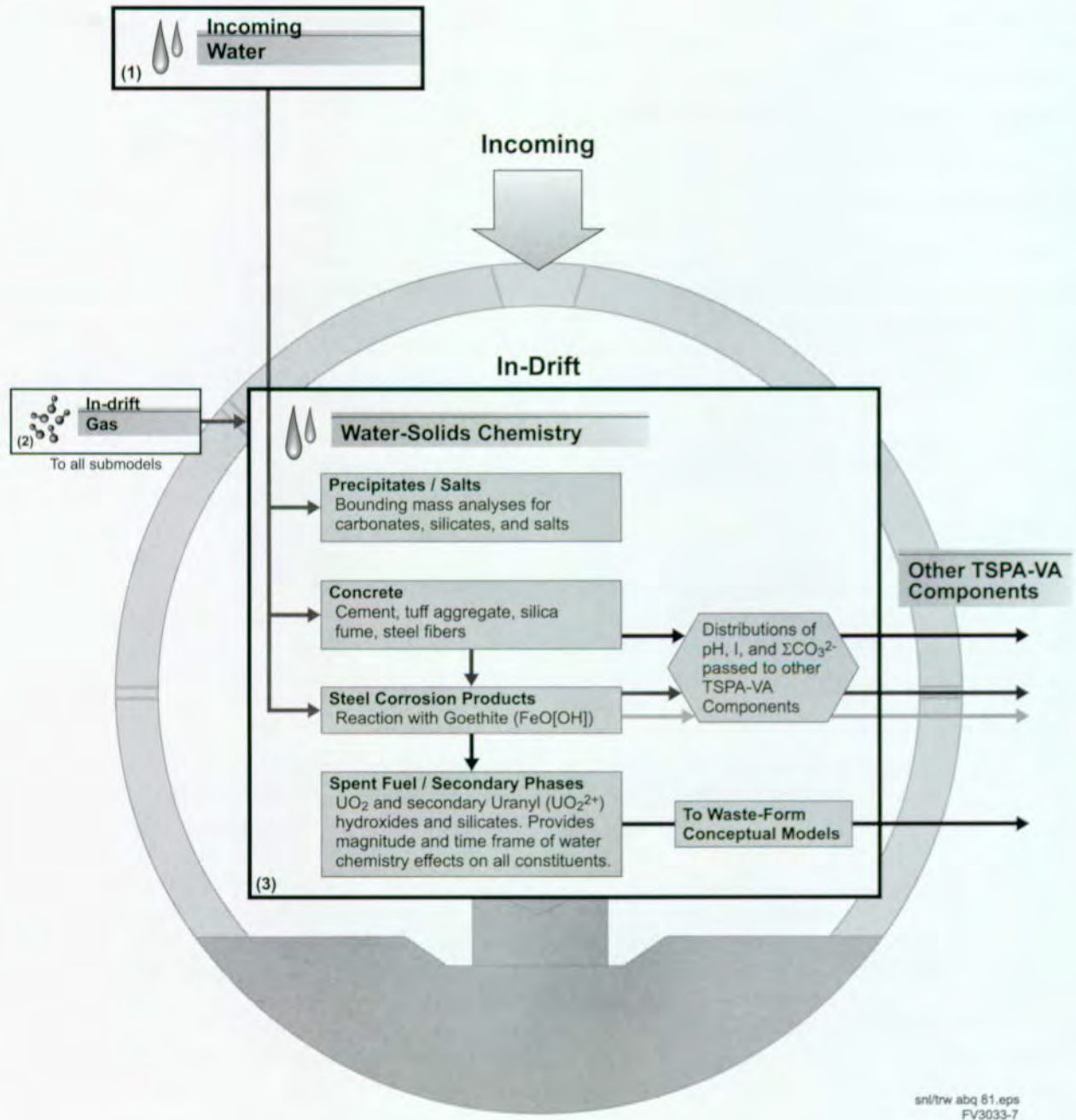


Figure 3-33. Connections Among the In-Drift Water-Solids Chemistry Sub-Models  
This is a detailed depiction of Model 3 in Figure 3-28. Various conceptual pathways for water-solids reactions are shown by the arrows.

perhaps with small fractures (Figures 3-32a, 3-32b, and 3-32c, Insets B and C), but does not correspond to reaction along large, highly permeable fractures through the system. Fast flow along such pathways would result in less pronounced changes to fluid composition. Two conceptual pathways for the incoming water were defined.

**Corrosion Products.** In the first pathway, water does not react with concrete, but drips directly onto the waste package through gaps in the lining during early time frames (Figure 3-32a), or through the area from which the concrete lining has collapsed during later time frames (Figures 3-32b and 3-32c). Because there will likely be water-flow pathways without concrete after the drift lining collapses (CRWMS M&O 1998c, Section 2.2), the water compositions calculated for this corrosion products only pathway are used as the base case fluids. This leg of the pathway is represented by iron oxides, (goethite,  $\text{FeO}(\text{OH})$ ) because the bulk of water that gets into the waste must encounter corroded package material. The primary effect on water chemistry from this reaction is to increase the dissolved iron content of the fluid. The resulting water composition is used as the initial fluid composition for calculating the effects of reaction with spent nuclear fuel during the active alteration period and at later stages when secondary uranium phases are reacting.

**Concrete.** The second pathway is the concrete conceptual pathway, which was not part of the base case, but considered as a sensitivity case (see Sections 5.3, 5.4, and 5.6). As shown in Figures 3-32b and 3-32c, concrete adjacent to the waste package could provide concrete-modified fluid compositions through diffusive migration of alkaline components into the waste package. Such fluids could then affect the waste package corrosion and possibly change waste form behavior (Figure 3-32b, Inset B). Along this conceptual pathway, water will react with corrosion products after reaction with concrete.

The concrete within the potential drifts will be comprised of tuff aggregate, sand, cement, and steel fibers (CRWMS M&O 1998i, Section 4.3 and 4.4). The alkaline components of cement, in

particular the calcium content, will represent a large compositional change to the system. The phases that produce high pHs are primarily portlandite ( $\text{Ca}(\text{OH})_2$ ) and calcium-silicate-hydrate phases formed by reaction of the silica with portlandite in the cement. Reaction of the incoming water with these constituents will continue to cause high pH in the resulting fluids until the cement phases are neutralized by carbonation via reaction with water and gas. Until the alkaline cement compounds are neutralized, water compositions may be mostly affected by reaction with the concrete. Reaction rates for this neutralization process are assumed to be relatively fast; however, availability of carbon dioxide will tend to constrain the time frame for this process. In addition, the cement contains sulfate phases that will tend to control the concentration of dissolved calcium, silica, and sulfate through mineral equilibria in a manner different from the interaction of water with tuff.

**Spent Fuel.** Once inside the waste package, water can react with exposed fuel. The effects of this reaction have been calculated with a model (CRWMS M&O 1998i, Chapter 6) that couples the flow rate of water through the package with the kinetics of spent nuclear fuel dissolution and the formation of secondary phases. Because the base case waste package failures occur primarily after the boiling period, this submodel for spent nuclear fuel, iron oxide reacted water shows reaction with  $\text{UO}_2$  at two different temperatures during the cooling period. The cladding and basket materials within the package were assumed to be inert. This reactive-transport model is not part of the base case, but its effects are examined in a sensitivity study discussed in Section 5.5.

The spent nuclear fuel is conceptualized as a porous medium, with an initial porosity equal to the porosity inside a waste package. The water flux through the spent nuclear fuel is assumed to be the long-term average seepage flux through the drift (CRWMS M&O 1998i, Section 3.1), taken directly or modified for the breached area of the waste package; flow rates depend on the evolution of porosity within the system. The water drips into the top of the waste package and then reacts with

spent nuclear fuel along a 1.56-m (5.12-ft) path, after which it leaves the waste package. The transport of dissolved constituents through the system includes advection, diffusion, and dispersion in the solution. The water composition at the outlet of the system is the primary focus of this submodel for the near-field geochemical environment.

In the model, the waste form dissolves as oxidized uranyl (uranium) species with secondary uranium phases precipitating at the carbon dioxide and oxygen-gas conditions determined for the cooling periods (from the in-drift gas model). Carbonate equilibria and calcite precipitation and dissolution are included in this submodel. The uranium solids considered for precipitation are four secondary uranyl (uranium) minerals: uranophane, sodium-boltwoodite, schoepite, and soddyite. These phases are commonly observed in alteration of uranium ore deposits and in laboratory tests of spent-fuel dissolution (CRWMS M&O 1998c, Section 6.5; CRWMS M&O 1998m, Section 6.3). In addition, after conversion of  $UO_2$  to secondary phases, the dissolution of those secondary phases occurs more slowly because they are closer to equilibrium with the fluid entering the waste package. The effects on water composition of the secondary phases are evaluated to provide a boundary on the magnitude of the entire suite of chemical changes.

**Precipitates/Salts.** Mineral deposits will develop as refluxed water drips through fractures and possibly onto the waste packages throughout the boiling period. The degree of boiling and evaporation of the water will cause various minerals to saturate within the solution. These precipitating minerals will change with time as the water composition changes. The major purpose of this model is to assess the magnitude of mineral precipitation and salt formation, the length of time to redissolve the soluble salts, and the amount of concentrated salt solutions from these processes. Although the amount of salt precipitation was assessed in the near-field geochemical environment component, it was not directly used (CRWMS M&O 1998i, Sections 4.4 and 4.6). The effect of salt on waste package degradation was

only used indirectly (see Section 3.4). The potential effects of salt on waste package degradation are discussed briefly in Section 3.4 and in more detail in Chapter 5 of the *Total System Performance Assessment-Viability Assessment (TSPA-VA) Analyses Technical Basis Document* (CRWMS M&O 1998i), but have not been directly incorporated into the TSPA-VA analyses. The effect of solution composition and concentration on the degradation of Alloy 22 was considered in the Waste Package Degradation Expert Elicitation (CRWMS M&O 1998b) and formed part of the basis of the elicited corrosion-rate uncertainty distributions. Data on the effect of salt build-up on stress-corrosion cracking of Alloy 22 is quite limited at present, but as it becomes available between VA and LA, it will be incorporated into the waste package modeling.

**Colloids in the Drift.** Another consideration in the evolution of the in-drift chemistry is colloids in the drift. The in-drift colloids are comprised of both the clay colloids entering the drift (Figure 3-32 Inset A), and the iron-oxyhydroxy colloids produced within the drift from the steel components of the design materials (Figure 3-32, Inset C). Because these colloids act to sorb and transport radionuclides, the amounts of these colloids affect the amounts of radionuclides that can be transported. The concentration of these colloids depends on the ionic strength of the solution; water with higher ionic strength causes colloids to coagulate and drop out of solution (Triay et al. 1996; CRWMS M&O 1998m, Section 6.3.6). Radionuclide sorption to these colloid types and the transport of colloids through the engineered barrier system are discussed in more detail in Section 3.5.

**In-Drift Microbial Communities.** In-drift microbial communities are also considered as part of the in-drift chemistry. Microbial activity exists at low levels in the host rock (CRWMS M&O 1998c, Section 7). Throughout the drift, microbes will use the nutrients and available energy from chemical oxidation and reduction reactions. The nutrients and energy are present because of system heating, fluid movement, and materials emplaced in the drifts. In the repository environment, many

different microbes could grow and provide a plethora of potential chemical processes that may affect the bulk chemistry within the emplacement drifts (CRWMS M&O 1998c, Section 7). A large source of potential nutrients for microbes is the organic material in concrete ground supports. The waste package materials represent reduced metals that can be oxidized to provide energy for microbes to thrive, and the waste forms themselves contain both nutrient and energy sources for microbes.

A model was developed to assess the possible magnitude of such effects on the system's total chemistry by bounding the magnitude of development of microbial communities (CRWMS M&O 1998c, Section 7; CRWMS M&O 1998i, Sections 4.4 and 4.6). This model uses constraints on the supply rates of both the energy available from oxidation and reduction reactions in the drift and the nutrients used to build an idealized microbial composition, comprised of carbon, nitrogen, sulfur, and potassium in addition to the

water components. Other constraints on microbial growth are temperature and relative humidity thresholds in the model that limit the start of microbial activity until the boiling period is over. Even though microbes could be sterilized out of the drifts during the highest temperature period, because they are present in the water-rock system they will return as water drips back into potential drifts. Microbes could also be sterilized in high radiation fields, but microbes would be reintroduced from the geosphere once the radiation field decays to lower levels. This model was not directly used in the base case, but provided first-order limits on potential microbial effects.

### 3.3.2 Implementation of the Near-Field Geochemical Environment Models

The input, output, and bases for the models in the near-field geochemical environment component are shown as the flow chart in Figure 3-34. The major input parameters come from the unsaturated

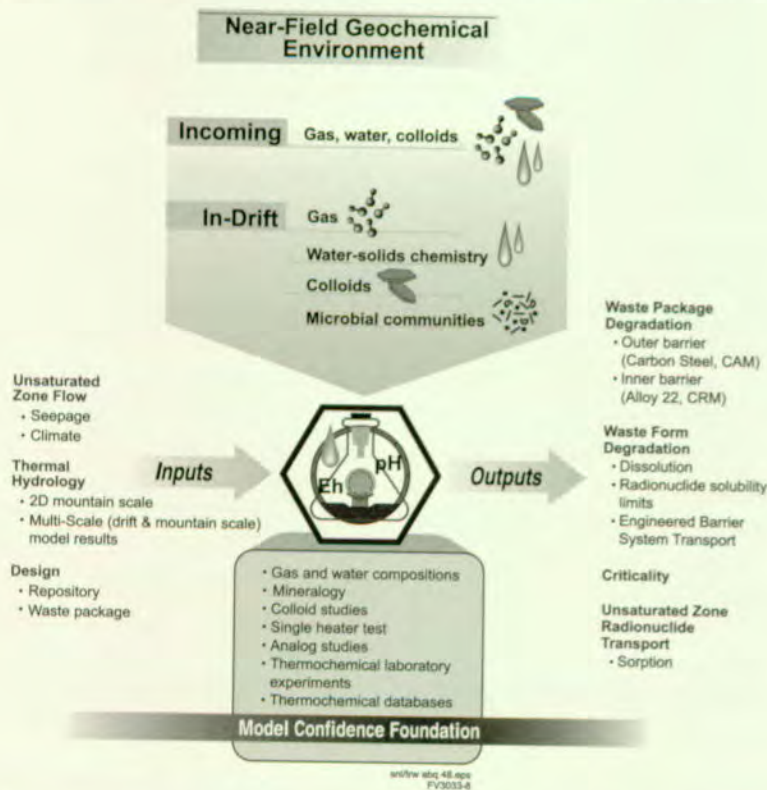


Figure 3-34. Inputs, Outputs, and Bases for the Total System Performance Assessment for the Viability Assessment Near-Field Geochemical Environment Component  
The types of studies that have supplied data/concepts to constrain the models are listed. (CAM—corrosion allowance material; CRM—corrosion resistant material)

zone flow and thermal-hydrology components and from the VA design. The primary outputs of the near-field geochemical environment are water and gas compositions provided to the waste package and waste form components. Additional input for conceptual scenarios is provided to the criticality, waste form, and unsaturated zone transport component analyses. In the latter two cases, sensitivity studies were conducted based on scenario development in the near-field geochemical environment (see Section 3.3.3). The bases for the conceptual models and parameter sets defining the near-field geochemical environment models discussed in Section 3.3.1 are in five general categories: site measurements, site experiments, site analog, laboratory experiments, and data analysis and compilation (Figure 3-34). The implementation for each of the near-field geochemical environment models is discussed in this section. The connections among the near-field geochemical environment models are shown in Figure 3-35.

### **3.3.2.1 Incoming Gas, Water, and Colloids**

The submodels of incoming gas, water, and colloids in the near-field geochemical environment component provide both the time-dependent boundary conditions for the gas, water, and colloids compositions and the cumulative fluxes of gas and water constituents entering the emplacement drift. For all the models in the near-field geochemical environment component, the abstracted evolution of system conditions is based on the thermal-hydrologic changes. However, because the total system analyses use time steps of 100 years, explicit coupling of the near-field geochemical environment evolution with the time-dependent thermal changes only captures the coarse behavior of the system. The development of the abstracted periods used in the process-level calculations for the near-field geochemical environment is discussed in the following paragraphs.

**Model Implementation for Incoming Gas.** The model implementation for incoming gas combines a model of the "air" composition in the mountain with the results of the thermal-hydrology calcula-

tions for gas flux. This combination determines changes to the air-mass fraction values caused by boiling water. The thermal-hydrology models evaluate a two-component gas phase (steam and air, see Section 3.2). The air portion represents the fraction of all non-condensable gas components (i.e., everything that is not steam), given by the air-mass fraction (which is 1 minus the steam fraction). The thermal-hydrologic results include the effects of boiling and gas flow on the mix of air and steam in the gas phase but none of the chemical interactions.

The two-dimensional thermal-hydrology model at the mountain scale provides both the air mass fraction and the gas flux through the drifts as continuous functions of time to 100,000 years. After that time, the system is considered to have returned to ambient conditions. These results were provided at the center and edge of a two-dimensional cross section running east to west through the middle of the repository (Section 3.2). The air-mass-fraction variations and the changes in air fluxes were used to delineate a number of periods for which gas compositions can be approximated as constant values with step changes at the transition points. For each of these periods, constant average values for air mass fraction were abstracted from the more continuous thermal-hydrologic results resulting in a stepped representation that captures the major variations that occur. Because most of the variation is caused by boiling effects during the early, higher temperature conditions (boiling regime), these earlier times are divided at a finer scale than the later periods that represent below boiling conditions (cooling regime). The thermal-hydrologic results for gas flux into the drift were used with the air mass fractions to constrain the cumulative flux of air into the drift for the defined periods. Combining these with the air composition defined for each period (as discussed below) allowed derivation of cumulative fluxes of each air constituent per meter of drift.

In general, the abstracted air mass fractions return to constant ambient values in only hundreds to a few thousand years after the boiling regime. Therefore the air mass fractions do not provide

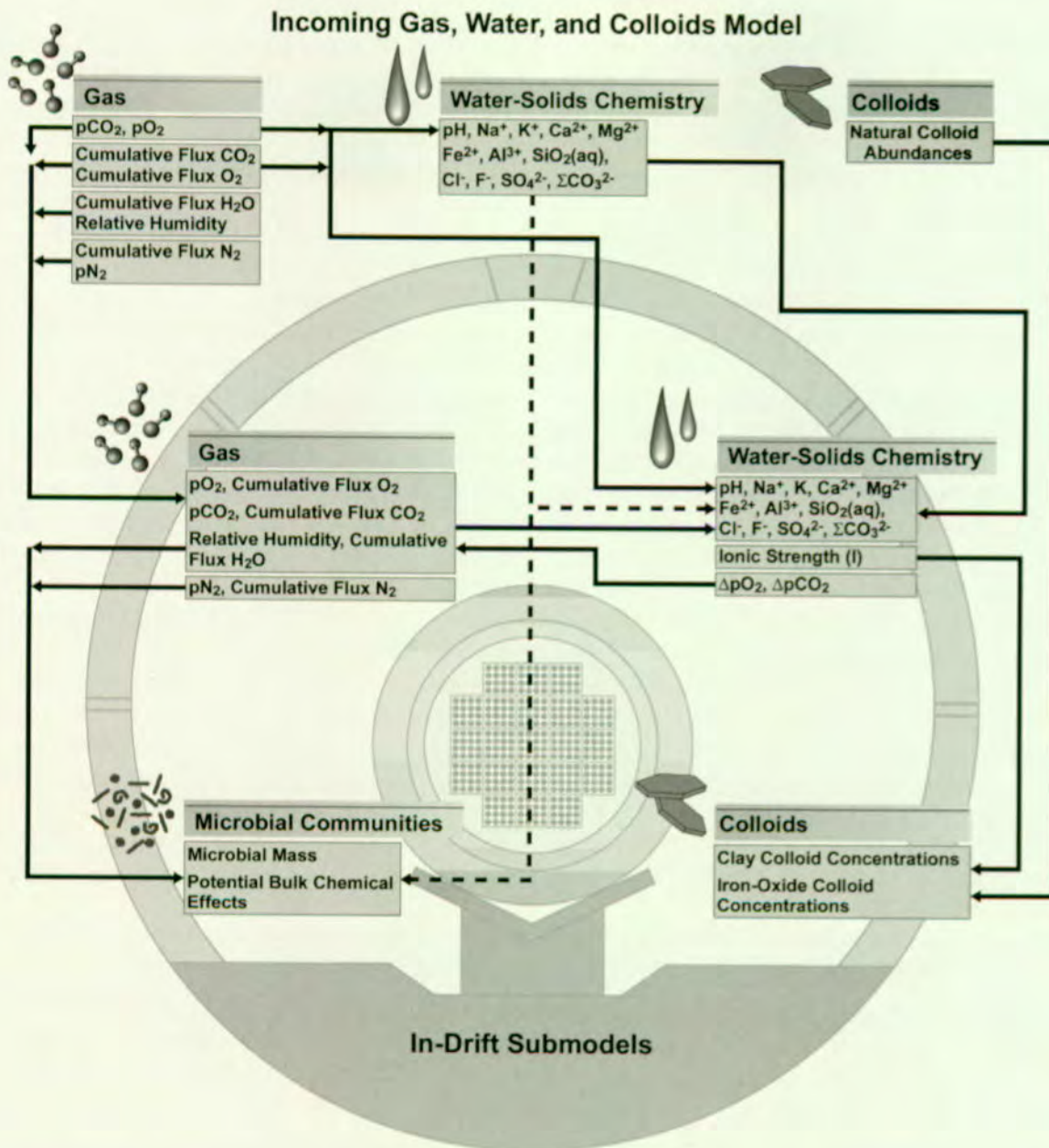


Figure 3-35. Flow Diagram Depicting the Parameter Exchanges Among all Near-Field Geochemical Environment Models

This figure provides a more detailed representation of the flow of information presented in Figure 3-28.

a useful basis for delineating abstracted periods after that point. For later times, variations in temperature were used to develop an additional set of abstracted periods representing the transition from boiling to cooling and the temperature decrease during the cooling regime. The time above boiling was defined based on the drift wall temperature because, for gas-water-rock reactions, the water boiling in the host rock is most important. During the boiling regime, any reaction of gas with fracture water was assumed to occur at 95°C (203°F), just below the boiling temperature), approximating reflux water reacting just before re-evaporation. The cooling regime was divided into temperatures of 70°C (158°F) and 30°C (86°F) to capture coarsely the intermediate- and lower-temperature conditions for reaction in the system.

The two dimensional, thermal-hydrology model at the mountain scale uses a smeared heat source and provides temperatures in the rock a small distance from the drift wall (Section 3.2). The model does not give an accurate drift wall temperature history, including the transition time to below boiling conditions. Instead, the drift-scale results of the multiscale (drift plus mountain scale) thermal-hydrologic models were used because they provided a more accurate thermal history of the drift wall. The multiscale thermal-hydrologic calculations provided average thermal evolutions for six repository regions (Section 3.2). These six regions were classified as center-like (Region CC), edge-like (Region SW), and intermediate (the other four regions) to determine how to link their

average thermal evolutions with the center and edge results from the two-dimensional, mountain-scale model. The time that average drift wall temperatures are above boiling is given by drift-scale results of the multiscale (drift plus mountain scale) thermal-hydrologic model for Region CC. The abstracted periods defined for the system based on this thermal history overlap somewhat with those based on the air-mass fraction. These two sets of abstracted periods were synchronized by ensuring that the break between the boiling and cooling regimes corresponded to the end of the last boiling period as defined by air-mass fraction changes.

Because the duration of the thermal change is greatest for the central portion of the repository, the near-field geochemical environment analyses were focused on this portion of the system. For the repository center, the time-period abstractions created three boiling periods which were defined as Period A (0–200 years), Period B (200–1,000 years), and Period C (1,000–2,000 years), and three cooling periods which were defined as Period D (2,000–4,000 years), Period E (4,000–10,000 years), and Period F (10,000–100,000 years). The boiling-regime periods are assigned the same temperatures, but they have various gas constraints (air mass fractions and air fluxes). The cooling-regime periods have different temperature and gas constraints (gas fugacities and cumulative fluxes). The conditions that result from this submodel (CRWMS M&O 1998i, Section 4.5) are summarized in Table 3-10. For the repository edge areas,

Table 3-10. Abstracted Periods, Temperatures, Gas Fugacities and Cumulative Gas Fluxes (Per Meter of Drift) Used for the Near-Field Geochemical Environment Component

| Boiling Regime    |                |                   |                               |                                       |                              |                                      |
|-------------------|----------------|-------------------|-------------------------------|---------------------------------------|------------------------------|--------------------------------------|
| Abstracted Period | Time Years     | Temperature °C/°F | CO <sub>2</sub> Fugacity ppmv | ΣCO <sub>2</sub> gas flux Moles/Meter | O <sub>2</sub> Fugacity ppmv | ΣO <sub>2</sub> gas flux Moles/Meter |
| A                 | 0-200          | 95/203            | 1x10 <sup>2</sup>             | 180                                   | 2 x 10 <sup>2</sup>          | 510                                  |
| B                 | 200-1,000      | 95/203            | 1x10 <sup>-4</sup>            | 190                                   | 2x10 <sup>-2</sup>           | 1000                                 |
| C                 | 1,000-2,000    | 95/203            | 1x10 <sup>1</sup>             | 270                                   | 2x10 <sup>3</sup>            | 25,000                               |
| Cooling Regime    |                |                   |                               |                                       |                              |                                      |
| Abstracted Period | Time Years     | Temperature °C/°F | CO <sub>2</sub> Fugacity ppmv | ΣCO <sub>2</sub> gas flux Moles/Meter | O <sub>2</sub> Fugacity ppmv | ΣO <sub>2</sub> gas flux Moles/Meter |
| D                 | 2,000-4,000    | 70/158            | 1x10 <sup>2</sup>             | 810                                   | 2x10 <sup>4</sup>            | 170,000                              |
| E                 | 4,000-10,000   | 70/158            | 1x10 <sup>3</sup>             | 2,100                                 | 2x10 <sup>5</sup>            | 530,000                              |
| F                 | 10,000-100,000 | 30/86             | 1x10 <sup>3</sup>             | 4,500                                 | 2x10 <sup>5</sup>            | 1,200,000                            |

ppmv—parts per million by volume

the time in the boiling regime is much shorter than it is in the central portion of the repository, and the return to ambient conditions occurs more rapidly. Because the thermal change is shorter in the edge and intermediate regions, the evolution of the near-field geochemical environment in these regions is bounded by modeling only the central portion of the repository. The TSPA-VA results are put into the general context of these periods in Section 2.4.

The incoming gas submodel defines the air composition. The model air composition description is based on the ambient pore gas (which differs from atmospheric air in carbon-dioxide content), with inclusion of a limited period of elevated carbon dioxide values for the early behavior of the heated system. This early change in carbon dioxide content reflects primarily potential mineral sources of carbon dioxide in the rock. The model of air composition is implemented only as a logical model (there is not a code that calculates the values); the values are assigned directly for the specific periods in the system evolution. The values used are atmospheric, about 20 percent oxygen and 80 percent nitrogen gases, through all periods with the partial pressure of the nitrogen gas adjusted to offset the increased carbon dioxide in certain conditions. For carbon dioxide, as discussed in Section 3.3.1, the ambient value is taken as 1,000 parts per million by volume. A value of 100,000 parts per million by volume, or 10 percent, is designated for the first 200 years (Period A) to reflect reaction of heated calcite and silica to form a calcium-silicate mineral and release carbon dioxide (Figure 3-30, Inset B). Combining the air-composition model and the abstracted air mass fractions from the thermal-hydrology model provides the incoming gas compositions within the near-field geochemical environment.

#### **Model Implementation for Incoming Water.**

The model implementation for incoming water included process-level calculations using the EQ3/6 geochemical modeling code package (Wolery 1992a; 1992b; Wolery and Daveler 1992). The calculations are discussed below and details of the analyses are given in Section 4 of the *Total System Performance Assessment-Viability Assessment (TSPA-VA) Analyses Technical Basis Document*

(CRWMS M&O 1998i, Section 4). For each of the abstracted periods, the conditions for gas composition and temperatures shown in Table 3-10 were used in calculations of water compositions. For each period, calculations were performed for reaction and equilibration of the heated water with the minerals and the gas phase. The two types of temperature regimes, a boiling regime and a cooling regime, were again recognized here. The additional processes considered during boiling regime calculations required a slightly different model implementation than the implementation for cooling regime calculations. The specific differences between these two implementations are detailed in the following paragraphs.

Despite some differences in the methods of calculation, the boiling and cooling regime implementations have many factors in common. Both of these implementations consider the same dissolved constituents in the aqueous phase: pH, sodium ( $\text{Na}^+$ ), potassium ( $\text{K}^+$ ), calcium ( $\text{Ca}^{2+}$ ), magnesium ( $\text{Mg}^{2+}$ ), iron ( $\text{Fe}^{2+}$ ), aluminum ( $\text{Al}^{3+}$ ), silica ( $\text{SiO}_2$ ), chloride ( $\text{Cl}^-$ ), fluoride ( $\text{F}^-$ ), carbonate ( $\text{CO}_3^{2-}$ ) and sulfate ( $\text{SO}_4^{2-}$ ). These constituents comprise the total masses of these components within the fluid and may be represented by a number of different species in solution. In process-level calculations, initial concentrations for many of these constituents are taken from the average composition of the groundwater sampled at Well J-13 for the saturated zone tuff aquifer (CRWMS M&O 1998c, Section 6.2; CRWMS M&O 1998i, Section 4.5). In addition, the equilibrium oxidation potential of the system was constrained by the oxygen fugacity, and the total dissolved carbonate was set to equilibrium with the carbon dioxide fugacity. The total  $\text{Ca}^{2+}$  content of the solution was set to be in equilibrium with the mineral calcite, and the system pH was calculated by charge balance constraints.

Calculations for the two temperature regimes, as given in Table 3-10, differ in the mineralogical constraints on the fluid composition and in the calculation method for the final fluid composition. The cooling regime implementation is simpler; for each of the periods in the cooling regime, a single model calculation was performed

using the EQ3NR code (Wolery 1992a; 1992b). In these calculations, the average J-13 water composition was equilibrated with the gas phase and a set of minerals at the appropriate temperature. In addition to the common constraints listed in the previous paragraph, the cooling regime calculations had dissolved silica set to equilibrium with alpha-cristobalite,  $Al^{3+}$  set to equilibrium with calcium-montmorillonite,  $Fe^{2+}$  set to equilibrium with calcium-nontronite, and  $Mg^{2+}$  set to equilibrium with calcium-saponite. These mineral constraints represent the silica and clay minerals resulting from alteration of the primary phases in the tuff (CRWMS M&O 1998c, Section 5; CRWMS M&O 1998i, Section 4.5).

In the calculations for the boiling-regime fluids, the water is not simply equilibrated with the changed gas compositions and minerals. Instead, to represent some of the effects of concentration via boiling, calculations were done to evaporate 90 percent of the water, allowing mineral phases to precipitate as the solution becomes more concentrated. Equilibrated water compositions were calculated using the strategy proposed in the *Near-Field/Altered-Zone Models Report* (CRWMS M&O 1998c, Section 6.2), modified with appropriate gas compositions and temperatures for each of the three boiling regime periods in Table 3-10. Equilibration of the initial J-13 water composition was calculated at the appropriate temperature and gas conditions with dissolved silica set to alpha-cristobalite equilibrium, in addition to the common constraints listed earlier. Then, the evaporation of water was simulated at the same temperature and gas conditions using the resulting fluid from the previous calculation. Quartz, tridymite, and talc are suppressed, or prevented from precipitating for these analyses, to reflect kinetic constraints in the system (CRWMS M&O 1998c; CRWMS M&O 1998i, Section 4.5). Conservative elements that are not precipitated in minerals have their final concentrations increased to 10 times the starting J-13 concentration. However, final concentrations of elements such as  $Ca^{2+}$  are controlled by phases that precipitate during the evaporation and boiling process.

**Incoming-Colloids Model.** The incoming-colloids model is a qualitative assessment of the types of colloids that may enter the drift and general constraints on the amounts of those colloid types. This model provides those qualitative constraints to the in-drift colloids model, in the form of a potential source of clay colloids. The in-drift colloid model is the only source of colloid abundances that are used by the other performance-assessment models. Therefore, the implementation of the model for incoming colloids (i.e., calculated abundances of clay colloids) was handled within the model for in-drift colloids discussed in Section 3.3.2.2. In brief, this entailed the use of site measurements on naturally occurring colloids in Yucca Mountain groundwaters (Triay et al. 1996, Table I) to show that a relation universally observed for colloids is relevant for the Yucca Mountain site (CRWMS M&O 1998m, Section 6.3.6; CRWMS M&O 1998i, Section 4.5). This relationship was implemented directly within the TSPA computer program RIP (Golder Associates, Inc. 1998) in the engineered barrier system cells (CRWMS M&O 1998i, Section 6).

### 3.3.2.2 Evolution of the In-Drift Chemistry

**Model Implementation for In-Drift Gas.** The model implementation for in-drift gas used the incoming gas compositions and fluxes directly to define in-drift gas constituents through time. There are two related major assumptions underlying this model. The first is that the in-drift gas composition is not affected substantially by reaction with the in-drift solids, and the second is that gas migration and mixing in the drift is rapid enough to maintain a homogeneous gas composition throughout the environment. The second assumption is relatively robust because gaseous diffusion alone is rapid enough to ensure homogeneity on these scales. The first assumption precludes generation of local changes to the in-drift gas composition from reaction with materials that are abundant compared to the gas. However, this assumption was evaluated to be reasonable for oxygen and carbon dioxide, the two major gas constituents of interest.

The first assumption was evaluated using mass-balance calculations. For these calculations, the in-drift materials were first assessed for their ability to act as either source or sinks of oxygen and carbon dioxide, and then relative masses for the sink and the source were compared. For oxygen, the major sink was taken to be oxidation of the iron content of the steels in both waste package and ground support materials. No major sources of oxygen from in-drift materials have been identified. The large mass of calcium in the concrete that would need to be carbonated to prevent extensive development of alkaline water in the drift was used for the mass-balance assessment for carbon dioxide. A simple mass-balance calculation was performed for each of these cases in which the cumulative flux of the constituent was compared with the mass that potentially could be removed by the material. Results of both the mass-balance and reaction-path analyses are presented in Section 3.3.3.

**In-Drift Water-Solids Chemistry.** For model implementation of in-drift, water-solids chemistry, the incoming water composition is used as the starting composition for reaction. In most cases, the reaction of this initial fluid with in-drift materials, including spent nuclear fuel, was evaluated at the temperature and gas conditions of the appropriate abstracted period (Table 3-10).

**Corrosion Products.** These analyses were implemented to simulate the equilibration of the incoming water with goethite,  $\text{FeO}(\text{OH})$ . This oxidized-iron phase was used to represent the corrosion products of the iron in steel (CRWMS M&O 1998i, Section 4.5). The calculations were done for each period at the appropriate temperature and gas composition as given in Table 3-10, with the initial dissolved concentrations specified as those from the incoming water composition except for the total dissolved iron constraint which was set to equilibrium with goethite. The output results are discussed in Section 3.3.3 and represent the base case for water that may enter the waste package. The resulting water compositions are used in the base case analyses and provided to the spent-fuel submodel as shown in Figure 3-33.

**Concrete.** The model calculations to evaluate the geochemical effects of concrete on the water composition were performed as reaction-path calculations using the EQ6 code (Wolery 1992a; Wolery and Daveler 1992). These calculations were performed as titration calculations where mineral constituents in the concrete progressively react with the incoming water compositions at the gas constraints and temperature conditions given in Table 3-10. The carbon dioxide and oxygen gas concentrations were specified initially but, as the reaction progressed, the gas composition could change in response to the water-mineral reactions. This flexibility was provided to evaluate whether available carbon dioxide could neutralize concrete alkalinity (high pH).

Design information on the concrete compositions was used to define reactant materials for these analyses (CRWMS M&O 1998i, Sections 4.3, 4.5). The concrete consists of cement, coarse and fine tuff aggregate, and steel fiber (iron) (CRWMS M&O 1998c, Sections 6.3, 7.2; CRWMS M&O 1998i, Section 4.5). The cement and tuff consist of multiple phases. The mineral assemblage used for the cement is for a relatively young cement that has not undergone much chemical or thermal alteration. This mineral assemblage consists of ettringite, calcium-silicate hydrate, brucite, hydrogarnet, and portlandite, with the relative amounts calculated based on the oxide composition (CRWMS M&O 1998i, Sections 4.3, 4.5). Both the coarse and fine aggregate are composed of Topopah Spring tuff and were represented by a normative modal mineral assemblage consisting predominantly of alkali feldspar, alpha-cristobalite and quartz (CRWMS M&O 1998c, Section 6.3; CRWMS M&O 1998i, Sections 4.3, 4.5). These minerals reacted with the incoming water composition at relative rates assigned to represent relatively fast dissolution of the cement phases and slower dissolution of the tuff aggregate phases and steel fiber.

Results of the analyses for water reaction with concrete are given in Section 3.3.3. Because the concrete lining is expected to collapse within the first few hundred years (see Section 3.3.1), concrete-modified water is not used in the base

case. The collapse of the concrete lining would remove it from much of the potential pathways of dripping water above waste containers. However, because the collapsed concrete mass will still be available to react with water on the lower portion of the waste package for a long time, these water compositions are evaluated in a sensitivity study (see Section 5.3). In addition, the possibility that these fluids could migrate through the unsaturated zone, causing large changes to radionuclide sorption, is examined in Section 5.6.

**Spent Fuel.** Because the spent nuclear fuel represents a large material mass, its capacity to affect the bulk fluid composition was evaluated for the near-field geochemical environment. The tool used for these analyses is the general reactive-transport code AREST-CT (Chen et al. 1995; 1996; 1997a; 1997b; Chen 1998). Using this program, this evaluation considers both equilibrium and kinetically controlled chemical reactions between solid phases, aqueous solutions, and gas under flowing conditions.

These analyses were done to reflect conditions within either Period E or Period F (Table 3-10) for both active alteration of spent-fuel to secondary phases, and subsequent dissolution and alteration of the secondary phases to a tertiary set of uranium minerals. These periods were chosen because only a few base case waste packages fail before 4,000 years (Section 3.4). For these calculations, both the oxygen and carbon dioxide fugacities were set to their ambient compositions (Table 3-10). The spent nuclear fuel is represented as a one-dimensional porous medium with various specific surface areas (CRWMS M&O 1998i, Section 4.4).

The chemical system is a subset of the water composition reacted with corrosion products and consists of the components pH, sodium ( $\text{Na}^+$ ), calcium ( $\text{Ca}^{2+}$ ), silica ( $\text{SiO}_2$ ), chloride ( $\text{Cl}^-$ ), and carbonate ( $\text{CO}_3^{2-}$ ), with the addition of the spent nuclear fuel components uranium ( $\text{UO}_2^{2+}$ ) and neptunium ( $\text{NpO}_2^+$ ). These constituents comprise the total masses of these components within the fluid and may be represented by a number of different species in solution. The kinetic rate of the spent nuclear fuel dissolution reaction was

constrained by the rate model based on observations for  $\text{UO}_2$  dissolution rates (CRWMS M&O 1998i, Section 4.4). Besides the  $\text{UO}_2$  dissolution reaction, the simulation also considered the kinetically controlled precipitation of four secondary uranium ( $\text{UO}_2^{2+}$ ) mineral reactions. The concentration of neptunium that may enter a secondary uranium phase was also constrained by data from dissolution testing of secondary phases developing within waste under dripping water conditions (CRWMS M&O 1998i, Section 4.4).

Four simulations were carried out to evaluate the effects of water composition during the active period of primary waste form alteration and subsequent effects of secondary-phase dissolution. The four simulations were carried out at  $70^\circ\text{C}$  ( $158^\circ\text{F}$ ) and  $30^\circ\text{C}$  ( $86^\circ\text{F}$ ) with two different percentages of cladding failure (two different amounts of spent nuclear fuel available to react with water; 1 percent and 100 percent). The bulk composition of the water at the end of the one-dimensional pathway was assumed to be the resulting water composition for consideration in the near-field geochemical environment. These results for spent nuclear fuel effects on water composition are discussed in Section 3.3.3. The results of the evolutions of the waste form and secondary uranium phases, and the release and retention of neptunium by these phases, are discussed more fully in Section 3.5.

**Precipitates and Salts.** This submodel was used to evaluate a set of bounding analyses of the mass and timing of precipitated minerals build up on the waste package surface and the capacity for generation of highly concentrated brines during the boiling period. These analyses were not used directly within the calculations but were used to assess the need for future work in this area (CRWMS M&O 1998i, Section 4.6).

**Model Implementation for In-Drift Colloids.** The model implementation for in-drift colloids calculated colloid concentrations as a function of ionic strength based on a statistical fit of measured colloid concentrations. This statistical fit of measured colloid concentrations was calculated for particles greater than 100 nm in groundwaters of

various ionic strengths from around the world (CRWMS M&O 1998m, Section 6.3.6; CRWMS M&O 1998i, Section 4.4). Although colloids smaller than 100 nm exist, the available data to constrain the colloid abundance relation are most accurate for the greater than 100 nm colloids (CRWMS M&O 1998m, Section 6.3.6.1; CRWMS M&O 1998i, Section 4.4). This relation may therefore not include an amount of colloids that potentially could account for about 10–40 percent of colloidally transported radionuclides (CRWMS M&O 1998i, Section 4.4). The colloid abundance relation and its associated uncertainty were implemented directly as part of the waste form engineered barrier system source-term cells.

For each of the abstracted periods, the ionic strength of fluids calculated from the submodel for the in-drift water-solids chemistry was used with this relationship to assess the stability and concentration of the suspended colloids reacting with the waste form. Other than this connection, the in-drift colloid model is relatively independent of the other near-field geochemical environment submodels (Figure 3-35). The amounts of iron-oxyhydroxide and clay colloids were assessed by this method directly within the system integration program RIP (CRWMS M&O 1998i, Section 4.5). They are used as input to the colloid sorption and transport model for plutonium, which is discussed within Section 5.5 and the *Total System Performance Assessment-Viability Assessment (TSPA-VA) Analyses Technical Basis Document* (CRWMS M&O 1998i, Section 6).

**Model Implementation for In-Drift Microbial Communities.** The model implementation for in-drift microbial communities was intended to be a bounding assessment on the masses of produced microbes. The model is implemented with a code (Ehrhorn and Jolley 1998; CRWMS M&O 1998i, Sections 4.4, 4.6) for microbial impacts to the near-field geochemistry and uses an idealized approach to assess the biomass production. At each time step, the analysis determines whether biomass production is limited based on the available energy in the system or the nutrient supply for microbes. The microbial production for that time step is the lower of the two values. The production rate and

the cumulative biomass can then be tracked for the time of the analysis to determine the biomass yield and system limitations. These analyses were not used directly within the calculations but were used to assess the need for potential future work in this area (CRWMS M&O 1998i, Section 4.6).

### 3.3.2.3 Major Uncertainties Within the Models

This section provides a general discussion of sources of uncertainties in the near-field geochemical environment models that are described in greater detail in the *Total System Performance Assessment-Viability Assessment (TSPA-VA) Analyses Technical Basis Document* (CRWMS M&O 1998i, Sections 4.4–4.6). Much of the uncertainty for the near-field geochemical environment stems from conceptual model uncertainties. This is particularly true for models of in-drift materials that use thermochemical data (equilibrium and kinetic parameters). The coupling among geochemical effects and physical processes in real systems cannot be incorporated comprehensively into the current near-field geochemical environment submodels. The inability to represent this coupling is another large contributor to conceptual uncertainty in these models; this is particularly the case for the evolution of the gas composition in this system. Thermal-hydrologic processes interact strongly to drive gas flow and generation of certain gas constituents. However, reactions among the gas, water, and minerals occurring simultaneously in this flowing system are only coupled in a limited manner in the near-field geochemical environment component. Limited representation of coupling is also true for the models of concrete effects that do not explicitly evaluate system flow or address permeability changes of the concrete caused by mechanical evolution or precipitation of alteration phases.

Further conceptual uncertainty is related to the inability to observe processes for geologic time spans, which introduces uncertainty about the appropriate time scale for applying those processes. Observations of analogs provide some insight, particularly into the state that a system has

evolved to over geologic time. However, only portions of the system can be observed generally (usually only the solids), and chemical and flow conditions must be inferred to extract quantitative information from the analogs. Applying observations of analogs to another system that may not be governed by the same conditions is another source of conceptual uncertainty.

Part of the conceptual uncertainty for coupled processes stems from limitations of the modeling tools applied to these types of systems. In general, a tradeoff must be made between tools that allow evaluation of a more comprehensive chemical system and those that allow an idealized geochemistry to be coupled to the thermal-hydrology. Uncertainty in the mathematics of the model, or representational uncertainty, is generally relatively small for the geochemical aspects of the near-field geochemical environment submodels in comparison to the conceptual uncertainties. However, computer codes that provide a representation more closely coupled to the hydrology of the system, tend to have larger mathematical or numerical uncertainties.

Parameter uncertainty may be large for models using thermochemical data if well constrained measurements are not available or are not available for the conditions needed (e.g., higher temperature). Lack of data for the appropriate species in a system is a type of conceptual uncertainty because the chemical processes involving those species cannot be included in the model.

The general approach to the large amount of conceptual uncertainty in the geochemical system is to separate the major potential contributors to water compositional changes into various subsystem models (e.g., gas phase, concrete, and microbes). These separate models can be used individually to assess the relative capacities of these processes to alter compositions of various chemical phases at various times. Such uncoupled models facilitate identification of the processes that may control the bulk chemistry for various time frames. Then, the dominant processes can be assigned to the appropriate time frames, or the models that need to be coupled can be identified.

A first level of coupling can be achieved by identifying conceptual scenarios that link the various processes along a pathway for water reaction. These pathways can be examined both with and without a particular subsystem model included as a means to bound the conceptual uncertainty in that subsystem model. For example, modeling scenarios for the in-drift water-solids chemistry with and without concrete capture the major portion of the conceptual uncertainty in the effects of concrete ground support. This approach does not encompass all sources of conceptual uncertainties because they also exist within each model, for example, the local equilibrium assumption in the water-solids submodel. These additional submodel conceptual uncertainties, together with parameter and representational uncertainties, are reflected in the parameter output distributions generated by the various submodels for each scenario (e.g., concreted versus no-concrete) analyzed in the TSPA-VA.

### **3.3.3 Results and Interpretation**

The results of the near-field geochemical model analyses are presented in sections that follow. The focus is on results that provide quantitative inputs either for other TSPA-VA component models or for the TSPA model, and are therefore incorporated into the system-level performance assessment results (e.g., see Sections 3.4 and 5.3). Other analyses conducted in this near-field geochemical environment component of the TSPA-VA provide preliminary constraints on the potential magnitude of additional issues having large uncertainties. The results of those analyses are used to evaluate the potential need for incorporation of those additional processes into system-level assessments. Such analyses also provide a basis for planning and directing process-level and performance-assessment-level investigations and model enhancements to be used in future analyses of performance. All of the results discussed below are described in detail in the *Total System Performance Assessment-Viability Assessment (TSPA-VA) Analyses Technical Basis Document* (CRWMS M&O 1998i, Sections 4.5, 4.6).

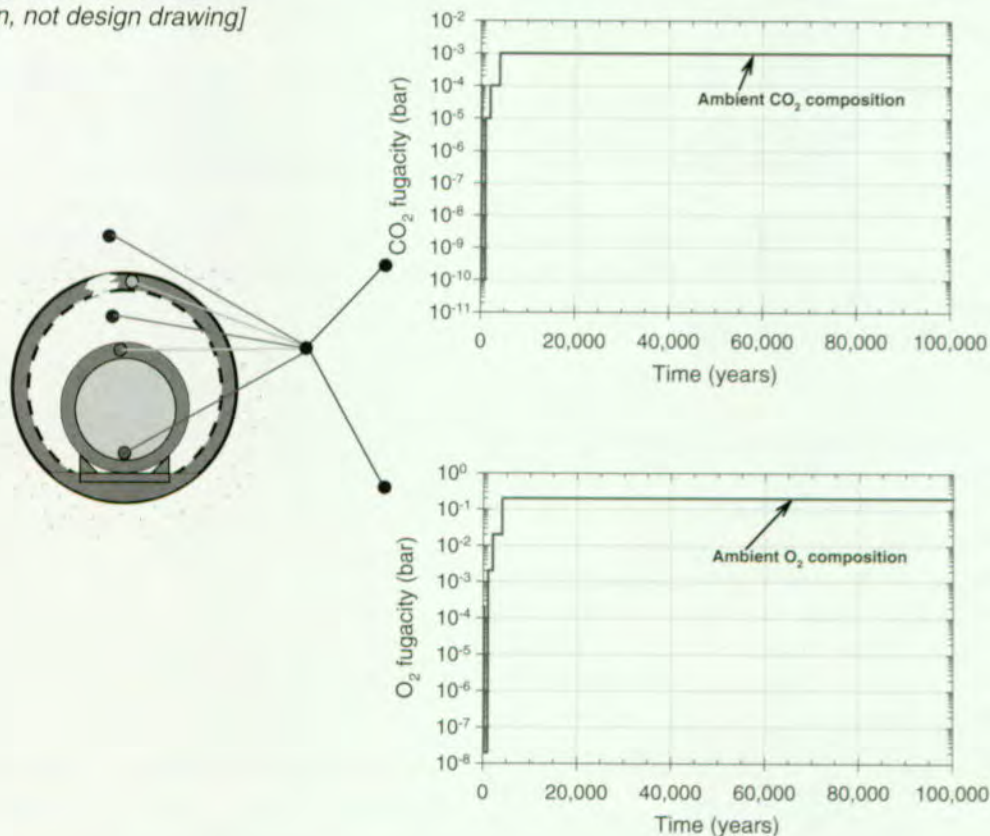
### 3.3.3.1 Gas Compositions

Time variation in gas composition (carbon dioxide and oxygen) provided by submodels of the near-field geochemical environment component are shown in Figure 3-36. These gas compositions apply to the entire region near the drift, within and outside the drift. During the boiling period (0-2,000 years for the center portion of the modeled repository), these gas components are diluted by steam generation. A relatively large decrease in the levels of these gases can be seen from 200 to 1,000 years, which corresponds to the peak boiling conditions. Although there are several smaller changes after 1,000 years, the model values of carbon dioxide and oxygen fugacities return to ambient levels at around 4,000 years. The

reduction in oxygen content may provide some benefit to any degradation processes dependent on oxidation (waste package, cladding, or waste form). However, because this reduction occurs primarily at conditions above boiling, no waste package degradation would be expected (see Section 3.4). For the corresponding edge areas, the return to ambient gas composition occurs around 1,000 years. On the 100,000-year time scale shown in Figure 3-36, the effects of gas composition are relatively short lived.

A simple bounding, mass-balance calculation was used to evaluate the likelihood of depletion of oxygen during package corrosion producing reducing conditions for waste form reactions. To decrease the oxygen fugacity to a reducing

[Schematic of reference design, not design drawing]



FV3033-10

Figure 3-36. Near-Field Geochemical Environment Gas Composition Results for Carbon Dioxide and Oxygen from Time of Waste Emplacement to 100,000 Years

As indicated by reference to the schematic of a drift cross-section and waste package. These gas compositions apply to the entire region within and near the drift, including inside of the waste package.

condition (reduced by at least two orders of magnitude), the waste packages must be able to use effectively all of the oxygen as it is supplied. The cumulative mass flux of oxygen from both the gas and water flux indicates that oxygen levels may be low during the peak boiling period (out to about 1,000 years). By 4,000 years the cumulative oxygen gas flux is up to about  $1.7 \times 10^5$  moles of oxygen gas per meter of drift, or about 450 percent of the oxygen gas needed for full oxidation. At 100,000 years, about seven times that mass of oxygen has been fluxed through the drifts. Therefore, reducing conditions in the drift do not appear very likely as a result of this mechanism.

A mass-balance analysis also assessed whether the amount of carbon dioxide entering the drifts was sufficient to completely carbonate the cement.

This mass-balance analysis was based on the assumption that all the calcium in the cement must bond with carbonate to prevent an increase in alkalinity. The cumulative mass flux of carbon dioxide from both the gas and water flux provides about 51,300 moles of carbon dioxide per meter of tunnel fluxed through the drift over the first 100,000 years. Most of this carbon dioxide is supplied as dissolved materials in the groundwater. At 10,000 years, only about 4,200 moles of carbon dioxide have passed through the drift, and the gas and water fluxes contribute about equally to this mass. To form calcite, one mole of carbon dioxide is needed for every mole of calcium. Based on the mass of concrete in the tunnel, there are about 20,000 total moles of calcium per meter of tunnel. Therefore, there is more than twice as much carbon dioxide than is necessary to carbonate all the cement in 100,000 years. However, only about 20 percent of the carbon dioxide needed to carbonate the cement will have been supplied to the drift in 10,000 years. Other reactions will need to play a major role in neutralizing the alkaline capacity of the large masses of concrete planned for ground support, or alkaline fluids will be likely over at least the first 10,000 years.

### 3.3.3.2 Water Compositions

Figures 3-37a, 3-37b, and 3-37c show water composition results for the near-field geochemical environment through the first 100,000 years for pH, total dissolved carbonate, ( $\Sigma\text{CO}_3^{2-}$ ), and ionic strength (I), respectively. In the figures, different modeled results apply to the different regions, both within and outside the drift. During the boiling period, (0–2,000 years for the center portion of the modeled repository), pH values are near 10 for both incoming water and water that has reacted with iron oxides. Later, the pH values drop. The total dissolved carbonate ( $\Sigma\text{CO}_3^{2-}$ ) values show a large decrease until about 1,000 years. This decrease is caused mainly by changes to gas compositions as shown in Figure 3-36. The ionic strength of these fluids is about 10 times higher until about 2,000 years, primarily because of concentration by boiling.

By 10,000 years, the calculated pH values are near 8 for both incoming water and water reacted with iron oxides, which is in the range of measured ambient pH at the site. However, for the water that reacted with concrete and iron oxides, the pH values remain close to 11 for the entire 10,000-year period, and the total dissolved carbonate ( $\Sigma\text{CO}_3^{2-}$ ) and ionic strength values are lower than for the incoming fluid. These lower values are caused primarily from interaction of water with the alkaline and sulfate components of cement in the concrete; even with additional reactions that bind calcium included, such as silicate-mineral formation, the alkaline components of the concrete still influence water pH.

For the period from 10,000 to 100,000 years, pH values are projected to be about midway between 7 and 8 for water that reacted with concrete and iron oxides. This range is slightly lower than for the cases without concrete. The total dissolved carbonate ( $\Sigma\text{CO}_3^{2-}$ ) and ionic strength values are also slightly lower. These differences also result from the different bulk chemistry in the system with concrete, with the calcium content of the solids and fluid playing a primary role.

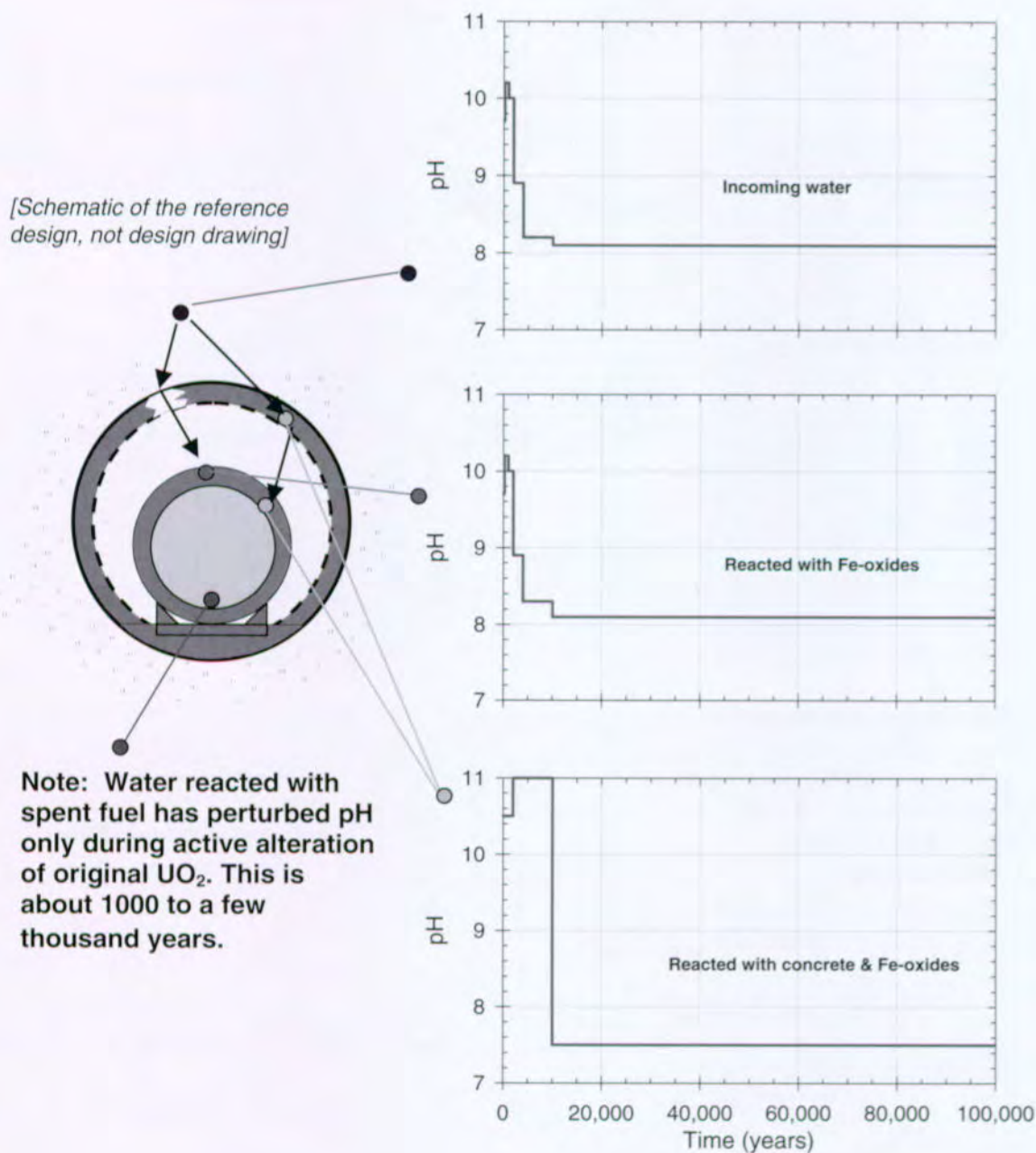


Figure 3-37a. Near-Field Geochemical Environment Water Composition Results, pH Values, for the Time Frame from Time of Waste Emplacement to 100,000 Years  
The region where the results of each plot applies is indicated by reference to a schematic of a drift cross-section with a waste package.

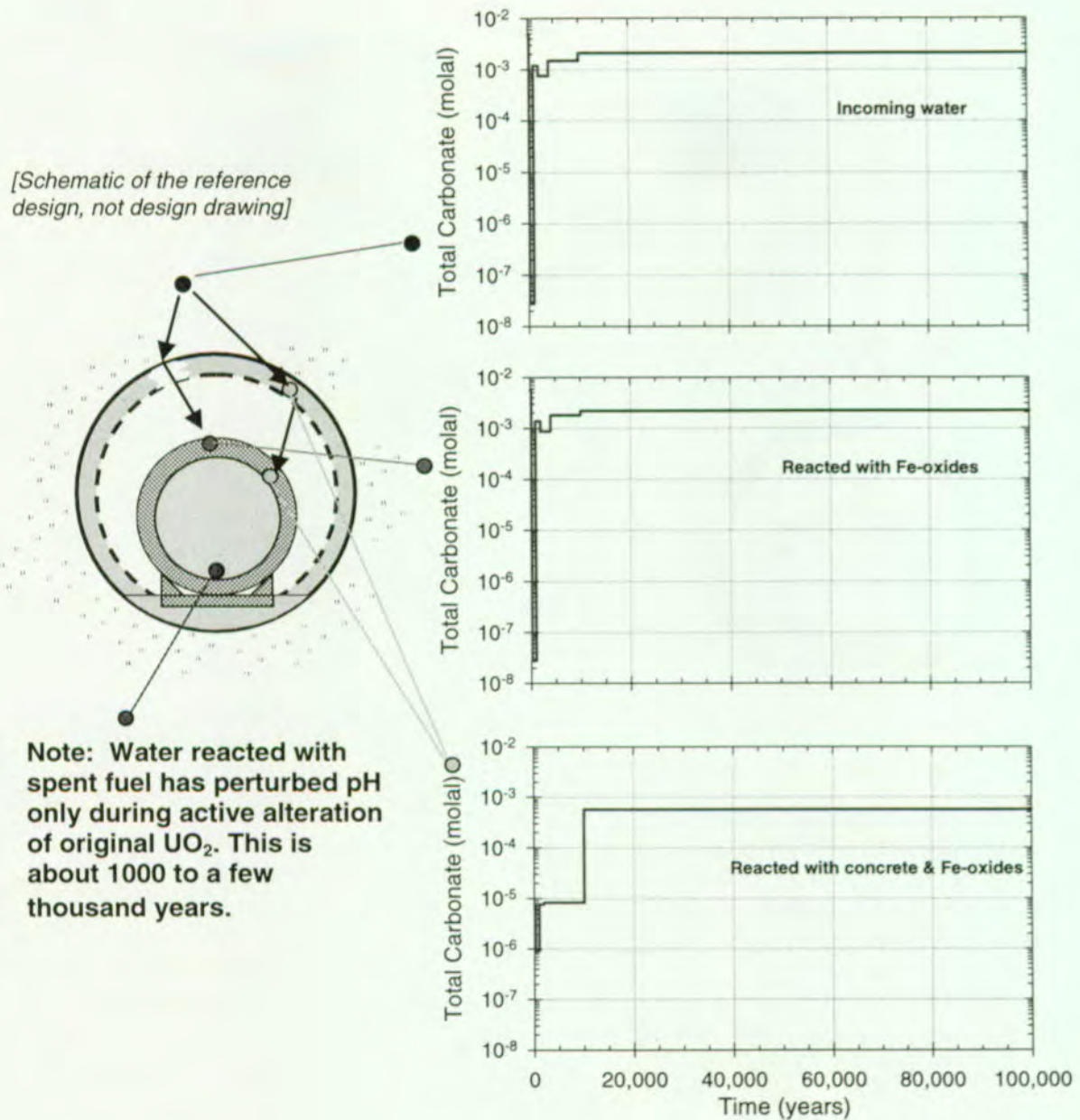
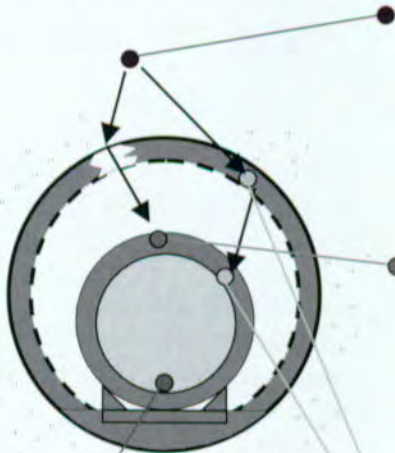


Figure 3-37b. Near-Field Geochemical Environment Water Composition Results, Total Dissolved Carbonate Values ( $\Sigma CO_3^{2-}$ ), for the Time Frame from Time of Waste Emplacement to 100,000 Years  
The region where the results of each plot applies is indicated by reference to a schematic of a drift cross-section with a waste package.

[Schematic of the reference design, not design drawing]



Note: Water reacted with spent fuel has perturbed pH only during active alteration of original  $UO_2$ . This is about 1000 to a few thousand years.

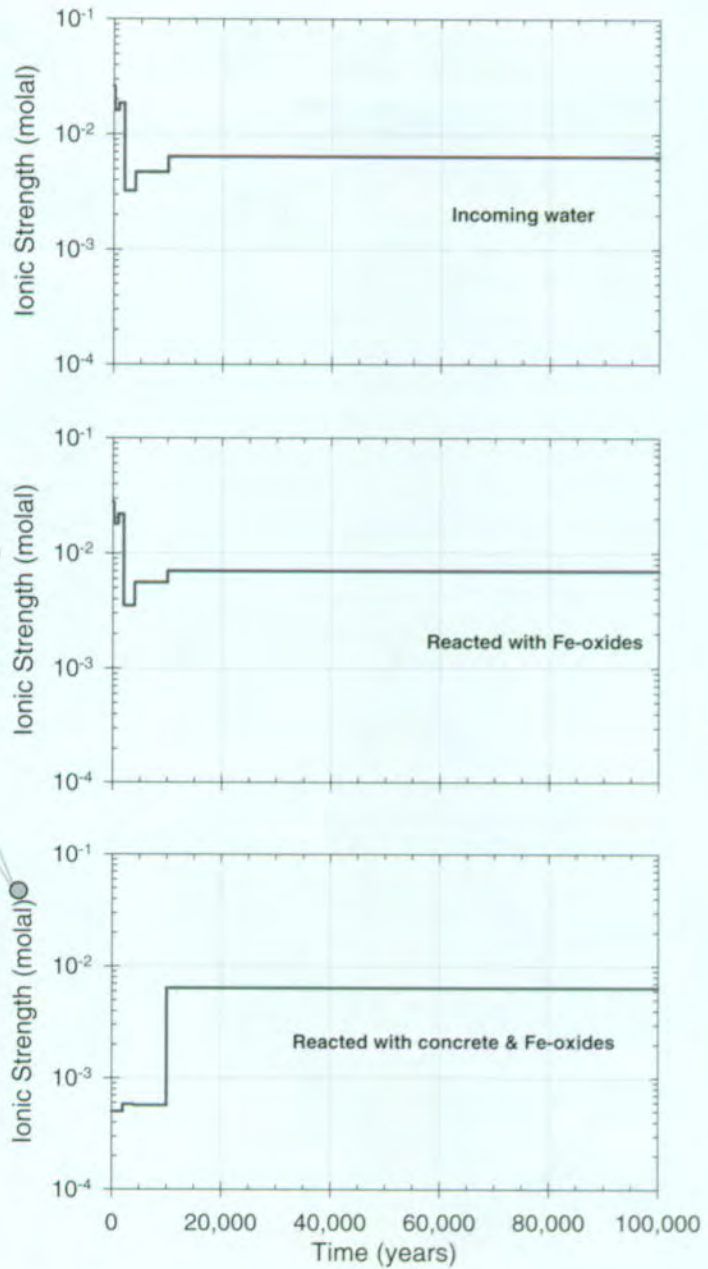


Figure 3-37c. Near-Field Geochemical Environment Water Composition Results, Ionic Strength Values, for the Time Frame from Time of Waste Emplacement to 100,000 Years  
The region where the results of each plot applies is indicated by reference to a schematic of a drift cross-section with a waste package.

The model values shown for gas compositions in Figure 3-36, and for water compositions in Figures 3-37a–3-37c, were assumed to represent the expected values of those parameters. However, because processes in the near-field geochemical environment have a large amount of associated uncertainty, these deterministic results were also used to generate probability distributions for the base case. The uncertainties assessed for the model results (see Section 3.3.2 of this volume; CRWMS M&O 1998i, Section 4.5) were used to construct the distributions, which were defined as log normal for dissolved constituents (this corresponds to a normal pH distribution). Figure 3-38 shows an example of the inputs from the near-field geochemical environment component showing the probability density functions for pH conditions within the drift at various times. These probability distributions are used to explicitly include some of the uncertainty in the modeled pH conditions within the analyses. The probability density functions are shown at the final time of their appli-

cability to the system. For example, the probability density function shown at 100,000 years is applicable from 10,000 years to 100,000 years

The expected values for the distributions (i.e., the peaks) are given by the results shown in Figure 3-37 for water reacted with iron oxides, together with ambient site values applied after 100,000 years. The uncertainties reflect a standard deviation of 0.3 pH units (i.e., one order of magnitude on either side of the expected value should capture 99 percent of the uncertainty). The use of these data for waste package corrosion models, waste form dissolution models, and unsaturated zone transport models is detailed in Sections 3.4, 3.5, and 3.6, respectively, with discussion of the results of those applications in the form of sensitivity studies given in Sections 5.3 through 5.6.

### 3.3.3.3 Consideration of Spent Fuel Alteration and Secondary Phase Effects on Near-Field Geochemical Environment

One set of results for simulations of water reacting with spent nuclear fuel within the waste package over 5,000 years is shown in Figure 3-39. The plot depicts the evolution of pH for fluid that has reacted with spent nuclear fuel. The water composition effects are shown during the active primary alteration stage at early times in which  $UO_2$  is converted to the first set of secondary phases. At both higher (70°C, or 158°F) and lower (30°C, or 86°F) temperatures, the water chemistry is affected to a larger extent if all of the fuel is exposed to reaction.<sup>4</sup> At 70°C (158°F), the ability of the spent nuclear fuel to alter the pH (and other characteristics of the water) begins to decrease almost immediately and is almost entirely dissipated after about 2,000 years. The calculation predicts that exposed spent nuclear fuel will be consumed in about 2,000 years, converted to the major secondary phase, schoepite. Once the exposed spent nuclear fuel is converted to schoepite, the water composition tends to revert to the incoming

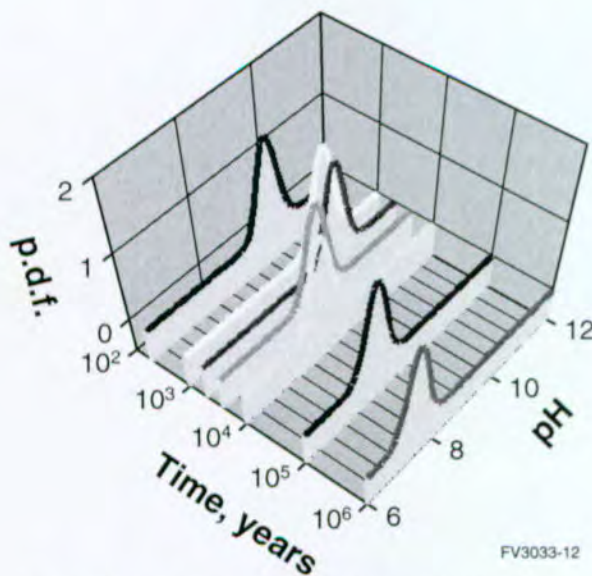
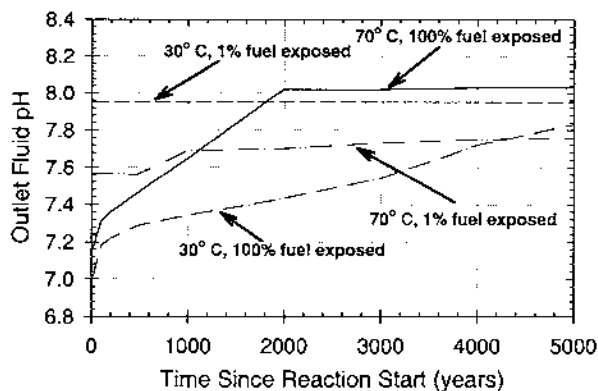


Figure 3-38. Example of Input to the Total System Performance Assessment for the Viability Assessment from the Near-Field Geochemical Environment Component Showing Distributions of pH for Incoming Water Reacted with Iron-Oxides Distributions are shown as probability density functions. (p.d.f.—probability density functions)

<sup>4</sup> The initial pH at of water entering the waste package is about 8.2.



FV3033-13

Figure 3-39. Results of Simulations for Primary Spent Fuel Reacting with Water to Form Secondary Alteration Phases

The plot depicts the evolution of pH of fluid that has reacted with spent nuclear fuel at both higher (70°C) (158°F) and lower (30°C) (86°F) temperatures, as well as for small amounts of exposed fuel (cladding failure = 1 percent) and completely exposed spent nuclear fuel (100 percent cladding failure).

composition. This conversion takes longer at 30°C (86°F), because the reaction rates are lower than at 70°C (158°F).

Additional analyses that specifically included neptunium in the secondary phases indicate that the pH of incoming water is changed by less than about two tenths of a unit during secondary phase dissolution. Although the dissolved calcium content decreases greatly, only small (about 10 percent) changes occur for dissolved carbonate and silica, and for ionic strength. These small effects indicate that the behavior of the secondary phases may be primarily controlled by the composition of the fluid entering the waste package. Because the major effects on fluid composition from spent nuclear fuel reaction appear either large but relatively short lived or minor for many constituents (depending on temperature and percentage of exposed fuel), the only aspect of the performance assessment that was modified to address these effects was the waste form component itself. This modification was accomplished in a sensitivity analysis by using the alteration rate of secondary uranium phases to assess the concentration of neptunium in the resulting fluids. These analyses

are discussed in detail in Section 3.5, and the performance assessment sensitivity results are presented in Section 5.5.

### 3.3.3.4 Colloid Amounts

The relation derived for colloid abundance as a function of ionic strength was used directly within the system integration program RIP (CRWMS M&O 1998i, Sections 4.4, 4.5). External to the system code, the relation was used to generate colloid amounts for values of ionic strength to ensure that the fit coefficients reproduce the data used and produce reasonable values for the amounts of clay and iron-oxyhydroxy colloids in the drift. A couple of examples are provided here. Using the relation indicates that an ionic strength of about  $3 \times 10^{-2}$  molal (boiling regime) corresponds to a colloid concentration of about  $8 \times 10^{-6}$  mg/mL, and ionic strength of  $5 \times 10^{-3}$  molal (cooling regime and ambient) corresponds to about  $6 \times 10^{-5}$  mg/mL. These values correspond to about  $1 \times 10^6$  and  $7 \times 10^6$  particles per milliliter, respectively (CRWMS M&O 1998i, Section 4.5). The performance-assessment-level results of the colloid model for release at the edge of the engineered barrier system, at the water table, and at the accessible environment are discussed in Sections 5.5, 5.6, and 5.7, respectively.

## 3.4 WASTE PACKAGE DEGRADATION

The waste package is a significant component in the overall performance of the repository system. Until the waste package is breached, it provides environmental isolation of the radionuclides in the waste forms within the waste package. As the waste package ultimately degrades with time, it will still provide substantial containment and will delay radionuclide releases to the rest of the engineered barrier system.

The waste package degradation modeling studies and analyses presented in this section were prepared with the view of addressing selected aspects of the NRC Key Technical Issue on Container Life and Source Term (NRC 1998b). Specifically, the information presented is pertinent to one of the four subissues of this key technical

issue consisting of effects of corrosion on the lifetime of the containers and the release of radionuclides to the near-field environment.

Waste package failure occurs when the waste package is breached by at least one perforation, allowing gaseous or aqueous release of radionuclides. Failure or first breach of the waste package may occur through perforations created by localized corrosion of the corrosion-resistant inner barrier. However, high performance, corrosion-resistant alloys such as the candidate inner barrier material are expected to undergo degradation mainly through general corrosion processes (CRWMS M&O 1998b). An additional small fraction of waste packages may fail prematurely, experience "juvenile failures," caused by processes other than corrosion including material imperfections, manufacturing defects, handling effects, and rockfall.

Evaluating waste package degradation is an important component of TSPA because the waste package must fail before any dissolution and

release of the waste form can occur. Important aspects of the evaluation of waste package degradation include determining the processes that cause degradation and finding an appropriate approach for evaluating degradation over long simulated periods.

The current design for the reference waste package is discussed in detail in Volume 2, Section 5.1.2. In summary, the reference design calls for a multi-barrier system consisting of a 10-cm (4-in.) outer barrier and a 2-cm (0.8-in.) inner barrier. The outer barrier is composed of corrosion-allowance material and is intended to provide structural strength and initial corrosion resistance; the inner barrier is composed of a corrosion-resistant material and is intended to withstand the environmental conditions within the drift. Carbon steel (Alloy A516) (ASTM 1990) is the reference material for the corrosion-allowance outer barrier, and nickel-base Alloy 22 is the reference material for the corrosion-resistant inner barrier (CRWMS M&O 1998I). The waste package characteristics are shown in Figure 3-40. The waste packages will

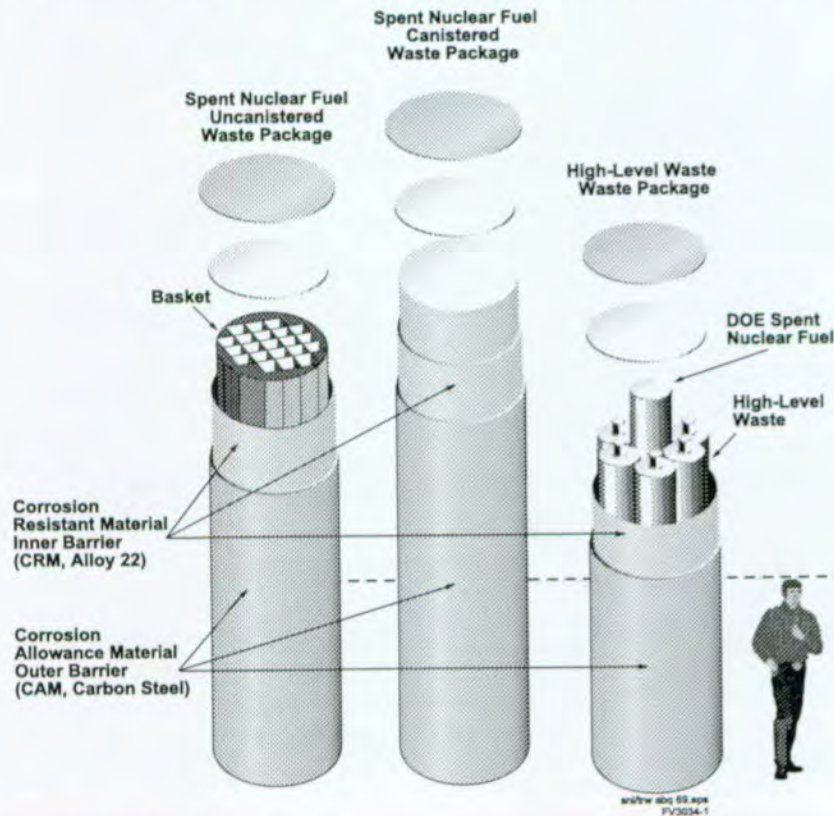


Figure 3-40. Waste Package Reference Design

be emplaced in the engineered barrier system on carbon-steel support assemblies located on concrete segments put in the bottom of the round emplacement drift to provide a level floor, as shown in Figure 3-41.

Most waste packages are expected to be exposed to high temperature, humid air conditions for a period after emplacement (see Section 3.2). These conditions will result in slow degradation of the waste packages. A small fraction of the waste packages may be emplaced in drifts with fractures that periodically drip water. Water may drip on these packages after emplacement. The dripping rate, frequency of drip periods, and water chemistry, especially pH and chloride concentration, will significantly contribute to waste package degradation.

Waste package degradation is shown schematically in Figure 3-42. Outer barrier corrosion is followed by corrosion of the inner barrier, leading to penetration of the waste package. This penetration allows either vapor or liquid water to enter the waste package and begin degrading and mobilizing

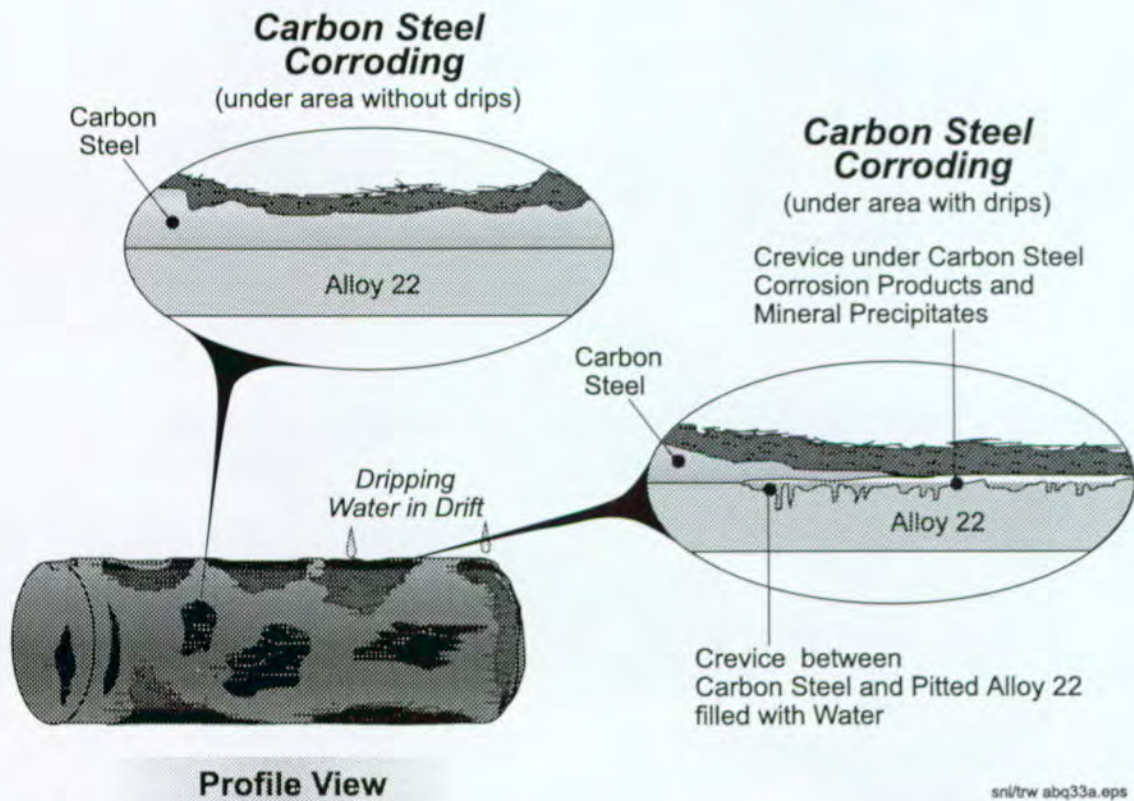
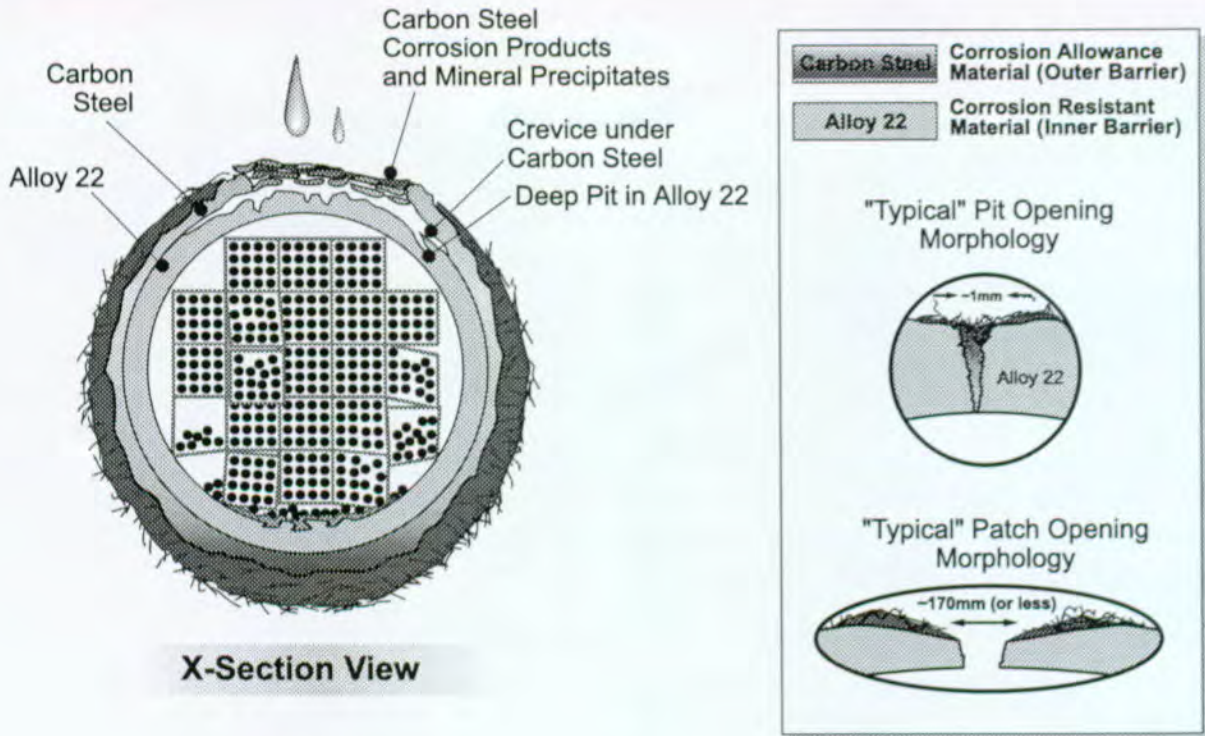
the waste form inside the waste package (see Section 3.5).

The degradation rate of the waste package depends on many things, including the waste package materials and the thermal-chemical-hydrologic regime close to the emplacement drifts. Important parameters of this regime are temperature, relative humidity, and those related to dripping effects and chemical and redox conditions. Analysis of waste package degradation requires information from all of these areas. In particular, waste package design defines the shape and materials used in the degradation and lifetime analyses. Thermal-hydrologic modeling defines the dripping conditions, temperature, and relative humidity input for the analyses. Near-field geochemical modeling provides the basis for the chemical conditions used in the analyses. In overall system modeling, information about waste package failure affects the modeling of waste form degradation and, ultimately, radionuclide transport from the breached waste package.

The detailed modeling of the carbon-steel waste package supports was not conducted for the TSPA-



Figure 3-41. Engineered Barrier System Reference Design



snl/trw abq33a.eps  
FV3034-3

Figure 3-42. Waste Package Degradation Schematic

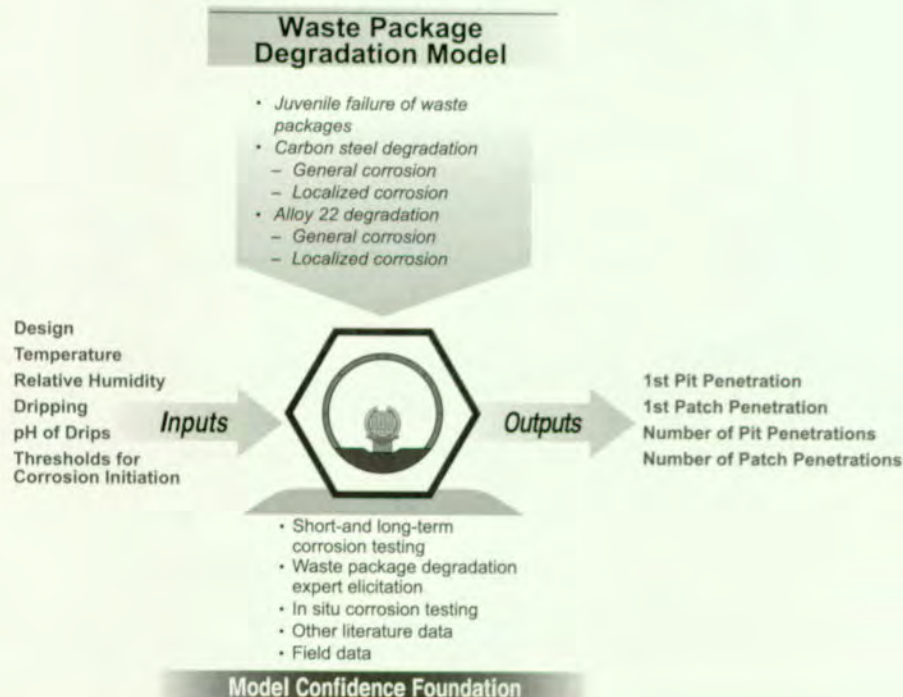
VA. The degradation of the supports with time, their potential contribution to wicking moisture from the invert to the waste package, their potential role as a trap for salts from evaporating water could lead to different waste package lifetimes and transport characteristics. However, due to the expected short lifetime of the supports relative to the repository lifetime, these effects were considered to be inconsequential.

The remainder of this section deals with construction of the conceptual model for waste package degradation, followed by a discussion of implementation of the waste package degradation model in the performance assessment model, and evaluation of some of the key aspects of waste package degradation relative to performance. Additional information on the waste package component can be found in Chapter 5 of the *Total System Performance Assessment-Viability Assessment (TSPA-VA) Analyses Technical Basis Document* (CRWMS M&O 1998i).

### 3.4.1 Construction of the Conceptual Model

The conceptual model for waste package degradation incorporates the important modes of corrosion of both the outer and inner waste package barriers. Several corrosion modes are evaluated for the variety of environments expected in the repository. Figure 3-43 is a summary of the conceptual model used for waste package degradation. The figure identifies the conceptual model input and output, degradation modes considered, and bases for the model. Figure 3-44 shows the degradation modes and thresholds included and the logic flow for the waste package degradation model discussed in detail in Section 3.4-2. As discussed below, the base case conceptual model was developed based on the information from the expert elicitation results (CRWMS M&O 1998b).

Juvenile failures and degradation of corrosion-allowance and corrosion-resistant material are included in the base case. Degradation modes that impact waste package lifetime, those included as well as those not included in the base case model, are discussed in Section 3.4.1.2.



snl/trw abq 41.eps  
FV3034-4

Figure 3-43. Waste Package Degradation Information Flow

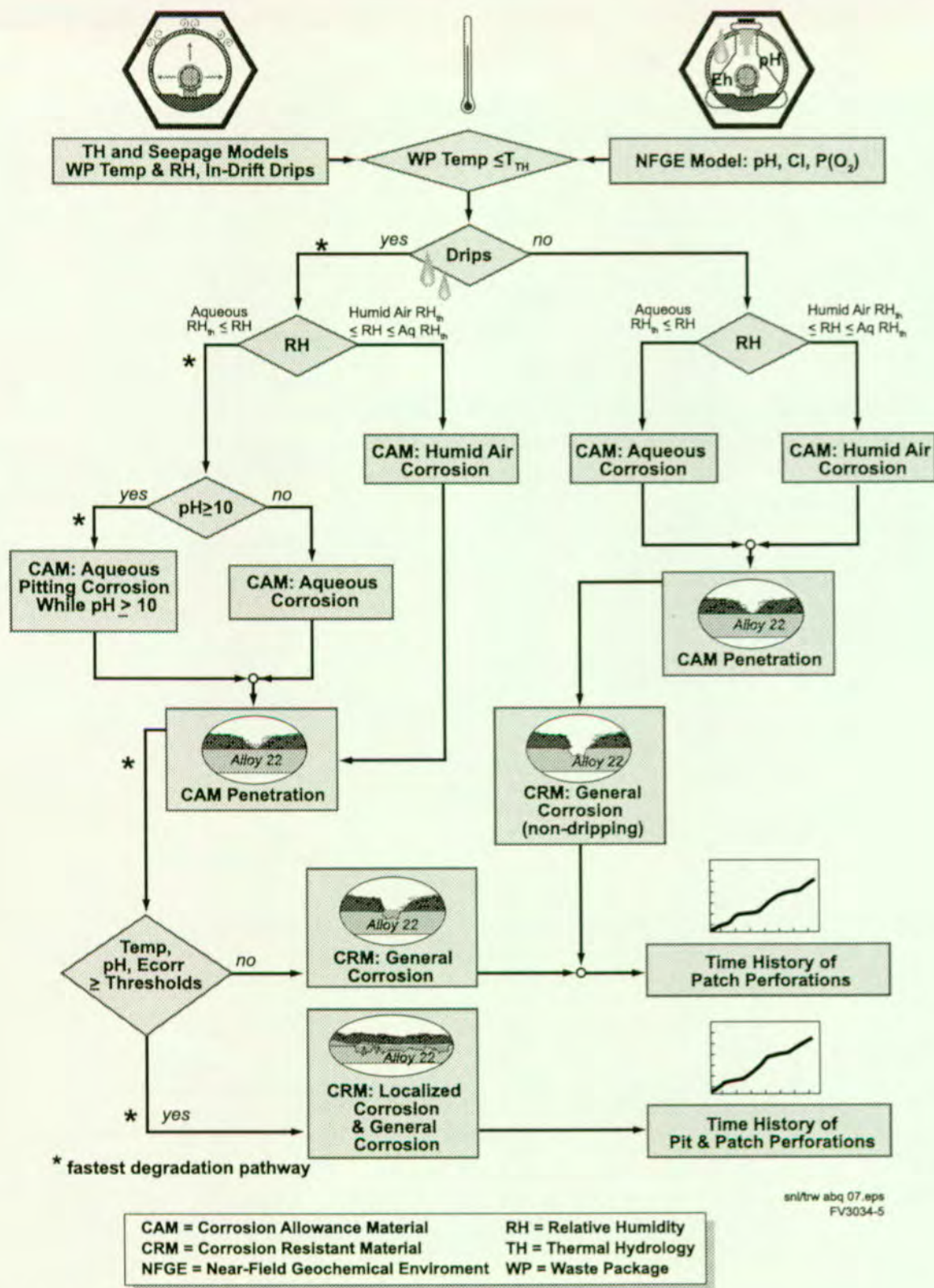


Figure 3-44. Waste Package Degradation Model Logic Diagram

The waste package degradation abstraction and testing workshop was held in early 1997 and focused on the project capabilities to evaluate the degradation modes of the waste package. A summary of the prioritization criteria, high priority issues relative to those criteria, and analysis plans from the workshop is presented in Table 3-11.

### 3.4.1.1 Waste Package Degradation Expert Elicitation

Data on corrosion of the candidate materials and their process models are being developed in conjunction with the comprehensive corrosion testing programs at Lawrence Livermore National Laboratory (McCright 1998). However, long-term test data are not yet available under expected repository conditions and, as a result, the models for waste package performance contain large uncertainties. An expert elicitation was conducted to develop additional information and models that are needed for evaluating waste package degradation for the TSPA-VA (CRWMS M&O 1998b). The major goal of the expert elicitation was to quantify the uncertainties involved in assessing degradation modes for the waste package, including uncertainty in both the models used to represent the degradation modes and the parameter values used in those models. The process followed the procedures and approaches for eliciting expert judgments that have been formalized in documents such as DOE guidance for the formal use of expert judgment by the YMP (DOE 1995 p. 1) and the NRC branch technical position on the use of expert elicitation in the high-level radioactive waste program (Kotra et al. 1996 pp. 3, 4, 7). The assessments and probability distributions that resulted from the expert elicitation provide a reasonable aggregate representation of the knowledge and uncertainties about issues in evaluating waste package degradation. For details of the ranges of values and opinions, see the expert elicitation report (CRWMS M&O 1998b).

During the elicitation, the experts provided an overview of the modes for waste package degradation in the repository, taking into consideration possible evolution of the exposure conditions in the

Table 3-11. Waste Package Degradation Abstraction/Testing Workshop

| <b>Waste Package Degradation<br/>Abstraction/Testing Workshop</b><br>January 8-10, 1997, Las Vegas, Nevada<br>(CRWMS M&O 1997h)   |  |
|---|--|
| <b>PRIORITIZATION CRITERIA</b>  |  |
| How significantly does the process/issue affect   |  |
| <ul style="list-style-type: none"> <li>• The time of waste package failure?</li> <li>• The rate of failure of waste packages?</li> <li>• The rate of waste package perforations and thus the rate of radionuclide release from the waste package?</li> </ul>  |  |
| <b>HIGHEST PRIORITY ISSUES</b>  |  |
| <ul style="list-style-type: none"> <li>• Carbon-steel outer barrier corrosion and salt-scale deposit effect:                             <ul style="list-style-type: none"> <li>- Refluxing and concentration of electrolyte (Cl<sup>-</sup>, pH, etc.)</li> <li>- Microbiological</li> <li>- Temperature dependence on corrosion</li> <li>- Model of salt buildup</li> <li>- Critical relative humidity (transition from dry oxidation to humid-air corrosion)</li> <li>- Critical relative humidity (transition from humid-air to aqueous corrosion)</li> <li>- Aqueous corrosion</li> <li>- Flow rate and episodicity of water</li> <li>- General corrosion in humid-air environment</li> </ul> </li> <li>• Nickel-based material inner-barrier corrosion:                             <ul style="list-style-type: none"> <li>- Aqueous corrosion</li> <li>- Crevice corrosion (geometry, etc.)</li> <li>- Cathodic (or galvanic) protection</li> <li>- Choice of waste package materials</li> <li>- Barrier interface environment</li> </ul> </li> <li>• Galvanic coupling effect:                             <ul style="list-style-type: none"> <li>- Barrier materials (alloy choice)</li> <li>- Water chemistry versus time</li> <li>- Threshold for galvanic protection cessation</li> <li>- Crevice corrosion (including welds)</li> <li>- Electrode area ratio</li> <li>- Ionic conductivity at interface</li> <li>- Fabrication process (contact effectiveness)</li> <li>- Water-contact mode inside container and outside container</li> </ul> </li> <li>• Microbiologically influenced corrosion                             <ul style="list-style-type: none"> <li>- Water variability</li> <li>- Amount of nutrients</li> <li>- Susceptibility of inner barrier</li> </ul> </li> <li>• Preferential weld susceptibility</li> <li>• Container material (microconstituents)</li> <li>• Rockfall, premature failure, and structural failure</li> <li>• Timing of rockfall</li> </ul> |  |
| <b>ANALYSIS PLANS</b>   |  |
| <ul style="list-style-type: none"> <li>• Carbon-steel outer-barrier corrosion</li> <li>• Corrosion-resistant inner-barrier corrosion</li> <li>• Microbiologically influenced corrosion</li> <li>• Effects of variability in near-field conditions, manufacturing, and materials on waste package degradation</li> </ul>   |  |

emplacement drifts. Then the experts evaluated the parameters of various important degradation modes and corrosion models for the corrosion-allowance material and the corrosion-resistant material forming the outer and inner barriers. The

information from the elicitation was used to develop the base case model for waste package degradation. Experts also evaluated the parameters of the corrosion processes and models that are components of the base case waste package degradation model discussed above. The following parameters were evaluated by the expert panel:

- The temperature threshold for starting corrosion of the corrosion-allowance material.
- Relative humidity thresholds for starting corrosion of the corrosion-allowance material by humid air and water.
- Roughness factors (see Section 3.4.1.6) for corrosion of corrosion-allowance material by humid air and neutral-pH water.
- Parameters for models that simulate pitting of corrosion-allowance material in alkaline conditions (pH greater than or equal to 10).
- Density of pits in corrosion-allowance material in alkaline conditions.
- General corrosion rate of corrosion-resistant material as a function of temperature under nondripping conditions.
- Three local exposure conditions on corrosion-resistant material under dripping conditions (pH of 3–10 and moderately oxidizing, acidic and moderately oxidizing, and acidic and highly oxidizing) and the probability of their occurrence. Note: These conditions are for in-crevice chemistry, not bulk chemistry as discussed in section 3.3.
- General corrosion rate of corrosion-resistant material as a function of temperature for each of three local exposure conditions.
- Probability of initiating pitting, and crevice corrosion rate of corrosion-resistant material as a function of temperature for each of three local exposure conditions.

- Density of pits in corrosion-resistant material.

In addition to evaluating these parameters, the expert panel also evaluated uncertainties in the parameter values.

#### **3.4.1.2 Model Input and Output**

The inputs to the modeling of waste package degradation include waste package design and expected environment, including the near-field geochemical environment, dripping conditions, and temperature and relative humidity. Additional information from corrosion data from short- and long-term testing of the reference and similar materials and expert elicitation results provided the basis for both input and confidence in the model.

The output from the modeling of waste package degradation is a time dependent quantitative assessment of waste package degradation and failure. The output is the time to initial breach for each of the waste packages, either a small hole, or pit, made by localized corrosion or a large opening, or patch, formed by general corrosion, and the subsequent perforation of the waste packages. The time of the initial breach corresponds to the start of waste form degradation inside the breached waste package. The perforated or opened area on the waste package provides the opening through which radionuclide transport out of the package can occur. The number of waste package failures plotted as a function of time (failure distribution) provides a time-dependent description of waste package failures. Additional output from the model include the uncertainty and spatial variability of the degradation information both on a package and at different repository locations.

#### **3.4.1.3 Modeled Degradation Modes**

The conceptual model incorporates significant degradation modes associated with waste package lifetime. Many factors influence the ways that corrosion can affect candidate materials. These include metallurgical factors (alloy composition and alloy microstructure); physical factors (temperature, relative humidity, and mode of water contact); chemical factors (pH and concentration of

aggressive species such as chloride, sulfate, nitrate, and carbonate); and mechanical factors such as stress (McCright 1998).

Degradation modes for the candidate barrier materials that are potentially important in the near-field repository environment at Yucca Mountain are identified by McCright (1998) as general corrosion; pitting corrosion; crevice corrosion; stress corrosion cracking; galvanically enhanced corrosion; microbiologically influenced corrosion; radiation-induced corrosion; corrosion in welded materials; and low-temperature oxidation.

Some of the unincorporated degradation modes are discussed later in this section. Degradation modes not analyzed in the base case for this TSPA that may negatively affect performance include late-time structural failure, microbiologically induced corrosion (see Section 3.4.1.7); stress corrosion cracking of Alloy 22, especially on closure welds (see Section 3.4.1.7), and hydrogen embrittlement of Alloy 22. Also, the potential for migration of molybdenum to grain boundaries exists, especially in those areas with high temperatures (e.g., weld areas). This can lead to additional stress, cracking, and generally poor corrosion resistance.

#### 3.4.1.4 Early Waste Package Failure (Juvenile Failure)

With the large number of waste packages to be manufactured and emplaced in the potential repository, there is the potential for degradation modes or factors other than the anticipated corrosion degradation to cause failure of the waste packages at relatively early time. These degradation modes or factors could include materials defects, human-induced factors (manufacturing including welding, handling and transportation), placement on active displacement faults, shifts during emplacement, rockfalls, shaking of waste packages by seismic activity, etc. Early failure from such processes or factors is called juvenile failure. Quantification of waste package juvenile failure is highly uncertain. The analyses for this TSPA attempt to include this potential failure mode based on information gained from available sources.

The initial analyses of juvenile failure included assessment of weld failures, discussed below. Other factors that could contribute to juvenile failure were incorporated into the probability of juvenile failure by expanding the range of failures. In an early study related to a nuclear waste program, the probability of a waste package being initially perforated was assessed based on data for simple pressure vessel components (Doubt 1984 p.7). Based on failure data among about 20,000 pressure vessels that were examined, a failure rate of  $8.5 \times 10^{-4}$  per vessel (17 out of 20,000) was estimated. That is, about 1 in 1,000 among a heterogeneous mixture of high-quality pressure vessels can be expected to fail early because of an undetected critical defect. The analysis was to suggest an upper limit to the probability of early waste package perforation, caused by undetected defects. Doubt (1984) indicated that in a large population of geometrically simple waste disposal containers subjected to highly standardized inspection procedures, the proportion containing critical undetected defects should be much lower. In a recent analysis for the potential repository, assuming independence between inner and outer barrier weld failures, a probability of  $5.8 \times 10^{-6}$  through-wall defects per waste package was estimated (CRWMS M&O 1997q). Based on approximately 10,500 total waste packages and the estimated frequency of waste package through-wall defects, the probability that there will be one waste package with a through-wall manufacturing defect in the potential repository was estimated to be  $6.3 \times 10^{-2}$ . This indicates less than one waste package potentially fails by weld failures in the expected case. The model used for this TSPA assumes one package failure for the expected case ( $10^{-4}$ ) with a range of one to ten packages potentially failing. The failure time is assumed to be 1,000 years.

#### 3.4.1.5 General Corrosion

General corrosion normally causes a relatively uniform thinning of materials without significant localized corrosion. The carbon steel (Alloy A516) outer barrier would be affected mostly by this corrosion mode; however, exposure of carbon steel to alkaline water (i.e., caused by the presence

of concrete) could reduce its resistance to corrosion, allowing the steel surface to be corroded locally with high-aspect ratio pitting (Marsh et al. 1988). This type of pit is a deep pit with a small diameter pit mouth.

The general corrosion rate of carbon steel in water is also strongly affected by temperature, with maximum corrosion rates at temperatures of about 60° to 80° C (140° to 176°F) (Figure 3-45). Such behavior is commonly observed in corrosion processes governed by the reduction of dissolved oxygen. An increase in temperature enhances both mobility or diffusivity of oxygen molecules and reaction rates, but at the same time decreases the solubility of oxygen gas. The net mass transport of

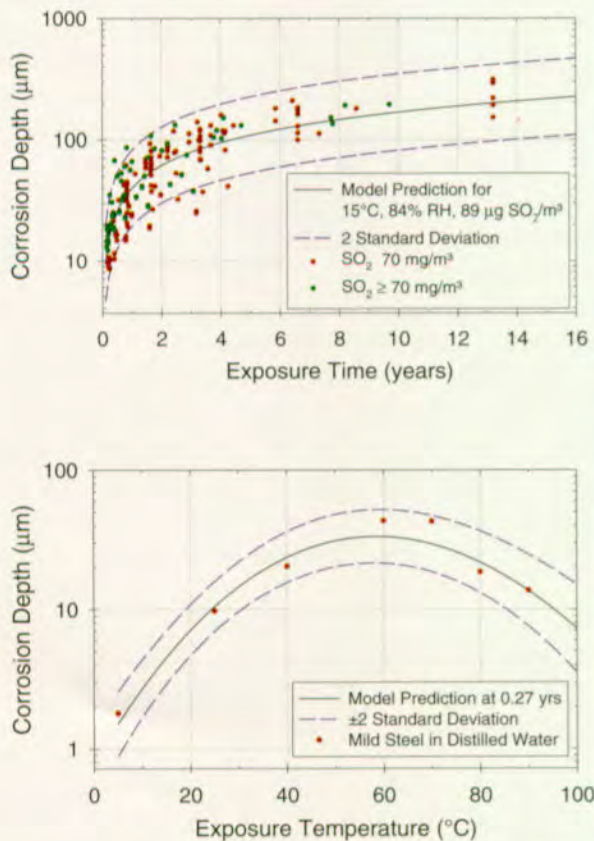
oxygen increases with temperature until it reaches a maximum where the oxygen concentration begins to decrease. In other words, the corrosion rate reaches a maximum and then decreases with further increase in temperature (Boden 1994, p. 2:18).

Alloys such as Alloy 22 with a high nickel, chromium, and molybdenum content are not expected to undergo localized corrosion under repository conditions. Consequently, the mechanism for degradation of these alloys is expected to be significant general passive corrosion and is expected to proceed at very low rates (CRWMS M&O 1998b). The factors affecting degradation of Alloy 22 include temperature, salt concentration (sodium and ferric chloride), and pH.

### 3.4.1.6 Localized Corrosion

Localized corrosion, or pitting and crevice corrosion, is induced by local variations in the electrochemical potential or driving force for corrosion on a micro-scale over small regions. Variations in electrochemical potential may be caused by localized irregularities in the structure and composition of usually protective passive films on metal surfaces and in the electrolyte composition of the solution that contacts the metal (McCright 1998; Henshall 1992; Henshall et al. 1993). Complex electrochemical processes associated with these factors strongly influence the initiation of pitting and pit growth processes. In general, metal pitting is caused by complicated interactions among many factors and appears to be random. As a result, stochastic approaches have been used in waste package degradation modeling to represent and quantify localized corrosion processes.

In neutral pH water, local variations of the depth of general corrosion of carbon steel are commonly represented with a roughness factor, that is defined as the ratio of the local general corrosion depth to the average general corrosion depth considered over the entire sample surface at a given exposure time. A roughness factor was used in modeling local variations of the general corrosion of carbon steel. However, when in contact with alkaline pH



FV3034-6

Figure 3-45. Corrosion Allowance Material Corrosion Rates and Data

Corrosion data are given for general corrosion in humid air and aqueous corrosion (in the presence of liquid water such as from drips). Corrosion allowance material is composed of carbon steel and is the material of the outer waste package layer.

water, carbon steel could undergo pitting corrosion with high-aspect ratio pits. A pit growth law was suggested for modeling pitting corrosion of carbon steel in alkaline water (CRWMS M&O 1998b). However, the one-year test results in concentrated repository-groundwater conditions in which the test solutions are maintained at approximately a pH of 9.7, showed no such pitting corrosion for the carbon steel samples (McCright 1998).

If the carbon steel outer barrier is penetrated, a number of factors determine the probability that localized corrosion of the inner barrier will begin. These factors include the availability of water and its pH, temperature, and chloride ions, ferric ions, and dissolved oxygen content which affect the corrosion potential of the material. The probability that localized corrosion of the inner barrier will begin is essentially the probability that an aggressive environment will exist relative to these factors. The availability of water to initiate localized corrosion of the inner barrier will vary depending on whether water drips onto the waste package. When the outer barrier is penetrated, crevices could form under the following conditions: between the inner barrier and the uncorroded carbon steel, or under a thick layer of material from the corrosion of carbon steel. For this reason, crevice corrosion of the inner barrier is considered a more probable process than pitting, and this process can begin at lower temperatures than pitting. For example, crevice corrosion may begin if the temperature is between 80° and 100°C (176° and 212°F) when the outer barrier fails. Once begun, crevice corrosion will grow similar to corrosion described by the pit growth law. If the temperature is below the threshold, no exposed site would initiate crevice corrosion, and the inner barrier can be assumed immune to localized corrosion. Under these conditions, the inner barrier will only experience general corrosion. The conditions required for crevice corrosion are necessary to sustain the process, as well. The data used to develop the localized corrosion model of the corrosion-resistant material include 38 experimental observations of Alloy 22.

### 3.4.1.7 Other Degradation Modes for Waste Packages

Several processes have not been included in the model for waste package degradation. These processes include dry oxidation, galvanic protection, stress corrosion cracking, microbiologically influenced corrosion, radiation-induced corrosion, and late-time structural failure. These processes are briefly discussed below.

**Dry Oxidation.** At the moderately elevated temperatures expected at the waste package surface in the repository, the corrosion-allowance material may be degraded by dry oxidation. A previous study concluded that the impact of oxidizing the candidate barrier materials under repository conditions is insignificant (Henshall 1997; CRWMS M&O 1998b). Because of this, the dry oxidation process is not included in the base case model.

**Galvanic Coupling.** Galvanic coupling of the inner and outer barriers may be an important process in the waste package degradation. Galvanic protection of the inner barrier may occur because of interaction between the outer and inner barriers. However, the panelists of the *Waste Package Degradation Expert Elicitation* (CRWMS M&O 1998b) noted that, while there could be galvanic protection of the inner barrier as the outer barrier is penetrated, the effect will be small and of short duration relative to the time scale of interest for repository performance. Thus, this effect is not incorporated in the base case. A recent analysis (Farmer and McCright 1998) showed that the galvanic coupling keeps the crevice solution chemistry from being extremely acidic and aggressive, conditions that are observed in crevices of single material nickel-based alloy. There is a potential for enhanced corrosion of carbon steel if it is single material coupled galvanically to Alloy 22 but this essentially protects the Alloy 22. Another potentially adverse effect from the galvanic coupling is hydrogen embrittlement of Alloy 22 from the production of hydrogen at the cathodic sites of the Alloy 22 surface and hydride phase formation in the alloy. This process is not included in the base case model, and is potentially non-conservative.

**Stress Corrosion Cracking.** This is a crack propagation process caused by the combined and synergistic interaction of mechanical stress and corrosion reactions. Recent bounding analyses using linear elastic fracture mechanics (McCright 1998) showed that, except for very high aspect ratio, the critical crack size for stress corrosion cracking is always larger than the thickness of both the barriers for the stresses (245 MPa for carbon steel and 410 MPa for Alloy 22) and aspect ratios that are considered. The expected stress in the design basis metals is expected to be (McCright 1998) much lower than the stress range studied here; therefore, there would be no stress corrosion cracking in the design basis metals (carbon steel and Alloy 22). Because of potential technical difficulties associated with relieving stresses in the closure welds of the double-walled waste package, stress corrosion cracking of the closure welds could be a potential degradation mode. Another potential degradation mode is the development of wedging stresses on the corrosion-resistant material. This may occur because of accumulation of corrosion-allowance material corrosion products in the gap between the inner and outer barriers, when the corrosion-allowance material is breached at early times and a substantial thickness of the corrosion-allowance material remains. Because of the low probability of occurrence, this process is not included in the base model.

**Microbiologically Influenced Corrosion.** This is caused by the metabolic activity of microorganisms. Microbiologically influenced corrosion may occur throughout the life of the repository, especially after the near-field temperature of the repository cools down. Microbial metabolism produces corrosive chemicals. Although 300-series stainless steels are known to be susceptible to microbiologically influenced corrosion, the nickel-based alloys such as Alloy 22 seem to be immune to this type of corrosion (CRWMS M&O 1998b). The panelists of the *Waste Package Degradation Expert Elicitation* (CRWMS M&O 1998b) discussed various aspects of potential microbial activity and microbiologically influenced corrosion in the repository. The experts generally agreed that, until the repository has cooled to temperatures below 100°C (212°F) and relative humidity is above 60 percent, microbiolog-

ically influenced corrosion would not occur. Also, significant microbiologically influenced corrosion was deemed unlikely if there is no dripping onto the waste package. The panelists concluded that the importance of microbiologically influenced corrosion is to increase pit and crevice density and the probability that localized corrosion will start, rather than to affect the rate once corrosion has begun is low. Further, they noted that Alloy 22 has not been associated with documented cases of microbiologically influenced corrosion. Thus, this process is not included in the base model.

**Radiolysis-Induced Corrosion.** This is another potentially important degradation process for waste packages in the repository. If irradiated by gamma radiation, fixed nitrogen may exist in the liquid phase as nitrite and nitrate ions that are corrosive to metals. Nitrogen fixation in water, as used here, is a process to transform nitrogen gas to a stable (fixed) form in water. The total amount of nitrite and nitrate that can be formed in a liquid phase is limited by the gamma radiation dose rate and the volume of irradiated air. If a thin film of water on the waste package container in contact with a relatively thicker air space is irradiated, there can be a significant concentration of nitrate in the relatively small amount of water in the film (Van Konyneburg et al. 1995 p. 8, vol. 3). This process is not included in the base model because the thickness of the waste package reduces the gamma flux, therefore reducing the amount of radiolysis to negligible levels.

**Structural Failure.** Sometime after closure of the repository and significant degradation of the concrete linings, rocks are expected to fall in the emplacement drift. A degrading waste package hit by falling rocks will experience a dynamic load initially. The degrading waste package will experience a static load from the weight of the rocks remaining on the waste package, the waste package itself and the waste inside. After a certain degree of degradation, the waste package will lose structural stability. A recent analysis reported results for the thinning of waste packages and how thinning relates to structural failure (CRWMS M&O 1996a). The structural analyses in the report provide a basis for determining the structural capabilities of waste package containment barriers

at various levels of uniform thinning degradation. The analysis results indicate that if the thickness of the carbon steel outer barrier and an inner barrier of Alloy 625 (a nickel-based alloy with lower molybdenum content than Alloy 22) is reduced, the waste package maintains containment even when the entire outer barrier and more than half of the inner barrier have been removed because of corrosion. That is, 9.5 mm of the original 20 mm remains. The analysis assumed no support from the basket assembly inside the waste package. While the analyses were conducted using Alloy 625 as the inner barrier, the results should also be valid for the Alloy 22 inner barrier. This degradation mode is not included in the base model.

### 3.4.2 Implementation of Waste Package Degradation Model

The waste package degradation model includes both juvenile failures (as described in Section 3.4.1.4) and degradation with time according to corrosion processes. The range of probability of juvenile failures is based on the analysis of weld failures but is expanded to cover other potential conditions that may lead to early failure. The evaluation of waste package degradation with time is incorporated into a computer code that is based on a probabilistic approach (CRWMS M&O 1998j; Lee et al. 1997). The code has the capability for modeling various designs, waste package materials, and degradation mechanisms. Figure 3-46 shows the degradation models and thresholds included and the logic flow for the model. The model tracks waste package degradation by first defining the environmental inputs to the system, then checking for dripping and pH conditions, followed by degradation of the corrosion-allowance material and the corrosion-resistant material. The model simulates degradation of both the corrosion-allowance material and the corrosion-resistant material because of general and localized, or pitting corrosion. The model divides the waste package into discrete corrosion patches for general corrosion. The corrosion patches are 310 cm<sup>2</sup> (48 in<sup>2</sup>) regions in which corrosion properties are assumed to be homogeneous.

Several environmental parameters affect degradation of the corrosion-allowance material:

- Relative humidity. The threshold at which relative humidity initiates corrosion is based on the distributions developed from the *Waste Package Degradation Expert Elicitation* (CRWMS M&O 1998b). This relative humidity threshold was used for all waste packages, even those in dripping conditions, to initiate humid air corrosion. For dripping conditions, aqueous corrosion was initiated after relative humidity reached a certain threshold (85–100 percent relative humidity).
- Temperature. The temperature at the waste package surface must be below a threshold temperature that represents the boiling point for corrosion to initiate. No dry oxidation corrosion is included in these analyses.
- Dripping conditions. Dripping conditions are assumed for a certain fraction of the waste packages based on water seepage into the drift (see Section 3.1 for discussion of the seepage model). If water drips onto a waste package, it is assumed to be 100 percent wet from the dripping. The sensitivity of the analysis to changes in these conditions is discussed in Section 5.4.
- pH of incoming water. The pH of the incoming water in the base case does not change because of interaction with concrete because the concrete lining is assumed to have fallen in at an early time and is not important over the performance period (see Section 3.3 for discussion of the development of the pH values as a function of time). The sensitivity of the analysis to changes in this parameter is discussed in Section 5.4.
- Other drift conditions not included in the base case. Other geochemical parameters are not included in the base case analyses of waste package degradation, because of modeling constraints. However, omitting chloride concentration is potentially not

conservative, while omitting oxygen partial pressure is probably conservative in terms of system performance.

The model for degradation of corrosion-resistant material was developed from existing data with significant input from the panelists of the *Waste Package Degradation Expert Elicitation* (CRWMS M&O 1998b). Figure 3-46 shows the elicited general corrosion rates for the corrosion-resistant material along with the data for degradation of Alloy 22. Data about variability and uncertainty were also elicited from the panel (CRWMS M&O 1998b). The base case definition assumes that uncertainty and variability are evenly divided in determining the general corrosion rates for the corrosion-resistant material under dripping conditions.

A temperature threshold is used for initiation of localized corrosion of Alloy 22 after the outer barrier is breached. The threshold for an Alloy 22 patch is sampled from a uniform distribution between 100° and 80°C (212° and 176°F) when a patch of corrosion-allowance material fails. Three local (in crevice) exposure conditions (not bulk near-field chemistry) on the inner barrier defined in the *Waste Package Degradation Expert Elicitation Project* (CRWMS M&O 1998b) are represented in the following model:

- 84 percent of the area that is dripped on is assumed to be in moderately oxidizing conditions, with pH of 3 to 10 and 340 mV standard hydrogen electrode
- 13 percent of the area that is dripped on is assumed to be in acidic and moderately oxidizing conditions, pH of 2.5 and 340 mV standard hydrogen electrode
- 3 percent of the area that is dripped on is assumed to be in acidic and highly oxidizing conditions, pH of 2.5 and 640 mV standard hydrogen electrode

These are the local environments the expert panel felt were representative of potential conditions in crevices on the waste package, not bulk pH values.

The experts provided cumulative distribution functions of general corrosion rates for corrosion-resistant material at three temperatures (25°, 50°, and 100°C; or 77°, 122°, and 212°F) for each local exposure condition (a total of nine cumulative distribution functions for corrosion rates).

The elicited cumulative distribution functions (indicating the spread in general corrosion rate values) of corrosion rates for the corrosion resistant material included both uncertainty and variability. There is uncertainty in the rates because of lack of extensive experimental information on the rates. There is variability in the rates because of the range of environments and material conditions that will be present in the repository (package to package variability) and on a package (patch to patch variability). The uncertainty and variability in corrosion rates was split up for dripping and no-dripping general corrosion conditions, as well as for the localized corrosion conditions to attempt to bound the effect of these parameters. The variability in the corrosion rates was further split up between package to package and patch to patch variability to attempt to bound the effect of these parameters. The full discussion of the approach to uncertainty/variability allocation is found in Chapter 5 of the *Total System Performance Assessment-Viability Assessment (TSPA-VA) Analyses Technical Basis Document* (CRWMS M&O 1998i).

The primary stochastic parameters used in the model are the following (CRWMS M&O 1998j):

1. Fraction of variability assigned to waste package to waste package and patch to patch.
2. The roughness factor multiplier for corrosion-allowance material is a bounded normal distribution with a mean equal to 1.5, standard deviation equal to 0.25, lower bound equal to 1, and upper bound equal to  $1 \times 10^6$  (in other words, no upper bound).
3. In the high pH model for corrosion-allowance material,  $D = Bt^n$ , where  $D$  = pit depth,  $B$  = pit depth when time is 1,  $t$  =

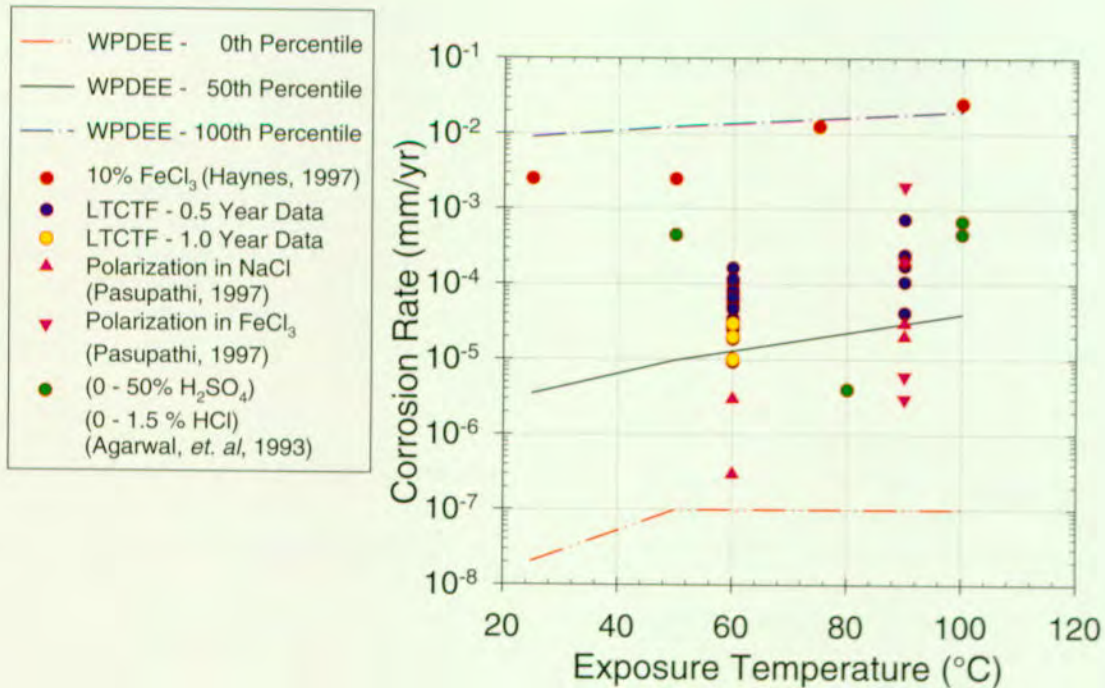
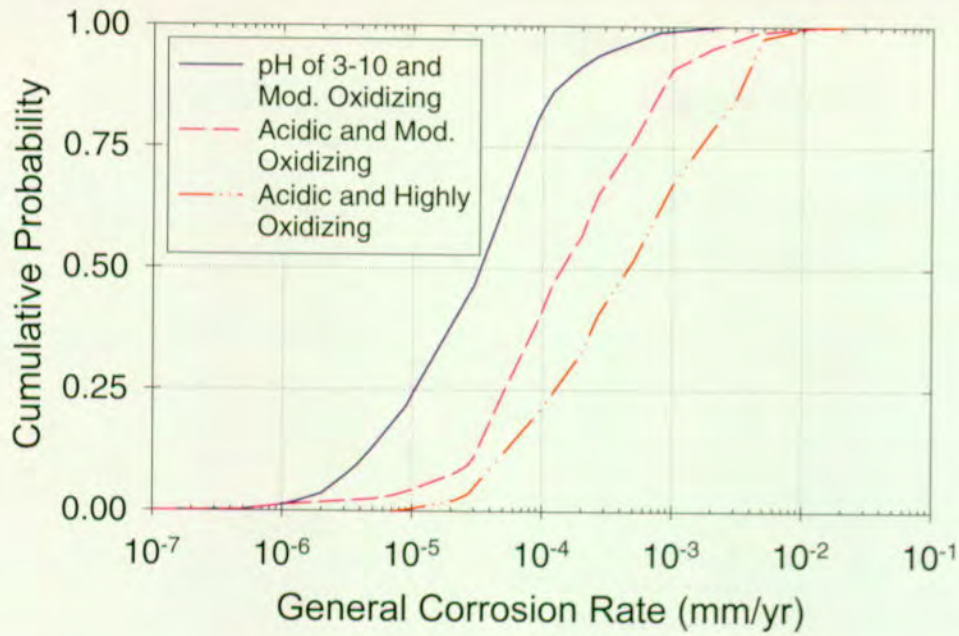


Figure 3-46. Abstracted General Corrosion Rate Distributions of Alloy 22  
Abstracted general corrosion rate distributions for the corrosion-resistant material for three different local exposure conditions at 100°C, and the comparison of the abstraction with the literature data for varying exposure conditions at different temperatures.

time, and  $n$  is between 0 and 1,  $B$  and  $n$  have cumulative distribution functions.

4. Drip and no drip conditions for general corrosion of the corrosion-resistant material, three cumulative distribution functions at three user-defined temperatures (25°, 50°, and 100°C; or 77°, 122°, and 212°F).

The results are provided as input to the total system performance analyses in the form of lookup tables. The tables contain cumulative distribution functions that represent the first breach time distribution for the waste package and the variation with time of the average number of pit and patch penetrations per failed waste package. These distributions are used to determine the time at which waste form degradation occurs and radionuclide release begins, and the effective area through which release can occur.

### 3.4.3 Results and Interpretation: Evaluation of Key Issues and Importance to Performance

The results of using the waste package degradation model to estimate performance of the waste package for the base case are presented in this section. These results point out the importance of various parameters in the modeling and the effects of some of the assumptions.

The results of using the waste package degradation model to estimate performance of the waste package provide a quantitative analysis of the initial failure of the waste packages and their degradation through time. Figure 3-47 shows the failure curves for the various aspects of failure when water drips on waste packages. The breach curve for corrosion-allowance material indicates when the first penetrations occur in the outer-barrier material. These breaches start at approximately 1,000 years and continue until the corrosion-allowance material fails for all packages at approximately 6,000 years. This curve for corrosion-allowance material shows that breaching occurs significantly before the simulated failure of the corrosion-resistant material. The first-breach

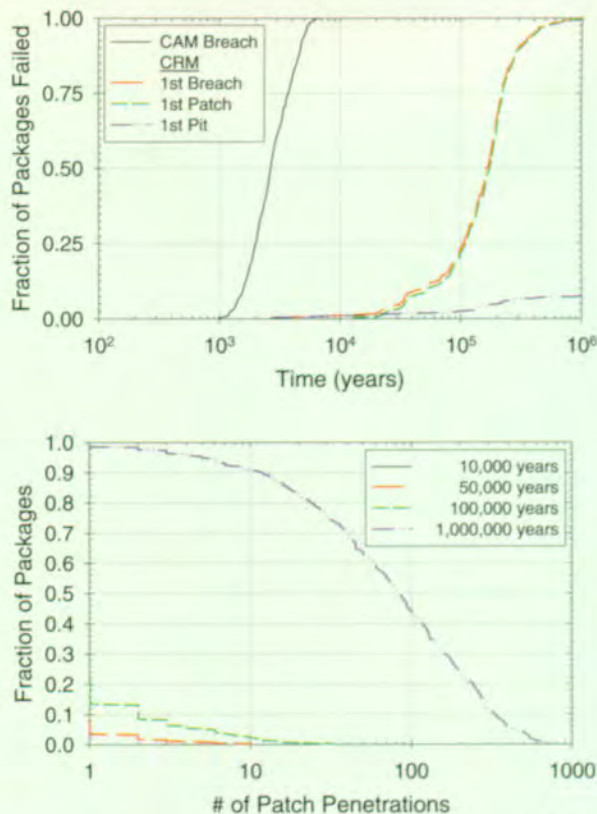


Figure 3-47. Waste Package Degradation History of Packages Exposed to Drips  
The top figure shows the failure rate history of packages for a period of 1 million years and the bottom figure shows the number of patch penetrations at different time periods. (CAM—corrosion-allowance material [waste package outer layer]; CRM—corrosion-resistant material [waste package inner layer])

curve indicates the time of first penetration completely through a waste package, whether it is because of a pit or a patch. This curve is primarily from patch failures, with a few initial pit penetrations, and shows that failures start at 3,000 years. All waste packages that are dripped on fail by 1 million years. The first-patch curve basically follows the first-breach curve because not many packages fail through pitting. The overall degradation of the waste package through patch failure is shown in Figure 3-47. At 1 million years, 50 percent of the packages that are dripped on have approximately 80 patch perforations.

The base case analyses incorporate both dripping and nondripping conditions. The effect of these

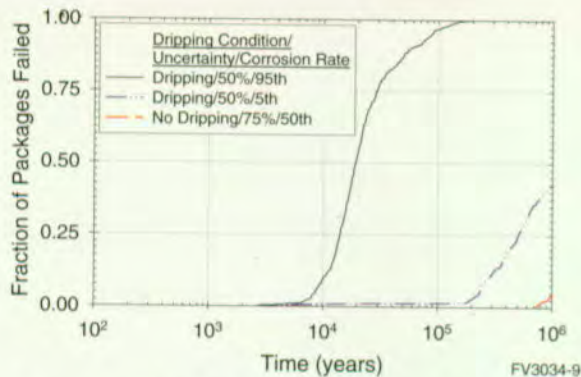


Figure 3-48. Dripping Versus No-Dripping Effect on Waste Package Degradation  
Exposure to dripping accelerates failure of packages.

two drift environments on waste package degradation is shown in Figure 3-48. The waste packages that are dripped on have a higher percentage of failures and fail much earlier than the waste packages that are only exposed to humid air conditions within the drift.

The waste packages will be exposed to different dripping environments within the drifts. The effect of alternate dripping environments is shown in Figure 3-49. The waste package failures are higher for the wetter climates, because of the effect of dripping on Alloy 22 corrosion. All of these dripping scenarios are included in the base case.

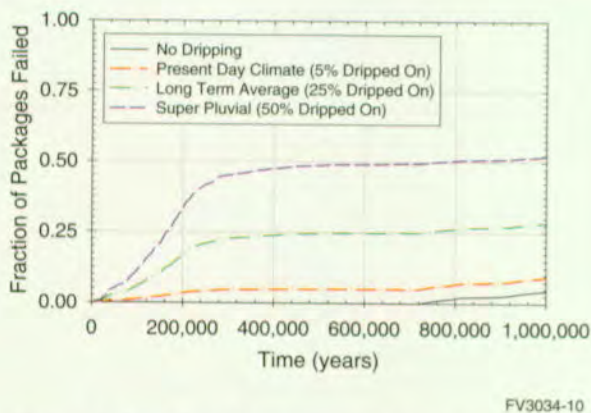


Figure 3-49. Effect of Alternative Dripping Scenarios on Waste Package Degradation  
This figure shows fraction of packages failed for three dripping scenarios including present-day climate, long-term-average climate, and superpluvial climate as well as a no-dripping comparison.

The impact of waste package performance on the overall system is potentially quite significant. The overall corrosion rate for corrosion-resistant material and the number of waste packages that get wet are significant determinants to the overall release of radionuclides from the system. A sensitivity analysis shows that system performance is highly dependent on the corrosion rate for corrosion-resistant material.

Based on previous results from the waste package degradation computer code and conceptual understanding of corrosion degradation processes for waste packages, a ranked list of potentially important parameters for evaluating waste package degradation was developed. The ranking looks at parameters that affect waste package failure, including first penetration of the waste package and the number of pit and patch penetrations that directly affect radionuclide releases from the waste packages. The ranking is as follows:

1. Allocation of the model variance, especially for corrosion-resistant material, to uncertainty and variability of waste package degradation
2. Local chemical and electrochemical exposure conditions for corrosion-resistant material
3. General corrosion rate for corrosion-resistant material under dripping conditions
4. Initiation threshold for localized corrosion of corrosion-resistant material
5. Localized corrosion rate for corrosion-resistant material

Other potentially important model parameters follow:

- Surface area of a waste package that is wetted under drips
- Allocation of the total variability to waste package-to-waste package and patch-to-patch variability

- Roughness factor for corrosion-allowance material

The overall strength of the model is that a significant amount of data has been reviewed to determine corrosion rates for corrosion-allowance material. The primary weakness of the model is the overall reliance on expert elicitation rather than on long-term test data of corrosion rates for corrosion-resistant material. These rates significantly affect overall system performance but are based on limited data for environments unlike those expected at Yucca Mountain.

The model provides highly uncertain analyses of corrosion of corrosion-resistant material because data are so limited. Providing additional defense of these analyses for the LA will require laboratory testing data for general and localized corrosion of Alloy 22 and for stress corrosion cracking, as well as further process model development.

### 3.5 WASTE FORM ALTERATION, RADIO-NUCLIDE MOBILIZATION, AND TRANSPORT THROUGH THE ENGINEERED BARRIER SYSTEM

The waste forms emplaced in the repository will initially be contained in and protected by the waste packages. Location of the waste forms in the overall repository system is shown in Figure 2-2. The major processes effective in this part of the repository system are identified in Figure 3-50. After degradation and failure of the waste packages, spent nuclear fuel assemblies and high-level radioactive waste canisters will be exposed to the drift environment including air, water vapor and, possibly, dripping water. After waste package failure, radionuclides are not available for release and transport until three things have occurred:

1. Failure of the fuel cladding, (the tubular material surrounding the fuel matrix), or high-level radioactive waste canister. (Note: The extra performance provided by the canisters is not accounted for in TSPA-VA.)
2. Degradation of the solid waste form

3. Mobilization of radionuclides into aqueous solution, aqueous colloidal suspension, (interaction with particles 0.001 to 1 micron in size through sorption and other chemical mechanisms), or gaseous form, (Note: No gaseous transport was considered in TSPA-VA because it was not a significant release mode in previous TSPAs.)

Mobile radionuclides are transported out of the degraded waste package and through the engineered barrier system to the unsaturated zone. Transport occurs through one of two mechanisms:

- Movement of dissolved or colloidal material because of random molecular, or thermal, motion along continuous water pathways within the waste package (diffusive transport)
- Movement of dissolved or colloidal material because of the bulk flow of a fluid, which in this case is water, through the waste form and waste package (advective transport)

Waste form degradation and radionuclide mobilization depend on the initial waste form type and amount, the initial design of the system and the processes occurring in the drift environment. Thermal history and package lifetime determine the temperature of the waste forms when they are exposed to degrading processes. Composition of the gas phase and aqueous chemistry of incoming water, along with the waste temperature, control the rates of waste form degradation and the nature of mobilized products available for transport.

The engineered barrier system is comprised of all components of the repository within the drifts. The analysis of transport of radionuclides within the engineered barrier system requires definition of numerous parameters and models. This transport is influenced by waste package degradation; waste form degradation, including cladding degradation; the thermal-hydrologic and chemical environment; and design of the engineered barrier system. Radionuclides released from the engineered barrier system enter the natural system for transport through the unsaturated and saturated zones to the

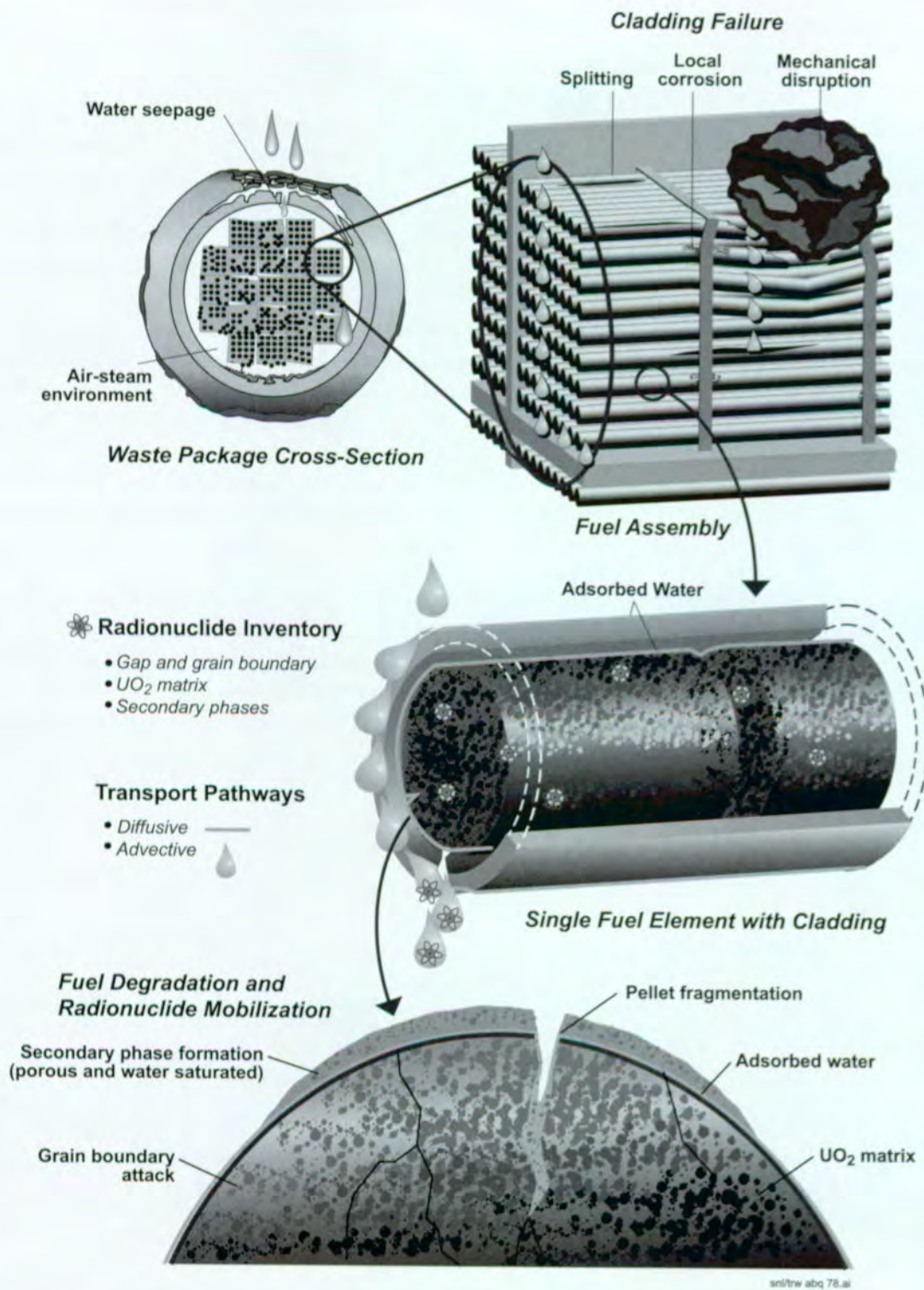


Figure 3-50. Schematic of Waste Form/Waste Package/Engineered Barrier System

accessible environment where overall repository performance is measured.

The waste form degradation and engineered-barrier-release modeling studies presented in this section were prepared with the view of addressing selected aspects of the NRC Key Technical Issues on Container Life and Source Term (NRC 1998b), Evolution of the Near-Field Environment (NRC 1997c), and Total System Performance Assessment and Integration (NRC 1998a). Specifically, the information presented is pertinent to the container life and source term subissue on contribution of spent nuclear fuel resistance to degradation towards controlling radionuclide releases to the near-field environment, the near-field environment subissue on effects of coupled processes on rate of release of radionuclides from breached waste packages and the TSPA integration subissue on model abstraction.

The remainder of this section deals first with construction of the conceptual model for waste form degradation, radionuclide mobilization, and transport through the engineered barrier system. This is followed by a discussion of the implementation of the engineered barrier system model in the

performance assessment model, and the evaluation of some of the key aspects of the subsystem relative to performance. Additional information on the waste form degradation, radionuclide mobilization, and engineered barrier system transport component can be found in Chapter 6 of the *Total System Performance System Assessment-Viability Assessment (TSPA-VA) Analyses Technical Basis Document* (CRWMS M&O 1998i).

### 3.5.1 Construction of the Conceptual Model

The conceptual model for waste form degradation, radionuclide mobilization, and transport through the engineered barrier system incorporates the key processes expected to occur in the engineered barrier system. Figure 3-51 provides a summary of this model. The figure identifies input and output, key components of the model, and the bases for confidence in the model.

The waste form degradation and mobilization abstraction/testing workshop was held in February 1997 and focused on the key issues for this topic. The prioritization criteria, high priority issues relative to those criteria, and analysis plans from



Figure 3-51. Waste Form Degradation/Mobilization/Engineered Barrier System Conceptual Model

the workshop are presented in a summary in Table 3-12.

An expert elicitation was conducted to consider issues, including processes, parameter ranges, alternative models and uncertainties, related to waste form degradation and radionuclide mobilization and transport through the engineered barrier system. A six-member panel was selected to represent a range of expertise. Members were from both from within and outside of the YMP. Results from this elicitation were not available for the TSPA-VA base case, but preliminary input influenced both construction of the base case and some of the sensitivity analyses. Issues

Table 3-12. Waste Form Degradation and Radionuclide Mobilization Abstraction/Testing Workshop

| <b>Waste Form Degradation and Radionuclide Mobilization Abstraction/Testing Workshop</b><br>February 19-21, 1997, Livermore, CA<br>(CRWMS M&O 1997c)  |  |
|---|--|
| <b>Prioritization Criteria</b>  |  |
| Does the process/issue affect the   |  |
| <ul style="list-style-type: none"> <li>• Radionuclide concentration at the waste form?</li> <li>• Mass release rate of radionuclides from the engineered barrier system?</li> <li>• Time and spatial variability in mass release rate?</li> <li>• Form of radionuclides entering the unsaturated zone for transport?</li> </ul>   |  |
| <b>Highest Priority Issues</b>  |  |
| <ul style="list-style-type: none"> <li>• Spent nuclear fuel:                             <ul style="list-style-type: none"> <li>- Dissolution rate</li> <li>- Time dependent evolution of solution and alteration layer</li> <li>- Representation of evolution of the near-field</li> <li>- Exposed spent nuclear fuel surface area</li> <li>- Cladding degradation model</li> </ul> </li> <li>• High-level radioactive waste (glass) and other wastes                             <ul style="list-style-type: none"> <li>- Time dependent evolution of solution and alteration layer</li> <li>- Vapor hydration</li> <li>- Evolution of near-field environment</li> <li>- Dissolution rate</li> </ul> </li> <li>• Solubilities and engineered barrier system transport:                             <ul style="list-style-type: none"> <li>- Physical processes—water contact mode</li> <li>- Mobilization—colloids</li> <li>- Chemical processes—mobilization—fluid dependence</li> <li>- Physical processes—transport paths</li> <li>- Chemical processes—mobilization—solid dependence</li> </ul> </li> </ul> |  |
| <b>Analysis Plans</b>   |  |
| <ul style="list-style-type: none"> <li>• Cladding and canister credit</li> <li>• Spent nuclear fuel dissolution</li> <li>• Spent nuclear fuel dissolution water chemistry and precipitated phases</li> <li>• High-level radioactive waste glass degradation and release</li> <li>• Solubility limits</li> <li>• Engineered barrier system transport and release</li> </ul>  |  |

considered, preliminary suggestions from the elicitation panel, and advice incorporated in the TSPA-VA include the following:

- Exposed, wet, and active surface areas—The experts suggested several approaches to bounding values, with the TSPA representation being on the conservative side.
- Cladding degradation—The experts expressed concern about assuming the cladding provides waste isolation benefits because of the large uncertainties and limited available data. The panelists suggested several long-term degradation modes that were incorporated into the TSPA.
- Dissolution rate for spent nuclear fuel—The experts suggested several alternative approaches, but the results would effectively be consistent with the model currently being used for the TSPA.
- Radionuclide solubilities—The experts gave a range of opinions on radionuclide solubilities, with substantial support for conservative bounds.
- Secondary-phase retention of radionuclides—The topic of secondary phase evolution and retention of radionuclides created a variety of input, with support for pursuing this credit for sensitivity studies and for licensing.
- Rapid-release fractions—The experts suggested revision of rapid-release fractions, but doing so would not cause significant change in release rates for the TSPA-VA analysis.
- Dissolution rate for high-level radioactive waste—The panelists suggested additional sophistication in the dissolution model, but the TSPA model was found to be acceptable in providing a usable bound.
- Colloid formation—The panelists supported including colloidal mobilization processes

and discussed several approaches for providing bounds guided by the limited data.

The results of the expert elicitation are documented in the *Waste Form Expert Elicitation* (CRWMS M&O 1998k).

### 3.5.1.1 Input

The important input to the waste form degradation and mobilization models include the following:

- The inventory of radionuclides
- Thermal-hydrologic modeling results: temperature at the waste package surface, relative humidity at the waste package surface, and liquid saturation in the invert
- Results from waste package degradation
- Results from cladding degradation
- Water ingress to the system
- Amount of exposed fuel surface area caused by cladding degradation
- Near-field geochemical conditions

The following are key inputs to the transport model for the engineered barrier system:

- Parameters relating to mobilization of radionuclides from the waste form
- Flux and chemistry of the water moving through the system
- Retardation in and permeability of the engineered barrier system materials, for example, the waste package and the invert, or emplacement drift flooring

### 3.5.1.2 Output

The output from the modeling of waste form degradation, radionuclide mobilization, and engineered barrier system transport is a release of radionuclides from the engineered barrier system into the

geosphere. These releases are in both aqueous and gaseous form (although TSPA-VA does not model gaseous release), along with a colloidal fraction.

### 3.5.1.3 Components of the Models

The components of the models include the following:

- The initial inventory
- Degradation of the cladding on commercial spent nuclear fuel
- Dissolution rates for the waste forms
- Solubility constraints on radionuclide mobilization
- Formation of colloids and secondary mineral phases
- Flow and diffusion of radionuclides through the system and sorption within the system

### 3.5.1.4 Bases for Confidence in the Model

The model is based on a substantial amount of data in some cases, and reliance on expert elicitation in others. In particular, the waste inventory and the dissolution rates are based on data and testing that have been in progress for over 14 years. Values for radionuclide solubility have been obtained from a combination of testing and expert evaluation. The cladding model is based on evaluation of cladding degradation processes, zirconium experiments, and literature data. Colloid parameters are based on a range of laboratory experiments and field observations. Sorption parameters are based on both site-specific data and expert elicitation. For the TSPA-VA, natural analogs have been used to corroborate dominant processes related to waste form degradation and engineered barrier system transport.

Several issues pertaining to the engineered barrier system have not been fully evaluated. These issues include the effects of lining and tunnel collapse on engineered barrier system transport and thermal-mechanical effects on the engineered barrier system.

### 3.5.1.5 Inventory

The following waste forms are to be included in the potential Yucca Mountain Repository:

- Commercial spent nuclear fuel; irradiated uranium dioxide pellets encased in cladding
- High-level radioactive waste; canistered borosilicate glass waste
- DOE spent nuclear fuel; primarily canistered irradiated uranium encased in cladding
- Plutonium waste forms; mixed oxide spent nuclear fuel and canistered ceramic waste forms

The waste form for commercial spent nuclear fuel to be emplaced in the repository is comprised of 63,000 MTHM from both pressurized water reactor and boiling water reactor commercial reactors. The high-level radioactive waste is comprised of canisters of glass from four sources:

- Hanford Site
- Savannah River Site
- West Valley
- Idaho National Engineering and Environmental Laboratory

The canisters of glass contribute 4,667 MTHM equivalent to the repository. Each source of high-level radioactive waste was assumed to contribute the same MTHM percentage (46 percent) of their total high-level radioactive waste to the repository, because the total inventory (10,110 MTHM) is well over the repository allocation of 4,667 MTHM. The DOE spent nuclear fuel consists of over 250 different types of spent nuclear fuel (Duguid et al. 1997, p. A-2) and will contribute 2,333 MTHM to the total repository (Table 3-13). The major contributor to this waste form is the N-Reactor fuel currently stored at the Hanford Site. This waste form also includes 65 MTHM of naval spent nuclear fuel. The 50 metric tons of plutonium is

assumed to be disposed in a combination of mixed-oxide fuel and ceramic waste forms.

There are over 200 radionuclides in the waste inventory. However, for evaluation of postclosure performance, the number of radionuclides considered can be reduced based on several characteristics of the radionuclides:

- Decay of radionuclides with short half-lives
- Sorption characteristics
- Low biosphere dose conversion factors

The inventory that is used in the analysis is crucial in defining which radionuclides are released from the system and their concentrations. Based on these considerations and previous TSPA results (Wilson et al. 1994; Andrews et al. 1994), a limited number of dominant radionuclides were chosen for analysis. The inventory for the nine radionuclides included in the base case inventory for each of the three waste forms is presented in Table 3-14. The inventory includes ingrowth of radionuclides because of the decay of parent radionuclides that are not included in the analyzed inventory. For example, all of the americium-241 and plutonium-241 in the waste is assumed to decay to neptunium-237 when the waste is emplaced to determine the initial inventory of neptunium-237. Radionuclide decay of the nine radionuclides is accounted for during the analysis, but daughter product ingrowth has been incorporated into the initial inventory. Also a simplified approach is used that adjusts the radionuclide source term to compensate for the production of the radionuclides neptunium-237, uranium-234, and protactinium-231. In the case of neptunium-237 and uranium-234, where the parents of concern have a shorter half-life, it was assumed that the parents had decayed to the isotopes of interest at the start of the simulation. However, for protactinium-231 the half life is much shorter than that of the parent, uranium-235. To allow for the neglect of decay, it was assumed that the protactinium was, at all time, in secular equilibrium with the uranium parent, that is, for every curie of uranium in the waste form there was a curie of protactinium. A portion of the inventory is expected to be in the void space between the fuel and the cladding, allowing for rapid release of

Table 3-13. U.S. Department of Energy Spent Nuclear Fuel Categories, Typical Spent Fuel in Each Category, and Metric Tons Heavy Metal in Each Category

| Category                                    | Typical Spent Fuel  | MTHM               |
|---|---|--------------------|
| 1. Uranium metal                            | N-Reactor   | 1979.88            |
| 2. Uranium-Zirconium alloy                  | Heavy Water Component Test Reactor                            | 0.04               |
| 3. Uranium-Molybdenum alloy                 | Enrico Fermi Reactor  | 3.51               |
| 4. Uranium oxide                            | Commercial Pressurized Water Reactor                          | 92.06              |
| 5. Uranium oxide (disrupted clad)           | Three Mile Island core debris                                 | 81.18              |
| 6. Uranium-Aluminum alloy                   | Advanced Test Reactor   | 8.15               |
| 7. Uranium silicide                         | Foreign Research Reactor-Materials Test Reactor               | 10.78              |
| 8. Uranium-Thorium carbide (high integrity) | Fort St. Vrain  | 23.01              |
| 9. Uranium-Thorium carbide (low integrity)  | Peach Bottom  | 1.55               |
| 10. Uranium-Thorium carbide (non-graphite)  | Fast Flux Test Facility carbide                               | 0.14               |
| 11. Mixed oxide                             | Fast Flux Test Facility oxide                                 | 11.49              |
| 12. Uranium-Thorium oxide                   | Shippingport Light Water Breeder Reactor                      | 46.30              |
| 13. Uranium-Zirconium hydride               | Training Research Isotope-General Atomic                      | 1.89               |
| 14. Sodium-bonded <sup>a</sup>              | Will be treated prior to disposal                             |                    |
| 15. Naval spent nuclear fuel                | Naval Nuclear Propulsion Uranium Based with Zircaloy Cladding | 63.00 <sup>b</sup> |
| 16. Miscellaneous                           | Not specified   | 10.01              |
| Total <sup>c</sup>                          |   | 2332.99            |

Source: CRWMS M&O 1998i, Section 6.

<sup>a</sup>Sodium-bonded spent nuclear fuel was not analyzed.

<sup>b</sup>At the time of publication of this document, the intent is to allow 65 MTHM of naval fuel into the repository; however, at the time the TSPA-VA analyses were completed, the direction was to only emplace 63 MTHM (CRWMS M&O correspondence, Robert W. Andrews, Duke Engineering & Services, Las Vegas, Nevada from E.P. Stroup of Lockheed Martin Idaho Technologies Company, Idaho Falls, ID, May 4, 1998). Therefore, all of the TSPA-VA analyses have been completed with the assumption of 63 MTHM of naval fuel. The difference between these two numbers would have a negligible effect on the outcome of the analyses.

<sup>c</sup>The total amount of DOE spent nuclear fuel is approximately 2,496 MTHM which was reduced by about 7 percent to reach 2,333 MTHM.

Table 3-14. Inventories for Various Waste Forms

| Radionuclide     | Waste Package Type                     |                                       |                                 | Half-Life (Years)  |
|------------------|--|---------------------------------------|---------------------------------|--------------------|
|                  | Commercial Spent Nuclear Fuel (Ci/pkg) | High-Level Radioactive Waste (Ci/pkg) | DOE Spent Nuclear Fuel (Ci/pkg) |                    |
| Carbon-14        | 11.7                                   | 0                                     | 0.31                            | $5.73 \times 10^3$ |
| Iodine-129       | 0.29                                   | 0.0000417                             | 0.00567                         | $1.57 \times 10^7$ |
| Neptunium-237    | 11.4                                   | 0.735                                 | 0.153                           | $2.14 \times 10^6$ |
| Protactinium-231 | 5.08 <sup>b</sup>                      | 0.0364                                | 0.661                           | $3.30 \times 10^4$ |
| Plutonium-239    | 3050                                   | 24.3                                  | 115                             | $2.41 \times 10^4$ |
| Plutonium-242    | 17                                     | 0.02                                  | 0.114                           | $3.87 \times 10^5$ |
| Selenium-79      | 3.72                                   | 0.286                                 | 0.0885                          | $6.50 \times 10^4$ |
| Technetium-99    | 118                                    | 29.5                                  | 2.55                            | $2.13 \times 10^5$ |
| Uranium-234      | 21.1                                   | 0.898                                 | 0.541                           | $2.45 \times 10^5$ |

Source: (CRWMS M&O 1998i)

<sup>b</sup>gm/waste package

Note: These inventories are for 30-year old fuel.

these radionuclides when the cladding fails (CRWMS M&O 1998i, Chapter 6).

The waste form inventory was abstracted to allow appropriate analyses. Figure 3-52 shows the abstraction of the inventory. This abstraction allows representation of the inventory as three separate waste forms in the total system analyses.

### 3.5.1.6 Cladding

The evaluation of cladding degradation includes the processes expected to affect the cladding over long periods of time. The analysis assumes a small fraction, 0.1 percent, of the commercial spent nuclear fuel rods to have failed from reactor operations. This is actually two times higher than data reported by the Electric Power Research Institute (EPRI 1997, p. 4-1). A small fraction, 1.15 percent, of the commercial spent nuclear fuel waste has stainless steel cladding. This cladding is assumed to fail immediately after the waste package fails because of rapid corrosion of stainless steel relative to the time scale being considered. Additional mechanisms in the cladding model include creep failure, which is primarily only an issue at high temperatures, and general and localized corrosion failure. Another long-term failure mechanism for fuel rods is mechanical disruption. After the waste package has lost structural integrity, mechanical loads caused by rocks falling from the drift walls and ceiling and disruption of the fuel support structure may break the fuel rods (CRWMS M&O 1998a, p. 45).

### 3.5.1.7 Dissolution Rates

The dissolution rate of the waste forms is another aspect of the system that requires analysis because this process provides the rate at which the radionuclides are made available for mobilization and release. Because the three major waste forms analyzed in TSPA-VA have different characteristics, it is essential to have a unique dissolution model for each waste form.

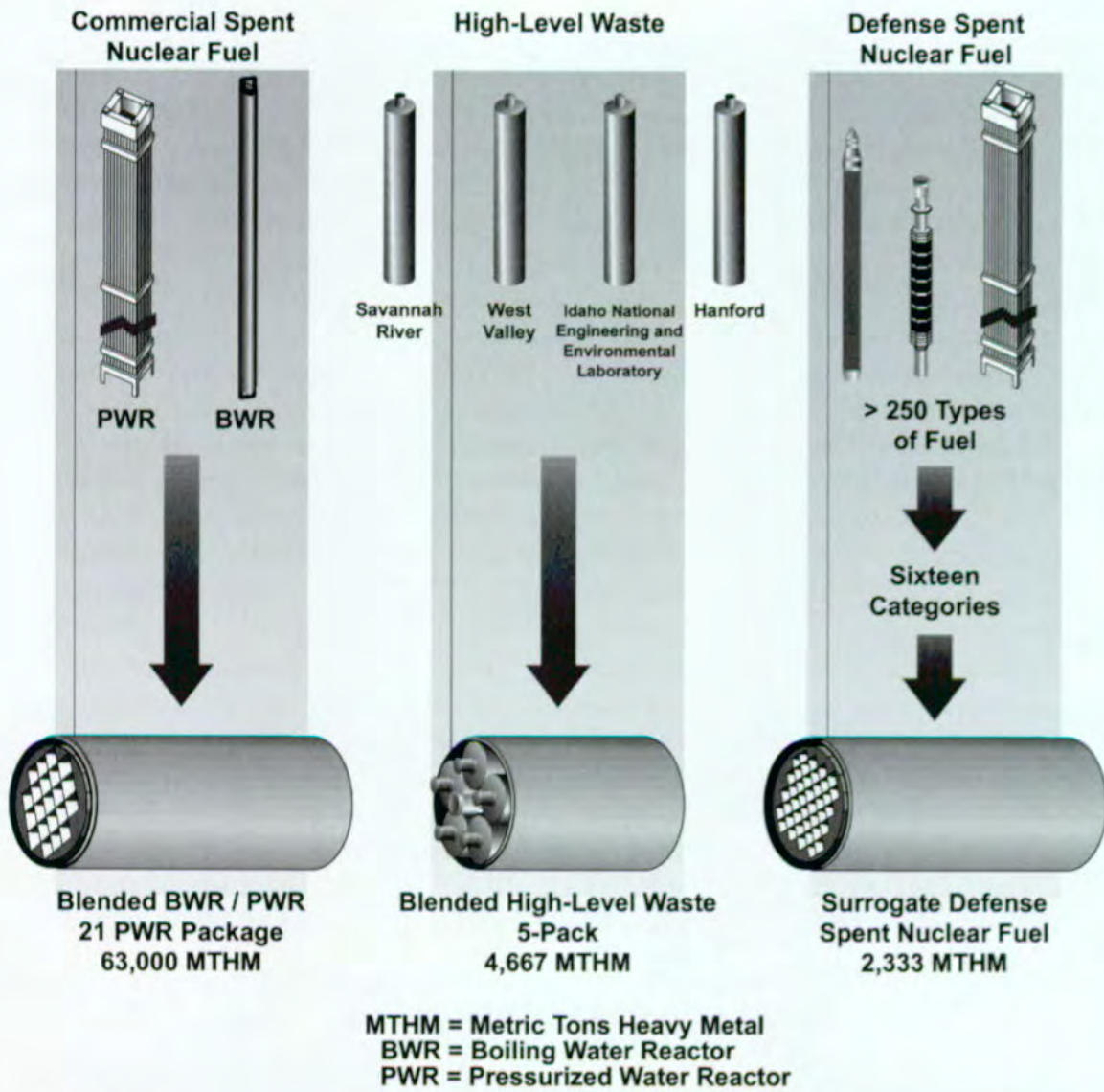
The dissolution rate for commercial spent nuclear fuel is a parametric equation that has been fitted to high flow-rate experimental data on commercial

spent nuclear fuel and uranium oxide. This fit provides dependence on temperature, pH, total carbonate ( $[\text{CO}_3]_{\text{T}}$ ), burnup, and oxygen potential. The rate is expressed in mass dissolved from a given surface area in a given time. The effective surface area is derived from experimental observations and accounts for fracturing of fuel pellets and some grain boundary activity. The dissolution rate is used as a conservative upper bound for the availability of radionuclides to mobilize. This dissolution rate does not account for solubility limits or retention of radionuclides in secondary phases that may form (see Section 3.5.1.8).

The model developed for high-level radioactive waste dissolution is based on or is consistent with several types of tests that are used to define the processes, fit rate parameters, or confirm general behavior. The forward reaction rate parameter used in the model is developed from data from laboratory tests that monitor a single flow across fuel material. The saturation term comes from chemical kinetic theory and is consistent with the results of static tests. The temperature effect is based on single pass flow through tests performed from 25° to 70°C (77° to 158°F) and is consistent with static tests done at temperatures up to 250°C (482°F). The evolution of secondary phases and dissolution rates under low flow conditions is consistent with low flow rate drip tests and vapor hydration tests.

The DOE spent nuclear fuel included in the repository is comprised primarily of N-Reactor fuel. In the base case a surrogate is used for the DOE spent nuclear fuel that is composed of 2,333 MTHM with a radionuclide inventory that is a weighted average of Categories 1, 4, 5, 6, 8, and 11 (as defined in Table 3-13). These categories were found to contribute significantly to dose from all DOE spent nuclear fuel (Duguid et al. 1997). A reasonable dissolution-rate model for this surrogate waste form is the metallic fuel model. The uranium metal fuel radionuclide release rate is expected to be very close to the uranium matrix dissolution or corrosion rate. The dissolution rate model was developed by fitting a response surface to the available data. When the repository temperature is below 100°C (212°F), water was assumed

## Waste Form Inventory Abstraction



|  |                          |  |
|--|--------------------------|--|
| $\frac{1}{2}$ 12 PWR 10.48 kW<br>1 21 PWR 2.91 kW<br>1 21 PWR 17.85 kW<br>2 x 44 BWR 6.44 kW | 1 Co-Disposal<br>4.06 kW | $\frac{1}{2}$ Direct-Disposal<br>0.73 kW |
|--|--------------------------|--|

**Inventory Abstraction for Thermal Hydrology Drift-Scale Model**  
 (One Drift Segment. See Section 3.2 for Explanation)

Figure 3-52. Inventory Abstraction

to be present on the waste form (wet oxid conditions) and humid air conditions are assumed for all other times.

### 3.5.1.8 Solubility Limits

The concentration of each radionuclide mobilized from the waste form cannot exceed the radionuclide solubility limit, unless suspended colloids are included. The solubility-limit model is a hybrid of solubility-limit distributions determined by expert elicitation (Wilson et al. 1994, pp. 9-1-9-11), previous assessments (EPRI 1992; Golder Associates 1993), and a reassessment of measured neptunium concentrations (CRWMS M&O 1997v; CRWMS M&O 1998c). Including the observed concentration for neptunium from waste form dissolution studies in the model is an initial attempt to incorporate the effect of secondary precipitation phases into the evaluation of release from the waste

form. Some of the elicited solubility constraints (americium, neptunium, plutonium) were also described as functions of temperature and pH (CRWMS M&O 1995). The neptunium solubility constraints currently range from a minimum value just below the maximum values based on spent-fuel drip tests (Finn et al. 1995) to a maximum value that encompasses the minimum values developed through the expert elicitation (CRWMS M&O 1998i). Additional work will refine this uncertainty in the future. Along the transport pathways through the engineered barrier system, the radionuclide concentrations are checked against the solubility limit. Table 3-15 lists the solubility distributions used in TSPA-VA analysis.

### 3.5.1.9 Colloids

Colloids may be important to performance for two reasons: they may increase the release of radionu-

Table 3-15. Solubility Limit Distributions

| RN | Distribution Type | Distribution Variable | Minimum Value<br>g/m <sup>3</sup> & [mol/L] | Maximum Value<br>g/m <sup>3</sup> & [mol/L] | Mean or Peak<br>g/m <sup>3</sup> & [mol/L] | C.V.            | Source                               |
|----|-------------------|-----------------------|---|---|--|-----------------|--------------------------------------|
| C  | ---               | ---                   | ---   | ---   | 1.2e4<br>[1.0]                             | ---             | Project Elicitation                  |
| I  | ---               | ---                   | ---   | ---   | 1.27e5<br>[1.0]                            | ---             | Project Elicitation                  |
| Np | beta              | log (Concen.)         | log(1.2e-2)<br>[log(5e-8)]                  | log(2.4e+1)<br>[log(1.0e-4)]                | log(3.4e-1)<br>[log(1.4e-6)]               | 1.20<br>[0.099] | CRWMS M&O 1998i                      |
| Pa | uniform           | log(Concen.)          | log(2.3e-5)<br>[log(1.0e-10)]               | log(2.3)<br>[log(1.0e-5)]                   | log(7.3e-3)<br>[log(3.2e-8)]               | ---             | Project Elicitation                  |
| Pu | uniform           | Concen.               | 2.4e-3<br>[1.0e-8]                          | 2.4e-1<br>[1.0e-6]                          | 1.2e-1<br>[5.1e-7]                         | ---             | Project Elicitation*                 |
| Se | triangular        | log(Concen.)          | log(7.9e+2)<br>[log(1.0e-2)]                | log(5.5e+5)<br>[log(7.0)]                   | log(7.9e+3)<br>[log(1.0e-1)]               | ---             | Golder Associates 1993,<br>EPRI 1992 |
| Tc | triangular        | log(Concen.)          | log(3.5e-2)<br>[log(3.6e-7)]                | log(9.9e+5)<br>[log(1.0e+1)]                | log(1.0e+2)<br>[log(1.0e-3)]               | ---             | Golder Associates 1993,<br>EPRI 1992 |
| U  | beta              | log(Concen.)          | log(2.4e-3)<br>[log(1.0e-8)]                | log(2.4e+3)<br>[log(1.0e-2)]                | log(7.6)<br>[log(3.2e-5)]                  | 1.02<br>[0.2]   | Project Elicitation                  |

log—refers everywhere in the table to the base 10 logarithm.

RN—radionuclide

Mean or Peak—The values listed are the arithmetic mean for all distributions *except* log triangular distributions where the values listed correspond to the peak of the distributions. NOTE: For any distribution of log (concen.), the value of the mean is *not equivalent* to the log (mean) for the corresponding distribution of concentration.

C.V.—Coefficient of Variation, which equals the absolute value of the ratio of the Standard Deviation to the Mean. Values given only for log beta distributions.

e+ represents positive power(s) of ten

e- represents negative power(s) of ten

\*—indicates modifications to original source information

Project Elicitation—Conducted at Sandia National Laboratory on April 13, 1993.

clides from the waste package, and they may increase the transport velocity of radionuclides. When a radionuclide concentration is solubility limited, transport as mobile colloids increases the release of the radionuclide from the waste package. The transport velocity of radionuclides attached to colloids may be faster than that of dissolved radionuclides because colloids may travel in the faster parts of the flow paths, and colloids may sorb to host rock less than dissolved radionuclides.

While many radionuclides have the potential for colloidal transport, this initial colloid analysis focused on plutonium. Plutonium is a major part of the waste inventory, has low solubility and high sorption onto host rock, and is the radionuclide most likely to be affected by colloidal transport. As more data are obtained, colloidal transport of additional radionuclides will be investigated.

Many types of colloids are expected to be present in the Yucca Mountain repository system, but only four types were chosen for explicit modeling: clay, iron corrosion products, spent nuclear fuel colloids, and glass waste colloids. The spent nuclear fuel and glass waste colloid types refer to all colloids that are produced during the degradation of the waste forms containing these waste types. The four colloid types were chosen because they may be present in significant concentrations and have enough attached plutonium to affect repository performance. The effect, however, will depend on the transport properties of the colloids, for example, velocity, filtration, and sorption, and the reversibility of the plutonium attachment to colloids.

For this initial modeling of colloids, transport was assumed to be unretarded through the fracture continuum. The reversibility of plutonium attachment to colloids has been investigated at Los Alamos National Laboratory. Their studies of sorption/desorption of plutonium (IV) and plutonium (V) on hematite, goethite, and clay show fast attachment and slow detachment. Therefore, sorption of dissolved plutonium onto the major near-field and far-field colloids is expected to be reversible on the time scale of transport to the accessible environment (hundreds to millions of years). The reversibility of attachment to waste

form colloids, however, has not been determined. Co-precipitation, in particular, has the potential to create colloids having radionuclides encapsulated by stable minerals. Workers at Argonne National Laboratory have observed radionuclide-containing phosphate minerals co-precipitated with clays in their glass dissolution experiments for high-level radioactive waste. These colloids may be able to move large distances without giving up their radionuclides. It is not clear what fraction of waste form colloids may have irreversibly attached radionuclides. Experiments are planned to address this issue.

### **3.5.2 Implementation of the Waste Form Degradation and Mobilization Model**

The various components of the waste form degradation and mobilization model are included in the TSPA analyses as abstractions from the observed data or expert elicitation. This section discusses the major models included in the analyses: cladding, waste form dissolution, solubility, colloids, and engineered barrier system transport.

#### **3.5.2.1 Cladding Model Abstraction**

Most of the commercial spent nuclear fuel is encased in Zircaloy cladding that isolates it from the environment. Models were developed to describe cladding degradation from creep, corrosion, and mechanical failure, or rockfalls. The model assumed cladding was failed at the time of emplacement in the repository for the stainless-steel-clad fuel (1.15 percent of inventory; CRWMS M&O 1998a, p. 30) and for fuel with defective cladding from reactor operation (0.1 percent; EPRI 1997, p. 4-1). The latter type of failure is termed "juvenile" cladding failure. Both creep and delayed hydride cracking, a process where hydrides facilitate cracking of the cladding, were modeled, but neither contributes significantly to the amount of fuel available for dissolution. Hydride embrittlement was also evaluated. If the assumption is made that the waste package failed after 100 years (during high temperature period), the amount of hydrogen taken up from the cladding corrosion is less than 50 ppm. This level of uptake of hydrogen is expected to have negligible effect on the cladding fracture toughness. For instance,

Kreyns et al. (1997, p. 766) showed that the fracture toughness decreased from 42 MPa-m<sup>0.5</sup> to 8 MPa-m<sup>0.5</sup> as the hydrogen content increased from zero to 4,000 ppm, a hydrogen uptake value much higher than is expected for the cladding.

One cause of cladding already being failed when it arrives at the repository is the type of cladding used in early fuel designs. Fuel design for commercial reactors has been evolving. Eight of the earlier reactors used stainless steel cladding, but no operating reactor currently uses this type of cladding. This type of fuel represents a total of 723 MTU, 1.15 percent of the estimated 63,000 metric tons of commercial fuel to be placed in the repository. Because the stainless steel cladding is expected to corrode rapidly relative to Zircaloy, this fraction of the fuel is likely to be exposed for dissolution when the waste package fails.

The failure rate for commercial fuel that is clad in Zircaloy has improved with time. Reactor cores prior to 1985 had an individual fuel rod or pin failure rate from 0.02 percent to 0.07 percent (EPRI 1997, p. 4-1). The pin failure rate has decreased to the current rate of 0.006–0.03 percent, (EPRI 1997, p. 4-2) with an average pin failure rate for both time periods of 0.01–0.05 percent. Occasionally, a specific core will have a higher failure rate, with the highest reported rate being 0.4 percent. For this analysis, the pin failure rate is intended to represent a conservative average, and not the extreme damage to a single core or assembly. The analysis assume an average of 0.1 percent of all pins are damaged to some degree. This is approximately twice the rate of failures in EPRI (1997, p. 4-1).

In the early stages of postclosure (first 50 years), the cladding could be damaged by creep or strain failure if the temperature (and, therefore, cladding stress) is high enough. This failure mode leads to a pinhole or hairline crack. This type of failure is not predicted to occur for pins in the average waste package and does not significantly contribute to the source term.

The fraction of fuel exposed for dissolution is used directly in the RIP computer program that

integrates the components of the repository system. The type of pin damage from reactor operation can be characterized as follows (EPRI 1997, pp. 4-3,):

- Pinhole and hairline cracks 80–90 percent
- Intermediate condition 0–20 percent
- Severe damage 0.04–0.9 percent

The fuel damaged by creep failure has either a pinhole or a hairline crack, exposing a very limited amount of fuel. The fuel temperatures are too low to produce U<sub>3</sub>O<sub>8</sub> and cladding unzipping, or tearing open. Therefore, only a limited amount of fuel is exposed for dissolution. The analysis assumes that the exposed fuel from juvenile failures, 0.1 percent of total fuel, has no cladding and is available for dissolution. This amount is added to the amount of fuel exposed because of the failure of stainless steel cladding, yielding a total of 1.25 percent of commercial fuel available for dissolution when the waste package fails. This approach is potentially non-conservative because it spreads the release over a larger area than if all stainless steel clad fuel was packaged together. The overall effect on performance however is negligible because of the mixing in the unsaturated zone.

Zirconium corrosion has been studied since 1946 when commercial grades became available. Rothman (1984, p. 11) compared the oxidation rates for Zircaloy, an alloy of zirconium, assessed by six different authors and predicts corrosion amounts that vary from 4 to 53 microns for cladding exposed for 10,000 years at 180°C (356°F). Rothman assumed (for both the pressurized-water reactor and the boiling-water reactor) that fuel was 10 years old, loaded to 44 kW/acre, 3.3 kW/package. Cladding temperatures start out at about 330°C (626°F) and cool to about 100°C (212°F) in about 1,000 years. The water used was J-13. All of the corrosion rate models use a temperature dependency that predicts near zero corrosion rates at long-term repository temperatures. Using recent correlations by four different authors, Einziger (1994, p. 556) for dry oxidation, VanSwam and Shann (1991, p. 771) for wet oxidation, Hillner et al. (1998, p. 6) for the most recent naval spent nuclear fuel wet correlation, and Hillner et al. (1998, p. 23 eg. 6) for this

widely used EPRI sponsored model, an analysis of the hottest pin in an average waste package exposed to the temperature history predicted at YMP gives corrosion depth from 1 to 5 microns if the waste package is assumed to have a breach at emplacement. The hottest pin in the hottest waste package would have from 38 to 93 microns of oxidation depending on the correlation used and again assuming that the waste package had a breach at emplacement. If the hottest waste package stays sealed for 50 years and then is breached, the hot pin cladding will oxidize to a depth of 2–10 microns. Such depths are small compared to the cladding thickness, which is typically 570 microns.

Yau and Webster (1987, pp. 707-708) reviewed the aqueous corrosion of Zircaloy in various chemical environments. While it is corrosion resistant in typical environmental conditions, Zircaloy is susceptible to corrosion by fluoride ions (greater than 100 ppm and pH dependent); hydrofluoric acid; and aqua regia, which is a mixture of nitric and hydrochloric acids. Yau and Webster (1987, pp. 709, 717) reported that Zircaloy is resistant to crevice corrosion, which is corrosion facilitated by conditions in a crevice between two pieces of metal. If the Zircaloy oxide layer is removed, Zircaloy is susceptible to galvanic corrosion if coupled to a more noble metal, either platinum, gold, graphite, titanium, or silver. It has a corrosion rate of 18 microns per year in a 3.5 percent boiling sodium chloride solution containing 500 ppm of copper ions at a pH equal to 5; however, there was no observed corrosion at a pH equal to 6 (Yau and Webster 1987, p. 717, Table 13). Zircaloy is susceptible to pitting from ferric chloride ions. Ferric chloride pitting requires ferric ions, and the pH must be less than 3. Current analysis of the water chemistry inside the waste package predicts that the pH is above 7.0. However, the chemistry within the waste package, hence the long term performance of Zircaloy cladding, is not well understood and has considerable uncertainty. Stress corrosion cracking has been observed in fuel pin locations that have high local stresses from pellet interactions. Such interactions are not expected after reactor discharge when the pellet contracts from the cladding.

Corrosion of Zircaloy was modeled using the waste package degradation computer code. This model assumes corrosion occurs after 100,000 years. Experimental results are available for corrosion of Zircaloy and high-nickel alloys such as Alloy 22, (other types of material used for cladding), under very severe conditions of hot, concentrated acids. Corrosion rates for the Zircaloy tend to be from ten to many thousands of times slower than the high-nickel alloys such as Alloy 22 under extreme acid conditions.

The Zircaloy corrosion model calculated the fraction of cladding patches that are 75 percent corroded using the Alloy 22 general corrosion model with the corrosion rate decreased by a factor of 10 (upper limit) and 1,000 (lower limit). For each realization, corrosion of the Zircaloy starts at the first penetration of the waste package, and the fuel area exposed (fraction of failed patches) is calculated as a function of time. Fuel exposure is initiated at about 30,000 years after the first patch penetrates the waste package. After one million years, the amount of fuel that could be exposed with this model ranges from 0.3 percent to 40 percent.

Rockfall onto the fuel after a waste package has experienced general corrosion causes mechanical failure. The assumed sequence of events leading to mechanical failure is the following:

- Rocks fall onto the upper surface of the waste package.
- The inner supports of the waste package fail and the fuel falls to the bottom of the waste package.
- Rocks fall 20 cm (8 in.) from the top of the waste package to the top of the fuel.

A separate statistical analysis of Zircaloy mechanical failure caused by falling rocks predicts that 0.2 percent to 11 percent of the fuel is exposed by this mechanism over 1 million years (CRWMS M&O 1998a, p. VIII-9). Mechanical failures are expected to begin to occur at 100,000 years as the loss of waste package integrity becomes significant. The failure rate is assumed to continue

linearly on a logarithmic time scale to 1 million years.

### 3.5.2.2 Dissolution Rates

#### Commercial Spent Nuclear Fuel Dissolution.

The dissolution of spent nuclear fuel and radionuclide release are not thermodynamic equilibrium processes, so the development of a dissolution rate model uses concepts from nonequilibrium thermodynamics. The objective is to derive an equation for the dissolution rate consistent with quasi-static thermodynamic processes and laboratory data. Currently, detailed knowledge is not available for the sequence of chemical and electrochemical reaction steps to describe the dissolution process over the range of spent nuclear fuel inventory, potential water chemistries, and temperatures. The current approach is to obtain an experimental database of dissolution rates for a subset of specific spent nuclear fuels over a range of controlled, aggressive water chemistries and temperatures. These data are then used to evaluate empirical parameters in a rate law to describe the dissolution rate of spent nuclear fuel (Stout and Leider, 1997, p. 3.4.2-1).

The test data for dissolution response were best represented by a model, in the form of a rate law as a product polynomial of the bulk water chemistry concentrations and temperature. This follows the form of the Butler-Volmer equation, which is commonly used in correlation of corrosion and electrochemical rate data. In the above approach, thermodynamic nonequilibrium was assumed for the dissolution process. By substituting the traditional chemical potentials that include a logarithmic dependence on activities or concentrations for the chemical potential changes in the Butler-Volmer-like model form, the classic chemical kinetic rate law was derived.

Burnup was represented as a concentration term as well, because it is proportional to the aggregated production and concentration of fission products. For regression purposes, the model was linearized by taking logarithms of each term, and fitting that equation, and allowing cross and quadratic terms to explain interactions and nonlinearities. This model describes features of the chemical dissolution

processes far from thermodynamic equilibrium and provides a reasonably good fit to the available data. Depending on the terms and coefficients in the model, extrapolation outside the measured independent variable space could cause large prediction errors. The TSPA-VA model does not extrapolate outside the range of measured values.

#### High-Level Radioactive Waste Dissolution.

Experimental and modeling work on aqueous alteration of borosilicate glass shows that the most important parameters in predicting glass alteration rates are temperature, exposed surface area, solution pH, and dissolved silica concentration in solution (O'Connell et al. 1997, p. 2; Bourcier et al. 1994). Long-term dissolution models for borosilicate glass employ a rate equation that includes these parameters and is consistent with transition state theory. The rate equation indicates that the dissolution rate will slow down as the dissolution process of the borosilicate glass adds to the silica in solution. As the glass dissolves, secondary phases begin to precipitate. A fraction of the silica contained in the glass will be trapped in the secondary phases. Thus only a fraction of silica in altered glass actually dissolves in the solution. That fraction depends on the types and amounts of alteration minerals that form during the glass alteration process.

The experimental data for several glass compositions show that even when the solution is saturated with silica after a long period of time, there persists a residual dissolution rate, as evidenced by the continuously increasing concentrations of certain highly soluble elements of the glass composition (Grambow 1987, pp. 34-37). This requires an additional parameter to the rate equation which accounts for this residual reaction rate under silica saturated conditions. The TSPA-VA analyses do not include any performance credit for the stainless steel canister for the glass waste form. The analyses assume failure of the canister after waste package failure.

### 3.5.2.3 Solubility Limits

The waste form dissolution model initially provides calculated upper and lower boundary values on the aqueous concentration of radionu-

clides in groundwater that has reacted with the waste form. Subsequently, these values are filtered by comparing them with solubility-limited values that are sampled from either a distribution of solubility limits for radionuclide-bearing minerals or a functional form for the solubility limit for each radionuclide considered. If the sampled solubility-limited value is lower for the given radionuclide than its derived concentration from the waste form dissolution model, then the aqueous concentration is set to the solubility-limited value and the difference in mass is calculated to precipitate out of solution. These solubility-limited values place constraints on the aqueous concentration of the particular radionuclide element considered, with each isotope of that element present in proportion to its isotopic abundance.

### 3.5.2.4 Colloids

Colloids are particles that are small enough to become suspended and transported in a liquid. Based on experiments and observations to date, plutonium attachment to colloids can vary from relatively fast and reversible to effectively irreversible. However, the necessary parameter values for modeling plutonium attachment to colloids are not available. In addition, the performance assessment computer codes for modeling radionuclide transport currently cannot accommodate the complexity needed for these calculations. Instead, plutonium attachment to colloids has been modeled using the two extremes: instantaneously reversible attachment and totally irreversible attachment as shown in Figure 3-53. Partitioning of plutonium into these two categories is treated as a sampled parameter.

The reversible model assumes instantaneous equilibrium between dissolved radionuclides and colloid particles and was available within the RIP code for use in the near-field and the FEHM code for use in the far-field. The RIP model defines the amount of radionuclide mobilized in colloidal form as the product of the dissolved radionuclide concentration, the dissolved-colloid sorption partitioning coefficient ( $K_d$ ), and the colloid concentration. The colloid concentration was calculated as a function of the ionic strength of the fluids as

described in Section 3.3.3.4. The FEHM model combines the  $K_d$  and colloid concentration parameters into a single parameter; the aqueous-colloid partitioning coefficient,  $K_c$ . The parameter ranges used in the calculations are summarized in Table 3-16.

The irreversible model was also included in the calculation to capture the possibility of a fraction of the radionuclides moving rapidly through the transport system irreversibly attached to colloids. At the Benham nuclear test site at the Nevada Test Site, rapid transport of colloid-associated plutonium may have occurred (Thompson et al. 1998, pp. 13, 18). At 1.3 km (0.8 mile) from the blast site,  $1 \times 10^{-14}$  M colloid-associated plutonium was detected 30 years after the blast. It is not clear what fraction of the transport was caused by transport on colloids, injection through fractures at the time of the blast, or transport as dissolved plutonium. However, fracture injections have not been observed to extend beyond a few hundred meters and dissolved plutonium is expected to sorb strongly to the fracture surfaces. In fracture systems, colloids that are repelled from the host material walls may move even faster than nonsorbing dissolved species because they remain in the faster flowing portions of the flow paths. This behavior was seen in a fraction of specially designed colloids pumped through 32 m (105 ft) of fractured tuff near Yucca Mountain (CRWMS M&O 1997f). These observations suggest that some small fraction of colloid-associated plutonium may travel relatively quickly through water-filled fractures, but these observations do not adequately define the uncertainty in this process.

Table 3-16. Parameters Used in Reversible Attachment Model

|                                | $K_d$ (mL/g)  | Effective $K_c$          |
|--------------------------------|---------------|--------------------------|
| Near-field colloids            |               |                          |
| Clay                           | $10^3 - 10^5$ | $\sim 10^{-5} - 10^{-2}$ |
| Iron oxyhydroxy colloids       | $10^4 - 10^6$ | $\sim 10^{-4} - 10^{-1}$ |
| Spent fuel waste form colloids | $10^2 - 10^8$ | $10^{-5} - 1$            |
| Glass waste form colloids      | $10^2 - 10^9$ | $10^{-5} - 10$           |
| Far-field colloids             |               | $10^{-5} - 10$           |

Notes:

bold: as input

italic: effective value in calculation

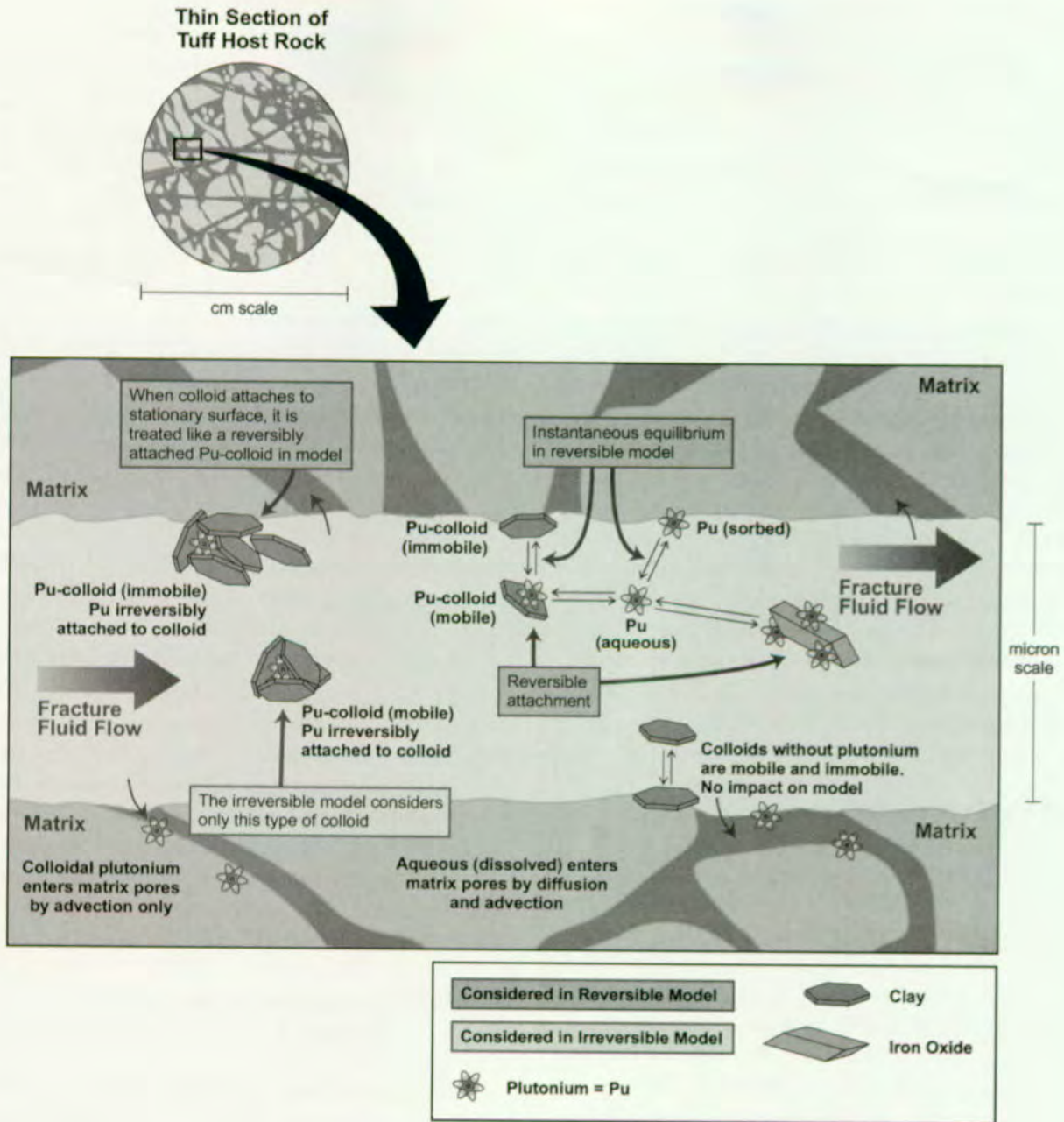


Figure 3-53. Colloidal Plutonium Transport

Specifics of colloid properties such as surface charge, size distribution, and stability in expected groundwaters, and of the transport and filtration properties in the pathways within the fractured tuff, and are not adequately known for accurate prediction at this time. These observations, however, were used to guide the selection of a large range for sensitivity studies. Based on the expected value plutonium solubility of  $5 \times 10^{-7} M$  and the observed  $1 \times 10^{-14} M$  colloidal plutonium concentration 1.3 km (0.8 mile) from the blast site, DOE has estimated that about  $1 \times 10^{-7}$  of the plutonium has attached irreversibly to colloids and also moved quickly. Because this estimate is quite uncertain and because the applicability of this estimate to transport within the Yucca mountain site is unknown, a three order of magnitude range was added to either side of this estimate. While this fraction includes effects from both source term and transport, it was implemented into the calculations at the interface between the engineered barrier system and the natural barrier system. The "irreversible plutonium" mass flux from the engineered barrier system to the unsaturated zone was calculated as the "reversible plutonium" mass flux times this irreversible plutonium fraction. Once passed to far-field, the "irreversible plutonium" was treated as a nonsorbing, slowly diffusing tracer.

### 3.5.2.5 Secondary Phase Analyses

Laboratory experiments (Wronkiewicz et al. 1992, p. 125) and field observations (Percy et al. 1994, pp. 713, 716, 718, 722, 724) demonstrate that when nuclear spent nuclear fuel is contacted by groundwater, it starts to dissolve and forms uranyl (uranium) minerals. The major secondary phases are schoepite, uranophane, Na-boltwoodite, and soddyite. Both theoretical prediction (Burns et al. 1997, pp. 1, 3-5, 8) and laboratory measurements (Buck et al. 1998, pp. 87, 91-93) indicate that neptunium would be incorporated into the structure of secondary phases during dissolution of spent nuclear fuel. Therefore, neptunium release would be controlled by the dissolution rate of secondary

phases. Based on this concept, a computer model has been built to calculate the release rate of neptunium using a reactive-transport simulator (Chen et al. 1995, p. 8-24; 1996, pp. 1051-1052).

The simulations start with schoepite, which is allowed to dissolve and precipitate uranophane, Na-boltwoodite<sup>5</sup>, and soddyite. The model assumes that the molar ratio of neptunium to uranium in schoepite is 0.0016, the same as that in the initial spent nuclear fuel inventory (with americium-241 and plutonium-241 grouped with neptunium-237). Two scenarios were considered: all of the neptunium released from schoepite dissolution goes into aqueous solution; and released neptunium is also incorporated into uranophane, Na-boltwoodite, and soddyite with the same uranium to neptunium ratio. Simulations with different temperature (30° and 70°C, or 86° and 158°F) and different cladding failure (1 percent and 11 percent) were carried out.

Simulated neptunium concentration at the bottoms of waste packages ranges from  $1 \times 10^{-9}$  to  $1 \times 10^{-6}$  mol/kg of solution. Based on the simulation results, a log-uniform distribution ranging from  $1 \times 10^{-9}$  to  $1 \times 10^{-6}$  mol/kg with a expected value of  $1 \times 10^{-7.5}$  mol/kg was proposed for a sensitivity study. This effort was the first attempt at including the attenuation of neptunium release because of the incorporation of neptunium in secondary phases. The lower limit of these simulations is consistent with the drip tests conducted at Argonne National Laboratory that reported neptunium concentrations of  $10^{-9}$  mol/kg (Finn et al. 1995, pp.65, 67).

### 3.5.2.6 Engineered Barrier System Transport

Radionuclide transport out of the waste form and waste package, through the invert system, and into the unsaturated zone is dependent on several events. The waste package must degrade, providing a path out of the waste package. The waste form must also degrade to allow radionuclide release. The primary transport medium is

<sup>5</sup> Unlike Argonne National Laboratory's drip tests, no Na-boltwoodite was seen in the simulations. It is believed to be caused by the inaccuracy in the thermodynamic data of Na-boltwoodite.

water, as previously discussed. Either a water film or moving water is necessary for radionuclide transport out of the waste package and through the remainder of the engineered barrier system. Gaseous releases were not analyzed in TSPA-VA.

The waste packages that are emplaced in repository areas with dripping water will degrade more rapidly. Also, radionuclide releases from degraded waste packages will be more rapid in repository areas with dripping water. If water is not dripping on a waste package, then a water film on a waste form and waste package can cause diffusive release, but this process is significantly slower than release caused by water moving through the waste package.

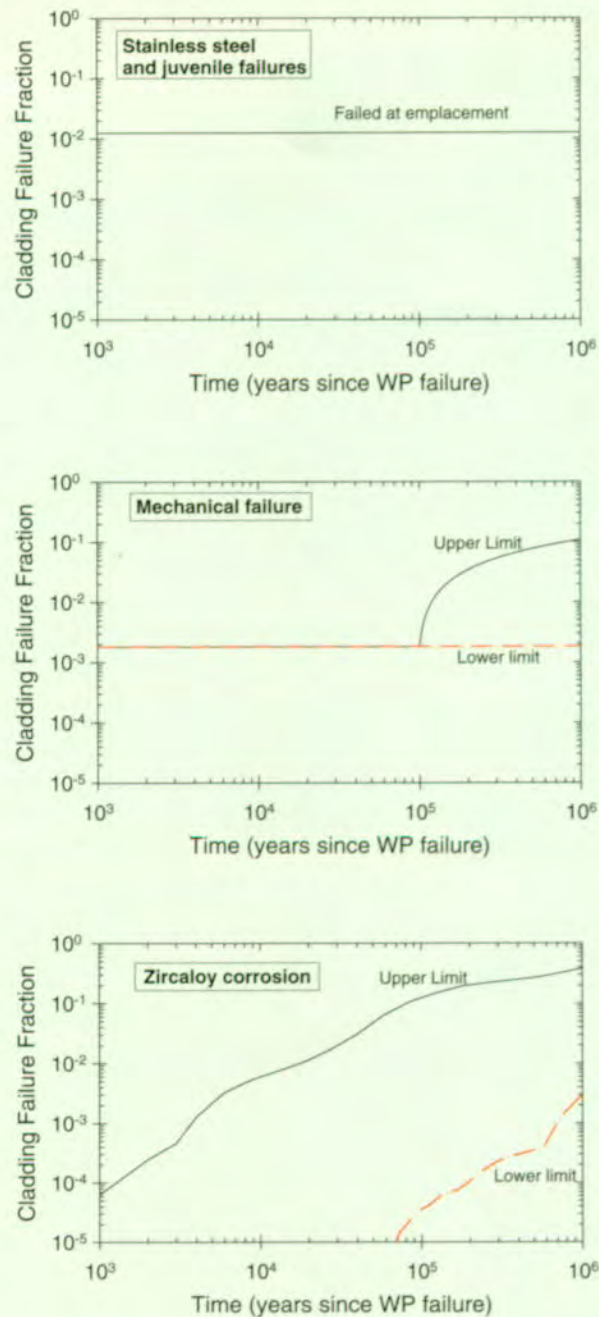
Transport through the invert can also occur because of advection and/or diffusion. Retardation in the concrete invert slows the transport. No degradation or reduction of permeability of the invert is modeled in these analyses.

### 3.5.3 Results and Interpretation: Evaluation of Issues Important to Performance

The model for waste form degradation, radionuclide mobilization, and transport through the engineered barrier system is an important part of the overall performance analysis of the repository system. The rate at which the waste forms degrade and the quantity of radionuclides that can be mobilized and moved out of the waste packages and through the engineered barrier system into the unsaturated zone provide the magnitude of release from the engineered barrier system. This release is reduced by decay and transport characteristics of the natural barrier system before reaching the accessible environment.

#### 3.5.3.1 Cladding Degradation

Several mechanisms can cause cladding degradation, as previously described. The resulting exposed surface area of the waste forms through time is shown in Figure 3-54. The two main causes of cladding degradation in the TSPA-VA analyses are mechanical failure and corrosion failure. These mechanisms are expected to be present, but the magnitude and timing of their effect on cladding



FV3035-5

Figure 3-54. Fraction of Commercial Spent Nuclear Fuel Surface Area Exposed as a Function of Time  
Fraction of commercial spent nuclear fuel surface area exposed as a function of time for the TSPA-VA base case, for several different failure mechanisms (see text). (WP—waste package)

degradation is uncertain. Section 5.5 provides sensitivity analyses of the effect of cladding on repository performance. Both the maximum and minimum values of exposed surface area through time are shown in Figure 3-54. Sampling between the maximum and minimum values using a log-uniform distribution is performed within the repository integration computer program. Before 60,000 years, the stainless steel clad fuel in breached waste packages and in defective waste packages will be available for dissolution when the waste package is breached. At about 100,000 years, waste packages that fail through both mechanical failure and corrosion will begin to expose more fuel for dissolution. At one million years, about 31 percent of the spent nuclear fuel in failed waste packages will be available for dissolution in the base case cladding model.

### 3.5.3.2 Waste Form Degradation

Under repository conditions, degradation of the commercial spent nuclear fuel occurs within a few thousand years, while degradation of the high-level radioactive glass waste form occurs over a period of 8,000 to 10,000 years. Thus, the degradation rates of both waste forms are not identified as key parameters in controlling long-term repository performance. This lack of importance of degradation rate could change if retention in less soluble secondary phases is considered, as is observed in dissolution tests at low flow rates that are currently underway. Another aspect of this is the radioactive decay of the initial inventory through time. Figure 3-55 presents the decay as a function of time to show the key long-lived radionuclides, especially neptunium, and the other important radionuclides initially present in the inventory.

### 3.5.3.3 Doses from DOE Spent Nuclear Fuel

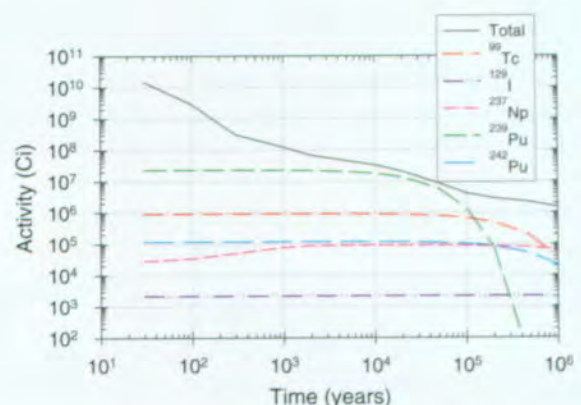
The DOE spent nuclear fuel is comprised of multiple waste form types with unique characteristics. The base case uses a surrogate for the many different types of waste in the DOE spent nuclear fuel inventory. A comparison of the surrogate DOE spent nuclear fuel to the spent nuclear fuel total is presented in Section 5.5.7.

### 3.5.3.4 Releases from Plutonium Waste Forms, High-Level Radioactive Waste, and the Commercial Spent Nuclear Fuel Waste Form

The comparison of releases from the plutonium waste form with the high-level radioactive waste and commercial spent nuclear fuel waste forms is also presented in Section 5.5.

### 3.5.3.5 Releases from Naval Spent Nuclear Fuel

One of the types of DOE-owned spent nuclear fuel to be disposed of in the potential repository is naval spent nuclear fuel. There will be approximately 65 MTHM of naval spent nuclear fuel. Because naval nuclear fuel is designed and built to meet demanding warship operating requirements, naval spent nuclear fuel cladding would outperform commercial spent nuclear fuel cladding in a repository environment. Through the repository environmental impact statement (EIS) data collection effort, the Naval Nuclear Propulsion Program provided values for the extremely small expected releases from naval spent nuclear fuel waste packages (Beckett 1998, Attachment A, p. 2).



FV3035-6

Figure 3-55. Activity as a Function of Time  
The reduction of activity for the total and some of the key radionuclides affecting the performance of the system is shown.

### 3.5.3.6 Remaining Uncertainties in Engineered Barrier System Analyses

There are several remaining areas in the analysis of the engineered barrier system that are not fully analyzed in the TSPA:

- The invert is assumed not to degrade with time but to retain the same transport characteristics of concrete for the duration of the analyses. However, the chemistry of the invert will probably change as the system is heated during the thermal period. Heating may alter the transport characteristics of the invert. Likewise, the invert sorption characteristics are not well known and are under study. The impact of more complex invert analysis on overall system performances is not expected to be significant because of the small transport length involved relative to the total transport length.
- The base case does not fully account for rock falling into the drift at later times, which is an expected condition. The cladding model attempts to evaluate some effect of rockfall on the cladding, but the rest of the analyses do not incorporate rockfall at later times. Rockfall may alter the thermal-hydrologic characteristics and enhance waste package degradation. Its effect on overall performance is uncertain.
- The effect of the secondary phases on subsequent radionuclide transport is not fully analyzed in the TSPA. Neither the dissolution rate of the secondary phase nor the identity of radionuclides that will become fixed in the secondary phases has been well characterized. This process could have the effect of delaying radionuclide releases, which may prove improved overall system performance.
- The amount of seepage into the waste package and onto the waste form has been previously discussed and is a significant factor in releases from the engineered barrier system. How much water actually enters the

waste package once it is breached is highly uncertain. The TSPA-VA analyses are conservative in this area.

- Diffusive transport out of a locally failed fuel rod is not explicitly considered and could significantly reduce release rates.

### 3.6 UNSATURATED ZONE TRANSPORT

As described in Volume 1, the repository is located in Yucca Mountain in the unsaturated zone, about midway between the ground surface and the regional water table. In the unsaturated zone, available voids in the rock, in the form of rock matrix pores and fractures, are filled partially with water and partially with air. The regional water table is the top of the saturated zone, below which the rock voids are fully saturated with water. Water movement is primarily downward through the unsaturated zone at Yucca Mountain, with possible lateral flow in certain regions such as perched water. The sequence of hydrogeologic units, their hydrologic and geochemical characteristics, and the imposed infiltration flux control radionuclide transport in the unsaturated zone. The unsaturated zone transport component of the TSPA evaluates the migration of radionuclides from their introduction at the edge of the engineered barrier system to the water table (Figure 3-56). Definitions of technical terms used in Volume 3 are available in the VA glossary.

The unsaturated zone transport modeling studies and analyses presented in this section were prepared with the view of addressing selected aspects of the NRC Key Technical Issues on Unsaturated and Saturated Flow under Isothermal Conditions (NRC 1997e; 1997f) and Total System Performance Assessment and Integration (NRC 1998a). Specifically, the information presented is pertinent to the unsaturated zone flow and transport under isothermal conditions subissue on the groundwater percolation through the repository horizon and the ambient flow conditions in the saturated zone, and the TSPA integration subissue on model abstraction.

Yucca Mountain was formed from a sequence of volcanic ash flows and ash falls that created a

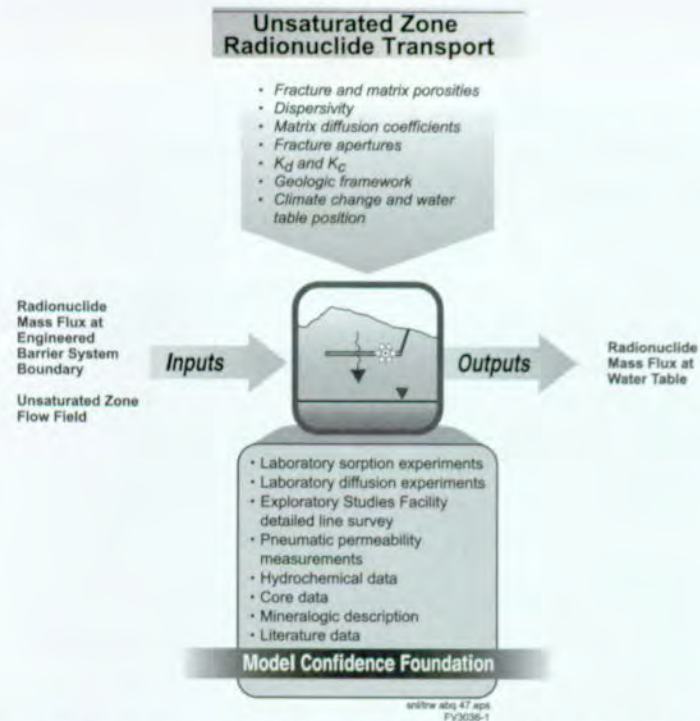


Figure 3-56. Coupling of Unsaturated Zone Radionuclide Transport to Other Total System Performance Assessment for the Viability Assessment Components

lithostratigraphic sequence of welded and nonwelded tuffs (Sawyer et al. 1994), as shown in Figure 3-57. The welded tuffs, formed by massive ash flows, are dense, brittle rocks with relatively low matrix porosity and a high fracture density. The nonwelded tuffs, formed from smaller ash flows and ash falls, are a more porous and elastic rock having relatively high matrix porosity and lower fracture density. The nonwelded tuffs can have either high or low matrix permeabilities depending primarily on the degree of alteration of the rock minerals into zeolites. Zeolitic units are common in the lower portions of the unsaturated zone and have matrix permeabilities similar to those in the welded tuffs. Nonwelded tuffs that have not been altered to zeolite, such as the nonwelded vitric tuffs, have much larger matrix permeabilities. Hydrogeologic stratigraphy of the unsaturated zone at Yucca Mountain is illustrated in Figure 3-57. The Calico Hills nonwelded unit may be further divided into vitric and zeolitic units.

An important characteristic of both the welded tuffs and nonwelded zeolitic tuffs is the difference in permeability between the fractures and the matrix. The fractures typically have permeabilities

that are several orders of magnitude larger than the matrix permeabilities, and fracture porosities that are orders of magnitude smaller than the matrix porosities. The differences are important characteristics of these tuffs because the high permeability, low porosity fractures can provide a much more rapid transport pathway to the water table than the matrix. On the other hand, the unaltered, or nonwelded, tuffs have larger matrix permeabilities that are of the same order of magnitude as the fracture permeabilities. These tuffs play an important role in the hydrologic behavior of the unsaturated zone because fracture flow is strongly attenuated, transport velocities are much slower, and contact of dissolved materials with the rock matrix is enhanced.

Perched water has been observed in some boreholes penetrating the repository, mainly in the northern area of the repository and along the western border of the Ghost Dance fault (see Figure 3-57). Perched water is a localized saturated zone that lies above unsaturated rock and the regional water table and typically forms on top of hydrogeologic units that have relatively low permeability. When present, perched water is

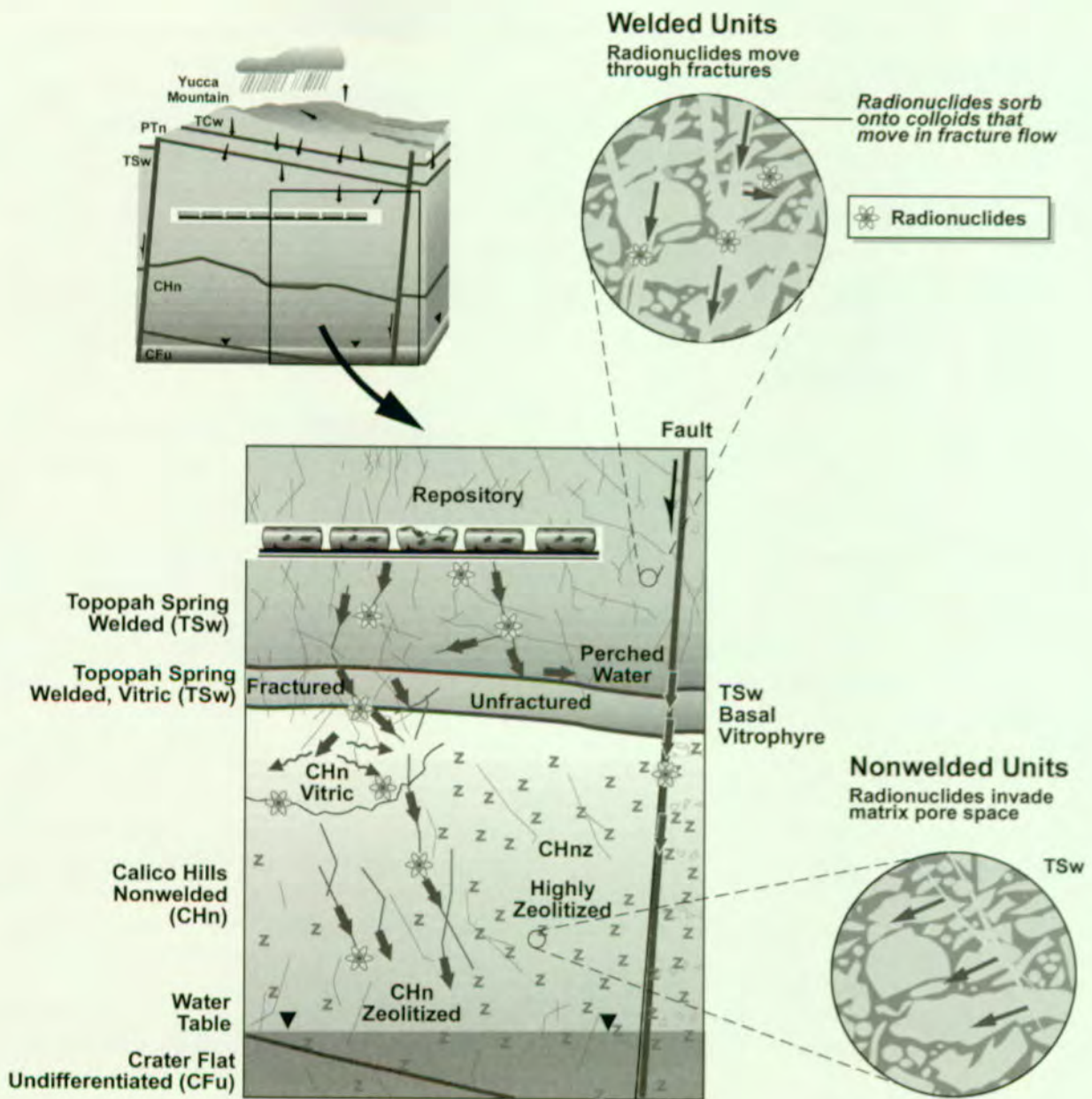


Figure 3-57. Conceptual East-West Hydrogeologic Section Through the Unsaturated Zone  
Conceptual east-west hydrogeologic section through the unsaturated zone at Yucca Mountain and process diagram for unsaturated zone radionuclide transport.

typically found at the base of the Topopah Spring welded unit and in areas of the Calico Hills zeolitic unit. These perched water bodies are believed to have formed by alteration of minerals in fractures to low permeability minerals that effectively block flow through the fractures (Bodvarsson et al. 1997, Section 13.5 pp. 13-13 and 13-14). This blockage of fracture flow will lead to lateral diversion of radionuclide transport if the percolation flux is sufficiently large. See Section 3.1 for additional information on unsaturated zone flow. Under nominal and most disruptive scenarios, transport of radionuclides through the unsaturated zone is one of several processes that impede the release of radioactive waste to the accessible environment after repository closure. The radioactive waste may migrate in unsaturated zone groundwater as a dissolved molecular species or associated with particles called colloids. Colloids are fine particles, between 0.001 and 1 micron that can interact with radionuclides through sorption and other chemical mechanisms, and are potentially mobile. Colloids reduce the interaction of the aqueous species with the rock matrix and enhance advective transport of the radionuclides, which is described below. Colloid interaction with radionuclides may be described in terms of reversible and irreversible interactions. Reversible interactions allow the radionuclide to detach from the colloid. For irreversible interactions, the radionuclide is attached to the colloid for the duration of the transport process.

Five processes affect the movement of dissolved or colloidal radionuclides: advection, diffusion, dispersion, sorption, and radioactive decay (de Marsily 1986, Chap. 10) (Figure 3-57). These processes are described below.

Advection is the movement of dissolved or colloidal material because of the bulk flow of a fluid, which in this case is water. This key transport mechanism can readily carry radionuclides through the approximately 300 m (984 ft) of unsaturated rock between the potential repository and the water table. Advection is also an important mechanism for radionuclide movement between fractures and rock matrix. In many of the hydrogeologic units, advection through fractures is expected to dominate transport behavior, primarily

because the expected flow rates through these systems exceed the matrix flow capacity under a unit gravitational gradient. Advection through fractures is fast because of high permeability and low porosity, with few opportunities for radionuclides to contact rock matrix. A few of the hydrogeologic units have much larger matrix permeability and are expected to capture most of the fracture flow by advection from the fractures to the matrix, causing much slower transport velocities and closer contact of the radionuclides with the matrix. Advective transport pathways result from and therefore follow the flow pathways, which are predominately downward. However, lateral diversion is expected along hydrogeologic unit contacts having strong contrasts in rock properties, particularly in areas of perched water. Flow that is diverted laterally ultimately finds a pathway to the water table through more permeable zones, which may be faults.

Diffusion is the movement of dissolved or colloidal material because of random thermal motion at the molecular scale. Diffusion results in mass flux at the continuum scale when the dissolved or colloidal material is nonuniformly distributed, that is, exhibits concentration gradients. It is not an effective mechanism for transport between the repository and the water table because of the large distance involved (about 300 m, or 984 ft). However, diffusion can play an important role in radionuclide exchange between fractures and rock matrix. Diffusion from fractures to the rock matrix can slow the advance of radionuclides undergoing advective transport through fractures.

Dispersion is a transport mechanism caused by localized variations in the radionuclide transport velocity due to localized variations in the flow field and molecular diffusion. These variations cause dispersion of the radionuclides both along and transverse to the average flow direction. Variations in both the magnitude and direction of the radionuclide velocity contribute to the overall dispersion. The dispersion resulting from variations in the flow field, under certain limiting conditions, can act in a manner analogous to diffusion, in which mass flux is proportional to the concentration gradient. Dispersion is most important where concentration gradients are the largest—near the front of a propa-

gating plume or along the lateral edges of the concentration field. Dispersion smears sharp concentration gradients and can reduce the breakthrough time, or arrival time at a specific point, for low concentration levels of an advancing concentration front.

Sorption is a general term for describing a combination of chemical interactions between the dissolved radionuclides and the solid phases, that is, either the immobile rock matrix or colloids. Any given sorptive interaction is caused by a set of specific chemical interactions such as surface adsorption, precipitation, and ion exchange. However, the sorption approach does not require identifying the specific underlying interactions. Instead, batch sorption experiments are used to identify the overall partitioning between the aqueous and solid phase, characterized as a sorption or distribution coefficient ( $K_d$ ). The strength of the sorptive behavior is a function of the chemical element, the rock type involved in the interaction, and the geochemical conditions of the water contacting the rock. Sorption reduces the rate of advance of a concentration front in advective and diffusive transport, and amplifies the effects of diffusive flux of radionuclides from the fractures to the rock matrix through its influence on the concentration gradient. In this context, sorption acts to retard the movement of solutes. The sorption coefficient,  $K_d$ , is generally combined with other terms in transport equations to give a retardation coefficient. This coefficient expresses the increase in effective pore volume that is provided by partitioning between the aqueous and the solid phases.

Radioactive decay is a process that affects the concentration of radionuclides during transport through the unsaturated zone. For simple decay, the radionuclide concentration decreases exponentially with time, creating decay products that are stable. Chain-decay adds another layer of complexity because of the ingrowth of new radionuclides created from the decay of a parent radionuclide. One aspect of potential significance with respect to chain-decay is that daughter products may have significantly different sorption behavior

than the parent radionuclide, thus affecting transport.

To reach the accessible environment, radionuclides must traverse the unsaturated zone to water table, and then migrate through the saturated zone. An exception to this would be radionuclides that partition into the gas phase in the unsaturated zone, and therefore may potentially escape the unsaturated zone at the ground surface. Very few radionuclides are expected to be able to move in the gas phase. These radionuclides are carbon-14 (as  $\text{CO}_2$ ) and perhaps chlorine-36 and iodine-129 (as  $\text{Cl}_2$  and  $\text{I}_2$ , respectively). Even if these radionuclides do manage to transport in the gas phase, the dose consequences for such releases are expected to be inconsequential (National Research Council 1995). Therefore, gas-phase radionuclide transport is not modeled in the TSPA.

Because radionuclide movement is almost exclusively in water, radionuclides tend to migrate with the unsaturated zone flow, which is mainly vertical. After movement through the unsaturated zone, radionuclide transport is primarily horizontal through the saturated zone to the location where repository performance is measured. The primary role of the unsaturated zone (below the engineered barrier system) for performance is to delay radionuclide movement. If the delay is long enough that a given radionuclide will decay considerably, then the unsaturated zone can have a large effect on decreasing the dose from that radionuclide at the accessible environment. The amount of delay strongly depends on the climate (infiltration) and sorptive interaction between the radionuclide and the rock matrix in the unsaturated zone.

### 3.6.1 Construction of the Conceptual Model

The conceptual model for radionuclide transport in the unsaturated zone is a combination of conceptual models for the processes described in the previous section: unsaturated zone flow, or advection; diffusion; dispersion; sorption; colloid-facilitated transport; and radioactive decay (Figure 3-57).

The primary vehicle for formulating the conceptual models for these processes was the workshop on unsaturated zone radionuclide transport held in Albuquerque, New Mexico, on February 5-7, 1997 (CRWMS M&O 1997p). The workshop addressed the attributes of radionuclide transport within the unsaturated zone that may impact the long-term performance of a geologic repository at Yucca Mountain. Issues related to unsaturated zone radionuclide transport were reviewed and prioritized. Methods to capture the key processes in performance assessment models were discussed and problem formulations were proposed (see Table 3-17).

The results of the workshop led to investigations of the following subjects:

- Fracture/matrix interaction and sensitivities
- Transient flow and transport
- Colloid-facilitated radionuclide transport
- The linear sorption model relative to more complex geochemical interaction models
- The effects of dispersion and fine-scale heterogeneity

The results of these investigations formed part of the basis for the unsaturated zone radionuclide transport model discussed below.

### 3.6.1.1 Unsaturated Zone Flow Model

The detailed geometry of fractures and matrix pore spaces at Yucca Mountain is far too complex to be modeled explicitly. Nevertheless, it is important to capture the larger-scale spatial variability, such as differences between welded and nonwelded hydrogeologic units, and the differences in fracture and matrix properties at the local scale. To show this variability, a dual-permeability model is used for fractured rock. In the dual-permeability model, the fractures and matrix are distinct interacting continua that coexist at every point in the modeling domain. Each continuum is assigned its own hydrologic properties such as permeability and porosity, which may also vary spatially. In general,

the fractures are modeled as a highly permeable continuum having low porosity; the matrix is modeled as a much less permeable continuum having higher porosity. The dual-permeability model offers a bimodal approximation to the true spectrum of fracture and matrix properties. More importantly, the dual-permeability model can capture the effects of fast pathways for radionu-

Table 3-17. Unsaturated Zone Radionuclide Transport Abstraction/Testing Workshop

| <b>UNSATURATED ZONE RADIONUCLIDE TRANSPORT<br/>ABSTRACTION/TESTING WORKSHOP<br/>February 5-7, 1997, Albuquerque, NM<br/>(CRWMS M&amp;O 1997p)</b>  |  |
|--|--|
| <b>PRIORITIZATION CRITERIA</b>   |  |
| <ul style="list-style-type: none"><li>• Does the process/issue affect the<ul style="list-style-type: none"><li>- Radionuclide concentration?</li><li>- Radionuclide velocity?</li><li>- Water flux?</li><li>- Spatial and temporal distribution of travel times to the water table?</li></ul></li></ul>  |  |
| <b>HIGHEST PRIORITY ISSUES</b>   |  |
| <ul style="list-style-type: none"><li>• Physical transport processes:<ul style="list-style-type: none"><li>- What conceptual model should be used for fracture/matrix interactions?</li><li>- How should long-term transient flow be included in unsaturated zone radionuclide transport modeling?</li><li>- What range and dependencies should be used for the fracture/matrix interaction parameter?</li></ul></li><li>• Chemical interactions and repository-perturbed environment:<ul style="list-style-type: none"><li>- Is the minimum <math>K_d</math> approach an appropriate modeling approach for unsaturated zone radionuclide transport?</li><li>- Are colloids expected to play an important role in unsaturated zone radionuclide transport?</li><li>- Is thermal-chemical alteration of existing minerals expected to be important for unsaturated zone radionuclide transport?</li></ul></li><li>• Heterogeneity:<ul style="list-style-type: none"><li>- Is lateral diversion of radionuclide pathways expected to be important for unsaturated zone radionuclide transport?</li><li>- Is a more detailed stratigraphy below the repository expected to be important for unsaturated zone radionuclide transport?</li><li>- Are areal variations in abundance and composition of zeolites expected to be important for unsaturated zone radionuclide transport?</li></ul></li><li>• Model calibration:<ul style="list-style-type: none"><li>- What are the criteria and methods for model calibration?</li></ul></li></ul> |  |
| <b>ANALYSIS PLANS</b>  |  |
| <ul style="list-style-type: none"><li>• Fracture/matrix interaction</li><li>• Transient flow and transport</li><li>• Colloid-facilitated radionuclide transport</li><li>• Sorption models for radionuclide transport</li><li>• Effects of dispersion and fine-scale heterogeneity on radionuclide transport</li></ul>  |  |

clide transport from the repository to the water table. This feature is an important improvement over single-continuum models (Robinson et al. 1996, Section 9.5.3; Robinson et al. 1995, Section 8.3).

The conceptual model for unsaturated zone transport is strongly tied to the conceptual model for unsaturated zone flow. As described above, advective transport because of flow is the main transport mechanism that can move radionuclides from the repository to the water table. Conceptual models for unsaturated zone flow are commonly based on a continuum relationship, known as Darcy's law, which relates volumetric flow rate and the gradient of hydraulic potential. In the case of fractured, porous rock such as the volcanic rock that constitutes Yucca Mountain, these continuum relationships are extended to embrace two coexisting continua, fractures and rock matrix, that interact according to the same constitutive relationships that govern flow in a single continuum.

From the standpoint of unsaturated zone transport, the need for explicit and separate representation of fracture and matrix flow arises because of the extreme disparity in transport velocities that can occur in the two continua. Travel times for radionuclides transported to the water table exclusively in fractures are expected to be about 10,000 times faster than travel times for radionuclides moving exclusively in the matrix. In addition, the transport velocities in the fractures may be sufficiently rapid that radionuclide concentrations in the fractures are in disequilibrium with concentrations in the matrix. For example, a high concentration of radionuclides entering fractures at the repository may penetrate the entire unsaturated zone before establishing a uniform, equilibrated concentration in the rock matrix. Therefore, a mechanistic and dynamic model of transport through the fractures and matrix, as well as exchange between the fractures and matrix, is needed to represent the system.

The dual-permeability model provides the necessary level of detail to capture the important differences between transport through fractures and matrix. There are other possible approaches to modeling flow in fractures and matrix rock. However, these other models, such as the equiv-

alent continuum model, do not recognize the important dynamic coupling between fractures and matrix. For these reasons, the flow and transport models for the unsaturated zone are based on dual permeability.

In general, flow in the unsaturated zone is time dependent or transient. One mechanism responsible for this time dependence is the time variations in the infiltration flux at the surface. The time variation of the infiltration flux may be approximated as occurring over short intervals characterized by changes in weather, resulting in episodic transient flows, or over much longer time periods corresponding to climate changes. Existing information concerning episodic transient flow seems to indicate that it may not be able to frequently penetrate through the unsaturated zone to the level of the repository because fracture flow tends to be absorbed by the matrix of the Paintbrush nonwelded hydrogeologic unit. This information also suggests that episodic transient flow appears to be localized in preferential pathways associated with through-going faults that breach the Paintbrush nonwelded unit (Robinson et al. 1997; p 6-15). Episodic transient flow propagating through fractures tends to be absorbed by the Paintbrush nonwelded unit, resulting in much slower drainage of the episodic flow events in hydrogeologic units at and below the repository level (Robinson et al. 1997, Section 6.13). Simulation results indicated that transport is not too different under episodic transient flow as compared with steady flow (CRWMS M&O 1998i, Section 7.6). Simulations show instances where breakthrough is faster for the steady flow case as compared to the episodic transient flow case (given the same average flow) and also the reverse. The reasons for this behavior are not understood. Therefore, the total quantity of water able to penetrate the unsaturated zone in the fracture system without interacting with matrix may, in fact, be larger for steady flow than for transient pulses, given the same average infiltration flux (CRWMS M&O 1998i, Section 7.6). For these reasons, episodic transient flows have not been incorporated into the TSPA-VA calculations. Changes in unsaturated flow because of longer-term changes in climate have a more pronounced influence on unsaturated zone flow than episodic transient flow. Sustained changes in infiltration

associated with climate change ultimately impact the entire flow field in the unsaturated zone. The actual transient period during which the unsaturated zone flow responds to a climate change, however, has been found to be less significant (Robinson et al. 1997, Section 8.11, pp. 8-47 and 8-48; CRWMS M&O 1998i, Section 7.4). The reason is that the change in flow in the fractures, which dominates the flux in most hydrogeologic units, responds relatively quickly to a change in infiltration. Therefore, the quasi-steady flow model was used to estimate the effects of climate change on radionuclide transport. In this model, infiltration rate is assumed to change abruptly when climate changes from one steady flow field to another. Transport calculations simply re-start when climate changes with radionuclides that were present in the unsaturated zone at the end of the previous climate included as an initial condition for the next climate. A distributed source of radionuclides throughout the unsaturated zone is derived from transport calculations using the flow field for the previous climate, and a new steady flow field is selected based on the new climate.

In addition to the change in the unsaturated zone flow field, the location of the water table is also assumed to change abruptly at the time of climate change. The three climate states—present day, long-term average, and superpluvial (see Section 3.1)—have successively higher water table elevations in response to the increasing infiltration. If the water table rises with the climate change, the radionuclides in the unsaturated zone between the previous and new water table elevations are immediately available for saturated zone transport. Water table elevations change by 80 m (262 ft) from present-day to long-term-average climates and by 120 m (394 ft) from present-day to superpluvial climates.

The flow field is expected to be mainly downward over large scales. However, local flow field variations are expected to be three-dimensional. The importance of these variations lies primarily in the kinds of rock units and fracture characteristics that dominate along the three-dimensional flow paths. A secondary consideration is that three-dimensional flow paths from the repository to the water

table will necessarily be longer than strictly vertical flow paths. Three-dimensional flow patterns are expected along rock unit contacts with contrasting properties, particularly in zones where these contrasts are believed to be features that create perched water (see Figure 3-57). To capture these effects, the flow and transport calculations are performed in three dimensions. Spatial variability is captured in the three-dimensional relationships of the hydrogeologic units and structural features, for example, faults, and in the variations in hydrogeologic and transport properties assigned to the hydrogeologic units.

### **3.6.1.2 Matrix Diffusion Model**

Matrix diffusion is one mechanism (the other is advection) that transports radionuclides between the fracture and matrix continua. Bulk diffusive flux occurs when concentration gradients are present because diffusion is driven by random molecular motion. In addition, matrix diffusion is a function of temperature, radionuclide mass, atomic or molecular dimension, and charge, as well as the matrix pore structure and water saturation. The temperature variations are expected to be small over the time period for radionuclide releases to the unsaturated zone. The effects of pore structure and water saturation have been shown to depend primarily on the volumetric water content of the rock (Los Alamos National Laboratory 1997, pp. VI-5 and VI-6). For rock in the unsaturated zone, the water content is relatively uniform spatially. Therefore, as a simplification, variations in the matrix diffusion coefficient are assumed to be primarily dependent upon the radionuclide type, that is, mass, size, complexation, and charge. In this case, measurements indicate that the primary difference is between cationic and anionic radionuclides (Triay et al. 1997, Section VI, pp. 189–198). Anionic radionuclides have lower matrix diffusion coefficients than cationic radionuclides, that is, they are transported more slowly by diffusion. Lower coefficients for anionic radionuclides are believed to be a result of size and charge exclusion from a portion of the pore structure. The surfaces of the pore minerals are generally negatively charged under the chemical conditions of the undisturbed environment.

In general, the direction of radionuclide transport by matrix diffusion between the fracture continuum and the matrix continuum depends on the direction of the concentration gradient. However, the most important influence of matrix diffusion is expected to be on radionuclide transport through fractures. The distance between an average radionuclide in the fractures and the matrix is small compared with the distance between an average radionuclide in the matrix from the fractures. This proximity is a result of the fracture and matrix geometry, where the ratio of fracture aperture to fracture spacing is small. Also, diffusive penetration of the matrix is proportional to the square root of the fracture transport time. Because of relatively fast transport through fractures, most radionuclides diffusing from fractures into the matrix do not penetrate far relative to the fracture spacing. For this reason, the effects of fracture spacing on matrix diffusion are expected to be negligible, and the effects of finite fracture spacing may be ignored. Similarly, because of the relatively small fraction of matrix affected by matrix diffusion, that is, diffusive movement from fractures into the matrix is relatively slow, an approximate representation can be made for fracture transport, including matrix diffusion, separately from the advection of radionuclides through the matrix. This is done in the transport model by having separate, noninteracting matrix regions for diffusive exchange with transport in the fracture continuum and for transport in the matrix continuum.

### 3.6.1.3 Sorption Model

Numerous rock-water chemical interactions may influence radionuclide transport:

- Ion adsorption: metal cations sticking to mineral surfaces due to London-van der Waals forces and hydrogen bonding
- Ion exchange: substitution of an aqueous cation for the cation in a mineral structure
- Surface complexation: coordination of an aqueous cation with a deprotonized metal hydroxide at the mineral surface
- Precipitation: generation of a bulk solid phase

The nature and strength of these rock-water interactions are highly dependent on the chemical composition of both the aqueous and solid phases. The conceptual model used to capture all these interactions and sensitivities is the minimum  $K_d$  model. This model bounds the distribution of radionuclides between the mobile, or dissolved in the aqueous phase, and immobile, attached to the solid phase, radionuclides using a linear, infinite-capacity partitioning model. In this model, the sorbed, or immobile, concentration is equal to the aqueous concentration times the partitioning coefficient ( $K_d$ ). Because of the numerous mechanisms and dependencies known to influence sorption, using a linear partitioning model with a single coefficient provides only a minimum bound for  $K_d$ , and hence the immobilized fraction.<sup>6</sup>

The range of pore-water compositions of the matrix of the undisturbed, that is, pre-repository, unsaturated zone is expected to overlap the combined range of groundwater compositions for the tuffaceous aquifer and the deeper carbonate aquifer (Meijer 1992, pp. 18–19). Therefore, sorption behavior investigated under this range of conditions is used to bound sorption in the unsaturated zone (Triay et al. 1997, p. 173). Under the assumptions of the model, the minimum  $K_d$  approach is conservative for radionuclide transport, except in the case of colloid-facilitated transport, which is discussed in Section 3.5 and is further discussed in Section 3.6.1.4.

The surfaces of fractures, often lined with minerals that differ from the bulk of the rock matrix, may be capable of sorbing many of the radionuclides (Triay et al. 1997, p. 173). However, there has been limited characterization of the distributions of

<sup>6</sup> Minimum bound means that the  $K_d$  used in the model represents the smallest reasonable ratio of radionuclides attached to the solid phase versus the aqueous phase. This assumption is conservative because it implies maximum transport of radionuclides in the aqueous phase.

the fracture-lining minerals and sorptive interactions with these minerals. For these reasons, it is conservatively assumed that there is no sorptive interaction with the fracture surfaces, and sorptive interactions are only possible for radionuclides in the matrix continuum.

Sorption is known to be sensitive to rock mineralogy and texture because these characteristics affect the types and available areas of different mineral surfaces. Although many different mineral types are present in Yucca Mountain, three basic rock types have been identified as having distinct sorptive interactions with the different elements of the waste form. These rock types are devitrified tuff, vitric tuff, and zeolitic tuff. Sorption coefficients for all radionuclides are specified for each of these rock types in the TSPA conceptual model.

Many of the investigated radionuclides are sorbed most strongly by the zeolitic tuff (CRWMS M&O 1998i, Table 7.5-1). Zeolitic tuff is primarily composed of clinoptilolite, and usually includes opal-CT (cristobalite - tridymite), quartz, and feldspar. Vitric tuffs, primarily composed of glass and feldspar, are generally less sorptive than zeolitic or devitrified tuffs. Devitrified tuff, also known as welded tuff, is primarily composed of alkali feldspar and tridymite. However, the importance of sorption in the different rock types is not only a function of the sorptive strength,  $K_d$ , but also the degree of exposure the radionuclides have with the rock matrix during transport through the unsaturated zone. The relative amount of radionuclide transport through the matrix is a strong function of the matrix permeability, where radionuclide transport is favored through a matrix with higher permeability. The vitric tuff is typically much more permeable than the devitrified or zeolitic tuffs, providing greater radionuclide contact with the vitric matrix.

Variations of geochemical conditions in time and space will affect the characteristics of radionuclide-rock interactions. Geochemical variability may be separated into two broad categories. One type of variability may be attributed to natural processes of the undisturbed environment that are observed in water samples from different locations.

The method for determining the appropriate minimum  $K_d$  is based on the range of geochemical conditions representative of this natural variability. Sensitivity studies suggest that future natural variations in geochemical conditions because of climate change will have little influence on radionuclide transport (Robinson et al. 1997, p. 11-48). A second type of variability is caused by the thermal-chemical interactions of the repository with the geochemical/mineralogical environment, disturbed environmental conditions. Although sensitivity studies indicate that transient thermal effects have little influence on radionuclide transport (Robinson et al. 1997, pp. 11-48 and 11-49), potential longer-term effects on geochemical and mineralogical conditions require further investigation (CRWMS M&O 1998i, Section 7.7).

#### 3.6.1.4 Colloid-Facilitated Transport Model

Colloids are potentially mobile in water flowing through the unsaturated zone. Colloids, because they are small solids, can interact with radionuclides through sorption mechanisms. Unlike sorption of radionuclides to the rock matrix, however, radionuclides sorbed on colloids are potentially mobile. Therefore, colloids can facilitate radionuclide transport through the unsaturated zone at a faster rate than the aqueous phase alone. Another form of colloidal radionuclide movement occurs when the radionuclide is an integral component of the colloid structure (see Section 3.5). In this case, the radionuclide is irreversibly bound to the colloid, as compared to the typically reversible sorption mechanism.

The transport equation of any aqueous radionuclide through fractures is expressed in terms of the previously mentioned processes of advection, sorption on fracture surfaces, if included, matrix diffusion, dispersion, and radioactive decay. If the radionuclide is sorbed on colloids, then additional terms are needed in the equation to describe the advection, sorption, dispersion, and decay of the radionuclides on colloids. Colloid particles themselves are not expected to experience any significant matrix diffusion because of the very low diffusion coefficients associated with colloids. It is assumed that sorption of radionuclides on

colloids may be approximated using the  $K_d$  conceptual model described above for sorption, except that the conservative bound now is the maximum  $K_d$ . A maximum  $K_d$  for sorption on the colloidal minerals is a conservative bound because more of the radionuclides are placed on the colloids. Advective radionuclide transport through the fractures is enhanced by reduced matrix diffusion and matrix sorption. Given a steady, uniform concentration of colloids and the  $K_d$  model for sorption, the ratio of the radionuclide mass in colloidal and aqueous form is a constant value ( $K_c$ ). Both the linear nature of the transport equations for aqueous and colloidal forms and the linear partitioning of the aqueous and colloidal concentrations allow simplification of the transport equation. The mathematical transport model for aqueous and colloidal radionuclides may be reduced to a single equation in terms of the aqueous radionuclide concentration (Robinson, et al. 1997, Section 8.10). Additionally, no new terms appear in this transport equation, as compared with strict aqueous transport. Therefore, the new transport equation for reversibly sorbed aqueous-colloidal transport has the same structure as that for strict aqueous transport. The difference is that the transport coefficients now include information concerning the colloidal partitioning.

Colloids may not be able to move through the rock matrix, particularly the welded and zeolitic rock types, because of colloid size relative to the matrix pore size. However, movement through the more permeable, nonwelded vitric rock in the Calico Hills may be possible. Advective, aqueous-phase transport of radionuclides between fractures and matrix is only a strong feature of the flow field in this higher-permeability unit. As an approximation to simplify the transport model, colloids are also allowed to move by advection with the aqueous-phase radionuclides between the fractures and matrix. However, colloids are not allowed to exchange between fractures and matrix through matrix diffusion (CRWMS M&O, 1998i, Section 7.4.5.1).

In some cases, radionuclides may be an integral part of the colloid structure itself, which can be approximated by an irreversible sorption model.

To model the transport of these irreversibly sorbed radionuclides, the transport model described above for reversibly sorbed, colloid-facilitated transport is modified to account only for transport processes that affect colloids. In other words, for this portion of the radionuclide mass, interaction with the aqueous phase and immobile rock phase is neglected. With this simplification, colloid transport is mathematically analogous to aqueous radionuclide transport with no matrix diffusion and no sorption (CRWMS M&O, 1998i, Section 7.4.5.2).

### 3.6.1.5 Dispersion Model

Dispersion is included in the transport conceptual model using a standard relationship based on Fick's law between mass flux and concentration gradient. The dispersion coefficient in the Fickian relationship is expressed as the product of the mixing length scale, or dispersivity, and the average linear velocity. Dispersion is independently represented in both the fracture and matrix continua. However, longitudinal dispersion is not expected to play an important role in the unsaturated zone transport. The repository emplacement area is very broad relative to the distance to the water table, and this geometrical arrangement tends to suppress longitudinal dispersion effects. Longitudinal dispersion becomes secondary to the explicitly modeled variations in transport velocities across the potential repository because of variations in infiltration. Also, the explicitly modeled variations in transport velocity caused by the fracture/matrix system also tend to dominate dispersion. Lateral dispersion may play a more important role, but is limited by the relatively short transport path from the repository to the water table compared with the size of the source.

### 3.6.1.6 Chain-Decay Model

Radioactive decay is modeled using simple exponential decay. For the base case, neptunium-237, uranium-234, and protactinium-231 are the only radionuclides significantly affected more than a few percent by the neglect of the chain-decay processes. Consideration of chain decay causes transport calculations to be more complex because

daughter radionuclides are created during transport of the parent isotope. The creation of progeny could be modeled in a complex calculation as a distributed source term throughout the modeling domain. However, the unsaturated zone transport model does not directly consider chain decay and progeny ingrowth. As discussed in Section 3.5.1.5, the effects of progeny ingrowth are included in the determination of the radionuclide inventory present. Therefore, the effects of chain decay and progeny ingrowth on unsaturated zone transport are approximately included through these adjustments to the radionuclide inventory. The accuracy of this approximation is affected by the relative degree of sorption for the parent radionuclides as compared with the daughter products. In most cases, the parent radionuclides are at least as sorptive as the daughter products. Therefore, the approximation is conservative.

### **3.6.2 Implementation of the Performance Assessment Model**

This section outlines the methods used to implement the models described in Section 3.6.1 for total system performance assessment calculations. The description of this implementation includes the mathematical models used, the connections with other TSPA models, and the basic data used to define model parameters.

#### **3.6.2.1 Finite Element Heat and Mass Particle Tracking**

The conceptual model described above has been implemented using a modified method for tracking the transport of particles. This modified method is used in the general-purpose, multi-phase flow and transport code FEHM (Zyvoloski et al. 1995). Particle tracking using FEHM is a cell-based approach in which particles move from cell to cell in a numerical grid. The finite-difference grid described below that computes the flow field also defines the cells. The movement from one cell to another requires a way to compute how long the particle will reside in the current cell and to select the next cell the particle will enter. The cell-to-cell routing is performed with sufficient time resolution that the next cell the particle will occupy is always an adjacent cell. The selection of the adjacent cell

is based on a mass-flux-weighted probability among adjacent cells that can have an outflow from the current cell, that is, particles cannot move into adjacent cells that are flowing into the current cell. The time that a particle will reside in a given cell is based on probabilistic distributions of residence time derived from mathematical models of the transport process (Robinson et al. 1997, Chapter 4, pp. 4-1, 4-6, and 4-7). Because the properties within a given cell are uniform, the mathematical development of residence time distributions may be carried out either analytically or semi-analytically, making the residence time calculations computationally efficient.

The particle tracking method is limited to transport conditions in which advection dominates dispersion, in the sense that the spread of an initially sharp concentration front is small compared with the distance that the front has advanced. This limitation is due to the nature of dispersive processes in which there is a finite probability for a particle to move into cells other than those adjacent to the current cell. Similarly, the assumption that cell-to-cell transfer is proportional to water flux also becomes inaccurate for dispersive-dominated transport. Advective-dominated transport is the expected condition in the unsaturated zone.

#### **3.6.2.2 Linkage with Other Models**

Radionuclide transport calculations for the three-dimensional, dual permeability model are directly coupled, that is, dynamically linked, with the computer program for total system integration (Golder Associates, Inc. 1998, Section 2.3.2). RIP provides the source term for radionuclide transport calculations in the unsaturated zone, that is, the radionuclide releases from the engineered barrier system as described in Section 3.5. Also, the FEHM particle tracker receives flow fields from an external flow calculation (see Section 3.1) and provides radionuclide mass flux values at the water table to the transport model for the saturated zone (see Section 3.7 and Figure 4-10).

For unsaturated zone transport, RIP directly accesses the FEHM particle tracker module (Robinson et al. 1997, Chapter 4, pp. 4-1 to 4-16)

to perform three-dimensional, site-scale transport calculations. The unsaturated zone flow fields required by the FEHM module are accessed separately by the program, as described below. For every simulation time step in RIP (for example, 100 years), source term radionuclide mass flux information is passed from the engineered barrier system cells to the FEHM module. The repository is divided into six regions in an attempt to capture the spatial variation for infiltration over the potential repository block (see Section 3.2.2.2). The radionuclide releases from a given region of the repository are assumed to be well mixed with the unsaturated zone flow through that region. The FEHM module then moves the particles as far as they would travel during that time step, based on the steady state velocity field in the fractures and matrix of the unsaturated zone rock units. The FEHM module sends back to RIP the amount of mass flux that leaves the unsaturated zone model domain in FEHM (i.e., the mass to be passed to the saturated zone model, which is the mass that enters the water table). The amount of radionuclide mass in the fractures is passed separately from that in the matrix so that intermediate results can be plotted. The two masses are mixed in a RIP code mixing cell, and the results are passed to the convolution integral function for the saturated zone<sup>7</sup>. The FEHM module also passes back the average fracture and matrix liquid fluxes in the six water table regions of the saturated zone model (see Figure 4-10).

For the TSPA, FEHM calculates transport dynamically. However, the flow fields used in the transport calculations are pre-generated with TOUGH2, a computer code that simulates three-dimensional flow of water and heat in porous and fractured media (Pruess 1991; Bodvarsson et al. 1997). The use of pre-generated flow fields implies the assumption of quasi-steady flow. There is a library of flow fields corresponding to the uncertainty in the unsaturated zone flow parameters and infiltration rate (see Section 3.1). For each realization, a different flow field is used based

on a random sampling of infiltration rate and key hydrogeologic parameters that are uncertain. Also, for each sampled flow field corresponding to present day climatic conditions, there are two corresponding flow fields that have a higher boundary condition at the surface for infiltration flux based on two future climate scenarios, long-term average and superpluvial. A detailed discussion of the unsaturated zone flow field, climate states, and generation methods is given in Section 3.1.

Based on the description of waste package groupings in Section 3.2.2.2, the radionuclide source term for the unsaturated zone transport model is divided into six distinct regions based on heterogeneity of infiltration flux. Therefore, there are six distinct sets of engineered barrier system cells in the computer program (see Section 4.1) that supply six distinct areas of the three-dimensional, unsaturated zone domain in the FEHM particle tracker. Radionuclide release within each of the six regions is spatially uniform over the common grid structure of the TOUGH2 flow code and FEHM particle tracker. The outflow of the unsaturated zone FEHM particle tracker is also divided into six distinct regions at the water table, based in part on the lithology of the geologic units intersecting the water table. These regions provide a coarse discretization of the radionuclide mass flux from the unsaturated zone as input to the saturated zone transport model. The six regions at the water table are unrelated to the six regions at the repository horizon. As mentioned above, fracture and matrix mass fluxes from these six distinct water table regions are supplied to six RIP mixing cells and then used for computation of saturated zone transport with the saturated zone convolution integral described in Section 3.7.2. Both solute and colloid mass are tracked throughout the models.

### 3.6.2.3 Parameter Inputs

The unsaturated zone transport model requires several parameter inputs to quantify the magni-

<sup>7</sup> For multi-realization simulations, RIP also passes an index parameter to FEHM that points to a row in a table of 100 realizations of the transport parameters in the unsaturated zone that are uncertain. The specific stochastic parameters that comprise these 100 vectors are discussed in Section 4.1.

tudes of matrix diffusion, sorption, dispersion, fracture aperture, and the aqueous-colloid partitioning coefficient. Because these parameter values have varying degrees of uncertainty, a probability distribution is identified for each parameter value that may be used in stochastic performance assessment calculations. The following descriptions summarize the data sources used to establish these parameter distributions (see Table 3-18).

Sorption  $K_d$ s have been quantified using results of batch sorption experiments for different radionuclides and rock types (Triay et al. 1997, Sections VA and VB, pp. 1-8). The results from batch sorption experiments were compared with those from experiments with crushed rock and whole rock columns for neptunium, plutonium, technetium, and selenium. The batch sorption technique provided conservative estimates for  $K_d$ . Of the eight elements considered in the base case,

three elements have little or no sorption: technetium, iodine, and carbon. These elements are modeled using a  $K_d$  of zero (ibid, p. 174). Of the remaining five elements, neptunium, uranium, and selenium have small but nonzero  $K_d$ s, with expected values less than or equal to 7 mL/g (ibid, p. 174). Only protactinium and plutonium have expected values of  $K_d$  greater than 10 mL/g (ibid, p. 174). As discussed for the conceptual model, sorption is identified for devitrified, vitric, and zeolitic rock types. Probability distributions for the  $K_d$ s, representing uncertainties in the parameter values, were identified through expert judgment (CRWMS M&O 1998i, Section 7.4). The assignment of  $K_d$  values were made on the assumption that their values are uncorrelated.

Matrix diffusion coefficients have been quantified in laboratory experiments for different radionuclides and rock types (Triay et al. 1997, p. 181). Anionic radionuclides have somewhat smaller

Table 3-18. Parameter Values Used for Unsaturated Zone Radionuclide Transport in Total System Performance Assessment for the Viability Assessment

| Parameter Description   | Distribution   |
|---|--|
| $K_d$ of $^{14}\text{C}$ in all units (mL/g)  | 0  |
| $K_d$ of $^{129}\text{I}$ in all units (mL/g)   | 0  |
| $K_d$ of $^{237}\text{Np}$ in devitrified units (mL/g)  | Beta; mean = 1.0, COV = 0.3, min = 0, max = 6.0  |
| $K_d$ of $^{237}\text{Np}$ in vitrified units (mL/g)  | Beta; mean = 1.0, COV = 1.0, min = 0, max = 15.0                                       |
| $K_d$ of $^{237}\text{Np}$ in zeolitic units (mL/g)   | Beta; mean = 4.0, COV = 0.25, min = 0, max = 12.0                                      |
| $K_d$ of $^{231}\text{Pa}$ in devitrified units (mL/g)  | Uniform; min = 0, max = 100  |
| $K_d$ of $^{231}\text{Pa}$ in vitrified units (mL/g)  | Uniform; min = 0, max = 100  |
| $K_d$ of $^{231}\text{Pa}$ in zeolitic units (mL/g)   | Uniform; min = 0, max = 100  |
| $K_d$ of $^{239}\text{Pu}$ and $^{242}\text{Pu}$ in devitrified units (mL/g)  | Beta; mean = 100, COV = 0.25, min = 20, max = 200                                      |
| $K_d$ of $^{239}\text{Pu}$ and $^{242}\text{Pu}$ in vitrified units (mL/g)  | Beta; mean = 100, COV = 0.25, min = 50, max = 200                                      |
| $K_d$ of $^{239}\text{Pu}$ and $^{242}\text{Pu}$ in zeolitic units (mL/g)   | Beta; mean = 100, COV = 0.25, min = 30, max = 200                                      |
| $K_d$ of $^{79}\text{Se}$ in devitrified units (mL/g)   | Beta; mean = 3, COV = 1.0, min = 0, max = 30   |
| $K_d$ of $^{79}\text{Se}$ in vitrified units (mL/g)   | Beta; mean = 3, COV = 1.0, min = 0, max = 20   |
| $K_d$ of $^{79}\text{Se}$ in zeolitic units (mL/g)  | Beta; mean = 2, COV = 1.0, min = 0, max = 15   |
| $K_d$ of $^{99}\text{Tc}$ in all units (mL/g)   | 0  |
| $K_d$ of $^{234}\text{U}$ in devitrified units (mL/g)   | Beta; mean = 2.0, COV = 0.3, min = 0, max = 4.0  |
| $K_d$ of $^{234}\text{U}$ in vitrified units (mL/g)   | Beta; mean = 1, COV = 0.3, min = 0, max = 3.0  |
| $K_d$ of $^{234}\text{U}$ in zeolitic units (mL/g)  | Beta; mean = 7, COV = 1.0, min = 0, max = 30.0   |
| Diffusion Coefficient ( $\text{m}^2/\text{s}$ ) of $^{237}\text{Np}$ , $^{239}\text{Pu}$ , $^{242}\text{Pu}$ , $^{234}\text{U}$ , $^{231}\text{Pa}$ | Beta; mean = $1.6 \times 10^{-10}$ , COV = 0.3125, min = 0, max = $1.0 \times 10^{-9}$ |
| Diffusion Coefficient ( $\text{m}^2/\text{s}$ ) of $^{99}\text{Tc}$ , $^{14}\text{C}$ , $^{129}\text{I}$ , $^{79}\text{Se}$                         | Beta; mean = $3.2 \times 10^{-11}$ , COV = 0.3125, min = 0, max = $1.0 \times 10^{-9}$ |
| $K_c$ of $^{239}\text{Pu}$ and $^{242}\text{Pu}$ in all units   | Log uniform; min = $1 \times 10^{-5}$ , max = 10                                       |
| Dispersivity (m) of both fracture and matrix units  | Normal; mean = 20, SD = 5.0  |
| Aperture (m) of fractures in all units  | Log normal; geometric mean = $1 \times 10^{-4}$ , geometric SD = 3.16                  |

matrix diffusion coefficients than cationic radionuclides. At least for technetium, the lower diffusion rate may be caused by its exclusion from some matrix pores because of the larger ion size and negative charge of the pertechnetate anion  $TcO_4^-$ , the predominant aqueous species of technetium for present-day conditions, as compared with tritium, for example. Matrix diffusion of sorbing, cationic radionuclides is estimated using the matrix diffusion coefficient for tritium. As discussed for the conceptual model, matrix diffusion is assumed to be a function of radionuclide type, although variations in matrix diffusion coefficients are expected with changes in bulk water content. These variations were estimated from the range of bulk water content in the unsaturated zone and a previously determined relationship between the matrix diffusion coefficient and bulk water content (Los Alamos National Laboratory 1997, pp. VI-5 and VI-6). These variations form the basis for the uncertainty range in matrix diffusion coefficients (CRWMS M&O 1998i, Section 7.4).

Dispersion coefficients are commonly modeled as a product of transport velocity and a mixing length scale called dispersivity. Dispersivity is a property of the flow geometry that is determined by the structure of the fracture paths, for dispersion in the fracture continuum, or pore structure, for the matrix continuum. There are no measured data at Yucca Mountain that can be directly applied to determining dispersivity in the unsaturated zone. However, a value of 20 m (66 ft) over the approximately 300 m (984 ft) of unsaturated zone travel distance is consistent with the dispersivity versus scale correlation of Neuman (1990). The base case distribution for dispersivity was selected to be normal with a mean of 20 m (66 ft) and a standard deviation of 5 m (16 ft), which captures a range of 7.5–32.5 m (25–107 ft) within the 99 percent probability limits. This dispersivity distribution applies to transport for both the fracture and matrix continua, but values for fracture and matrix are sampled independently for TSPA calculations. Sensitivity studies indicate that radionuclide transport in the unsaturated zone is insensitive to dispersivities over a range from 0 to 75 m (0–246 ft) (CRWMS M&O 1998i, Section 7.4).

One concern for implementation of a numerical transport model is numerical dispersion. Numerical dispersion is an artifact of numerical solution algorithms and has no physical basis. It is a function of spatial-grid size and time-step size. The effects of numerical dispersion on transport solutions are similar in character to physical dispersion. The particle tracking technique used here for unsaturated zone transport is formulated specifically to reduce numerical dispersion. For flow parallel to the grid, numerical dispersion is expected to be zero (Goode and Shapiro 1991). Benchmark tests have shown the accuracy of this technique for systems with low physical dispersion (Robinson et al. 1997, Section 4.6.1).

Fracture aperture plays a role in calculations of residence time distributions for matrix diffusion. Matrix diffusion between fractures and matrix is enhanced for fractures with smaller aperture. Fracture aperture is equivalent to the fracture volume per unit area of fracture/matrix contact. Hydraulic fracture apertures derived by Bodvarsson et al. (1997) mostly lie between about 100 to 200 microns, with some ranging up to 500 microns (Bodvarsson et al. 1997, Table 7.12). Therefore, as a first approximation a log-normal distribution is used with a geometric mean of 100 microns and a geometric standard deviation of 3.16, that is, a two standard deviation width is a factor of 10. (Specifically, this means that the ratio of the value one standard deviation above the mean to that value one standard deviation below the mean is 10.)

### 3.6.3 Results and Interpretations

This section presents results of the unsaturated zone transport model in terms of travel times and transport pathways, and sensitivities of the results to the conceptual model for unsaturated zone flow, matrix diffusion, and the sorptive characteristics of different rock types. A summary of the findings based on analyses of the unsaturated zone transport subsystem is provided, along with recommendations for additional work prior to LA.

### 3.6.3.1 Results for the Unsaturated Zone Transport Model

Simulations using the unsaturated zone transport model were performed to investigate the travel times and transport pathways from the various repository regions to the water table. The simulations used 100,000 particles released from each node in the repository to develop a travel time distribution for transport to the water table. The simulations were also used to identify the center of mass at the water table for releases from each repository node. This information indicates transport pathways through the unsaturated zone. The results presented here are for expected infiltration under long-term average climate, which averages about 40 mm/year (1.6 in./year) over the repository block. The long-term average climate is

expected during about 90 percent of the postclosure time period.

Figure 3-58 shows the contour plots of the repository region; color represents travel time to the water table. These calculations were done using hypothetical nonsorbing, non-diffusing particles to focus on the advective transport processes. Two plots are presented. Figure 3-58a shows the times for 0.1 percent of the released mass to arrive at the water table as a function of location within the repository. Figure 3-58b shows the times for 50 percent of the released mass to arrive at the water table. The general trend is for the travel time to increase from northeast to southwest through the repository. The shorter travel times in the northeast (less than 50 years for 0.1 percent; less than 200 years for 50 percent) are attributed to transport dominated by the fracture continuum.

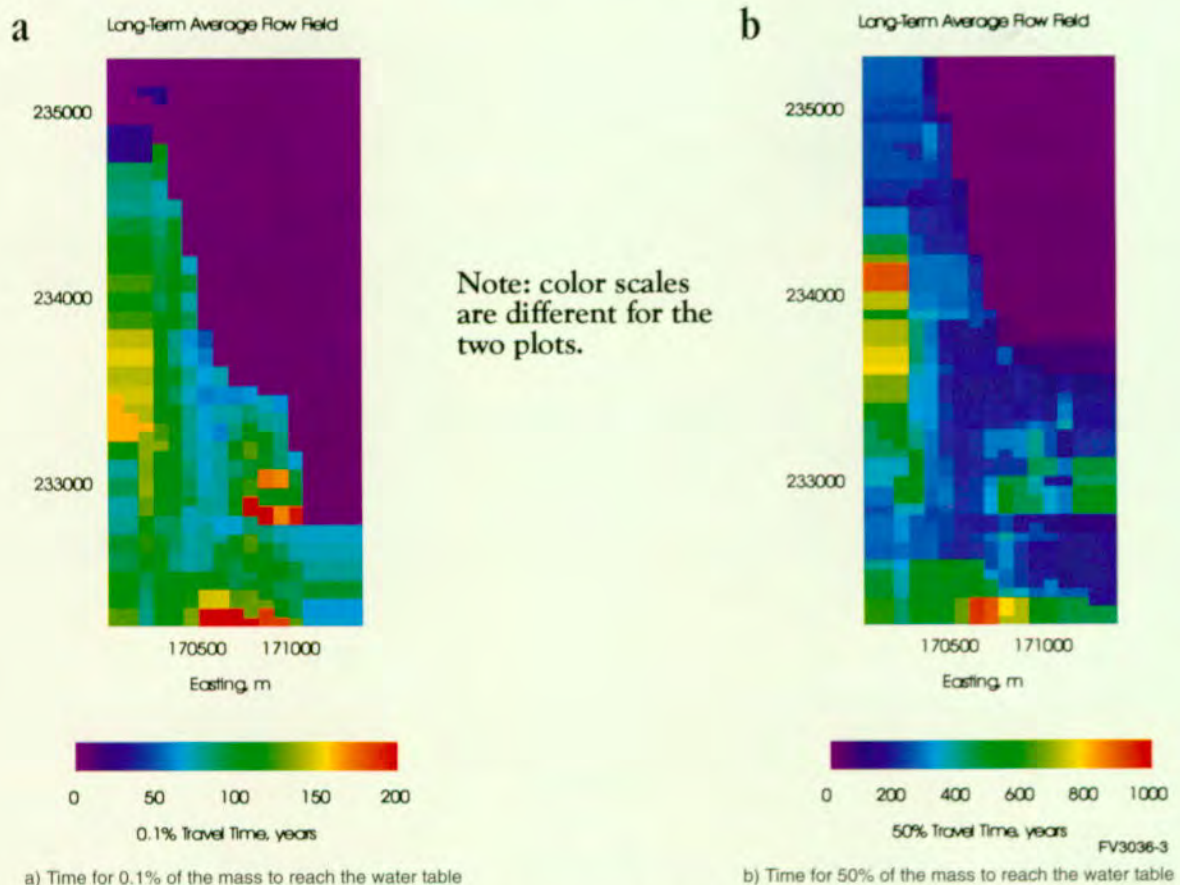


Figure 3-58. Color Contour Plot Showing Travel Times from the Repository to the Water Table for Hypothetical Nonsorbing, Nondiffusing Tracer Particles (100,000 particles per grid cell) Using the base case parameter set, long-term average climate and mean infiltration.

The northeast section is a zone in which site characterization studies have commonly found perched water along the basal vitrophyre of the Topopah Spring welded unit and upper zeolitic units in the Calico Hills nonwelded unit. The flow model has been calibrated to reproduce observations of perched water. This calibration was achieved by severely reducing fracture permeabilities in zones immediately underlying zones of observed perched water. This reduction in fracture permeability leads to lateral diversion of the flow through more permeable fracture pathways around the perched water. Further east, the diverted water eventually returns to flow pathways that are mainly vertical, either along the Ghost Dance fault or other fracture pathways. Another factor influencing travel times is the uneven distribution of infil-

tration over the repository block. Infiltration models predict higher infiltration rates in the northeast than in the southwest (CRWMS M&O 1998i, Chapter 2).

Figure 3-59 is a similar plot to Figure 3-58, but in this case the travel times are for particles having the transport characteristics of plutonium. In the base case, plutonium is assumed to interact with colloids both reversibly and irreversibly. Irreversible sorptive interaction with colloids causes particles to act as nonsorbing and nondiffusing, causing the travel times as shown in Figure 3-58. Reversible sorptive interaction with colloids causes different magnitudes and patterns for travel times. Similar qualitative trends in travel time are shown in Figure 3-59a as in Figure 3-58a (both for

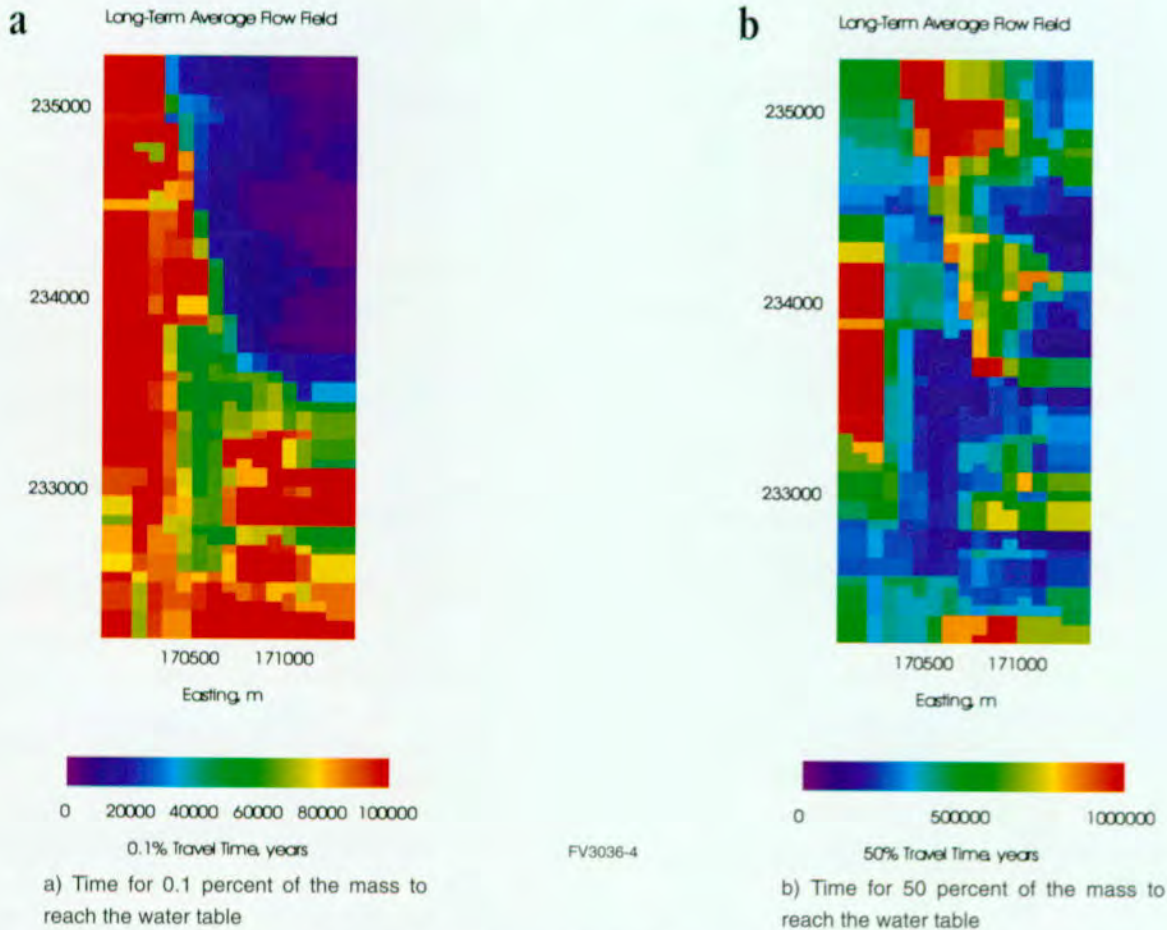


Figure 3-59. Color Contour Plot Showing Travel Times from the Repository to the Water Table for Hypothetical Tracer Particles Having the Characteristics of Plutonium (100,000 particles per grid cell) Using the base case parameter set; long-term average climate and mean infiltration.

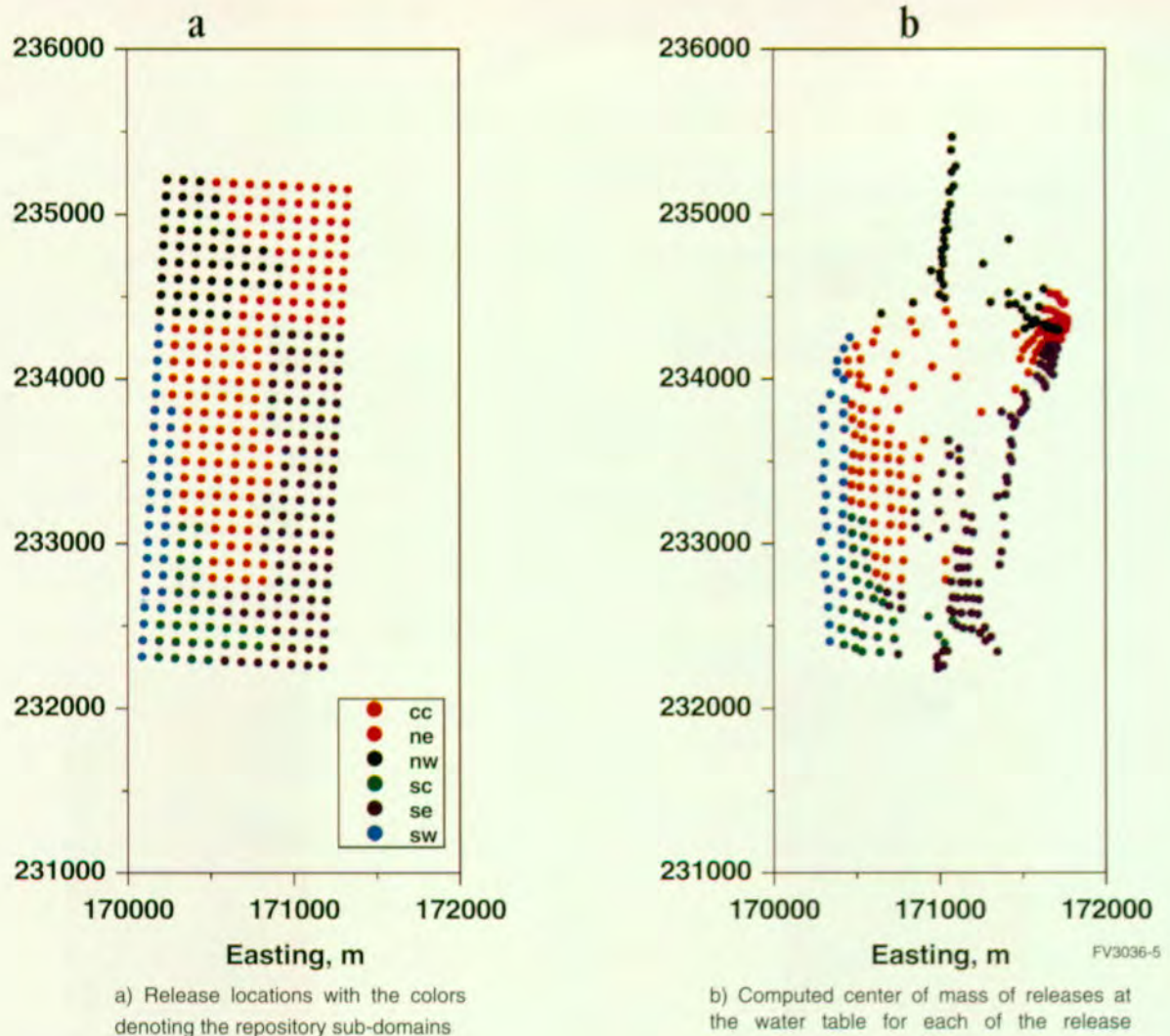
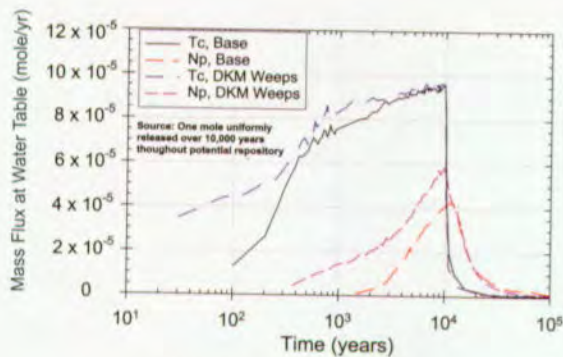


Figure 3-60. Average Locations for Hypothetical Releases from each Repository Grid Cell at the Water Table Using the base case parameter set; long-term average climate and mean infiltration.

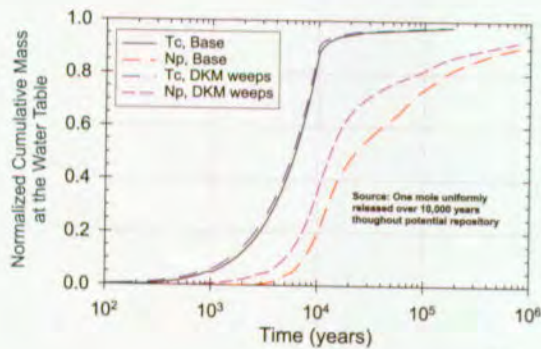
0.1 percent recovered mass). However, the magnitudes of the travel times are much larger for the plutonium case. Travel times approach 100,000 years for plutonium, compared with maximum travel times that are less than 200 years for the passive tracer. Travel times for 50 percent of the released plutonium are in excess of 100,000 years, and some exceed one million years. Also, the spatial trends in travel time have changed and are much less distinct.

Figure 3-60a shows the origin points of particle releases from the repository. These points have been color coded so that releases from the six zones (cc  $\equiv$  central; ne  $\equiv$  northeast; nw  $\equiv$  northwest; sc  $\equiv$  south central; se  $\equiv$  southeast; sw  $\equiv$

southwest) can be identified at the water table in Figure 3-60b. The colored dots in Figure 3-60b represent the center of mass of each of the releases upon arrival at the water table. Lateral diversion of releases from the northern portions of the repository is the most prominent feature. Some diversion is also seen from the southeast portion of the repository. The somewhat abrupt termination of lateral diversion eastward is attributed to the Ghost Dance fault (see Figure 3-1). The linear pattern of releases at the water table originating from the northwest portion of the repository (black dots) may result from the dip of the hydrogeologic units intercepting the water table or alternatively, a high-permeability feature is interrupting lateral diversion. Transport pathways from the southwest,



a) Mass flux at the water table



b) Cumulative mass recovered at the water table

Figure 3-61. Comparison of the Effects of Unsaturated Zone Flow Fields on Technetium and Neptunium Transport: Base Case Versus DKM Weeps Flow Models

Using the base case parameter set; long-term average climate with mean infiltration.

south central, and central-central regions are more nearly vertical.

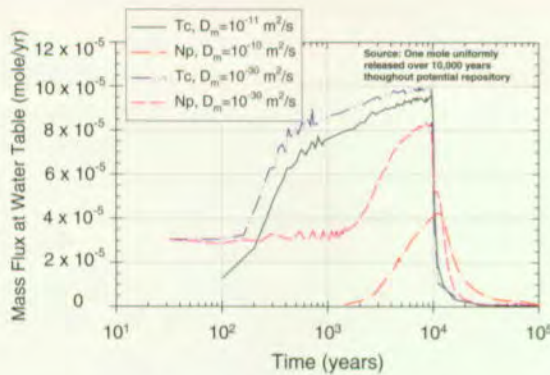
### 3.6.3.2 Influence of the Unsaturated Zone Flow Model

The use of alternative flow models for radionuclide transport in the unsaturated zone is shown in Figure 3-61 (see Section 3.1). In this simulation, one mole each of technetium and neptunium were released uniformly over the repository region for a period of 10,000 years. The calculations were performed for the mean infiltration under long-term-average climate. Technetium is assumed not to sorb, whereas neptunium has limited sorptive interaction with the different rock types. The mean flow field for the base case, and the dual-permeability/Weeps model using mean permeability (see

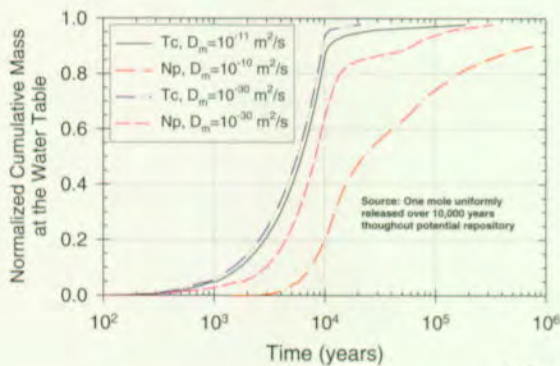
Section 3.1) are compared in Figure 3-61. The dual-permeability/Weeps model reduces flow interaction between fractures and matrix compared with the base case flow field. Figure 3-61a shows mass flux at the water table, and Figure 3-61b shows cumulative mass arrival. The primary difference in these flow fields is due to differences in the fracture/matrix coupling strength. This factor, discussed in Section 3.1, affects the magnitude of advective exchange between the fractures and the matrix. The dual permeability model with Weeps modeling reduces the amount of fracture/matrix exchange, causing transport behavior that has a greater tendency to be dominated by fracture flow. In Figure 3-61a, mass flux increases over time until 10,000 years, when the source is depleted. These results indicate that higher concentrations of technetium and neptunium arrive sooner for the flow field derived using the dual permeability model with Weeps. However, Figure 3-61b shows that the cumulative mass of technetium recovered at the water table is relatively insensitive to the different flow fields. Some differences are seen in the cumulative recovery of neptunium at the water table. Reduced fracture/matrix contact in the dual permeability model with Weeps modeling results in faster neptunium movement to the water table, although the differences are not large. Radionuclide decay is not modeled in this calculation.

### 3.6.3.3 Influence of Matrix Diffusion

Matrix diffusion is another mechanism that allows radionuclides moving through fractures to enter the matrix. In the simulation, one mole each of technetium and neptunium are released uniformly over the repository region for a period of 10,000 years. The calculations were performed using the mean flow field for the base case and mean infiltration for the long-term average climate. Figures 3-62a and 3-62b show the effects of matrix diffusion on the transport of technetium and neptunium in which, as before, technetium is nonsorbing and neptunium moderately sorbing. The mass flux plot in Figure 3-62a shows that early releases arrive at the water table sooner without matrix diffusion, that is, for  $D_m = 10^{-30}$  m<sup>2</sup>/s (this very low value has been used to represent zero



a) Mass flux at the water table



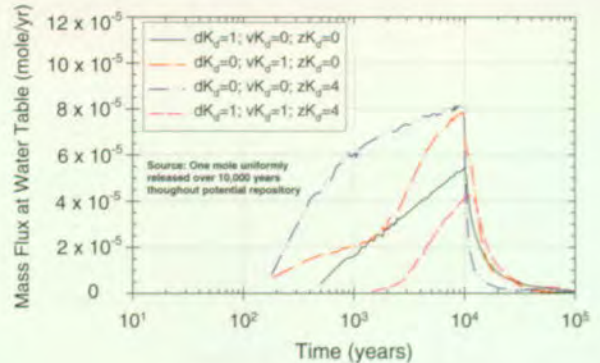
b) Cumulative mass recovered at the water table

Figure 3-62. Comparison of the Effects of Matrix Diffusion on Technetium and Neptunium Transport Using the base case parameter set; long-term average climate with mean infiltration.

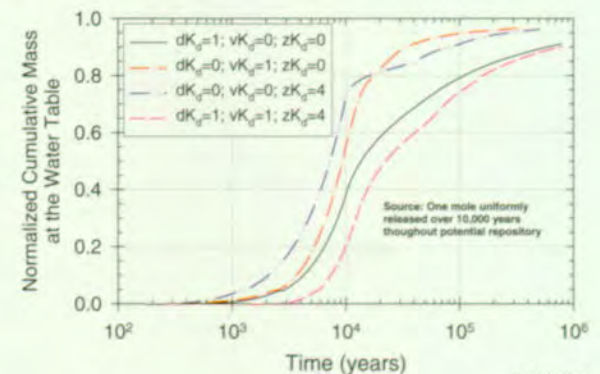
matrix diffusion). Differences in mass flux and in cumulative mass recovered are much larger for neptunium than technetium. These results suggest that matrix diffusion has little affect on nonsorbing radionuclides but is more important for sorbing radionuclides, because of sorption sites in the matrix which are accessed by matrix diffusion.

### 3.6.3.4 Influence of Rock Type

Differences in hydrogeologic and geochemical properties between the devitrified, vitric, and zeolitic rock types suggest that they may not affect transport in the same way. For this simulation, one mole of neptunium is released uniformly over the repository region for a period of 10,000 years. As before, the calculations were performed using the



a) Mass flux at the water table



b) Cumulative mass recovered at the water table

Figure 3-63. Comparison of the Influence of Sorption on Devitrified, Vitric, and Zeolitic Rock on Neptunium Transport

Using the base case parameter set; long-term average climate with mean infiltration;  $dk_d$  = sorption coefficient on devitrified rock;  $vk_d$  = sorption coefficient on vitric rock;  $zk_d$  = sorption coefficient on zeolitic rock, all in mL/g.

mean flow field for the base case and mean infiltration for the long-term average climate. The  $K_d$ s for neptunium sorption on the different rock types are 1 mL/g for devitrified rock, 1 mL/g for vitric rock, and 4 mL/g for zeolitic rock. Three transport calculations were conducted with sorption "turned on" in one layer only, that is,  $K_d$ s were equal to zero in the other layers, to see the influence of each individual rock type. A final calculation was done using all the base case  $K_d$ s "turned on." The results are shown in Figures 3-63a and 3-63b for the radionuclide mass flux and cumulative mass arrival, respectively, at the water table.

The conclusion based on this sensitivity calculation is that the Topopah Spring welded unit (with

sorption parameter  $dK_d$ , where the leading "d" stands for the devitrified rock type) is the most important unit in delaying radionuclide arrival at the water table. Flow through the Topopah Spring welded unit is nearly vertical throughout the repository domain, and this flow pattern causes longer residence times during transport through the fractures, allowing greater interaction with the matrix. On the other hand, large portions of the Calico Hills unit are bypassed because of lateral diversion. Therefore, in many areas the flux that does pass through the Calico Hills is relatively focused and residence times in these fracture pathways are short, leading to poor interaction with the matrix. The Calico Hills vitric unit generally has the next largest effect on radionuclide retardation because of high matrix permeability that attenuates fracture flow and causes greater radionuclide contact with the matrix.

### 3.6.3.5 Summary and Conclusions

Calculations for radionuclide transport in the unsaturated zone use a modified form of the particle tracking method implemented in the FEHM flow and transport code. This transport code is dynamically linked with RIP. The transport model uses a dual-permeability approach for computing radionuclide transport in a fracture/matrix system. For the particle tracking transport calculations, three-dimensional, steady flow fields in the unsaturated zone are computed using TOUGH2, the code platform of the unsaturated zone flow model. Changes in infiltration because of climate change are treated using a quasi-steady flow approximation. The transport model includes the effects of fracture/matrix interaction due to advective and diffusive exchange between the fracture and matrix continua. The effects of radionuclide sorption on the rock matrix are addressed using a bounding, minimum- $K_d$  modeling approach, but fracture sorption is not included. The effects of colloids on plutonium transport are included in two forms—reversibly sorbed to colloids and irreversibly bound in the colloid structure.

The results of investigations into radionuclide transport through the unsaturated zone lead to the following conclusions:

1. Under the dominant long-term average climate, releases of nonsorbing or weakly sorbing radionuclides from the northern portion of the repository have short travel times, only a few years, because of fracture-dominated transport.
2. Under the dominant long-term average climate, releases of nonsorbing or weakly sorbing radionuclides from the southern portion of the repository may have much longer travel times (hundreds of years).
3. For most of the mass of strongly sorbing radionuclides, such as plutonium, arrival at the water table is delayed tens to hundreds of thousands of years. Radionuclides that reversibly sorb onto colloids are also delayed; however, irreversibly bound radionuclides may behave as nonsorbing radionuclides.
4. Matrix diffusion has little effect on transport of nonsorbing radionuclides. However, combining matrix diffusion with sorption significantly retards radionuclides compared with sorption and no matrix diffusion.
5. The Topopah Spring welded unit is the primary barrier to radionuclide transport in the unsaturated zone because of slower fracture transport in this unit compared with the Calico Hills zeolitic unit, and its greater thickness and continuity compared with the Calico Hills vitric unit.
6. Alternative flow models like the dual-permeability model with Weeps modeling, which have smaller coupling strengths for effective fracture/matrix contact area, increase fracture-dominated transport, particularly for sorbing radionuclides. However, the magnitude of this effect is not large for weakly sorbing radionuclides.

### 3.7 SATURATED ZONE FLOW AND TRANSPORT

The saturated zone at Yucca Mountain is the region beneath the ground surface where rock pores and fractures are completely saturated with groundwater. The upper boundary of the saturated zone is called the water table. The repository is located in the unsaturated zone, which is above the saturated zone. The flow-and-transport component of the TSPA for the saturated zone evaluates the migration of radionuclides from their introduction at the water table below the repository to the release point to the biosphere (Figure 3-64). This component of the analysis is coupled with the transport calculations for the unsaturated zone that describe the movement of contaminants in downward percolating groundwater from the repository to the water table. This input to the saturated zone flow-and-transport calculations is the spatial and temporal distributions of simulated mass flux at the water table. The saturated zone

results are linked to the biosphere analysis by the simulated time history, or system response as a function of time, of radionuclide concentration in groundwater produced from a hypothetical well. The geosphere/biosphere interface is assumed to be located 20 km (12 miles) from the repository (Figure 3-65). Radionuclide concentrations in the hypothetical well water are used in the biosphere component to calculate radiation dose rates received by the public.

The saturated zone modeling studies and sensitivity analyses presented in this chapter were prepared with the view of addressing selected aspects of the NRC Key Technical Issues on Unsaturated and Saturated Flow under Isothermal Conditions (NRC 1997e; 1997f) and Total System Performance Assessment and Integration (NRC 1998a). Specifically, the information presented is pertinent to the unsaturated and saturated flow under isothermal conditions subissue on groundwater percolation through the repository horizon,

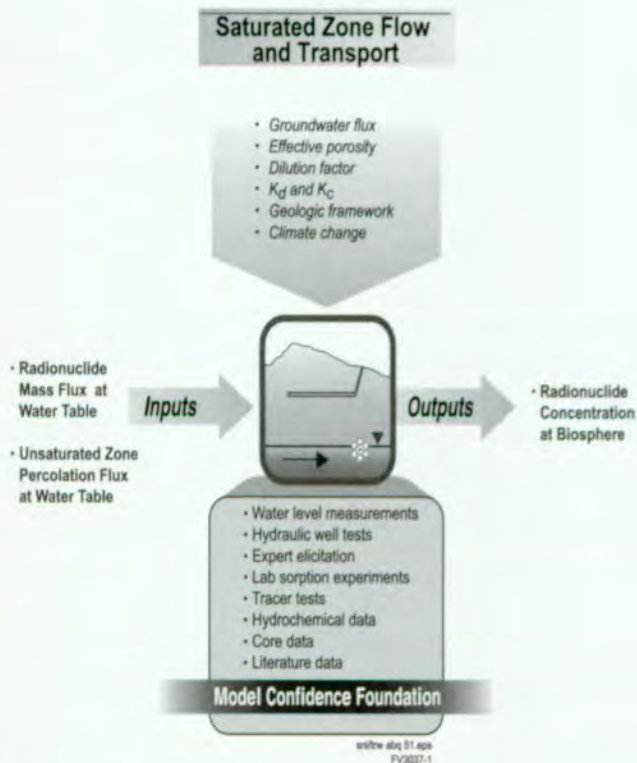
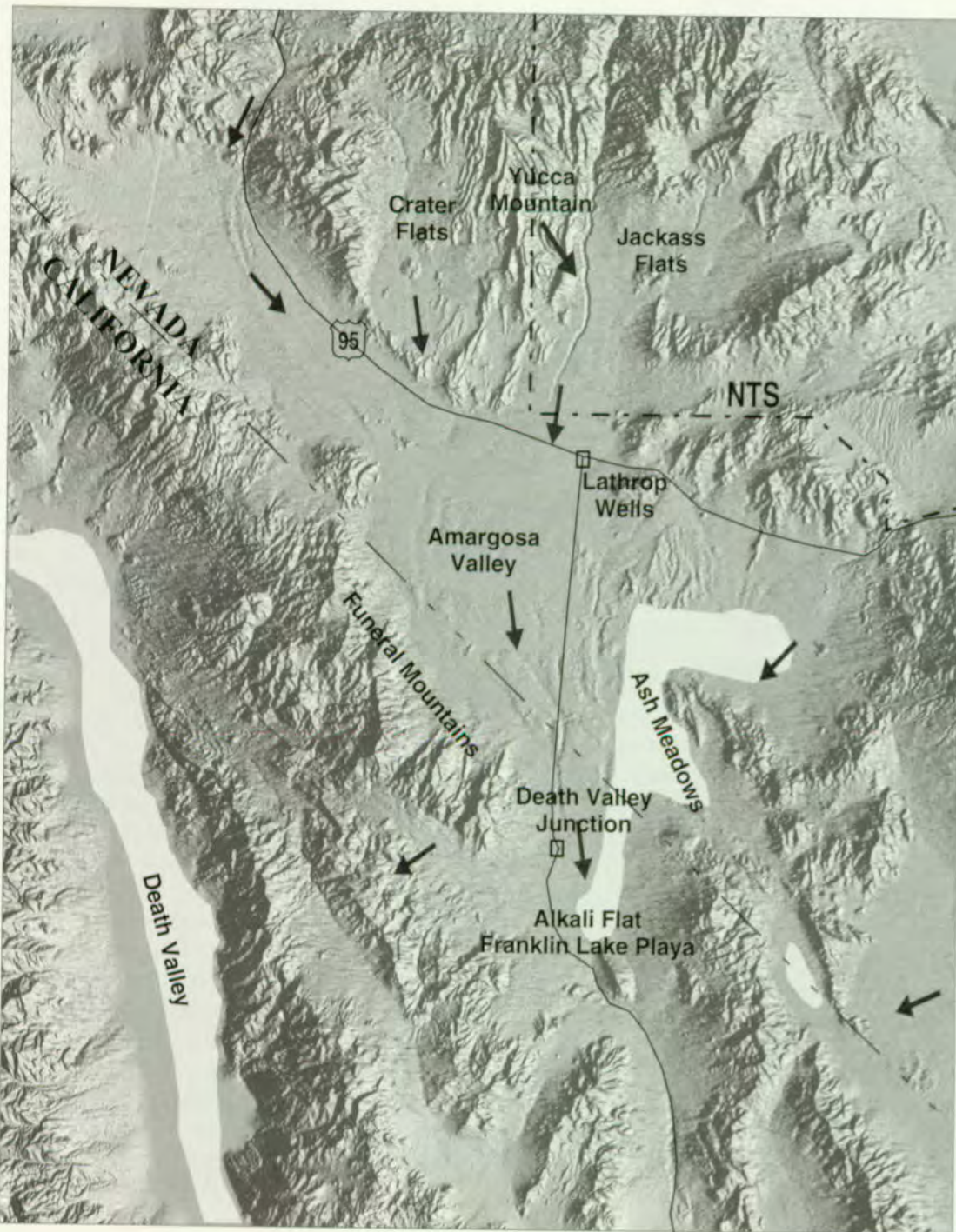


Figure 3-64. Summary of Inputs and Outputs for the Saturated Zone Flow and Transport Component of the Total System Performance Assessment for the Viability Assessment Analysis. Site characterization information that forms the basis of saturated zone flow and transport modeling is also indicated.



0 10 20 KILOMETERS

Figure 3-65. Regional Map of the Saturated Zone Flow System  
Arrows indicate general directions of groundwater flow in the saturated zone on a regional scale. Lighter area (Ash Meadows, Alkali Flat, Death Valley) indicates major areas of groundwater discharge by a combination of spring discharge and evapotranspiration by plants.

ambient flow conditions in the saturated zone, and the TSPA integration subissue on model abstraction.

### **3.7.1 Construction of the Conceptual Model**

This section describes the conceptual model of the flow-and-transport processes in the saturated zone that are relevant to radionuclide migration from the repository and shows how the model has been applied. Model application includes using judgment provided by panelists of an expert elicitation on processes in the saturated zone. Information from observations of the saturated zone system that forms the basis of the conceptual model is also summarized.

#### **3.7.1.1 Conceptualization of Saturated Zone Flow and Transport Processes**

Groundwater flow in the saturated zone below and directly downgradient of the repository at Yucca Mountain occurs in fractured, porous volcanic rocks at relatively shallow depths beneath the water table and in fractured carbonate rocks of Paleozoic age at much greater depths. At distances greater than about 10–20 km (6–12 miles) downgradient from the repository where the volcanic rocks thin and disappear under alluvium, groundwater flows either through the alluvium or the deep Paleozoic carbonates. Based on measured water levels in wells, the groundwater flow is generally to the southeast near the repository, with a transition toward the south and southwest farther south of the repository, as shown in Figure 3-65 (D'Agnese et al. 1997a, pp. 64 and 67). Groundwater that has flowed beneath Yucca Mountain is probably captured at pumping wells 20 km (12 miles) or more to the south in the Amargosa Valley under present conditions. Under predevelopment conditions (before pumping in the Amargosa Valley) and for the current climatic state, natural discharge of groundwater from beneath Yucca Mountain probably occurs further south at Franklin Lake Playa (Czarnecki 1990, p. 1-12), although spring discharge in Death Valley is a possibility (D'Agnese et al. 1997a, pp. 64 and 69). Under past wetter climatic conditions, groundwater discharge occurred at locations nearer to Yucca Mountain than Franklin Lake Playa.

Radionuclides migrating from the repository must be transported approximately 300 m (1,000 ft) downward by groundwater in the unsaturated zone to the water table, where they enter the saturated zone. Radionuclides are then carried downstream in the groundwater system. At 20 km (12 miles), the radionuclides reach the hypothetical water well located near the Amargosa Valley, where they could become a source of contamination in the biosphere (see Figure 3-66).

Important processes that must be considered in describing radionuclide travel time in the saturated zone include advection, transport by moving water; matrix diffusion, diffusion of contaminants into the rock pores; and sorption, capture of particles on rock surfaces by chemical processes (see Figure 3-66). The fractured, porous media of the volcanic units consist of an interconnected network of fractures and matrix material. The effective porosity is the porosity for the combination of fractures and matrix pores through which the radionuclides are carried. Effective porosity affects how fast the contaminants travel. Effective porosities are greater in porous media (e.g., alluvium) than in fractured media (e.g., volcanic tuffs), where contaminant movement is thought to occur primarily through the fractures. Because of the smaller effective porosity, travel times tend to be shorter in the fractured media than in the porous media. Matrix diffusion is the movement of dissolved radionuclides from groundwater flowing in fractures into the relatively immobile pore water of the matrix due to differences in concentration. Diffusion occurs at a small scale, probably not more than a few centimeters into the rock from fractures, and slows radionuclide movement by providing additional solute storage in the matrix pores. Geochemical retardation, through sorption of radionuclides on mineral grains, slows radionuclide migration in groundwater in both fractured and porous media. Processes such as sorption and matrix diffusion increase the residence time for certain radionuclides and allow reduction of dose by radioactive decay.

The most important process that influences radionuclide concentration in the saturated zone is dilution from hydrodynamic dispersion. Radionuclides are expected to move through the unsat-

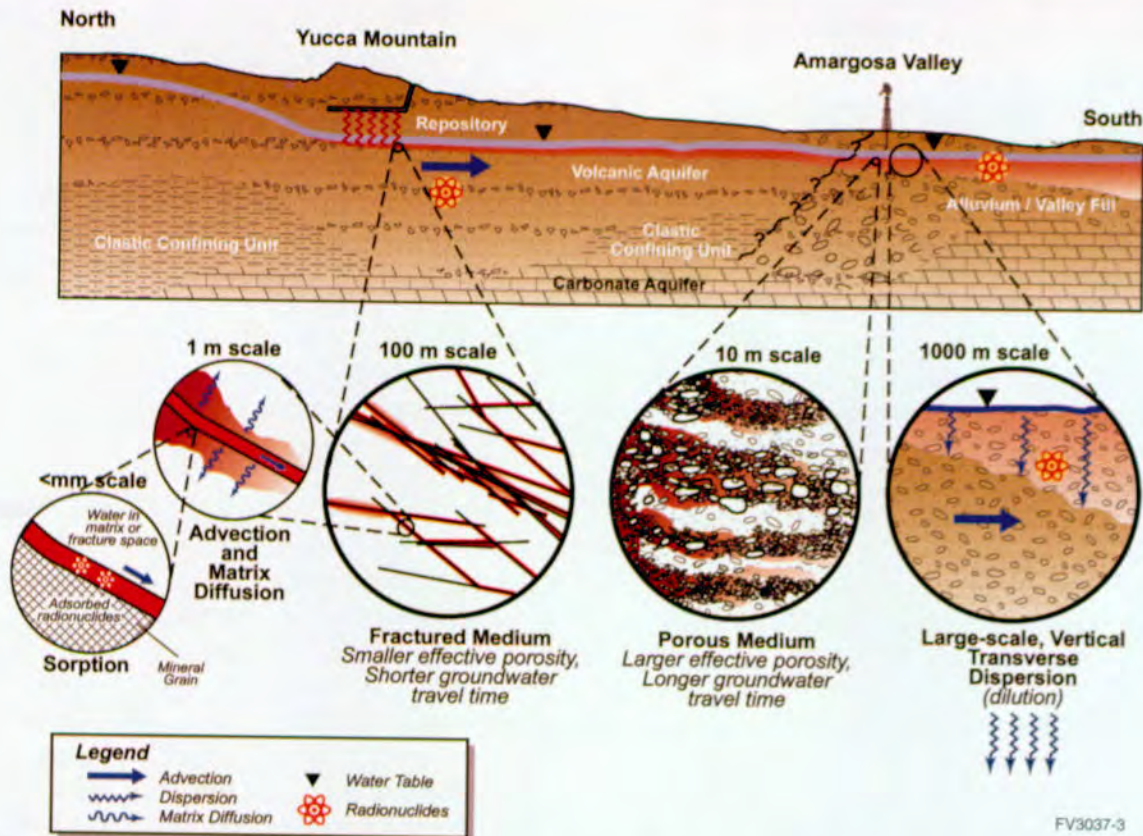


Figure 3-66. Conceptual Model of the Saturated Zone Groundwater Flow System and Processes Relevant to Performance of the Potential Repository at Yucca Mountain

Processes that affect radionuclide travel times in the saturated zone from beneath Yucca Mountain to potential pumping wells include advection, matrix diffusion and sorption. Processes that affect the concentration of radionuclides in groundwater include transverse dispersion of the contaminant plume and radioactive decay.

urated zone below the repository and enter the saturated zone in a well-defined plume, that is, as a flow system distinguishable from the surrounding flow because of differences in chemistry, temperature, concentration, or other parameters. Transverse dispersion, or horizontal and vertical spreading of the plume perpendicular to the travel path, causes dilution of radionuclide concentration. Longitudinal dispersion, or horizontal spreading in the direction of groundwater flow, decreases radionuclide concentrations if the source is varying with time. Transient changes in the direction of groundwater flow may contribute to apparent transverse dispersion and dilution. Transience in the saturated zone flow system could result from climatic variations over long time periods or from focused recharge on shorter time scales. Processes that cause dilution of radionuclides contribute directly to the attenuation of radiological dose by reducing radionuclide concentrations in groundwater.

### 3.7.1.2 Saturated Zone Flow and Transport Data

Numerous observations and scientific studies have provided both regional-scale and near-site knowledge about the saturated zone groundwater system at Yucca Mountain. Much of the information in the following summary is taken from the synthesis report of Luckey et al. (1996), from Czarnecki et al. (1997), and from D'Agnesse et al. (1997a).

The saturated zone flow system at Yucca Mountain is part of the Alkali Flat-Furnace Creek groundwater subbasin of the larger Death Valley groundwater flow system. Groundwater flows regionally from recharge areas at higher elevations in mountain ranges, most significantly, the Spring Mountains and Pahute Mesa, toward natural discharge areas at springs. Groundwater also

discharges through evapotranspiration at playas (see Figure 3-65). Significant quantities of groundwater are also currently being discharged from the regional saturated zone system by pumping in areas such as the Amargosa Valley.

Measurements of water levels in wells near Yucca Mountain indicate that north of the site is a region of possible large hydraulic gradient, potentially 150 m/km (790 ft/mile). An alternative interpretation is that the higher apparent heads in wells north of the site are the result of perched water. West of the site is a region of moderate hydraulic gradient, corresponding to a 45-m (150-ft) increase in water table elevation. Water level data indicate a small horizontal hydraulic gradient (0.1 to 0.3 m/km or 0.5 to 1.6 ft/mile) immediately southeast of the site. Groundwater flow from the repository site for a distance of 5 to 8 km (3 to 5 miles) is apparently to the southeast toward Fortymile Wash. From there, the apparent direction of groundwater flow for about 20 km (12 miles) is to the south-southwest. Hydraulic head is a measure of the driving potential for groundwater flow that is inferred from water level measurements in wells. Near the Yucca Mountain site, hydraulic head in the deeper volcanic units and in the Paleozoic carbonate aquifer, based on one well, are generally higher than in the shallower saturated zone, indicating the potential for groundwater to flow upward. Variations in temperature and heat flow measured in boreholes in the saturated zone suggest significant redistribution of heat by vertical groundwater movement in some areas. These observations suggest that there is (an imperfect) confining unit separating the shallow volcanic flow system from the deeper flow system.

Variations in water table elevations have been directly monitored for a few decades and inferred from geological and geochemical data over hundreds of thousands of years. Water level fluctuations in most wells have been small—on the order of a few decimeters—primarily in response to barometric variations and earth tides. Variations have been greater in the Amargosa Valley area because of pumping. Highly transient and longer-term variations in hydraulic head of a few meters to a few decimeters have been observed following earthquakes. Significantly higher water table

elevations (80–120 m or 260–390 ft higher than current elevations) at Yucca Mountain have been inferred from the locations of nearby paleospring deposits and from geochemical and mineralogical evidence from the unsaturated zone at the site. Higher water table elevations in the geologic past were apparently associated with wetter climatic conditions. From the perspective of performance assessment calculations, fluctuations of this magnitude in water table elevations suggest potentially significant alteration of radionuclide transport path lengths in the unsaturated zone on geologic time scales.

The aquifer in volcanic rocks has been hydraulically tested at many of the wells near the Yucca Mountain site, although there are no borehole data between approximately 10 and 20 km (6 and 12 miles) downgradient of the repository. Most of the available data are from single borehole tests using constant discharge, fluid injection, pressure injection, and radioactive tracer methods. From these tests, estimates of hydraulic conductivity (a factor that determines the amount of water that can flow through a material) in the fractured volcanic rocks of the saturated zone generally range over three orders of magnitude, depending on the depth and the particular hydrogeologic unit. The apparent hydraulic conductivity values determined from multiple borehole hydraulic tests at the C-hole complex tend to be much higher, by about two orders of magnitude, than the values from single-borehole tests for the same intervals (Geldon 1996, p. 59). The C-hole complex is located approximately 2.5 km (1.6 miles) to the southeast of the repository. Multiple-borehole hydraulic tests generally yield results that are more representative of large-scale hydraulic conductivity of the aquifer, suggesting that the single-borehole tests elsewhere at the site may have significantly underestimated the effective hydraulic conductivity (and thus the groundwater flow velocity) at those locations. Thus, results from the multiple-borehole tests were used in the saturated zone flow modeling for TSPA-VA. Surveys of flow in the deeper wells in the saturated zone near Yucca Mountain indicate that groundwater production in most of the wells occurred in a few discrete intervals within the volcanic units. For performance assessment calculations, these results

suggest that most groundwater flow in the fractured volcanic units is through only a small fraction of the saturated thickness.

Forced-gradient, cross-hole tracer tests conducted at the C-hole complex have provided data on in situ transport of the non-radioactive surrogate solutes and synthetic colloids in fractured, porous volcanic tuffs in the saturated zone (CRWMS M&O 1997f; Geldon et al. 1997, p. Background-2). These tests have been interpreted to indicate that the tracers diffused from fractures into the rock matrix and that sorption occurred. Test results that indicate relatively high flow porosity suggest that flow may have occurred in both fractures and the rock matrix during the tracer tests. There was relatively good agreement between tracer-test results and laboratory measurements of sorption coefficients ( $K_d$ ) for transport of lithium. Lower recovery of microspheres, a uniformly sized surrogate colloid with a neutral surface charge, suggests significant filtration over the 30-m (100-ft) transport distance. For the TSPA analyses, these results support accounting for matrix diffusion in fractured volcanic units and using laboratory measurements of the sorption coefficient parameter for sorbing radionuclides.

Groundwater sampling from fractured volcanic tuff in the saturated zone near the Benham underground nuclear test site on Pahute Mesa suggests that colloid-facilitated transport of plutonium in the saturated zone may be relatively rapid (Thompson et al. 1998, p. vii). Although some component of transport may have been associated with the underground nuclear test, low concentrations of plutonium, associated with colloidal material in groundwater samples, indicate transport in the saturated zone of at least 1,300 m (4,300 ft) in 28 years (Thompson et al. 1998, p. 13). For the TSPA, this observation was used to develop an alternative conceptual model for colloid-facilitated transport of plutonium (Section 3.7.2.2).

### 3.7.1.3 Saturated Zone Flow and Transport Modeling

Analyses of groundwater flow and radionuclide transport in the saturated zone use numerical

modeling results at different scales for site characterization and TSPA calculations. The regional-scale flow model (D'Agnese et al. 1997a) encompasses a large portion of southern Nevada and parts of eastern California. The regional-scale model was designed to use natural system boundaries so that estimates of groundwater flux through the model are constrained. The estimate of groundwater flux through the saturated zone flow system is based on the system's overall water budget. The regional-scale model has also been used to estimate the influence of climate change on changes to groundwater flux and flow direction in the saturated zone flow system (D'Agnese et al. 1997b).

A smaller-scale TSPA three-dimensional flow model for groundwater flow was developed to determine the flowpath from the repository footprint, or outline, at the water table to a distance 20 km (12 miles) downgradient, the approximate distance to the nearest domestic extraction of groundwater. Based on the simulation, the hydrogeologic units that were present along the contaminant travel path were determined as well as the percentage of the flowpath occupied by each unit. The travel distance through each hydrogeologic unit provided by this analysis was used to define the travel-path characteristics in the saturated zone for the TSPA one-dimensional transport, base case analysis (see Section 3.7.2).

The TSPA three-dimensional flow model used for this analysis incorporated an area of about 20 km × 36 km (12 miles × 22 miles) to a depth of 950 m (3,100 ft) below the water table. The model grid was a uniform orthogonal mesh with 500-m × 500-m × 50-m (1,600-ft × 1,600-ft × 160-ft) elements. The hydrogeologic framework in the model was based on a refined version of the regional geologic framework model used by D'Agnese et al. (1997a, p. 29-35). Seventeen different hydrogeologic units were represented in the model. Two linear, vertical features with low permeabilities to the west and north of Yucca Mountain were included to simulate the moderate and large hydraulic-gradient regions, respectively.

Flow was modeled as steady state through a single-continuum, porous medium. Focused recharge

along Fortymile Wash, consistent with USGS measurements, was included as a specified flux. Specified-pressure boundary conditions were applied to the lateral boundaries based on the interpolation of measured values of hydraulic head. Groundwater flow was not allowed to occur across the bottom boundary of the model. Permeability was assumed to be uniform within hydrogeologic units in the model domain, and average isothermal conditions were applied in the three-dimensional flow model for the saturated zone.

The TSPA three-dimensional model was calibrated by an iterative procedure, and the simulated hydraulic heads were compared with measured head values in the model domain. There was good agreement between the simulation results and most of the well measurements, particularly in the area downgradient of the repository. The differences between simulated and measured hydraulic head values were less than 5 m (16 ft) for shallow wells downgradient of the repository, within a 10 km (6 miles) distance. The direction of groundwater movement in this flow model is consistent with the conceptual model of the system and is evident in the plot of simulated particle paths shown in Figure 3-67.

Particle tracking in the simulated flow field of the TSPA three-dimensional flow model was used to estimate the flowpath lengths in the saturated zone through each of the hydrostratigraphic units downstream from the repository. In the model simulations, a swarm of particles was released at the water table and evenly distributed across the repository footprint. Flowpath lengths within the units were then tabulated. Flow was significant in four of the hydrostratigraphic units, and the resulting information was incorporated into the one-dimensional transport simulations used in the TSPA analyses (Section 3.7.2).

#### **3.7.1.4 Saturated Zone Workshop and Expert Elicitation**

To help understand how to best model saturated zone flow and transport for TSPA-VA, a workshop was held in Denver, Colorado (Table 3-19). The goal of the workshop was to bring together a number of experts in order to define issues related

to the saturated zone that were important to repository performance, in particular, issues concerning transport travel times and dilution. The issues were then evaluated to determine if they were sufficiently well understood and accounted for in the modeling. If not, analysis plans were developed to address the issue. Some analyses had an indirect effect on TSPA-VA; for example, the study of how structural controls, such as faults, influenced flow and transport aided in the development of, but did not explicitly produce, a distribution for effective porosity. Other analyses were specifically directed toward TSPA-VA modeling; for example, the convolution integral method (Section 3.7.2) was developed and tested as part of this effort. The analysis plan concerning climate directly led to modeling that derived the groundwater fluxes used in TSPA-VA for future climates.

In addition to the workshop, an expert elicitation was conducted to provide guidance for the saturated zone component of TSPA-VA. Five panelists participated in the expert elicitation to assess the uncertainty in conceptual models of processes and specific parameter values relevant to the saturated zone. The elicitation process consisted of the following:

- Written and oral presentation of data to the experts by researchers from the YMP
- Exchange of opinions and assessments among the panel members
- Formal interviews with the individual experts to elicit assessments of key issues

The experts expressed their general opinions about the appropriate conceptual models for flow and transport in the saturated zone and provided probabilistic distributions for some key parameters (CRWMS M&O 1998g, pp. 1-1 to 1-7).

The experts generally agreed that groundwater in the saturated zone flows from beneath the repository to the southeast and south primarily through fractured volcanic tuffs of the middle volcanic aquifer and the valley fill alluvium. Some panel members suggested that sorptive characteristics of

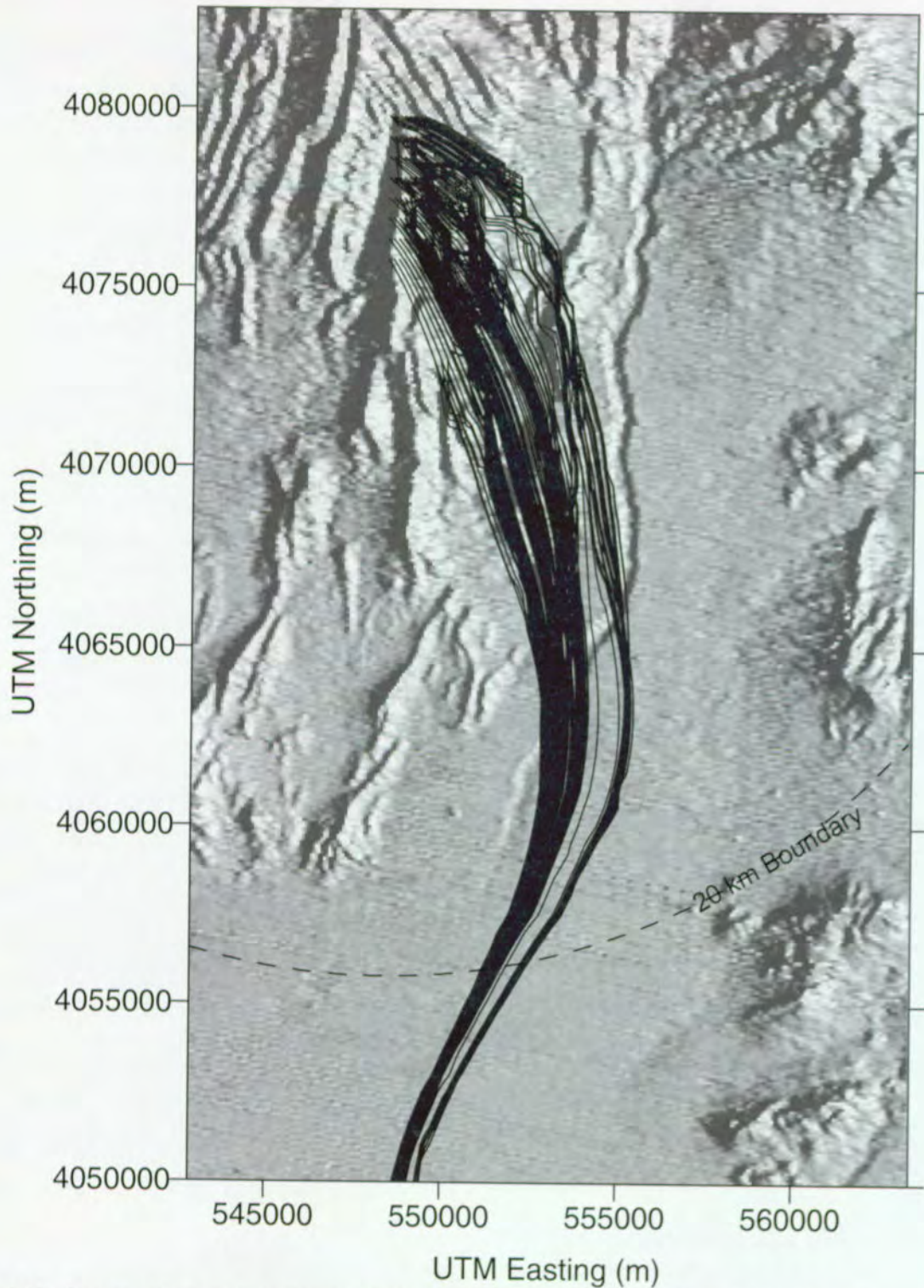


Figure 3-67. Simulated Particle Paths from the Total System Performance Assessment for the Viability Assessment Three-Dimensional Flow Model for the Saturated Zone  
The simulated pathlines are superimposed on a shaded relief map of the surface topography. The transport model results shown are for a hypothetical release of a nonsorbing radionuclide at 10,000 years following the introduction of a source evenly distributed over the footprint of the repository.

Table 3-19. Saturated Zone Flow and Transport  
Abstraction/Testing Workshop

|  |
|--|
| <p style="text-align: center;"><b>SATURATED ZONE FLOW AND TRANSPORT<br/>ABSTRACTION/TESTING WORKSHOP</b><br/>April 1-3, 1997, Denver, CO<br/>(CRWMS M&amp;O 1997s)</p> <p><b>PRIORITIZATION CRITERIA</b></p> <ul style="list-style-type: none"><li>• Does the process/issue affect the<ul style="list-style-type: none"><li>- Peak radionuclide concentration at 5 km from the repository?</li><li>- Peak radionuclide concentration at 30 km from the repository?</li><li>- Time to first arrival (1% of peak)?</li><li>- Spatial distribution of the plume (both horizontal and vertical)?</li><li>- Spatial distribution of groundwater flux (e.g., dilution at the unsaturated zone-unsaturated zone interface)?</li></ul></li></ul> <p><b>HIGHEST PRIORITY ISSUES</b></p> <ul style="list-style-type: none"><li>• Conceptual models of saturated zone flow:<ul style="list-style-type: none"><li>- Regional discharge</li><li>- Regional recharge</li><li>- Vertical flow</li><li>- Alternative conceptual models</li></ul></li><li>• Conceptual models of saturated zone geology:<ul style="list-style-type: none"><li>- Channelization in vertical features</li><li>- Properties of faults</li><li>- Channelization in stratigraphic features</li><li>- Distribution of zeolites</li><li>- Fracture network connectivity</li></ul></li><li>• Transport processes and parameters<ul style="list-style-type: none"><li>- Dispersivity</li><li>- Matrix diffusion (effective porosity)</li><li>- Matrix sorption</li><li>- Fracture sorption</li></ul></li><li>• Coupling to other components of TSPA<ul style="list-style-type: none"><li>- Climate change</li><li>- Unsaturated zone and saturated zone coupling</li><li>- Thermal and chemical plume</li><li>- Well withdrawal scenarios</li></ul></li></ul> <p><b>ANALYSIS PLANS</b></p> <ul style="list-style-type: none"><li>• Sensitivity study on uncertainties in site-scale saturated zone transport parameters and models</li><li>• Coupling unsaturated and saturated zone models</li><li>• The effects of large-scale channelization on effective transport parameters</li><li>• Determination of effective field-scale transport parameters using C-Wells testing results</li><li>• Past, present, and future saturated zone fluxes</li><li>• Geologic structure and processes affecting flow channelization</li></ul> |
|--|

the alluvium could significantly contribute to retardation of some radionuclides. They expected faults and fracture zones to have important impacts on flow in the volcanic units. The panel members offered alternative hypotheses for the large hydraulic gradient north of Yucca Mountain, and there was disagreement regarding the importance of this feature to repository performance. The

panel members did agree that any major transient change in the large hydraulic gradient is unlikely. The panel members generally concurred with interpretations of geochemical and paleospring data indicating water table rises of 80–120 m (260–390 ft) beneath the repository in response to past climatic variations.

For transport of contaminants in the saturated zone, the experts emphasized the limitations of processes that would cause dilution of contaminant concentrations. The experts believe that transport is by movement in vertically thin plumes through flow tubes beneath the repository. Dilution of contaminants occurs by vertical transverse dispersion and transient fluctuations in the direction of the hydraulic gradient. The experts generally rejected a mixed tank model in which contaminated flow from the unsaturated zone mixes on a large scale with uncontaminated groundwater in the saturated zone.

The dilution-factor distribution suggested by the experts was used to reduce the maximum concentration in the saturated zone at the source beneath the repository to the concentration in the groundwater approximately 20 km (12 miles) downgradient from the repository. The aggregate uncertainty in this parameter ranges from 1 to 100, with a median value of about 10. This range of values for dilution in the saturated zone represents a significant departure from previous TSPA analyses for Yucca Mountain (for example, CRWMS M&O 1995, pp. 7–23 and 7–25; Wilson et al. 1994, p. 11–35) in which effective values of dilution were typically orders of magnitude higher. The expert elicitation provided a median value for specific discharge in the saturated zone (0.6 m/year or 2 ft/year) that was used in the one-dimensional transport simulations for the TSPA-VA. Finally, the experts discussed what the effective porosity should be, that is, the fraction of the bulk volume of the aquifer that carries flow and solute transport. Some of the panel members believed that effective porosity for radionuclide transport in fractured volcanic rocks in the saturated zone could be as low as conservative estimates of fracture porosity, implying little diffusive interaction with the rock matrix. Consequently, the uncertainty distribution for effective porosity in fractured volcanic units

used in the TSPA-VA analyses has a maximum value equivalent to the average matrix porosity and a value of  $1 \times 10^{-5}$  at its lower end.

### 3.7.2 Implementation of the Performance Assessment Model

For the TSPA, a hierarchy of models was used to simulate the transport of radionuclides in the saturated zone. Explicit, three-dimensional modeling was not used to simulate radionuclide concentrations because it can generate numerical dispersion, which artificially lowers concentration. Three-dimensional modeling was used only to determine flow paths. One-dimensional transport modeling was used, based on the flow paths from the three-dimensional modeling, to determine concentration breakthrough curves at a distance of 20 km (12 miles) for unit releases of radionuclides. Then, within the TSPA calculations, the convolution integral technique described in Section 3.7.2.3 was used to combine the break-

through curves with the time-varying radionuclide sources from the unsaturated zone. Finally, the radionuclide concentrations were divided at 20 km (12 miles) by the dilution factor, which was sampled from the distribution suggested by the expert elicitation process described above. These final radionuclide concentrations, corresponding to groundwater contamination in a hypothetical well, were used to calculate dose in the biosphere model. No additional dilution in the pumping well was considered in the analysis (Section 5.8.2 addresses issues related to dilution from well pumping).

#### 3.7.2.1 One-Dimensional Flow and Transport Modeling

A diagrammatic representation of the conceptual model for saturated zone transport is shown in Figure 3-68. Simulations of radionuclide transport in the saturated zone for the TSPA calculations were performed with six one-dimensional flow tubes using FEHMN (Zyvoloski et al. 1995), a computer code for simulating heat and mass

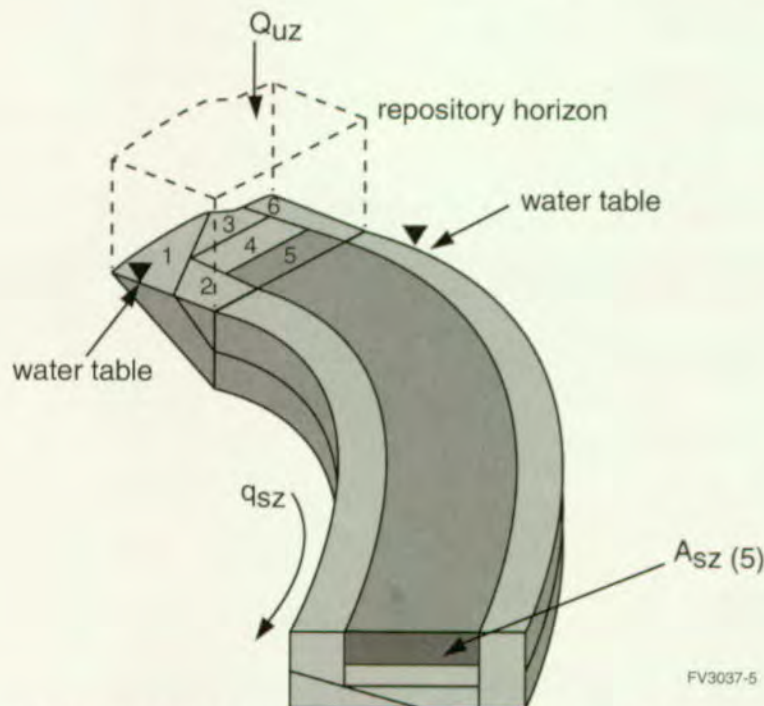


Figure 3-68. Schematic Diagram of the Conceptual Basis of the Total System Performance Assessment for the Viability Assessment One-Dimensional Transport Model for the Saturated Zone from Below the Repository to 20 km (12 miles) South

The six source subregions at the water table beneath the repository correspond to the six streamtubes in the saturated zone. The cross-sectional area of each streamtube (for example,  $A_{sz}(5)$ ) is proportional to the volumetric groundwater flux through that streamtube. The specific discharge for groundwater in the saturated zone is  $q_{sz}$ .

transfer with finite elements. Streamtubes are taken from a concept in classical fluid dynamics that is used to visualize and estimate the behavior of the elements of a flow system. Each of the six streamtubes is a continuation of a groundwater flow path from the repository in the unsaturated zone. Note that the six source subregions at the water table shown in Figure 3-68 were used to divide radionuclide mass and groundwater flow among the streamtubes. The shapes of these subregions were defined to capture potential variability in radionuclide releases (e.g., edge versus center of the repository) and to capture geologic variability (e.g., presence of welded Bullfrog tuff at the water table in source subregion 1). The volumetric flux of groundwater through each streamtube ( $Q_{UZ}$ ) was determined at the water table from flow simulations using the site-scale flow model developed by Bodvarsson et al. (1997) for the unsaturated zone (see Section 3.1). Transport simulations with the one-dimensional streamtube approach implicitly assume complete mixing of the radionuclide mass in the volumetric groundwater flux specified for each streamtube. The specific discharge within the streamtubes in the saturated zone ( $q_{SZ}$ ) was 0.6 m/year (2 ft/year) for current climatic conditions. The streamtubes are 20 km (12 miles) long, with a

regular grid spacing in the tubes of 5 m (16 ft). The four hydrostratigraphic units in the streamtubes are the middle volcanic aquifer, the upper volcanic aquifer, the middle volcanic confining unit, and the alluvium/valley fill. The lengths of these units within the streamtubes were defined by modeling particle transport using the TSPA three-dimensional flow model for the saturated zone described in Section 3.7.1.3.

### 3.7.2.2 Model Parameter Uncertainty

Uncertainty in radionuclide transport through the saturated zone was incorporated into the analysis by varying key transport parameters. The stochastic parameters used in the one-dimensional transport simulations were effective porosity in the volcanic units and the alluvium unit; distribution coefficients ( $K_d$ s) for sorbing radionuclides in the volcanic and alluvial units; the ratio of the radionuclide mass in aqueous and colloidal forms ( $K_c$ ) for colloid-facilitated transport of plutonium; longitudinal dispersivity; the fraction of flowpath through the alluvium; and the dilution factor (Table 3-20).

A broad range of uncertainty in effective porosity for fractured volcanic units was employed in the

Table 3-20. Stochastic Parameters for Saturated Zone Flow and Transport

| Parameter   | Distribution Type   | Distribution Statistics [Bounds]        |
|---|---------------------|---|
| Dilution Factor                                     | CDF                 | Median=10, [1., 100.] (Section 3.7.1.4) |
| Effective Porosity (Alluvium)                       | Truncated Normal    | Mean=0.25, SD=0.075 [0., 1.0]           |
| Effective Porosity (Upper Volcanic Aquifer)         | Log Triangular      | [1e-5, 0.02, 0.16]                      |
| Effective Porosity (Middle Volcanic Aquifer)        | Log Triangular      | [1e-5, 0.02, 0.23]                      |
| Effective Porosity (Middle Volcanic Confining Unit) | Log Triangular      | [1e-5, 0.02, 0.30]                      |
| Effective Porosity [Pu] (Volcanic Units)            | Log Uniform         | [1e-5, 1e-3]                            |
| $K_d$ [Np] (Alluvium) (mL/g)                        | Uniform             | [5., 15.]                               |
| $K_d$ [Np] (Volcanic Units) (mL/g)                  | Beta (Approx. Exp.) | Mean=1.5, SD=1.3, [0., 15.]             |
| $K_d$ [Pa] (Alluvium) (mL/g)                        | Uniform             | [0., 550.]                              |
| $K_d$ [Pa] (Volcanic Units) (mL/g)                  | Uniform             | [0., 100.]                              |
| $K_d$ [Se] (Alluvium) (mL/g)                        | Uniform             | [0., 150.]                              |
| $K_d$ [Se] (Volcanic Units) (mL/g)                  | Beta (Approx. Exp.) | Mean=2.0, SD=1.7, [0., 15.]             |
| $K_d$ [U] (Alluvium) (mL/g)                         | Uniform             | [5., 15.]                               |
| $K_d$ [U] (Volcanic Units) (mL/g)                   | Uniform             | [0., 4.]                                |
| $K_c$ [Pu] (All Units)                              | Log uniform         | [1e-5, 10.]                             |
| Longitudinal Dispersivity (All Units) (m)           | Log normal          | Logmean=2.0, LogSD=0.753                |
| Fraction Of Flowpath in Alluvium                    | CDF                 | [0., 0.3] (See Text)                    |

CDF—cumulative distribution function  
SD—standard deviation  
Approx. Exp.—Approximate Exponential

TSPA-VA analyses to reflect uncertainty in the underlying processes affecting contaminant travel times in the saturated zone. The effective porosity is the fraction of the bulk rock volume that is available for storage of dissolved radionuclides during transport in the saturated zone. The effective porosity approach is a simplified representation of the system that includes the influences of molecular diffusion from fractures into matrix pore water and the spacing between fractures with flowing groundwater. The effective porosity approach also implies potential limited access of contaminants to the sorptive capacity of the rock matrix, an effect accounted for in the TSPA-VA simulations.

Colloid-facilitated transport of plutonium in the saturated zone was simulated using a conceptual model based on both equilibrium, reversible sorption of plutonium onto colloids and the potential for irreversible sorption of plutonium onto some colloidal particles (see Section 3.5). These two components of plutonium transport were included in the analysis. A large fraction of the plutonium mass was simulated to move through the saturated zone assuming chemical equilibrium among dissolved plutonium, plutonium sorbed onto colloids, and plutonium sorbed onto the aquifer material. This conceptual model uses the partition coefficient ( $K_c$ ) to define the distribution of plutonium sorbed on colloids relative to the aqueous concentration of plutonium. The values of  $K_c$  were correlated in the saturated zone and unsaturated zone components of the TSPA-VA probabilistic calculations. A small fraction of the plutonium mass was simulated to be irreversibly attached onto colloids and transported relatively rapidly in the saturated zone, without significant retardation. This small fraction was defined to be consistent with the reduction in plutonium concentration inferred at the Benham site (Sections 3.5.2.4 and 3.6.1.4). The fraction of irreversibly sorbed plutonium used in the calculations implicitly considers partitioning of plutonium at the source and filtration during transport. Because attenuation of irreversible colloid-facilitated transport was implicitly included in characterization of the source term, filtration of colloids was not explicitly included in the saturated zone

transport model. Colloid transport occurred only within the fracture porosity of the volcanic units, so the uncertainty distribution of effective porosity for colloids varied only over the estimated range of fracture porosity.

The stochastic parameters in the probabilistic analyses for saturated zone-flow and transport are summarized in Table 3-20. The dilution factor was applied to radionuclide concentrations to implicitly account for transverse dispersion out of the one-dimensional streamtubes. The uncertainty distribution for the dilution factor was a product of the expert elicitation described in Section 3.7.1. The travel distance through the alluvium/valley fill unit was varied from 0 to 6.0 km (0 to 3.7 miles), with a 10 percent probability that no alluvium is present along the 20 km (12 miles) of travel path for radionuclides in the saturated zone. The uncertainty in the fraction of the flowpath in alluvium was included to account for uncertainty in the flow system, which was not explicitly evaluated with the TSPA three-dimensional flow model.

### 3.7.2.3 Integration of Transport Modeling with Total System Performance Assessment Calculations

The convolution integral method was used in the TSPA calculations to determine the radionuclide concentration in the outlets of the six streamtubes, 20 km (12 miles) downgradient of the repository as a function of the transient radionuclide mass flux at the water table beneath the repository. This computationally efficient method combines information about the unit response of the system, as simulated by the TSPA one-dimensional transport modeling, with the radionuclide source history to calculate transient system behavior, as shown in Figure 3-69. The most important assumptions of the convolution method are linear system behavior (i.e., doubling mass input results in doubling of concentration) and steady-state flow conditions in the saturated zone.

The effects of climate change on radionuclide transport in the saturated zone were incorporated into the analysis by assuming instantaneous change from one steady-state flow condition to another steady-state condition in the saturated zone.

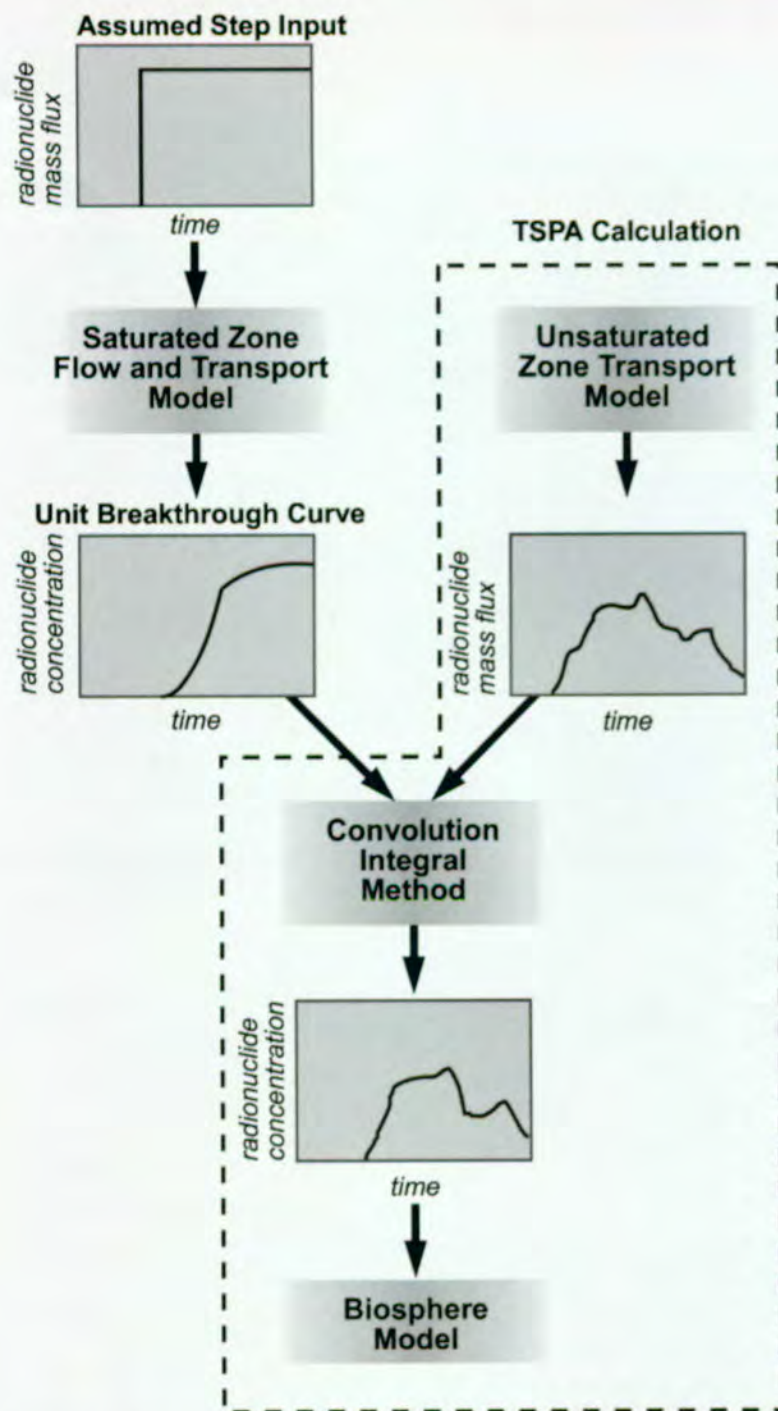


Figure 3-69. Flow Chart for Utilization of the Convolution Integral Method in Saturated Zone Flow and Transport Calculations in Total System Performance Assessment for the Viability Assessment

As illustrated in this flowchart, information on radionuclide travel times and concentrations in the saturated zone (contained in the unit breakthrough curve) is combined with information on radionuclide mass flux at the water table beneath the repository by the convolution integral method to calculate the radionuclide concentration history at 20 km (12 miles) downstream from the repository. The nature of the unit breakthrough curve varies significantly among Monte Carlo realizations (see Figure 3-71) to reflect uncertainty in the transport characteristics of the saturated zone.

Changes in climate state were assumed to affect the magnitude of groundwater flux through the saturated zone system but have a negligible impact on flowpaths. These effects were incorporated into the convolution method by scaling the velocity of radionuclide breakthrough curves proportionally to the change in saturated zone specific discharge. Also, the concentrations of the radionuclide breakthrough curves were scaled proportionally to the change in volumetric flux from the unsaturated zone into the streamtubes. The regional-scale flow model for the saturated zone provided estimates of the relative change in specific discharge in the saturated zone for future climate states (as summarized in e-mail message from Pat Tucci, 12/11/97; D'Agnesse et al. 1997b). The site-scale flow model for the unsaturated zone (Bodvarsson et al. 1997) provided estimates of changes in volumetric flux through the repository horizon. These estimates are summarized in Table 3-21. Radioactive decay was also applied to radionuclide concentrations calculated with the convolution integral computer program. Ingrowth of radionuclide daughter products was not included in the saturated-zone transport calculations, but the inventory at the repository was adjusted to account for progeny ingrowth (Section 3.5.1.5).

Table 3-21. Climatic Alterations to Saturated Zone Flow

| Climate State     | Saturated Zone Specific Discharge ( $q_{sz}$ ) (m/year) | Volumetric Flux Through Repository Horizon ( $Q_{Uz}$ ) ( $m^3/year$ ) |
|-------------------|---|--|
| Dry (Present)     | 0.6   | 26,900   |
| Long-Term Average | 2.3   | 146,300  |
| Superpluvial      | 3.7   | 395,000  |

The radionuclide concentrations in the six streamtubes were decreased by the dilution factor and then summed to obtain an estimate of the maximum concentration in the saturated zone at 20 km (12 miles) from the repository. For this approximation it is assumed that, in a conceptual sense, implicit spreading of radionuclide mass from individual streamtubes via dilution causes six plumes that essentially overlap. At each time step, the maximum estimated concentration was compared to the maximum undiluted concentration at the source in the saturated zone. The maximum estimated concentration was not allowed to exceed

the maximum undiluted concentration in any individual streamtube at the source (Section 5.7.3 contains an evaluation of methods for combining flow tubes).

### 3.7.3 Results and Interpretation

For the TSPA-VA, the results of the flow and transport analysis for the saturated zone are the radionuclide concentration histories at the geosphere/biosphere interface, which is a well head located 20 km (12 miles) downgradient in the Amargosa Valley region. These concentrations are directly proportional to the radiation dose rate calculated for possible future inhabitants.

A steady boundary condition for unit radionuclide mass flux was applied at the inlet of each streamtube for the TSPA one-dimensional transport simulations. The resulting unit breakthrough curves of concentration formed the basis for calculating radionuclide concentrations using the convolution integral method. The breakthrough curves for unit concentration for the nine radionuclides at 20 km (12 miles) from the repository are shown in Figure 3-70. These curves were generated using the expected parameter values. Differences in the arrival times of different radionuclides are because of variations in sorption among the radionuclides. Differences in the maximum concentration among radionuclides are because of radioactive decay during transport through the saturated zone system. To include parameter uncertainty in the TSPA, 100 breakthrough curves were simulated for each radionuclide by sampling parameter values from their respective probability distributions (see Section 3.7.2, Table 3-20). The impact of uncertainty in the one-dimensional transport simulations for the saturated zone is illustrated in Figure 3-71. This figure shows the unit breakthrough curves for technetium-99 concentrations for all 100 realizations used in the base case analyses. Travel times for the nonsorbing technetium-99 vary from a few hundred years to about 4,000 years; maximum concentrations, primarily influenced by the dilution factor, vary over two orders of magnitude among these simulations. The uncertainty in longitudinal dispersion is shown by variations in the slopes of the breakthrough curves in Figure 3-71.

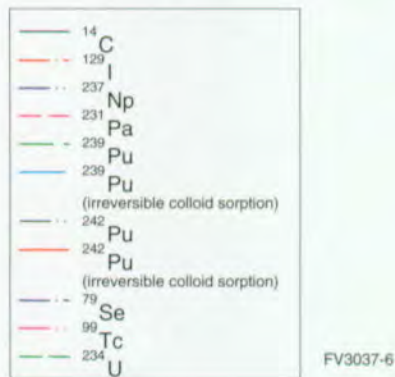
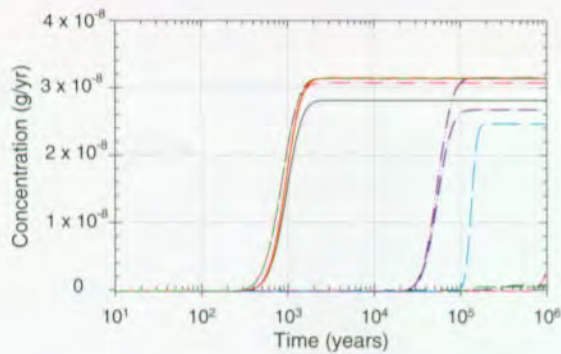
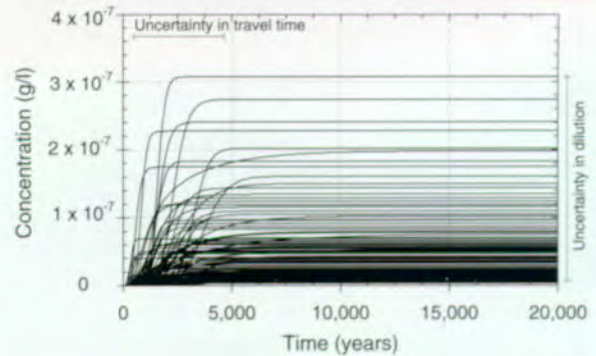


Figure 3-70. Unit Radionuclide Concentration Breakthrough Curves from the Total System Performance Assessment One-Dimensional Transport Modeling for the Saturated Zone at a Distance of 20 km (12 miles) for all Modeled Radionuclides. The radionuclide concentration breakthrough curves are shown for the expected parameter value case from source subregion 1 at the water table under dry climatic conditions, assuming a source mass flux of 1 g/year for each radionuclide spread over source subregion 1.

Radionuclide migration through the saturated zone affects total system performance in two ways. First, the saturated zone may function as a mechanism for significant delay in releasing radionuclides to the biosphere. Second, there may be significant dilution of radionuclide concentrations that occurs during transport in the saturated zone. Both impacts are functions of the distance between the repository and the point of release to the biosphere, which is assumed for the TSPA-VA to be 20 km (12 miles) from the repository.

Delays in radionuclide migration caused by processes in the saturated zone are potentially important to repository performance if the travel time for a radionuclide through the saturated zone system is long in comparison to its half life. For



FV3037-7

Figure 3-71. Unit Radionuclide Concentration Breakthrough Curves from the Total System Performance Assessment One-Dimensional Transport Modeling for the Saturated Zone at a Distance of 20 km (12 miles) for Technetium-99.

The radionuclide concentration breakthrough curves are shown from source subregion 1 at the water table under dry climatic conditions, assuming a source mass flux of 1 g/year spread over source subregion 1. The uncertainty bars indicate the range of variability in the important characteristics of the saturated zone system in the TSPA-VA analyses.

example, in the expected-value case shown in Figure 3-70, the maximum concentrations of plutonium-239 (equilibrium colloid sorption) and selenium-79 are significantly attenuated relative to the other radionuclides because of radioactive decay. Delay in radionuclide migration in the saturated zone may also be significant if the travel time through the system is long relative to the time period of concern. For example, the travel time of unretarded radionuclides such as technetium-99 (see Figure 3-71) may be relevant to repository performance in a 10,000-year time frame. However, the delay in radionuclide release from the saturated zone for a period of 100,000 years for unretarded radionuclides would be insignificant. Retardation in the saturated zone for most of the radionuclides that experience sorption is highly uncertain, particularly with regard to sorption characteristics of the alluvium/valley fill material.

The dilution of radionuclide concentrations in the saturated zone is handled in a straightforward manner in the TSPA-VA calculations through the dilution-factor parameter. Although there is significant uncertainty in this parameter and complexity in the underlying processes that lead to dilution, the relationship between the dilution factor and

radiation dose rate is a simple linear function for a steady radionuclide source from the unsaturated zone. Transient peaks in the radionuclide concentration at the source in the saturated zone are also attenuated by longitudinal dispersion during transport in the saturated zone.

### 3.8 BIOSPHERE

The biosphere is that part of the earth where all living organisms reside, including all components of the environment, such as soil, water, and air. Of interest is how a potential high-level radioactive waste repository at Yucca Mountain could affect the biosphere. In particular, it is important to know how radionuclides move through the biosphere and how they might eventually impact the human inhabitants of the region. The primary measure of the repository performance is the annual dose of radiation that would be received by an individual living in the region.

The biosphere scenario adopted for the base case assumes a reference person who is living 20 km (12 miles) from a potential repository at Yucca Mountain, in the Amargosa Valley region. The 20-km (12-mile) distance is not a regulatory boundary, as no performance regulation presently exists for a repository at Yucca Mountain; it was selected for TSPA-VA because it marks the closest present-day habitation to Yucca Mountain. People living in the community of Amargosa Valley are considered to be the group of people most likely to be affected by radioactive releases (the critical group), because of their proximity to Yucca Mountain, and because the Amargosa valley region is hydraulically down-gradient from the potential repository site (Luckey et al. 1996, p. 14). The reference person is intended to be representative of this group: an adult who lives year-round at this location, uses a well as the primary water source, and otherwise has habits, such as the consumption of local foods, that are similar to those of inhabitants of the region. Because changes in human activities over millennia are beyond current capabilities to predict, the present-day reference person is also assumed to be typical of future inhabitants.

A survey was conducted of inhabitants residing within an 80-km (50-mile) grid centered on Yucca Mountain to collect information for several programs, with a primary emphasis on biosphere modeling. Over one thousand interviews were completed for the survey, including 43 percent of the households in the Amargosa Valley. The survey collected dietary and lifestyle information on adults and was used to define the food consumption of the reference person.

Incorporation of the biosphere into the TSPA-VA calculations involved two steps. The first step was creating a model of the reference person and the biosphere pathways that might direct radionuclides to that person. The model was implemented in an accepted computer program for predicting radiation dose, GENII-S (Leigh et al. 1993). Model parameters were quantified using the regional survey, other site-specific data, and data from accepted national and international sources. The model uses a unit concentration of a radionuclide in water as the input, and produces a biosphere dose conversion factor for that radionuclide as the output. The biosphere dose conversion factor includes the effects of various pathways through the environment (e.g., irrigation and uptake of a contaminant by vegetables, then ingestion by the reference person), as well as various pathways through the reference person (e.g., the fraction of the contaminant that is taken up by the reference person, where it is accumulated in the body, and its retention time).

The second step required calculating radionuclide concentrations in the groundwater and multiplying them by the appropriate biosphere dose conversion factors. The end product of these calculations is prediction of the annual radiation dose to the reference person, the primary performance measure for TSPA-VA.

An overview of how the biosphere component fits in TSPA-VA is depicted in Figure 3-72.

In addition to the biosphere scenario considered for the base case, comparative analyses were performed to examine the impact of several assumptions. In addition to a typical Amargosa Valley adult resident, two other types of inhabitants

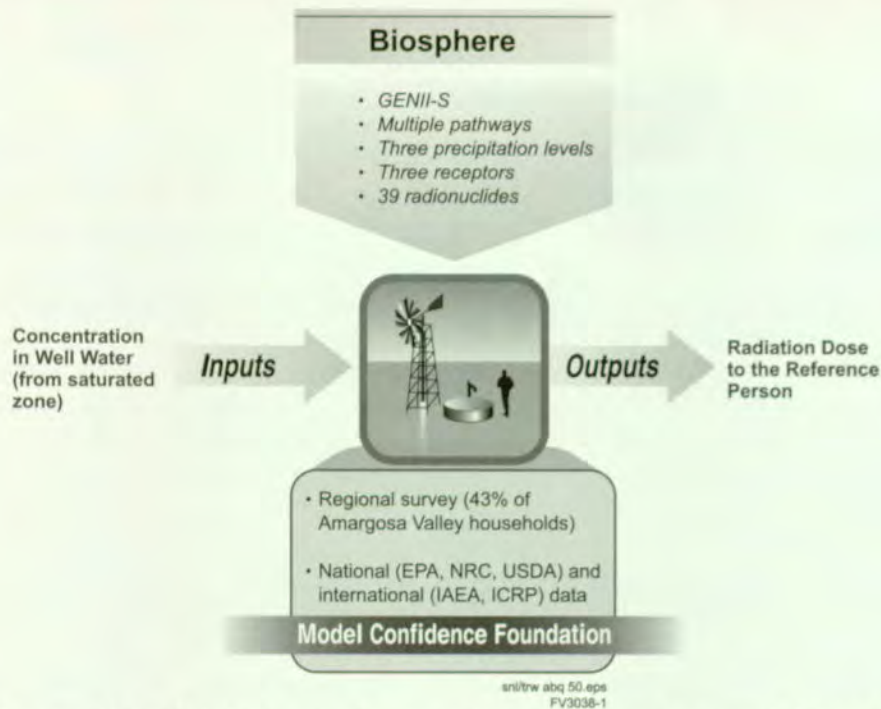


Figure 3-72. Overview of the Modeling Process Employed in the Biosphere Component of Total System Performance Assessment for the Viability Assessment

were considered. One was a subsistence farmer who takes all drinking water from a local well and only consumes locally produced foodstuffs. The other was a resident farmer whose food consumption is 50 percent locally grown but who still gets all drinking water from the well. Also, scenarios involving climate change and a volcanic eruption (Section 4.4.2) at Yucca Mountain were considered.

The biosphere pathway/dose modeling studies and analyses presented in this section were prepared with the view of addressing selected aspects of the NRC Key Technical Issues on Total System Performance Assessment and Integration (NRC 1998a) and Unsaturated and Saturated Flow under Isothermal Conditions (NRC 1997e; 1997f). Specifically, the information presented is pertinent to the TSPA integration subissue on model abstraction and on the unsaturated and saturated zone flow and transport subissue of ambient flow conditions in the saturated zone as those conditions affect evaluations of dilution caused by pumping.

### 3.8.1 Construction of the Conceptual Model

Yucca Mountain lies in a semi-arid, sparsely populated region between the Great Basin and the Mojave Deserts in southern Nevada. The local vegetation is primarily desert scrub and grasses. The mean annual precipitation in the area is about 170 mm/year (6.7 in./year) and the mean annual temperature is about 16°C (61°F). The nearest community in the direction of flow of groundwater is Amargosa Valley (Figure 3-73), an area of approximately 500 miles<sup>2</sup> defined as a tax district by the Nye County commissioners in the early 1980s. Within this district the closest inhabitants to Yucca Mountain are approximately 20 km (12 miles) south at the intersection of US 95 and Nevada State Route 373, in the location known as Lathrop Wells. There are about eight inhabitants at this location. The closest agricultural area and where the majority of the people live is the Amargosa Farms area located approximately 30 km (20 miles) to the south of Yucca Mountain. The Amargosa Farms area is a triangle of land bounded by the Amargosa Farm Road to the north, Nevada State Route 373 to the east, and the California border running from the northwest to the



Figure 3-73. Present-Day Biosphere in the Amargosa Valley  
The upper photograph shows a view of the Amargosa Valley looking eastward from the edge of the Funeral Mountains. The lower picture is the general store in the community.

southeast. The next community in the direction of groundwater flow is across the California state line in Inyo County. The community known as Death Valley Junction is about 60 km (40 miles) south of Yucca Mountain and has a permanent population of less than 10. Evaluation of water flow and wind patterns suggests that any contamination from a repository at Yucca Mountain could spread south and east into this region.

The Amargosa Valley region is primarily rural agrarian in nature (Figure 3-74). Agriculture is mainly directed toward growing livestock feed, for example, alfalfa; however, gardening and animal husbandry are common. Water for household uses, agriculture, horticulture, and animal husbandry is primarily acquired from local wells. Although sparsely populated, the Amargosa Valley region does support a population of 1,270 in approximately 450 households (CRWMS M&O 1997k, Section 2.4; CRWMS M&O 1997i). Commercial agriculture in the Amargosa Valley farming triangle area includes a relatively large dairy that operates with approximately 4,500 milk cows and employs approximately 50 people, a garlic farm that produces about 2,000 lbs. of garlic per year, and a catfish farm that sustains approximately 15,000 catfish. The area contains approximately 1,800 acres planted in alfalfa, 30 acres in oats, 80 acres in pistachios, and 10 acres in grapes. There is a general store, community center, senior center, library, medical clinic, elementary school, restaurant, hotel-casino, and a motel.

To help understand how to best model the biosphere for TSPA-VA, a workshop was held in Las Vegas, Nevada (Table 3-22). The workshop primarily reinforced the modeling strategy that was initially developed for the YMP—to investigate the radiological effects on a “reference person” (the person likely to be exposed to radionuclides released from a repository at Yucca Mountain) living near Amargosa Valley. Analyses were defined that would direct the modeling more toward the goals of TSPA-VA, especially in defining the habits of the reference person that would be modeled and the climates that would be modeled. No expert elicitation was conducted for the biosphere component of TSPA-VA.

Table 3-22. Biosphere Abstraction/Testing Workshop

| <b>BIOSPHERE ABSTRACTION/TESTING WORKSHOP</b><br>June 2-3, 1997, Las Vegas, NV<br>(CRWMS M&O 1997a) |   |
|---|---|
| <b>PRIORITIZATION CRITERIA</b>  |   |
| •   | To what extent does the issue/process affect the following: <ul style="list-style-type: none"><li>- Individual dose?</li><li>- Population dose?</li><li>- The range or uncertainty in the resultant biosphere dose conversion factor?</li></ul>                                   |
| <b>HIGHEST PRIORITY ISSUES</b>  |   |
| •   | Critical group: <ul style="list-style-type: none"><li>- Extrapolation of present habits to the future</li><li>- Location of critical group</li><li>- Habits of critical group</li></ul>   |
| •   | Biosphere pathways: <ul style="list-style-type: none"><li>- Which radionuclides</li><li>- Soil build up</li><li>- Climate change effects as it impacts pathways only</li></ul>  |
| •   | Geo-biosphere interface—present and future: <ul style="list-style-type: none"><li>- Location and definition of bio/geosphere interface</li><li>- Climate change effects as it impacts interface only</li><li>- Important radionuclides transferred by disruptive events</li></ul> |
| <b>ANALYSIS PLANS</b>   |   |
| •   | Critical group definition <ul style="list-style-type: none"><li>- Biosphere pathways variability</li><li>- Climate</li></ul>  |

### 3.8.1.1 Model Basis

The strategy used to conceptualize the Amargosa Valley environment for the TSPA-VA biosphere component was to be consistent with similar activities being pursued by the international scientific community. In this regard, guidance was taken from the National Research Council (National Research Council 1995) and the Biosphere Model Validation Study II Steering Committee (BIOMOVS II 1994). The steering committee established a reference biosphere working group to develop consensus on an approach to evaluating long-term effects of radioactive-waste disposal systems (BIOMOVS II 1996). In developing the model basis for the biosphere component of TSPA-VA, the recommended methodology for biosphere analysis and the list of features, events, and processes developed by the international participants of the steering committee and the working group were used. The TSPA-VA biosphere component focuses on an individual—the

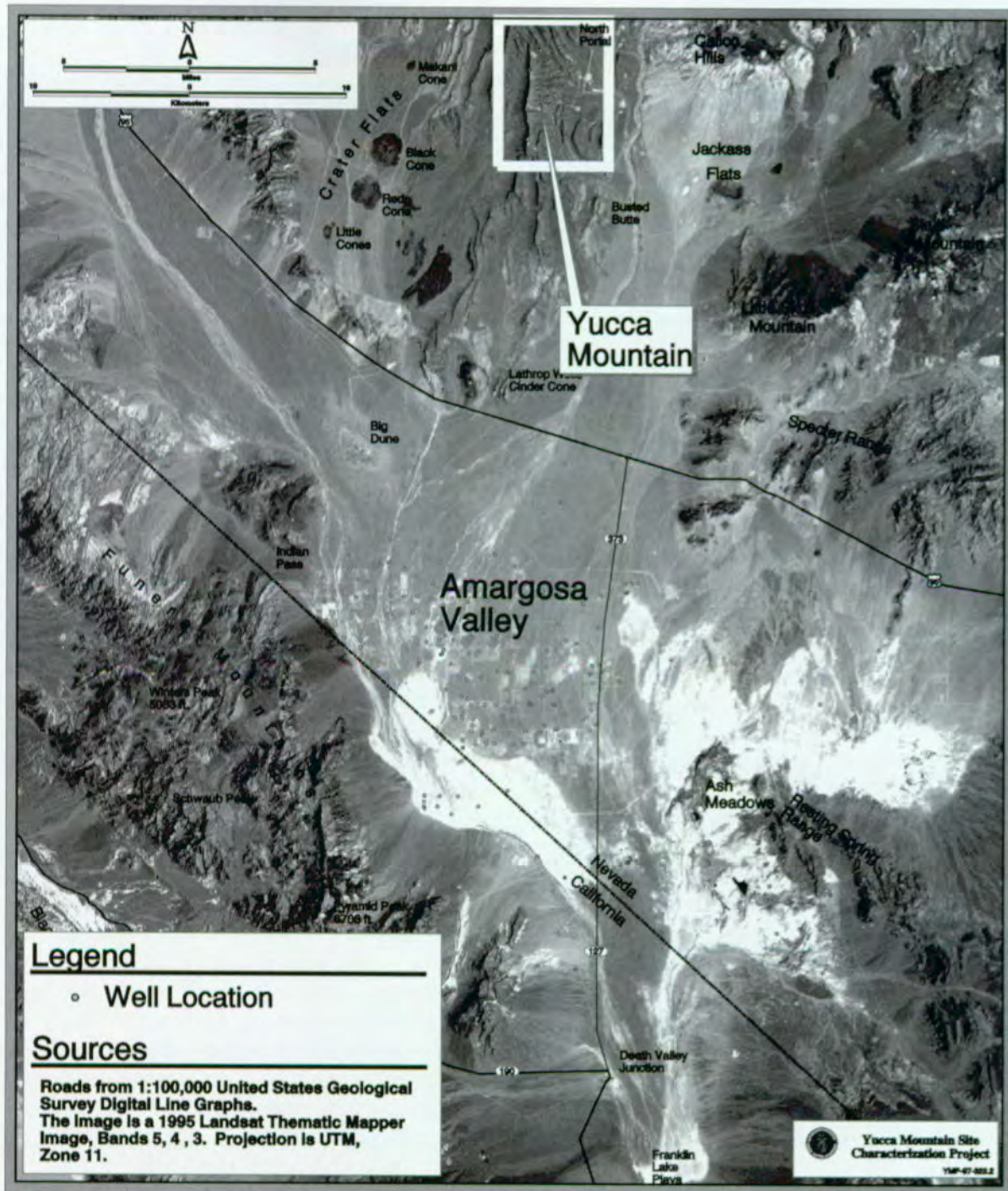


Figure 3-74. Satellite Image Showing the Yucca Mountain Area Including the Amargosa Valley Area. Amargosa Valley is the nearest populated area to Yucca Mountain that would be affected by radionuclide release and subsequent transport by groundwater from the repository.

reference person—living in an Amargosa Valley environment that might change over time. Consistent with guidance from the National Research Council (National Research Council 1995, p. 52), this reference person is defined as the average member of the “critical group,” where the critical group is composed of those individuals expected to receive the highest doses as a result of the discharges of radionuclides from a repository. Because predicting future human technologies, lifestyles, and activities are beyond this TSPA effort, it is assumed that the present-day inhabitants of the region are similar to future inhabitants. This assumption has been accepted in similar international efforts at biosphere modeling, and is preferable to developing a model for a future society.

Climate conditions could become wetter in the future, so two other climates were considered: a long-term average climate, which is colder and wetter than the present climate; and a superpluvial climate, which is much colder and wetter than the present (Section 3.1). The mean annual precipitation rate for the long-term average climate is estimated to be about twice the present-day rate; the mean annual precipitation rate for the superpluvial is estimated to be about three times the present-day rate. The major impact of these different climates on the reference person is to reduce the amount of well water required for irrigation. Other climate effects, for example, a rise in the water table and the appearance of springs, seeps, or other surface water, are not directly considered (although by assuming no dilution in the well withdrawal, the end result would be the same as if the water came from a spring).

The reference person is an adult; children are not considered in TSPA-VA. The closest distance people presently live to Yucca Mountain is just over 20 km (12 miles). In this area, groundwater depth is approximately 100 m (328 ft). Closer to Yucca Mountain, groundwater is at a depth of greater than 200 m (656 ft), which imposes economic constraints on agricultural uses of land. The reference person lives year-round on a farm or in a similar domicile. The person has a garden and livestock and access to locally grown food. The

person consumes locally grown food in types and amounts typical of present-day inhabitants. The person takes all water for agriculture and domestic uses from wells.

Except for releases associated with volcanism (Section 3.8.3.3), the assumption is that contaminated well water is the only way that radionuclides from the repository can reach the reference person. It is also assumed that the reference person takes all water from a well at the point of the highest concentration of radionuclides at the distance under consideration. A further assumption is that no dilution of the contaminated water occurs during pumping of the well. (Section 5.8.1 contains an investigation of the effects of some of these assumptions.)

### **3.8.1.2 Pathways**

Radiation dose to the reference person occurs via exposure pathways. A pathway is the route taken by a contaminant through the biosphere from its source until it interacts with a human. For example, one pathway is from well water to soil via irrigation, from soil to dust via resuspension, from dust to human lungs via inhalation. Exposure pathways fall in three principal categories: ingestion pathways, inhalation pathways, and external exposure pathways (Figure 3-75).

Primary ingestion pathways include the consumption of drinking water, the consumption of locally produced crops irrigated with contaminated water, and the consumption of meat and dairy products from livestock given contaminated water and fodder. Major uncertain or variable factors that affect the ingestion pathways include the leaf interception fraction, uptake of radionuclides by plants and animals, and the amounts of contaminated foodstuffs consumed. In the biosphere model, livestock and poultry are sustained only by locally grown feed, for example, pasture and seasonally harvested alfalfa. These animals are exposed to the groundwater-derived radionuclides by watering and by consuming radionuclides present in the plant tissues. Alfalfa is the predominant crop produced in the Amargosa Valley and alfalfa and forage grasses comprise a major proportion of Nye County agricultural land

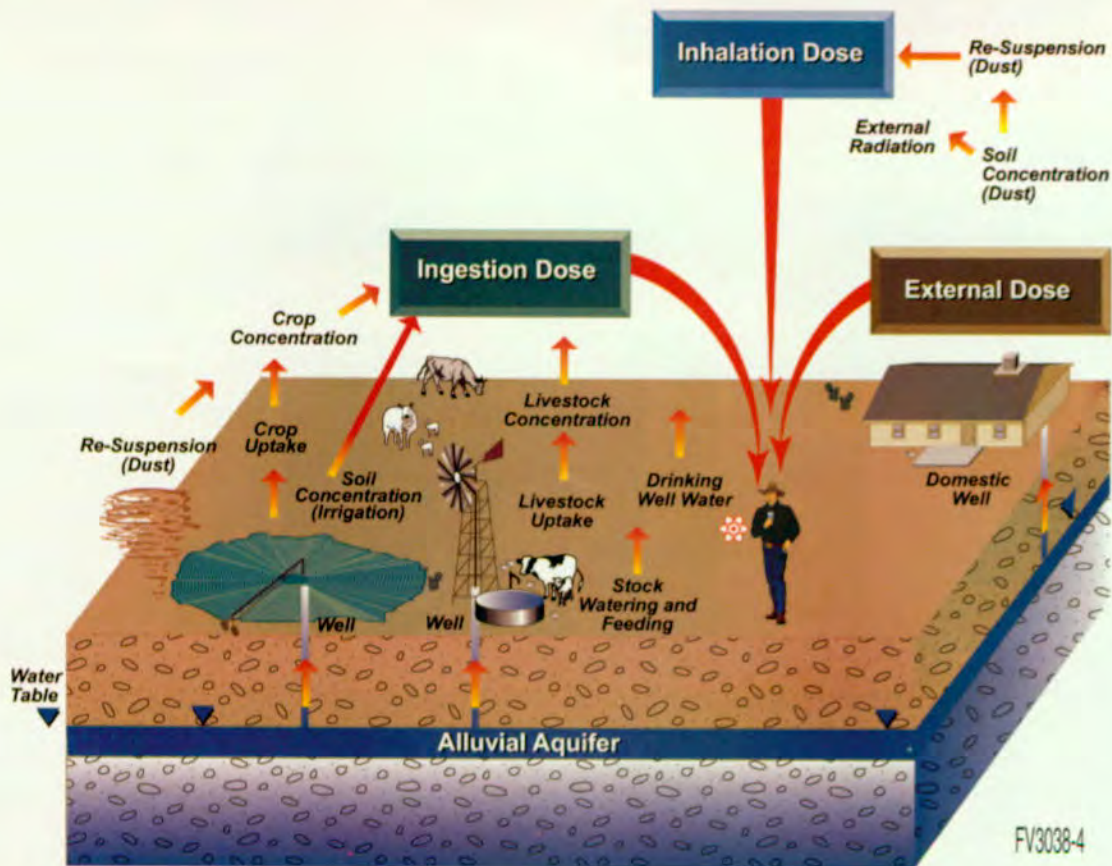


Figure 3-75. Illustration of the Biosphere Modeling Components and Pathways Contributing to Three Major Dose Categories to Humans  
The categories are the ingestion of contaminated food and water, the inhalation of contaminants, and the direct exposure to contaminated soil.

(LaPlante and Poor 1997, p. 2-6). Another ingestion pathway is the inadvertent ingestion of contaminated soil, such as while eating vegetables.

The inhalation pathways involves breathing dust during outdoor activities such as farming and recreation. Uncertainty in the parameters describing this pathway results from difficulties establishing quantities of radionuclides associated with the suspended particles as well as the quantities of material inhaled by residents in the Amargosa Valley. Some of the factors that affect dust resuspension are the density and mineralogical composition of the soil particles and their effects on radionuclide binding, changes in binding and retention of the sorbed radionuclides through time, and the amount of time residents spend outdoors.

The external exposure pathway results from proximity to a radiation source that is external to the body. This pathway is also called "ground shine" when the contaminants are on the ground; but the pathway includes submersion when the contaminants are in the atmosphere, or immersion when in water. Again, there is uncertainty in the dose from this pathway due to differing habits, such as time spent outdoors, time working irrigated crops, or time bathing/showering.

### 3.8.1.3 Regional Survey

A survey of people living in the area was completed in 1997. Among other reasons, the survey was designed to permit an accurate representation of dietary patterns and lifestyle characteristics of residents within the 80-km (50-mile) radiological monitoring grid surrounding Yucca